

Ice Flow Shift, Drumlin, and Bedrock Topography Effects on Glacial Dispersal from Kimberlites  
in the Lac de Gras Region, Northwest Territories, Canada

by

Rebecca Abigail Stirling

A thesis

presented to the University of Waterloo

in fulfillment of the

thesis requirement for the degree of

Master of Science

in

Earth Sciences

Waterloo, Ontario, Canada, 2022

© Rebecca Abigail Stirling 2022

### **Author's Declaration**

This thesis consists of material all of which I authored or co-authored: see Statement of Contributions included in the thesis. This is a true copy of the thesis, including any required final revisions, as accepted by my examiners.

I understand that my thesis may be made electronically available to the public.



## Statement of Contributions

Co-author name	Contribution
Dr. Martin Ross	Helped with the research design, field work, photos, provided guidance, and helped with data interpretation and writing
Dr. Sam Kelley	Helped with the research design, field work, GPS coordinates, photos, initial GIS set-up including layers for surficial geology, lakes, GSC ice flow indicators, data interpretation, and provided guidance
Barrett Elliott	Provided HWRC dataset, and helped further understand the context of the HW dataset, some aspects of diamond exploration, bedrock geology
Dr. Jean Richardson	Provided guidance on QA/QC, data organization, application to industry
Robert Janzen	Provided MS Excel help to draw control lines on QA/QC graphs (Appendix G) and some formatting

## Abstract

Glaciations of the Quaternary Period have had a profound impact on the Canadian landscape and surficial sediments. Understanding glacial landforms and sediments has thus helped develop fundamental knowledge of past glaciations and how they affected landscapes, sediments, and climates. Because Quaternary Period sediments and landforms are ubiquitous in many regions of Canada, studying and understanding them is also important for numerous applications such as mineral exploration. Successful diamond exploration in the Northwest Territories, Canada, for instance, requires detailed knowledge of the glacial history, including ice flow phases and the net effect of several glacial processes. This is because glacial sediments often cover bedrock of interest, and because they can be used for tracing certain minerals, referred to as indicator minerals, back to a buried source. Traditional and proven exploration techniques using glacial sediments evolved from tracing mineralized boulders back to their source to a greater diversity of methods using indicator minerals and geochemical pathfinders. Typically, regional scale programs involve collecting surface samples of glacial sediment (till) and analyzing compositional patterns of interest, sometimes in combination with geophysics to find the most promising bedrock targets. However, this analysis becomes a complex 3D problem in areas of variably thick till. There is also a temporal component often involving shifts in ice flows and thus of sediment transport directions. To address these issues, companies sometimes use a grid-style drilling strategy where till samples are collected vertically at different depths. However, this is a costly and time-consuming approach that may be applied with incomplete knowledge of the full glacial history and/or with limited understanding of bedrock topographic effects and changing subglacial conditions on 3D dispersion. To address this knowledge gap, this research uses a large reverse circulation (RC) drilling and hand-sampling dataset from the Harry Winston (HW) camp south of Lac de Gras in the Northwest Territories to improve our understanding of how till thickness and bedrock topography control or affect sediment dispersal from known kimberlites in areas that were affected by shifting ice flow phases during the last glaciation.

Two study areas were selected to investigate two different problems. The first problem is about the effect of subglacial landform forming processes on till composition and 3D dispersal patterns. For example, recent models about drumlin formation (aka drumlinization) suggest they could be dominantly erosional, raising the possibility for the preservation of dispersal patterns inherited from ice flow phases that preceded drumlinization. The second problem is related to kimberlites that did not produce a clear dispersal train in glacial sediments. Here, the research investigates the specific case of a kimberlite (Big Blue) nested in a bedrock topographic high consisting of more resistant rocks (granitoids) than the surrounding lower terrain (metasediments). In both study areas, landform-scale and outcrop-scale ice flow indicators record a clockwise shift in ice flow from southwest to west, to northwest. Although the most dominant and youngest ice flow is to the northwest, there are still erosional evidence leftover (e.g., roches moutonnées) from the oldest and greater sediment-generating ice flow phases. RC drilling is not sensitive enough to determine the detailed vertical till stratigraphy. Nonetheless, useful insights can be obtained from compositional data about the possible occurrence of relict till preserved at the base of deeper boreholes, or increasingly inherited till at depth, such as at the core of drumlins or in lee-side deposits. The research problems were investigated by analysing

and interpreting clast lithology and kimberlite indicator mineral (KIM) patterns at depth and at surface throughout the two selected study areas within the large HWRC dataset.

Kimberlite indicator mineral patterns in the east study area demonstrate well-preserved isolated 3D sediment dispersal in a drumlin field that persists through the full thickness of the till column. Field observations and satellite imagery of landforms and ice flow indicator measurements constrain till and indicator mineral provenance, while multiple datasets, including KIM grain counts (peridotitic and eclogitic pyrope, olivine, Cr-diopside, chromite, and picroilmenite), pathfinder geochemistry (Ni, Cr, Co Nb, Ba, Rb), and clast lithology (granitoid pebble counts %), indicate high inheritance in the thicker till within the drumlin field associated with the oldest SW ice flow phase. In addition, partial overprinting and till re-entrainment by the younger W and NW ice flow events reshaped the landscape thereby fragmenting and smearing older dispersal trains that are preserved in the subsurface sediments. Although the surficial till in the drumlin field could be a discontinuous till cap, erosional processes could have exposed relict till at the surface.

Bedrock topography protected till at depth in the west study area, preserving a weak till dispersal train from a distal kimberlite at the base of a bedrock topographic high, whereas the lack of a dispersal train from the subcropping Big Blue kimberlite nested in a granitoid knob may be explained by the formation of a lee-side cavity, causing the glacier to pass over the kimberlite. Lee-side cavity filling and the formation of a crag-and-tail landform around the granitoid knob are considered the main mechanisms for explaining till thickness variations and vertical compositional changes identified from deeper boreholes. Further analysis of other settings with soft rock bodies nested in bedrock knobs would need to be conducted to determine whether the lack of surficial dispersal trains is common in this situation, or if it is due to specific or rare local conditions. Field observations and satellite imagery of glaciofluvial corridors that wrap around Big Blue as well as small channels that run overtop of the granitoid knob could have received sediment supply from the kimberlite, or alternatively the corridors could have re-entrained and mobilized till containing inherited indicator minerals sourced from distal kimberlites up the older up-ice ice flow direction (NE).

Overall, this study further refines and constrains the local ice-flow history south of Lac de Gras, characterizes a well-preserved palimpsest dispersal train in a drumlin field, and provides a model for explaining the lack of a clear dispersal train from a known kimberlite nested in a bedrock topographic high. Till deposited during earlier ice flow phases appear to have been better preserved within drumlins and other areas of thicker till, such as down-ice bedrock steps. Steps in bedrock topography served to prevent erosion of pre-existing lee-side sediment, as well as of a nested kimberlite, to the extent of preventing a surficial dispersal train from forming down-ice of the kimberlite. This study thus provides a conceptual model for explaining why, in certain cases, kimberlites that intersect the bedrock surface may not produce a clear dispersal train at surface. Results from this research suggest there is an opportunity to re-examine subsurface till dispersal patterns in legacy datasets in the Lac de Gras region to better consider effects of ice flow shifts, drumlin formation, and bedrock topographic effects. This could potentially lead to new discoveries.

## **Acknowledgements**

This research was funded by the Northwest Territories Geological Survey (NTGS) as part of the Slave Province Surficial Materials and Permafrost Study (SPSMPS) supported by the Canadian Northern Economic Development Agency's (CanNor) Strategic Investments in Northern Economic Development (SINED) program. Additional financial support was provided by thesis supervisor, Dr. Martin Ross, and by the University of Waterloo. This research was made possible with the donation of the large HWRC dataset containing mineral exploration results from Dominion Diamond Mines and North Arrow Minerals Inc.

I want to thank Drs. Martin Ross and Sam Kelley for their help and mentorship during field work, and the support of Barrett Elliot with logistical support. Dr. Sam Kelley's mentorship preparing for my first conferences and guidance in scholarship applications was invaluable. Fellow research group members Bob, Jessey, Thomas, Grant, and Caroline consistently supported me while I prepared for conference talks and the 3MT competition and were there for those presentations. Jessey's mentorship in the office, Bob's help with specific technical issues, Grant's support with ArcGIS, Roger's special studies class, and Andrea's introduction to the lab were priceless. Dr. Jean Richardson was amazing in her support when the pandemic broke out and checked in daily with Skype visits. Elisabeth and Jessica were also fantastic encouragers and resources. I also want to thank my Toastmasters club for the priceless feedback and confidence I received from them to prepare me for giving talks in front of audience members. Ultimately, it was the understanding of my committee members and Dr. Martin Ross's constant enthusiastic support for my research and compassion as I navigated the grief of losing my sister that helped me complete this project.

## **Dedication**

To the amazing John Dawson: the biggest positive influence in my adult life. Thank you for sharing part of your remarkable life and wisdom with me.

## Table of Contents

Author's Declaration.....	ii
Statement of Contributions .....	iii
Abstract .....	iv
Acknowledgements.....	vi
Dedication .....	vii
List of Figures .....	xii
List of Tables .....	xx
CHAPTER 1: Introduction .....	1
1.1 Scientific Rationale.....	1
1.2 Background.....	4
1.2.1 Subglacial Erosion, Transport, and Deposition .....	4
1.2.1.1 Abrasion and quarrying.....	4
1.2.1.2 Landform processes .....	6
1.2.1.3 Subglacial drainage.....	8
1.2.1.4 Regelation intrusion and englacial transport.....	9
1.2.1.5 Subglacial sediment deformation.....	10
1.2.1.6 Till deposition .....	11
1.2.2 Drift Prospecting.....	11
1.2.2.1 Drift prospecting using till .....	12
1.2.3 Indicator Minerals .....	12
1.2.3.1 Kimberlite indicator minerals .....	13
1.2.4 Till Matrix Geochemistry .....	13
1.2.4.1 Geochemical pathfinder elements.....	14
1.2.5 Palimpsest Dispersal .....	15

1.3 Study Areas .....	17
1.3.1 Regional and Local Bedrock Geology .....	18
1.3.2 Surficial Geology and Ice-Flow History in Study Areas .....	19
1.3.3 Bedrock Topography and Drift Thickness.....	21
1.4 Specific Research Problems and Thesis Objectives .....	21
1.5 Methodology .....	22
1.5.1 Fieldwork .....	22
1.5.2 Ice-Flow Indicators .....	23
1.5.3 Sediment Sampling .....	24
1.5.4 Sedimentological and Geochemical Analyses .....	24
1.5.5 Sample Preparation and Grain Size Measurements.....	25
1.5.5.1 Clast lithological classification .....	26
1.5.5.2 QA/QC and analytics .....	26
1.5.6 Geochemical Sample Processing .....	27
1.5.6.1 Element analysis .....	27
1.5.6.2 QA/QC and analytics .....	29
1.5.7 Indicator Minerals Sample Processing.....	30
1.5.7.1 Kimberlite indicator extraction and electron microprobe analysis.....	31
1.5.8 HW Dataset.....	31
1.5.8.1 HW data processing .....	32
1.5.9 Mapping and Data Integration .....	33
1.5.9.1 Provenance study .....	34
1.6 Thesis Structure .....	34
CHAPTER 2: Preserved three-dimensional sediment dispersal in a drumlin field, southeast of Lac de Gras, Northwest Territories.....	35

2.1 Introduction.....	35
2.2 Study Area .....	36
2.3 Methodology.....	40
2.3.1 Fieldwork.....	41
2.3.2 Sediment and Geochemical Analysis.....	41
2.3.3 HW Dataset.....	41
2.3.4 Data Analysis and Mapping.....	42
2.4 Results and Interpretations.....	43
2.4.1 Field-based Ice Flow Indicators and Till Characteristics .....	43
2.4.2 Kimberlite Indicator Minerals.....	48
2.4.3 Till Texture, Clast Lithology, and Till Matrix Geochemistry .....	53
2.4.3.1 Till texture.....	54
2.4.3.2 Pebble lithology .....	55
2.4.3.3 Surficial till matrix geochemistry .....	59
2.5 Discussion.....	62
2.5.1 Role of Till Thickness Variability on Dispersal Patterns .....	65
2.5.2 Implications for Drift Prospecting .....	65
2.6 Conclusions.....	66
CHAPTER 3: Bedrock topographic effects on down-ice three-dimensional sediment dispersal patterns, south of Lac de Gras, Northwest Territories .....	67
3.1 Introduction.....	67
3.2 Study Area .....	68
3.3 Methodology.....	72
3.3.1 Field Work.....	72
3.3.2 Sediment and Geochemical Analysis.....	73



3.3.3 HW Dataset.....	73
3.3.4 Data Analysis and Mapping.....	74
3.4 Results and Interpretations.....	74
3.4.1 Field-based Ice Flow Indicators and Landscape Characteristics .....	74
3.4.2 Kimberlite Indicator Minerals.....	79
3.4.3 Sample Texture, Clast Lithology, and Geochemistry .....	83
3.5 Discussion.....	92
3.5.1 Role of Bedrock Topography and Multiple Ice Flows on Dispersal Trains and Till Thickness .....	94
3.5.2 Implications for Drift Prospecting .....	98
3.6 Conclusions.....	99
CHAPTER 4: Conclusions .....	100
4.1 Identifying Potential Effects related to Bedrock Topography and Till Thickness Variations on Till Dispersal Trains .....	100
4.1.1 Thesis Contributions .....	100
4.1.2 Research Questions:.....	101
4.1.3 Drift Prospecting in Areas with Variable Till Thickness and Bedrock Topography.....	102
4.1.4 Future Work.....	103
References.....	105
Appendix A: UW field sample and sample type.....	118
Appendix B: Ice flow indicator field measurements.....	121
Appendix C: KIM results for UW and HW data, and HW KIM data processing.....	124
Appendix D: Sediment texture results for UW data .....	140
Appendix E: Clast lithology results for UW and HW data.....	161
Appendix F: Geochemistry results for UW data.....	200
Appendix G: QA/QC results for UW and HW data.....	231

## List of Figures

<b>Figure 1.1:</b> Ice advance over a pre-existing till sheet creates a continuum of inheritance and overprinting. A) Layered stratigraphy due to net deposition during several ice flow phases B) Till with unidirectional indicators and provenance consistent with the latest ice flow phase; prior deposits have been completely reworked C) High overprinting of pre-existing sediment during a younger ice flow phase, minor inheritance at surface D) Mix of inheritance and overprinting from two or more phases E) Limited overprinting, high inheritance from earlier phases F) Complete preservation of earlier phases (modified from Trommelen et al., 2013).....	2
<b>Figure 1.2:</b> Location of the general study area in the Lac de Gras region in the Northwest Territories, Canada (Image credit: Google Earth). .....	3
<b>Figure 1.3:</b> Initiation and optimization of quarrying on lee slopes at planes of weakness in main bedrock structures (after Gordon, 1981; modified from Benn and Evans, 2010).....	5
<b>Figure 1.4:</b> Roche moutonnée in the eastern study area. Shovel pointed in direction of younger (NW) ice flow (295°). .....	7
<b>Figure 1.5:</b> Drumlin core cross-section decreasing in complexity (palimpsest) from A to E. A) Layered stratigraphy; B) layered stratigraphy with minor inheritance; C) overprinting with minor inheritance; D) complete reworking with internal deformations, and E) complete preservation of till/bedrock (modified from Stokes et al., 2013).....	8
<b>Figure 1.6:</b> Subglacial cavity systems are variably connected and pressurized depending on ice-overburden pressure. Channelized systems can develop during instability, such as periods of deglaciation (modified from Hooke, 2005; after Kamb, 1987). .....	9
<b>Figure 1.7:</b> Model of the regelation intrusion process. $H_s$ = thickness of regelated sediment, $V_r$ = intrusion rate, $P_i$ = pressure of the ice, $P_w$ = pore water pressure (after Iverson, 1993). .....	10
<b>Figure 1.8:</b> 2D surficial palimpsest dispersal trains and the ice flow phases that could create them (modified from Parent et al., 1996).....	16
<b>Figure 1.9:</b> The overall study area within the regional bedrock geology context mapped at 1:250 000 scale (bedrock geology compilation by Kjarsgaard et al. (2002)). Bedrock within the study area is Archean in age, except for a small mafic intrusive body, Proterozoic in age, near the northeast corner of the map. The dashed box outlines view extent in <b>Fig. 1.10</b> , <b>Fig. 1.11</b> and <b>Fig. 1.12</b> .....	19

**Figure 1.10:** Surficial geology by Ward et al. (1997) draped over the Arctic Digital Elevation Model (ArcticDEM) (Porter et al., 2018). Inset shows a clockwise ice flow shift based on GSC measurements and relative age relationships. Study areas outlined in dashed boxes. The combined surficial geology and ArcticDEM highlights the relationship between till blanket and drumlin fields (especially between Lac de Gras and Mackay Lake). Surficial geology unit codes: O (organics) GFf (glaciofluvial outwash fan sediments) GFr (eskers) Tv (till – veneer) Tb (till – blanket) Th (till – hummock). Dotted white boxes show the two study areas..... 20

**Figure 1.11:** Quaternary Period sediment thickness model from Kelley et al. (2019b) modelled at 1:250,000 with 30-meter resolution highlights west study area bedrock topographic high (expressed as bedrock) and east study area drumlin field. Dotted black boxes outline the two study areas..... 21

**Figure 1.12:** Location of UW surficial (large purple) and HWRC borehole (small black) sample sites, with publicly available kimberlite locations on surficial geology by Ward et al. (1997). Dotted white boxes outline the two study areas..... 23

**Figure 1.13:** Workflow for UW samples returned to UW Quaternary research lab for mechanical preparation, and provenance analysis ..... 25

**Figure 1.14:** HWRC Dataset organization and available information contains descriptive and measured data..... 31

**Figure 2.1:** Conceptual cross-section of a stratified drumlin with hypothetical RC drill holes represented by dashed boxes. Drilling in a grid pattern through areas of thicker till could sample till of different provenance, making data interpretation challenging..... 36

**Figure 2.2:** Google Earth image of the broad region with diamond mines and study areas. Approximately 300 km NE of Yellowknife, Ekati mine developed in late 1990s, Diavik mine in early 2000s; Snap Lake mine developed over mid-2000s, and Gahcho Kué mine developed over mid-2010s. The east study area is outlined in dashed white box..... 37

**Figure 2.3:** Landscape of areal scouring with zones of bedrock outcrops (grey) and zones of till and other surficial sediments (brown and green)...... 38

**Figure 2.4:** Flat topped esker. Reworked esker provides evidence of shoreline reworking (and glacial lake inundation) in the study area. Shoreline reworking of surficial till in the study area is also expected. .... 39

**Figure 2.5:** Surficial geology and distribution of HW drillhole locations and the local study area (white dashed outline). Drumlin corridor is a predominant feature, extending from southeast at the northern tip of MacKay Lake, to northwest at the southern edge of Lac de Gras. .... 40

**Figure 2.6:** Eleven ice flow indicator measurements taken at six locations are consistent with GSC measurements from Ward et al. (1997), indicating a clockwise shift in ice flow from southwest to northwest..... 44

**Figure 2.7:** Rose diagram displaying 11 ice flow indicator measurements collected for this study..... 44

**Figure 2.8:** Ice flow indicators on outcrop and whalebacks. A) Stoss-lee relationship indicating ice flow from left to right; B) Polished surface with striations and grooves towards the NW; C) relative age relationship (older = 259° and younger = 284°) established on the basis of protected polished surface and upper (top of outcrop) indicators; Till veneer covering striae better protects striae from subsequent glacial movement, while the exposed top of the whaleback is striated in direction of youngest ice flow, aligned with the Brunton compass pointed in the down-ice direction (right of photo, adjacent magnetic variation-corrected annotation). .... 44

**Figure 2.9:** Roches moutonnées. A) Roches moutonnées formed by the earlier SW flow phase are well preserved in the northeast of the study area. B) Shovel pointed in direction of younger (NW) ice flow (309°). C) Pluck faces formed during older (SW) ice flow (259°). .... 46

**Figure 2.10:** Whalebacks present down ice of DO-40/DO-41. Previous pluck face smoothed during subsequent ice flow. Marker pointed in down-ice direction where till buried old lee-side of landform..... 46

**Figure 2.11:** Till samples collected from frost boils on drumlin tops. (A) Sample site 17-RS-001-B after clearing surface organics (B) and after extracting sample material for a KIM and geochemical/textural sample. (C) Sample site 17-RS-011-B contained sandy pebble till with micas collected from the southeast side of a small truncated drumlin. The top of the pit contained oxidized material with dark-brown large gravel and small cobbles where the matrix was washed out. Sample material was collected from below this oxidized zone. (D) Sample site 17-RS-012-B contained sandy pebble till collected from the southwest side of a drumlin along a scarp face. There were exposed large cobbles and some boulders on the surface (both metasedimentary with some chocolate-brown oxidation in felsic boulders) where fines were washed down-slope. (E)

Sample site 17-RS-014-B contained very sandy angular pebble till collected from the northeast side of a drumlin. Small boulders and large cobbles were exposed on surface..... 47

**Figure 2.12:** Scarped drumlin flanks visible from the air, possibly eroded from glaciolacustrine wave washing. Dashed lines and circles outline scarp flanks to make them easier to see. .... 48

**Figure 2.13:** Drumlins, especially their southwest side, have eroded flanks..... 49

**Figure 2.14:** KIM count results normalized to 10kg samples. On previous page: A) KIM counts from within base of borehole depth interval on sediment thickness map. Moving up the borehole depth interval; B) HW lower-mid depth interval; On this page: C) HW upper-mid depth interval; and D) HW top depth interval, displayed with UWaterloo KIM count results on surficial geology map. Dashed black lines outline clusters of KIM grains. Surficial geology unit codes: O (organics) Gff (glaciofluvial outwash fan sediments) GFr (eskers) Tv (till – veneer) Tb (till – blanket) Th (till – hummock)..... 52

**Figure 2.15:** Map containing publicly available surface KIM data from NTGS Data Hub, and all publicly known kimberlites (subcropping and an intercept depth of up to 30 feet at 90 degree dip angle) in the area (Kjarsgaard, 2007). Dashed white box outlines the study area. Dashed black ovals roughly outline potential dispersal trains using total KIM grain counts from NTGS Data Hub KIDD data <datahub-ntgs.opendata.arcgis.com>. .... 53

**Figure 2.16:** Cumulative weight percent textural analysis curve. Samples collected within the drumlin field in the western portion of the study area are separated from samples collected in the zone of till veneer in the northern portion of the study area. Samples that have associated indicator analysis are represented with dashed lines. Textural samples were also collected adjacent a lake beach setting from one location where layered sand was observed. .... 55

**Figure 2.17:** Example of lithology classification using sample 17-RS-018-B. Several other examples are in Appendix E. .... 56

**Figure 2.18:** Granitoid clast lithology at depth using data from HWRC Dataset. On previous page: A) base depth interval of borehole granitoid clast estimates are higher than expected and the cluster persists moving up the borehole to B) HW lower-mid depth interval. On this page C) HW upper-mid depth interval, D) HW top depth interval, displayed with UWaterloo granitoid clast count results, shows cluster of higher granitoid clasts persists through the till column..... 58

**Figure 2.19:** Distribution of selected geochemical results from UWaterloo surficial till samples. On previous page: A) Percentiles of Ni, Co, Cr, Nb (total digestion) also display a cluster of

elevated values in the drumlin field. B) Rubidium. On this page: C) Barium total digestion results display a cluster of elevated values in the drumlin field, as well as in the direction of the youngest ice flow from a known kimberlite source. C) Surficial geology unit codes described in **Fig. 2.14**..... 61

**Figure 2.20:** Q-Q plots used for assessing thresholds and elevated (See sections 1.2.4.1 and 1.5.6) values in pathfinder elements. Ba and Cr used ICP-OES total digestion method, and Rb, Ni, Co, Nb used ICP-MS total digestion method..... 62

**Figure 2.21:** Interpretation of surficial KIM dispersal patterns, and higher granitoid clast lithology and geochemical pathfinder values superimposed on till thickness model by Kelley et al. (2019b). The black dashed outlines are interpreted from UW and HW KIM grains. The green dashed outlines are interpreted from the public KIM surface dataset. The pink dashed outline is interpreted from the UW and KIM granitoid clast lithology. The brown dashed outline is interpreted from UW Ni, Cr, Co, Nb geochemical results. The orange dashed outlines are interpreted from the Rb and Ba geochemical results. Till was initially transported to the southwest across the study area during the oldest known ice flow phase. The till was then eroded into drumlins and only partially re-entrained to the northwest. Thicker and mostly relict till from the southwest ice flow phase is thus preferentially preserved in the core of drumlins. Elsewhere, northwest entrainment and/or re-entrainment was more important during the younger northwest ice flow phase. .... 64

**Figure 3.1:** Approximately 300 km NE of Yellowknife, Ekati mine developed in late 1990s, Diavik mine in early 2000s; Snap Lake mine developed over mid-2000s, and Gahcho Kué mine developed over mid-2010s (Google Earth Images). The west study area is outlined in dashed white box..... 69

**Figure 3.2:** Bedrock geology (Kjarsgaard et al., 2002) map highlights major lithologies overlain on ArcticDEM (Porter et al., 2018) with dashed outline of study area. Samples collected for this thesis work are purple points, while the donated dataset are black points. .... 70

**Figure 3.3:** Panorama of granitoid knob with Big Blue Kimberlite nested in a bowl-shaped depression (under the lake), looking in the up-ice direction towards the knob. .... 71

**Figure 3.4:** Panorama of meltwater corridor with kames, looking westward..... 71

**Figure 3.5:** Twenty-two ice flow indicator measurements taken at ten locations are consistent with regional GSC measurements from Ward et al. (1997) indicating a clockwise shift in ice flow from southwest to northwest. Ice flow summary provided as inset in results maps..... 75

**Figure 3.6:** Rose diagram displaying ice flow indicator measurements collected for this study. N=22 ..... 76

**Figure 3.7:** Striation cross cutting relationships on a metasedimentary outcrop located on the west side of the study area. Oldest flow (1) = 253°, intermediate flow (2) = 269°, and youngest flow (3) = 324°. Note that although this specific outcrop could be in a possible area of deflection during the youngest flow, the cross-cutting relationships are well represented. .... 77

**Figure 3.8:** Large topographic high consisting of granitoid bedrock. The Big Blue kimberlite is nested within a depression within a local bedrock knob on the topographic high. Glaciofluvial corridors are outlined in orange dash marks. In addition, small channels cut across the local rock knob surrounding Big Blue. Note the absence of the pond covering the Big Blue kimberlite in study area maps, because it is relatively too small to map. Surficial geology polygons from Ward et al. (1997). .... 78

**Figure 3.9:** A) Kame within a glaciofluvial corridor covered with cobbles and small boulders. B) Perched boulders in meltwater corridor. C) Cross-section of esker within meltwater corridor crosscut by creek. D) Discontinuous esker within glaciofluvial channel, possibly washed by glaciolacustrine processes. .... 79

**Figure 3.10:** Normalized KIM counts from the HW till samples displayed as intervals classified into borehole depth intervals superimposed on sediment thickness map (Kelley et al., 2019b). On previous page: A) base, B) lower-mid. On this page: C) upper-mid, and D) top (surface). A pattern of indicator minerals along base of topographic high persists through the till column.... 82

**Figure 3.11:** Normalized KIM counts for UW samples collected at surface for this study. They include one till sample (orange triangle) and five glaciofluvial samples (circles). Glaciofluvial corridor outlined in yellow..... 83

**Figure 3.12:** Examples of till sample sites collected for geochemical, lithological, and textural analysis. A) Oxidized and unoxidized till zones at sample site 17-RS-030-B. B) Sample site 17-RS-025-B was collected immediately up-ice of Big Blue from a frost boil. C) 17-RS-023-B was collected down-ice of the kimberlite (in a zone of thicker till) and contained finer grained sand, few pebbles, and few large cobbles. D) 17-RS-039-B was collected near the confluence of two

meltwater channels to the west northwest of the Big Blue. Nearby is a boulder balanced on washed out till perched on cobbles. Despite the proximity to the meltwater channels,, this sample was collected from a till mound, containing unoxidized fine-sandy pebble till with cobbles and small boulders. .... 84

**Figure 3.13:** Curves in blue represent glaciofluvial sediment sample texture, curves in green represent till sample texture, and curves in red are washed till. The outlying sample with the highest coarse-grained material came from a sample site that was collected from the side of a drumlin that appeared wave washed. .... 85

**Figure 3.14:** On previous page: A) top map shows granitoid clast content in the base interval of sediment thickness (adjacent bedrock) in the HW dataset is low. B) Granitoid content in the lower-mid interval. On this page: C) granitoid clast content in the upper mid-interval. D) Granitoid content in the top interval (surface). .... 88

**Figure 3.15:** Box plots highlight lower granitoid clast content (compared to metasediment clast content) at the base of the boreholes compared to the surface. .... 89

**Figure 3.16:** Till matrix geochemistry QQ plots do not indicate outliers of note. Ba and Cr used ICP-OES total digestion method, and Rb, Ni, Co, Nb used ICP-MS total digestion method. .... 90

**Figure 3.17:** Till matrix geochemistry across the study area. A) Rubidium and B) Barium results for till (n=14) and glaciofluvial samples (n=2). Sample result from flank of a wave washed drumlinoid is outlined in black dashed box (A)..... 91

**Figure 3.18:** Till matrix geochemistry across the study area (n=14). Metals results, calculated as normalized percentile sums (Grunsky, 2010), used as pathfinder elements for kimberlites are low in the youngest ice flow direction. Glaciofluvial results are not displayed due to mobility and density issues associated with water transport. Sample result from flank of a wave washed drumlinoid is outlined in black dashed box. .... 92

**Figure 3.19:** NTGS datahub publicly available total grain count does not show significant KIM grains on the bedrock topographic high. The data set does not contain any sample weights, and therefore samples cannot be normalized to 10kg in the same way as the HW or UW KIM data. Distances from distal subcropping kimberlites are provided along dotted white lines (20 km and 30 km in the older and youngest ice flow directions, respectively, while 30 km and 35 km ranges are given down ice of Big Blue, a distance consistent with other dispersal train lengths known subcropping kimberlites to the east). Blue arrows outline the oldest and youngest ice flow



directions from Big Blue as a centre point. KIM grain counts from NTGS Data Hub KIDD data <datahub-ntgs.opendata.arcgis.com>. .... 94

**Figure 3.20:** ArcticDEM (Porter et al., 2018) image draws attention to the bedrock protrusion to the east of the kimberlite (dashed red) an ideal configuration for the development of a cavity (dashed orange) over the kimberlite. Steep pluck faces on the lee-side in the oldest ice flow direction and drumlinization from subsequent ice flow phases are also visible. .... 95

**Figure 3.21:** Small channels cross the granitoid knob probably drained into lateral channels on occasion, possibly mobilizing some material from the Big Blue kimberlite. .... 96

**Figure 3.22:** Model of nested kimberlite within granitoid knob with small subglacial cavity over the kimberlite. .... 97

**Figure 3.23:** Sediment thickness model (Kelley et al., 2019b) highlights thicker till in both down ice directions from the bedrock knob, and also down-ice the broad granitoid topographic high (NW corner of the map). It is possible there are two crag-and-tail features at two scales (red dashed outline and yellow dashed outline). .... 98

## List of Tables

<b>Table 1.1:</b> Geochemical pathfinder elements for diamondiferous kimberlites in the Northwest Territories and Lac de Gras area ( <sup>1</sup> Wilkinson et al., 2001a; <sup>2</sup> McClenaghan et al., 2002; <sup>3</sup> McClenaghan and Kjarsgaard, 2007; <sup>4</sup> McClenaghan et al., 2018). .....	15
<b>Table 1.2:</b> Northwest Territories diamond mine production summary (see websites in bottom row for information). .....	18
<b>Table 1.3:</b> SRC geochemical analysis summary. ....	28
<b>Table 1.4:</b> Standardized depth interval assigned to bins for 3D analysis.....	32

## CHAPTER 1: Introduction

### 1.1 Scientific Rationale

Drift prospecting is a mineral exploration technique that focuses on tracing mineralized boulders, indicator minerals, and geochemical pathfinders in surficial sediments back to their buried source (e.g., McClenaghan and Paulen, 2018). In Canada, surficial sediments are predominantly glacial in origin (Fulton, 1995); therefore, the technique is particularly focused on glacial processes, such as subglacial erosion of mineralized bedrock, entrainment and comminution, and deposition of sediments by ice sheets during the glaciations of the Quaternary Period (e.g., DiLabio and Coker, 1989; Kujansuu and Saarnisto, 1990; Shilts, 1996; McMartin and Paulen, 2009). The technique typically focuses on surficial till samples collected within the shallow subsurface (~0.3-0.5m) and assumes that the material captures the erosion and dispersal history of the prospective diamond area. This assumption may be valid in areas characterized by an ice flow record that can be summarized by relatively simple curvilinear flowlines (e.g., McClenaghan, 2005; Strand et al., 2009; Sharpe et al., 2017). However, several studies have led to a realization that most areas experienced complex ice flow shifts due to changes in the configuration of the ice sheet over time (c.f. Dyke and Prest, 1987; Boulton and Clark, 1990ab; McClenaghan, 1994; Clark, 1999; McMartin and Henderson, 2004; Stea et al., 2009; Paulen et al., 2014; Hodder et al., 2016; Gauthier et al., 2019). Regions in the Canadian Shield, for example, far from the margins of the last glacial maximum extent, still bare erosional and depositional evidence of multiple ice flow phases (Shilts, 1991; Stea et al., 2009; Hodder et al., 2016; Rice et al., 2019).

As a result of complex ice flow, tills of hybrid compositions were produced due to re-entrainment of earlier sediments and mixing with newly-produced sediments: processes which create inheritance or overprinting of till composition (e.g., Parent et al., 1996; Stea and Finck, 2001; Trommelen et al., 2013). Compositional and sediment fabric inheritance or overprinting appear to vary along a continuum (**Fig. 1.1**). This continuum increases the complexity of discerning end-member and hybrid till units across a study area (Trommelen et al., 2013). In areas of higher sediment supply and deposition, till stratigraphy could be generated whereby the surface till only captures the last till production event (**Fig. 1.1**), whereas underlying tills could have protected subcropping mineralized bedrock. Essentially, we now know that the sediment constituting a surficial till across an area could be variably inherited from earlier ice flow phases, which could form fragmented dispersal compositional patterns that are not fully consistent with the dominant ice flow direction recorded in the surficial landscape (e.g., Parent et al., 1996; Stea and Finck, 2001; Trommelen et al., 2013). Additional complications could also affect dispersal patterns, such as where till thickness and bedrock topography vary by several meters (e.g., Kelley et al., 2019a). In summary, multiple factors could affect till dispersal and resulting dispersion patterns which can complicate interpretation of results leading to difficulties in identifying a buried mineralized source.

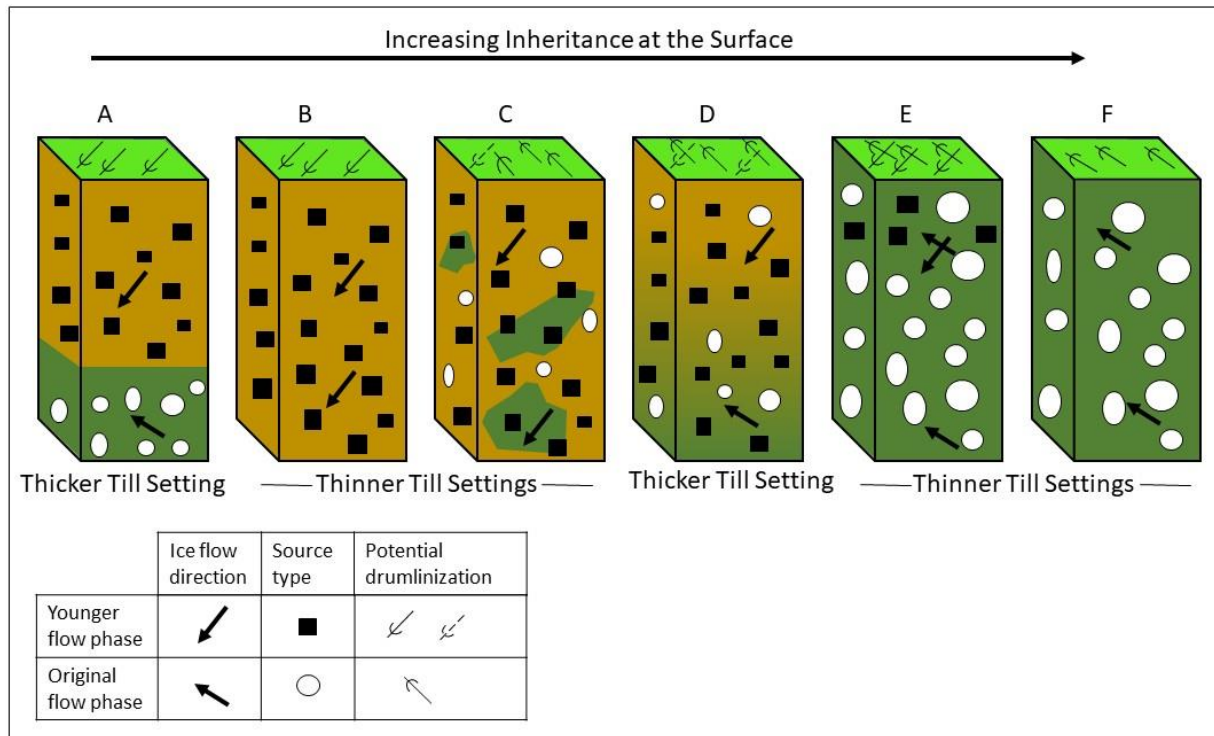


**Figure 1.1:** Ice advance over a pre-existing till sheet creates a continuum of inheritance and overprinting. A) Layered stratigraphy due to net deposition during several ice flow phases B) Till with unidirectional indicators and provenance consistent with the latest ice flow phase; prior deposits have been completely reworked C) High overprinting of pre-existing sediment during a younger ice flow phase, minor inheritance at surface D) Mix of inheritance and overprinting from two or more phases E) Limited overprinting, high inheritance from earlier phases F) Complete preservation of earlier phases (modified from Trommelen et al., 2013).

We still know little about the effect of till thickness and bedrock topography variations on till dispersal patterns, both at the surface (2D) and in the subsurface (3D). In the Lac de Gras region, in the Northwest Territories, Kelley et al. (2019a) analyzed surface and subsurface dispersal patterns originating from two kimberlites located close to each other (DO-18 and DO-27 kimberlites). This is the first published research on 3D dispersal patterns down-ice of known kimberlite deposits, which provided useful insights into bedrock topography effects on till dispersal. Kelley et al. (2019a) found that bedrock topography had multiple effects on the dispersal of material from the kimberlite sources, as well as on the preservation of older patterns at depths. Firstly, it was demonstrated that an elongated depression down-ice of one of the kimberlites had a clear effect on the till dispersal of kimberlitic material. Secondly, a bedrock topographic high had a shielding effect in the down-ice dispersal direction from the second kimberlite, limiting and deflecting dispersal from that kimberlite. Finally, down-ice from that bedrock high, an older till at depth showed evidence of dispersal related to an older ice flow direction; bedrock topography clearly had played a role in protecting that till from subsequent re-entrainment by younger ice flows. Despite these findings, important questions remain about the effect of bedrock and till thickness on dispersal trains, especially in different settings. Subglacial landforms, such as drumlins, also occur variably on till surfaces and exhibit a wide range of spatial characteristics, such as density, elongation, and amplitude (e.g., Fowler et al., 2013;

Hillier et al., 2013; Ely et al., 2016, 2018; Clark et al., 2018; Sookhan et al., 2021). Some studies have investigated variations of the direction of shear in till across a drumlin field (Menzies et al., 2016; Iverson, 2017), but few have looked specifically at the effect of these fields of subglacial landforms on till compositional patterns. The recent study by Sookhan et al. (2021) looks at this problem of till dispersion in a drumlin field in the context of ice streaming and strong overprinting using detailed geomorphological analysis of drumlins, but with limited pebble lithological counts from surficial samples. There is thus still limited knowledge about the effects of shifting ice flow and drumlinization of layered till stratigraphy on 2D and 3D dispersal patterns, and how drift prospecting strategies could take these landforms, and the processes related to their formation, into account.

My research addresses these knowledge gaps by investigating till composition across an area (**Fig. 1.2**) that is known to have been affected by different ice flow phases, which has variable till thickness and bedrock topography, and whose till surface is also variably drumlinized. The selected area is also a prospective area for diamond. It is thus important to mention that diamond exploration in Canada has applied drift prospecting techniques extensively since the 1990s, during which time a suite of indicator minerals and geochemical pathfinders was developed for this commodity (e.g., McClenaghan and Kjarsgaard, 2007).



**Figure 1.2:** Location of the general study area in the Lac de Gras region in the Northwest Territories, Canada (Image credit: Google Earth).

In addition, the large HWRC dataset (Dominion, 2022) covering the study area and containing surface and subsurface indicator mineral results from a large industry-led drilling exploration program was donated to the Government of the Northwest Territories, which then made it available to us for further study. This dataset, alongside other publicly available data and new

targeted data collected as part of this thesis research (see below), provides an opportunity to explore and understand the relationships between ice flow shifts and variable till thickness and bedrock topography in an unprecedented way.

## 1.2 Background

To understand the problem of till dispersion in more details, it is useful to review the main concepts surrounding subglacial erosion, entrainment by ice, deposition, and landforms, as well as the main concepts and strategies of drift prospecting. This section provides an overview of these concepts, processes, and methods.

### 1.2.1 Subglacial Erosion, Transport, and Deposition

Two important erosional processes occur at the ice-bed interface when wet basal ice is sliding on hard bedrock: abrasion and quarrying (Benn and Evans, 2010). These two processes create particles of varying sizes at the site of erosion. At that point, various processes can be involved which can act on the newly generated particles, and any pre-existing particles, to facilitate their evacuation from the erosion site. These ‘entrainment’ processes may be viewed as part of the erosion process as they are required to set particles into motion and remove them from the site. Other processes could then become important to keep particles in motion until deposition. The main processes are described and explained below.

#### 1.2.1.1 Abrasion and quarrying

Abrasion wears rock surfaces on particle- to landform-scales through the processes of scouring and polishing. At the bedrock scale, the rate of abrasion ( $\dot{A}$ , in  $\text{m}^{-1}$ ) can be quantitatively modeled for the subglacial case using wear laws, assuming no pre-existing sediment between debris-rich sliding ice and bedrock and abrading particles that are harder than the underlying bedrock (Iverson, 1995):

$$\dot{A} = F_N \dot{\gamma}_{cbc} u_c c_r \quad (1.0)$$

where  $F_N$  is the normal force at the contact between an abrading particle and the bedrock;  $\dot{\gamma}_{cbc}$  is a term that includes the hardness of the particle relative to that of bedrock and the geometry of the particle/bedrock contact,  $u_c$  is the average particle velocity, and  $c_r$  is the basal debris concentration. It is important to note that there are some feedbacks between these parameters. For instance, basal debris concentration could increase friction at the ice-bed interface, which could then decrease the basal particle velocity and thus affect abrasion rate. Therefore, abrasion rate does not increase continuously with basal debris concentration.

Quarrying is a mechanism that takes place at naturally weaker areas in rock, such as joints, fractures, microcracks, foliation, bedding, or cleavage planes in rocks or minerals at many scales (Rea, 2007) (**Fig. 1.3**). The orientation of these linear and planar features, to the forces exerted by ice-flow movement, contributes significantly to the failure of rock. Some rocks fail more easily than others. For example, metasediment rocks can exhibit bedding and cleavage planes at an optimal orientation for quarrying processes than granitoid rocks with minimal joint spacing. Optimal conditions for quarrying include relatively thin, fast flowing ice over irregular bedrock, which are especially present during deglacial phases (Iverson, 1991; Hallet, 1996). These conditions will favor the development of lee-side cavities down-ice a bedrock step, which could be connected to a linked-cavity system of meltwater drainage. Pressure fluctuations within these cavities generate intense stress gradients and fluctuations at the tip of a bedrock obstacle and, especially in the presence of pre-existing sub-vertical joints, will lead to failure of the step. For a 2D case and assuming the substrate consists of irregular bedrock, with water-filled cavities at the ice-bed interface, the rate of quarrying may be expressed using the following equation (from Iverson, 2012)

$$\dot{E}_q = \frac{ukh}{2L} \left(1 - \frac{S}{L}\right) \quad (1.1)$$

where  $u$  is the basal ice sliding velocity,  $k$  is a probability of step failure and erosion,  $h$  is the step height,  $L$  is the length from one step to the next in the down-ice direction, and  $S$  is the cavity length. The cavity length  $S$  depends on the step height ( $h$ ), sliding velocity ( $u$ ), and normal effective stress, which corresponds to the ice overburden pressure minus the water pressure in the cavity. The greater the velocity, the larger/longer the cavities. This is further enhanced under high water pressures, which will promote ice-bed decoupling (or separation). In the latter case, the area of contact between ice and the bed is reduced, which leads to stress concentration at the top of the bedrock step (Iverson, 2012). Then, if the pressure suddenly drops in the cavity, the stress will suddenly increase at the top of the step, before cavity closure, which explains why failure is more likely to occur at that location.

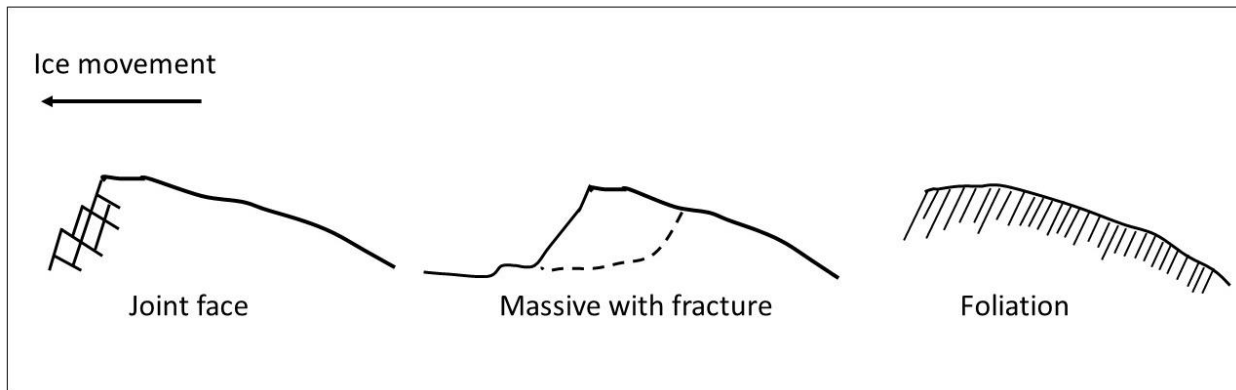


**Figure 1.3:** Initiation and optimization of quarrying on lee slopes at planes of weakness in main bedrock structures (after Gordon, 1981; modified from Benn and Evans, 2010).

### 1.2.1.2 Landform processes

As previously discussed, erosion, entrainment, and deposition of glacial material by ice and water through subglacial processes over time generates landforms. Controls and influences at the ice-bed interface integral to the formation of erosional landforms include physical characteristics of the bed itself; such as jointing, permeability, and composition; glaciological and topographic variables, such as ice characteristics, stresses, bed thermal conditions, and bed morphology like bed roughness; and changes of these variables through time.

Erosional landform features created by abrasion and quarrying can be used to determine ice flow direction, including roches moutonnées, whalebacks, and drumlins (e.g., Trommelen et al., 2012). Typically, most features reflect the youngest strong basal ice flow event, but older features are sometimes preserved on surfaces that were protected from that younger flow due to the shape of the outcrop. Numerous studies have used this approach to establish ice flow relative chronology in different regions of Canada (e.g., Parent et al., 1995; Veillette et al., 1999; Gauthier et al., 2019; Rice et al., 2019). Occasionally, a set of landforms is partially overprinted by a younger oblique set, which together represent evidence for ice flow shift (e.g., Stroeven et al., 2006; Stokes et al., 2006; Stokes et al., 2009).

Roches moutonnées are formed by plucking of the lee side of a bedrock protrusion where cavities are forming (**Fig.1.4**). Formation efficiency increases with steep down-ice dipping foliation and fractures, and cavities with fluctuating water pressure that enhances the quarrying process (e.g., Iverson 1991; Sugden et al., 1992; Cohen, 2006).





**Figure 1.4:** Roche moutonnée in the eastern study area. Shovel pointed in direction of younger (NW) ice flow (295°).

Whalebacks are also glacially sculpted rock outcrops, but without a quarried face. Whalebacks could have been sculpted from pre-existing bedrock relief (Lindström, 1988; Glasser et al., 2005), or bedrock lithology not conducive to quarrying (Gordon, 1981). Anundsen (1990) suggests whalebacks could have formed from pre-existing landforms, such as roches moutonnées in regions that experienced palimpsest ice flow.

Drumlins are oval-shaped erosional and depositional subglacial bedforms on the scale of meters to hundreds of meters, where the long axis is aligned with the direction of ice flow, the stoss side has higher relief, and the lee side tapers (Stokes et al., 2013). Their shape and dimension vary along a continuum (Ely et al., 2016), and their length to width ratios have been used as an indicator of relative basal ice flow velocity (Ely et al., 2016). Drumlin formation has been highly debated because the complete formation of drumlins has never been observed directly. Any complete theory of drumlin formation needs to explain the varied composition of these landforms from bedrock to stratified and unstratified sediments and combinations in between (Stokes et al., 2011). In addition, it is likely that erosional and depositional processes work together to sculpt these landforms, which could exist in clusters or individually (Shaw and Sharpe, 1987; Fowler et al., 2013). Drumlins with rock cores are anchored, while sediment

moves around them; and sediment drumlins can migrate, scavenge, and amalgamate nearby drumlins, especially in areas that experienced palimpsest ice flow (**Fig. 1.5**) (Hermanowski et al., 2019). Sampling drumlins could be challenging if successive glacial events combine older drumlins and preferentially erode or preserve material.

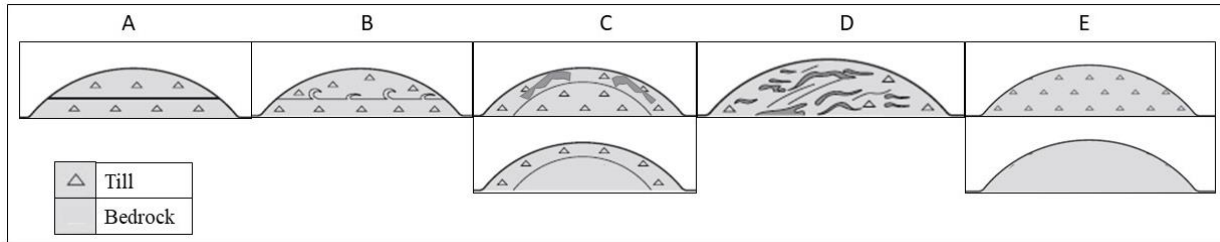


**Figure 1.5:** Drumlin core cross-section decreasing in complexity (palimpsest) from A to E. A) Layered stratigraphy; B) layered stratigraphy with minor inheritance; C) overprinting with minor inheritance; D) complete reworking with internal deformations, and E) complete preservation of till/bedrock (modified from Stokes et al., 2013).

### 1.2.1.3 Subglacial drainage

During deglaciation, for example, larger low-pressure cavities can receive water from connected higher pressure cavities, enhancing the growth of larger cavities (**Fig. 1.6**). An increase of pressurized water can result in ice-bed decoupling resulting in optimal quarrying conditions (Hallet, 1996). However, Sharp et al. (1989) concluded that cavities are not always connected, and the network of cavities and openings vary based on the volume of water stored in the system. In areas where this kind of drainage persists, channels could develop, leading to an instability of the drainage system, and a more channelized system could form. Linked-cavity systems are therefore enhanced when 1) there is low effective pressures, 2) there is little input into the system, such as when available meltwater is produced basally; and 3) ice moves faster over rough beds.

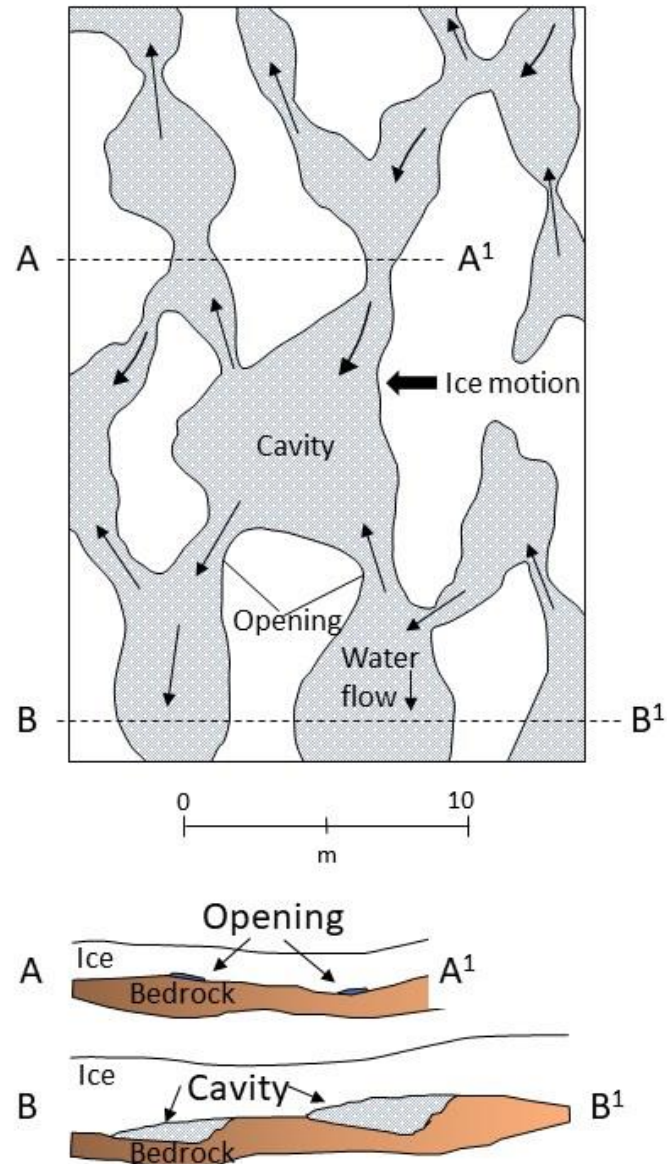


**Figure 1.6:** Subglacial cavity systems are variably connected and pressurized depending on ice-overburden pressure. Channelized systems can develop during instability, such as periods of deglaciation (modified from Hooke, 2005; after Kamb, 1987).

#### 1.2.1.4 Regelation intrusion and englacial transport

Regelation intrusion is considered the dominant mechanism for incorporation of debris produced by quarrying and abrasion, as well as any pre-existing sediment, into moving basal ice. It is therefore an important process for initiating particle entrainment.

Regelation intrusion is the process by which basal ice penetrates by pressure melting into subglacial sediments and refreezes around the particles (**Fig. 1.7**). The process requires the ice-overburden pressure to be greater than the water pressure in the pore space. (Iverson, 1995;



2007; Clark, 2005). Iverson (2000) describes the regelation intrusion process with the following formula:

$$v_r = K_s (P_i - P_w) / H_s \quad (1.3)$$

where the vertical (downward) intrusion rate ( $v_r$ ) is directly proportional to the difference between the pressure of the ice ( $P_i$ ) and pore water ( $P_w$ ) (the normal effective pressure  $N$ ) times the constant  $K_s$  based on sediment porosity and thermal conductivity, and inversely proportional to the effective thickness of regelated sediment ( $H_s$ ). Infiltration rates decrease if the regelated layer gets too thick, or the effective normal pressure  $N$  is reduced.

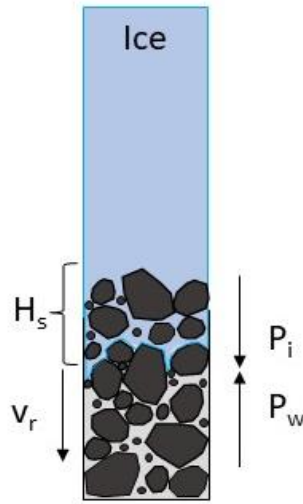


**Figure 1.7:** Model of the regelation intrusion process.  $H_s$  = thickness of regelated sediment,  $V_r$  = intrusion rate,  $P_i$  = pressure of the ice,  $P_w$  = pore water pressure (after Iverson, 1993).

If basal ice is moving horizontally, the regelation intrusion process leads to net erosion and entrainment. Following Hildes et al. (2004) and Melanson et al. (2013), transport and deposition of regelated (englacial) sediment is described by changes of englacial debris concentration ( $C$ ) near the base of the ice with respect to time ( $t$ ):

$$\frac{\partial C}{\partial t} = -\nabla \cdot C \vec{v}_i - \frac{\partial(C\dot{V}_{net})}{\partial z} + V_{mix} \quad (1.4)$$

where  $v_i$  is the horizontal ice velocity,  $V_{net}$  is the net entrainment/deposition which depends on regelation intrusion and basal melting rates, and  $V_{mix}$  is a term that takes into account ductile deformation (e.g., folding) within basal ice.

### 1.2.1.5 Subglacial sediment deformation

Subglacial sediment deformation occurs when ice couples with underlying material, and the forces of shear traction and sediment yield strength are equal (Boulton and Hindmarsh, 1987).

Soft-bed deformation occurs under relatively low basal shear stresses (Alley, 1991; Murray, 1997; Alley, 2000; Evans et al., 2006), which can transport sediment tens to hundreds of kilometers down ice (Boulton, 1996; Clark and Pollard, 1998; Larson, 2005). The volume of sediment advected down-ice depends on the thickness of the deforming layer, which can vary over time depending on the subglacial conditions. Based on Melanson et al. (2013), changes in the thickness of the deforming layer ( $h_{sed}$ ) with respect to time ( $t$ ) can be expressed as:

$$\frac{\partial h_{sed}}{\partial t} = -\nabla \cdot \vec{Q}_s + \dot{E} - V_{net} \quad (1.5)$$

where  $\vec{Q}_s$  is the deformation flux of the deforming layer,  $\dot{E}$  is the rate of erosion from abrasion and quarrying, and  $V_{net}$  is the net entrainment/deposition rate.

### 1.2.1.6 Till deposition

As indicated in eqs. 1.4 and 1.5, till deposition occurs when basal melt rate exceeds regelation intrusion rate or when the base of the deforming layer moves up to coincide with the ice-bed interface (i.e., the deforming layer decreases over time to a thickness of zero). Basal melting can occur passively if the basal ice velocity is equal to zero (i.e., the ice is stagnant) or by pressure melting due to moving ice pressing horizontally against a rigid obstacle. Till deposition can also occur when frictional drag of debris-rich basal ice is greater than the shear stress from moving ice (Boulton, 1975, 1982). The process that leads to deposition by mechanical frictional processes and the plastering of debris onto a hard substrate is referred to as ‘lodgement’ (Dreimanis, 1989). Particles can get lodged against asperities when there is a rigid bed with an element of bed roughness (Drewry, 1986), which can produce grooves, or in resistive deformable beds, particles could plough through soft sediments and become lodged in sediments (Thompson and Iverson, 2008). Whole slabs of basal ice debris can become lodged when basal frictional drag is greater than the pressure of overlying ice, or when a decollement plane develops due to a difference in rheological properties (Benn and Evans, 2010).

### 1.2.2 Drift Prospecting

The processes of subglacial erosion, transport and deposition described in the previous sections can be used in glaciated regions to trace indicators of mineralization of interest back to their buried bedrock source. It is therefore a type of ‘inverse problems’ where the mineralogy of the source region is determined and traced back from downstream, or down-ice, sediment composition (Lipp et al., 2021). By systematically collecting a specific kind of material, typically till, across a glaciated landscape, and by looking at spatial trends of till compositional data, a mineral source could be discovered.

### **1.2.2.1 Drift prospecting using till**

Drift prospectors explore for commodities by examining glacial drift material. Drift is a term that refers to all surficial sediments. It can include material sourced from glacial erosion (till) or reworked through fluvial or lacustrine processes, for example. Till is the preferred sampling medium for drift prospectors in glaciated terrains, because it is widespread at the surface of those regions and is directly related to the glacial history, which can be reconstructed in a way that allows constraining sediment provenance. It is also comprised of unsorted sediment from clay-sized particles to boulder-sized clasts, which offers several possibilities for analysis (boulder tracing, indicator minerals, geochemistry). These various particle size fractions can indeed be analyzed separately to gain insights into parent bedrock type and potential sediment provenance, which could also provide information about sediment transport distance from the source (Dreimanis, 1971). In the early days of drift prospecting, predating the 1940s, the focus was on mineralized glacial erratics (boulders) and related boulder-tracing methods, but it later evolved to include heavy mineral analysis and trace element geochemistry of the finer fractions (Hawkes, 1957; DiLabio, 1979; Miller, 1984; Kujansuu and Saarnisto, 1990; Shilts, 1996). Today, due to these highly successful efforts, diagnostic assemblages of indicator minerals and geochemical pathfinders exist for several mineral deposit types including diamondiferous kimberlites (Fipke et al., 1995; McClenaghan et al., 2000), VMS deposits (McClenaghan et al., 2015; McClenaghan and Peter, 2016), gold and uranium deposits (DiLabio, 1979; McClenaghan, 1994; Earle, 2001), copper porphyry deposits (Plouffe et al., 2016) and others (McClenaghan et al., 2018). Heavy mineral analysis used in drift prospecting is applied to sand-size particle fractions, optimally <125 µm or <250µm, while trace element geochemistry is generally applied to the finest till matrix fraction (sand- to clay-size particles; typically, <180µm, < 63µm, or <2µm). It is out of the scope of this thesis to review all the techniques and mineral assemblages used in drift prospecting. However, since the research uses the large HWRC dataset of kimberlite indicator minerals, as well as some till matrix geochemistry data, the following sub-sections provide a brief overview of the main indicator minerals and geochemical pathfinders used in drift prospecting for diamondiferous kimberlites in Canada.

### **1.2.3 Indicator Minerals**

Indicator minerals are used as an exploration tool because of their physical and chemical properties, which allow them to persist through harsh conditions such as glaciation and surface weathering (McClenaghan, 2005). Due to their physical and chemical properties, most indicator minerals can be easily separated from other host rock material, making the work involved in processing these grains more efficient (McClenaghan, 2005). Indicator minerals can represent mineralization, alteration, or bedrock lithology (depending on the mineral and environment) and can indicate that a mineralized source is nearby. Their presence in glacial sediments also provide a larger footprint, due to glacial transport, that can augment the search area (McClenaghan, 2005; Leshner et al., 2017). Indicator minerals were innovated for diamond exploration during the 1990s (Schulze, 1993; Schulze, 1999).

### 1.2.3.1 Kimberlite indicator minerals

Kimberlite indicator minerals are specific to kimberlite deposits, which may or may not be diamond-bearing. Building on seminal work by Schulze (1993) primary signature kimberlite were determined to include indicator minerals include xenocrysts from peridotite and eclogite mantle xenoliths and include Cr-pyrope garnet, eclogitic pyrope-almandine garnet, Cr-diopside, Cr-spinel, olivine, enstatite, omphacitic pyroxene, and diamond (McClenaghan et al., 2002; McClenaghan and Kjarsgaard, 2007). Kimberlite indicator minerals also include megacrysts of low Cr-Ti pyrope, Mg-ilmenite, phlogopite, zircon and olivine, and phenocrystals of olivine and spinel (McClenaghan et al., 2002; McClenaghan and Kjarsgaard, 2007). Diamond indicator minerals include high Cr-Mg picrochromites, and high Na-Ti pyrope-almandine garnet (McClenaghan et al., 2002; McClenaghan and Kjarsgaard, 2007). Diamond indicator minerals have been narrowed down to specific species of minerals and detailed classifications have been developed, such as the Grütter classification scale, where G10 garnets (harzburgitic garnets with 1.0-22.0 wt% Cr<sub>2</sub>O<sub>3</sub>, <3.375 wt% calcium, and 0.75-0.95 MgO content) and G10D garnets (further constrained ranges: Cr<sub>2</sub>O<sub>3</sub> ≥ 5.0 +0.94\*CaO, or Cr<sub>2</sub>O<sub>3</sub> < 5.0 +0.94\*CaO and MnO <0.36) indicate a diamondiferous kimberlite, inasmuch as the temperature-pressure and compositional association with diamond are strong (Grütter et al., 2004).

Kimberlite indicator mineral abundances vary between regions and kimberlite fields within a region (McClenaghan and Kjarsgaard, 2007). For example, Cr-pyrope (G9/G10 garnets) and Cr-diopside comprise the highest counts of indicator minerals in the central Slave, while Mg-ilmenite is prevalent in the north Slave (McClenaghan and Kjarsgaard, 2007). Kimberlite indicator minerals for the Lac de Gras region (central Slave) include, in decreasing order of abundance: Cr-pyrope, Cr-diopside, Cr-spinel and Mg-ilmenite (McClenaghan et al., 2000). Kimberlite indicator mineral counts can vary within regions in the Lac de Gras area; therefore, delineation of dispersal trains can be based on just a few grains of kimberlite indicator minerals to hundreds of grains per 10 kg normalized sample (McClenaghan, 2005). By mapping the concentrations of kimberlite indicator minerals specific to a local area, a dispersal train can help lead drift prospectors to a kimberlite source (McClenaghan et al., 2000).

### 1.2.4 Till Matrix Geochemistry

Till matrix geochemistry provides useful information on the general provenance of tills and, sometimes, clear dispersal patterns can be deciphered through careful analysis. Geochemical analysis performed on the silt and clay fractions can be used to identify contrasting trace element compositions between the host-rock of a deposit and the deposit itself (McClenaghan et al., 2013). Certain elements could be sufficiently enriched in the deposit of interest, relative to the surrounding host rocks, to form what is referred to as ‘anomalous’ concentrations (Rose et al., 1979). In contrast, other elements in the deposit could be depleted relative to most rocks in an area and these elements may be used with the anomalous ones to form a distinct signature that could be detectable in till.

#### 1.2.4.1 Geochemical pathfinder elements

Regional geochemical patterns in till vary depending on geographic area, due to regional and local lithology, alteration zones, and mineralization at the bedrock surface; thus, till contains suites of chemical elements specific to the area that was glacially eroded to produce the till (McClenaghan et al., 2002; McClenaghan and Kjarsgaard, 2007). Chemical element values are measured through geochemical laboratory analytical testing of the till matrix to determine a baseline and to subsequently determine whether elevated element content values exist above regional background (baseline) values (McClenaghan et al., 2013). Assemblages of elevated element values corresponding to a particular type of mineralization in a geographic area are known as pathfinder element suites.

The geochemical pathfinder element method is a relatively quick and cost-effective method to identify prospective economic mineral areas (McClenaghan and Kjarsgaard, 2007). Regions with elevated values of pathfinder element suites have a greater potential for hosting mineral deposits rather than areas without elevated values (e.g., Litinski, 1961; McClenaghan et al., 2002; McClenaghan and Kjarsgaard, 2007). Relationships already established in mineral exploration case studies helps drift prospectors interpret their till geochemical data and narrow down locations that are more likely to contain a mineralized source.

McClenaghan et al. (2018) reviewed Canadian case studies published by McClenaghan et al. (2002), McClenaghan and Kjarsgaard (2007), and Nowicki et al. (2007) and summarizes the pathfinder elements for diamondiferous kimberlites in the Northwest Territories, which include Ba, Cr, K, LREE, Mg, Nb, Ni, P, Rb, Sr, Ta, Ti. Compatible elements, such as Ni, Cr, Co, are associated with ultramafic rocks found in the deep mantle, which host kimberlite deposits. In the Lac de Gras area, Wilkinson et al. (2001a) determined that the best kimberlite pathfinders include Ba, Ce, Cr, La, Mg, Nb, and Ni; and potentially Hf and Ta. In areas where till does not contain detritus derived from ultramafic volcanic and diabase dyke rocks, elevated values of Bi, Ca, Co, Fe, K, Mn, Nd, and Rb can be considered additional pathfinder elements (Wilkinson et al., 2001a). Interestingly, Wilkinson et al. (2001a) noted differences in till composition in areas of thin till compared to thick till, which they attributed to detritus derived from small sources may not have as much contribution towards voluminous thick till as it would in thin till due to greater dilution of material from the more prevalent bedrock source. Specifically, surficial till in areas of thick till tends to be characterized by higher values of pathfinders Ba, Cr, Mg, and Ni, and lower values of La and Ce compared to thinner tills. In other cases, such as the Ranch Lake deposit north of Lac de Gras, Ni, Cr, Ba, Co, Sr, K, Mg, and Mn are the typical pathfinder elements. Table 1.1 presents a summary of the most useful pathfinder suites from the different studies above.



**Table 1.1:** Geochemical pathfinder elements for diamondiferous kimberlites in the Northwest Territories and Lac de Gras area (<sup>1</sup>Wilkinson et al., 2001a; <sup>2</sup>McClenaghan et al., 2002; <sup>3</sup>McClenaghan and Kjarsgaard, 2007; <sup>4</sup>McClenaghan et al., 2018).

<sup>1</sup> Generally enriched elements in Lac de Gras kimberlites	Ba, Ce, Cr, La, Mg, Nb, and Ni; and potentially Hf, Ta
<sup>1</sup> Enriched elements associated with kimberlites in Lac de Gras where till is lacking ultramafic volcanic and diabase dyke material	Bi, Ca, Co, Fe, K, Mn, Nd, Rb
<sup>1</sup> Geochemical pathfinder elements in Lac de Gras areas with thicker tills	Ba, Cr, Mg, and Ni, and lower values of Ce, La
<sup>2</sup> Enriched elements for the Ranch Lake kimberlite north of Lac de Gras (granitoid host rock)	Ba, Co, Cr, K, Mg, Mn, Ni, Sr
<sup>2</sup> Depleted elements in the Ranch Lake kimberlite north of Lac de Gras	Ba, Ce, Cr, Th
<sup>3</sup> Geochemical pathfinder elements in the Northwest Territories	Ba, Ca, Co, Cr, Fe, K, Mg, Nb, Ni, Rb, REE, Sr, Ta, Ti
<sup>3,4</sup> Canadian case study geochemical pathfinder elements	Ba, Cr, K, LREE, Mg, Nb, Ni, P, Rb, Sr, Ta, Ti

### 1.2.5 Palimpsest Dispersal

Multiple shifts of ice-flow directions can form complex surficial dispersal trains if anomalous patterns from an old till are partially preserved after re-entrainment by a subsequent ice flow. These old, remnant patterns are referred to as ‘palimpsest dispersal trains’ in reference to the term used to refer to old manuscripts, which were re-used, but the original text can still be seen, although faintly, under the new text; one of the best-known examples of such text is the Archimedes palimpsest (e.g., Netz and Noel, 2007). Palimpsest dispersal trains are common (Parent et al., 1996; Paulen et al., 2013) and notably, palimpsest dispersal exhibits a variety of shapes including fan, lobate, and amoeboid shapes (**Fig. 1.8**). Palimpsest dispersal is common in areas of complex glacial geology where ice flow shifts and/or changes in subglacial conditions occurred (Trommelen et al., 2013). They reveal key insights into fundamental aspects of the local/regional glacial geology (e.g., ice flow history, subglacial processes) with implications for sampling programs and data interpretation in glaciated terrain (McClenaghan, 2005).

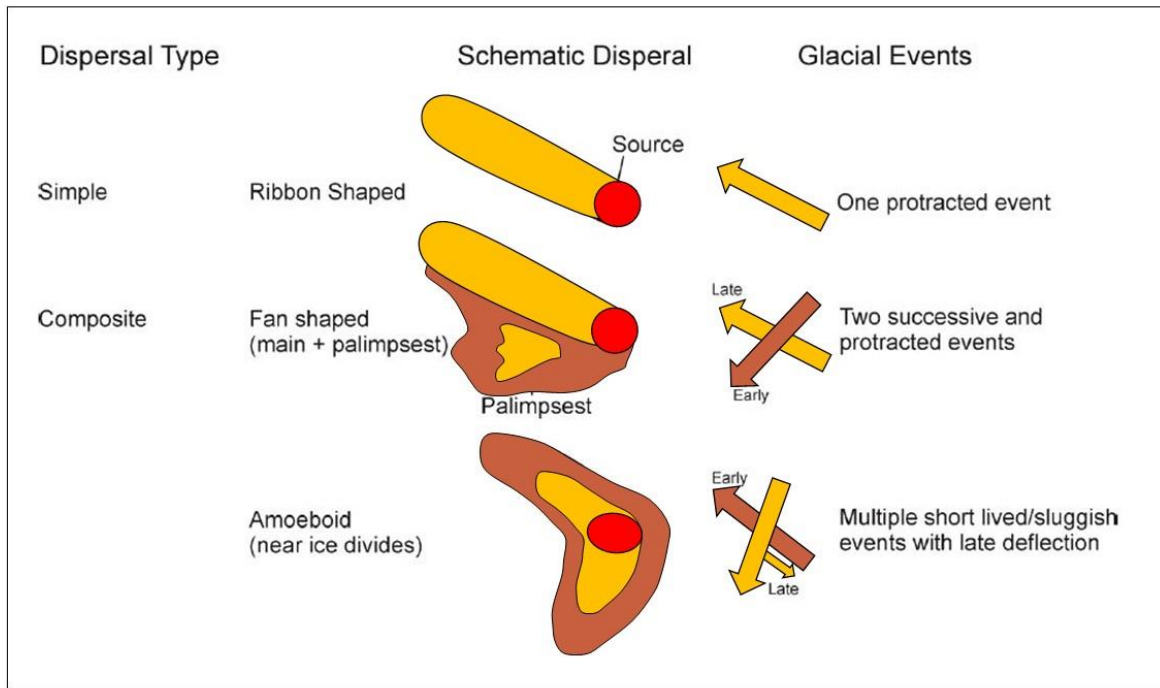


**Figure 1.8:** 2D surficial palimpsest dispersal trains and the ice flow phases that could create them (modified from Parent et al., 1996).

Simple, ribbon-shaped trains are the result of sediment entrainment from a relatively small source in a single ice flow direction. Fan shaped dispersal trains result from shifting ice flow and relatively continuous erosion at the source, as well as continuous entrainment and deposition (Klassen, 1997; Stea et al., 2009). Amoeboid dispersal trains have been documented near ice divides (e.g., Klassen and Thompson, 1993) where opposite movement directions can occur as a result of ice divide migration over a source area (Rice et al., 2019). Recently described lobate palimpsest dispersal trains are outlined as amalgamated lobes, generally resulting from faster flowing multiple ice-flow events (Trommelen et al., 2013). Palimpsest dispersal patterns reflect the direction, number, intensity, and succession of ice flow phases (Parent et al., 1996).

Problems arise when shifting ice-flow directions re-entrain previously deposited material from older glacial events (Stea et al., 2009). One problem is the dilution effect caused by incorporation of material not derived from the source rock of interest (Stea et al., 2009). For instance, till from a different source area or sediment from a different depositional environment (e.g., glaciolacustrine), if re-entrained and mixed with newly produced particles from a source rock of interest, could dilute the signature of that source. Another problem is that portions of a pre-existing dispersal train could also be buried at depth below newly produced till from a different source. Drilling and 3D analysis are necessary to identify buried dispersal trains (Stea et al., 2009; Kelley et al., 2019a).

McClenaghan et al. (2000) identified the need to understand regional and local ice-flow history when designing a till sampling program. Efficient till sampling should take into account a

dispersal pattern hypothesis. In the case of one ice flow direction, till sampling from the source and in the direction of sediment transport (ice flow direction) should identify decreasing trends (Klassen, 1997; Stea et al., 2009). In the case of shifting ice-flow directions depositing multiple layers of till, then discerning which till layers were formed during a single ice flow event is essential. Buried mineralized dispersal trains could also be present beneath non-mineralized till, as in the case of skip zones (Klassen, 1997) or multi-till stratigraphy (Bustard, 2016). Understanding ice-flow history and developing dispersal pattern hypotheses become essential during drilling programs in areas where multilayer stratigraphy exists.

### 1.3 Study Areas

For this research, the study is subdivided into two separate study areas (**Fig. 1.10**) located in the Northwest Territories approximately 300 km northeast of Yellowknife, south of Lac de Gras. The study areas are approximately 30 kilometers apart (west-east) and are herein referred to as the west study area and the east study area (**Fig. 1.10**). The Archean central Slave hosts the Lac de Gras Kimberlite field and 4 producing and past producing diamond mines (Ekati, Diavik, Snap Lake, and Gahcho Kue ), all of which are less than 120 km from the study areas. Operating diamond mines have contributed billions of dollars to the economy, yet are nearing end of life (See Table 1.2). The benefit of a mature mining district with continuing prospectivity is a wealth of data and knowledge already exist (regional sediment compositional datasets, airborne geophysics, geological maps) to support research and new exploration. Some of that information is publicly available through the government, such as regional surficial and bedrock maps, ice-flow indicators, various geophysical maps, geochemical databases, and kimberlite drilling data ([www.nwtgeoscience.ca](http://www.nwtgeoscience.ca)).

Drift prospecting using heavy mineral till sampling made it possible to trace indicator mineral trains back to prospective targets to test with drilling or conduct airborne geophysics to narrow in on targets to drill. In spite of 30 years of successful diamondiferous kimberlite discoveries, some known kimberlites did not generate a dispersal train or characteristic geophysical signature and it is possible buried kimberlites have been overlooked. The study areas are surrounded by operating mines and could hold the answers to some important questions.

**Table 1.2:** Northwest Territories diamond mine production summary (see websites in bottom row for information).

Mine	Ekati	Diavik	Snap Lake	Gahcho Kue
Owner	Arctic Canadian Diamond Company and North Arrow Minerals Inc.	Rio Tinto	De Beers	De Beers, Mountain Province Diamonds Inc
Year discovered	1991	1992	1997	1995
Production start	1998	2003	2008	2016
Discovery methods	Heavy mineral till sampling, drilling	Heavy mineral till sampling, airborne geophysics, drilling	Heavy mineral till sampling, drilling	Heavy mineral till sampling, drilling, airborne geophysics
In production	Yes	Yes	No	Yes
Current mine life	2028	2025	2015	2028
Annual production	5 million carats/year current	6.7 million carats/year (2019)	1.4 million carat capacity	6.5 million carats (fiscal 2020)
Contribution to economy	\$2.2 billion in 2019	10% of NT's GDP	\$1.7 billion over mine life	\$2.5 billion (2006-2020)
Distance from study area kimberlites (km)	40	15 (east) 25 (west)	80	120
Company websites	arcticcanadian.ca	riotinto.com	canada.debeersgroup.com	

### 1.3.1 Regional and Local Bedrock Geology

Two main Archean lithologies are exposed at the surface in the vicinity of both study areas (**Fig. 1.9**). The metasedimentary rocks of the Yellowknife Supergroup (YKSG) Itchen Formation, and the granitoid rocks of both the syn-YKSG (2.65 to 2.608 Ga) and the post-YKSG (2.599 to 2.582 Ga) (Kjarsgaard et al., 2002). Up-ice of the east study area, Proterozoic diabase dykes cut these lithologies, including Malley dykes (2.33 Ga; 20 to 40 meters wide) which trend around 45 degrees; Mackay dykes (2.21 Ga; 30 to 50 meters wide) which trend at 80 degrees; and less common Mackenzie dykes (1.27 Ga; 20 to 50 meters wide) which trend at 320-340 degrees (Wilkinson et al., 2001b). In the west study area, Malley, Mackay, and Mackenzie dykes outcrop up-ice, as well as Lac de Gras dykes (2.03 Ga; 30 to 40 meters wide) that trend around 10 degrees (Wilkinson et al., 2001b).

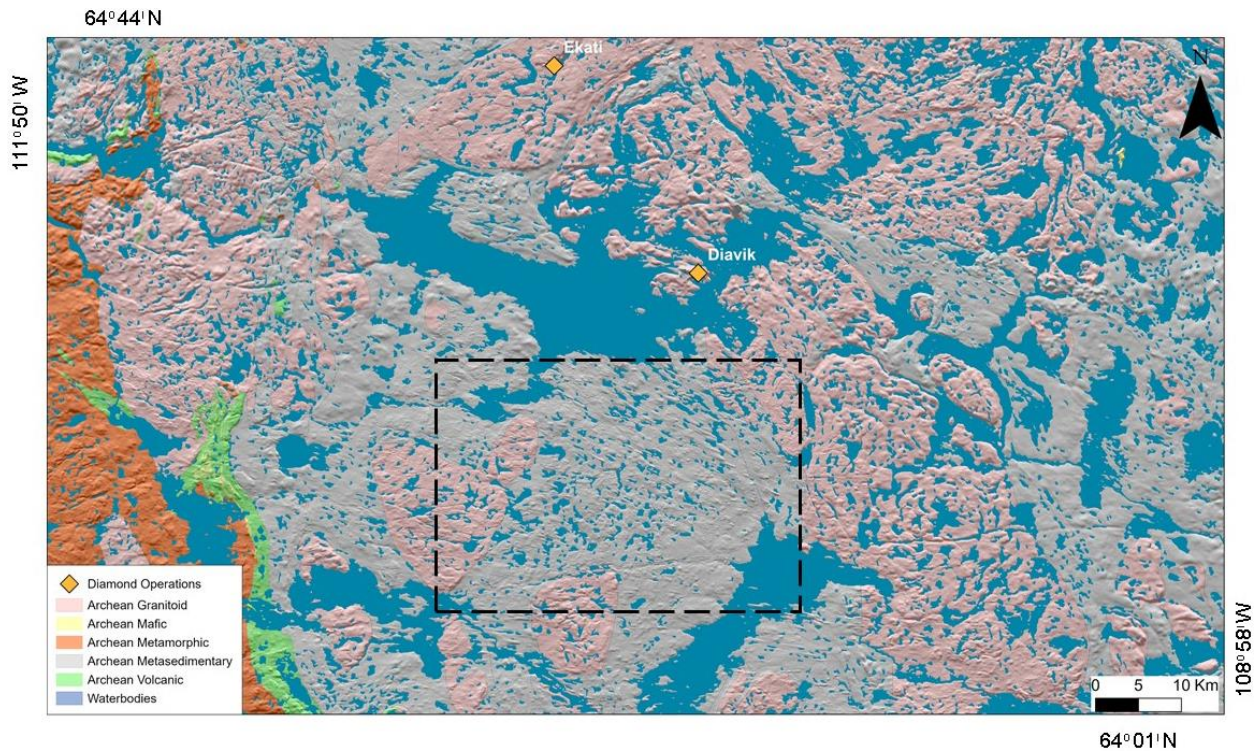


**Figure 1.9:** The overall study area within the regional bedrock geology context mapped at 1:250 000 scale (bedrock geology compilation by Kjarsgaard et al. (2002)). Bedrock within the study area is Archean in age, except for a small mafic intrusive body, Proterozoic in age, near the northeast corner of the map. The dashed box outlines view extent in Fig. 1.10, Fig. 1.11 and Fig. 1.12.

Kimberlites in this region are Cretaceous to Eocene in age, but some could be as old as Cambrian further south of the study areas (Kjarsgaard et al., 2002). According to Davis and Kjarsgaard (1997) kimberlites were emplaced between 74-47 Ma, with economic kimberlites emplaced between 55-52 Ma. Locally, in the west study area, similar YKSG metasedimentary rocks are the dominant rock type, while hornblende granitoid rocks of the syn-YKSG host the known MO2 (aka Big Blue) kimberlite deposit (Kjarsgaard et al., 2002) in the eastern part of the west study area. In the east study area, biotite schists and cordierite porphyroblastic schists compose the YKSG (Kjarsgaard et al., 2002). Biotite and muscovite-biotite monzogranites from post-YKSG outcrop at surface and hosts a known kimberlite subcrop in the northeast corner of the east study area (Kjarsgaard et al., 2002).

### 1.3.2 Surficial Geology and Ice-Flow History in Study Areas

The study is located within the Keewatin sector of the Laurentide Ice Sheet, which is an interior region of the ice sheet that covered, at the Last Glacial Maximum, mainland Nunavut and the Northwest Territories (Dyke and Prest, 1987). According to Dredge et al. (1994), the Lac de Gras region is characterized by a discontinuous till sheet comprised of a single stratigraphic unit that was deposited during the Late Wisconsinan (~25-10 ka). Regional erosional ice-flow indicators and their cross-cutting relationships indicate shifting ice-flow phases in a clockwise



direction (Ward et al., 1997). Shifting ice flow is attributed to the migrating Keewatin Ice Divide (Dyke et al., 2002). A 1:125,000 scale surficial geology map based on regional fly-over surveys and air photo interpretation is available for the study area (Ward et al., 1997). Southeast of Lac de Gras, this surficial map depicts notable landforms, such as low relief drumlins and exposed bedrock aligned with the youngest ice-flow direction to the NW. Discontinuous till veneer occurs in washed zones to the west, and eskers mainly occur along exposed bedrock, or follow along fault structures in a direction oblique to late-stage ice flow indicators (Ward et al., 1997; Kjarsgaard et al., 2002). Till associated with granitoid bedrock source is sandier than till from YKSG bedrock (Dredge et al., 1994).

Based on the map by Ward et al. (1997), and a more recent elevation model (Porter et al., 2018), the east study area is characterized in part by a drumlin field and a well-defined esker to the east outside the drumlin field, as well as whalebacks by roches moutonnées adjacent the drumlin field, in an area of discontinuous till veneer (**Fig. 1.10**). The west study area contains abundant exposed bedrock and few isolated drumlins, hummocks, and a glacial outwash corridor. For the most part, this study area has thin tills, especially over the large topographic high composed of granitoid bedrock. The regional GSC erosional ice-flow indicator measurements in the west study area are consistent with those in the east study area.

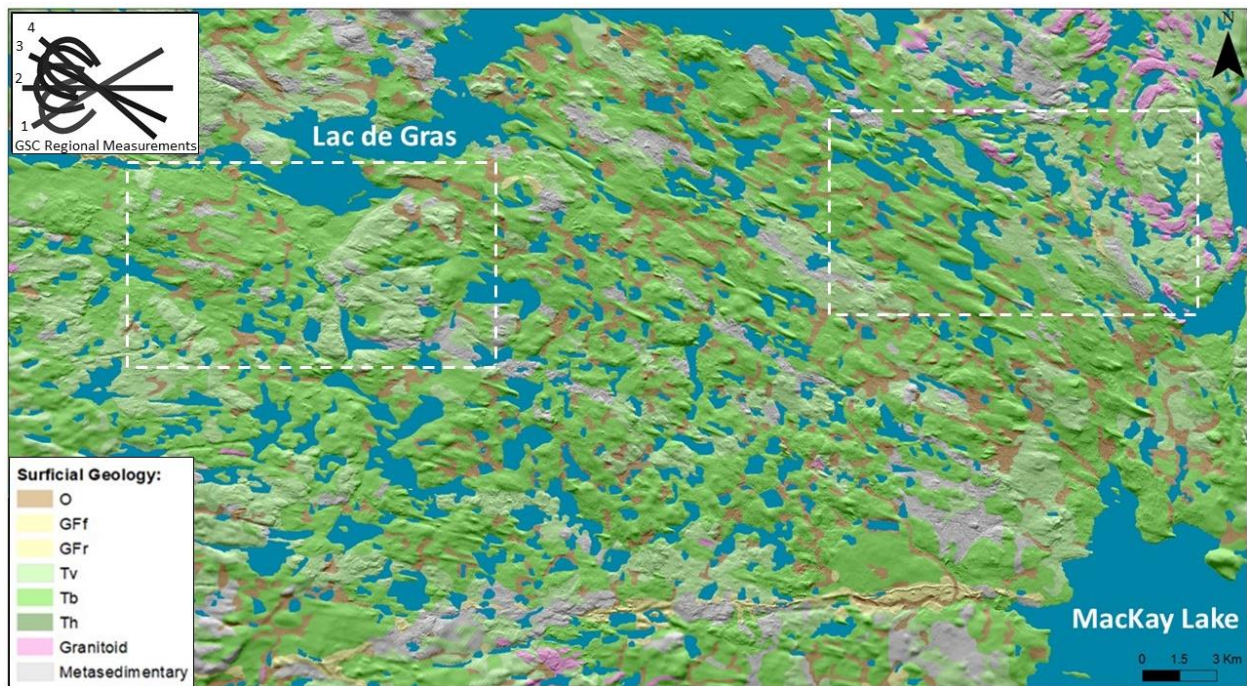


**Figure 1.10:** Surficial geology by Ward et al. (1997) draped over the Arctic Digital Elevation Model (ArcticDEM) (Porter et al., 2018). Inset shows a clockwise ice flow shift based on GSC measurements and relative age relationships. Study areas outlined in dashed boxes. The combined surficial geology and ArcticDEM highlights the relationship between till blanket and drumlin fields (especially between Lac de Gras and Mackay Lake). Surficial geology unit codes: O (organics) GFf (glaciofluvial outwash fan sediments) GFr (eskers) Tv (till – veneer) Tb (till – blanket) Th (till – hummock). Dotted white boxes show the two study areas.

### 1.3.3 Bedrock Topography and Drift Thickness

Bedrock topographic highs in the study areas are consistent with bedrock type. The west study area contains a topographic high comprised of exposed granitoid bedrock and perched on top is a granitoid knob with a kimberlite pipe nested within a bowl-shaped depression (Ward et al., 1997; Kjarsgaard et al., 2002). The topographic high steps down to topographically lower metasedimentary bedrock ([livingatlas2.arcgis.com/arcticdemexplorer](http://livingatlas2.arcgis.com/arcticdemexplorer)). Till veneer is more common over more elevated granitoid bedrock, whereas thicker tills cover metasedimentary bedrock (Ward et al., 1997); this is also where large drumlin fields occur. The regional drift thickness map by Kelley et al. (2019b) after Kerr and Knight (2007) also provide insights into till thickness patterns (**Fig. 1.11**).

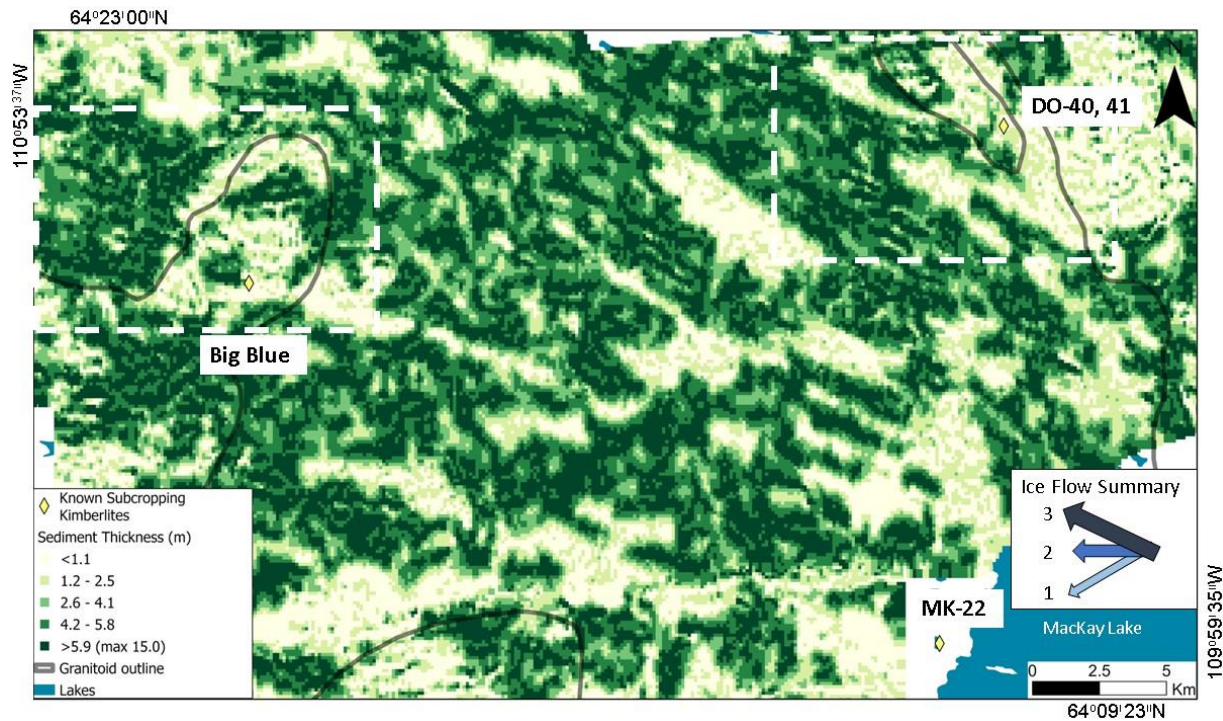


**Figure 1.11:** Quaternary Period sediment thickness model from Kelley et al. (2019b) modelled at 1:250,000 with 30-meter resolution highlights west study area bedrock topographic high (expressed as bedrock) and east study area drumlin field. Dotted black boxes outline the two study areas.

### 1.4 Specific Research Problems and Thesis Objectives

As mentioned in Sect. 1.1, there is limited understanding of the effect of till thickness, landforms, and bedrock topography variations on till dispersion patterns, both at the surface (2D) and in the subsurface (3D). These knowledge gaps are addressed in this research by investigating till composition across the two selected areas described above. The two selected study areas offer contrasting surficial geology settings within an area presumably affected by the same glacial history. The west study area is characterized by variable bedrock topography and thin till, whereas the east study area is characterized by thicker tills within a well-defined drumlin field

and less pronounced bedrock topography. **The general objective** of this research is to gain insights into the potential local effects of bedrock topography, till thickness variations and related landforms on local till dispersal trains in the two study areas. More specifically, the objectives of this research are as follows:

Specific objective 1: Refine and further constrain the local ice-flow history of the two selected study areas;

Specific objective 2: Analyze the 3D dispersion patterns of kimberlite indicator minerals and clast lithology in the two selected study areas in order to determine the extent and strength of palimpsest dispersal at depth;

Specific objective 3: Analyze the surficial dispersion patterns of kimberlite indicator minerals, selected lithologies, and geochemical pathfinders in the two study areas to determine whether there is a link between the surface and subsurface dispersal patterns;

Specific objective 4: Compare dispersal patterns obtained in (2) and (3) and investigate the potential effects related to bedrock topography and till thickness variations, as well as related subglacial processes (i.e., erosion, sediment entrainment/deposition, ice flow shifts);

Specific objective 5: Explore and discuss implications for mineral exploration

## **1.5 Methodology**

To achieve objective 1, field work included a series of traverses across areas with known bedrock outcrop to refine and confirm the regional ice-flow measurements and to ground truth surficial geology features published in the regional surficial geology map of Ward et al. (1997). To achieve objectives 2 and 3, field work aimed to collect surface samples to complement the large HWRC dataset. New surface samples were collected and through laboratory analysis of indicator minerals, lithological and geochemical pathfinders, and till texture, surficial dispersal patterns were identified. In addition, subsurface data contained in the reverse circulation dataset was also analyzed and dispersal patterns from that data were investigated. Finally, to achieve objective 4, both the surficial and subsurface dispersal patterns were compared to investigate the effects of bedrock topography, till thickness variation, and subglacial processes on dispersal. The following sub-sections describe the methodology in more detail.

### **1.5.1 Fieldwork**

Two weeks of fieldwork provided an opportunity to traverse both study areas by foot, measure ice flow indicators, describe and collect information (e.g., photos) about surficial sediments, and collect surficial samples for further laboratory analysis. Drumlins in the east study area were



strategically transected to test the possibility for multi-till stratigraphy exposed at surface due to the drumlinization process (Fig. 1.12). Transects to collect UW samples and make surficial observations were also designed to match the HWRC borehole transects while also considering the known kimberlites in the area, as well as access and surface conditions (Fig. 1.12).

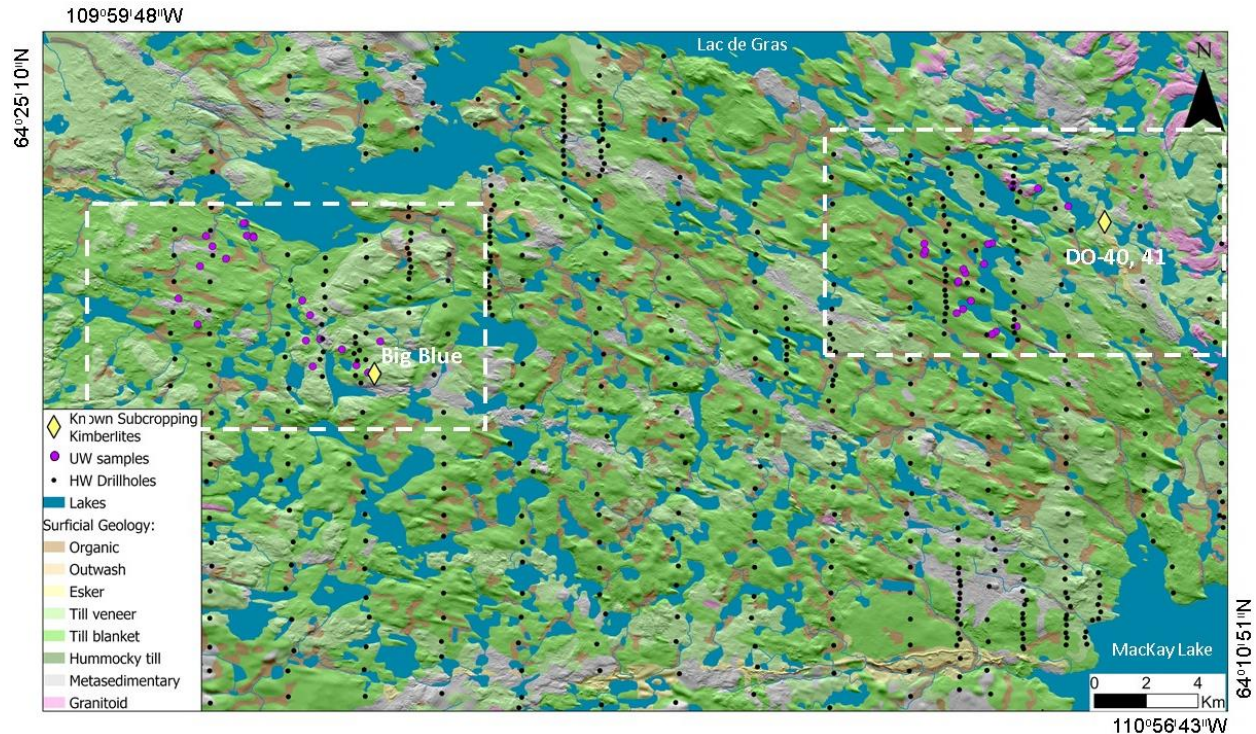


**Figure 1.12:** Location of UW surficial (large purple) and HWRC borehole (small black) sample sites, with publicly available kimberlite locations on surficial geology by Ward et al. (1997). Dotted white boxes outline the two study areas.

### 1.5.2 Ice-Flow Indicators

To refine the ice flow history (cf. Sect 1.5.2), several bedrock outcrops were visited and carefully examined for evidence of erosional glacial activity. For this type of investigations, preference is given to outcrops at the top of ridges or those located on laterally extensive flat areas, which are less likely to have been affected by local topographic effects than the ones in narrow valleys or depressions. Outcrop-scale ice-flow indicators, such as roches moutonnées, grooves, chattermarks, and striations were found at 16 outcrops and measured to determine ice-flow directions using stoss-lee relationships. Specifically, many outcrops exhibit an asymmetric profile (e.g., roche moutonnée) characterized by a gently-sloping up-ice abraded surface and a steeper down-ice plucked face. At these sites, relative age chronology of ice flow phases can be determined using established methods (Klassen and Bolduc, 1984; Parent et al., 1995; Veillette et al., 1999; and Paulen et al., 2013). Landforms, such as drumlins and whalebacks, also provide important information about past ice-flow directions at the landscape scale. These landforms were observed using satellite imagery and the ArcticDEM obtained from Porter et al. (2018).

### 1.5.3 Sediment Sampling

One of the specific objectives (specific objective 2; Sect. 1.6) is to analyze the surficial dispersion patterns of selected lithologies and geochemical pathfinders in the two study areas. To this end, new sediment samples were needed whose sites were strategically selected to both complement and correspond to the RC dataset. At all new sample locations, coordinates were collected in decimal degrees in the WGS 1984 coordinate system; landform associations and characteristics of the area surrounding the sample site were noted; presence, size, and lithology of boulders were listed and observations of interest were recorded.

Samples were collected by first removing all visible humus by way of scraping with a shovel when required. Some sample locations required exhuming with a metallic shovel before desirable sample material could be reached. When necessary, additional sample pits were exhumed and examined to confirm sediment material before samples were collected. Samples collected from the top of subglacial bedforms were taken from frost boils following techniques detailed in McMartin and Paulen (2009). All 51 samples collected for geochemical or kimberlite indicator mineral analyses were obtained using a hard plastic garden trowel to deposit material into a poly-ore bag and assigned a unique ID. The majority of KIM samples were collected at the same site as geochemistry samples. Samples were sealed to prevent leakage during transport back to camp. At camp, samples were inventoried and placed into labelled buckets for shipping. The larger (average 12.6 kg) KIM samples (n=12) were shipped to Saskatchewan Research Council (SRC) Laboratories and the smaller (average 2.7 kg) samples (n=39) collected for sedimentology and geochemical analyses were shipped to UW.

### 1.5.4 Sedimentological and Geochemical Analyses

Grain size analysis and lithological analysis of clasts greater than 4 mm diameter were performed at the UW Quaternary research lab and small sample aliquots of the silt and clay fraction were also separated for geochemical analysis. **Fig. 1.13** details the workflow of geochemical sample preparation and analysis performed at the UW Quaternary research lab.

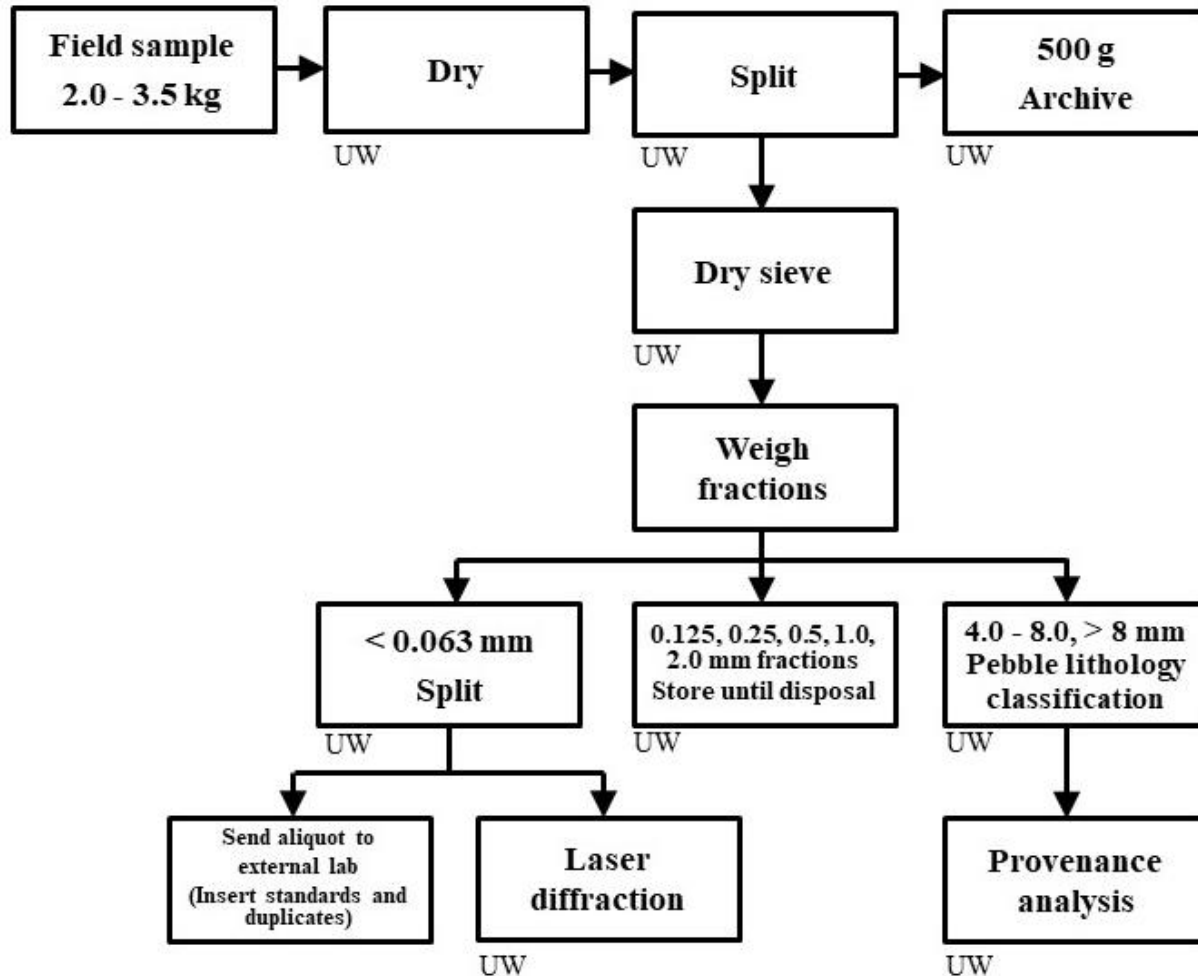


**Figure 1.13:** Workflow for UW samples returned to UW Quaternary research lab for mechanical preparation, and provenance analysis

### 1.5.5 Sample Preparation and Grain Size Measurements

At the UW Quaternary research lab, mechanical processing was performed on all samples, including drying, splitting, and sieving, and the general process to follow was given on an instruction sheet. Samples were weighed and described before being disaggregated and dried in a glass pan in a small oven at the lowest temperature setting, which is approximately 85 degrees Celsius, using a VWR Scientific 1350 degrees F forced air oven. Samples were dried four at a time and stirred using one of four firm silicone spoons every four hours. Remaining aggregations were further broken down as needed using a rubber mallet. Pans and stirring spoons were washed and dried thoroughly between samples. Sample dry-weight was recorded.

Archive samples (500g) were split from the main sample for archival purposes using a Humboldt Testing Equipment H-3987 (1/06, ASTM) riffle splitter with 2.5 cm spacing. The riffle splitter was thoroughly washed and dried between each sample. These archived samples can be accessed through the thesis supervisor up to 2030.

Samples were sieved into 9 fractions in two batches using Canadian and US Standard Sieve Series (from W.C. Tyler Company of Canada, Ltd) mounted on a Fritsch vibratory sieve shaker (Analysette 3 Spartan). A vibration amplitude of 2.0 mm for 15 minutes was applied. Mesh sizes included 0.063 mm, 0.125 mm, 0.250 mm, 0.50 mm, 1.00 mm, 2.00 mm, 4.0 mm, 8.0 mm. Sieves were cleaned thoroughly between every use using an Elmasonic S 300 for 30 minutes using concurrent sweep and degas settings. Sieve pans were allowed to dry for 24 hours to prevent moisture inherent in the sieve pan's rubber O-ring from aggregating fine sediment along the edges of the screens along where the rubber sits. Sample fractions were then bagged independently and labelled with the sample number and individual fraction size. Each fraction weight was recorded.

Sediment <0.063 mm collected in the pan were then further split and an aliquot (<1 gram) was analyzed using a laser diffractometer. A Fritsch Analysette 22 with a range from 0.08  $\mu\text{m}$  to 2000  $\mu\text{m}$  was used to measure the silt and clay particle fractions. To measure this fine fraction, less than a gram of sample material was combined with 16 ml of 4% solution of deflocculant agent sodium metaphosphate and deionized water for at least 1 minute, using a Scholar 171 Corning Stirrer at fast setting, before the mixture was slowly poured into the Analysette in specific quantity that optimizes laser diffractions and calculations and subsequent estimates of grain sizes. Once all sample results were obtained, the values from the longest measurement of a particle were summed, and the proportion of silt and clay were incorporated into the cumulative weight percent curve with the larger sieve fractions. More details about the sample preparation for the Analysette 22 are in Appendix G.

Finally, a 50g aliquot was taken using a metal scoopula and the cone and quarter method (Gerlach et al., 2001) from the <0.063 mm fraction and placed into a small twist tie bag and given a unique lab ID. A total of 40 samples, including two samples of 1179 – Till-3 certified reference material from CANMET ([www.ccrmp.ca](http://www.ccrmp.ca)), were inserted at a 1:20 interval in the sample batch sent to SRC for geochemical analysis of 50 elements.

#### **1.5.5.1 Clast lithological classification**

Sediment particles ranging 4.00 to 8.00 mm and >8.00 mm were categorized into major lithology classes, including white granitoid, pink granitoid, metasedimentary, quartz, and other. After sample clasts were categorized based on bare eye and microscope checks, clasts were counted and arranged for photograph documentation with a label (See Appendix E). Samples were randomly reclassified for consistency.

#### **1.5.5.2 QA/QC and analytics**

Every run in the Analysette is duplicated, and the first 20 samples used in the Analysette are duplicated or triplicated to ensure repeatability of results. Once the <0.063 mm silt/clay

proportion is calculated, grain size analysis curves are finalized based on cumulative weight percent and compared based on study area, depth of excavation, landform from which the sample was exhumed, underlying lithology, and dispersal pattern inclusion. Outliers in the grain size curves are further investigated to see if field or lab methods establish a reason for the lack of consistency. Data with quality issues are excluded from analysis but still noted as being excluded.

## **1.5.6 Geochemical Sample Processing**

### **1.5.6.1 Element analysis**

Samples were processed at SRC and subject to a partial and total digestion before being analyzed by Inductively Coupled Plasma Optical Emission Spectroscopy (ICP-OES) or Inductively Coupled Plasma Mass Spectrometry (ICP-MS) to determine the quantities of various elements (See table 1.3). The full methodology for the Basement Exploration Package (ICP-MS 2) can be found on the SRC website <<https://www.src.sk.ca/services/minerals-analysis>>.

**Table 1.3:** SRC geochemical analysis summary.

	ICP-Optical	ICP-MS Total	ICP-MS Partial
Lab number	537	537	537
Accreditation status	Not audited ISO 17025 standard	Not audited ISO 17025 standard	Not audited ISO 17025 standard
Analytical technique	ICP-OES	ICP-MS	ICP-MS
Elements used in this study	Ba, Cr	Co, Nb, Ni, Rb	None
Instrument used	Perkin Elmer ICP-OES (models: Optima 5300DV, 8300DV, and Avio 500DV)	Perkin Elmer Sciex Elan DRC II ICP-MS	Perkin Elmer Sciex Elan DRC II ICP-MS
Detection Limit - Ba	1 ppm	-	-
Detection Limit - Cr	1 ppm	-	-
Detection Limit - Co	-	0.02 ppm	0.01 ppm
Detection Limit - Nb	-	0.1 ppm	0.01 ppm
Detection Limit - Ni	-	0.1 ppm	0.01 ppm
Detection Limit - Rb	-	0.1 ppm	0.01 ppm
Reason used	Predetermined	Predetermined	Not used in this study: not as effective as total. Analysis performed at the request of the funding body.
Sample size	0.125 g	0.125 g	0.5 g
Digestion technique	Digested to dryness in a Teflon tube within a hot block digestion system using a mixture of concentrated HF:HNO <sub>3</sub> :HClO <sub>4</sub> . The residue is dissolved in dilute HNO <sub>3</sub> .	Digested to dryness in a Teflon tube within a hot block digestion system using a mixture of concentrated HF:HNO <sub>3</sub> :HClO <sub>4</sub> . The residue is dissolved in dilute HNO <sub>3</sub> .	Digested in a mixture of concentrated nitric: hydrochloric acid (HNO <sub>3</sub> :HCl) in a test tube in a hot water bath, then diluted using deionized water.
Lab internal standard	DCB01	DCB01	DCB01
UW standard - international reference material provided for this study	1179 Till 3	1179 Till 3	1179 Till 3
Fit for purpose - Ba	Yes	-	-
Fit for purpose - Cr	Yes	-	-
Fit for purpose - Co	-	Yes	-
Fit for purpose - Nb	-	Yes, considering detection limit	-
Fit for purpose - Ni	-	Yes, but I must be cautious	-
Fit for purpose - Rb	-	Yes	-

### 1.5.6.2 QA/QC and analytics

#### Quality Assurance

SRC kimberlite indicator results in the UW dataset were performed in a manner that was independently audited by the Standards Council of Canada's professionals to be consistent with the ISO 17025 standard. Within that quality standard, a number of quality assurance principles are mandated and audited. SRC has seven methods in their scope of accreditation and their quality management system (including documentation, reporting, and record keeping) is also accredited. Although the ICP-OES and ICP-MS methods are not audited to the ISO 17025 standard, quality processes are standard throughout the laboratory. C.F. Minerals Research Ltd. performed kimberlite indicator mineral analysis in 2013 for the full HW dataset. This lab is not accredited to ISO 17025, but instead they report they are certified ISO 9001:2015, and have been certified since 2010. The methods used by C. F. Minerals Research Ltd. are in confidential and proprietary, but may be obtained from C. F. Minerals Research Ltd. upon request. The methods used by the UW Quaternary research lab are described in sections 1.5.3, 1.5.4 and 1.5.5. Pictures of the UW Quaternary research lab process for sample preparation and texture analysis can be sourced from the author ([linkedin.com/in/rebecca-stirling-711931162](https://www.linkedin.com/in/rebecca-stirling-711931162)).

#### Quality Control

To test for quality control, lab duplicates and CANMET (Certificate of Analysis 1179 Till 3 in Appendix G) standard reference material are inserted into the samples sent to SRC at a frequency of 1:10. In addition, SRC included standard reference material (DCB01) as part of their in-house program (See Appendix G). Duplicate scatterplots, Thompson-Howarth Short Method, the average coefficient of variation, and relative percent difference methods are used for statistical analysis as part of the quality control procedure to determine errors (Piercey, 2014). Results that pass the QA/QC procedure are used with confidence. Although these methods are used for many trace elements analyzed for this study, only the six elements presented in this study are provided in Appendix G.

Duplicates are inserted to detect error in sample preparation, and bias and precision in the analysis of samples. In this study, duplicate samples (n=2) are included with samples sent to SRC. SRC also inserted in-house duplicates and performed repeat analysis (n=2) as part of their in-house QA/QC program (See Appendix G). Using these results (n=4) compared to the original samples, a 90% confidence interval is established to test the precision and accuracy of the duplicates. A scatterplot uses the original lab value as the independent variable and the duplicate value as the dependent variable and displays control lines to outline a 90% confidence window. Data lying between the control lines are precise, while data deviating outside the control lines are imprecise or exhibit bias (possibly due to sample preparation, analysis, statistical assumptions).

The Thompson-Howarth Short Method is then used to confirm the precision of the duplicate scatterplots when there are fewer than 50 samples. This method uses the mean as the independent variable and standard deviation as the dependant variable, assuming a normal distribution of

random errors below a chosen threshold. In this study a 90<sup>th</sup> percentile, meaning 90% of the data should be below the control line. However, geochemical data often contains errors does not necessarily follow a normal distribution (Davis and Sampson, 1986) and therefore tends to underestimate the precision of the data (Stanley and Lawie, 2007; Abzalov, 2008; Piercey, 2014).

Average coefficients of variation determine the best practice and acceptable values of results that do not follow a normal distribution (Stanley and Lawie 2007; Abzalov, 2008; Piercey, 2014). There are best practice and acceptable average coefficients of variation values for mineral deposits that typically range from 3 (e.g., copper in a porphyry deposit) to 10 (e.g., gold in coarse grained deposit) and can be extrapolated to other commodities (Piercey, 2014). Abzalov (2008) suggests pulp and analytical duplicates should be less than 5-7.5%.

Relative percent difference is calculated to compare standard results to certified values. Results are considered to have excellent accuracy (+/- 0-3%) very good accuracy (+/- 3-7%) good accuracy (+/-7-10) and not accurate (above +/-10) following Jenner (1996) and Piercey (2014).

Quantile-Quantile (Q-Q) plots are created to determine anomalous values within the dataset. Measured values that are greater than those predicted are considered anomalous (Wilk and Gnanadesikan, 1968; Kürzl, 1988). Q-Q plots are used for assessing thresholds and elevated values in pathfinder elements. Q-Q plots are also useful to identify outliers, which could be due to laboratory measurement errors or other issues.

### **1.5.7 Indicator Minerals Sample Processing**

The larger (average 12.6 kg) KIM samples (n=12) were shipped directly from the field to SRC for KIM processing.

At SRC, heavy mineral separation for a KIM study involves the following procedure: 1- Samples are first sieved into 0.25-0.50 mm, 0.5-1.00 mm, and >1.00 mm fractions. 2 - Dense media separation (micro-DMS) separates material with densities greater than 2.7 g/cm<sup>3</sup>. This sink material is dried and weighed. 3- Heavy liquid processing through methylene iodide then concentrates material that sinks between 3.23 and 3.3 g/cm<sup>3</sup>. 4- Sink material is then magnetically separated. 5- Leftover non-magnetic material is then placed under a microscope for indicator mineral observation.

After grains are separated and sorted, indicator mineral grains are mounted on a glass slide and additional features are identified, such as surface textures (e.g., frosted surfaces, “orange peel” textures (from pit impressions of pyroxene crystals) the presence of kelyphite rims or other mineral adherence to indicator grains, and occasionally grain morphology (McClenaghan et al., 2005; McClenaghan and Kjarsgaard, 2007). Morphological features can also aid in estimating the distance of transport and identifying whether transport occurred via water or ice (McClenaghan, 2005).



### 1.5.7.1 Kimberlite indicator extraction and electron microprobe analysis

At SRC, pyrope (peridotitic and eclogitic), olivines, Cr-diopside, chromite, and magnesium ilmenite are counted under the microscope. For quality assurance, ten percent of samples are recounted by a lab supervisor. These minerals were probed through electron probe microanalysis to assist in determining mineral species and signatures that are associated with economic deposits. Kimberlite indicator mineral discrimination plots are in Appendix G. The full methodology for KIMTILLS can be found on the SRC website <<https://www.src.sk.ca/services/minerals-analysis>>.

### 1.5.8 HW Dataset

The large HWRC dataset was donated by Dominion Diamond Corporation and North Arrow Minerals to the Northwest Territories Geological Survey (NTGS), which was then made available for this research. This dataset provides valuable information about subsurface KIM distribution, depth to bedrock, and sediment characteristics that can be used in combination with surficial maps and surficial data collected in this research to develop a 3D understanding of surficial geology, bedrock topography, and 3D KIM dispersal patterns (**Fig. 1.14**).

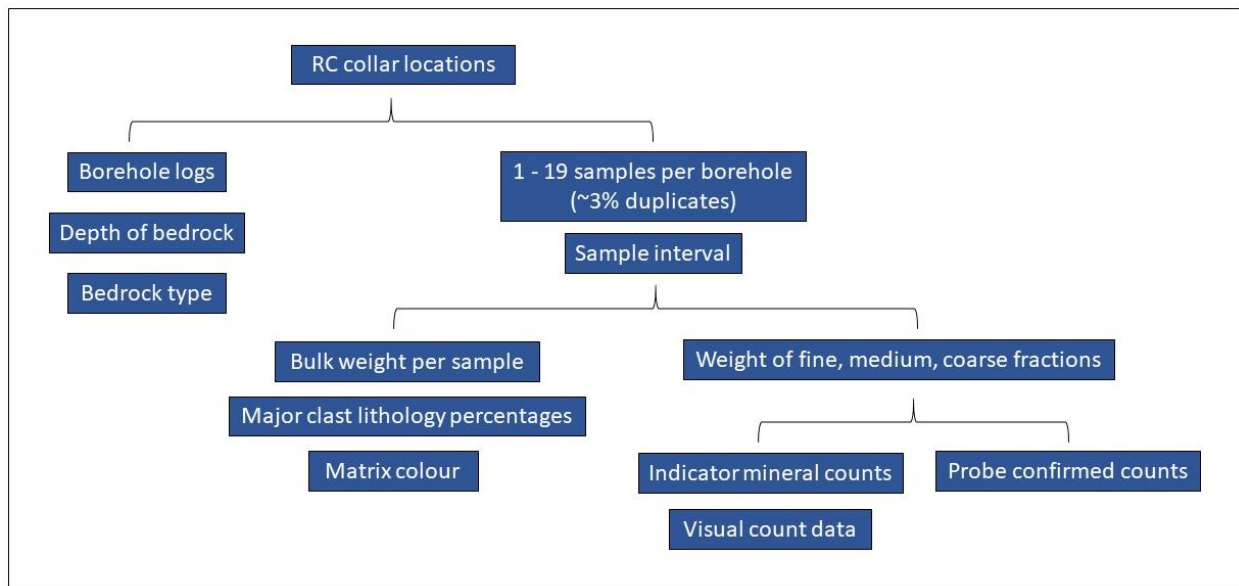


**Figure 1.14:** HWRC Dataset organization and available information contains descriptive and measured data.

The RC dataset contains results from samples obtained by Northspan Drilling during diamond exploration programs. Data includes GPS collar locations, borehole depths, sample weights and intervals, sample interval descriptions, matrix descriptions, main minerals descriptions, KIM counts, probed mineral compositions, and fraction weights. This visually picked and probe confirmed KIM dataset was processed at C. F. Minerals Inc. in 2013 (See Appendix C).

The dataset containing 757 boreholes and 5097 results is contained in an excel file with 17 tabs that organize various sample data in various ways, including borehole collar data, lab results, borehole logs, etc. Borehole sampling intervals were typically 1.5 meters, but significantly varied in depth of interval near the surface. Each borehole contains 1 to 14 samples, which were weighed, then sieved into three fractions (fine (0.25-0.5 mm) medium (0.5-1.0 mm) and coarse (1.0-2.0 mm)) before KIMs were counted. KIM counts for 34 abbreviated mineral types (namely ALM, CP2, CP3, CP5, CP6, CP9, CPX, CR, CR04, CR05, G 3, 5, G 9, G 9-1, G10-2, G10-3\*, G10-4, G10-5\*, G10-6, G10-7\*, G10-9\*, G11, G11-1, GT, OLV, OLV-FORS, OP1, OP2, OP4, OP5, OPX, PERVMgSi, PIL, SPNL) are summed into 5 categories (namely Garnets, Ilmenites, Spinels, ChromeDiopsides, Olivines). These KIM count results are used to build a 3D subsurface model, as well as granitoid clast lithology content. Each sample interval in a borehole contained clast percentage estimates for granitoid (ClastsPctGr) and metasedimentary (ClastsPctVS) rock.

### 1.5.8.1 HW data processing

Some minerals in the HW database were not picked in the UW samples; therefore, only the garnets, ilmenites, Cr-diopsides, and olivines were used. Then, the coarse fraction (1.0-2.0 mm) was removed from the analysis (n=15 counts) to be more consistent with UW sample analysis, which did not include this coarse size fraction. Next, the extent of the study region and both west and east study areas were defined using Esri's ArcGIS version 10.5 software. The remaining fine and medium fractions from the same sample were added together, since they come from the same post-weighed sieved sample. Bulk sample weight is used (no archived split) to be consistent with UW KIM sample weights available, as no table feed weights are provided by SRC Laboratories. Then, samples containing KIM grains were normalized to 10 kg (nKIM) and checks were performed to ensure the results are reasonable and accurate. Duplicate sample results included in the dataset (n=13) were averaged before ranking samples in each borehole. Ranks were assigned by depth within a borehole using a standardization method via the following calculation:

$$\text{Standardization} = (\text{rank}-0.5) / (N) \quad (1.6)$$

where N is the total number of samples in a borehole. Finally, these standardized depth intervals were classified into bins (Table 1.4).

**Table 1.4:** Standardized depth interval assigned to bins for 3D analysis.

Bin	From Interval	To Interval	Notes
4	0.00	0.25	Top
3	0.26	0.50	Upper-mid
2	0.51	0.75	Lower-mid
1	0.75	1.00	Base

For the boreholes containing five or more samples, for example, intervals can contain more than one nKIM result in the same bin; therefore, an average nKIM counts were calculated for the bin (See Appendix C). Then, based on study area, bins were saved in separate spreadsheets based on bin number (to represent a slice through the relative depth within a borehole) to import in ArcGIS. The purpose of using four bins of standardized depth interval values is to allow mapping all the sample results of one standardized depth interval on the same map even if they are in fact at different real depths. The subsurface data is thus sliced in a way that is conformable to the bedrock topography instead of slicing at constant depth. For instance, the KIM counts from the basal till interval in a 5m deep borehole are mapped together with the 'basal' interval of a 10m deep borehole, as opposed to being mapped with its middle depth interval.

A model of the bedrock topography and till thickness developed by Kelley et al. (2019b) after Kerr and Knight (2007) was also used. This is particularly useful to investigate the potential effects of bedrock topography and till thickness variations on 3D dispersal trains analyzed in this study.

### **1.5.9 Mapping and Data Integration**

Ice-flow indicator measurements from striations and grooves were plotted on a histogram and visually sorted into groups of measurements. Cross-cutting relationships recorded in these ice-flow indicator measurements were noted to establish relative ages among ice flow phases. Rose diagrams were constructed for a visual representation of the local ice flow phases and compared to regional GSC measurements from Ward et al. (1997).

Clast lithological analysis was performed on each clast in the UW dataset in the 4-8 mm and >8 mm fractions. Clasts >8mm were used to help identify major lithologies, while the 4-8 mm clasts were examined using a microscope if needed to categorize into the same lithologies. Every sample was photographed with labels showing the lithologies. Clast results within the HW dataset contain estimated granitoid percentage results for every sample interval. It is assumed (due to adjacent columns in the database) that these estimates were made on the clast or pebble size fractions of at least 2 mm diameter. No other information is available for how clast content was determined in the HW dataset.

Preliminary data investigations were completed to inform subsequent data interpretations. Data were examined for till texture trends, landform associations, and spatial patterns among selected field samples. These trends and patterns were then compared to the RC dataset to test patterns and trends at depth.

Surficial dispersal patterns were delineated based on elevated KIM counts; and multiple lines of evidence, such as clast lithology and geochemistry, were used to support the dispersal pattern interpretation. Subsurface dispersal patterns were delineated based on elevated KIM counts. Ice-flow indicator measurements were used to put the surface and subsurface dispersal patterns into the glacial history and potential sediment transport context.

### **1.5.9.1 Provenance study**

Multiple lines of evidence were used to determine the provenance of all the different indicators described above. These include ice-flow data, grain size analysis, and compositional analysis (including geochemical, indicator mineral, and pebble lithological analysis). Ice-flow data are used to constrain directions of sediment transport. Grain size analysis is used to determine the till texture and glaciofluvial texture, which could give insights into the depositional setting and processes that affected the sediment. Pebble lithological analysis on the two largest clast fractions provides information about the main bedrock sources for the till, while geochemistry is used to fingerprint the possible bedrock sources for the fine matrix of the till. The KIM grains data could form dispersal patterns that could be linked to known kimberlites in the study areas.

## **1.6 Thesis Structure**

This thesis is structured as a paper-based thesis. The first chapter contains an introduction to the research. Chapters 2 and 3 are written as manuscript for submission to scientific journals, while Chapter 4 serves as the conclusion chapter of the thesis.

Chapter 1 includes the scientific rationale for the research, background information on glaciology pertinent to this research, research objectives, and methods. Chapter 2 presents an investigation of a well-preserved 3D dispersal train in a drumlin field, southeast of Lac de Gras, Northwest Territories, and includes results and interpretations from available lithological, indicator mineral, and geochemical data in the east study area. Chapter 3 investigates bedrock topographic effects on down-ice 3D dispersal patterns, south of Lac de Gras, Northwest Territories, and will include results and interpretations from the west study area, as well as provide a contrast and comparison between both east and west study areas. Chapter 4 provides a summary of the main findings and contributions of this research by synthesizing and summarizing chapters 2 and 3, and it also provides recommendations to industry and government. Future work and questions will also be included in this section.

## CHAPTER 2: Preserved three-dimensional sediment dispersal in a drumlin field, southeast of Lac de Gras, Northwest Territories

### 2.1 Introduction

The effect of till thickness and landforms on till dispersion patterns, both at the surface (2D) and in the subsurface (3D) has gaps in our understanding that can be addressed by investigating till composition across a selected study area with contrasting surficial geology settings presumably affected by the same glacial history (See section 1.1).

Recent advances have been achieved in establishing the relationship between drumlin elongation and distance of subglacial transport of tracer lithologies. For instance, a study by Sookhan et al. (2021) investigated the relationship between drumlin elongation and transport distance of indicator clasts (quartzites of the Silurian Grimsby Fm). To this end, they digitized quartzite counts from 135 till samples from Homes (1952) containing between 200-800 clasts per sample from 75-100 yard spacing in small pockets within the larger study area. They showed that the longest dispersal distance of quartzites to their bedrock source is greater in drumlin corridors (called flow units) consisting of more elongated drumlins than in corridors where drumlins are less elongated. Despite these advances, our understanding of the full 3D dispersion in drumlin fields, where till is of variable thickness, is still limited.

As previously described (See section 1.2.5) palimpsest ice flow along a continuum through overprinting and inheritance can be generalized in areas of thin and thick tills. In areas of relatively continuous thick till, sediment and landforms from an earlier ice flow phase, or glaciation, tend to be partly preserved and landforms are sometimes reshaped by the youngest direction of ice flow, thus requiring consideration when determining the provenance of till (e.g., Hirvas, 1991; Stea and Finck, 2001; Trommelen et al., 2013; McClenaghan et al., 2018). Therefore, till material originating from a source not aligned with the youngest ice flow event can create problems with 3D data interpretation in areas with thicker tills. Furthermore, till stratigraphy crosscut during RC drilling could contain hybrid end-member tills, consisting of till variably inherited and overprinted from various ice flow events (**Fig. 2.1**). Despite this general knowledge, only few studies about palimpsest trains have considered the full thickness of the till sheet(s) (Kelley et al., 2019a).

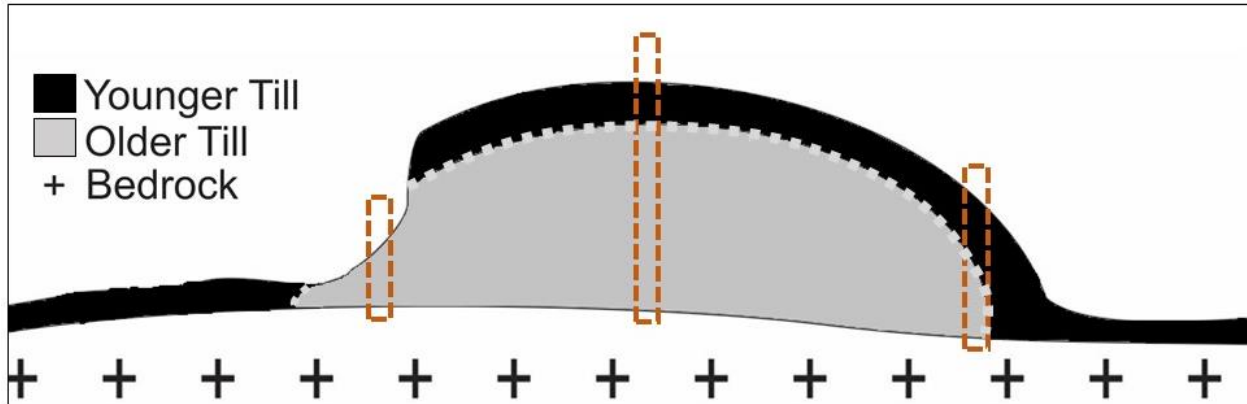


**Figure 2.1:** Conceptual cross-section of a stratified drumlin with hypothetical RC drill holes represented by dashed boxes. Drilling in a grid pattern through areas of thicker till could sample till of different provenance, making data interpretation challenging.

In summary, it is still unclear whether there is a surface and subsurface connection in dispersal trains experiencing complex ice flow shifts. Therefore, the purpose of this chapter is to gain insights into the potential net effect of till thickness variations in a drumlin field and related landforms on local 3D till dispersal trains in an area that was affected by ice flow shifts (See section 1.3.2).

More specifically, the objectives of this chapter will refine and further constrain the ice-flow history of the drumlin field in this study area and provide an analysis of the 3D patterns of kimberlite indicator minerals to determine the extent and strength of the palimpsest dispersal at depth, and analysis of the surficial dispersion of lithologies and geochemical pathfinders to determine whether there is a link between the surface and subsurface dispersal patterns. This is done by mapping 3D dispersal patterns of indicator minerals, lithological and geochemical pathfinders, and landforms.

## 2.2 Study Area

The Lac de Gras district in the Northwest Territories contains 3 current producers and 1 past producing mines within 120 km of the study areas. This is a highly prospective area to target harder-to-find kimberlites, not only because of proven deposits nearby, but also because exploration in the surrounding areas has been widespread and there are a lot of data available to reinterpret to discover the next viable diamond-bearing target (**Fig. 2.2**). South of Lac de Gras, in the Harry Winston (HW) camp region, Dominion Diamond Mines and North Arrow Minerals, Inc. implemented a large reverse circulation drilling program to further define the geology of the area in 2013. Then, the ArcticDEM was released (Porter et al., 2018) which provides a significant amount of detail about the topography of the area.



**Figure 2.2:** Google Earth image of the broad region with diamond mines and study areas. Approximately 300 km NE of Yellowknife, Ekati mine developed in late 1990s, Diavik mine in early 2000s; Snap Lake mine developed over mid-2000s, and Gahcho Kué mine developed over mid-2010s. The east study area is outlined in dashed white box.

The east study area includes 135 km<sup>2</sup> in the highly prospective (for diamonds) Lac de Gras kimberlite field, hosted by the Archean central Slave craton (Fipke et al., 1995), south of Lac de Gras, Northwest Territories (NT) approximately 300 km northeast of Yellowknife, NT. Kimberlites subcrop in the northeast of the study area within Archean Post-Yellowknife Supergroup muscovite-biotite monzogranites (ca 2599-2582) referred to as granitoids in this study, whereas the drumlin field overlays Archean Yellowknife Supergroup metasediments from the Itchen Formation, containing either biotite schists or cordierite +/- andalusite porphyroblastic schists (ca 2637, +8 -7 Ma) referred to as metasediments in this study (Kjarsgaard, 2007).

The area was overlain by the Keewatin Sector of the Laurentide Ice Sheet (Dyke and Prest, 1987) as further described in section 1.2.2. While the northeast quadrant of the study area is characterized by streamlined landforms interspersed with discontinuous till veneer (**Fig. 2.3**) and an esker trending northeast along the east of the study area (**Fig. 2.4**), the predominant feature in the study area is a drumlin corridor oriented in the youngest ice flow direction to the northwest (**Fig. 2.5**). Till thickness varies in the drumlin field, from the tops of higher amplitude drumlins to swales of bedrock overlain by a veneer of till or organics or exposed bedrock.



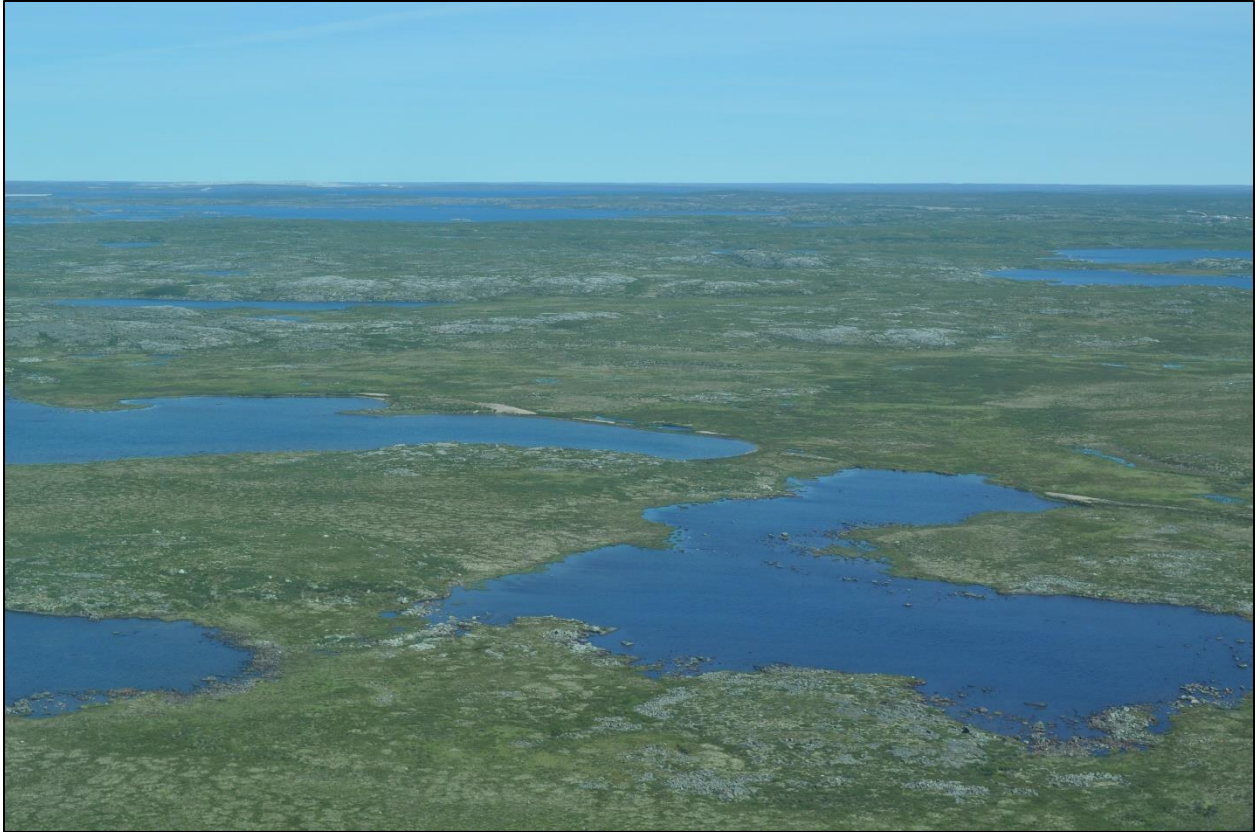


**Figure 2.3:** Landscape of areal scouring with zones of bedrock outcrops (grey) and zones of till and other surficial sediments (brown and green).





**Figure 2.4:** Flat topped esker. Reworked esker provides evidence of shoreline reworking (and glacial lake inundation) in the study area. Shoreline reworking of surficial till in the study area is also expected.

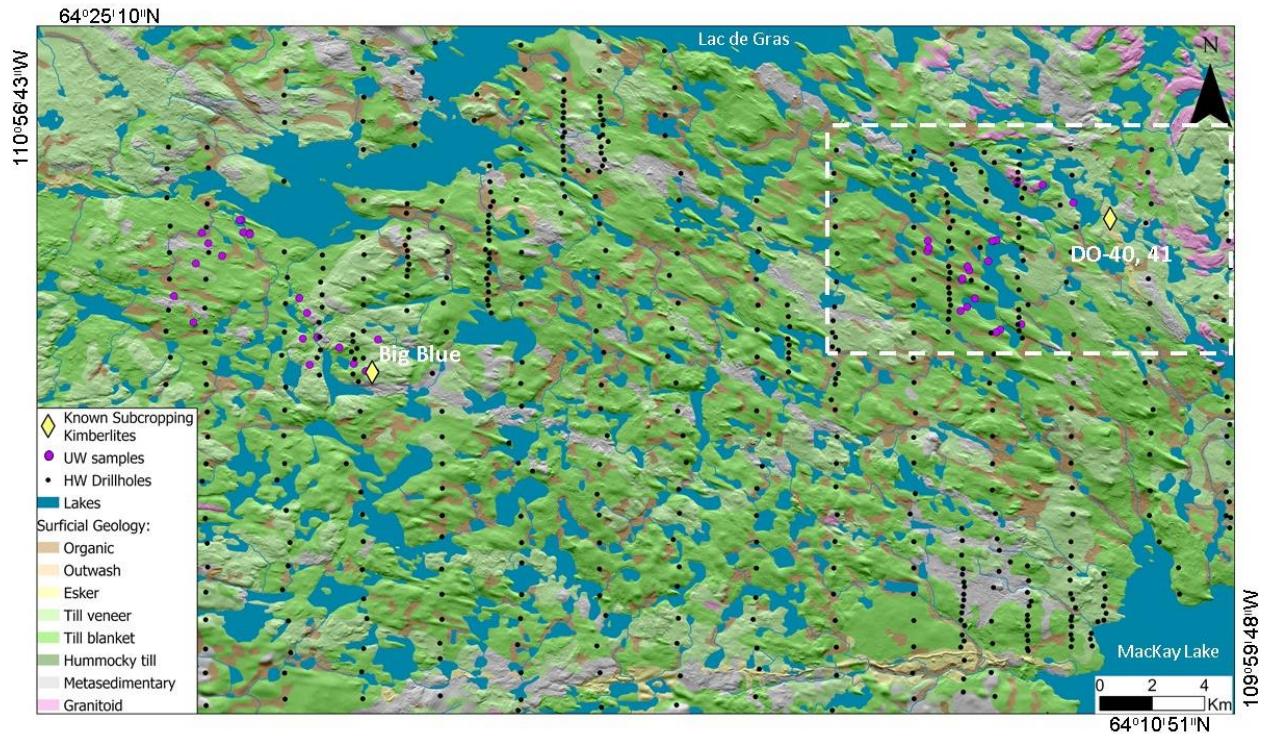


**Figure 2.5:** Surficial geology and distribution of HW drillhole locations and the local study area (white dashed outline). Drumlin corridor is a predominant feature, extending from southeast at the northern tip of MacKay Lake, to northwest at the southern edge of Lac de Gras.

### 2.3 Methodology

The large HWRC result database provided for this study by the Northwest Territories Geological Survey, the regional surficial geology map (Ward et al., 1997) regional bedrock geology map containing known kimberlites (Kjarsgaard 2007) and a high resolution (2m) ArcticDEM (Porter et al., 2018) provided an opportunity to study till thickness variability and its effect on dispersion in the proximity of known kimberlites (DO-40, DO-41).

Because the region experienced complex ice flow events (Ward et al., 1997; Kelley et al., 2019a Janzen, 2020), it was hypothesized that a continuum of till compositional, inheritance and overprinting (see **Fig. 1.1**) within a drumlin corridor produced palimpsest sediment dispersal. If true, it could have important implications for till dispersal pattern interpretation. To test this hypothesis, a field traverse crossed the drumlin field while collecting new ice flow indicator measurements, to augment pre-existing regional measurements, and till samples for KIM and geochemical analysis. Ice flow indicators, such as striations and stoss-lee outcrop shapes (i.e., small roches moutonnées) were measured on exposed bedrock in the northeast of the study area and between the swales in the drumlin field. In addition, KIM, geochemical, and textural samples were collected during the planned traverse that aimed to transect and examine drumlin features. These samples were collected from the tops of drumlins, the swales between drumlins, and from pits dug into the flanks of drumlins, aiming to sample deeper into the core of the drumlins (**Fig.**

**2.1).** Textural samples were also collected to examine the sediment at the edge of a water body to compare to the texture of samples from drumlins. KIM samples collected at surface were compared to results from the RC database to determine palimpsest dispersal at depth. Geochemical samples were analyzed for surficial dispersion of lithologies and geochemical pathfinders to determine whether there is a link between the surface and subsurface dispersal patterns to investigate the potential effects related to till thickness variations and related subglacial processes.

### **2.3.1 Fieldwork**

Ice flow indicator measurements were taken at every opportunity on exposed outcrop and in places where till veneer was carefully removed from outcrop suspected of preserving striae. Striae and stoss-lee relationships were identified, and multiple measurements were taken from outcrops to increase confidence in observations. Care was taken to avoid measuring striae in areas where ice flow could be deflecting around the sides of the landform. Where present, cross cutting striae were ordered in relative age and noted on the outcrop from 1 (oldest) to youngest.

Geochemical samples were collected across the study area, and six KIM samples were collected at strategic geochemical sample sites to transect drumlin features. Organic debris was cleared from a sample site. This included moss, lichen, and plant material. Sample material was scrutinized to determine if it was till, and if the till material was oxidized. If till material was too oxidized, another sample site was established nearby. More details about sampling can be found in Chapter 1 (Section 1.4.3).

### **2.3.2 Sediment and Geochemical Analysis**

Twenty geochemical till samples were processed for texture and clast lithology at the UW Quaternary Geology lab. Texture was determined using a series of sieves and particle laser analyzer, then the largest fractions were categorized for clast lithology (see Section 1.5.4, 1.5.5 for details). An aliquot (50 g) of the clay and silt fractions were sent for geochemical testing at the Saskatchewan Research Council (SRC) (See section 1.5.5 and 1.5.6.1). Samples for KIM processing were sent from the field to SRC to be visually picked and probe confirmed for pyrope, Cr-diopside, olivine, chromite, and picroilmenite. An additional three textural samples were collected from separate layers at same sample site to examine the sediment at the edge of a water body to compare to the texture of geochemical samples from drumlins.

### **2.3.3 HW Dataset**

The study area encompasses 111 drill holes from the HW dataset (n= 757). Drill holes contain descriptive logs, depth to bedrock, major clast lithology percentages, matrix colour, and probe confirmed indicator mineral visual counts. In this study, 228 samples were used, with up to 19

samples per hole, with an average sample interval length of 1.5 meters. Although each sample was processed in three fractions, namely 0.25-0.5 mm, 0.5-1.0 mm, 1.0-2.0 mm, best practices from McClenaghan et al. (2013) recommends using results 1.0 mm and under, and so the dataset was prepared using the 0.25-0.5 mm and 0.5-1.0 mm fractions (See section 1.5.8.1) to be consistent with best practices and method used by SRC. HW samples were visually picked for minerals including pyrope, Cr-diopside, olivine, chromite and picroilmenite, and probe confirmed by C.F. Minerals. Every borehole interval was analyzed in the same way, for both indicator mineral counts and lithological counts. Clast lithology data was calculated into bins and recorded in an Excel database (See Appendix E).

### **2.3.4 Data Analysis and Mapping**

The HW dataset was prepared by geoscientists and provided to the NTGS. It is assumed QA/QC was performed on the data, and the data was validated before it was presented to the NTGS. Till composition pebble counts were estimated in the HW dataset, while till clast lithology counts were performed on the UW samples.

Duplicate and repeat (n=4) trace element results in the UW dataset presented in this study (including Ni, Cr, Co, Nb, Ba, Rb) are precise to a 10% confidence interval in both scatterplots and the Thompson-Howarth Short Method. Average coefficients of variation are less than 3.5, following Piercey (2014) and are well below the suggested pulp and analytical duplicate average coefficient of variation value of 5-7.5% (Abzalov, 2008) (Appendix G).

Standard results (1179 Till 3) compared to certified values using relative percent differences have excellent accuracy (+/- 0-3%) (n=2) and very good accuracy (+/- 3-7%) (n=2) following Jenner (1996) and Piercey (2014). However, two standard reference values (Ni (LOD 0.1 ppm) and Nb (LOD 0.1 ppm)) were not accurate (they are above +/- 10%, following Jenner (1996) and Piercey (2014)). Although the data is not precise according to the CANMET published results for total digestion, standard reference material inserted by SRC (DBC01) has very good accuracy for Nb and excellent accuracy for Ni (See Appendix G). Given the importance of these metals as geochemical pathfinders for kimberlites, Ni and Nb results are further tested for error, bias, and precision using duplicate scatterplots, Thompson-Howarth Short Method, and average coefficients of variation. Duplicate scatterplots, Thompson-Howarth Short Method, and average coefficients of variation tests show the data is precise and generally fit-for-purpose. Due to low analytical values, Nb is precise to the detection limit (-11%) and still fit-for-purpose. Nickel values are over-valued at 20%. However, since values are low and the relative percent difference does not significantly change the values, the data is still fit-for-purpose, but used with caution. Furthermore, results presented in this study are calculated as percentiles (Grunsky, 2010) which further mitigates the error.

HW and UW sample locations and results were added to ArcGIS Pro 2.9 as layer files to spatially examine 3D patterns of geochemical data, KIM data, and clast lithological content in the context of ice flow indicator measurements collected in the field and published by Ward et al. (1997) to test patterns and trends at depth.



To present 3D data in 2D space while eliminating depth bias, borehole intervals were divided into quarters based on depth of hole (See section 1.5.8.1). Single-sample boreholes (typically in shallow till less than 1 meter thick) are represented only in the top depth interval, two-sample boreholes are represented in the top and base depth interval, and three-sample boreholes are represented at the base, upper-mid and surface depth intervals. The deepest boreholes could contain as many as two to three samples per depth interval. All KIM results are normalized to 10 kilograms.

## 2.4 Results and Interpretations

### 2.4.1 Field-based Ice Flow Indicators and Till Characteristics

Six locations provided new ice-flow indicators, which consist of 10 striation measurements and two stoss-lee relationship measurements (**Fig. 2.6**). Ice-flow indicator measurements from striations were plotted on a histogram and visually sorted into groups of measurements used to construct a rose diagram (**Fig. 2.7**) and an ice flow summary diagram in ArcGIS. These measurements are consistent with ice-flow indicator measurements of the older, intermediate and young flow phases (SW, W and NW) presented on the regional surficial geology map (Ward et al., 1997), and also more recently by Kelley et al. (2019a) and Janzen (2020).

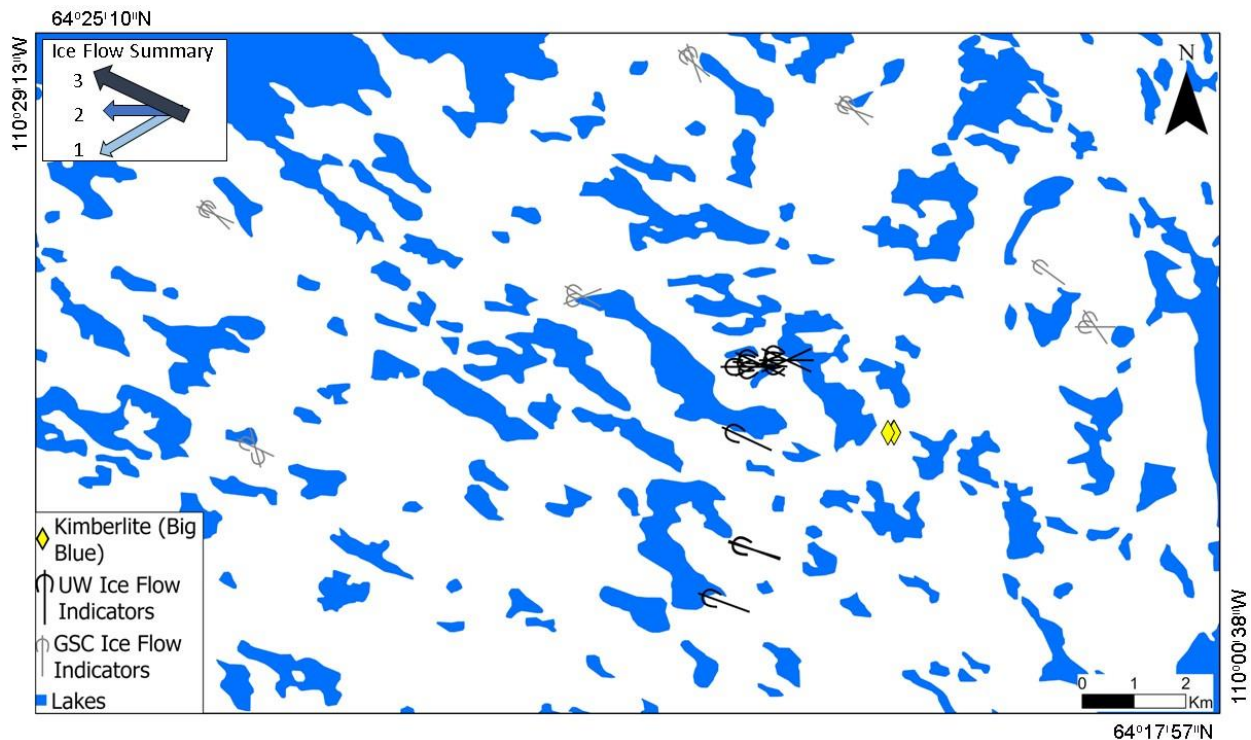


**Figure 2.6:** Eleven ice flow indicator measurements taken at six locations are consistent with GSC measurements from Ward et al. (1997), indicating a clockwise shift in ice flow from southwest to northwest.

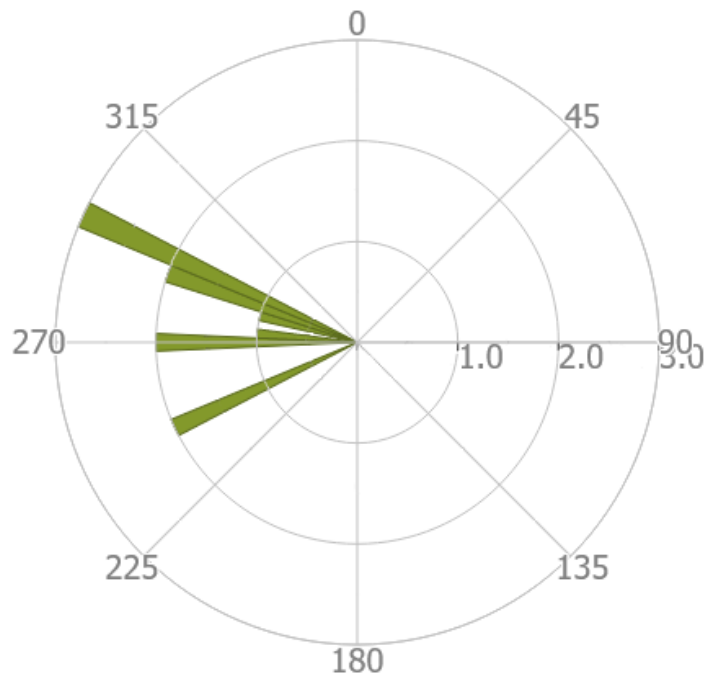


**Figure 2.7:** Rose diagram displaying 11 ice flow indicator measurements collected for this study.

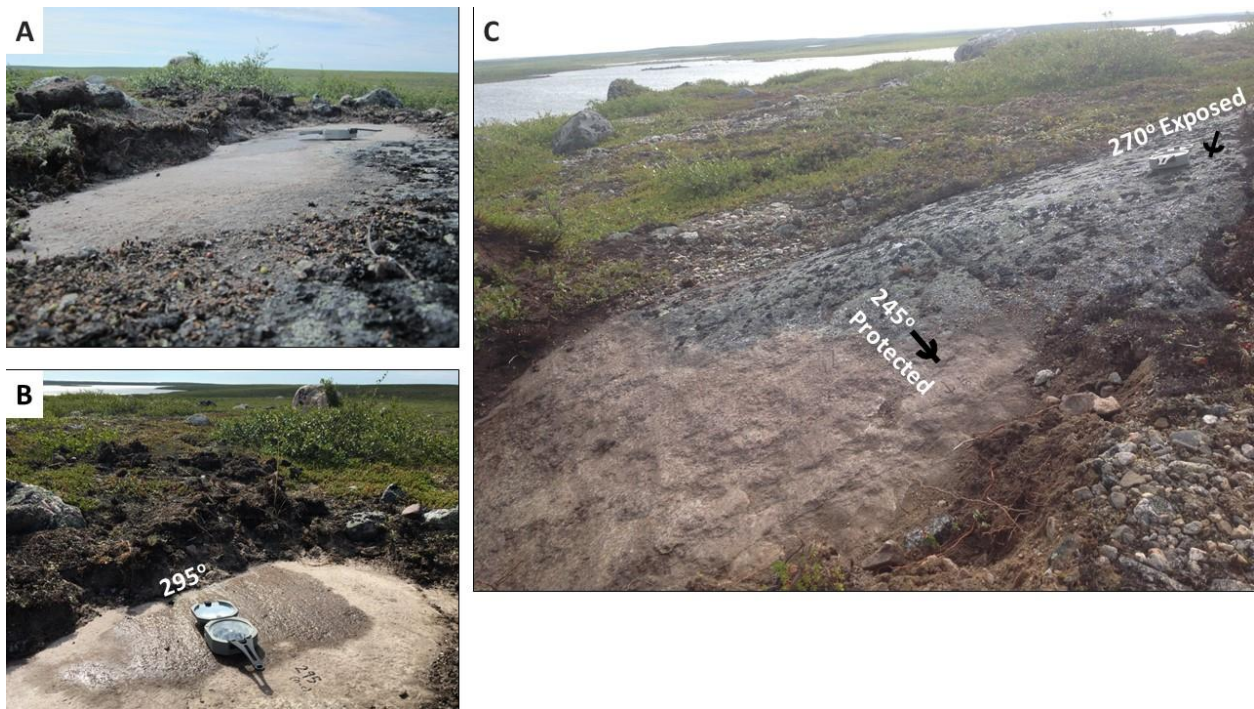


**Figure 2.8:** Ice flow indicators on outcrop and whalebacks. A) Stoss-lee relationship indicating ice flow from left to right; B) Polished surface with striations and grooves towards the NW; C) relative age relationship (older = 259° and younger = 284°) established on the basis of protected polished surface and upper (top of outcrop) indicators; Till



veneer covering striae better protects striae from subsequent glacial movement, while the exposed top of the whaleback is striated in direction of youngest ice flow, aligned with the Brunton compass pointed in the down-ice direction (right of photo, adjacent magnetic variation-corrected annotation).

The largest drumlin dimensions in the corridor within the study area is 2700 meters long, 500 meters wide, and up to 21 meters in amplitude. Underlying bedrock topographic relief is subdued in the drumlin corridor, due to the erodibility of metasedimentary rock. The northeast quadrant of the study area and beyond is characterized by exposed bedrock in the form of roches moutonnées and whalebacks (**Figs. 2.8, 2.9, 2.10**) interspersed with discontinuous till veneer. The erosional bedrock landforms that were traversed, down ice of the kimberlite, were significantly smaller and on the scale of a few meters. In addition, an esker with a flattened top meanders its way across the kimberlite deposit from southeast to northwest (**Fig. 2.4**).

Glaciolacustrine wave wash evidence is visible across this study area, including flattened top eskers, scarped drumlin flanks, and oxidized sediment and or washed fines exposed in hand dug sample pits (**Fig. 2.11, 2.12, 2.13**). Wave washed scarps were eroded into the southwest flanks of drumlins in the drumlin corridor and are clearly visible in areal view (**Fig. 2.12**). Elevation measurements of these scarped features, or terraces, during foot traverses were noted across the study area. It is possible the finest sediments were deposited at lower elevations in what is now present-day Lac de Gras. Glaciolacustrine processes are out of the scope of this thesis, but are still important to note, as the effects on sedimentological and landform characteristics in the study area cannot be ignored.

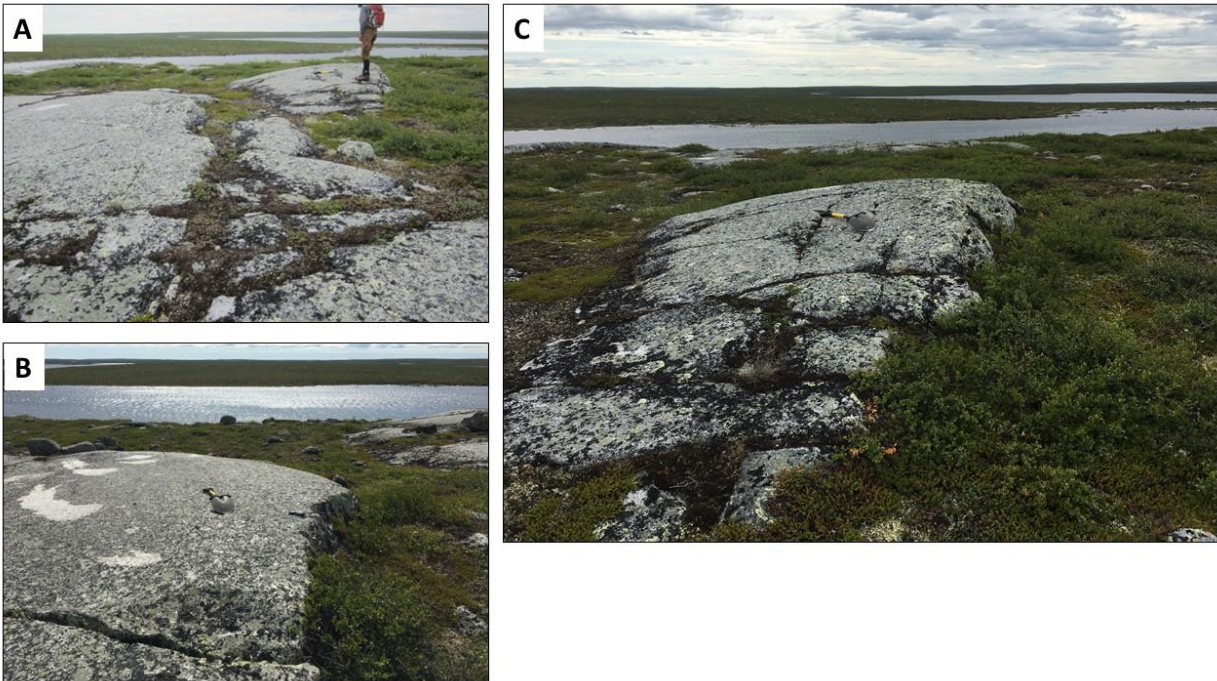


**Figure 2.9:** Roches moutonnées. A) Roches moutonnées formed by the earlier SW flow phase are well preserved in the northeast of the study area. B) Shovel pointed in direction of younger (NW) ice flow (309°). C) Pluck faces formed during older (SW) ice flow (259°).



**Figure 2.10:** Whalebacks present down ice of DO-40/DO-41. Previous pluck face smoothed during subsequent ice flow. Marker pointed in down-ice direction where till buried old lee-side of landform.

Overall, the general sedimentological characteristics observed in the field included unoxidized light tan/grey sandy pebble till with occasional micas, and small felsic boulders and felsic cobbles (**Fig. 2.11**). These characteristics were consistent within and outside the drumlin. Occasionally, finer grained sand was observed, greater clay content, or rarely dark brown oxidized boulders/gravel were associated with the sample site. Most samples were collected from either frost boils on the tops of drumlins (2-10 cm depth), or wave cut or reworked flanks of drumlins (up to 70 cm depth) that were observed at a similar elevation across the study area (**Fig. 2.12**). Along drumlin flank sample sites, the top of the pit contained oxidized material and care was taken to avoid sampling oxidized material wherever possible.



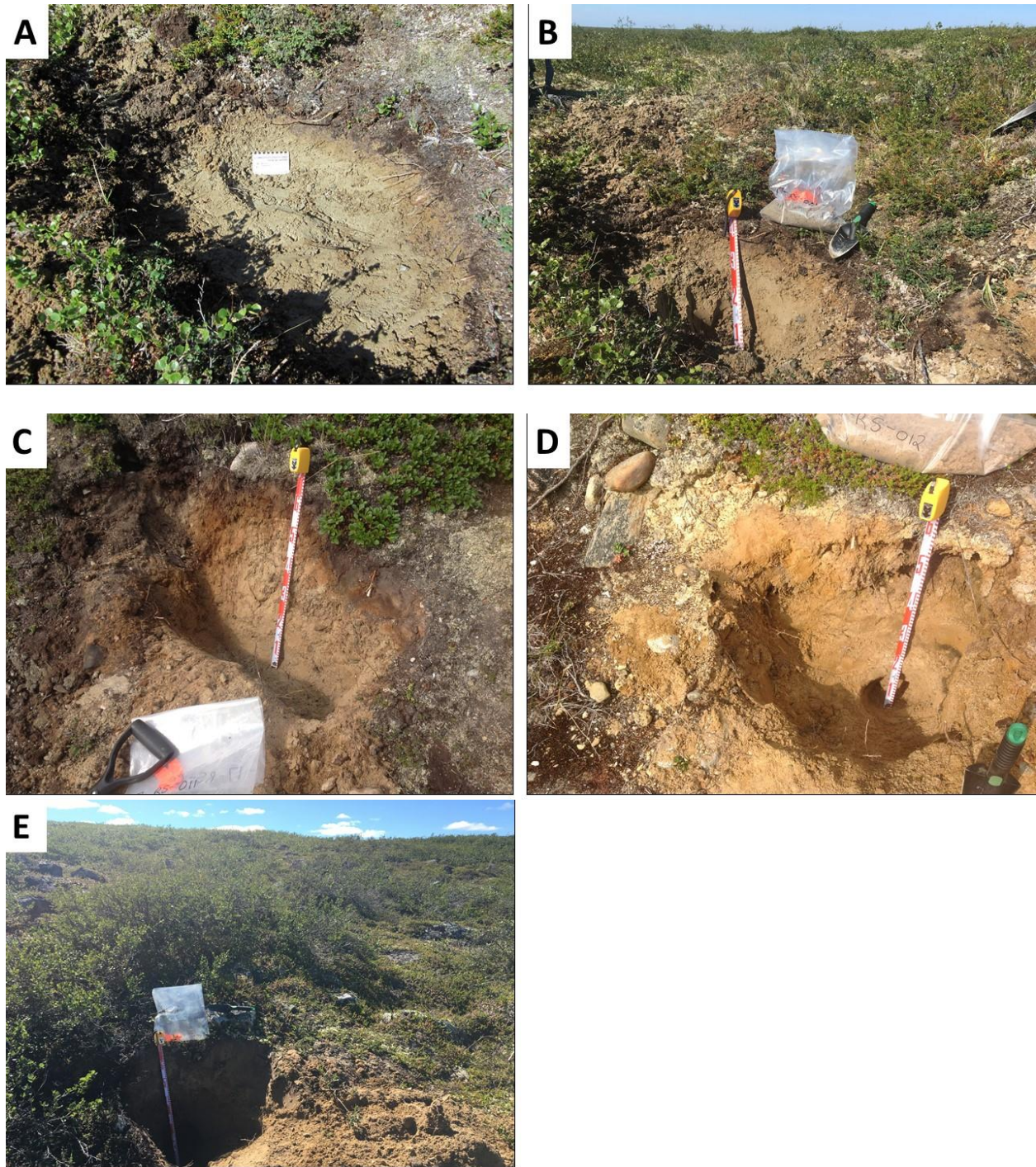


**Figure 2.11:** Till samples collected from frost boils on drumlin tops. (A) Sample site 17-RS-001-B after clearing surface organics (B) and after extracting sample material for a KIM and geochemical/textural sample. (C) Sample site 17-RS-011-B contained sandy pebble till with micaceous material collected from the southeast side of a small truncated drumlin. The top of the pit contained oxidized material with dark-brown large gravel and small cobbles where the matrix was washed out. Sample material was collected from below this oxidized zone. (D) Sample site 17-RS-012-B contained sandy pebble till collected from the southwest side of a drumlin along a scarp face. There were exposed large cobbles and some boulders on the surface (both metasedimentary with some chocolate-brown oxidation in felsic boulders) where fines were washed down-slope. (E) Sample site 17-RS-014-B contained very sandy angular pebble till collected from the northeast side of a drumlin. Small boulders and large cobbles were exposed on surface.





**Figure 2.12:** Scarped drumlin flanks visible from the air, possibly eroded from glaciolacustrine wave washing. Dashed lines and circles outline scarp flanks to make them easier to see.

#### **2.4.2 Kimberlite Indicator Minerals**

Six KIM samples, averaging 13 kilograms of till material, were collected from sites including the tops of drumlins at a 1 cm depth, the swales between drumlins, and from pits dug up to a meter into eroded scarp faces along the flanks of drumlins, aiming to sample deeper into the core of the drumlins (**Fig. 2.13**).



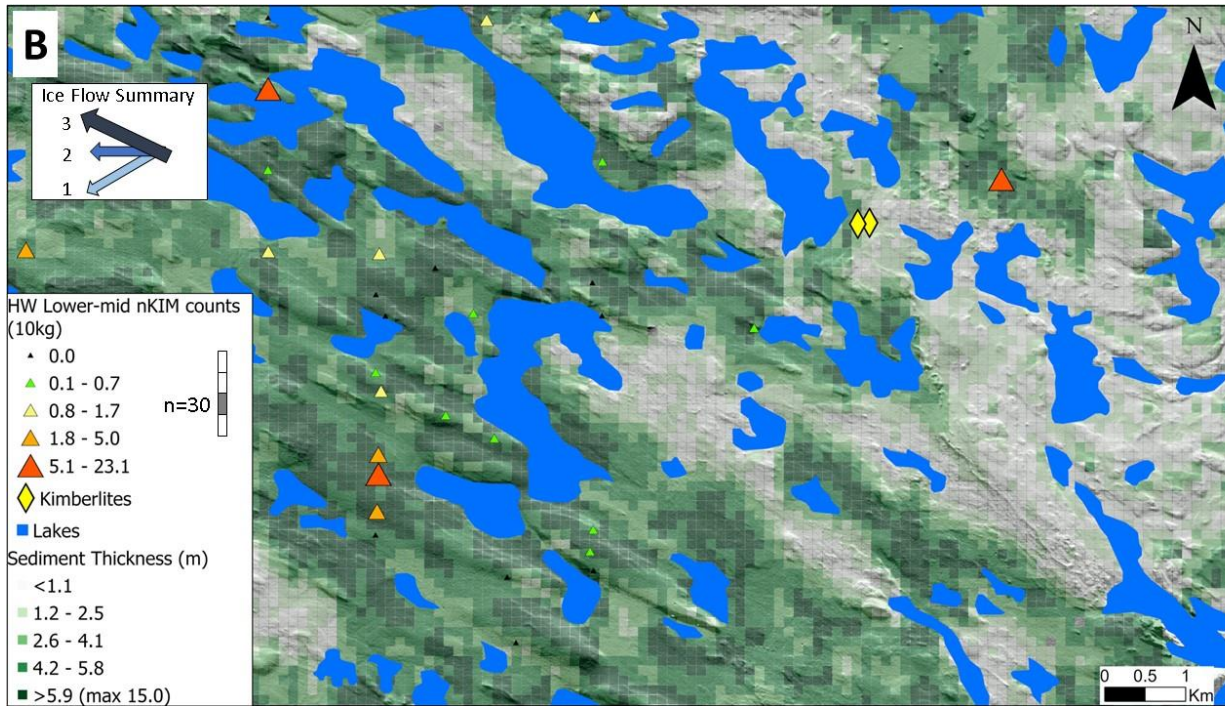
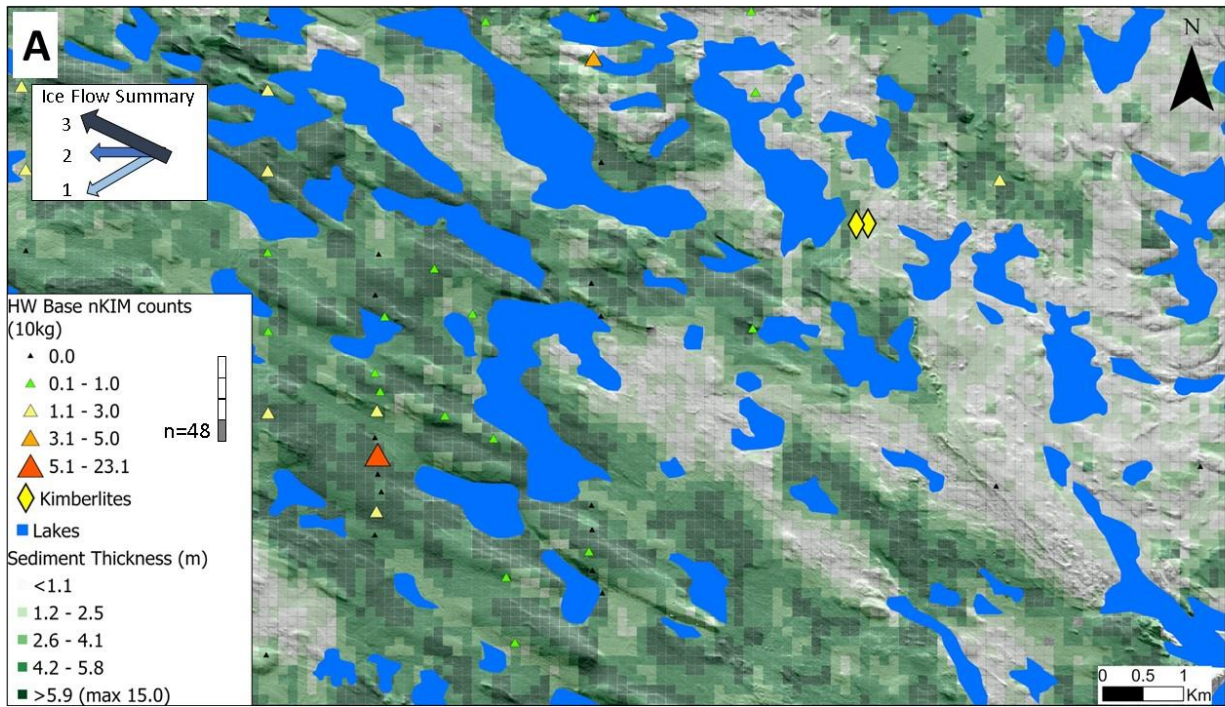
**Figure 2.13:** Drumlins, especially their southwest side, have eroded flanks.

It is assumed that subcropping kimberlites DO-41/40 are the source of kimberlite indicator material within this local area (**Fig. 2.14**), because they are the closest source of kimberlitic material in the area in all known up-ice flow directions. KIM grain morphological analysis provided by SRC suggests that KIM grains were transported some distance, albeit not substantial distances (See section 1.5.7 and Appendix C). All chromite grains were pitted and shiny, only 1 olivine grain was striated, and all peridotite pyrope grains were pitted and fragmented with half of the grains having pyrite present, and a kelyphite rim was identified on one grain.

At the base depth interval of the boreholes, KIM indicators are found within the drumlin field (**Fig. 2.14A**). Moving upwards through the borehole, the clusters of KIM grains persist through the upper-mid depth interval, and KIM indicators along the north of the study area start to increase (**Fig. 2.14B, C**). On surface, there are three clusters of KIM indicators (**Fig. 2.14D**). These clusters are spatially consistent between the RC drilling results and UWaterloo surface sample results. A large cluster spans the study area, while two smaller clusters are seen within the drumlin field. Based on these observations, a 3D dispersal pattern, detached from any known source, is present in the drumlin field. The closest known source is in the older ice flow direction

to the northeast, suggesting the cluster of KIM grains in the drumlin field represent a palimpsest train.







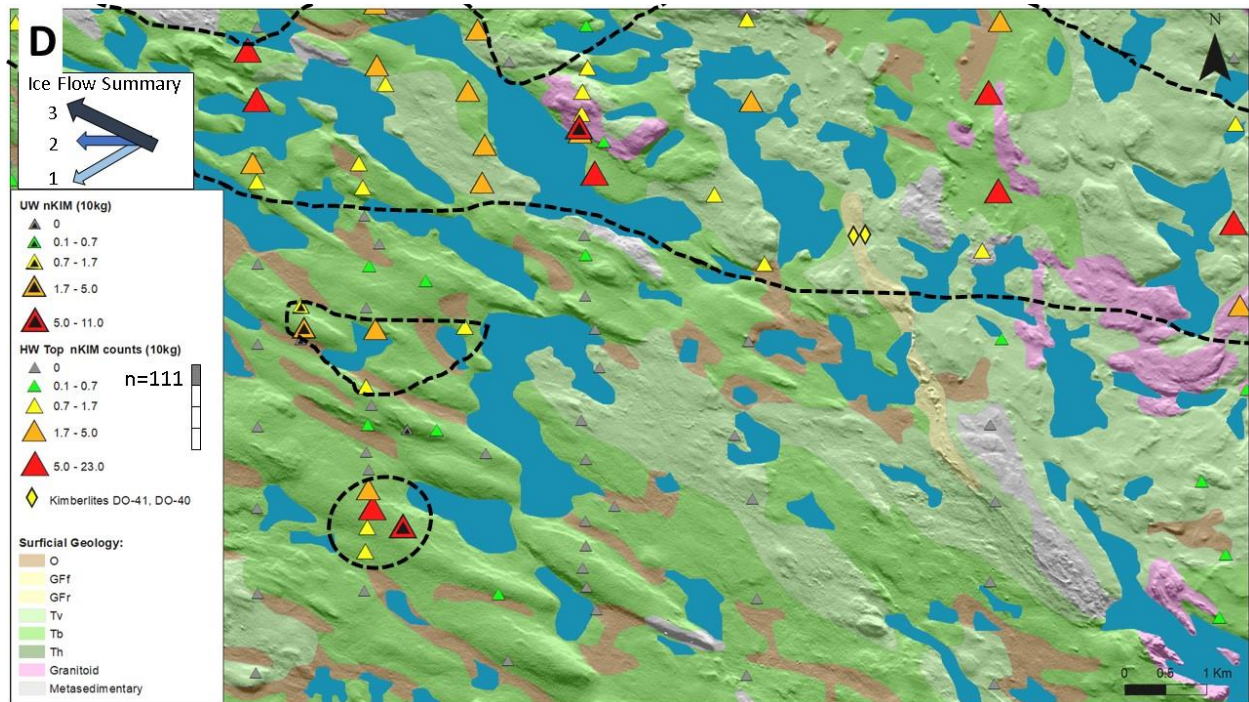
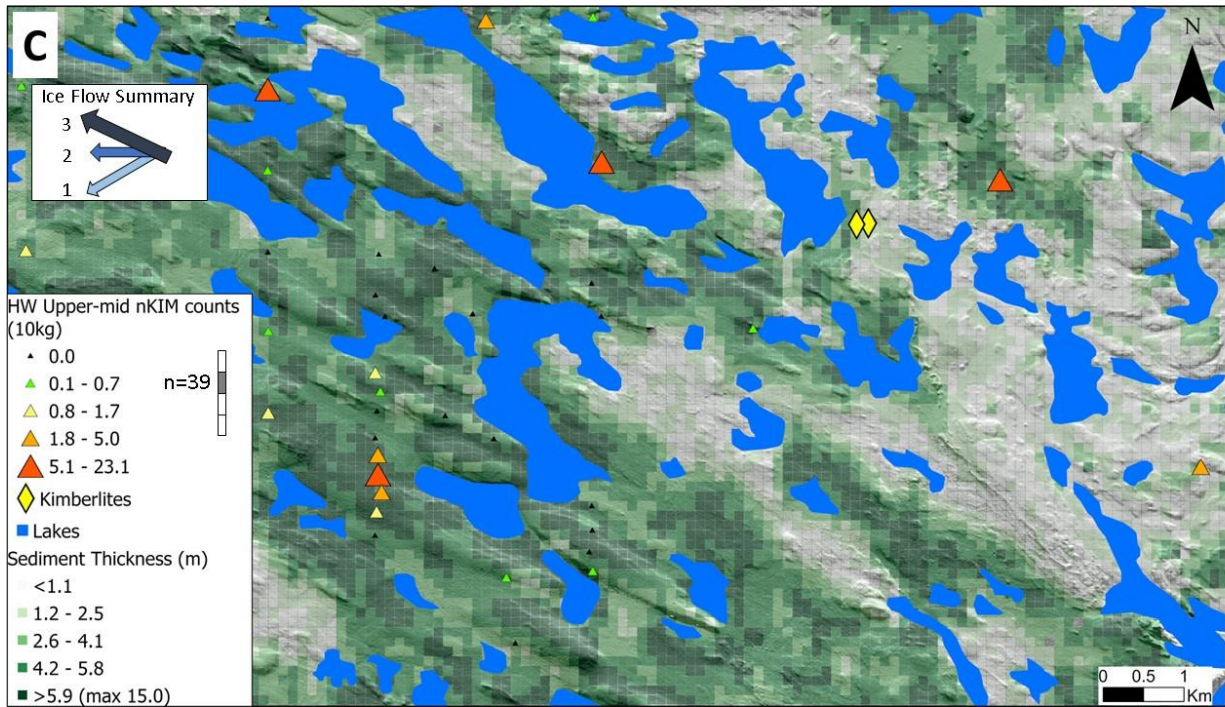


**Figure 2.14:** KIM count results normalized to 10kg samples. On previous page: A) KIM counts from within base of borehole depth interval on sediment thickness map. Moving up the borehole depth interval; B) HW lower-mid depth interval; On this page: C) HW upper-mid depth interval; and D) HW top depth interval, displayed with UWaterloo KIM count results on surficial geology map. Dashed black lines outline clusters of KIM grains. Surficial geology unit codes: O (organics) GFf (glaciofluvial outwash fan sediments) GFr (eskers) Tv (till – veneer) Tb (till – blanket) Th (till – hummock).



A regional examination (using publically available kimberlite data through NTGS Data Hub) shows an emerging pattern (**Fig. 2.15**). Total KIM grain counts are displayed in **Fig. 2.15**, but are not normalized to a 10 kg sample, and therefore cannot be directly compared to the HW and UW results, but the overall pattern is similar. A dispersal train crosses the northern portion of the study area, which extends 30 km from the closest subcropping kimberlites (DO-18, and DO-27, DO-29) aligned in the youngest ice flow direction and possibly rejuvenated by the kimberlites within the study area (DO-41/40). More importantly, there are detached and relatively small clusters of KIM grains within the drumlin field, characteristic of palimpsest sediment dispersal trains.

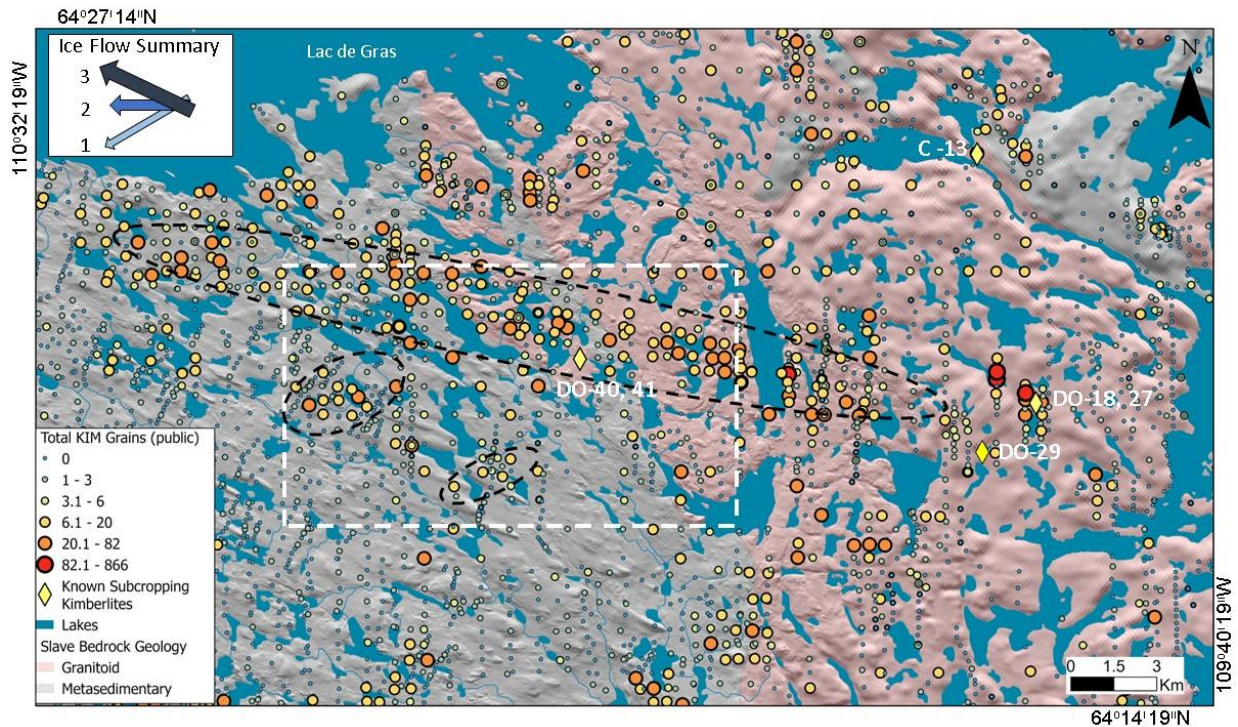


**Figure 2.15:** Map containing publicly available surface KIM data from NTGS Data Hub, and all publicly known kimberlites (subcropping and an intercept depth of up to 30 feet at 90 degree dip angle) in the area (Kjarsgaard, 2007). Dashed white box outlines the study area. Dashed black ovals roughly outline potential dispersal trains using total KIM grain counts from NTGS Data Hub KIDD data <datahub-ntgs.opendata.arcgis.com>.

### 2.4.3 Till Texture, Clast Lithology, and Till Matrix Geochemistry

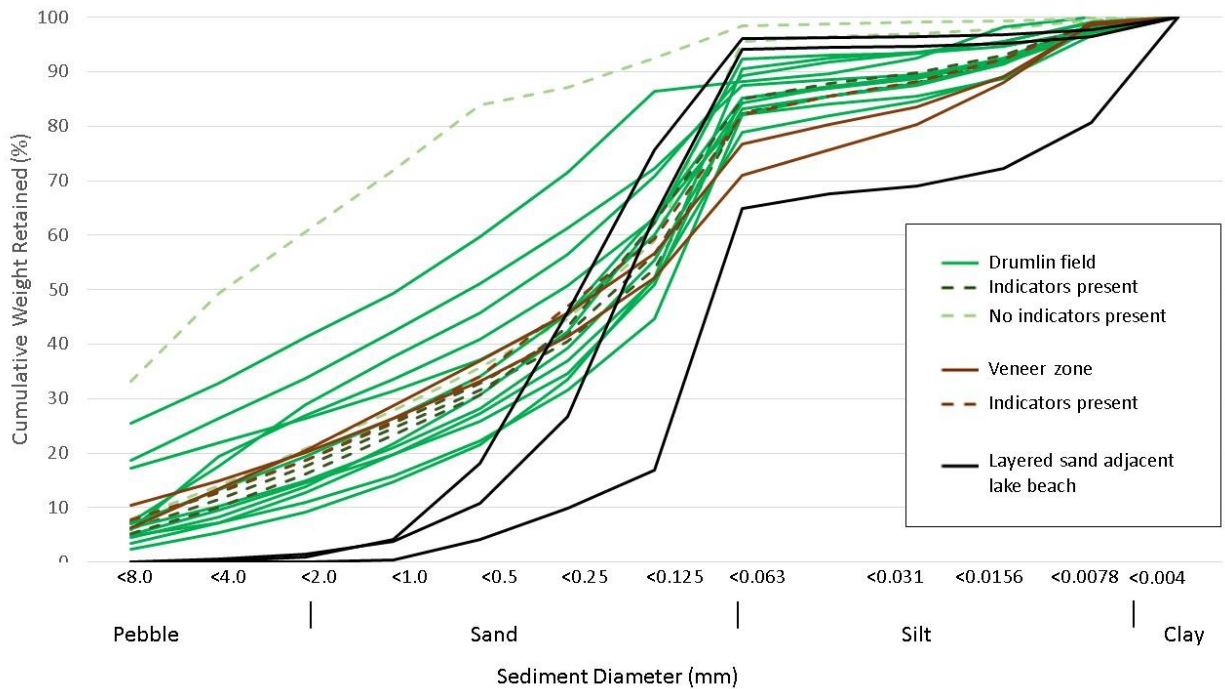
Twenty samples weighing an average of 2.7 kilograms were collected for texture analysis and detailed lithological estimations. In addition, three samples weighing an average of 0.23 kilograms were collected for textural analysis only. First, textural and lithologic analysis results and interpretations are given, followed by geochemical results and interpretations.

### 2.4.3.1 Till texture

**Fig. 2.16** represents till texture from samples across the study area. Samples collected within the drumlin field in the western portion of the study area are separated from samples collected in the northern portion of the study area. Samples that have associated indicator mineral analysis are represented with dashed lines. Samples were also collected adjacent a lake beach setting from one location where layered sand was observed for the purpose of textural analysis. Within this sample location, till was observed below the layered sand. The sample collected adjacent this till layer was the finest of the three textural samples collected.

Till texture in the drumlin field appears to have been affected by lacustrine processes. The coarsest samples were collected from the southwestern flanks of drumlins where scarp faces allowed deeper penetration into the drumlin. It is important to note these scarp faces are thought to be caused by wave water erosion, likely washing away finer sediment. The textural samples collected along a lake between drumlins has an increased amount of fines and could indicate incorporation of lacustrine sediments possibly originating from sediments washed from drumlins. Most of the finer samples were collected from the tops of drumlins, suggesting possible dilution by incorporation of glacial lake fines. The two texturally finest samples collected in the drumlin field were collected from a sample pit within the water table, and the second from what appeared to be a terraced step on the side of a drumlin, possibly created when the lake level was higher.

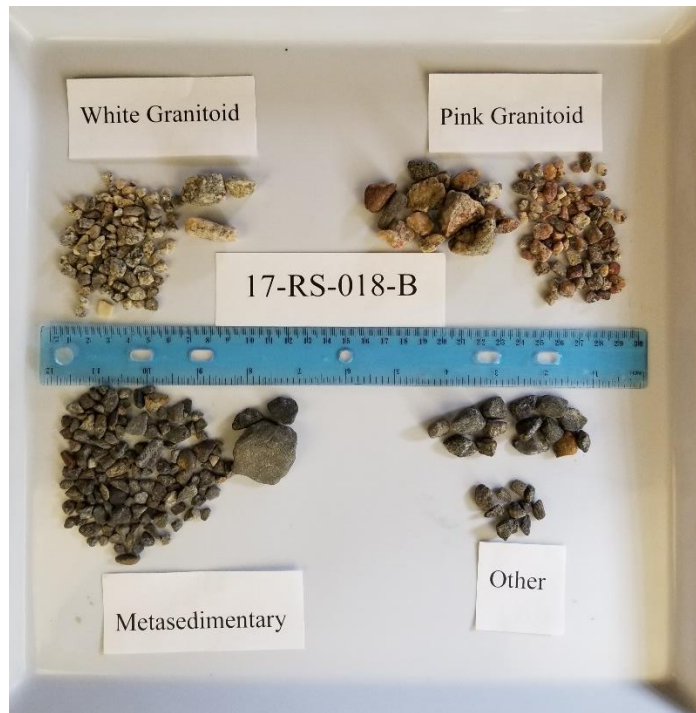




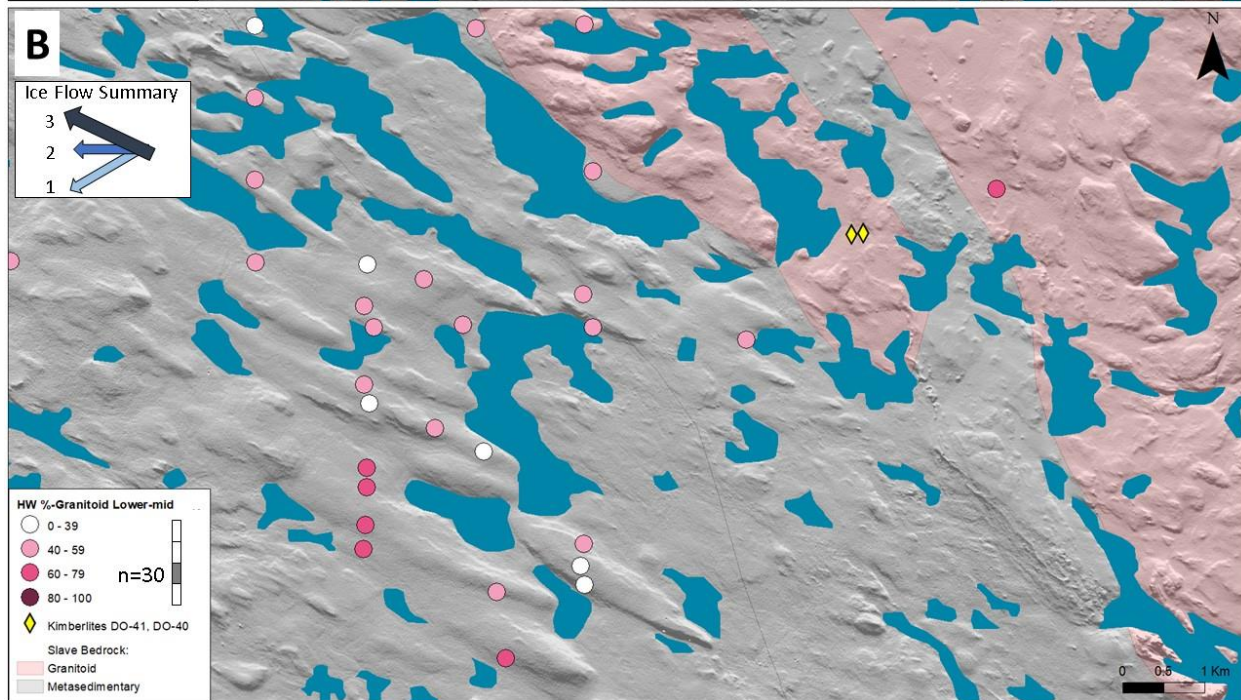
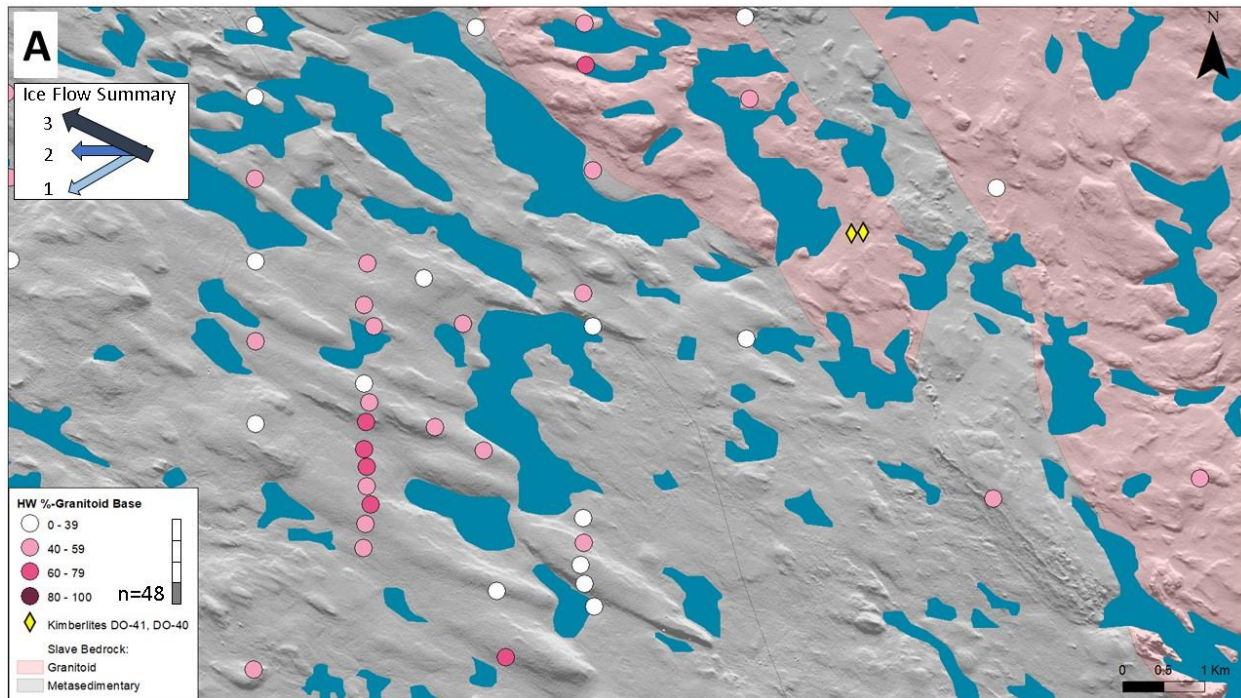
**Figure 2.16:** Cumulative weight percent textural analysis curve. Samples collected within the drumlin field in the western portion of the study area are separated from samples collected in the zone of till veneer in the northern portion of the study area. Samples that have associated indicator analysis are represented with dashed lines. Textural samples were also collected adjacent a lake beach setting from one location where layered sand was observed.

### 2.4.3.2 Pebble lithology

Granitoid pebble lithologies are presented (**Fig. 2.17**) At the base of the boreholes, there is a high percentage of granitoid clasts found within the drumlin field associated with the higher amplitude drumlins (**Fig. 2.18A**). Metasediment foliation is steeply dipping to the northwest, meaning the conditions are favourable for quarrying, and so granitoid and kimberlite material would be quickly diluted with metasedimentary rock. The high (40-80%) granitoid clast percentages are therefore significant, and most likely come from the closest granitoid source, which is aligned in the direction of the older ice flow event to the NE. There is granite to the southeast, about 15-kilometers away, and so if the granitoids were generated during the northwest flow, then granitoid clast content should be more prevalent in the other samples as well. Moving upward through the till column, this cluster of higher granitoid material persists and so does the granitoid clast content within the borehole intervals (**Fig. 2.18B, C**). On surface, UWaterloo samples, where every clast was counted, are consistent (within 10%) with the estimated drilling results (**Fig. 2.18D**). There is also a strong relationship between the lithological count results and the KIM indicator mineral results in the drumlin field. Specifically, high granitoid counts correspond spatially to high KIM indicator mineral counts suggesting that the source of the KIM is from a kimberlite hosted in granitoids and is likely the closest one with that characteristic (most likely DO-41/40).



**Figure 2.17:** Example of lithology classification using sample 17-RS-018-B. Several other examples are in Appendix E.





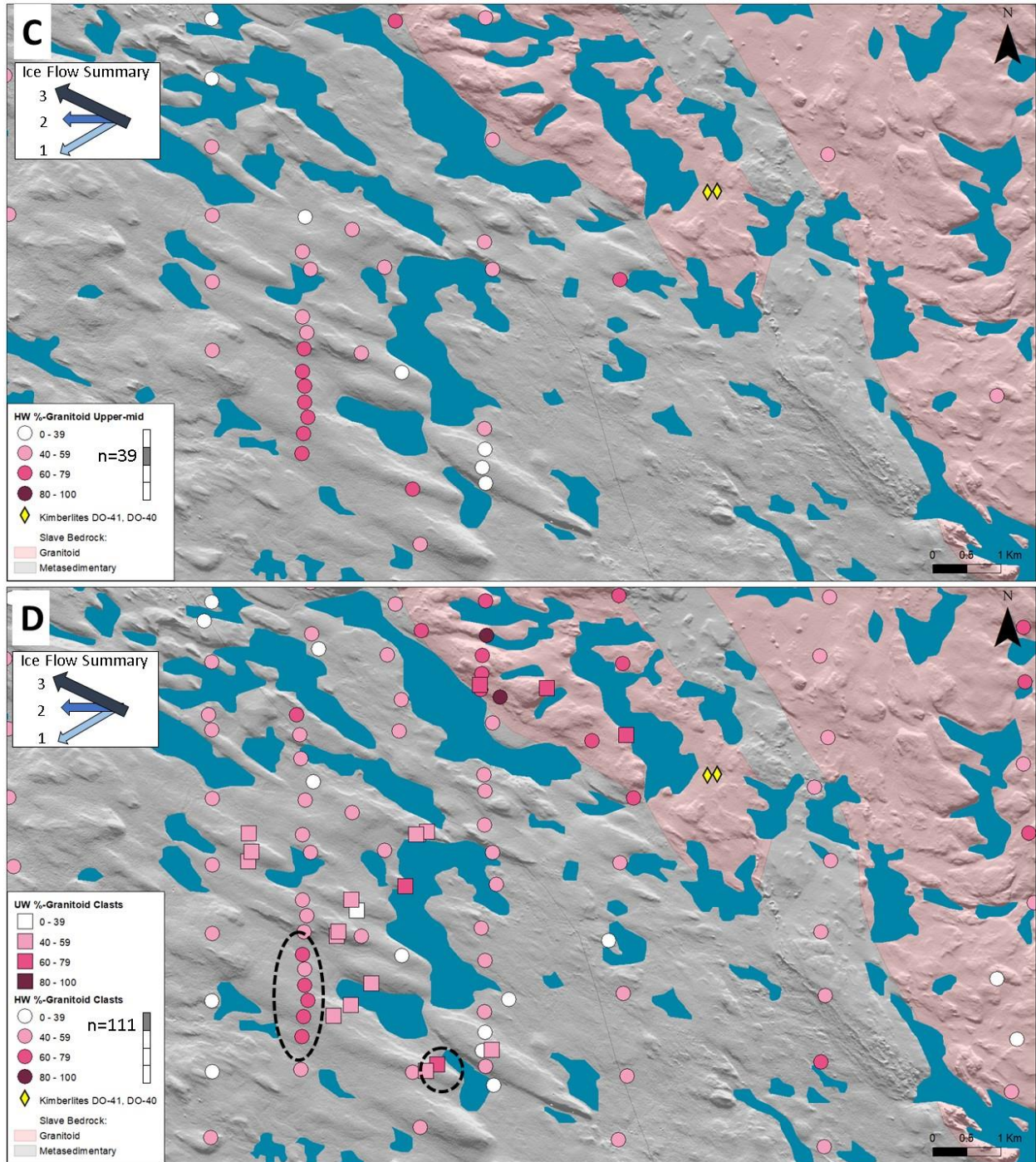


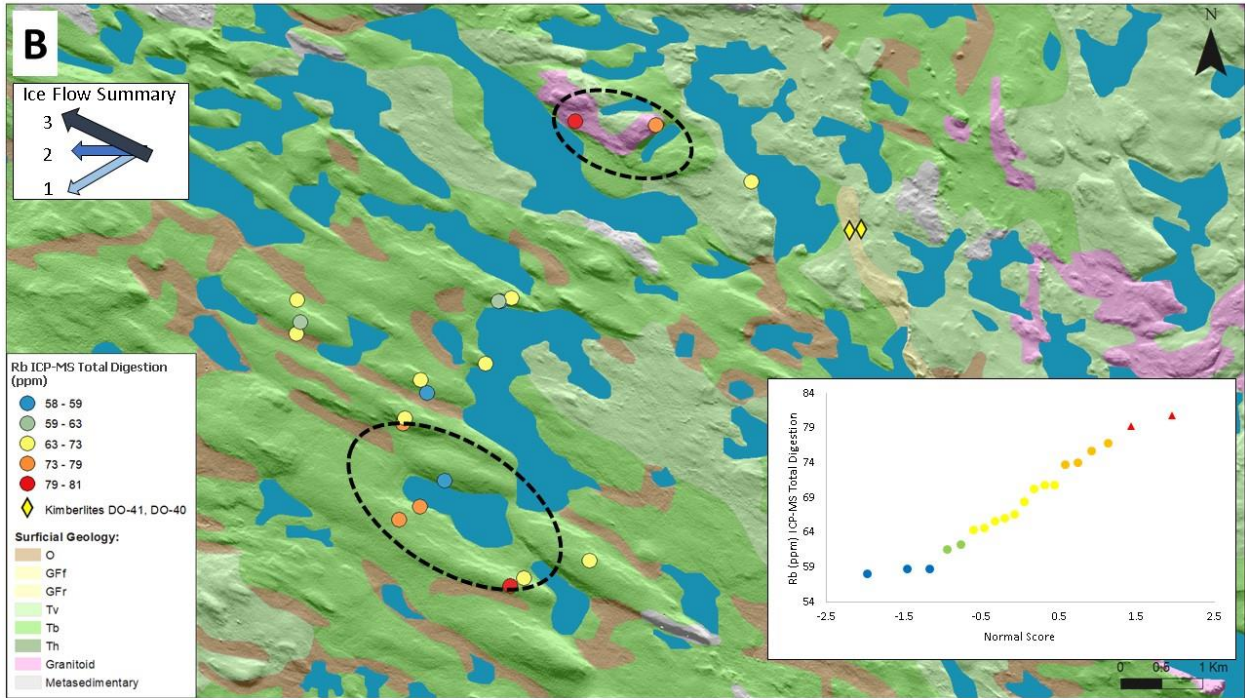
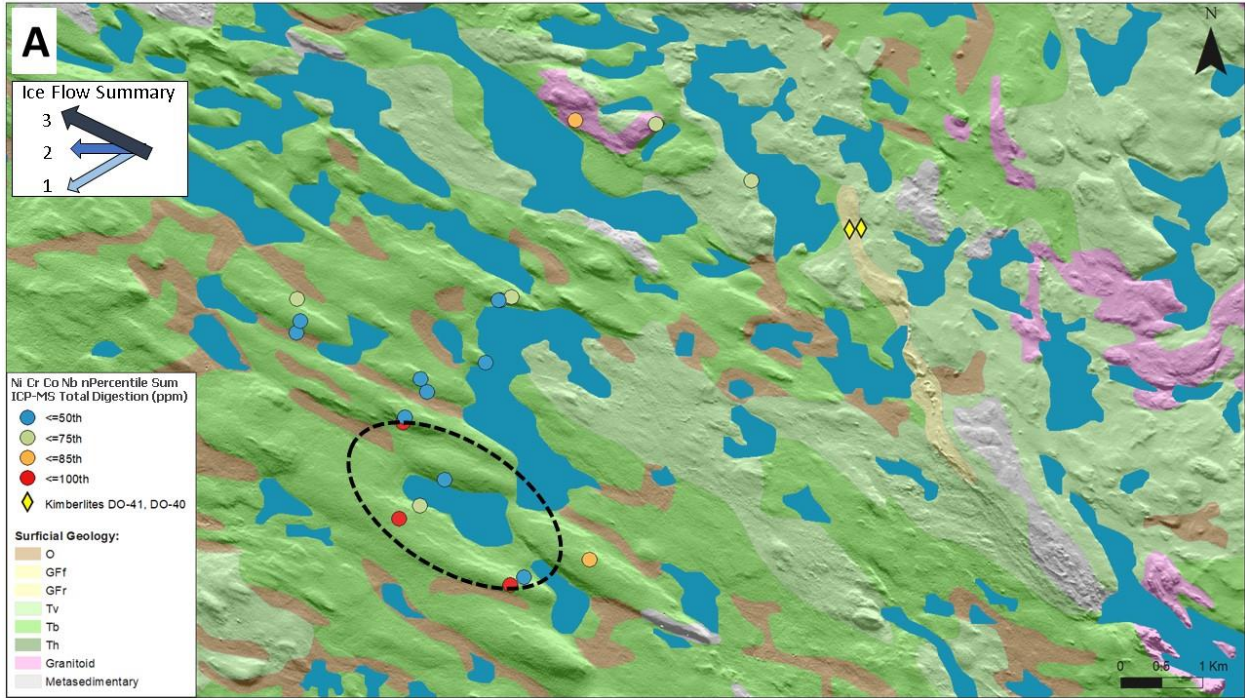
**Figure 2.18:** Granitoid clast lithology at depth using data from HWRC Dataset. On previous page: A) base depth interval of borehole granitoid clast estimates are higher than expected and the cluster persists moving up the borehole to B) HW lower-mid depth interval. On this page C) HW upper-mid depth interval, D) HW top depth interval, displayed with UWaterloo granitoid clast count results, shows cluster of higher granitoid clasts persists through the till column.

### 2.4.3.3 Surficial till matrix geochemistry

Nickel (Ni), chromium (Cr), cobalt (Co), and niobium (Nb) are pathfinder metals associated with kimberlite deposits. These elements were determined to be fit-for-purpose (See sections 1.5.6.1, 1.5.6.2, 2.3.4). These trace elements were calculated as percentiles and summed for an even graphical representation of all four elements. Elevated values (identified as the highest summed percentiles in the east study area dataset) are spatially consistent with the cluster of KIM indicator minerals within the drumlin field. These geochemical elements display a similar surficial trend within the drumlin field (**Fig. 2.19A**).

Rubidium (Rb) and barium (Ba) are enriched in granitic rocks relative to metasediments (Rose et al., 1979), so this study uses Rb and Ba as a proxy for the granitoids (**Fig. 2.19B, C**). However, kimberlites within the Lac de Gras region are also enriched in Rb and Ba (Wilkinson et al., 2001a; McClenaghan et al., 2002; McClenaghan and Kjarsgaard, 2007; McClenaghan et al., 2018). Therefore, Rb and Ba are geochemical pathfinders for granitoid and/or kimberlite sources (**Fig. 2.19B and C**). If Rb and Ba correlate to metals, it is normally because there is a kimberlite signal. The elevated values of both Rb and Ba, as determined using Quantile-Quantile plots (See sections 1.2.4.1 and 1.5.6), in the drumlin field can be attributed to granitoid and/or kimberlitic rock sources to the northeast. Elevated values were determined using Q-Q plots (**Fig. 2.20**). It is also important to note the occurrence of elevated values over granitoid rocks and down the youngest ice flow direction of the known kimberlites **Fig. 2.19B, C**).





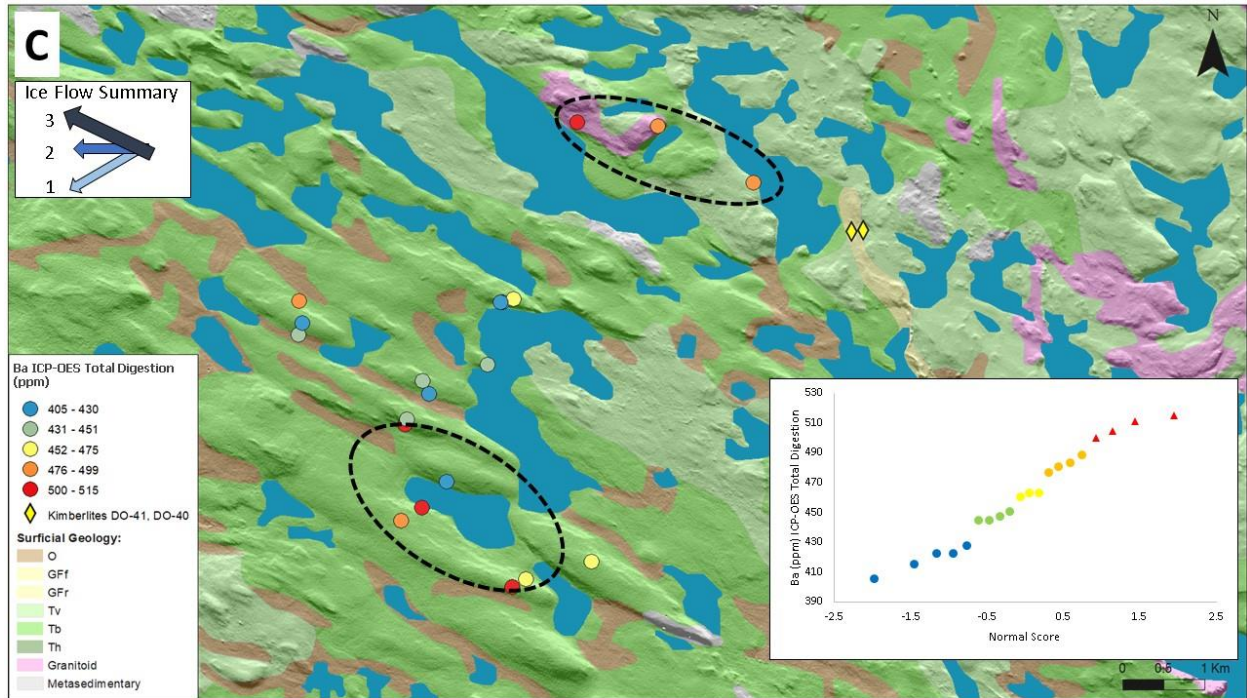


**Figure 2.19:** Distribution of selected geochemical results from UWaterloo surficial till samples. On previous page: A) Percentiles of Ni, Co, Cr, Nb (total digestion) also display a cluster of elevated values in the drumlin field. B) Rubidium. On this page: C) Barium total digestion results display a cluster of elevated values in the drumlin field, as well as in the direction of the youngest ice flow from a known kimberlite source. C) Surficial geology unit codes described in **Fig. 2.14**.

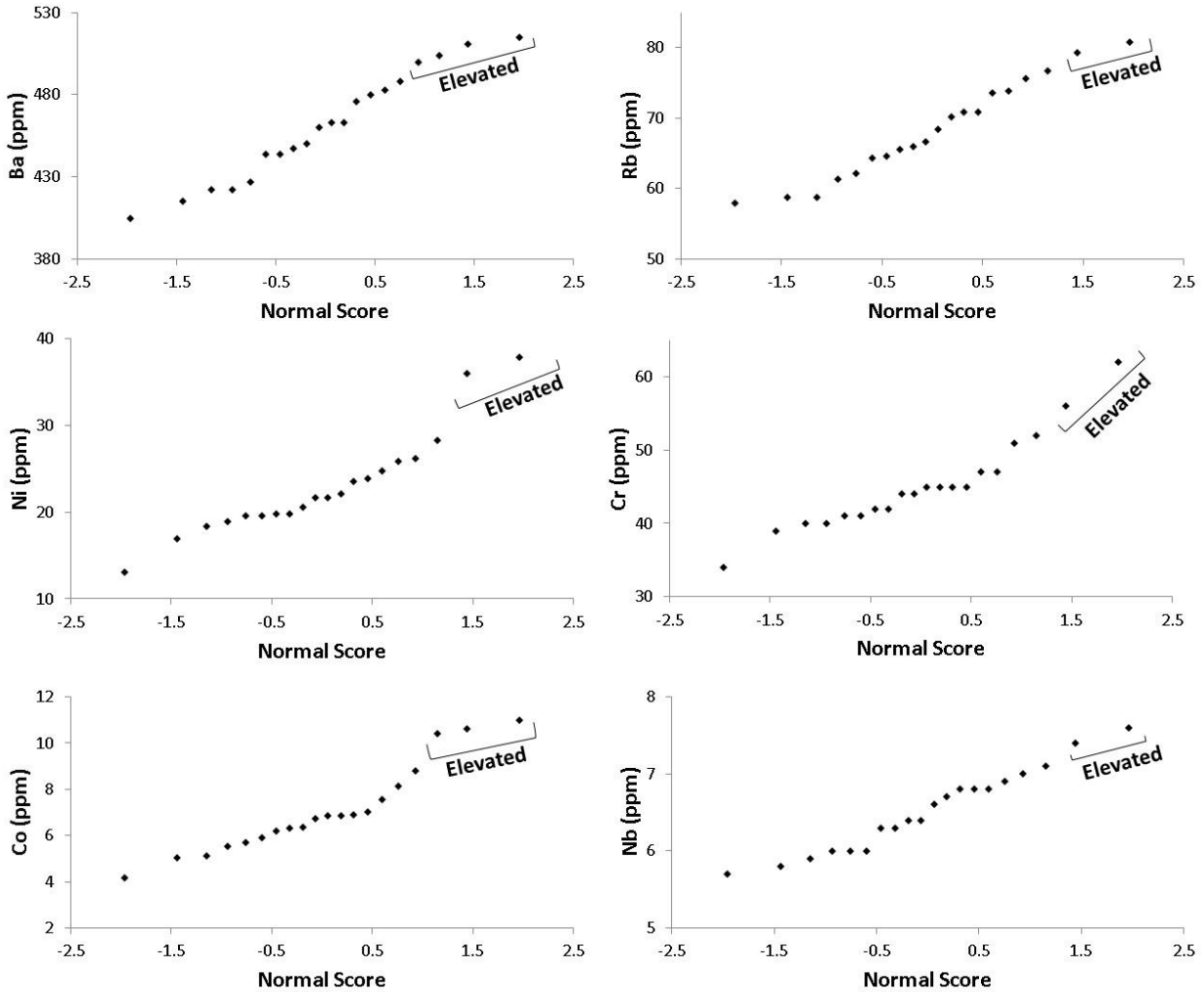


**Figure 2.20:** Q-Q plots used for assessing thresholds and elevated (See sections 1.2.4.1 and 1.5.6) values in pathfinder elements. Ba and Cr used ICP-OES total digestion method, and Rb, Ni, Co, Nb used ICP-MS total digestion method.

## 2.5 Discussion

Ice-flow indicator measurements are used to constrain surface and subsurface dispersal patterns. Surficial dispersal patterns are delineated based on elevated KIM grain counts and multiple lines of evidence, including clast lithology and matrix geochemistry. Subsurface dispersal patterns are delineated based on elevated KIM grain counts. The isolated cluster of KIM grains within the drumlin field (**Fig. 2.14**) persists throughout the till column of the HW dataset and it also exists in the other two independent datasets of surficial till KIM results: the public KIM total grain counts (**Fig. 2.15**), and in the UWaterloo KIM normalized grain counts (**Fig. 2.14**). This isolated region of KIM grains in the drumlin field is located southwest of the closest known kimberlites. The interpretation follows that it represents a palimpsest, detached fragment of a dispersal pattern that was initially formed during the early ice flow phase to the southwest.



The provenance of KIM indicators and KIM pathfinders of the persistent zone of relict till is thus assumed to be the subcropping kimberlite deposit within the study area (**Fig. 2.21**). The detrital particles within that till were mostly entrained during the oldest ice flow event. However, this material was likely re-entrained during subsequent ice flow events, such as the northwest ice flow responsible for creating the drumlin field. The surficial patterns indeed support this interpretation. The surficial patterns within the drumlin field appear to be smeared in the northwest direction and there is also strong surficial dispersal to the NW elsewhere, such as just to the north of the drumlin field. The KIM grains over that northern portion of the study area are part of a longer dispersal train, which is distinguishable in the regional dataset (inset map of **Fig. 2.20**) and is also clearly elongated in the youngest NW ice flow direction.

To verify the hypothesis of a relict till in the drumlin field that was only partially re-entrained by the younger northwest ice flow in its uppermost portion, clast lithology and till matrix geochemistry were also examined. Isolated clusters of elevated granitoid clasts in the till (**Fig. 2.18**) and co-located elevated values in pathfinders related to either granitoid or kimberlite rocks (**Fig. 2.19**) provide supporting evidence that the surficial till within these clusters in the drumlin field is mostly 'relict', i.e., produced during the early southwest ice flow phase (**Fig. 2.21**). It should be noted that granitoid clasts have a higher hardness than the fractured metasediments underlying the drumlin field, and this could have affected the relative proportions of both lithologies. However, it is also clear that metasediments have survived glacial transport as elevated proportions occur outside the identified isolated clusters of elevated granitoid rocks. In addition, the till matrix geochemistry (all 6-elements used were determined to be fit-for-purpose) is also consistent with a greater signal from a granitoid source, which would not be expected if most metasediments would have been comminuted to the finer till matrix fraction. Finally, the closest granitoid outcrops to the southeast, which would be the source direction if particles had been transported only during the youngest NW flow phase, are located at about 11 km. There are three publicly known kimberlites subcrop approximately 20 km to the east southeast (**Fig. 2.15**). In contrast, the possible sources to the northeast for all these indicators and pathfinders are only about 5.5 km away. Altogether, the results suggest the presence of a relict zone of till in the drumlin field that was initially produced by the old southwest ice flow phase, and whose surficial portion was likely re-entrained in the direction of the youngest ice flow to the northwest.

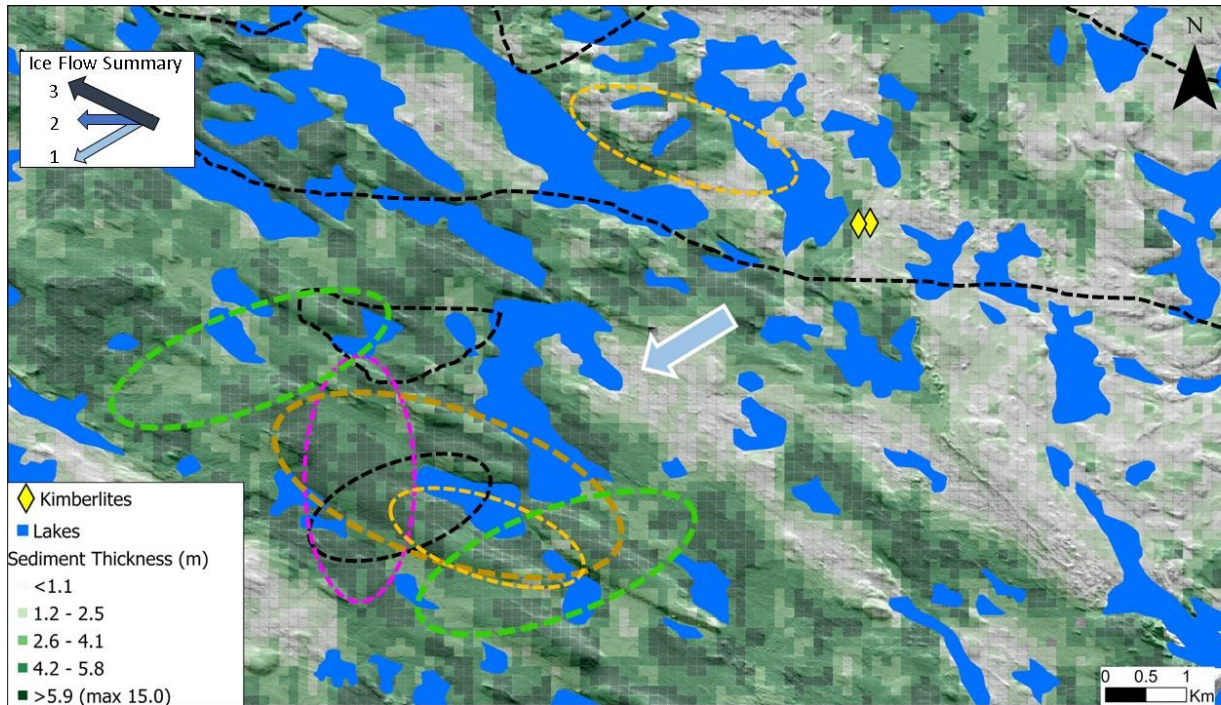


**Figure 2.21:** Interpretation of surficial KIM dispersal patterns, and higher granitoid clast lithology and geochemical pathfinder values superimposed on till thickness model by Kelley et al. (2019b). The black dashed outlines are interpreted from UW and HW KIM grains. The green dashed outlines are interpreted from the public KIM surface dataset. The pink dashed outline is interpreted from the UW and KIM granitoid clast lithology. The brown dashed outline is interpreted from UW Ni, Cr, Co, Nb geochemical results. The orange dashed outlines are interpreted from the Rb and Ba geochemical results. Till was initially transported to the southwest across the study area during the oldest known ice flow phase. The till was then eroded into drumlins and only partially re-entrained to the northwest. Thicker and mostly relict till from the southwest ice flow phase is thus preferentially preserved in the core of drumlins. Elsewhere, northwest entrainment and/or re-entrainment was more important during the younger northwest ice flow phase.

To put this research in the bigger context of the drumlin discussion, evidence points to erosional drumlinization. Other studies have concluded that erosion is an important, or the dominant process in drumlin formation (e.g., Kerr and Eyles, 2007; Eyles et al., 2016; Ely et al., 2018). Specifically, pre-existing sediments that were subsequently drumlinized have been studied for decades (e.g., Menzies 1979; Knight and McCabe, 1997). As for palimpsest drumlins, Stea and Brown, 1989 used whole rock geochemistry for their Nova Scotia study to determine provenance from two ice flow phases, and others (Charbonneau and David, 1993; Klassen and Thompson, 1993; Parent et al., 1996) determined that older dispersal trains containing indicator minerals were reshaped by younger ice flow phases. A recent study by Sookhan et al. (2021) looked at ice streaming and strong overprinting using detailed geomorphological analysis of drumlins. While they were able to establish a relationship between distance of transport of a lithological tracer (quartzite) from its bedrock source and drumlin elongation, the study could not investigate palimpsest trains through the full till column in the drumlin field.

### **2.5.1 Role of Till Thickness Variability on Dispersal Patterns**

The till and the associated dispersal patterns in both 3D and 2D represent the net effect of a complex ice flow history and shifting subglacial processes. The young ice flow events produced new sediment, but also re-entrained older material, which created a hybrid till with an inherited and overprinted composition across the study area. As a result, fragmented palimpsest dispersal patterns have been preserved across the landscape and at depth. These signals can be interpreted by understanding the full regional ice flow history. In some places, relict till mostly occur in the subsurface (e.g., Kelley et al., 2019a) and could thus be missed using only surficial till samples. However, it appears that the erosional processes involved in drumlinization were sufficient to expose the relict till at surface in the study area even though the ‘signal’ of the relict till appears to be stronger at depth.

### **2.5.2 Implications for Drift Prospecting**

Drift prospectors working in erosional drumlin fields should expect high inheritance in the till in areas with complex ice flow movement. Constraining till compositional patterns with regional ice flow indicator measurements and comparing data available from the full thickness of the till column can more efficiently determine the provenance of till material in areas with variable till thickness and reduce difficulties in identifying a buried mineralized source. Younger, stronger ice flow events can reshape landforms and expose older ‘relict’ till at surface, which could be challenging to interpret. Taking subglacial processes into account, developing a good understanding of the full ice flow history, and paying attention to isolated (possibly) detached dispersal trains can help unravel the complexity in drumlinized areas. With the ArcticDEM (Porter et al., 2018) to help identify landforms, reinterpreting legacy datasets could lead to new targets.

Due to the dominant erosional phase of the drumlinization process (e.g. Eyles et al., 2016), older till may become exposed at surface. Isolated surficial dispersal patterns of KIM grains and clast lithology in drumlin fields may thus be related to patches of high inheritance till reflecting dispersal from earlier ice flow phases. These isolated clusters of higher count values could also extend into the subsurface depending on till stratigraphy and thus caution should be taken to interpret these isolated patches as having the same sediment provenance as surrounding surficial till. According to this study, to define more specific targets, older ice flow phases identified through erosional or depositional measurements in the local area can lead to a better understanding of the full ice flow history, which is crucial for a more accurate interpretation of these isolated patches. The oldest erosional evidence can be overprinted or buried by subsequent ice flow events leaving few ice flow indicators available to measure, but this stage of ice flow may contribute to sediment at the base of the till column and can increase the complexity of the interpretation, even of surficial till due to exposed relict or inherited till at the surface. Future work can test for palimpsest dispersal in other till-core drumlin fields.

## 2.6 Conclusions

This study identified a well-preserved but fragmented (isolated) palimpsest train within a drumlin field that persists from the surface and through the full till thickness of the till column. Field observations and satellite imagery of landforms and ice flow indicator measurements, as well as examination of till composition, including multiple datasets containing KIM grain counts, clast lithology and matrix geochemistry, led to the identification of a high inheritance within the thicker till in a drumlin field. Evidence of partial overprinting and till re-entrainment by a younger ice flow is also recognized in the surficial till. The younger ice flow reshaped the landscape and fragmented an older dispersal train recorded in subsurface sediments. Finally, few surficial samples show a clear impact of post-depositional reworking in the proglacial environment (e.g., glacial lake). The surficial till in a drumlin field that is related to the drumlinization could be thin and discontinuous. Erosional processes involved in the drumlin-forming process could expose relict till at the surface. Dispersal patterns in a drumlin field could thus partly reflect an earlier ice flow phase rather than the one that created the drumlins. This has important implications for provenance studies such as the ones applied in drift prospecting, and implications for reinterpreting legacy datasets to discover new targets.

## **CHAPTER 3: Bedrock topographic effects on down-ice three-dimensional sediment dispersal patterns, south of Lac de Gras, Northwest Territories**

### **3.1 Introduction**

Bedrock topography influences subglacial erosion, sediment transport and deposition (e.g., Kelley et al., 2019a), and thus it partly controls till thickness variations. As a result, bedrock topography and till thickness affect the occurrence and shape of compositional dispersal patterns in till. Kelley et al. (2019a) documented some of these bedrock and till thickness effects on till dispersal patterns down ice of known kimberlites in the Lac de Gras area. They determined that bedrock topography influenced dispersal at the surface while contributing to preservation of dispersal patterns at depth from older ice flow events. However, questions remain about the effect of bedrock and till thickness on dispersal trains in different geologic settings. For instance, since kimberlites generally weather at surface, they tend to form depressions surrounded by more competent, and thus more elevated host rocks. However, there are cases where kimberlites and other soft intrusive bodies (e.g., carbonatites), while still forming depressions in the bedrock surface, are also nested within more elevated resistant rock knobs relative to surrounding softer rocks. In these cases, the intrusive body, despite siting in a depression within the rock knob, intersect the bedrock surface at a higher elevation than the average elevation of the widespread soft rocks surrounding the topographic high. There is some evidence that dispersal trains could still be produced from these more elevated nested source rocks, but documented examples are characterized by relatively wider and less topographically isolated source rocks than typical kimberlites of the Lac de Gras region. A good example are the large carbonatite bodies nested within inliers of Canadian Shield rocks forming a few hills in the lower Laurentians of southern Quebec, from which fan-shaped dispersal trains of rare earth elements have been documented (Ross, 2004; Ross et al., 2006). It is, however, unclear whether smaller and more isolated kimberlites nested within a hard rock knob would have generated a dispersal train in a down-ice direction.

In addition to the above problem, bedrock hills also have other effects on subglacial processes and glacial sediment deposition. For instance, thicker glacial sediment commonly occurs immediately down-ice of a rock knob forming what is referred to as ‘crag-and-tail’ landforms. The tail is thought to have escaped glacial erosion from the ice flow phase aligned parallel to the tail long axis. The formation of crag-and-tails has been attributed to pressure shadows resulting from warm-based and possibly faster-flowing ice (Evans and Hansom, 1996) wrapping around the resistant ‘crag’, but not enough to fully remove the sediments in the down-ice (lee-side) of the obstacle; the tail of sediment on the lee-side is sometimes just streamlined by the flow. In this case, pre-existing sediment down-ice of a rock knob were largely shielded from glacial erosion and were thus mostly preserved, whereas most of that pre-existing material was removed elsewhere around the obstacle during the ice flow phase. Boulton (1982) also described depositional processes whereby debris and debris-rich ice fall into subglacial cavities that sometimes form down-ice of bedrock hills (e.g., Iverson, 1991, Evans et al., 2006). These two mechanisms are used to explain most situations where glacial sediments end-up being thicker

immediately down-ice of a rock knob. However, the two cases have different implications for till provenance and dispersal patterns. For the crag-and-tail situation, the lee-side till could have been produced and deposited during an older ice flow phase that was flowing in a different direction than the younger phase that formed the crag-and-tail landform. Therefore, provenance of indicator minerals in that till would be from a different source region than up the ice flow direction indicated by the crag-and-tail. In a nearby study, Kelley et al. (2019a) used slope aspect of a bedrock surface and till thickness and compositional data from drilling to reveal preferential preservation at depth of till in a crag-and-tail. This till was correlated to an older ice flow phase, which would have brought material from a kimberlite located up the older ice flow direction, which was oblique relative to the ice flow phase that had produced the final shape of the crag-and-tail. In addition, another kimberlite located just on the opposite side of the tail, thus up the younger ice flow, did not produce a clear dispersal pattern at surface during the younger ice flow phase, probably due to the kimberlite being quite deep and with a steep adverse slope from the rock knob just in front of it. A different dispersal pattern would have been expected if the till on the lee-side of the rock knob consisted of lee-side cavity till produced during the younger ice flow phase. In this case, the kimberlite indicator minerals (KIM) would not be expected to occur only at depth in the tail. There are also questions about the potential role of subglacial meltwater on the reworking of kimberlite indicators around these hills.

In summary, while progress has been made in our understanding of the effect of rock knobs on till preservation and glacial sediment dispersal patterns, much remain to be learned about dispersal trains from elevated sources nested in rock knobs, as well as on the preservation of palimpsest trains in till at depth on the lee-side of crag-and-tail landforms. In this Chapter, I investigate the problems described above to improve knowledge on bedrock topography effects and subglacial processes on till thickness and dispersal trains by investigating till composition in an area characterized by a kimberlite nested within a rock knob surrounded by relatively softer bedrock and thicker till. The area also experienced multiple ice flow phases similar to what is documented in the nearby study by Kelley et al. (2019a).

The specific objectives of this chapter are twofold: 1- document glacial sediment dispersion from an isolated kimberlite nested in a rock knob to improve our understanding of this particular setting, and 2- analyze till dispersion at depth down the younger ice flow direction from the rock knob to understand the effect of possible crag-and-tail and/or lee-side cavity fills. This is done by mapping 3D dispersion patterns of indicator minerals, lithological and geochemical pathfinders, and landforms.

### **3.2 Study Area**

Northeast of Yellowknife, NT, the Lac de Gras region was overlain by the Keewatin Sector of the Laurentide Ice Sheet (Dyke and Prest, 1987). The highly prospective diamond Lac de Gras kimberlite field, hosted by the Archean central Slave craton, has been heavily explored for diamond bearing kimberlites using drift prospecting (Fipke et al., 1995). Drift prospecting has



been highly successful in narrowing down targets in this area, leading to 4 diamond mines that contributed billions of dollars to the local and federal economy. As these mines are nearing their end of life and discovering the next viable target in this area becomes increasingly urgent, their legacy datasets can be reinterpreted using new knowledge about areas with complex settings. The large HWRC dataset containing results from exploration programs was donated for further study. One area (**Fig. 3.1**) was found to be particularly promising to investigate the problem stated above. The area of approximately 135 km<sup>2</sup> is characterized by variable bedrock topography and till thickness, and a known kimberlite is nested in a large rock knob surrounding lower terrain. The area was thus selected for the study.



**Figure 3.1:** Approximately 300 km NE of Yellowknife, Ekati mine developed in late 1990s, Diavik mine in early 2000s; Snap Lake mine developed over mid-2000s, and Gahcho Kué mine developed over mid-2010s (Google Earth Images). The west study area is outlined in dashed white box.

The bedrock map (Kjarsgaard et al., 2002) and the ArcticDEM (Porter et al., 2018) highlight granitoid rocks forming a topographic high as the predominant feature in the study area (**Fig. 3.2**). A kimberlite, known as Big Blue (De Beers, 2010), is perched on - and nested within - a granitoid knob perched on the topographic high from the Archean Syn-Yellowknife Supergroup (ca. 2650-2605 Ma). A topographic step at the western edge of the bedrock topographic high marks a transition to Archean Yellowknife Supergroup metasediments from the Itchen Formation, containing either biotite schists or cordierite +/- andalusite porphyroblastic schists (ca 2637, +8 -7 Ma) referred to as metasediments in this study.

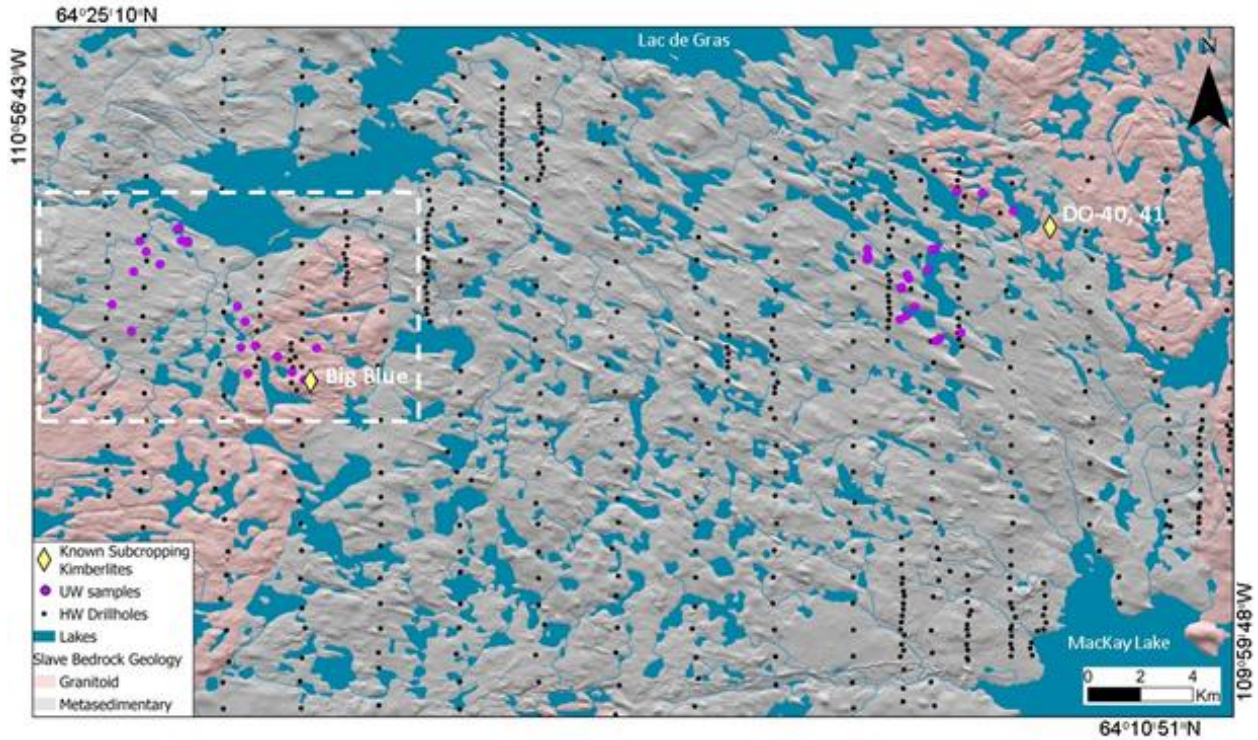


**Figure 3.2:** Bedrock geology (Kjarsgaard et al., 2002) map highlights major lithologies overlain on ArcticDEM (Porter et al., 2018) with dashed outline of study area. Samples collected for this thesis work are purple points, while the donated dataset are black points.

Bedrock topography varies up to 35 meters correlated with resistant granitoid, the predominant feature in the area, and a bedrock knob rising 4 meters above the nested kimberlite underlying a small lake (**Fig. 3.3**). This topographic high steps down to softer metasedimentary bedrock, covered by thicker till deposits. Elsewhere, till thickness is patchy with variable drumlinization throughout the study area. In addition, glaciofluvial landforms cover the landscape, including a meltwater corridor down-ice of the bedrock topographic high (**Fig. 3.4**). The corridor contains boulders perched on top of pebbles on outcrop, continuous and truncated eskers formed in the subglacial environment, and kames and mounds formed in the supraglacial environment. For a broader surficial geology context, see section 1.3.2.





**Figure 3.3:** Panorama of granitoid knob with Big Blue Kimberlite nested in a bowl-shaped depression (under the lake), looking in the up-ice direction towards the knob.



**Figure 3.4:** Panorama of meltwater corridor with kames, looking westward.

There is evidence the region experienced different ice flow phases, which appear to have deposited at least two till sheets (Kelley et al., 2019a; Janzen 2020), although uncertainties about the stratigraphy persist. Given the proximity to these other studies, it is assumed the area was affected by the same ice flow phase sequence (clockwise shift from SW to NW), with possible corresponding till stratigraphy preserved locally.

### **3.3 Methodology**

The surficial geology down-ice of the Big Blue kimberlite is complex. Nonetheless, a better understanding of the surficial landscape can be determined by traversing the landscape, ground-truthing regional data, collecting local ice-flow indicators and samples, and by carefully analyzing all available datasets. A field work program including a foot traverse was therefore planned across the local study area. The main landforms were visited, described, and photographed. In addition, a small number of till samples were also collected. Surficial sampling was limited due to the remoteness of the site and the fact that samples had to be carried on foot. Nonetheless, this small sampling program was useful to get new data about surficial till properties and composition. The main datasets used in this study were the large HWRC dataset, as well as the ArcticDEM and the regional surficial maps. The following sub-sections present these different methods and datasets as they were used in this specific study area. More details can be found in Chapter 1 (see Section 1.5).

#### **3.3.1 Field Work**

Fieldwork included measuring outcrop-scale ice flow erosional indicators, and sampling till and glaciofluvial sediment. Twenty-two ice flow indicators were collected at ten different sites from exposed bedrock and included stoss-lee relationships from glacially sculpted bedrock outcrops, striations (including nailhead striations) on bedrock abraded surfaces, as well as grooves, pressure cracks or chattermarks, and crescentic scour marks. Measured ice flow directions were mainly obtained from striations and grooves. For sampling, it was critical to be aware of the landforms being sampled and to describe sediment facies to aid in a more accurate interpretation of the results, since the study area contained ‘primary’ subglacial till, washed till, and glaciofluvial material. Glaciofluvial sediments are transported and deposited by completely different mechanisms than till; it is thus important to group samples by sediment type before analyzing and interpreting results (McClenaghan and Paulen, 2018). Evidence of glaciolacustrine processes were observed in flat top eskers, wave washed landforms, such as drumlins, and at times in sediment dug from pits.

A total of 16 samples (14 till and 2 glaciofluvial), weighing an average of 2.7 kg, were collected in the field during this study. In addition, six larger samples (1 till and 5 glaciofluvial) weighing an average 12.1 kg were also collected for KIM counts. Sample sites avoided ground squirrel

habitat as much as possible to avoid reworking and sampling a thicker profile, and possibly slightly sorted sediment, than at other undisturbed sites. Some samples were collected from frost boils after careful scraping away of organic contaminants. Cobble sized clasts were removed from sample material, since they would not be used in geochemistry or texture studies. Samples taken from glaciofluvial kame-type landforms were collected downslope from the top of the feature. The smaller samples (n=16) were sent first to the University of Waterloo Quaternary Geology lab for preparation and texture analysis, and a 50-gram aliquot of the silt and clay fraction was sent later to Saskatchewan Research Council, while the larger KIM samples (n=6) were sent directly to Saskatchewan Research Council to be visually picked and probe confirmed for pyrope, chromium-diopside, olivine, chromite, and picroilmenite.

### **3.3.2 Sediment and Geochemical Analysis**

The 16 glacial sediment samples were processed for texture at the UW Quaternary Geology lab using a series of sieves and particle laser diffractometer (See sections 1.5.4, 1.5.5), while an aliquot of the clay and silt fractions were sent for ICP-MS (package 2) geochemical testing at the Saskatchewan Research Council (See section 1.5.5, 1.5.6.1 for details). Fractions 4-8mm and >8mm were classified at the UW Quaternary lab for clast lithology (see Section 1.5.5.1 for details).

### **3.3.3 HW Dataset**

The study area encompasses 73 “boreholes” from the HW dataset (n= 757) which are described in the borehole log as till. Boreholes contained up to 11 samples per hole, for a total of 355 samples used in this study (See section 2.3.3). Although each sample was processed in three fractions, namely 0.25-0.5 mm, 0.5-1.0 mm, 1.0-2.0 mm, best practices from McClenaghan et al. (2013) recommends using results 1.0 mm and under, and so the dataset was prepared using the 0.25-0.5 mm and 0.5-1.0 mm fractions (See section 1.5.8.1) to be consistent with best practices and methods used by Saskatchewan Research Council. HW samples were visually picked for a combined 33 minerals of clinopyroxene, chromite, garnet, olivine, orthopyroxene, perovskite, picroilmenite, and spinel, then probe confirmed by C.F. Minerals. Indicator minerals were selected to be consistent with Saskatchewan Research Council results containing data on pyrope, chromium-diopside, olivine, chromite, and picroilmenite. To compare KIM grains between samples, all KIM grain counts were normalized to 10 kg samples, with each bulk weight sample weighing an average 17 kg, to be consistent with the available UW sample weights used to normalize those indicator mineral counts. In addition to indicator mineral grains, the dataset also contains major clast lithology percentages from each sample, which were also categorized into borehole depth intervals (See section 1.5.8.1). Borehole logs also recorded bedrock type, depth to bedrock, and bulk sample weight (See **Fig. 1.14**).

### 3.3.4 Data Analysis and Mapping

The large HWRC dataset obtained from NTGS is assumed to have been validated and checked for quality by industry geoscientists, before the data was provided in MS Excel format for this study. UW geochemical data is tested for precision and error using duplicates and standard reference material. Duplicate scatterplots and follow-up Thompson-Howarth Short Method results are precise to 10% confidence interval, following Piercey (2014). The average coefficient of variation for the six elements used in this study are under 3.5, within the best practice and acceptable values suggested by Abzalov (2008). Although relative percent difference calculations for the 1179 Till-3 reference material determined there is either a bias or results are not accurate for Ni and Nb, the DCB01 standard reference material have very good accuracy for Nb and excellent accuracy for Ni (See Appendix G). These metals are important geochemical pathfinders, and are determined to be precise using scatterplot and Thompson-Howarth methods in duplicate and repeat results (See section 1.5.6.2 and 2.3.4). Due to low analytical values, Nb is precise to the detection limit (-11%) and still fit-for-purpose. Nickel values are over-valued at 20%, though since values are low and the relative percent difference does not significantly change the values, the data is still fit-for-purpose, but used with caution. Therefore, Ni and Nb percentiles are calculated from the results and presented in this study with Co and Cr.

MS Excel spreadsheets were used to organize and prepare data from the HW dataset at depth and UW samples collected from surface for this study. Three-dimensional data presented in 2-D space necessitated eliminating depth bias via dividing boreholes into 4 intervals based on depth of hole (See section 1.5.8.1). These data were imported into Esri software (ArcGIS Pro version 2.6) to map all results. The indicator mineral data was used to analyze dispersal from known kimberlites, whereas clast lithology counts and geochemical data provide information about other bedrock sources from the region. Provenance of all this material is constrained by the ice flow history from ice flow indicator measurements taken from the field and publicly available data from Ward et al. (1997). The bedrock map compilation by Kjarsgaard et al. (2002) were compared to bedrock data in the HW dataset. A sediment thickness map was compiled by Kelley et al. (2019b) using this HW dataset. ArcGIS was used to spatially examine data to identify trends and patterns.

## 3.4 Results and Interpretations

### 3.4.1 Field-based Ice Flow Indicators and Landscape Characteristics

Ten locations provided new ice-flow indicators, which consist of 22 striation and groove measurements (**Fig. 3.5**). Additional indicators include pressure cracks and crescentic gouges. Ice-flow indicator measurements from striations were plotted on a rose diagram for a visual representation of the local ice flow phases (**Fig. 3.6**). These measurements are consistent with ice-flow indicator measurements available from the GSC (Ward et al., 1997). In addition, one



location recorded cross-cutting striations which established relative age relationship between an older and younger ice flows (**Fig. 3.7**). The oldest ice flow was to the southwest, followed by a clockwise shift to the west and then northwest. The old striations were preserved on the abraded surface at those sites presumably because they are incised deeper into the rock, whereas the younger ones are shallower and seemed to have only partially abraded and eroded the surface, not obliterating the pre-existing ice flow indicators (**Fig. 3.7**).

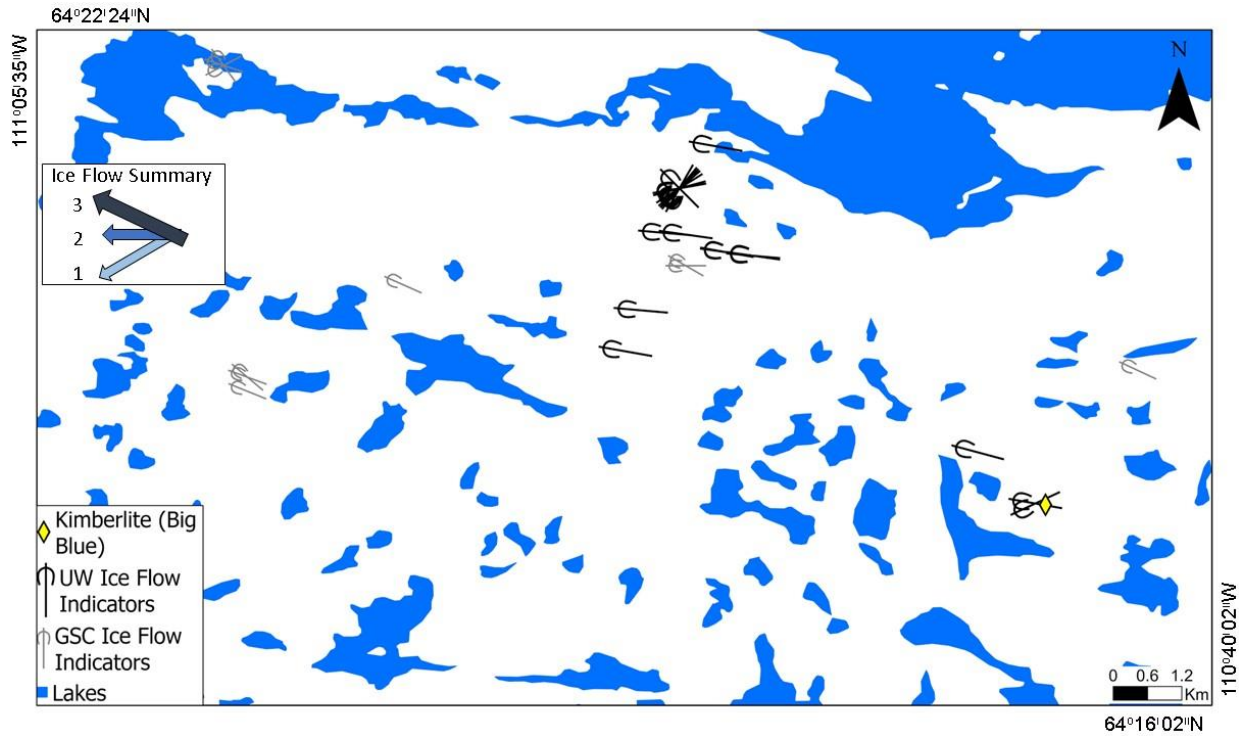


**Figure 3.5:** Twenty-two ice flow indicator measurements taken at ten locations are consistent with regional GSC measurements from Ward et al. (1997) indicating a clockwise shift in ice flow from southwest to northwest. Ice flow summary provided as inset in results maps.

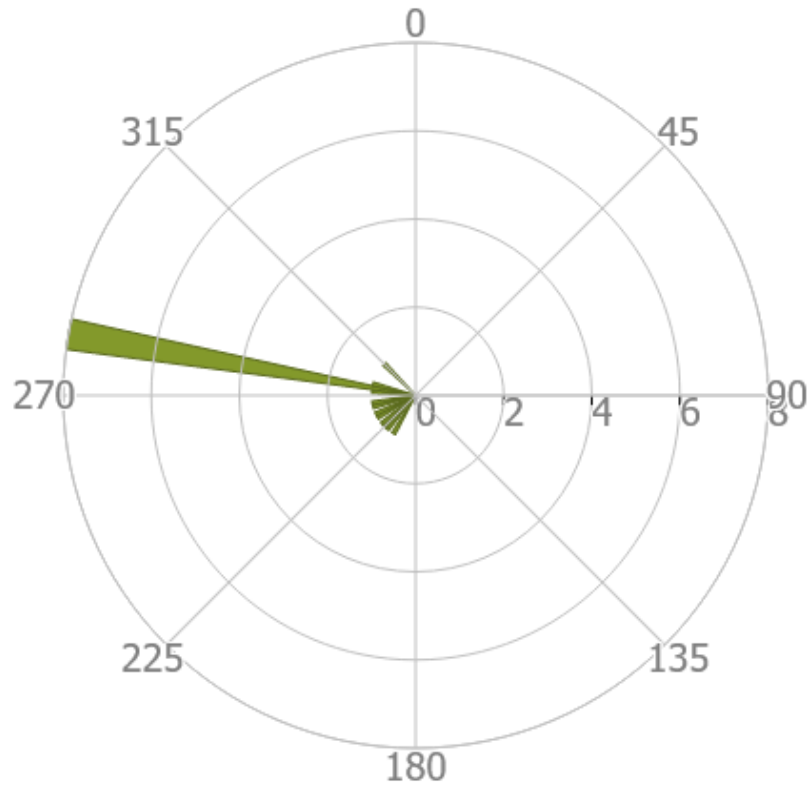


**Figure 3.6:** Rose diagram displaying ice flow indicator measurements collected for this study. N=22



**Figure 3.7:** Striation cross cutting relationships on a metasedimentary outcrop located on the west side of the study area. Oldest flow (1) = 253°, intermediate flow (2) = 269°, and youngest flow (3) = 324°. Note that although this specific outcrop could be in a possible area of deflection during the youngest flow, the cross-cutting relationships are well represented.

The Big Blue kimberlite is nested within a granitoid knob, at least 4 meters in elevation above the lake level, on the granitoid topographic high (approximately 35 meters above the surrounding terrain). The HW data indicate till thickness on the local rock knob ranges from 0 to 0.2 meters. Till is also thicker, averaging about 3.3 meters, immediately to the NW side of the knob (n=5) in the direction of the youngest ice flow phase in the study area. Till is thickest at the base of the topographic step, with boreholes penetrating 7.5 meters to 16.4 meters deep. As seen in **Fig. 3.8**, the till surface is also variably drumlinized, aligned with the young ice flow direction (to the NW).



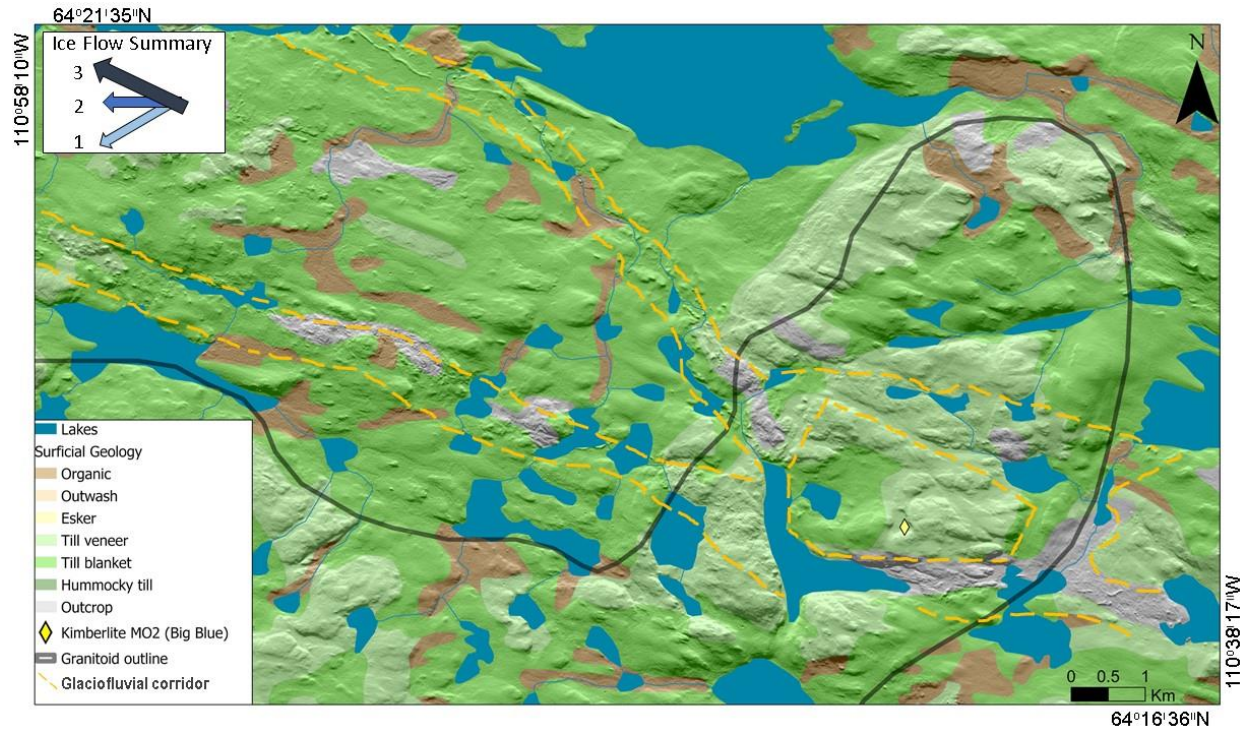


**Figure 3.8:** Large topographic high consisting of granitoid bedrock. The Big Blue kimberlite is nested within a depression within a local bedrock knob on the topographic high. Glaciofluvial corridors are outlined in orange dash marks. In addition, small channels cut across the local rock knob surrounding Big Blue. Note the absence of the pond covering the Big Blue kimberlite in study area maps, because it is relatively too small to map. Surficial geology polygons from Ward et al. (1997).

Additionally, a meltwater corridor split into two distinct channels around the bedrock topographic high extending towards the northwest (**Fig. 3.8**). One glaciofluvial corridor continued west northwest and contains abundant kames of various shapes and sizes, truncated eskers and perched boulders (**Fig. 3.9A, B**), whereas the second corridor extends north northwest and contains a more continuous esker (**Fig. 3.9C, D**).

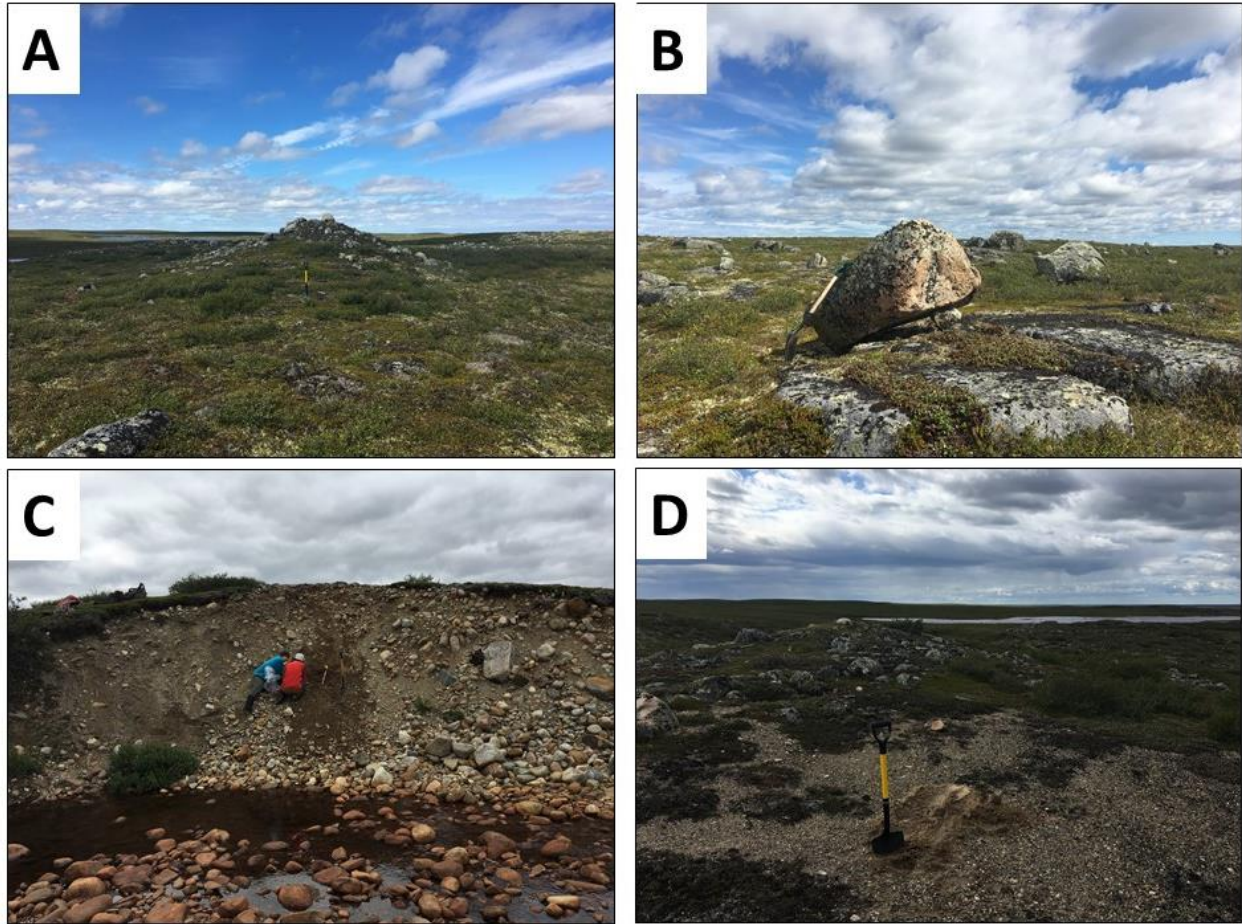


**Figure 3.9:** A) Kame within a glaciofluvial corridor covered with cobbles and small boulders. B) Perched boulders in meltwater corridor. C) Cross-section of esker within meltwater corridor crosscut by creek. D) Discontinuous esker within glaciofluvial channel, possibly washed by glaciolacustrine processes.

Glaciolacustrine wave wash evidence is seen intermittently across this study area, including truncated eskers, scarped drumlin flanks, and oxidized sediment and or washed fines exposed in hand dug sample pits (e.g., **Fig. 3.12D**). It is possible the finest sediments were transported and redeposited in present day Lac de Gras. Glaciolacustrine processes are out of the scope of this thesis, but are still important to note, as the effects on sedimentological and landform characteristics in the study area cannot be ignored.

### 3.4.2 Kimberlite Indicator Minerals

Borehole intervals were divided into quarters based on depth of hole (see Sections 1.5.8.1) and normalized to 10 kilograms. Single-sample boreholes (typically in shallow till less than 1 meter thick) are represented only in the top depth interval, two-sample boreholes are represented in the top and base depth interval, and three-sample boreholes are represented at the base, upper-mid

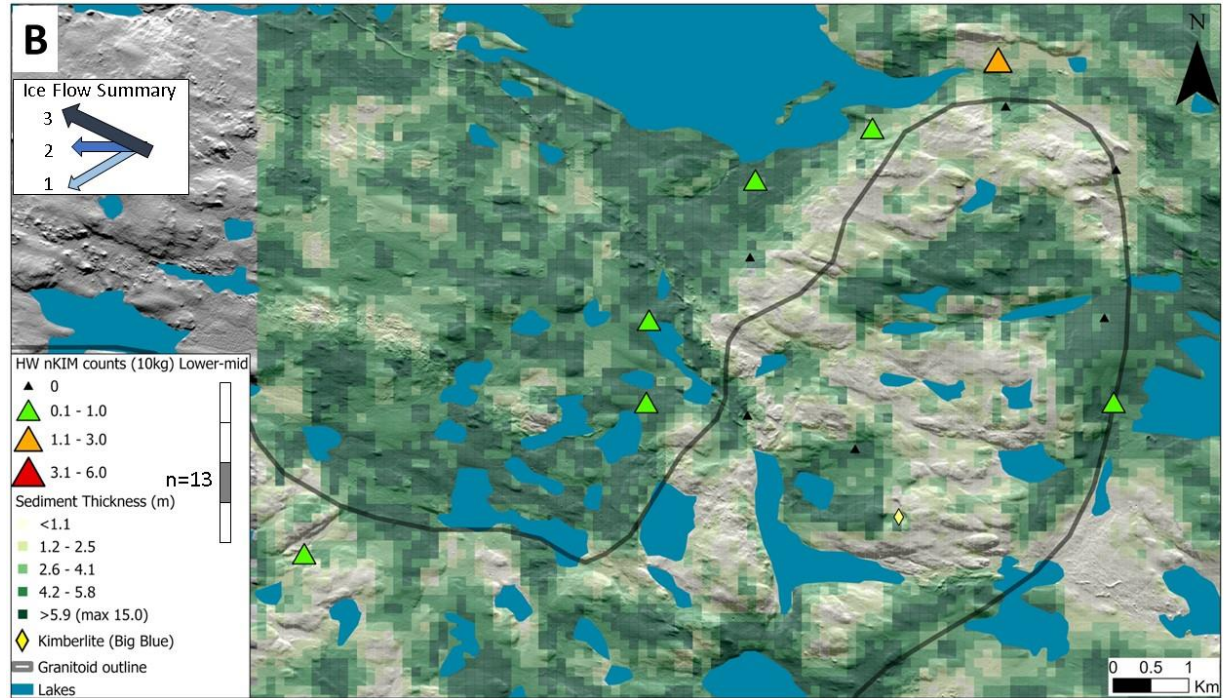
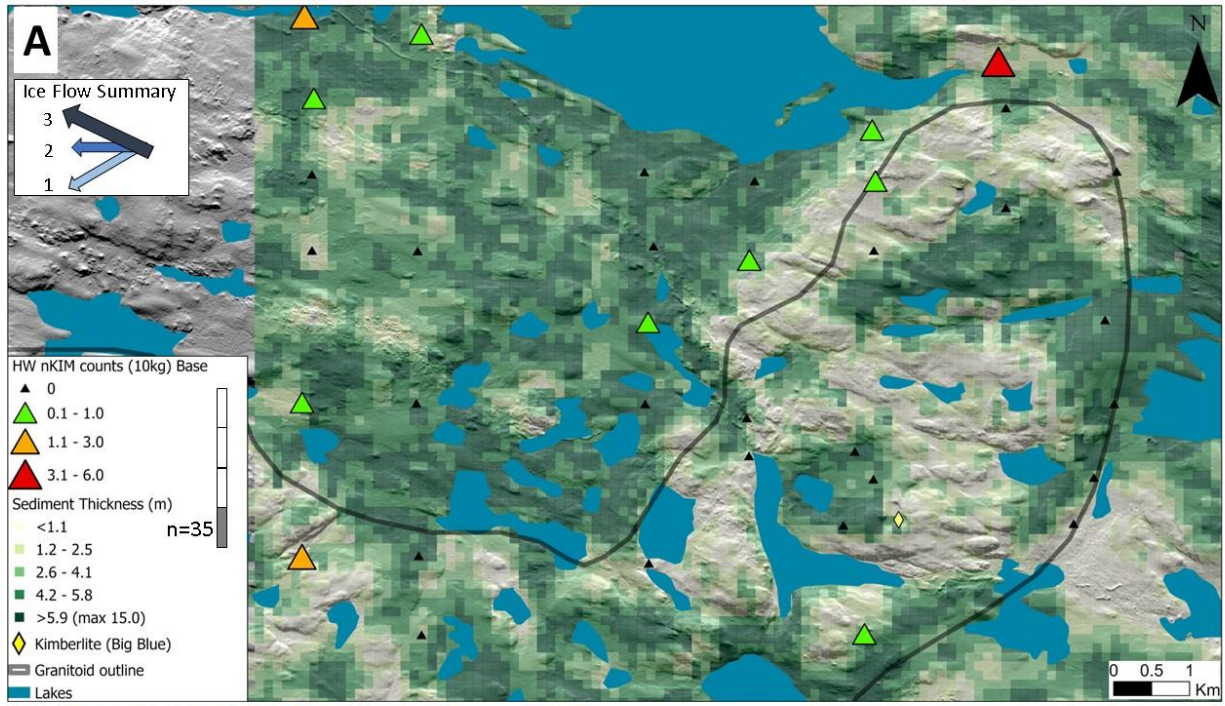
and surface depth intervals. The deepest boreholes could contain as many as two to three samples per depth interval.

At the base of the boreholes (**Fig. 3.10A**, first depth interval adjacent bedrock), there are a few scattered indicator mineral grains. Moving up the borehole (**Fig. 3.10B, C**) a pattern of buried indicators aligns with the base of the topographic step. However, at the surface (**Fig. 3.10D**, uppermost or last borehole depth interval), there are no indicator mineral grains and there is no defined dispersal train down-ice of the Big Blue kimberlite. However, there is a cluster of indicator mineral grain counts on the granitoid bedrock located north of the kimberlite, which are not sourced from the Big Blue kimberlite according to the known ice flow history. This cluster of indicator mineral grains is from the top depth interval of HW samples collected 0.5-2.8 meters from surface.

To the immediate northwest of the kimberlite, in the down ice of the youngest flow phase, a thicker layer of till (2.0-7.5m) has no indicator mineral grains at depth and contains less than 1 mineral grain in normalized samples within the top depth interval. The sample containing the highest amount of indicator mineral grains in the study area (5.6 grains/10kg) was collected from the surface to a depth of 0.75 meters approximately 6.3 kilometers to the southwest of the kimberlite (**Fig. 3.10D**). Relatively high counts were also obtained from another HW drillhole located approximately 1 km south of Big Blue; outside the predicted envelope of a Big Blue dispersal train (**Fig. 3.10D**).

Most of the boreholes with relatively higher indicator mineral grain counts at depth were drilled deeper than the other boreholes without indicator mineral grain counts. Material at the base of the topographic step, the deepest boreholes in the study area (7.5-16.4 m) could be derived from a distal kimberlitic source, due to low indicator mineral counts (0.3 to 3.9 grains/10kg) and therefore could be part of a distal tail end of a dispersal train sourced from the older ice flow direction to the NE.







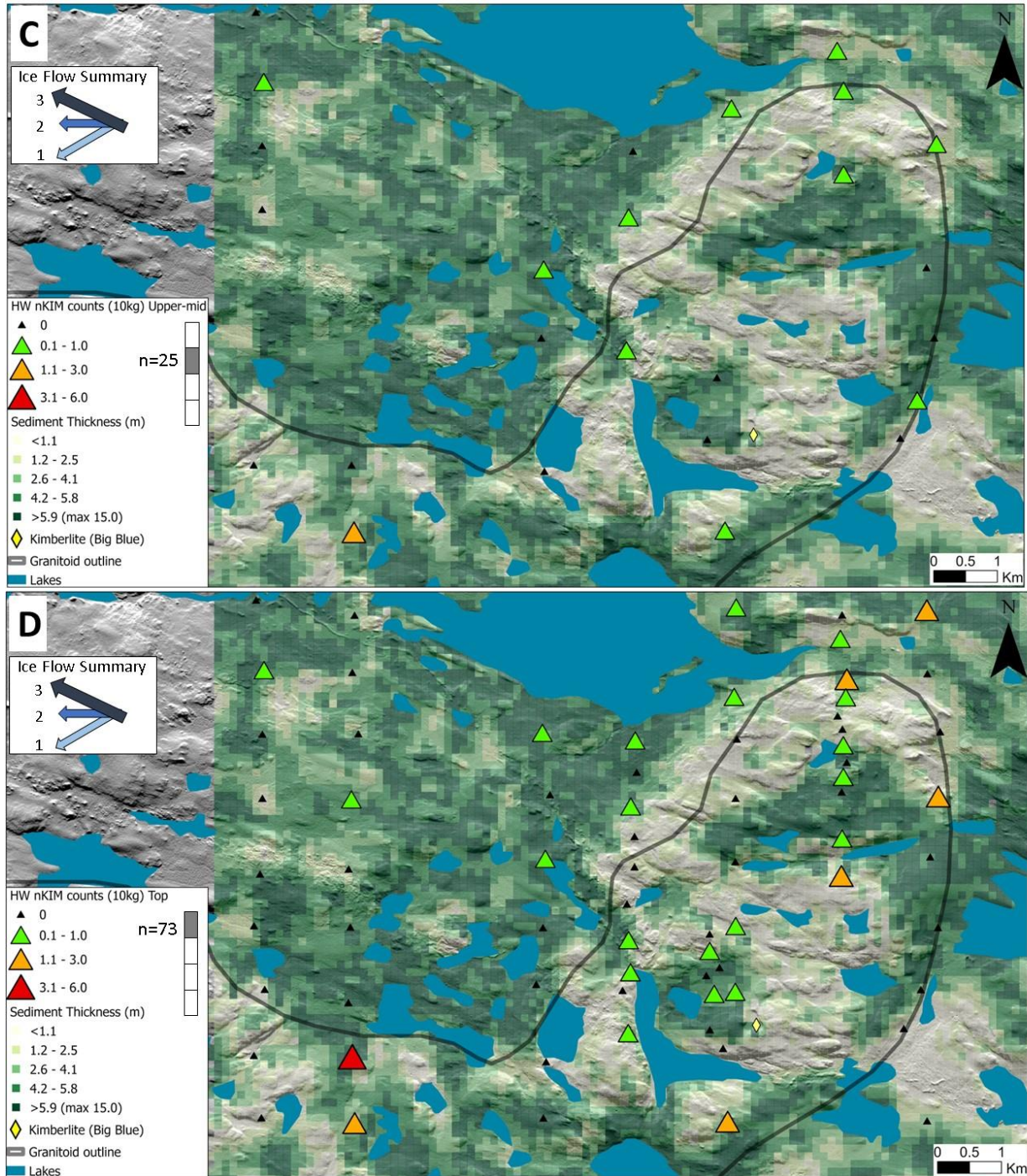


**Figure 3.10:** Normalized KIM counts from the HW till samples displayed as intervals classified into borehole depth intervals superimposed on sediment thickness map (Kelley et al., 2019b). On previous page: A) base, B) lower-mid. On this page: C) upper-mid, and D) top (surface). A pattern of indicator minerals along base of topographic high persists through the till column.



Glaciofluvial KIM samples in the UW dataset contained relatively higher normalized indicator mineral counts (average 4.0 grains/10kg, n=3) compared to the one till KIM sample collected (2.6 grains/10kg) (**Fig. 3.11**). These KIMs in the glaciofluvial corridor are interpreted to be mostly derived from the erosion of the till because the corridors are erosional along their entire path and seem to go around Big Blue. The higher counts are expected because most KIMs are resistant minerals that can survive both intense meltwater transport and post-glacial oxidizing conditions, which leads to an enrichment relative to many other, more labile heavy minerals. In the HW dataset, samples collected within the glaciofluvial corridors were described in the borehole logs as till, and so there are no separate glaciofluvial results. HW till results collected in the glaciofluvial corridor are all below 1.0 grains/10kg, except for one sample in the base depth interval collected near the edge of Lac de Gras (1.8 grains/10kg) (**Fig. 11A**).

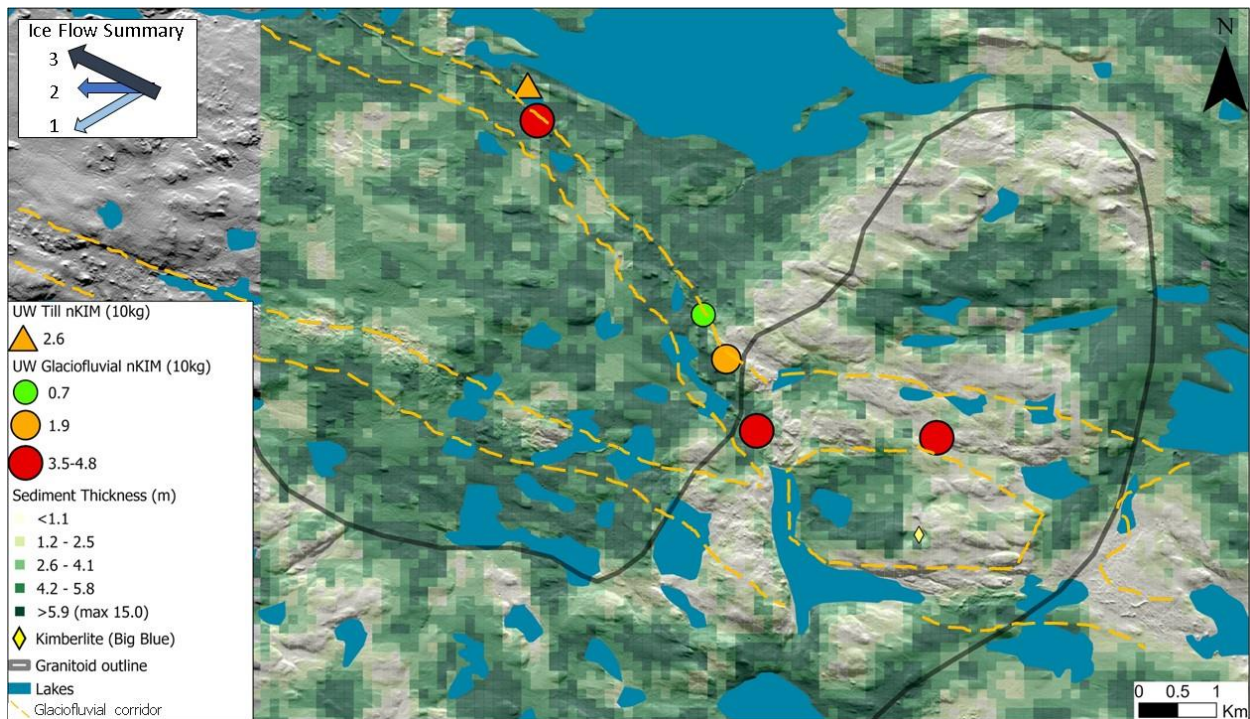


**Figure 3.11:** Normalized KIM counts for UW samples collected at surface for this study. They include one till sample (orange triangle) and five glaciofluvial samples (circles). Glaciofluvial corridor outlined in yellow.

### 3.4.3 Sample Texture, Clast Lithology, and Geochemistry

Samples collected from frost boils (**Fig. 3.12A, B, C**) were taken centimetres from the surface, yet convection within frost boils are thought to churn till from within the till column through the active layer, which is at least about a meter thick in the study area. Overall, the general sedimentological characteristics of the till down-ice of the bedrock topographic high appear to be relatively similar at all sampling sites (**Fig. 3.13**). The till in the study area has a sandy pebble texture occasionally with finer grained sand. Cobbles and boulders are predominately rounded to subrounded and consisting mostly of felsic igneous rocks. Boulders are often perched on finer sediment or bedrock within 1-5 meters distance of the sample pit. Glaciofluvial samples (**Fig.**



3.12D) were mainly coarse sandy material collected from eskers, truncated eskers, or down slope from the top of kame/hummock features.

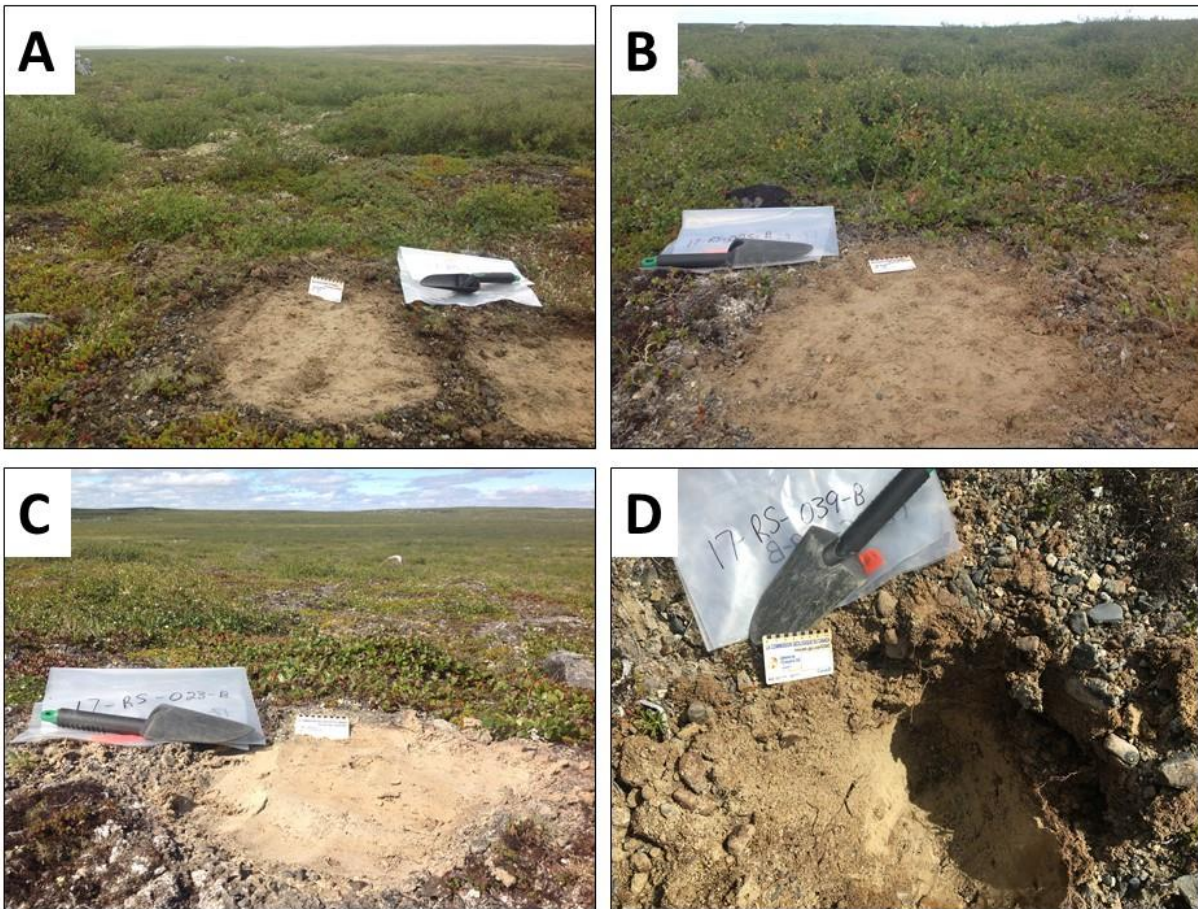


**Figure 3.12:** Examples of till sample sites collected for geochemical, lithological, and textural analysis. A) Oxidized and unoxidized till zones at sample site 17-RS-030-B. B) Sample site 17-RS-025-B was collected immediately up-ice of Big Blue from a frost boil. C) 17-RS-023-B was collected down-ice of the kimberlite (in a zone of thicker till) and contained finer grained sand, few pebbles, and few large cobbles. D) 17-RS-039-B was collected near the confluence of two meltwater channels to the west northwest of the Big Blue. Nearby is a boulder balanced on washed out till perched on cobbles. Despite the proximity to the meltwater channels, this sample was collected from a till mound, containing unoxidized fine-sandy pebble till with cobbles and small boulders.

Till and glaciofluvial material were examined independently but are occasionally presented on the same map or figure with symbology to distinguish between the two. Texture across till and glaciofluvial samples were rather consistent, with some overlap (**Fig. 3.13**). One till sample collected from the flank of a wave washed drumlinoid form contained significantly more clasts over 8mm in diameter and less silt material than samples in this study area (**Fig. 3.13**). The glaciofluvial sample with significantly less fine material than other samples was collected in the glaciofluvial corridor immediately down ice of the bedrock topographic high. On average, samples contain one third fine sand (0.125-0.25mm) material by weight.

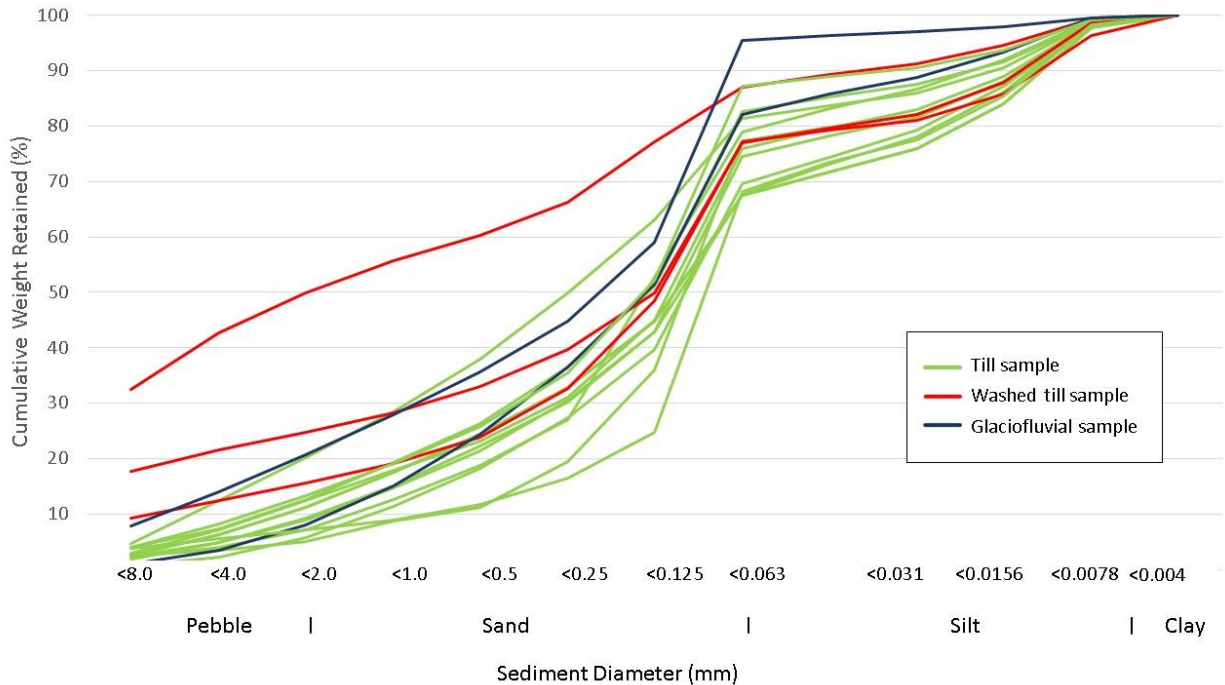


**Figure 3.13:** Curves in blue represent glaciofluvial sediment sample texture, curves in green represent till sample texture, and curves in red are washed till. The outlying sample with the highest coarse-grained material came from a sample site that was collected from the side of a drumlin that appeared wave washed.

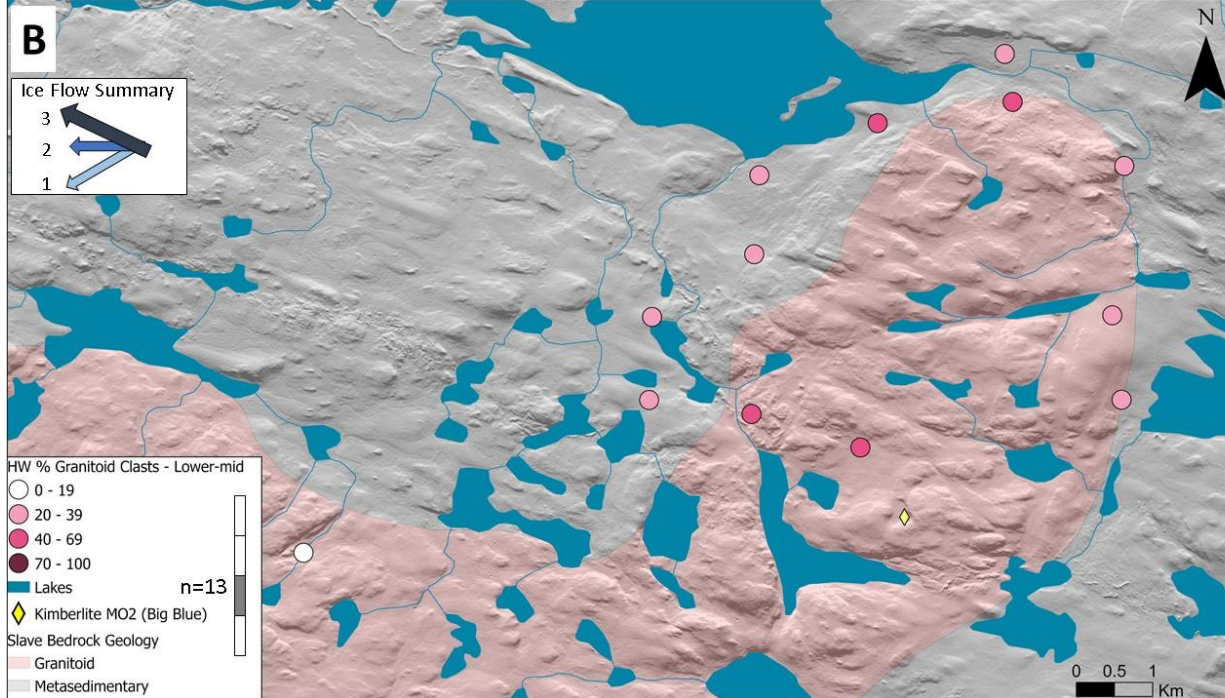
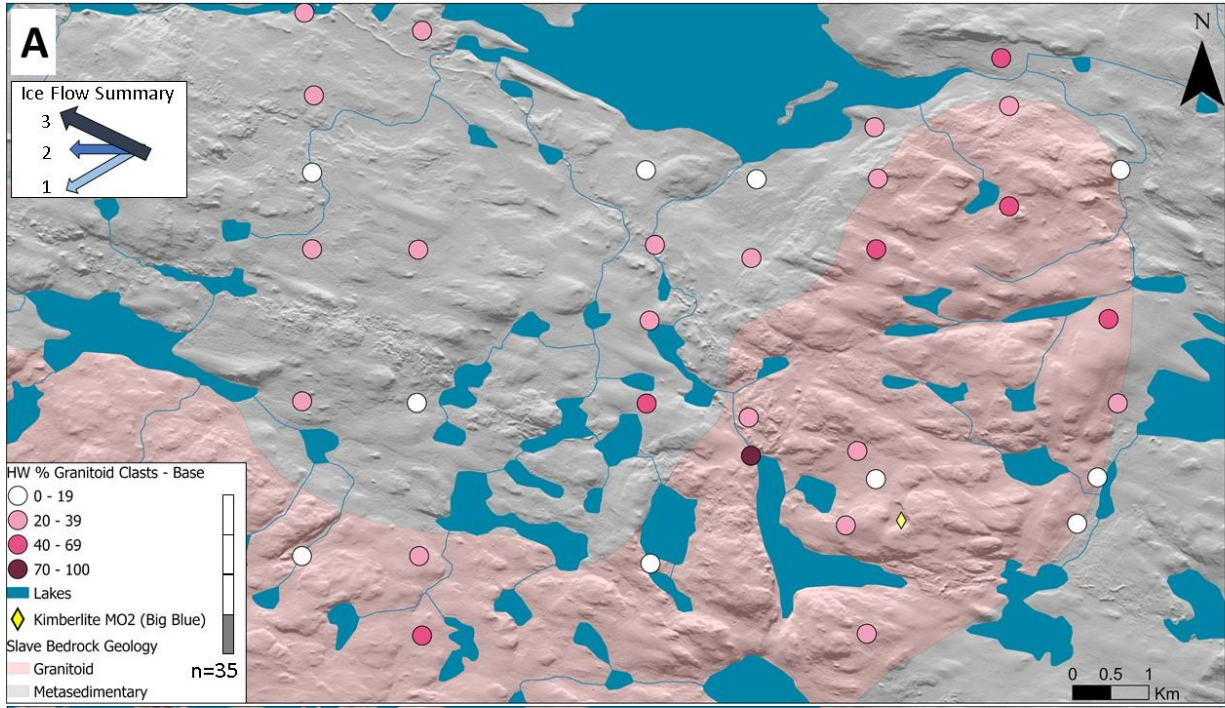
Clast lithology in the first depth interval (base of borehole) across the study area contained few granitoid clasts (0-40%) compared to metasedimentary clasts (**Fig. 3.14A**). In the western portion of the study area underlain by metasedimentary bedrock, till is patchy and boreholes are fairly shallow (0.1- 3.75m) compared to the younger lee-side of the topographic high, where boreholes are up to 9 meters deep. Adjacent the kimberlite nested within a granitoid knob, till at the base of boreholes (2.0-7.5m) also contained few granitoid clasts compared to metasedimentary clasts. Metasediment bedrock extends to the northeast, in the older ice flow direction. The softer nature of the metasediments and foliation orientation available to quarrying quickly inundates the sediment load compared to granitoid derived sediment. Till overlying metasedimentary bedrock maintains a greater proportion of metasedimentary clasts through the mid-depth intervals, whereas granitoid clast content on the granitoid topographic high increases through the mid-depth intervals (**Fig. 3.14B, C**).

Interestingly, a zone of thicker till (2.0-7.5m deep) to the west and northwest of the kimberlite contains few granitoid clasts (10-30%) in the base depth interval (**Fig. 3.14A**). In this 1.5-kilometer-wide zone of thick till down-ice of the kimberlite in the youngest ice flow direction, the lower-mid and upper-mid depth intervals display increasing granitoid clast content (40-50%) up to 80% granitoid clast content in one sample in the top depth interval (**Fig. 3.14B, C, D**). In contrast, the median granitoid content in the till in the study area is 30%, leading to the assumption that there is a certain degree of mixing, because the binning process is unlikely to

have separated till sheets perfectly, and the stratigraphy is unknown due to the lack of detail available in the borehole samples (**Fig. 3.15**).

The variable depth and thickness of the intervals between boreholes (see Section 1.5.8.1 for details) represent a challenge for the interpretation. For example, the top depth interval in one borehole may be 3 meters thick, while the base depth interval may be 0.4 meters thick; while the top depth interval in next drill hole may represent 3 meters of material and the base one 1.5 meters of material. A third borehole may be a single surface sample representing 0.1 meters of material. Ultimately, the variable borehole length leading to intervals of different thickness in the HW dataset creates some issues and limitations for the interpretation. Nonetheless, overall trends between the base and surface are helpful: there is greater metasediment clasts content at the base of the boreholes across the study area, and a greater granitoid clast content near and at the surface (**Fig. 3.15**). With the inconsistent sampling depth, it is more challenging to determine the depth of relict till and mixing, but there appears to be a vertical change with depth suggesting changing till composition, which could indicate till stratigraphy or increasing inheritance from older till towards the base of boreholes. Similar observations were reported by Janzen (2020) in a study area located further down-ice.







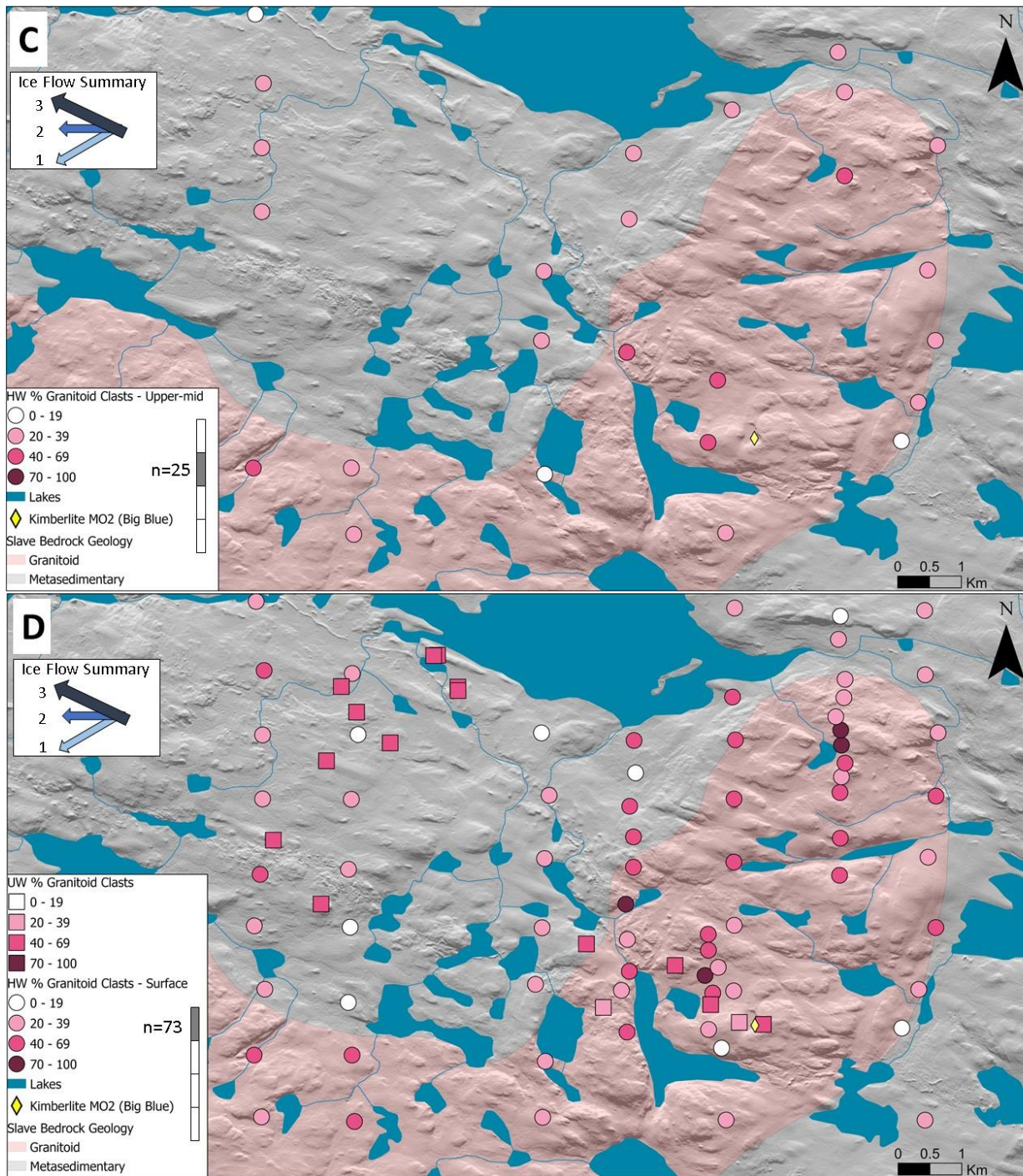


**Figure 3.14:** On previous page: A) top map shows granitoid clast content in the base interval of sediment thickness (adjacent bedrock) in the HW dataset is low. B) Granitoid content in the lower-mid interval. On this page: C) granitoid clast content in the upper mid-interval. D) Granitoid content in the top interval (surface).



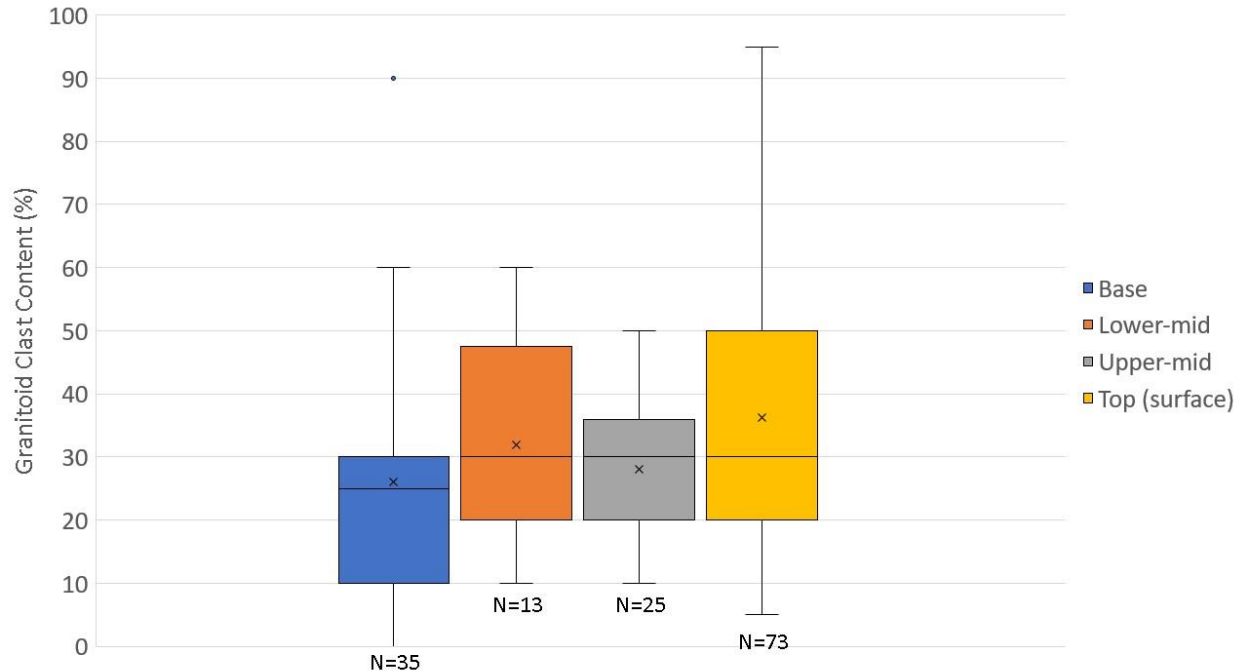


**Figure 3.15:** Box plots highlight lower granitoid clast content (compared to metasediment clast content) at the base of the boreholes compared to the surface.

Till matrix geochemistry lacks outliers and distinguishable patterns across the study area (**Fig. 3.16, 3.17, 3.18**), probably due to the low number of samples. Elements of interest include pathfinder metals associated with kimberlites, including Ni, Cr, Co, and Nb. These trace elements were calculated as percentiles and summed for an even graphical representation of all four elements (**Fig. 3.18**). Rubidium and barium are also associated with kimberlites within the Lac de Gras region (Wilkinson et al., 2001a; McClenaghan et al., 2002; McClenaghan and Kjarsgaard, 2007; McClenaghan et al., 2018), but they are also enriched in granitic rocks relative to metasediments (Rose et al., 1979). One sample, the sample collected from the flank of a wave washed drumlinoid form exhibiting the coarsest texture curve, consistently ranks as the highest value of Rb, Ni, Cr, Co, and is also among some of the highest in the study area for Ba and Nb (**Fig. 3.16, 3.18**).

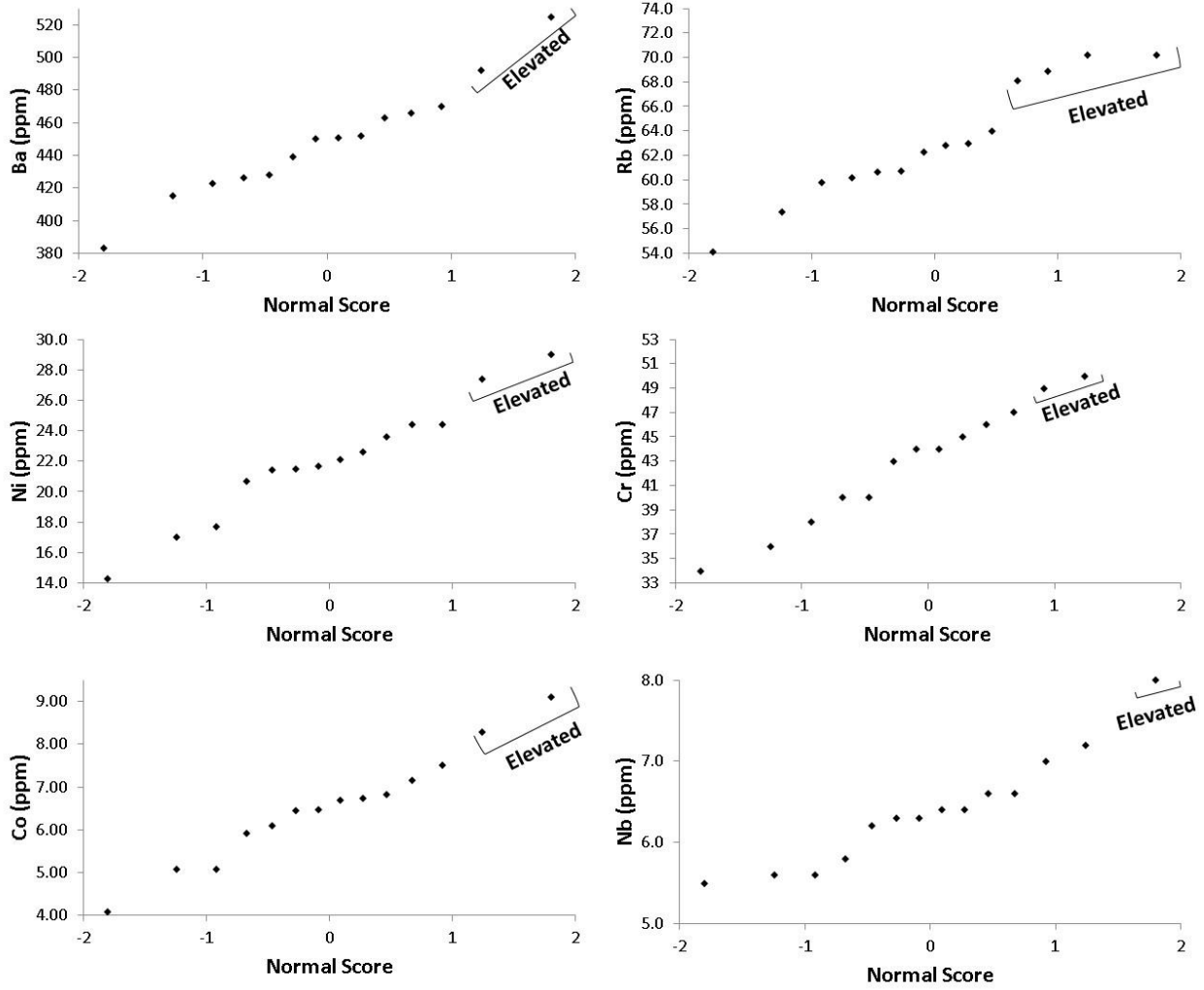


**Figure 3.16:** Till matrix geochemistry QQ plots do not indicate outliers of note. Ba and Cr used ICP-OES total digestion method, and Rb, Ni, Co, Nb used ICP-MS total digestion method.

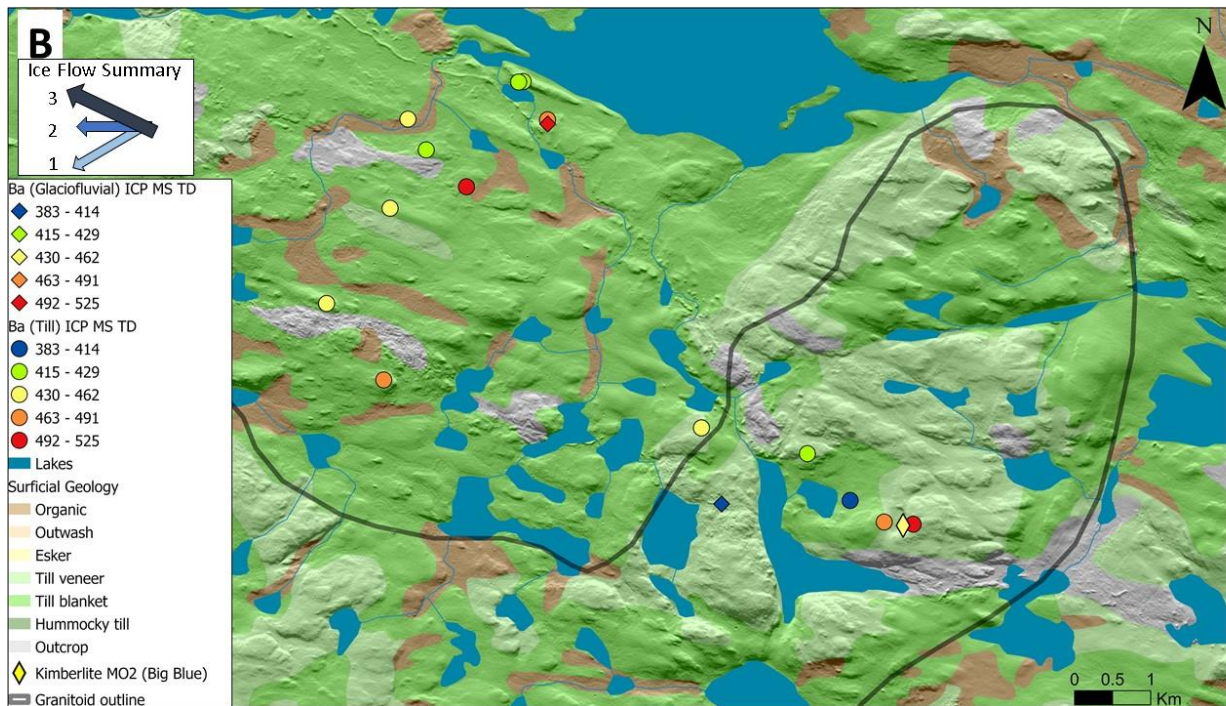
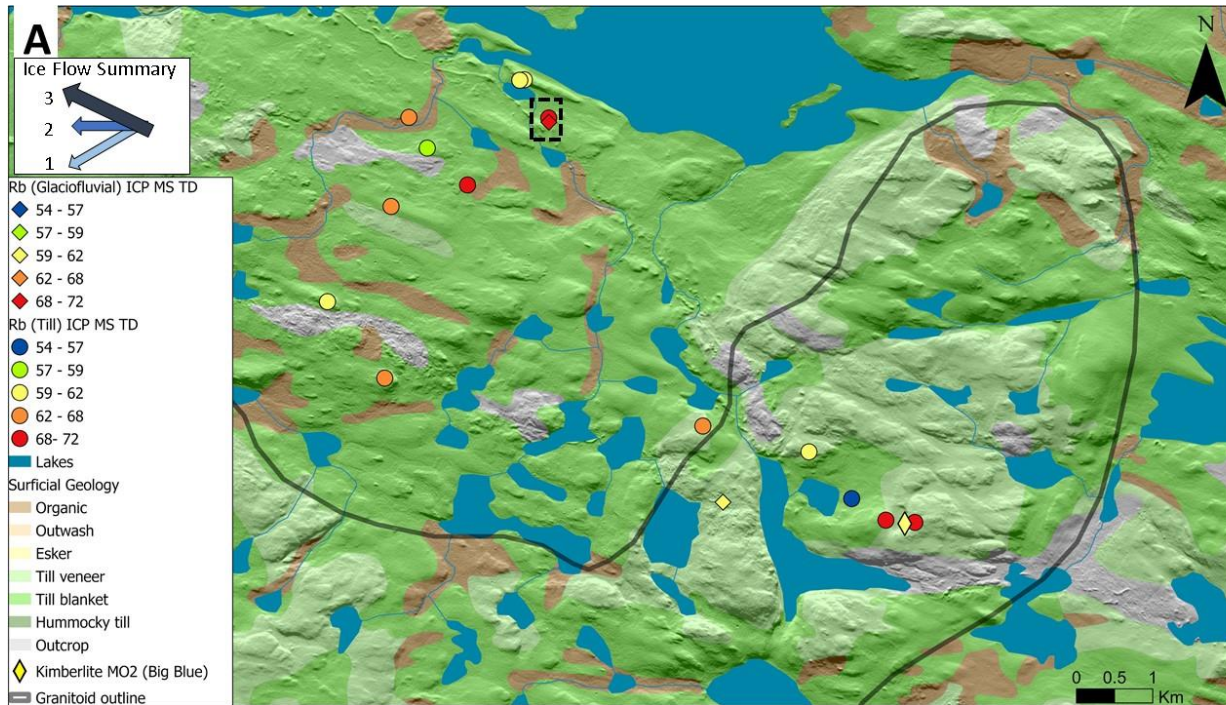


**Figure 3.17:** Till matrix geochemistry across the study area. A) Rubidium and B) Barium results for till (n=14) and glaciofluvial samples (n=2). Sample result from flank of a wave washed drumlinoid is outlined in black dashed box (A).



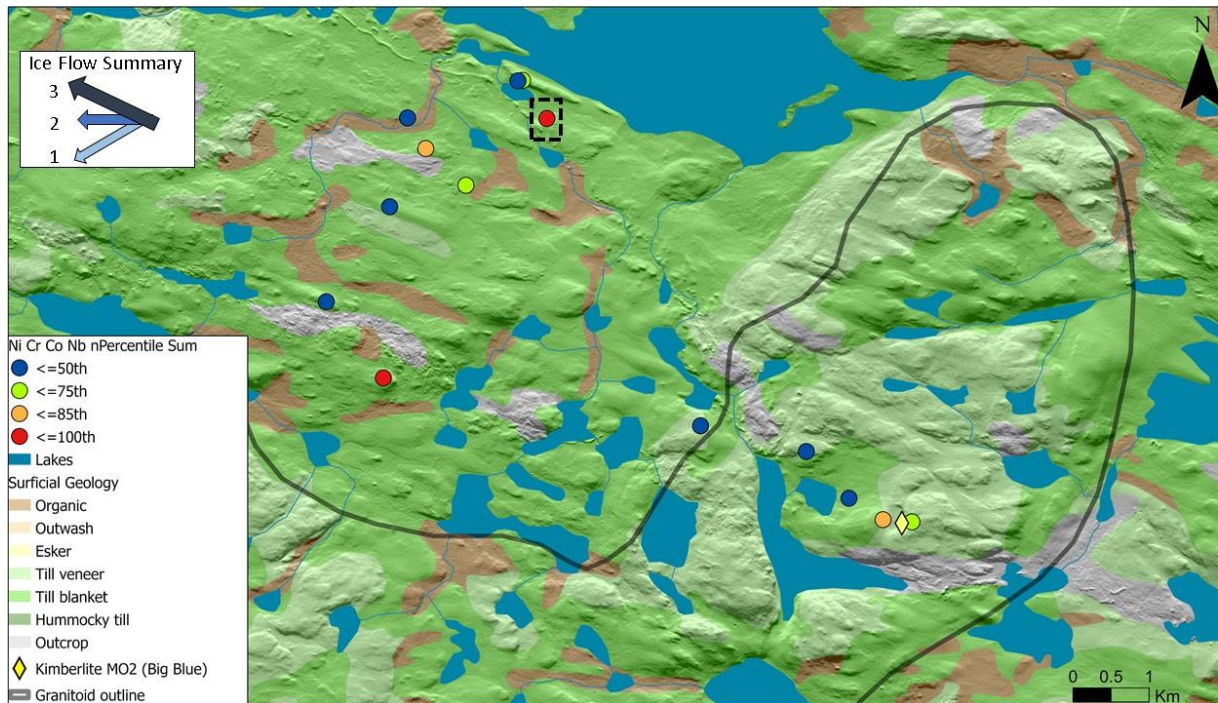


**Figure 3.18:** Till matrix geochemistry across the study area (n=14). Metals results, calculated as normalized percentile sums (Grunsky, 2010), used as pathfinder elements for kimberlites are low in the youngest ice flow direction. Glaciofluvial results are not displayed due to mobility and density issues associated with water transport. Sample result from flank of a wave washed drumlinoid is outlined in black dashed box.

### 3.5 Discussion

The sediment-landform assemblages in the study area show a complex sequence of events. The oldest ice flow event generated till, as evidenced by stoss-lee characteristics and eroded surfaces on outcrop and landforms. The till in the first (lower) depth interval of the HW data has a higher KIM content than the overlying intervals suggesting the presence of an older remnant dispersal train that does not intersect the surface in that area. The possibility that these buried KIMs come from the Big Blue kimberlite cannot be excluded, but based on the ice flow history, the relative position at depth of the KIMs, as well as the low normalized counts (0.3 to 3.9 grains/10kg), it is more likely that the KIMs are part of the distal tail end of a dispersal train, probably derived from a different kimberlitic source located up the older ice flow direction to the NE.

From a regional perspective, looking at the NTGS Data Hub publicly available total grain count data along the youngest ice flow direction (**Fig. 3.19**), the closest kimberlite in the youngest ice flow direction is 30 km away, moderately aligned with a dispersal train ending 15 km short of the topographic high. A second kimberlite located 20 km away in the older ice flow direction is better aligned with the indicator grains recovered from the HW drillcores, but is intercepted 30 meters below the surface, with an unknown depth of overlying sediments (outside the sediment thickness model). The surficial dispersal train ends on the outside edge of the drumlin field, about 10 km away from the first HW KIMs. The source of the indicators, both at depth and on the topographic high is inconclusive. However, the KIMs from the top of the granitoid



topographic high are located north of Big Blue and are thus very unlikely sourced from that kimberlite.

Based on the ice flow history and the location of the other kimberlites to the NE, it seems more likely that these KIMs at the top of the topographic high are sourced from the NE. Of note is the public dataset does not contain indicators on the topographic high like the HWRC dataset, probably because the top drill samples include upwards of 1-3 meters into the till, whereas the public dataset is likely primarily surficial samples, which suggests the drill samples either penetrated an older till or the till at the bottom has higher compositional inheritance from an older till due to incomplete reworking and mixing. In addition, the single surficial till sample collected for this study also has a relatively higher KIM count compared to the surrounding HW top depth interval (surface till) results. Additional support for subsurface till sourced from the NE includes the vertical trend of greater metasediment clast content at depth, likely sourced from the long distance of metasedimentary rocks to the NE, compared to the top depth interval (surface till) with higher granitoid content supplied by the local granitoid source. This could also mean the thicker till at the base of the lee-side bedrock step could also contain till from the old SW ice flow phase.

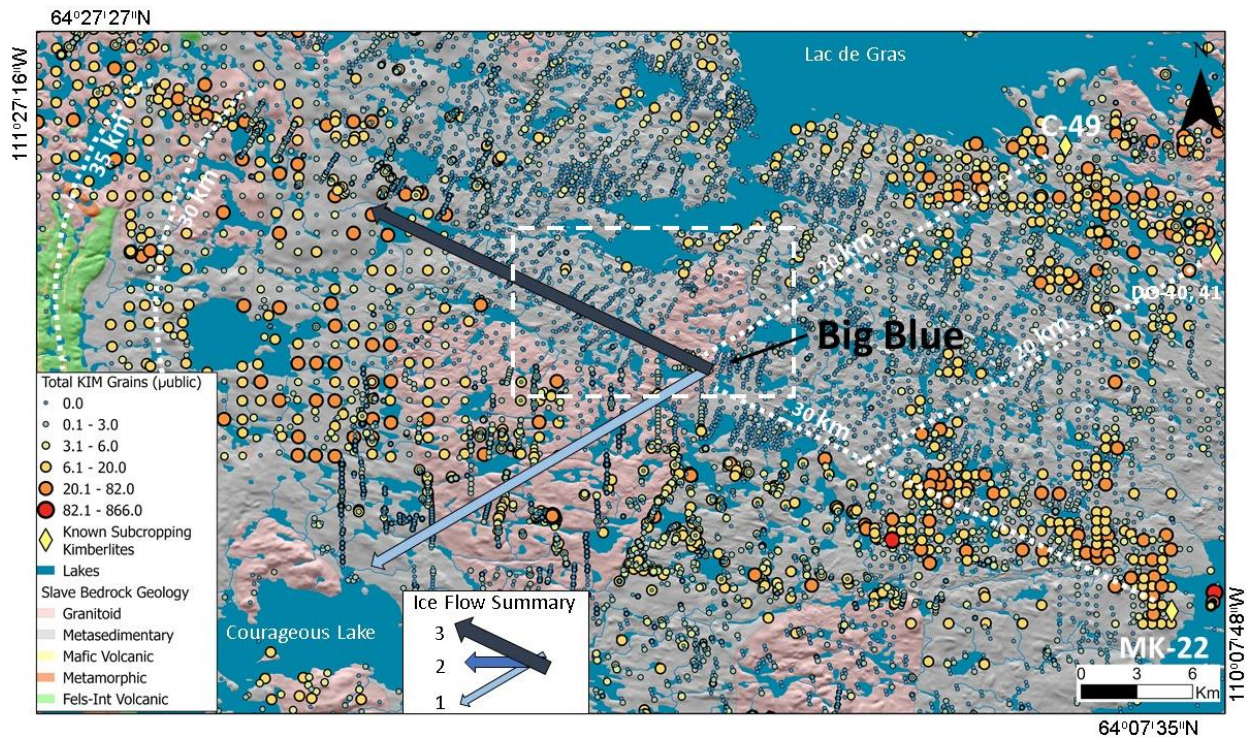


**Figure 3.19:** NTGS datahub publicly available total grain count does not show significant KIM grains on the bedrock topographic high. The data set does not contain any sample weights, and therefore samples cannot be normalized to 10kg in the same way as the HW or UW KIM data. Distances from distal subcropping kimberlites are provided along dotted white lines (20 km and 30 km in the older and youngest ice flow directions, respectively), while 30 km and 35 km ranges are given down ice of Big Blue, a distance consistent with other dispersal train lengths known subcropping kimberlites to the east). Blue arrows outline the oldest and youngest ice flow directions from Big Blue as a centre point. KIM grain counts from NTGS Data Hub KIDD data <datahub-ntgs.opendata.arcgis.com>.

### 3.5.1 Role of Bedrock Topography and Multiple Ice Flows on Dispersal Trains and Till Thickness

The Big Blue kimberlite, nested in a resistant rock knob, does not appear to have created a dispersal train in the upper till layer down the youngest ice flow to the northwest. While it cannot be ruled out that some KIM grains in the HW dataset are derived from Big Blue, it can be confidently stated that Big Blue did not generate a large and well-defined dispersal train. It therefore appears the kimberlite was not accessible to glacial erosion during most (if not all) of the northwest flow phase. The interpretation is that the granitoid protrusion in the up-ice direction of the kimberlite played a major role in causing the basal ice to skip the kimberlite (Fig. 3.20). This setting would have favored the formation of a small subglacial cavity over the kimberlite, resulting in basal ice skipping over the kimberlite (Fig. 3.21). Additionally, if there was a pressure cavity over the kimberlite, there might have been subglacial meltout till deposited. This would protect the pipe from erosion by covering it with sediment.

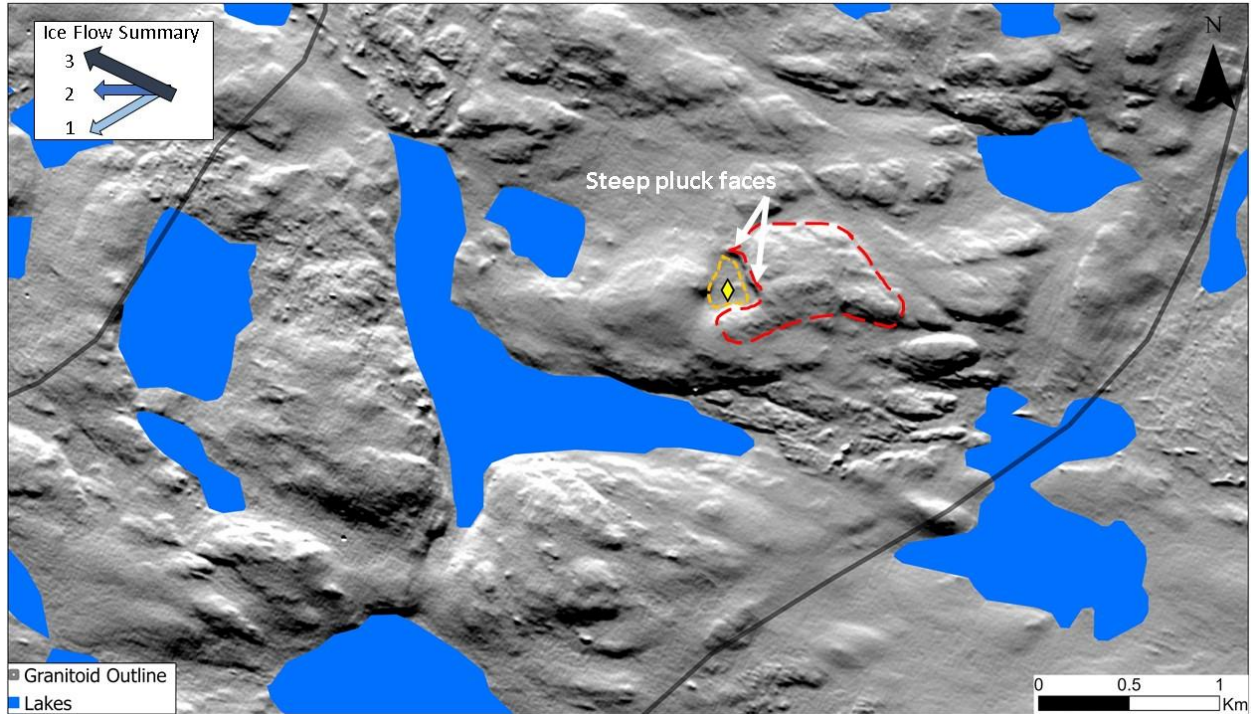


**Figure 3.20:** ArcticDEM (Porter et al., 2018) image draws attention to the bedrock protrusion to the east of the kimberlite (dashed red) an ideal configuration for the development of a cavity (dashed orange) over the kimberlite. Steep pluck faces on the lee-side in the oldest ice flow direction and drumlinization from subsequent ice flow phases are also visible.

Pressure differentials caused by an advancing glacier can create subglacial cavities due to changes in underlying lithology, or especially under conditions of thinner and or faster flowing ice, such as conditions experienced during deglaciation periods (e.g., Iverson, 1991; Hallet, 1996; Evans et al., 2006). The ArcticDEM also highlights a series of small channels that cross the topographic high, possibly draining meltwater to lateral channels (**Fig. 3.20, 3.21**).





**Figure 3.21:** Small channels cross the granitoid knob probably drained into lateral channels on occasion, possibly mobilizing some material from the Big Blue kimberlite.

In an effort to explain the lack of a KIM dispersal pattern in the till down-ice of Big Blue, a conceptual model is proposed (**Fig. 3.22**) showing the presence of the topographic high and the local rock knob located just up-ice of the Big Blue kimberlite. In the subglacial environment, these obstacles lead to compressive stress on their up-ice side. This situation can bring the ice-bed interface to above the pressure melting point on the up-ice side, as well as to the development of a subglacial cavity on the down-ice side, which here would have been over the kimberlite. The meltwater generated on the up-ice side would have flowed down ice to the cavity on the lee-side of the knob. Cavities like this are often connected to a drainage system called ‘linked-cavity’ system (Benn and Evans, 2010; section 3.4.3). The cavity could at times be full of water, but it would also occasionally drain, thus reducing the water pressure in the cavity. This situation could lead to freezing of water in the joints and to an increase in the effective stress at the edge of the bedrock step. This would promote failure of the step, thus contributing to the quarrying process (Iverson, 2012). The presence of a relatively stable (or growing) cavity over the kimberlite would have locally ‘decoupled’ the ice/bed interface, thus effectively preventing the erosive base of the glacier from being in direct contact with the top of the soft kimberlite. This model seems to explain the lack of a KIM dispersal pattern in the till down-ice of Big Blue. More investigations are needed in other soft-rock bodies nested in rock knobs to verify if the lack of a surficial dispersal train is a common feature for this type of setting, or if the conditions at Big Blue are rare.



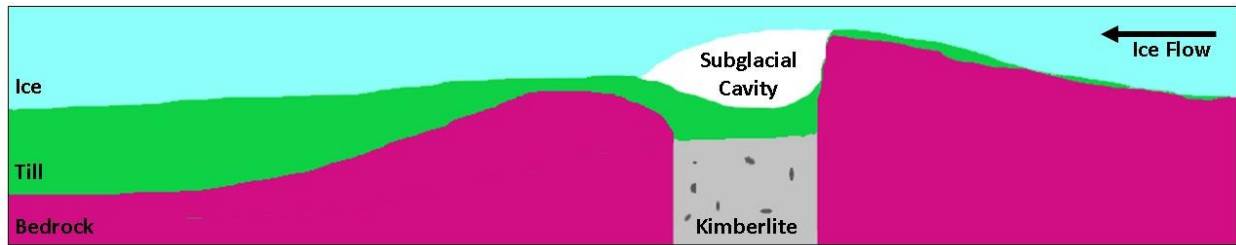


**Figure 3.22:** Model of nested kimberlite within granitoid knob with small subglacial cavity over the kimberlite.

The sediment thickness model, developed by Kelley et al. (2019b) using the HW dataset, highlights the area of thicker sediments to the west and northwest of the kimberlite (**Fig. 3.23**). The proportion of granitoid clasts (4-8mm) at the base of the thicker till area is low relative to the local surficial till, which means metasediment clasts are more abundant at depth than at surface. This could indicate the presence of relict till at depth and through most of the till column that would have been sourced from the northeast. It is possible the granitoid knob with the nested kimberlite formed a crag-and-tail down-ice at a coarser scale, while at a finer scale, it appears a smaller crag-and-tail also formed, superimposed on the larger crag-and-tail (**Fig. 3.23**). Pressure shadows resulting from warm-based faster-flowing ice that wrap about the crags helped preserve sediment in the down-ice lee-side from erosion. These lee-side sediment preservation processes could also explain the presence of KIM grains at the surface of the boreholes on top of the bedrock topographic high to the north of the kimberlite. To the southwest of the crag-and-tail landforms, there could be a remnant tail, possibly formed during the older ice flow event and subsequently drumlinized by the youngest ice flow event, then truncated by the glaciofluvial corridor. However, in the older ice flow direction, minimal sample results are available due to the proximity to the edge of the dataset. Overall, the surface of the study area appears variably drumlinized by the youngest ice flow event.

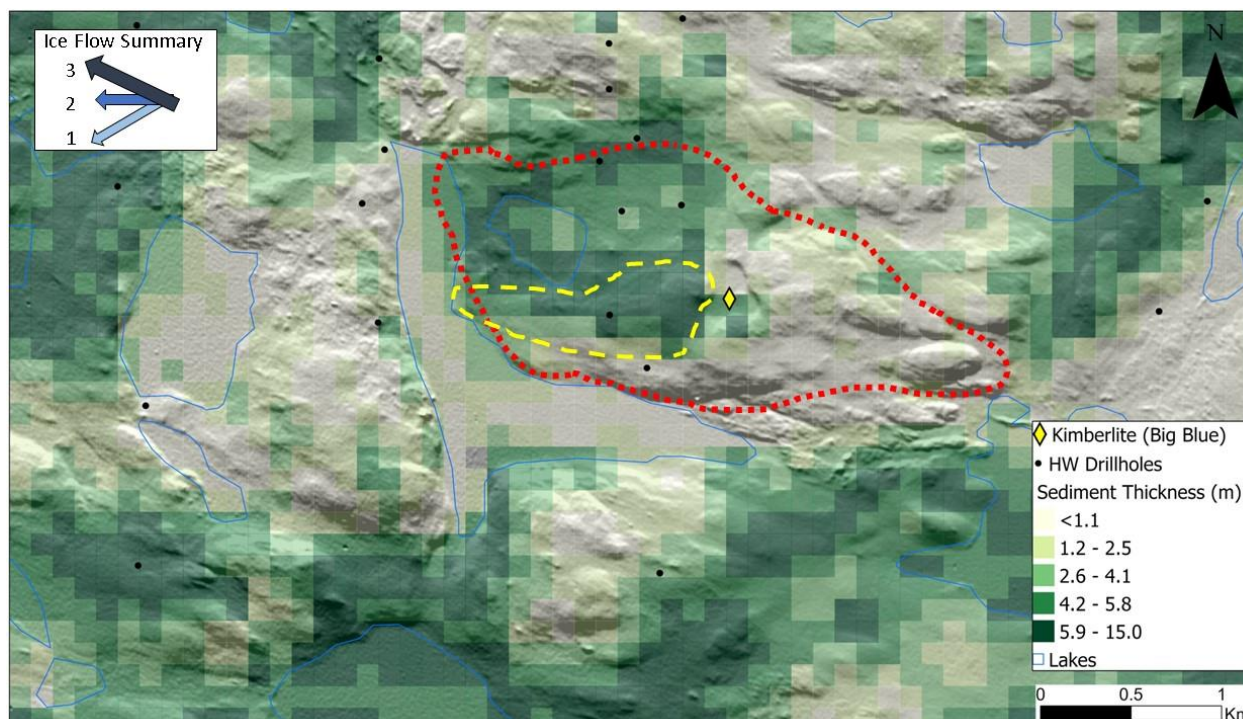


**Figure 3.23:** Sediment thickness model (Kelley et al., 2019b) highlights thicker till in both down ice directions from the bedrock knob, and also down-ice the broad granitoid topographic high (NW corner of the map). It is possible there are two crag-and-tail features at two scales (red dashed outline and yellow dashed outline).

### 3.5.2 Implications for Drift Prospecting

Drift prospectors working in areas with more elevated resistant rock knobs may not see a till dispersal train generated in the down-ice direction if the source of interest consists of soft rocks, which formed a depression nested in a rock knob, or if it is located just on the up-ice end of a rock knob as described in Kelley et al. (2019a). In addition, those working in areas with bedrock topography and variable till thickness should anticipate relict till preserved at depth. Being informed of the regional sequence of events of ice flow movement can help constrain till compositional patterns in the results and could identify an alternative explanation for indicator mineral grain counts, providing more efficient targets to explore. Taking into account the depositional and erosional potential of locally dominant ice flow phases by having good knowledge of subglacial processes can more efficiently determine the provenance of till material and reduce difficulties in identifying a buried mineralized source. Glaciofluvial corridors are erosional and can mobilize till material and rework it into glaciofluvial sediment with a different concentration of indicator minerals than the source till. Recording the landforms present during sampling, taking subglacial processes into account, and comparing data available from the full thickness of the till column adds an additional element to help unravel the complexity in areas with till variability. Legacy dataset reinterpretation using the ArcticDEM is a good first step for incorporating landforms into the interpretation. Understanding when dispersal trains may not be generated could be the key to unravelling the next viable target.

In addition, indicator mineral results from surficial till collected from a frost boil assumes convection of thawed material in the upper meter of the till column. Therefore, these results may not be comparable to the results from the first sample of an RC drilling program (commonly greater than 2 meters and occasionally as much as 3 meters) because drilling can penetrate till stratigraphy variably inherited from a different provenance. This observation was also made by Janzen (2020) in work done using a different RC dataset 20-40 kilometers to the northwest.

### **3.6 Conclusions**

Ice flow patterns were further refined and constrained in the study area through 22 ice flow indicator measurements from 10 different sites, while relative age chronology was established at only one location confirming the clockwise shift in ice flow directions (from SW to NW), in agreement with legacy measurements from Ward et al. (1997). In summary, an oldest ice flow towards the SW shifted towards the west and, finally, the northwest (youngest). In addition, this study identified areas of thicker till exhibiting vertical compositional changes, which are interpreted to reflect either till stratigraphy, with a relict till in deeper drillholes, or increasing compositional inheritance towards the base of the till column across the study area as seen in both the KIM and clast lithology datasets. Despite the presence of a kimberlite, till matrix geochemistry did not indicate any anomalous material in the study area. To the NE of Big Blue at the surface, a shallow cap of discontinuous till contains indicator mineral grains, likely from the tail end of a till dispersal train sourced from a distal kimberlite.

In areas protected by bedrock topography, weak till dispersal trains are preserved at depth. A granitoid protrusion created a lee-side cavity over the Big Blue kimberlite, allowing the glacier to skip over the kimberlite. The presence of protrusions may have also lead to possible cavity lee-side fill and crag-and-tail landforms at various scales, creating till stratigraphy observed in boreholes. This situation is thought to explain the lack of a clear and strong till dispersal train coming off Big Blue. This study therefore provides a conceptual model for explaining why, in certain cases, kimberlites that intersect the bedrock surface do not produce a clear dispersal train at surface. More settings characterized with kimberlites or other soft rock bodies nested in rock knobs would need to also be investigated to verify if the lack of a surficial dispersal train is a common feature in this setting, or if the local conditions at Big Blue are rare or unique.

Field observations and satellite imagery of landforms identified glaciofluvial corridors containing landforms such as eskers, kames, and perched boulders. Samples collected from a corridor splitting to the northwest contained some of the highest number of indicator mineral grains in the study, suggesting these corridors possibly re-entrained and mobilized a younger cap till. Glaciofluvial corridors could have truncated relict landforms, and subsequent drumlinization could mask relict landforms. This has significance for provenance studies such as the ones applied in drift prospecting, and especially when reinterpreting legacy data while taking landforms into consideration.

## **CHAPTER 4: Conclusions**

### **4.1 Identifying Potential Effects related to Bedrock Topography and Till Thickness Variations on Till Dispersal Trains**

To achieve the objectives (see sect. 1.3) of this study, the large HWRC dataset was used to target two kimberlites in different surficial geology settings which experienced the same ice flow history. Additional field data was collected to complement the dataset and used to refine and further constrain the ice flow history and till provenance. This study addressed knowledge gaps related to shifting ice flows and till thickness and bedrock topographic variation on till dispersal trains from kimberlites in the Northwest Territories. Addressing these gaps required reconstructing the ice flow history, as well as establishing till provenance in each study area. One important assumption in many till provenance studies is that compositional data from surficial till samples capture the full subglacial sediment transport history, even in regions affected by major ice flow shifts. In areas where till is of variable thickness, this assumption may not be valid. In the context of mineral exploration, another common assumption is that dispersal trains of indicator minerals exist down-ice kimberlites and mineralized bodies, as long as they intersect the bedrock surface, regardless of local conditions (e.g., bedrock topography). Therefore, this research was designed with five objectives. 1) Refine and further constrain the local ice-flow history of the two selected study areas; 2) analyze the 3D dispersion patterns of indicator minerals in the two study areas to determine the extent and strength of complex dispersal at depth; 3) analyze the surficial dispersion patterns of selected lithologies and geochemical pathfinders in the two study areas to determine whether there is a link between the surface and subsurface dispersal patterns; 4) compare dispersal patterns obtained in the previous two objectives and investigate the potential effects related to bedrock topography and till thickness variations, as well as related subglacial processes, such as erosion, sediment entrainment and sediment deposition and ice flow shifts; and 5) explore and discuss the implications for mineral exploration. These objectives rendered information from each study area that was used to understand the connection between shifting ice flow, sediment, and landforms. This information was used to improve the gaps in understanding in how till thickness and bedrock topographic variation controls till dispersal trains. This knowledge can be used by drift prospectors to improve interpretations from new and legacy datasets to resolve complex problems between surface and subsurface patterns variably expressed on surface in drumlin corridors or from mineral sources nested in resistant bedrock knobs. The main contributions of the thesis are detailed in the next section.

#### **4.1.1 Thesis Contributions**

The following contributions are made possible by the research conducted in this study:

- 1) Ice flow history was refined and further constrained in both study areas (11 measurements from 6 sites from the east study and 22 measurements from 10 sites in the



west study area, with one relative age chronology site in each study area). This new data is consistent with Ward et al. (1997) mapped at a 1:125,000 scale.

- 2) Surficial dispersion patterns of indicator grains, clast lithology counts, and geochemical pathfinders identified a widespread, albeit discontinuous surficial till related to the youngest NW ice flow phase.
  - a. Three-dimensional dispersion patterns of indicator mineral grains and clast lithology in areas of thicker till exhibited vertical compositional changes, recording either a relict till at the base of the till column or increasing compositional inheritance towards the base of the till column. Isolated clusters of higher KIM and clast lithology counts have been identified in a drumlin field and appears to be associated with the higher amplitude drumlins. These clusters persists through the full till thickness of the till column and could thus reflect an earlier ice flow phase rather than the one that created the drumlins. Erosional processes involved in the drumlin-forming process are thought to be responsible for exposing relict or highly inherited till at the surface.
  - b. Preserved relict till in thicker tills on the lee-side of a granitoid bedrock topographic high have also been identified. During the youngest NW ice flow phase, a tail of till was preserved down-ice where the granitoid topographic high ends. This is thought to explain why there is increased inheritance from older ice flow in the deepest till.
- 3) A new model provides an explanation for the lack of a clear dispersal train down-ice of the Big Blue kimberlite. The model involves the formation of a lee-side cavity over the kimberlite, down-ice of a granitoid rock knob, which would have allowed the glacier to skip over the kimberlite during the younger ice flow phase to the NW.

#### **4.1.2 Research Questions:**

- Are palimpsest till dispersal trains preserved in drumlin corridors (See section 2.6)?

A zone of either high inheritance or relict till was identified in the drumlin corridor in the east study area in three different data sets (UW, HW, NTGS Data Hub) and in three lines of evidence (KIM, clast lithology, and geochemical pathfinder) through the full thickness of the till column that aligned in the older ice flow direction.

- Are dispersal trains generated from nested kimberlites within resistant rock knobs (See section 3.5.1)?

Results show that a buried dispersal train sourced from the Big Blue kimberlite is not recorded in the study area after considering ice flow history constraints. Due to the resistant bedrock topographic high surrounding the Big Blue, it appears that lee-side cavity formation prevented the erosion, entrainment, and deposition of kimberlitic material, Kimberlite indicator mineral grains present on surface appear to have been sourced from other kimberlites.

- Are palimpsest till dispersal trains preserved on the lee-side of crag-and-tail landforms (See section 3.6)?

Relict, or inherited till was preserved at the base of the topographic step in the west study area where thick till overlays softer bedrock. Due to ice flow history and low number of mineral grains, this material appears to be the tail end of a dispersal train sourced in the older ice flow direction. Bedrock topography shielded till from the erosive effects of the subglacial environment.

- What is the potential role of subglacial meltwater on the reworking of kimberlite indicators around resistant bedrock hills (See section 3.6)?

The west study area contained subglacial meltwater corridors. One of those corridors was sampled for KIMs, and those samples had some of the highest grain counts found in the study area. The leading edge of the bedrock topographic high presented an obstacle to the base of an overriding glacier, increasing pressure on that leading edge, which could have increased basal melting and contributed to the formation of a meltwater corridor. The meltwater channels left evidence of flowing around the bedrock knob and overtop of the knob. It is possible meltwater mobilized KIM material from the lee-side of the bedrock knob where the nested kimberlite was embedded. It is also possible the meltwater corridors remobilized a till cap containing KIM grains from another provenance and concentrated them in the meltwater corridors. The presence of KIMs in till north of the Big Blue kimberlite lends support to this interpretation.

#### **4.1.3 Drift Prospecting in Areas with Variable Till Thickness and Bedrock Topography**

Successful drift prospecting in the diamondiferous Lac de Gras region has been ongoing since the 1990s, but now new knowledge and new strategies are needed to discover more elusive targets.. This study combined subsurface and surface results to provide new insights into ice flow events, till thickness, and bedrock topographic variation and to determine their potential net effects on till dispersal trains. It is clear the surficial landscape was sculpted by the younger ice flow event in the study area, which variably eroded and deposited till. In the studied drumlin field, this study has shown that the till had largely been deposited during earlier ice flow phases and was subsequently partially eroded during drumlinization. Whether drumlin fields commonly contain older or inherited till through most of their thickness remains uncertain, but this study suggests it could be a characteristic of at least certain drumlin fields, especially those characterized by relatively high amplitude till-cored drumlins like the ones studied herein. One

potential implication is that surficial palimpsest trains could be common in drumlin fields, due to net erosion during drumlinization. Therefore, it is imperative to take landforms into account, not only in the design of till sampling surveys, but also in the interpretation of results.

This study also provides an explanation for kimberlites lacking a dispersal train, especially the ones that are nested in a topographic high consisting of more resistant bedrock than the larger area around. The model involves the development of a lee-side cavity, which would have decoupled the erosive base of the sliding glacier from the top of the soft kimberlite, thus effectively preventing erosion and entrainment/incorporation of kimberlitic material into the till.

Legacy datasets can thus be reinterpreted with new considerations in specific surficial geology settings by taking into consideration shifting ice flow, till thickness and bedrock topographic controls on the formation of 3D till dispersal trains. Perhaps a re-interpretation of legacy data could lead to new kimberlite discoveries in the Lac de Gras region, and maintain Canada's status as one of the top three diamond producers in the world.

Due to the dominant erosional phase that can expose older till at surface during the drumlinization process, interpreting the full thickness of the till column, using at least KIM grains and clast lithology, can identify clusters of higher values, that can be found within a drumlin field. These isolated clusters of higher values may represent till stratigraphy and caution should be taken to interpret these isolated patches as having the same sediment provenance as surrounding till. According to this study, to define more specific targets, older ice flow phases identified through erosional or depositional measurements in the local area can lead to a better understanding of the full ice flow history, which is crucial for a more accurate interpretation of these isolated patches. The oldest erosional evidence can be overprinted or buried by subsequent ice flow events leaving few ice flow indicators available to measure, but this stage of ice flow may contribute to sediment at the base of the till column and can increase the complexity of the interpretation of exposed relict or inherited till at the surface. Future work can test for palimpsest dispersal in other till-core drumlin fields.

#### **4.1.4 Future Work**

Electron microprobe data and grain morphology results are available in the UW dataset, and probe data is available in the HW dataset. These data can augment this study if the geochemical fingerprint of Big Blue, DO-40 and DO-41 are available. In the west study area along the base and on top of the topographic high, as well as to the southwest of the Big Blue kimberlite, the geochemical fingerprint of these KIM grains can be compared to the geochemical fingerprint of Big Blue. It is unclear at this time if this kimberlite has a geochemical fingerprint analysis available for use. In the east study area, the geochemical fingerprint of KIM grains found in the detached clusters can and in the composite train, can be compared to the DO-40 and DO-41 kimberlite geochemical fingerprint to test whether the KIM grains in the detached clusters are sourced predominantly from these local kimberlites. Another opportunity for future work is testing the interpretation of fragmented palimpsest dispersal in other drumlin fields where there was shifting ice flow. Investigating more settings with kimberlites or other soft rock bodies

nested in rock knobs would be needed to verify if the lack of a surficial dispersal train is a common feature in this setting, or if the local conditions at Big Blue are rare or unique.

Suggestions for future drilling include consideration of sonic drilling instead of RC drilling. Sonic drilling preserves stratigraphy and can collect undisturbed drillcores, whereas RC drilling uses vacuum pressure to lift sediments within the borehole and transport in to sampling containers. Therefore, a large proportion of fine material is lost, and it is often in the fractions that are used most for analysis. A more pressing matter is the sampling interval depth of drilling. RC drilling samples at a minimum of 1.5-meter intervals, and too often up to 3 meters. The loss of clarity in the data can hamper the information contained in till stratigraphy.



## References

- Abzalov, M. 2008. Quality control of assay data: A review of procedures for measuring and monitoring precision and accuracy. *Exploration and Mining Geology*, **17**: 131-144.
- Alley, R.B. 1991. Deforming-bed origin for southern Laurentide till sheets? *Journal of Glaciology*, **37**: 67-76.
- Alley, R.B. 2000. Continuity comes first: recent progress in understanding subglacial deformation. Geological Society, London, Special Publications, **176**: 171-179.
- Anundsen, K. 1990. Evidence of ice movement over southwest Norway indicating an ice dome over the coastal district of west Norway. *Quaternary Science Reviews*, **9**: 99-116.
- Benn, D.I., and Evans, D. 2010. *Glaciers and Glaciation*. 802 pp. Hodder Education, London.
- Boulton, G.S. 1982. Subglacial processes and the development of glacial bedforms. *In Research in Glacial, Glacio-Fluvial and Glacio-Lacustrine Systems. Proceedings of the 6th Guelph Symposium on Geomorphology, 1980*. Pp 1-31.
- Boulton, G.S. 1996. Theory of glacial erosion, transport and deposition as a consequence of subglacial sediment deformation. *Journal of Glaciology*, **42**: pp.43-62.
- Boulton, G.S. and Hindmarsh, R.C.A. 1987. Sediment deformation beneath glaciers: rheology and geological consequences. *Journal of Geophysical Research: Solid Earth*, **92**: 9059-9082.
- Boulton, G.S., Wright, A.E. and Moseley, F. 1975. Processes and patterns of subglacial sedimentation: a theoretical approach. *In Ice ages: ancient and modern* **6**: 7-42). Seel House Press, Liverpool.
- Bustard, A. 2016. Fingerprinting and tracing the signature of basement-hosted unconformity-type uranium alteration through thick Quaternary tills: an example from the Thelon Basin, Nunavut. Master's thesis, University of Waterloo.
- Charbonneau, R., and David, P.P. 1993. Glacial dispersal of rock debris in central Gaspésie, Quebec, Canada. *Canadian Journal of Earth Sciences*, **30**: 1697-1707.
- Clark, C.D., Ely, J.C., Spagnolo, M., Hahn, U., Hughes, A.L., and Stokes, C.R. 2018. Spatial organization of drumlins. *Earth Surface Processes and Landforms*, **43**: 499-513.

Clark, P.U. and Pollard, D., 1998. Origin of the middle Pleistocene transition by ice sheet erosion of regolith. *Paleoceanography*, **13**: 1-9.

Clarke, G.K.C. 2005. Subglacial Processes. Annual review of earth and planetary sciences, **33**: 247-276.

Cohen, D., Hooyer, T.S., Iverson, N.R., Thomason, J.F. and Jackson, M. 2006. Role of transient water pressure in quarrying: A subglacial experiment using acoustic emissions. *Journal of Geophysical Research: Earth Surface*, **111**.

Davis, J.C. and Sampson, R.J. 1986. Statistics and data analysis in geology. Wiley, New York, pp 238-244.

Davis, W.J., and Kjarsgaard, B.A. 1997. A Rb-Sr isochron age for a kimberlite from the recently discovered Lac de Gras Field, Slave Province, Northwest Canada. *Journal of Geology*, **105**: 503-510.

DiLabio, R.N.W. 1979. Drift prospecting in uranium and base-metal mineralization sites, District of Keewatin, Northwest Territories, Canada.

DiLabio, R.N.W., and Coker, W.B. 1989. Drift prospecting. Energy, Mines and Resources Canada.

Dominion Diamond Mines ULC and North Arrow Minerals Inc. 2022. Lac de Gras Joint Venture Overburden Drilling and Kimberlite Indicator Mineral Data, Dominion Diamond Mines ULC and North Arrow Minerals Inc., compiled by Aurora Geosciences Ltd, NWT, Open Report 2022-006. <https://doi.org/10.46887/2022-006>

Dredge, L.A., Ward, B.C., and Kerr, D.E. 1994. Glacial geology and implications for drift prospecting in the Lac de Gras, Winter Lake, and Aylmer Lake map areas, central Slave Province, Northwest Territories. Current research, 1994-C: 33-38.

Dreimanis, A. 1989. Tills: their genetic terminology and classification. Genetic classification of glacial deposits. Pp.17-83.

Dreimanis, A. and Vagners, U.J. 1971. Bimodal distribution of rock and mineral fragments in basal tills. In Till, a Symposium. Edited by R.P. Goldthwait, Ohio State University Press. pp. 237-250.

Drewry, D.J. 1986. Glacial geologic processes. E. Arnold, London.

Dyke, A.S. and Prest, V.K., 1987. Paleogeography of northern North America, 18,000-5,000 years ago. Geological Survey of Canada, Ottawa, Map 1703A, Scale 1:12 500 000.

Dyke, A.S., Andrews, J.T., Clark, P.U., England, J.H., Miller, G.H., Shaw, J., and Veillette, J.J. 2002. The Laurentide and Innuitian ice sheets during the last glacial maximum. *Quaternary Science Reviews*, **21**: 9-31.

Earle, S. 2001. Application of composite glacial boulder geochemistry to exploration for unconformity-type uranium deposits in the Athabasca Basin, Saskatchewan, Canada. Geological Society, London, Special Publications, **185**: 225-235.

Ely, J.C., Clark, C.D., Spagnolo, M., Hughes, A.L., and Stokes, C.R. 2018. Using the size and position of drumlins to understand how they grow, interact and evolve. *Earth Surface Processes and Landforms*, **43**: 1073-1087.

Ely, J.C., Clark, C.D., Spagnolo, M., Stokes, C.R., Greenwood, S.L., Hughes, A.L.C., Dunlop, P., and Hess, D. 2016. Do subglacial bedforms comprise a size and shape continuum? *Geomorphology*, **257**: 108-119.

Evans, D.J. and Hansom, J.D. 1996. The Edinburgh Castle crag-and-tail. *Scottish Geographical Magazine*, **112**: 129-131.

Evans, D.J.A., Phillips, E.R., Hiemstra, J.F., and Auton, C.A. 2006. Subglacial till: Formation, sedimentary characteristics and classification. *Earth-science Reviews*, **78**: 115-176.

Eyles, N., Putkinen, N., Sookhan, S. and Arbelaez-Moreno, L. 2016. Erosional origin of drumlins and megaridges. *Sedimentary Geology*, **338**: 2-23.

Fipke, C.E., Dummett, H.T., Moore, R.O., Carlson, J.A., Ashley, R.M., Gurney, J.J., and Kirkley, M.B. 1995. History of the discovery of diamondiferous kimberlites in the Northwest Territories, Canada. *In International Kimberlite Conference: Extended Abstracts*, Vol. 6, pp. 158-160.

Fowler, A.C., Spagnolo, M., Clark, C.D., Stokes, C.R., Hughes, A.L.C., and Dunlop, P. 2013. On the size and shape of drumlins. *GEM international journal on geomathematics*, **4**: 155-165.

Fulton, R J. 1995. Surficial materials of Canada, Geological Survey of Canada, "A" Series Map no. 1880A, Scale 1: 5 000 000.

Glasser, N.F., and Harrison, S. 2005. Sediment distribution around glacially abraded bedrock landforms (whalebacks) at Lago Tranquilo, Chile. *Geografiska Annaler. Series A, Physical Geography*, **87**: 421-430.

Gordon, J.E. 1981. Ice-scoured topography and its relationships to bedrock structure and ice movement in parts of northern Scotland and West Greenland. *Geografiska Annaler: Series A, Physical Geography*, **63**: 55-65

Grunsky, E.C. 2010. The interpretation of geochemical survey data. *Geochemistry: Exploration, Environment, Analysis*, **10**: 27-74.

Grütter, H.S., Gurney, J.J., Menzies, A.H., and Winter, F. 2004. An updated classification scheme for mantle-derived garnet, for use by diamond explorers. *Lithos*, **77**: 841-857.

Hallet, B., Hunter, L., and Bogen, J. 1996. Rates of erosion and sediment evacuation by glaciers: A review of field data and their implications. *Global and Planetary Change*, **12**: 213-235.

Hawkes, H.E. 1957. Principles of geochemical prospecting: contributions to geochemical prospecting for minerals. Geological Survey Bulletin 100-F. US Government Printing Office, Washington, USA.

Hermanowski, P., Piotrowski, J.A., and Szuman, I. 2019. An erosional origin for drumlins of NW Poland. *Earth Surface Processes and Landforms*, **44**: 2030-2050.

Hildes, D.H., Clarke, G.K., Flowers, G.E. and Marshall, S.J. 2004. Subglacial erosion and englacial sediment transport modelled for North American ice sheets. *Quaternary Science Reviews*, **23**: 409-430.

Hillier, J.K., Smith, M.J., Clark, C.D., Stokes, C.R., and Spagnolo, M. 2013. Subglacial bedforms reveal an exponential size–frequency distribution. *Geomorphology*, **190**: 82-91.

Hodder, T.J., Ross, M., and Menzies, J. 2016. Sedimentary record of ice divide migration and ice streams in the Keewatin core region of the Laurentide Ice Sheet. *Sedimentary Geology*, **338**: 97-114.

Hughes, A.L., Clark, C.D., and Jordan, C.J. 2014. Flow-pattern evolution of the last British Ice Sheet. *Quaternary Science Reviews*, **89**: 148-168.

Hughes, T. 1996. Can ice sheets trigger abrupt climatic change? *Arctic and Alpine Research*, **28**: 448-465.



Iverson, N.R. 1991. Potential effects of subglacial water-pressure fluctuations on quarrying. *Journal of Glaciology*, **37**: 27-36.

Iverson, N.R., 1993. Regelation of ice through debris at glacier beds: Implications for sediment transport. *Geology*, **21**: 559-562.

Iverson, N.R. 1995. Processes of erosion. In *Modern Glacial Environments: Processes, Dynamics, and Sediments*. Edited by J. Menzies, J. Oxford. pp. 241-259.

Iverson, N.R. 2000. Sediment entrainment by a soft-bedded glacier: a model based on regelation into the bed. *Earth Surface Processes and Landforms: Journal of the British Geomorphological Research Group*, **25**: 881-893.

Iverson, N.R. 2012. A theory of glacial quarrying for landscape evolution models. *Geology*, **40**: 679-682.

Iverson, N.R. 2017. Determining glacier flow direction from till fabrics. *Geomorphology*, **299**: 124-130.

Janzen, R. 2020. An Analysis of Glacial Sediment Dispersion with Applications to Diamond Exploration, Lac de Gras, Northwest Territories. University of Waterloo.

Jenner, G. A. 1996. Trace element geochemistry of igneous rocks: Geochemical nomenclature and analytical geochemistry. *Trace Element Geochemistry of Volcanic Rocks: Applications for Massive Sulfide Exploration*. Pp. 51-77.

Kamb, B. 1987. Glacier surge mechanism based on linked cavity configuration of the basal water conduit system. *Journal of Geophysical Research: Solid Earth*, **92**: 9083-9100.

Kelley, S.E., Ross, M., Elliott, B., Normandeau, P.X. 2019. Effect of shifting ice flow and basal topography in shaping three-dimensional dispersal patterns, Lac de Gras region, Northwest Territories, Canada. *Journal of Geochemical Exploration*, **199**: 105–127.

Kelley, S.E., Ross, M., Elliott, B., and Normandeau, P.X. 2019a. Effect of shifting ice flow and basal topography in shaping three-dimensional dispersal patterns, Lac de Gras region, Northwest Territories, Canada. *Journal of Geochemical Exploration*, **199**: 105-127.

Kelley, S.E., Ross, M., Elliott, B., and Normandeau, P.X. 2019b. Glacial Sediment Thickness model for the southern Lac de Gras region. Unpublished report submitted to the Geological Survey of the Northwest Territories. 13 pages.

Kerr, D.E., and Knight, R.D. 2007. Modelling overburden thickness in glaciated terrain: Lac de Gras, Northwest Territories, Canada. *Geophysical Inversion and Modelling*. Geological Survey of Canada, Paper 97.

Kerr, M. and Eyles, N. 2007. Origin of drumlins on the floor of Lake Ontario and in upper New York State. *Sedimentary Geology*, **193**: 7-20.

Kjarsgaard, B A; Wilkinson, L; Armstrong, J. 2002. Lac de Gras kimberlite field, central Slave Province, Northwest Territories - Nunavut. Geological Survey of Canada, Open File 3238, Scale 1:250,000.

Klassen, R.A. 1997. Glacial history and ice flow dynamics applied to drift prospecting and geochemical exploration. *In Proceedings of Exploration 97: Fourth Decennial International Conference on Mineral Exploration*. Edited by A.G. Gubins. Prospectors and Developers Association of Canada. pp. 221-232.

Klassen, R.A. and Thompson, F.J. 1993. Glacial history, drift composition, and mineral exploration, central Labrador. Geological Survey of Canada, Bulletin 435. p.76.

Klassen, R.A., and Bolduc, A.M. 1984. Ice flow directions and drift composition, Churchill Falls, Labrador. *Current Research*. Geological Survey of Canada, Part A, Paper 84-1A: 255-258.

Knight, J. and McCabe, A.M. 1997. Identification and significance of ice-flow-transverse subglacial ridges (Rogen moraines) in northern central Ireland. *Journal of Quaternary Science*, **12**: 519-524.

Kujansuu, R., & Saarnisto, M. (1990). *Glacial indicator tracing*: AA Balkema.

Kürzl, H. 1988. Exploratory data analysis: recent advances for the interpretation of geochemical data. *Journal of Geochemical Exploration*, **30**: 309-322.

Larson, P. C., & Mooers, H. D. 2004. Glacial indicator dispersal processes: A conceptual model. *Boreas*, **33**: 238-249.

Larson, P. C., Mooers, H. D., Hildes, D. H. D., Clarke, G. K. C., Flowers, G. E., & Marshall, S. J. 2005. Comment on "Subglacial erosion and englacial sediment transport modeled for North American ice sheets" by D.H.D. Hildes, G.K.C. Clarke, G.E. Flowers, S.J. Marshall (multiple letters). *Quaternary Science Reviews*. **24**: 233-234.

Leshner, M., Hannington, M., Galley, A., Ansdell, K., Astic, T., Banerjee, N., Beauchamp, S., Beaudoin, G., Bertelli, M., and Bérubé, C. 2017. Integrated Multi-Parameter Exploration

Footprints of the Canadian Malartic Disseminated Au, McArthur River-Millennium Unconformity U, and Highland Valley Porphyry Cu Deposits: Preliminary Results from the NSERC-CMIC Mineral Exploration Footprints Research Network. In "Proceedings of Exploration 17: Sixth Decennial International Conference on Mineral Exploration". Edited by V. Tschirhart and M.D. Thomas, 2017, pp. 325–347.

Lindström, E. 1988. Are Roches Moutonnées Mainly Preglacial Forms? *Geografiska annaler. Series A, Physical Geography*, **70**: 323-331.

Lipp, A. G., Roberts, G. G., Whittaker, A. C., Gowing, C. J. B., & Fernandes, V. M. 2021. Source region geochemistry from unmixing downstream sedimentary elemental compositions. *Geochemistry, Geophysics, Geosystems*, **22**, e2021GC009838.

Litinski, V.A. 1961. On the content of Ni, Cr, Ti, Nb and some other elements in kimberlites and the possibility of geochemical prospecting for kimberlite bodies. *Geochemistry*, **9**: 813-821.

McClenaghan, M.B. 1994. Till geochemistry in areas of thick drift and its application to gold exploration, Matheson area, northeastern Ontario. *Exploration and Mining Geology*, **3**: 17-30.

McClenaghan, M.B. 2005. Indicator mineral methods in mineral exploration. *Geochemistry: Exploration, Environment, Analysis*, **5**: 233-245.

McClenaghan, M.B. Kjarsgaard, B.A. 2007. Indicator mineral and surficial geochemical exploration methods for kimberlite in glaciated terrain: examples from Canada. In *Mineral Deposits of Canada: A Synthesis of Major Deposit-Types, District Metallogeny, the Evolution of Geological Provinces, and Exploration Methods*. Edited by W.D. Goodfellow. Geological Association of Canada, Mineral Deposits Division, Canada, Special Publication No. 5, pp. 983-1006.

McClenaghan, M.B., and Paulen, R.C. 2018. Application of Till Mineralogy and Geochemistry to Mineral Exploration. Elsevier. Pp 689-751.

McClenaghan, M.B., and Peter, J.M. 2016. Till geochemical signatures of volcanogenic massive sulphide deposits: an overview of Canadian examples. *Geochemistry: Exploration, Environment, Analysis*, **16**: 27-47.

McClenaghan, M.B., Paulen, R.C., and Oviatt, N.M. 2018. Geometry of indicator mineral and till geochemistry dispersal fans from the Pine Point Mississippi Valley-type Pb-Zn district, Northwest Territories, Canada. *Journal of Geochemical Exploration*, **190**: 69-86.

- McClenaghan, M.B., Paulen, R.C., Layton-Matthews, D., Hicken, A.K., and Averill, S.A. 2015. Glacial dispersal of gahnite from the Izok Lake Zn-Cu-Pb-Ag VMS deposit, northern Canada. *Geochemistry: Exploration, Environment, Analysis*, **15**: 333-349.
- McClenaghan, M.B., Plouffe, A., McMartin, I., Campbell, J.E., Spirito, W.A., Paulen, R.C., Garrett, R.G., and Hall, G. 2013. Till sampling and geochemical analytical protocols used by the Geological Survey of Canada. *Geochemistry: Exploration, Environment, Analysis*, **13**: 285-301.
- McClenaghan, M.B., Thorleifson, L.H., DiLabio, R.N.W. 2000. Till geochemical and indicator mineral methods in mineral exploration. *Ore Geology Reviews*, **16**: 145-166.
- McClenaghan, M.B., Ward, B.C., Kjarsgaard, I.M., Kjarsgaard, B.A., Kerr, D.E., and Dredge, L.A. 2002. Indicator mineral and till geochemical dispersal patterns associated with the Ranch Lake kimberlite, Lac de Gras region, NWT, Canada. *Geochemistry: Exploration, Environment, Analysis*, **2**: 299-319.
- McMartin, I., and Henderson, P. 2004. Evidence from Keewatin (central Nunavut) for paleo-ice divide migration. *Geographie physique et Quaternaire*, **58**: 163-186.
- McMartin, I., and Paulen, R.C. 2009. Ice-flow indicators and the importance of ice-flow mapping for drift prospecting. In Application of Till and Stream Sediment Heavy Mineral and Geochemical Methods to Mineral Exploration in Western and Northern Canada. Edited by RC Paulen and I. McMartin. Geological Association of Canada. Short Course Notes, **18**: 15-34.
- Melanson, A. 2013. Numerical modelling of subglacial erosion and sediment transport and its application to the North American ice sheets over the Last Glacial cycle. M.Sc, Department of Physics and Physical Oceanography, Memorial University of Newfoundland, St. John's, Newfoundland.
- Menzies, J., Hess, D.P., Rice, J.M., Wagner, K.G., and Ravier, E. 2016. A case study in the New York Drumlin Field, an investigation using microsedimentology, resulting in the refinement of a theory of drumlin formation. *Sedimentary Geology*, **338**: 84-96.
- Miller, J.K. 1984. Model for clastic indicator trains in till. In Prospecting in areas of glaciated terrain. International symposium. Pp. 69-77.
- Murray, T., 1997. Assessing the paradigm shift: deformable glacier beds. *Quaternary Science Reviews*, **16**: 995-1016.
- Netz, R. and Noel, W. 2007. The Archimedes codex. Revealing the secrets of the world's greatest palimpsest, Great Britain. Weidenfeld & Nicolson.



- Nowicki, T., Porritt, L., Crawford, B., and Kjarsgaard, B. 2008. Geochemical trends in kimberlites of the Ekati property, Northwest Territories, Canada: Insights on volcanic and re-sedimentation processes. *Journal of Volcanology and Geothermal Research*, **174**: 117-127.
- Parent, M., Paradis, S. and Boisvert, E. 1995. Ice-flow patterns and glacial transport in the eastern Hudson Bay region: implications for the late Quaternary dynamics of the Laurentide Ice Sheet. *Canadian Journal of Earth Sciences*, **32**: 2057-2070.
- Parent, M., Paradis, S. and Doiron, A. 1996. Palimpsest glacial dispersal trains and their significance for drift prospecting. *Journal of Geochemical Exploration*, **56**: 123-140.
- Paulen, R. C. 2017. A revised look at Canada's landscape: Glacial process and dynamics. *In* New frontiers for exploration in glaciated terrain. *Edited by* R.C. Paulen and M.B. McClenaghan; Geological Survey of Canada, open file 7374, pp. 5-12.
- Paulen, R.C., and McClenaghan, M.B. 2015. Late Wisconsin ice-flow history in the Buffalo Head Hills kimberlite field, north-central Alberta. *Canadian Journal of Earth Sciences*, **52**: 51-67.
- Paulen, R.C., McClenaghan, M.B., and Hicken, A.K. 2013. Regional and local ice-flow history in the vicinity of the Izok Lake Zn–Cu–Pb–Ag deposit, Nunavut. *Canadian Journal of Earth Sciences*, **50**: 1209-1222.
- Piercey, S.J. 2014. Modern Analytical Facilities 2. A review of quality assurance and quality control (QA/QC) procedures for litho-geochemical data. *Geoscience Canada*, **41**: 75-88.
- Plouffe, A., Ferbey, T., Hashmi, S., and Ward, B.C. 2016. Till geochemistry and mineralogy; vectoring towards Cu porphyry deposits in British Columbia, Canada. *Geochemistry: Exploration, Environment, Analysis*, **16**: 213-232.
- Porter, C., et al. 2018. ArcticDEM. *In* Harvard Dataverse. V1 <https://doi.org/10.7910/DVN/OHHUKH>. (Accessed May 2019).
- Rea, B. 2007. Micro to Macro Scale Forms. *In* Scott A. Elias. *Edited by* Encyclopedia of Quaternary Sciences. Elsevier, **2**: pp. 853-864.
- Rice, J.M., Ross, M., Paulen, R.C., Kelley, S.E., Briner, J.P., Neudorf, C.M., and Lian, O.B. 2019. Refining the ice flow chronology and subglacial dynamics across the migrating Labrador Divide of the Laurentide Ice Sheet with age constraints on deglaciation. *Journal of Quaternary Science*, **33**: 519-535.

Rose, A., Hawkes, H.E., Webb, J.S. 1979. *Geochemical Mineral Exploration*. Second Edition, Academic Press, 657 pages.

Ross, M., Parent, M., and Lefebvre, R. 2005. 3D geologic framework models for regional hydrogeology and land-use management: a case study from a Quaternary basin of southwestern Quebec, Canada. *Hydrogeology Journal*, **13**: 690-707.

Ross, M., Parent, M., Benjumea, B., and Hunter, J. 2006. The late Quaternary stratigraphic record northwest of Montréal; regional ice-sheet dynamics, ice-stream activity, and early deglacial events. *Canadian Journal of Earth Sciences*, **43**: 461-485.

Schulze, D.J. 1993. An introduction to the recognition and significance of kimberlite indicator minerals. *Techniques in Exploration For Diamonds: Short Course Notes*, May, pp.13-14. Schulze, D.J. 1999. The significance of eclogite and Cr-poor megacryst garnets in diamond exploration. *Exploration and Mining Geology*, **6**: 349-366.

Sharp, M., Gemmell, J.C. and Tison, J.L., 1989. Structure and stability of the former subglacial drainage system of the Glacier de Tsanfleuron, Switzerland. *Earth Surface Processes and Landforms*, **14**: 119-134.

Sharpe, D.R., Kjarsgaard, B.A., Knight, R.D., Russell, H., and Kerr, D.E. 2017. Glacial dispersal and flow history, East Arm area of Great Slave Lake, NWT, Canada. *Quaternary Science Reviews*, **165**: 49-72.

Shaw, J., and Sharpe, D.R. 1987. Drumlin formation by subglacial meltwater erosion. *Canadian Journal of Earth Sciences*, **24**: 2316-2322.

Shilts, W.W. 1996. Drift Exploration. *In Past Glacial Environments, Sediments, Forms and Techniques*. Pp. 411-439.

Shilts, W.W., Franklin, J.M., and Duke, J.M. 1991. Principles of Glacial Dispersal and Sedimentation, **2**: 2-42.

Sookhan, S., Eyles, N., Bukhari, S., and Paulen, R.C. 2021. LiDAR-based quantitative assessment of drumlin to mega-scale glacial lineation continuums and flow of the paleo Seneca-Cayuga paleo-ice stream. *Quaternary Science Reviews*, **263**: pp. 1-17; 10.1016/j.quascirev.2021.107003.

Stanley, C.R., and Lawie, D. 2007. Average relative error in geochemical determinations: Clarification, calculation, and a plea for consistency. *Exploration and Mining Geology*, **16**: 267–275.

Stea, R.R., and Finck, P.W. 2001. An evolutionary model of glacial dispersal and till genesis in Maritime Canada. *In* Drift Exploration in Glaciated Terrain. *Edited by* M. B. McClenaghan, P. T. Bobrowsky, G. E. M. Hall, S. J. Cook. Geological Society, London, Special Publications, **185**: 237-265.

Stea, R.R., Johnson, M., and Hanchar, D. 2009. The geometry of KIM dispersal fans in Nunavut, Canada. *In* Application of Till and Stream Sediment Heavy Mineral and Geochemical Methods to Mineral Exploration in Western and Northern Canada. *Edited by* R.C. Paulen and I. McMartin, Geological Association of Canada, Canada, Short Course Notes 18, pp. 1-13.

Stokes, C.R., Clark, C.D., and Storrar, R. 2009. Major changes in ice stream dynamics during deglaciation of the north-western margin of the Laurentide Ice Sheet. *Quaternary Science Reviews*, **28**: 721-738.

Stokes, C.R., Clark, C.D., and Winsborrow, M. 2006. Subglacial bedform evidence for a major palaeo-ice stream and its retreat phases in Amundsen Gulf, Canadian Arctic Archipelago. *Journal of Quaternary Science*, **21**: 399-412.

Stokes, C.R., Spagnolo, M., and Clark, C.D. 2011. The composition and internal structure of drumlins: Complexity, commonality, and implications for a unifying theory of their formation. *Earth-science Reviews*, **107**: 398-422.

Stokes, C.R., Spagnolo, M., Clark, C.D., Cofaigh, C., Lian, O.B., and Dunstone, R.B. 2013. Formation of mega-scale glacial lineations on the Dubawnt Lake Ice Stream bed: 1. size, shape and spacing from a large remote sensing dataset. *Quaternary Science Reviews*, **77**: 190-209.

Strand, P., Banas, A., Baumgartner, M., Burgess, J., Paulen, R.C., and McMartin, I. 2009. Tracing kimberlite indicator mineral dispersal trains: an example from the Churchill Diamond Project, Kivalliq region, Nunavut. *In* Application of Till and Stream Sediment Heavy Mineral and Geochemical Methods to Mineral Exploration in Western and Northern Canada. *Edited by* RC Paulen and I. McMartin. Geological Association of Canada. Short Course Notes, **18**: 167-175.

Stroeven, A.P., Harbor, J., Fabel, D., Kleman, J., Hattestrand, C., Elmore, D., Fink, D., and Fredin, O. 2006. Slow, patchy landscape evolution in northern Sweden despite repeated ice-sheet glaciation. *Special papers-Geological Society of America*, **398**: 387.

Sugden, D.E., Glasser, N. and Clapperton, C.M., 1992. Evolution of large roches moutonnées. *Geografiska Annaler: Series A, Physical Geography*, **74**: 253-264.

Thomason, J.F. and Iverson, N.R., 2008. A laboratory study of particle ploughing and pore-pressure feedback: a velocity-weakening mechanism for soft glacier beds. *Journal of Glaciology*, **54**: 169-181.

Trommelen, M.S., Ross, M., and Campbell, J.E. 2012. Glacial terrain zone analysis of a fragmented paleoglaciologic record, southeast Keewatin sector of the Laurentide Ice Sheet. *Quaternary Science Reviews*, **40**: 1-20.

Trommelen, M.S., Ross, M., and Campbell, J.E. 2013. Inherited clast dispersal patterns: Implications for palaeoglaciology of the SE Keewatin Sector of the Laurentide Ice Sheet. *Boreas*, **42**: 693-713.

Veillette, J.J., Dyke, A.S., and Roy, M. 1999. Ice-flow evolution of the Labrador Sector of the Laurentide Ice Sheet: a review, with new evidence from northern Quebec. *Quaternary Science Reviews*, **18**: 993-1019.

Ward, B.C., Dredge, L.A., Kerr, D.E., and Kurfurst, D. 1997. Surficial geology, Lac de Gras, District of Mackenzie, Northwest Territories. Geological Survey of Canada, Scale 1:125 000.

Wilk, M.B., and Gnanadesikan, R. 1968. Probability plotting methods for the analysis for the analysis of data. *Biometrika*, **55**: 1-17.

Wilkinson, L., Harris, J., Kjarsgaard, B., McClenaghan, B., and Kerr, D. 2001. Influence of till thickness and texture on till geochemistry in the Lac de Gras area, Northwest Territories, with applications for regional kimberlite exploration. Natural Resources Canada, Geological Survey of Canada.

Wilkinson, L., Kjarsgaard, B.A., LeCheminant, A.N., and Harris, J. 2001. Diabase dyke swarms in the Lac de Gras area, Northwest Territories, and their significance to kimberlite exploration: initial results. Natural Resources Canada, Geological Survey of Canada.

## **Appendices**

Appendix A: UW field sample and sample type.....	118
Appendix B: Ice flow indicator field measurements.....	121
Appendix C: KIM results for UW and HW data, and HW KIM data processing.....	124
Appendix D: Sediment texture results for UW data .....	140
Appendix E: Clast lithology results for UW and HW data.....	161
Appendix F: Geochemistry results for UW data.....	200
Appendix G: QA/QC results for UW and HW data.....	231



## **Appendix A: UW field sample location and sample type**

UW field sample location and sample type

Sample ID	N	W	Elev	Type	Landform	Study_Area	Sample_Material	Easting	Northing
001-A	64.33839	110.2879	438	KIM	Swale (SW)	E	Till	534409.9009	7134915.516
002-A	64.33964	110.2869	443	KIM	Drumlin top	E	Till	534454.2398	7135055.322
003-A	64.34204	110.2876	435	KIM	Drumlin side NE	E	Till	534417.4217	7135322.381
006-A	64.32841	110.2612	440	KIM	Drumlin side SW	E	Till	535710.4843	7133818.121
018-A	64.31787	110.2624	442	KIM	Drumlin top	E	Till	535668.5276	7132642.982
020-A	64.36132	110.2166	440	KIM	Vineer	E	Till	537820.525	7137511.138
032-A	64.35078	110.8308	428	KIM	Drumlin side	W	Till	508172.9914	7136114.359
036-A	64.3465	110.8282	427	KIM	Esker	W	Glaciofluvial	508299.3723	7135637.741
038-A	64.30968	110.722	461	KIM	Esker	W	Glaciofluvial	513445.4079	7131552.775
040-A	64.31057	110.77	463	KIM	Kame	W	Glaciofluvial	511126.2	7131642.69
041-A	64.31887	110.778	464	KIM	Kame	W	Glaciofluvial	510733.6057	7132566.234
042-A	64.32401	110.7841	457	KIM	Kame	W	Glaciofluvial	510439.1198	7133138.013
001-B	64.33839	110.2879	438	CHEM	Swale (SW)	E	Till	534409.9009	7134915.516
002-B	64.33964	110.2869	443	CHEM	Drumlin top	E	Till	534454.2398	7135055.322
003-B	64.34204	110.2876	435	CHEM	Drumlin side NE	E	Till	534417.4217	7135322.381
004-B	64.34164	110.2362	430	CHEM	Drumlin side SW	E	Till	536899.6874	7135306.626
005-B	64.34201	110.2334	432	CHEM	Drumlin top	E	Till	537038.3269	7135349.531
006-B	64.32841	110.2612	440	CHEM	Drumlin side SW	E	Till	535710.4843	7133818.121
007-B	64.3221	110.2509	433	CHEM	Drumlin side SW	E	Till	536219.5185	7133120.846
008-B	64.32897	110.2607	446	CHEM	Drumlin top	E	Till	535733.9259	7133880.803
009-B	64.33173	110.2551	439	CHEM	Drumlin side SW	E	Till	536002.4409	7134191.532
010-B	64.33311	110.2566	442	CHEM	Drumlin top	E	Till	535928.149	7134344.46
011-B	64.33482	110.2401	430	CHEM	Drumlin side SE	E	Till	536723.7406	7134544.443
012-B	64.34169	110.2366	430	CHEM	Drumlin side SW	E	Till	536881.7453	7135311.983
013-B	64.3131	110.2145	442	CHEM	Drumlin top	E	Till	537988.3068	7132139.167
014-B	64.31131	110.2311	435	CHEM	Drumlin side NE	E	Till	537188.4044	7131929.897
015-B	64.31042	110.2345	445	CHEM	Drumlin top	E	Till	537024.6754	7131828.733
016-C1	64.31923	110.2572	430	Grain Analysis only	Swale below WT	E	Lacustrine	535917.7101	7132797.451
016-C2	64.31923	110.2572	430	Grain Analysis only	Swale below WT	E	Lacustrine	535917.7101	7132797.451
016-C3	64.31923	110.2572	430	Grain Analysis only	Swale below WT	E	Lacustrine	535917.7101	7132797.451
017-B	64.31923	110.2572	430	CHEM	Drumlin side NE	E	Till	535917.7101	7132797.451
018-B	64.31787	110.2624	442	CHEM	Drumlin top	E	Till	535668.5276	7132642.982
019-B	64.36077	110.1964	448	CHEM	Vineer	E	Till	538797.4547	7137462.039

Sample ID	N	W	Elev	Type	Landform	Study_Area	Sample_Material	Easting	Northing
020-B	64.36132	110.2166	440	CHEM	Vineer	E	Till	537820.525	7137511.138
021-B	64.35445	110.1723	430	CHEM	Vineer	E	Till	539970.1144	7136772.728
022-B	64.30698	110.7527	477	CHEM	Vineer	W	Till	511962.5927	7131245.765
023-B	64.30145	110.7412	467	CHEM	Swale	W	Till	512521.8921	7130631.736
024-B	64.29892	110.732	490	CHEM	Kimberlite - down-ice	W	Till	512970.1508	7130351.654
025-B	64.29863	110.7242	494	CHEM	Kimberlite - up-ice	W	Till	513348.2062	7130320.953
026-B	64.34645	110.8609	438	CHEM	Swale	W	Till	506721.2451	7135628.308
027-B	64.34283	110.8559	449	CHEM	Drumlin top	W	Till	506962.7215	7135225.439
028-B	64.33598	110.8657	461	CHEM	Drumlin top	W	Till	506488.9449	7134461.049
029-B	64.32481	110.883	471	CHEM	Drumlin top	W	Till	505655.7147	7133214.639
030-B	64.3158	110.8676	475	CHEM	Drumlin top	W	Till	506403.7466	7132212.05
031-B	64.35083	110.8295	431	CHEM	Drumlin top	W	Till	508234.3148	7136120.095
032-B	64.35078	110.8308	428	CHEM	Drumlin side	W	Till	508172.9914	7136114.359
033-B	64.34634	110.823	423	CHEM	Drumlin side	W	Till	508552.0594	7135620.604
034-B	64.34584	110.8229	433	CHEM	Kame Swale	W	Glaciofluvial	508555.1129	7135564.893
035-B	64.33849	110.845	449	CHEM	Drumlin rock	W	Till	507490.0176	7134743.038
037-B	64.31007	110.7815	470	CHEM	Swale	W	Till	510570.6395	7131585.011
039-B	64.3011	110.7761	474	CHEM	Kame	W	Glaciofluvial	510835.8377	7130586.332

## **Appendix B: Ice flow indicator field measurements**

UW ice flow indicator field measurements

Object-ID	DATE	N	W	EL	MEASUREMENT	LINEATION	Easting	Northing	NOTES
1	20-Jul	64.3479	110.2021	440	295	striation	538541	7136026	younger flow. Took measurements on whaleback. Metaseds. Just off foliation
2	23-Jul	64.3286	110.1996	433	290	striation	538688	7133879	Bedrock in felsenmeer. Metaseds. 287 striation 10-15 m away. Bedrock may have been pushed up by not rotated
3	23-Jul	64.3286	110.1996	433	287	striation	538688	7133879	Bedrock in felsenmeer. Metaseds. 287 striation 10-15 m away. Bedrock may have been pushed up by not rotated
4	23-Jul	64.3196	110.2121	431	290	striation	538099	7132868	Tried to uncover up ice outcrop exposure, but plucked surface and cracks prevent presence of rock
5	24-Jul	64.3614	110.1858	442	270	striation	539306	7137538	Felsic intrusive. 2 older striation measurements (SW flow - older). 295 (NW flow younger). Outcrop exposed with thin till, small boulders, large cobble. Old pluck faces filled with till makes older striations more convincing.
6	24-Jul	64.3614	110.1858	442	245	striation	539306	7137538	Felsic intrusive. 2 older striation measurements (SW flow - older). 295 (NW flow younger). Outcrop exposed with thin till, small boulders, large cobble. Old pluck faces filled with till makes older striations more convincing.
7	24-Jul	64.3614	110.1858	442	295	striation	539306	7137538	Felsic intrusive. 2 older striation measurements (SW flow - older). 295 (NW flow younger). Outcrop exposed with thin till, small boulders, large cobble. Old pluck faces filled with till makes older striations more convincing.
8	24-Jul	64.3608	110.1964	448	275	striation	538797	7137462	Top of ridge. Exposed bedrock with thin fill. Possible photo (see page 15) 245 pluck face with shovel in 295 direction
9	24-Jul	64.3608	110.1964	448	295	pluck face	538797	7137462	Top of ridge. Exposed bedrock with thin fill. Possible photo (see page 15) 245 pluck face with shovel in 295 direction
10	24-Jul	64.3608	110.1964	448	245	pluck face	538797	7137462	Top of ridge. Exposed bedrock with thin fill. Possible photo (see page 15) 245 pluck face with shovel in 295 direction
11	24-Jul	64.3603	110.2012	449	270	striation	538565	7137411	Pinhead striations 100 m along ridgetop. 270 real flow, not just microscale plastic flow
12	26-Jul	64.3070	110.7527	477	285	striation	511963	7131246	Adjacent sample 22B.
13	26-Jul	64.2989	110.7320	490	280	striation	512970	7130352	Adjacent sample 24B. Down ice of kimberlite peanut lakes. 245 pluck face
14	26-Jul	64.2989	110.7320	490	245	striation	512970	7130352	Adjacent sample 24B. Down ice of kimberlite peanut lakes. 245 pluck face
15	27-Jul	64.3485	110.8604	438	210	striation	506743	7135858	Metaseds. Younger flow (280). Protected area several striations. 1. (oldest) 220, 238, (range). 2. (fairly abundant from low surface) 255, 260. 3. Youngest 315. Possible area of deflection.
16	27-Jul	64.3485	110.8604	438	225	striation	506743	7135858	Metaseds. Younger flow (280). Protected area several striations. 1. (oldest) 220, 238, (range). 2. (fairly abundant from low surface) 255, 260. 3. Youngest 315. Possible area of deflection.



Object-ID	DATE	N	W	EL	MEASUREMENT	LINEATION	Easting	Northing	NOTES
17	27-Jul	64.3485	110.8604	438	230	striation	506743	7135858	Metaseds. Younger flow (280). Protected area several striations. 1. (oldest) 220, 238, (range). 2. (fairly abundant from low surface) 255, 260. 3. Youngest 315. Possible area of deflection.
18	27-Jul	64.3485	110.8604	438	220	striation	506743	7135858	Metaseds. Younger flow (280). Protected area several striations. 1. (oldest) 220, 238, (range). 2. (fairly abundant from low surface) 255, 260. 3. Youngest 315. Possible area of deflection.
19	27-Jul	64.3485	110.8604	438	238	striation	506743	7135858	Metaseds. Younger flow (280). Protected area several striations. 1. (oldest) 220, 238, (range). 2. (fairly abundant from low surface) 255, 260. 3. Youngest 315. Possible area of deflection.
20	27-Jul	64.3485	110.8604	438	255	striation	506743	7135858	Metaseds. Younger flow (280). Protected area several striations. 1. (oldest) 220, 238, (range). 2. (fairly abundant from low surface) 255, 260. 3. Youngest 315. Possible area of deflection.
21	27-Jul	64.3485	110.8604	438	260	striation	506743	7135858	Metaseds. Younger flow (280). Protected area several striations. 1. (oldest) 220, 238, (range). 2. (fairly abundant from low surface) 255, 260. 3. Youngest 315. Possible area of deflection.
22	27-Jul	64.3485	110.8604	438	315	Striation	506743	7135858	Metaseds. Younger flow (280). Protected area several striations. 1. (oldest) 220, 238, (range). 2. (fairly abundant from low surface) 255, 260. 3. Youngest 315. Possible area of deflection.
23	27-Jul	64.3413	110.8582	450	278	Striation	506853	7135050	Metaseds
24	27-Jul	64.3294	110.8745	464	275	Striation	506066	7133727	Striations and grooves. Metaseds, till veneer
25	27-Jul	64.3294	110.8745	464	275	Grooves	506066	7133727	Striations and grooves. Metaseds, till veneer
26	27-Jul	64.3230	110.8801	468	280	Striation	505797	7133010	Striations and S like grooves. Metasedimentary in felsenmeer
27	27-Jul	64.3415	110.8656	444	275	Striation	506494	7135078	Striations. Also at this location: pressure cracks, crescentic chips missing down ice
28	28-Jul	64.3379	110.8338	444	278	Striation	508031	7134680	Pinhead striations. Grooves at 275. Some slightly curved. Fissile metaseds
29	28-Jul	64.3379	110.8338	444	275	Grooves	508031	7134680	Pinhead striations. Grooves at 275. Some slightly curved. Fissile metaseds
30	28-Jul	64.3385	110.8433	453	279	Grooves	507574	7134740	Grooves. Very well defined. Fractures cross cut younger flow (fast flowing). Nail head x2 (curve)
31	28-Jul	64.3385	110.8433	453	280	Grooves	507574	7134740	Grooves. Very well defined. Fractures cross cut younger flow (fast flowing). Nail head x2 (curve)
32	28-Jul	64.3385	110.8433	453	278	Grooves	507574	7134740	Grooves. Very well defined. Fractures cross cut younger flow (fast flowing). Nail head x2 (curve)
33	29-Jul	64.3551	110.8473	400	280	Grooves	507374	7136594	iPhone compass. Groves at 280. Tensile cracks at 245. Crescentic cracks upslope 247. Be cautious

## **Appendix C: KIM results for UW and HW data, and HW KIM data processing**

UW SRC lab results: D-17-168

UW SRC lab results: EMPA Report AMC2018-013

UW KIM grain morphology

HW nKIM depth interval bin calculations

HW borehole depth interval boundaries

Report No: D-17-168

March 01, 2018

**University Of Waterloo**  


**Attn: Rebecca Stirling**

Test reports are the property of the customers. Publications of statements, conclusions or extracts from these reports are not permitted without prior written permission from the customer.

This document constitutes the **final official test report**. Liability for the SRC Geoanalytical Laboratories', if any, will be limited to the cost of analysis for samples in this test report. The results contained in this test report relate only to the items tested. It is the customer's responsibility to ensure that all interpretation of analysis is done using the data from this report.

The customer will not use the name of the Saskatchewan Research Council in connection with the sale, offer, advertisement or the promotion of any article, product, or company without the prior written consent of the SRC.

Results Reviewed and Approved by: \_\_\_\_\_



Cristiana Mircea  
Mineralogist/Geologist

University Of Waterloo

Attention: Rebecca Stirling

PO #/Product: SC455876

Samples: 12

**Test Report  
MicroDMS**

Date of Report: March 1, 2018

- 1) SWT : Original Sample Weight in kilograms
- 2) MWT Dry + : Mid Fraction -1.00+0.5mm Dry Weight in grams
- 3) MWT Dry - : Mid Fraction -0.5+0.25mm Dry Weight in grams
- 4) MicroDMS Sinks +0.5 : MicroDMS S -1.00+0.5mm Weight in grams
- 5) MicroDMS Sinks +0.25 : MicroDMS S -0.5+0.25mm Weight in grams
- 6) MIF+ : MI Floats SG<3.23 -1.00+0.5mm Weight in grams
- 7) MIF- : MI Floats SG<3.23 -0.5+0.25mm Weight in grams
- 8) MIS+ : MI Sinks SG>3.23 -1.00+0.5mm Weight in grams
- 9) MIS- : MI Sinks SG>3.23 -0.5+0.25mm Weight in grams
- 10) MAGS+0.5 : Mags -1.00+0.5mm Weight in grams
- 11) MAGS+0.25 : Mags -0.5+0.25mm Weight in grams
- 12) Pyr-p + : Pyrope Peridotitic Grains -1.00+0.5mm in Counts
- 13) Pyr-p - : Pyrope Peridotitic Grains -0.5+0.25mm in Counts
- 14) Pyr-e + : Pyrope Eclogitic Grains -1.00+0.5mm in Counts
- 15) Pyr-e - : Pyrope Eclogitic Grains -0.5+0.25mm in Counts
- 16) Chr D + : Chrome-Diopside Grains -1.00+0.5mm in Counts
- 17) Chr D - : Chrome-Diopside Grains -0.5+0.25mm in Counts
- 18) Olv + : Olivine Grains -1.00+0.5mm in Counts
- 19) Olv - : Olivine Grains -0.5+0.25mm in Counts
- 20) Picroilm + : Picroilmene Grains -1.00+0.5mm in Counts
- 21) Picroilm - : Picroilmene Grains -0.5+0.25mm in Counts
- 22) Chr + : Chromite Grains -1.00+0.5mm in Counts
- 23) Chr - : Chromite Grains -0.5+0.25mm in Counts
- 24) OBS+0.5 : Observation -1.00+0.5mm Weight in grams
- 25) OBS+0.25 : Observation -0.5+0.25mm Weight in grams
- 26) Observer
- 27) Repicker

Sample Number	SWT kg	MWT +0.5 g	MWT +0.25 g	MicroDMS Sinks +0.5 g	MicroDMS Sinks +0.25 g	MIF+0.5 g	MIF+0.25 g	MIS+0.5 g	MIS+0.25 g	MAGS+0.5 g	MAGS+0.25 g	Pyr-p + Counts	Pyr-p - Counts	Pyr-e + Counts	Pyr-e - Counts
17-RS-001-A	14.70	1233.9	1020.7	205.2	192.7	201.6262	188.1554	3.3281	4.1769	1.4342	1.3248	0	0	0	0
17-RS-002-A	11.75	1046.7	828.2	149.5	129.8	146.3712	125.9299	2.9313	3.6872	1.3612	1.2442	0	2	0	0
17-RS-003-A	12.55	1018.4	859.6	160.0	120.6	157.2079	117.0061	2.5774	3.4688	1.1546	1.2067	0	0	0	0
17-RS-006-A	13.95	847.0	688.8	130.1	86.2	127.0944	82.8572	2.6244	3.1022	1.1365	1.0644	0	0	0	0
17-RS-018-A	12.10	915.1	961.3	143.6	134.5	141.2304	131.1015	2.0201	3.1580	0.8916	1.0685	2	6	0	0
17-RS-020-A	13.45	1153.4	1055.6	168.4	127.8	164.783	122.6804	3.4736	4.7971	1.5945	1.4829	0	11	0	0
17-RS-032-A	11.70	677.1	844.5	118.7	108.8	117.0583	103.2808	1.4524	5.1700	0.7062	1.0642	0	0	0	0
17-RS-036-A	14.35	2688.5	889.8	548.5	141.1	528.0859	111.9938	19.7082	28.9064	7.6861	9.3494	2	1	0	0
17-RS-038-A	10.50	1236.6	973.2	199.1	132.2	195.5892	126.97	3.1747	5.0564	1.3383	1.4416	0	2	0	0
17-RS-040-A	10.65	1553.7	1532.9	282.4	216.9	278.3653	207.4588	3.6950	9.4754	1.6947	2.3729	0	4	0	0
14-RS-041-A	10.70	1117.8	1084.8	196.9	146.1	193.3323	140.12	3.5363	6.0517	1.3739	1.6711	0	0	0	0
17-RS-042-A	14.80	1949.1	1041.0	314.0	131.9	306.7824	122.7726	6.9325	9.1301	2.9126	2.8338	0	1	0	0

University Of Waterloo

Attention: Rebecca Stirling

PO #/Product: SC455876

Samples: 12

**Test Report  
MicroDMS**

Date of Report: March 1, 2018

Sample Number	Chr D + Counts	Chr D - Counts	Olv + Counts	Olv - Counts	Picroilm + Counts	Picroilm - Counts	Chr + Counts	Chr - Counts	OBS+0.5 g	OBS+0.25 g	Observer	Repicker
17-RS-001-A	0	0	0	0	0	0	0	0	1.8937	2.8613	JK	n/a
17-RS-002-A	0	0	0	0	0	0	0	0	1.5710	2.4440	JK	n/a
17-RS-003-A	0	0	1	0	0	0	0	0	1.4240	2.2634	JK	n/a
17-RS-006-A	0	0	0	0	0	0	0	0	1.4883	2.0378	JK	n/a
17-RS-018-A	0	0	1	3	0	0	0	1	1.1299	2.0881	JK	SR
17-RS-020-A	0	0	3	10	0	0	0	0	1.8801	3.3183	JK	SR
17-RS-032-A	0	0	0	3	0	0	0	0	0.7493	4.1078	JK	n/a
17-RS-036-A	0	0	0	1	0	0	0	1	12.0212	19.5585	JK	n/a
17-RS-038-A	0	0	0	1	0	0	0	2	1.8378	3.6171	SR	SR
17-RS-040-A	0	0	0	0	0	0	0	0	1.9990	7.1001	SR	JK
14-RS-041-A	0	0	1	0	0	0	0	1	2.1635	4.3830	JK	n/a
17-RS-042-A	0	0	0	0	0	0	0	0	4.0186	6.2973	JK	SR

All samples were MI processed at 3.30 S.G.



## EPMA Report AMC2018-013

SampleID	GrainNo.	Mineral	G-Class	SiO2	TiO2	Al2O3	Cr2O3	V2O3	FeO	MnO	NiO	ZnO	MgO	CaO	Na2O	K2O	Nb2O5	Total
GOR128	1			45.885	0.280	9.900	0.332	0.021	9.831	0.173	0.132	<0.005	26.098	6.217	0.570	0.037	<0.008	99.476
GOR128	2			46.000	0.281	9.928	0.330	0.018	9.909	0.176	0.137	<0.005	26.053	6.219	0.570	0.038	<0.008	99.660
GOR128	3			45.918	0.284	9.942	0.333	0.021	9.855	0.172	0.139	<0.005	25.939	6.203	0.572	0.036	0.011	100.523
GOR128	4			46.061	0.288	9.989	0.336	0.023	9.806	0.178	0.132	<0.005	25.891	6.218	0.577	0.033	0.013	99.543
GOR128	5			45.873	0.285	9.952	0.336	0.020	9.876	0.173	0.139	<0.005	26.113	6.235	0.578	0.035	0.009	99.621
17-RS-002-A PYR	1	garnet	G11	40.264	0.507	15.541	9.942	0.044	7.074	0.335	<0.004	<0.006	18.643	6.740	0.027	<0.001	<0.008	99.116
17-RS-002-A PYR	2	garnet	G9	40.298	0.257	16.393	9.372	0.040	7.493	0.376	<0.004	<0.005	18.254	6.539	0.019	<0.001	<0.008	99.040
17-RS-003-A OLV	1	olivine		40.533	0.003	0.020	0.068	<0.002	8.838	0.110	0.373	<0.005	49.980	0.066	0.016	0.002	0.019	100.028
17-RS-018-A PYR	1	garnet	G9	41.246	0.315	18.610	6.637	0.039	6.740	0.328	<0.004	<0.005	20.077	5.302	0.029	<0.001	0.013	99.337
17-RS-018-A PYR	2	garnet	G1	41.645	0.507	20.952	3.178	0.031	7.143	0.308	<0.004	<0.005	20.673	4.790	0.042	0.004	<0.008	99.272
17-RS-018-A PYR	3	garnet	G9	41.570	0.040	21.791	3.536	0.023	7.363	0.340	<0.004	<0.005	20.350	4.626	0.017	<0.001	<0.008	99.655
17-RS-018-A PYR	4	garnet	G9	40.646	0.137	17.667	7.974	0.045	7.274	0.337	<0.004	<0.005	18.720	6.414	0.013	0.002	<0.008	99.229
17-RS-018-A PYR	5	garnet	G9	40.474	0.310	17.561	8.280	0.038	7.296	0.384	<0.004	<0.005	18.802	5.874	0.041	<0.001	<0.008	99.062
17-RS-018-A PYR	6	garnet	G9	41.147	0.100	17.934	8.431	0.030	7.684	0.452	<0.004	<0.005	18.487	5.663	0.024	<0.001	<0.008	99.953
17-RS-018-A PYR	7	garnet	G10D	41.000	0.030	13.339	13.678	0.052	6.693	0.328	<0.004	<0.006	18.497	6.283	<0.002	<0.001	<0.008	99.900
17-RS-018-A PYR	8	garnet	G11	40.408	0.431	13.012	13.479	0.056	6.855	0.366	<0.004	<0.006	16.729	8.337	0.029	<0.001	<0.008	99.702
17-RS-018-A OLV	1	olivine		40.804	<0.002	<0.003	0.026	<0.002	7.352	0.088	0.351	<0.005	51.174	0.017	0.002	0.002	<0.008	99.816
17-RS-018-A OLV	2	olivine		40.090	0.023	<0.003	0.023	<0.002	9.623	0.126	0.296	<0.005	49.265	0.032	0.002	<0.001	<0.008	99.479
17-RS-018-A OLV	3	epidote		37.231	0.064	27.365	0.008	0.027	7.912	0.143	<0.004	<0.006	0.034	23.804	<0.002	0.002	0.013	96.602
17-RS-018-A OLV	4	olivine		40.189	0.006	<0.003	0.031	<0.002	8.804	0.099	0.376	<0.005	49.687	0.027	0.003	0.003	<0.008	99.225
17-RS-018-A CHR	1	chromite		0.023	0.165	7.568	52.619	0.057	33.681	1.102	0.006	1.556	0.901	0.002	0.092	<0.001	<0.009	97.771
17-RS-020-A PYR	1	garnet	G10D	40.333	0.071	16.513	10.240	0.042	6.973	0.440	<0.004	<0.005	19.359	5.057	0.016	<0.001	<0.008	99.045
17-RS-020-A PYR	2	garnet	G10	41.847	0.026	18.193	7.936	0.039	7.001	0.426	<0.004	<0.005	19.612	5.047	0.013	<0.001	<0.008	100.139
17-RS-020-A PYR	3	garnet	G11	41.202	0.779	18.085	6.207	0.051	8.179	0.414	<0.004	<0.005	16.992	7.896	0.060	<0.001	0.013	99.878
17-RS-020-A PYR	4	garnet	G11	40.934	0.525	19.144	5.959	0.037	7.239	0.345	<0.004	<0.005	19.562	5.332	0.057	<0.001	0.009	99.144
17-RS-020-A PYR	5	garnet	G11	40.961	0.564	19.401	5.151	0.041	8.516	0.405	<0.004	<0.005	17.872	6.524	0.053	0.004	<0.008	99.491
17-RS-020-A PYR	6	garnet	G11	41.774	0.547	19.887	4.934	0.049	7.116	0.332	<0.004	<0.005	19.662	5.381	0.054	<0.001	<0.008	99.735
17-RS-020-A PYR	7	garnet	G11	41.595	0.546	18.038	6.857	0.034	6.797	0.311	0.005	<0.005	19.503	5.801	0.026	<0.001	<0.008	99.513
17-RS-020-A PYR	8	garnet	G9	41.457	0.397	18.227	7.019	0.039	7.544	0.361	<0.004	<0.005	18.998	5.769	0.031	<0.001	<0.008	99.842
17-RS-020-A PYR	9	garnet	G9	41.918	0.120	19.999	5.375	0.031	6.775	0.309	<0.004	<0.005	19.954	5.293	0.008	<0.001	<0.008	99.783
17-RS-020-A PYR	10	garnet	G9	41.150	0.065	20.276	4.729	0.055	7.634	0.323	<0.004	<0.005	19.446	5.420	0.008	<0.001	<0.008	99.107
17-RS-020-A PYR	11	garnet	G9	41.191	0.187	20.901	4.147	0.047	7.146	0.332	<0.004	<0.005	20.106	5.122	<0.002	0.002	<0.008	99.180
17-RS-020-A OLV	1	olivine		40.374	0.004	0.008	0.043	<0.002	7.436	0.102	0.369	<0.005	50.830	0.028	0.003	0.002	<0.008	99.200
17-RS-020-A OLV	2	olivine		40.431	<0.002	<0.003	0.021	<0.002	8.312	0.090	0.365	<0.005	50.131	0.026	<0.002	0.002	<0.008	99.378
17-RS-020-A OLV	3	olivine		41.108	0.002	0.003	0.035	<0.002	8.977	0.112	0.371	<0.005	49.222	0.035	<0.002	0.004	<0.008	99.870
17-RS-020-A OLV	4	olivine		40.311	<0.002	<0.003	0.062	<0.002	7.507	0.103	0.358	<0.005	50.648	0.033	0.004	0.002	<0.008	99.028

SampleID	GrainNo.	Mineral	G-Class	SiO2	TiO2	Al2O3	Cr2O3	V2O3	FeO	MnO	NiO	ZnO	MgO	CaO	Na2O	K2O	Nb2O5	Total
17-RS-020-A OLV	5	olivine		41.425	<0.002	<0.003	0.042	<0.002	6.916	0.076	0.354	<0.005	50.908	0.014	<0.002	<0.001	0.019	99.753
17-RS-020-A OLV	6	olivine		41.222	<0.002	<0.003	0.028	<0.002	8.545	0.108	0.389	<0.005	49.815	0.031	0.002	0.003	0.021	100.163
17-RS-020-A OLV	7	olivine		40.355	0.006	<0.003	0.041	<0.002	7.598	0.102	0.376	<0.005	50.536	0.015	0.008	<0.001	<0.008	99.037
17-RS-020-A OLV	8	olivine		40.262	<0.002	<0.003	0.046	<0.002	8.409	0.121	0.386	0.019	49.981	0.033	<0.002	<0.001	<0.008	99.255
17-RS-020-A OLV	9	olivine		41.356	0.015	<0.003	0.038	<0.002	8.442	0.121	0.375	0.009	49.758	0.022	0.005	0.002	<0.008	100.144
17-RS-020-A OLV	10	olivine		41.381	<0.002	<0.003	0.013	<0.002	7.781	0.098	0.350	<0.005	50.258	0.013	<0.002	<0.001	<0.008	99.894
17-RS-020-A OLV	11	olivine		40.422	0.012	0.004	0.030	<0.002	7.926	0.093	0.398	<0.005	50.279	0.031	0.003	0.006	0.013	99.216
17-RS-020-A OLV	12	olivine		40.971	0.030	<0.003	0.016	<0.002	9.379	0.134	0.253	<0.005	49.077	0.026	0.002	<0.001	<0.008	99.887
17-RS-020-A OLV	13	olivine		41.024	<0.002	0.004	0.054	<0.002	8.868	0.113	0.389	<0.005	49.449	0.039	0.008	<0.001	<0.008	99.950
17-RS-032-A OLV	1	olivine		41.239	0.014	<0.003	0.045	<0.002	8.345	0.121	0.376	<0.005	49.788	0.019	0.009	0.001	0.013	99.971
17-RS-032-A OLV	2	olivine		41.216	0.007	<0.003	0.031	<0.002	8.865	0.109	0.403	<0.005	49.452	0.038	0.003	<0.001	<0.008	100.123
17-RS-032-A OLV	3	olivine		41.358	0.009	<0.003	0.029	<0.002	7.948	0.103	0.358	<0.005	50.119	0.019	0.004	0.003	<0.008	99.949
17-RS-036-A PYR	1	garnet	G9	42.365	0.236	21.018	3.965	0.032	6.537	0.298	<0.004	<0.005	20.762	4.728	0.016	0.003	0.010	99.968
17-RS-036-A PYR	2	garnet	G11	40.934	0.428	17.354	8.052	0.040	7.347	0.353	0.006	<0.005	18.622	6.242	0.035	<0.001	<0.008	99.414
17-RS-036-A PYR	3	garnet	G9	41.176	0.036	18.133	7.950	0.042	6.896	0.352	<0.004	<0.005	18.934	5.926	0.014	0.003	<0.008	99.462
17-RS-036-A OLV	1	olivine		40.994	0.010	0.013	0.030	<0.002	8.551	0.112	0.382	<0.005	49.716	0.043	0.009	<0.001	<0.008	99.858
17-RS-036-A CHR	1	chromite		0.030	0.336	12.089	48.784	0.138	27.787	0.317	0.139	0.053	8.445	<0.002	0.004	<0.001	<0.009	98.121
17-RS-038-A PYR	1	garnet	G9	41.479	0.073	18.781	7.257	0.035	6.710	0.353	<0.004	<0.005	19.323	5.795	0.012	<0.001	<0.008	99.818
17-RS-038-A PYR	2	garnet	G9	41.236	0.208	18.920	7.050	0.037	8.017	0.512	0.006	<0.005	18.203	5.793	0.041	<0.001	<0.008	100.022
17-RS-038-A OLV	1	olivine		41.435	0.016	<0.003	0.023	<0.002	7.673	0.088	0.376	<0.005	50.532	0.024	<0.002	<0.001	0.014	100.181
17-RS-038-A CHR	1	cr-spinel		<0.004	0.425	16.963	47.424	0.153	21.580	0.242	0.113	0.036	11.709	<0.002	<0.003	<0.001	<0.009	98.645
17-RS-038-A CHR	2	chromite		0.038	0.105	9.356	50.232	0.078	33.748	1.599	<0.005	2.249	0.522	<0.002	0.123	<0.001	<0.009	98.050
17-RS-040-A PYR	1	garnet	G9	41.948	0.348	21.567	3.259	0.023	8.048	0.365	<0.004	<0.005	19.721	4.818	0.046	<0.001	<0.008	100.143
17-RS-040-A PYR	2	garnet	G11	41.592	0.510	18.123	6.804	0.038	7.183	0.308	0.013	<0.005	19.675	5.563	0.029	<0.001	<0.008	99.837
17-RS-040-A PYR	3	garnet	G9	41.062	0.128	18.395	7.328	0.028	7.752	0.431	<0.004	<0.005	18.625	5.651	0.019	<0.001	<0.008	99.418
17-RS-040-A PYR	4	garnet	G9	41.728	0.264	20.161	4.769	0.037	7.834	0.350	<0.004	<0.005	19.431	5.365	0.012	<0.001	<0.008	99.951
17-RS-041-A OLV	1	olivine		41.236	0.018	<0.003	0.026	<0.002	8.341	0.090	0.394	<0.005	49.873	0.021	0.004	0.001	0.011	100.017
17-RS-041-A CHR	1	chromite		<0.004	0.258	8.978	52.800	0.123	29.931	0.308	0.162	0.383	5.060	0.007	0.023	0.007	<0.009	98.041
17-RS-042-A PYR	1	garnet	G12	41.262	0.460	19.849	4.640	0.044	8.514	0.416	0.005	<0.005	17.552	7.148	0.034	<0.001	<0.008	99.923

Kimberlite Indicator Mineral Grain Morphology Sheet											Group :	D-17-168
Sample Name	Quantity	Location	Fraction	Grain Type	Colour	Shape	Clarity	Lustre	Surface Feature	Comment	Date	Observer
17-RS-002-A	1	1	-0.50 / +0.25 mm	Pyr-p	Purple	Fragm	Transparent	Vitreous	Kelyphite Rim		12-Feb-2018	JK
17-RS-002-A	1	2	-0.50 / +0.25 mm	Pyr-p	Purple	Fragm	Transparent	Vitreous	Pitted		12-Feb-2018	JK
17-RS-003-A	1	1	-1.00 / +0.50 mm	Olv	Yellow	Irr	Translucent	Vitreous	None		13-Feb-2018	JK
17-RS-018-A	1	1	-0.50 / +0.25 mm	Chr	Black	Irr	Opaque	Shiny	Pitted		23-Feb-2018	JK
17-RS-018-A	1	1	-1.00 / +0.50 mm	Pyr-p	Purple	Fragm	Transparent	Vitreous	Pitted		14-Feb-2018	JK
17-RS-018-A	1	2	-1.00 / +0.50 mm	Pyr-p	Red-Purple	Fragm	Transparent	Vitreous	Pitted		14-Feb-2018	JK
17-RS-018-A	1	3	-0.50 / +0.25 mm	Pyr-p	Purple-Pink	Fragm	Transparent	Vitreous	Pitted		14-Feb-2018	JK
17-RS-018-A	5	4	-0.50 / +0.25 mm	Pyr-p	Purple	Fragm	Transparent	Vitreous	Pitted		14-Feb-2018	JK
17-RS-018-A	1	1	-1.00 / +0.50 mm	Olv	Yellow	Irr	Translucent	Vitreous	None		14-Feb-2018	JK
17-RS-018-A	3	2	-0.50 / +0.25 mm	Olv	Yellow	Irr	Translucent	Vitreous	None		14-Feb-2018	JK
17-RS-020-A	8	1	-0.50 / +0.25 mm	Pyr-p	Purple	Fragm	Transparent	Vitreous	Pitted	pyrite present	14-Feb-2018	JK
17-RS-020-A	3	9	-0.50 / +0.25 mm	Pyr-p	Purple-Pink	Fragm	Transparent	Vitreous	Pitted	pyrite present	14-Feb-2018	JK
17-RS-020-A	3	1	-1.00 / +0.50 mm	Olv	Yellow	Irr	Translucent	Vitreous	None	pyrite present	14-Feb-2018	JK
17-RS-020-A	9	4	-0.50 / +0.25 mm	Olv	Yellow	Irr	Translucent	Vitreous	None	pyrite present	14-Feb-2018	JK
17-RS-020-A	1	13	-0.50 / +0.25 mm	Olv	Yellow	Irr	Translucent	Vitreous	Striations	pyrite present	28-Feb-2018	JK
17-RS-032-A	3	1	-0.50 / +0.25 mm	Olv	Yellow	Irr	Translucent	Vitreous	None	#1 olv broken into 2 pieces	22-Feb-2018	JK
17-RS-036-A	1	1	-0.50 / +0.25 mm	Chr	Black	Irr	Opaque	Matte	Pitted	pyrite present	22-Feb-2018	JK
17-RS-036-A	1	1	-1.00 / +0.50 mm	Pyr-p	Purple-Pink	Fragm	Transparent	Vitreous	Pitted	pyrite present	22-Feb-2018	JK
17-RS-036-A	1	2	-1.00 / +0.50 mm	Pyr-p	Purple	Fragm	Transparent	Vitreous	Pitted	pyrite present	22-Feb-2018	JK
17-RS-036-A	1	3	-0.50 / +0.25 mm	Pyr-p	Purple	Fragm	Transparent	Vitreous	Pitted	pyrite present	22-Feb-2018	JK
17-RS-036-A	1	1	-0.50 / +0.25 mm	Olv	Yellow	Irr	Translucent	Vitreous	None	pyrite present	22-Feb-2018	JK
17-RS-038-A	1	1	-0.50 / +0.25 mm	Chr	Black	Octahedra	Opaque	Shiny	Pitted		01-Mar-2018	SR
17-RS-038-A	1	1	-0.50 / +0.25 mm	Chr	Black	Irr	Opaque	Shiny	Pitted		01-Mar-2018	SR
17-RS-038-A	2	1	-0.50 / +0.25 mm	Pyr-p	Purple	Fragm	Transparent	Vitreous	Pitted		21-Feb-2018	SR
17-RS-038-A	1	1	-0.50 / +0.25 mm	Olv	Yellow	Irr	Translucent	Vitreous	Striations		21-Feb-2018	SR
17-RS-040-A	1	1	-0.50 / +0.25 mm	Pyr-p	Red-Purple	Fragm	Transparent	Vitreous	Pitted	pyrite present	22-Feb-2018	SR
17-RS-040-A	2	2	-0.50 / +0.25 mm	Pyr-p	Purple	Fragm	Transparent	Vitreous	Pitted	pyrite present	22-Feb-2018	SR
17-RS-040-A	1	1	-0.50 / +0.25 mm	Pyr-p	Purple-Pink	Fragm	Transparent	Vitreous	Pitted	pyrite present	01-Mar-2018	SR
14-RS-041-A	1	1	-0.50 / +0.25 mm	Chr	Black	Irr	Opaque	Shiny	Pitted		22-Feb-2018	JK
14-RS-041-A	1	1	-1.00 / +0.50 mm	Olv	Yellow	Irr	Translucent	Vitreous	None		22-Feb-2018	JK
17-RS-042-A	1	1	-0.50 / +0.25 mm	Pyr-p	Purple-Pink	Fragm	Transparent	Vitreous	Pitted		27-Feb-2018	JK

## nKIM Calculations

SampleID	StudyArea	CollarEasting	CollarNorthing	From	To	nKIM	Depth Interval	Depth Interval Bin	Sample Count added	KIM sum	KIM avg	Notes
HWRC-040-01	e	533889	7129918	0	2	0.6	0.250	4	1	0.6	0.6	
HWRC-040-02	e	533889	7129918	2	2.5	0.0	0.750	1	1	0.0	0.0	
HWRC-041-01	e	533865	7130847	0	3	0.0	0.250	4	1	0.0	0.0	
HWRC-041-02	e	533865	7130847	3	3.5	0.0	0.750	1	1	0.0	0.0	
HWRC-042-01	e	533887	7131814	0	1	0.0	0.500	4	1	0.0	0.0	
HWRC-043-01	e	533876	7132854	0	1.8	0.0	0.500	4	1	0.0	0.0	
HWRC-044-01	e	533886	7133844	0	1.5	0.0	0.167	4	1	0.0	0.0	
HWRC-044-02	e	533886	7133844	1.5	3	1.1	0.500	3	1	1.1	1.1	
HWRC-044-03	e	533886	7133844	3	4.5	1.9	0.833	1	1	1.9	1.9	
HWRC-045-01	e	533889	7134856	0	1.5	0.0	0.167	4	1	0.0	0.0	
HWRC-045-02	e	533889	7134856	1.5	3	0.5	0.500	3	1	0.5	0.5	
HWRC-045-03	e	533889	7134856	3	4.4	0.5	0.833	1	1	0.5	0.5	
HWRC-046-01	e	533883	7135833	0.2	2	0.0	0.100	4	1	0.0	0.0	
HWRC-046-02	e	533883	7135833	2	3.5	0.0	0.300	3	2	0.0	0.0	
HWRC-046-03	e	533883	7135833	3.5	5	0.0	0.500	3	2			
HWRC-046-04	e	533883	7135833	5	6.5	1.6	0.700	2	1	1.6	1.6	
HWRC-046-05	e	533883	7135833	6.5	8.2	0.5	0.900	1	1	0.5	0.5	
HWRC-047-01	e	533881	7136842	0	1.5	1.3	0.100	4	1	1.3	1.3	
HWRC-047-02	e	533881	7136842	1.5	3	0.0	0.300	3	2	0.5	0.2	
HWRC-047-03	e	533881	7136842	3	4.5	0.5	0.500	3	2			
HWRC-047-04	e	533881	7136842	4.5	6	0.6	0.700	2	1	0.6	0.6	
HWRC-047-05	e	533881	7136842	6	7.8	1.3	0.900	1	1	1.3	1.3	
HWRC-048-01	e	533882	7137842	0	1.5	5.2	0.125	4	1	5.2	5.2	
HWRC-048-02	e	533882	7137842	1.5	3	13.9	0.375	3	1	13.9	13.9	
HWRC-048-03	e	533882	7137842	3	4.8	13.4	0.625	2	1	13.4	13.4	
HWRC-048-04	e	533882	7137842	4.8	6	1.9	0.875	1	1	1.9	1.9	
HWRC-049-01	e	530835	7137888	0	1.5	0.6	0.167	4	1	0.6	0.6	
HWRC-049-02	e	530835	7137888	1.5	3	0.7	0.500	3	1	0.7	0.7	
HWRC-049-03	e	530835	7137888	3	4.6	1.9	0.833	1	1	1.9	1.9	
HWRC-050-01	e	530929	7138776	0	0.2	0.7	0.500	4	1	0.7	0.7	
HWRC-051-01	e	533882	7138721	0	1.5	0.0	0.125	4	1	0.0	0.0	
HWRC-051-02	e	533882	7138721	1.5	3	0.0	0.375	3	1	0.0	0.0	
HWRC-051-03	e	533882	7138721	3	4.5	0.0	0.625	2	1	0.0	0.0	
HWRC-051-04	e	533882	7138721	4.5	5.4	0.0	0.875	1	1	0.0	0.0	
HWRC-052-01	e	530887	7136858	0	1.5	0.6	0.250	4	1	0.6	0.6	
HWRC-052-02	e	530887	7136858	1.5	2.8	2.4	0.750	1	1	2.4	2.4	
HWRC-053-01	e	530890	7135852	0	1	0.0	0.125	4	1	0.0	0.0	
HWRC-053-02	e	530890	7135852	2.5	3.2	1.0	0.375	3	1	1.0	1.0	
HWRC-053-03	e	530890	7135852	3.8	4.2	2.0	0.625	2	1	2.0	2.0	
HWRC-053-04	e	530890	7135852	4.6	4.8	0.0	0.875	1	1	0.0	0.0	
HWRC-054-01	e	530962	7134835	0	0.6	0.0	0.500	4	1	0.0	0.0	
HWRC-055-01	e	530939	7133753	0	1.8	0.0	0.500	4	1	0.0	0.0	
HWRC-056-01	e	530861	7132803	0	1.4	0.0	0.500	4	1	0.0	0.0	
HWRC-057-01	e	530779	7131825	0	1	0.0	0.500	4	1	0.0	0.0	
HWRC-059-01	e	530884	7129853	1	1.5	0.0	0.250	4	1	0.0	0.0	
HWRC-059-02	e	530884	7129853	1.5	3.2	0.0	0.750	1	1	0.0	0.0	
HWRC-166-01	w	515887	7128816	0	1.2	0.0	0.500	4	1	0.0	0.0	
HWRC-167-01	w	515789	7130868	0	2	0.0	0.167	4	1	0.0	0.0	
HWRC-167-02	w	515789	7130868	2	3	0.4	0.500	3	1	0.4	0.4	
HWRC-167-03	w	515789	7130868	3	4.5	0.0	0.833	1	1	0.0	0.0	
HWRC-168-01	w	516057	7131840	0	1.5	0.0	0.083	4	2	0.0	0.0	
HWRC-168-02	w	516057	7131840	1.5	3	0.0	0.250	4	2			
HWRC-168-03	w	516057	7131840	3	4.5	0.0	0.417	3	1	0.0	0.0	
HWRC-168-04	w	516057	7131840	4.5	6	0.5	0.583	2	2	1.0	0.5	
HWRC-168-05	w	516057	7131840	6	7.5	0.5	0.750	2	2			
HWRC-168-06	w	516057	7131840	7.5	9	0.0	0.917	1	1	0.0	0.0	
HWRC-169-01	w	515936	7132946	0	1.5	0.0	0.125	4	1	0.0	0.0	
HWRC-169-02	w	515936	7132946	1.5	3	0.0	0.375	3	1	0.0	0.0	
HWRC-169-03	w	515936	7132946	3	4.5	0.0	0.625	2	1	0.0	0.0	
HWRC-169-04	w	515936	7132946	4.5	5.6	0.0	0.875	1	1	0.0	0.0	
HWRC-170-01	w	516061	7133906	0	2	1.7	0.500	4	1	1.7	1.7	

SampleID	StudyArea	CollarEasting	CollarNorthing	From	To	nKIM	Depth Interval	Depth Interval Bin	Sample Count added	KIM sum	KIM avg	Notes
HWRC-171-01	w	516092	7134904	0	1.5	0.0	0.100	4	1	0.0	0.0	
HWRC-171-02	w	516092	7134904	1.5	3	0.0	0.300	3	2	0.5	0.3	
HWRC-171-03	w	516092	7134904	3	4.5	0.5	0.500	3	2			
HWRC-171-04	w	516092	7134904	4.5	6	0.0	0.700	2	1	0.0	0.0	
HWRC-171-05	w	516092	7134904	6	7	0.0	0.900	1	1	0.0	0.0	
HWRC-172-01	w	515891	7135813	0	1.8	0.0	0.500	4	1	0.0	0.0	
HWRC-173-01	w	515881	7136823	0	1.8	2.2	0.500	4	1	2.2	2.2	
HWRC-174-01	w	512898	7136861	0	1.2	0.5	0.500	4	1	0.5	0.5	
HWRC-175-01	w	512910	7134790	0	1.4	0.0	0.250	4	1	0.0	0.0	
HWRC-175-02	w	512910	7134790	1.4	2.6	0.5	0.750	1	1	0.5	0.5	
HWRC-176-01	w	512890	7133862	0	1.2	0.0	0.250	4	1	0.0	0.0	
HWRC-176-02	w	512890	7133862	1.2	2.2	0.0	0.750	1	1	0.0	0.0	
HWRC-177-01	w	512885	7132870	0	2	0.0	0.500	4	1	0.0	0.0	
HWRC-178-01	w	512891	7131876	0	1.4	0.5	0.500	4	1	0.5	0.5	
HWRC-179-01	w	512884	7130847	0	1.6	0.5	0.250	4	1	0.5	0.5	
HWRC-179-02	w	512884	7130847	1.6	3.4	0.0	0.750	1	1	0.0	0.0	
HWRC-180-01	w	512694	7129949	0	1	0.0	0.500	4	1	0.0	0.0	
HWRC-181-01	w	512765	7128818	0	1.5	1.2	0.167	4	1	1.2	1.2	
HWRC-181-02	w	512765	7128818	1.5	3	0.5	0.500	3	1	0.5	0.5	
HWRC-181-03	w	512765	7128818	3	4	0.6	0.833	1	1	0.6	0.6	
HWRC-204-01	w	509883	7128860	0	2	0.0	0.500	4	1	0.0	0.0	
HWRC-205-01	w	509925	7129741	0	1.5	0.0	0.167	4	1	0.0	0.0	
HWRC-205-02	w	509925	7129741	1.5	3	0.0	0.500	3	1	0.0	0.0	
HWRC-205-03	w	509925	7129741	3	5	0.0	0.833	1	1	0.0	0.0	
HWRC-206-01	w	509770	7130950	0	1	0.0	0.500	4	1	0.0	0.0	
HWRC-207-01	w	509876	7131838	0	1.45	0.0	0.083	4	2	0.0	0.0	
HWRC-207-02	w	509876	7131838	1.45	3	0.0	0.250	4	2			
HWRC-207-03	w	509876	7131838	3	4.5	0.0	0.417	3	1	0.0	0.0	
HWRC-207-04	w	509876	7131838	4.5	6	0.0	0.583	2	2	1.3	0.6	
HWRC-207-05	w	509876	7131838	6	7.5	1.3	0.750	2	2			
HWRC-207-06	w	509876	7131838	7.5	8.4	0.0	0.917	1	1	0.0	0.0	
HWRC-208-01	w	509913	7132927	0	1.5	1.1	0.045	4	3	1.6	0.5	
HWRC-208-02	w	509913	7132927	1.5	3	0.5	0.136	4	3			
HWRC-208-03	w	509913	7132927	3	4.5	0.0	0.227	4	3			
HWRC-208-04	w	509913	7132927	4.5	6	1.1	0.318	3	3	2.4	0.8	
HWRC-208-05	w	509913	7132927	6	7.5	0.6	0.409	3	3			
HWRC-208-06	w	509913	7132927	7.5	9	0.7	0.500	3	3			
HWRC-208-07	w	509913	7132927	9	10.5	0.6	0.591	2	2	1.2	0.6	
HWRC-208-08	w	509913	7132927	10.5	12	0.6	0.682	2	2			
HWRC-208-09	w	509913	7132927	12	13.5	0.0	0.773	1	3	1.1	0.4	
HWRC-208-10	w	509913	7132927	13.5	15	1.1	0.864	1	3			
HWRC-208-11	w	509913	7132927	15	16.4	0.0	0.955	1	3			
HWRC-209-01	w	509986	7133919	0	1.5	0.0	0.250	4	1	0.0	0.0	
HWRC-209-02	w	509986	7133919	1.5	2	0.0	0.750	1	1	0.0	0.0	
HWRC-210-01	w	509866	7134899	0	1.5	0.6	0.250	4	1	0.6	0.6	
HWRC-210-02	w	509866	7134899	1.5	1.6	0.0	0.750	1	1	0.0	0.0	
HWRC-211-01	w	506929	7136728	0	1.5	0.0	0.250	4	1	0.0	0.0	
HWRC-211-02	w	506929	7136728	1.5	2.9	0.7	0.750	1	1	0.7	0.7	
HWRC-212-01	w	506893	7135833	0	0.6	0.0	0.500	4	1	0.0	0.0	
HWRC-213-01	w	506987	7134872	0	1	0.0	0.500	4	1	0.0	0.0	
HWRC-214-01	w	506878	7133857	0	1.5	0.5	0.250	4	1	0.5	0.5	
HWRC-214-02	w	506878	7133857	1.5	3.5	0.0	0.750	1	1	0.0	0.0	
HWRC-215-01	w	506836	7132756	0	0.5	0.0	0.500	4	1	0.0	0.0	
HWRC-216-01	w	506862	7131848	0	1.5	0.0	0.250	4	1	0.0	0.0	
HWRC-216-02	w	506862	7131848	1.5	3.2	0.0	0.750	1	1	0.0	0.0	
HWRC-217-01	w	506831	7130665	0	1	0.0	0.500	4	1	0.0	0.0	
HWRC-218-01	w	506892	7129838	0	1.5	5.6	0.167	4	1	5.6	5.6	
HWRC-218-02	w	506892	7129838	1.5	3	0.0	0.500	3	1	0.0	0.0	
HWRC-218-03	w	506892	7129838	3	5.25	0.0	0.833	1	1	0.0	0.0	
HWRC-219-01	w	506929	7128796	0	1.5	1.8	0.167	4	1	1.8	1.8	
HWRC-219-02	w	506929	7128796	1.5	3	1.1	0.500	3	1	1.1	1.1	
HWRC-219-03	w	506929	7128796	3	5.25	0.0	0.833	1	1	0.0	0.0	
HWRC-226-01	w	505470	7128865	0.6	1.5	0.0	0.500	4	1	0.0	0.0	
HWRC-227-01	w	505353	7129839	0	1.5	0.0	0.125	4	1	0.0	0.0	



SampleID	StudyArea	CollarEasting	CollarNorthing	From	To	nKIM	Depth Interval	Depth Interval Bin	Sample Count added	KIM sum	KIM avg	Notes
HWRC-227-02	w	505353	7129839	1.5	3	0.0	0.375	3	1	0.0	0.0	
HWRC-227-03	w	505353	7129839	3	4.5	0.6	0.625	2	1	0.6	0.6	
HWRC-227-04	w	505353	7129839	4.5	5.5	2.1	0.875	1	1	2.1	2.1	
HWRC-228-01	w	505522	7130873	0	2	0.0	0.500	4	1	0.0	0.0	
HWRC-229-01	w	505355	7131869	0	1	0.0	0.250	4	1	0.0	0.0	
HWRC-229-02	w	505355	7131869	1.5	3.5	0.5	0.750	1	1	0.5	0.5	
HWRC-230-01	w	505449	7132678	0	0.3	0.0	0.500	4	1	0.0	0.0	
HWRC-231-01	w	505486	7133863	0.2	1.5	0.0	0.167	4	1	0.0	0.0	
HWRC-231-02	w	505486	7133863	1.5	3	0.0	0.500	3	1	0.0	0.0	
HWRC-231-03	w	505486	7133863	3	3.3	0.0	0.833	1	1	0.0	0.0	
HWRC-232-01	w	505485	7134867	0.2	1.5	0.0	0.167	4	1	0.0	0.0	
HWRC-232-02	w	505485	7134867	1.5	3	0.0	0.500	3	1	0.0	0.0	
HWRC-232-03	w	505485	7134867	3	3.3	0.0	0.833	1	1	0.0	0.0	
HWRC-233-01	w	505510	7135880	0	1.5	0.9	0.167	4	1	0.9	0.9	
HWRC-233-02	w	505510	7135880	1.5	3	0.7	0.500	3	1	0.7	0.7	
HWRC-233-03	w	505510	7135880	3	4.5	0.6	0.833	1	1	0.6	0.6	
HWRC-234-01	w	505387	7136965	0	1.5	0.0	0.167	4	1	0.0	0.0	
HWRC-234-02	w	505387	7136965	1.5	3	0.0	0.500	3	1	0.0	0.0	
HWRC-234-03	w	505387	7136965	3	4.8	1.8	0.833	1	1	1.8	1.8	
HWRC-269-01	w	512866	7135462	0	1.5	0.0	0.056	4	3	1.1	0.6	
HWRC-269-02	w	512866	7135462	1.5	3	1.1	0.167	4	3			
HWRC-270-01	w	515523	7130261	0	1.5	0.0	0.167	4	1	0.0	0.0	
HWRC-482-01	e	536774	7129893	0	2	0.0	0.167	4	1	0.0	0.0	
HWRC-483-01	e	536943	7131001	0	2	0.0	0.083	4	2	0.0	0.0	
HWRC-483-02	e	536943	7131001	2	3.5	0.0	0.250	4	2			
HWRC-484-01	e	536834	7131810	0	2	0.0	0.063	4	2	0.9	0.4	
HWRC-484-02	e	536834	7131810	2	3.5	0.9	0.188	4	2			
HWRC-485-01	e	536416	7135069	0	2	0.0	0.042	4	3	3.0	1.0	
HWRC-485-02	e	536416	7135069	2	3.5	1.0	0.125	4	3			
HWRC-485-03	e	536416	7135069	3.5	5	1.9	0.208	4	3			
HWRC-486-01	e	536077	7133811	0	1	0.5	0.036	4	4	1.5	0.4	
HWRC-486-02	e	536077	7133811	1	2	0.5	0.107	4	4			
HWRC-486-03	e	536077	7133811	2	3.5	0.5	0.179	4	4			
HWRC-486-04	e	536077	7133811	3.5	5	0.0	0.250	4	4			
HWRC-487-01	e	536677	7133526	0	2	0.0	0.071	4	2	0.0	0.0	
HWRC-487-02	e	536677	7133526	2	3.5	0.0	0.214	4	2			
HWRC-487-03	e	536677	7133526	3.5	5	0.0	0.214	4	2			
HWRC-488-01	e	535945	7135629	0	3	0.0	0.071	4	2	1.1	0.5	
HWRC-488-02	e	535945	7135629	3	5	1.1	0.214	4	2			
HWRC-489-01	e	536636	7136822	0	2.4	1.7	0.500	4	1	1.7	1.7	
HWRC-490-01	e	536666	7137283	0	0.2	1.8	0.500	4	1	1.8	1.8	
HWRC-491-01	e	536455	7137941	0	2.2	4.6	0.500	4	1	4.6	4.6	
HWRC-492-01	e	535449	7138029	0	0.2	1.5	0.500	4	1	1.5	1.5	
HWRC-493-01	e	533832	7137060	0	0.7	2.2	0.500	4	1	2.2	2.2	
HWRC-494-01	e	533768	7138443	0	0.4	5.1	0.500	4	1	5.1	5.1	
HWRC-495-01	e	535351	7138251	0	2	2.9	0.500	4	1	2.9	2.9	
HWRC-496-01	e	535335	7139007	0	1	2.8	0.500	4	1	2.8	2.8	
HWRC-497-01	e	536580	7138693	0	2	6.1	0.063	4	2	6.1	3.1	
HWRC-497-02	e	536580	7138693	2	3.5	0.0	0.188	4	2			
HWRC-498-01	e	536958	7138304	0	0.8	0.0	0.500	4	1	0.0	0.0	
HWRC-499-01	e	539865	7138821	0	2	1.5	0.250	4	1	1.5	1.5	
HWRC-500-01	e	539921	7137816	0	2	2.9	0.250	4	1	2.9	2.9	
HWRC-501-01	e	539470	7136684	0	0.6	1.0	0.500	4	1	1.0	1.0	
HWRC-502-01	e	540076	7135844	0	2.4	1.2	0.500	4	1	1.2	1.2	
HWRC-503-01	e	539884	7134889	0	2	0.0	0.100	4	1	0.0	0.0	
HWRC-504-01	e	539711	7133744	0	0.4	0.0	0.500	4	1	0.0	0.0	
HWRC-505-01	e	539928	7132967	0	0.5	0.0	0.500	4	1	0.0	0.0	
HWRC-506-01	e	539987	7131749	0	1.5	0.0	0.500	4	1	0.0	0.0	
HWRC-507-01	e	539856	7130818	0	0.6	0.0	0.500	4	1	0.0	0.0	
HWRC-508-01	e	539974	7129901	0	0.6	0.0	0.500	4	1	0.0	0.0	
HWRC-509-01	e	542716	7129910	0	0.5	0.0	0.500	4	1	0.0	0.0	
HWRC-510-01	e	542884	7130708	0	0.3	0.0	0.500	4	1	0.0	0.0	
HWRC-511-01	e	542833	7131961	0	0.2	0.0	0.500	4	1	0.0	0.0	
HWRC-512-01	e	542896	7132936	0	0.4	0.0	0.250	4	1	0.0	0.0	

SampleID	StudyArea	CollarEasting	CollarNorthing	From	To	nKIM	Depth Interval	Depth Interval Bin	Sample Count added	KIM sum	KIM avg	Notes
HWRC-513-01	e	542837	7133868	0	0.4	0.0	0.500	4	1	0.0	0.0	
HWRC-514-01	e	542979	7134917	0	0.6	0.6	0.500	4	1	0.6	0.6	
HWRC-515-01	e	542742	7135996	0	1.2	1.5	0.500	4	1	1.5	1.5	
HWRC-516-01	e	542939	7136728	0	1.5	22.2	0.100	4	1	22.2	22.2	
HWRC-517-01	e	542820	7137926	0	2.2	5.2	0.500	4	1	5.2	5.2	
HWRC-518-01	e	542962	7138795	0	0.2	2.0	0.500	4	1	2.0	2.0	
HWRC-519-01	e	545809	7138350	0	0.4	0.0	0.500	4	1	0.0	0.0	
HWRC-520-01	e	545840	7137544	0	0.4	0.9	0.500	4	1	0.9	0.9	
HWRC-521-01	e	545814	7136344	0	1.5	5.9	0.500	4	1	5.9	5.9	
HWRC-522-01	e	545891	7135326	0	0.4	2.3	0.500	4	1	2.3	2.3	
HWRC-523-01	e	545968	7134302	0	1.6	0.6	0.500	4	1	0.6	0.6	
HWRC-524-01	e	545422	7133178	0	1.5	0.5	0.167	4	1	0.5	0.5	
HWRC-525-01	e	545720	7132292	0	0.4	0.4	0.500	4	1	0.4	0.4	
HWRC-526-01	e	545641	7131521	0	0.2	0.5	0.500	4	1	0.5	0.5	
HWRC-527-01	e	545365	7130311	0	0.4	0.5	0.500	4	1	0.5	0.5	
HWRC-528-01	e	545835	7129364	0	0.8	0.0	0.500	4	1	0.0	0.0	
HWRC-626-01	e	538023	7131613	0	1.5	0.0	0.250	4	1	0.0	0.0	
HWRC-627-01	e	537901	7131891	0	1.5	0.0	0.056	4	2	0.0	0.0	
HWRC-627-02	e	537901	7131891	1.5	3	0.0	0.167	4	2			
HWRC-628-01	e	537858	7132128	0	1.5	0.0	0.036	4	4	0.0	0.0	
HWRC-628-02	e	537858	7132128	1.5	3	0.0	0.107	4	4			
HWRC-628-03	e	537858	7132128	3	4.5	0.0	0.179	4	4			
HWRC-628-04	e	537858	7132128	4.5	6	0.0	0.250	4	4			
HWRC-629-01	e	537897	7132397	0	1.5	0.0	0.083	4	2	0.0	0.0	
HWRC-629-02	e	537897	7132397	1.5	3	0.0	0.250	4	2			
HWRC-630-01	e	537889	7132698	0	1.5	0.0	0.167	4	1	0.0	0.0	
HWRC-631-01	e	538247	7132882	0	1	0.0	0.500	4	1	0.0	0.0	
HWRC-632-01	e	537898	7133451	0	1	0.0	0.500	4	1	0.0	0.0	
HWRC-633-01	e	537837	7133926	0	1.2	0.0	0.500	4	1	0.0	0.0	
HWRC-634-01	e	538062	7134569	0	1.6	0.0	0.500	4	1	0.0	0.0	
HWRC-635-01	e	538006	7135040	0	1.5	0.0	0.125	4	1	0.0	0.0	
HWRC-636-01	e	537888	7135447	0	1.5	0.0	0.125	4	2	0.0	0.0	
HWRC-636-02	e	537888	7135447	0	1.5	0.0	0.125	4	2			Duplicate
HWRC-637-01	e	537900	7135946	0	1.4	0.5	0.500	4	1	0.5	0.5	
HWRC-638-01	e	537881	7136183	0	0.5	0.0	0.500	4	1	0.0	0.0	
HWRC-639-01	e	538010	7136946	0	1.5	7.2	0.042	4	3	25.1	8.4	
HWRC-639-02	e	538010	7136946	1.5	3	8.2	0.125	4	3			
HWRC-639-03	e	538010	7136946	3	4.5	9.7	0.208	4	3			
HWRC-640-01	e	538119	7137327	0	1	0.6	0.500	4	1	0.6	0.6	
HWRC-641-01	e	537833	7137436	0	0.4	2.9	0.500	4	1	2.9	2.9	
HWRC-642-01	e	537852	7137666	0	0.2	0.9	0.500	4	1	0.9	0.9	
HWRC-643-01	e	537858	7137933	0	0.3	1.1	0.500	4	1	1.1	1.1	
HWRC-644-01	e	537916	7138232	0	1.5	1.4	0.250	4	1	1.4	1.4	
HWRC-645-01	e	537904	7138738	0	1.5	0.6	0.125	4	1	0.6	0.6	
HWRC-646-01	e	535127	7137062	0	0.4	1.3	0.500	4	1	1.3	1.3	
HWRC-647-01	e	535174	7136771	0	1	1.1	0.500	4	1	1.1	1.1	
HWRC-648-01	e	535188	7136420	0	0.4	0.0	0.500	4	1	0.0	0.0	
HWRC-649-01	e	535372	7136078	0	1.2	0.0	0.500	4	1	0.0	0.0	
HWRC-650-01	e	535255	7135807	0	1.5	0.0	0.083	4	2	0.6	0.3	
HWRC-650-02	e	535255	7135807	1.5	3	0.6	0.250	4	2			
HWRC-651-01	e	535214	7135302	0	1.5	0.0	0.036	4	4	0.0	0.0	
HWRC-651-02	e	535214	7135302	1.5	3	0.0	0.107	4	4			
HWRC-651-03	e	535214	7135302	3	4.5	0.0	0.179	4	4			
HWRC-651-04	e	535214	7135302	4.5	6	0.0	0.250	4	4			
HWRC-652-01	e	535331	7135036	0	1.5	2.7	0.125	4	1	2.7	2.7	
HWRC-653-01	e	535211	7134342	0	1.5	0.0	0.056	4	2	1.3	0.7	
HWRC-653-02	e	535211	7134342	1.5	3	1.3	0.167	4	2			
HWRC-654-01	e	535275	7134110	0	1.5	0.0	0.063	4	2	0.0	0.0	
HWRC-654-02	e	535275	7134110	1.5	3	0.0	0.188	4	2			
HWRC-655-01	e	535233	7133870	0	1.5	0.6	0.167	4	1	0.6	0.6	
HWRC-656-01	e	535211	7133536	0	1.5	0.0	0.167	4	1	0.0	0.0	
HWRC-657-01	e	535243	7133325	0	1.5	0.0	0.100	4	1	0.0	0.0	
HWRC-658-01	e	535244	7133083	0	1.5	4.8	0.056	4	2	4.8	2.4	
HWRC-658-02	e	535244	7133083	1.5	3	0.0	0.167	4	2			

SampleID	StudyArea	CollarEasting	CollarNorthing	From	To	nKIM	Depth Interval	Depth Interval Bin	Sample Count added	KIM sum	KIM avg	Notes
HWRC-659-01	e	535288	7132866	0	1.5	5.1	0.167	4	1	5.1	5.1	
HWRC-660-01	e	535227	7132623	0	1.5	0.7	0.056	4	2	1.8	0.9	
HWRC-660-02	e	535227	7132623	1.5	3	1.1	0.167	4	2			
HWRC-661-01	e	535208	7132332	0	1.5	1.4	0.125	4	1	1.4	1.4	
HWRC-662-01	e	535191	7131848	0	1.5	0.0	0.500	4	1	0.0	0.0	
HWRC-663-01	e	530738	7129256	0	1.2	0.0	0.500	4	1	0.0	0.0	
HWRC-664-01	e	530900	7130060	0	1	0.0	0.500	4	1	0.0	0.0	
HWRC-665-01	e	531006	7130255	0	1	0.0	0.500	4	1	0.0	0.0	
HWRC-666-01	e	530830	7130590	0	1.5	0.0	0.500	4	1	0.0	0.0	
HWRC-667-01	e	531003	7131149	0	0.8	0.0	0.500	4	1	0.0	0.0	
HWRC-668-01	e	530780	7131283	0	0.5	0.7	0.500	4	1	0.7	0.7	
HWRC-669-01	e	530891	7131642	0	1	0.0	0.500	4	1	0.0	0.0	
HWRC-670-01	e	530805	7132276	0	0.6	0.0	0.500	4	1	0.0	0.0	
HWRC-727-01	w	514544	7132663	0	0.5	1.3	0.500	4	1	1.3	1.3	
HWRC-728-01	w	514556	7133245	0	1	0.8	0.500	4	1	0.8	0.8	
HWRC-729-01	w	514556	7133245	0	1.5	0.6	0.500	4	1	0.6	0.6	
HWRC-730-01	w	514550	7133962	0	2.7	0.0	0.500	4	1	0.0	0.0	
HWRC-731-01	w	514575	7134210	0	2.25	1.0	0.500	4	1	1.0	1.0	
HWRC-732-01	w	514630	7134425	0	3	0.0	0.167	4	1	0.0	0.0	
HWRC-733-01	w	514575	7134706	0	2.8	0.9	0.500	4	1	0.9	0.9	
HWRC-734-01	w	514562	7134945	0	2.3	0.0	0.500	4	1	0.0	0.0	
HWRC-735-01	w	514487	7135153	0	1.5	0.0	0.500	4	1	0.0	0.0	
HWRC-736-01	w	514614	7135455	0	1.6	0.5	0.500	4	1	0.5	0.5	
HWRC-737-01	w	514630	7135742	0	3	1.1	0.100	4	1	1.1	1.1	
HWRC-738-01	w	514529	7136370	0	1.5	0.9	0.056	4	2	1.4	0.7	
HWRC-738-02	w	514529	7136370	1.5	3	0.5	0.167	4	2			
HWRC-739-01	w	514557	7136733	0	1.5	0.0	0.500	4	1	0.0	0.0	
HWRC-740-01	w	511319	7134780	0	3	0.4	0.083	4	2	0.4	0.2	
HWRC-740-02	w	511319	7134780	3	4.5	0.0	0.250	4	2			
HWRC-741-01	w	511342	7134271	0	2.9	0.0	0.500	4	1	0.0	0.0	
HWRC-742-01	w	511249	7133747	0	3	0.0	0.071	4	2	0.4	0.2	
HWRC-742-02	w	511249	7133747	3	4.5	0.4	0.214	4	2			
HWRC-743-01	w	511309	7133266	0	0.2	0.0	0.500	4	1	0.0	0.0	
HWRC-744-01	w	511309	7132790	0	3	0.0	0.500	4	1	0.0	0.0	
HWRC-745-01	w	511190	7132208	0	0.1	0.0	0.500	4	1	0.0	0.0	
HWRC-746-01	w	511215	7131655	0	3	0.6	0.083	4	2	1.1	0.6	
HWRC-746-02	w	511215	7131655	3	4.5	0.5	0.250	4	2			
HWRC-747-01	w	511245	7131153	0	3	0.6	0.250	4	1	0.6	0.6	
HWRC-748-01	w	511121	7130856	0	0.1	0.0	0.500	4	1	0.0	0.0	
HWRC-749-01	w	511209	7130199	0	0.1	0.5	0.500	4	1	0.5	0.5	
HWRC-750-01	w	512488	7130241	0	0.15	0.0	0.500	4	1	0.0	0.0	
HWRC-751-01	w	512488	7130241	0	1.5	0.0	0.167	4	1	0.0	0.0	
HWRC-752-01	w	512555	7130814	0	0.4	0.8	0.500	4	1	0.8	0.8	
HWRC-753-01	w	512432	7131089	0	2	0.0	0.500	4	1	0.0	0.0	
HWRC-754-01	w	512639	7131215	0	3	0.0	0.125	4	1	0.0	0.0	
HWRC-755-01	w	512485	7131486	0	1.2	0.5	0.500	4	1	0.5	0.5	
HWRC-756-01	w	512484	7131738	0	1.2	0.0	0.500	4	1	0.0	0.0	
HWRC-269-03	w	512866	7135462	3	4.5	2.3	0.278	3	3	2.8	0.9	
HWRC-269-04	w	512866	7135462	4.5	6	0.5	0.389	3	3			
HWRC-269-05	w	512866	7135462	6	7.5	0.0	0.500	3	3			
HWRC-270-02	w	515523	7130261	1.5	3	0.0	0.500	3	1	0.0	0.0	
HWRC-482-02	e	536774	7129893	2	3.5	0.0	0.500	3	1	0.0	0.0	
HWRC-483-03	e	536943	7131001	3.5	5	0.0	0.417	3	1	0.0	0.0	
HWRC-484-03	e	536834	7131810	3.5	5	0.5	0.313	3	2	0.5	0.2	
HWRC-484-04	e	536834	7131810	5	6.5	0.0	0.438	3	2			
HWRC-485-04	e	536416	7135069	5	6.5	0.0	0.292	3	3	0.0	0.0	
HWRC-485-05	e	536416	7135069	6.5	8	0.0	0.375	3	3			
HWRC-485-06	e	536416	7135069	8	9.5	0.0	0.458	3	3			
HWRC-486-05	e	536077	7133811	5	6.5	0.0	0.321	3	3	0.0	0.0	
HWRC-486-06	e	536077	7133811	6.5	8	0.0	0.393	3	3			
HWRC-486-07	e	536077	7133811	8	9.5	0.0	0.464	3	3			
HWRC-487-04	e	536677	7133526	5	6.5	0.0	0.357	3	2			
HWRC-487-05	e	536677	7133526	6.5	8	0.0	0.500	3	2	0.0	0.0	
HWRC-488-03	e	535945	7135629	5	6.5	0.0	0.357	3	2	0.0	0.0	

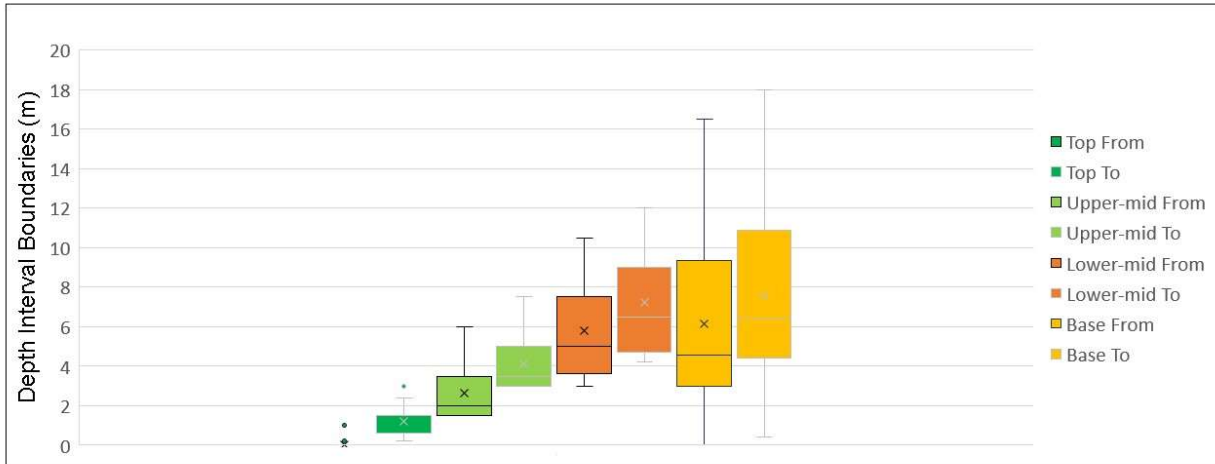
SampleID	StudyArea	CollarEasting	CollarNorthing	From	To	nKIM	Depth Interval	Depth Interval Bin	Sample Count added	KIM sum	KIM avg	Notes
HWRC-488-04	e	535945	7135629	6.5	8		0.0	0.500	3	2		
HWRC-497-03	e	536580	7138693	3.5	5		0.0	0.313	3	2	4.4	2.2
HWRC-497-04	e	536580	7138693	5	6.5		4.4	0.438	3	2		
HWRC-503-02	e	539884	7134889	2	3.5		0.5	0.300	3	2	0.5	0.3
HWRC-503-03	e	539884	7134889	3.5	5		0.0	0.500	3	2		
HWRC-516-02	e	542939	7136728	1.5	3		26.0	0.300	3	2	46.2	23.1
HWRC-516-03	e	542939	7136728	3	4.5		20.1	0.500	3	2		
HWRC-524-02	e	545422	7133178	1.5	3		2.4	0.500	3	1	2.4	2.4
HWRC-627-03	e	537901	7131891	3	4.5		0.0	0.278	3	3	0.7	0.2
HWRC-627-04	e	537901	7131891	4.5	6		0.7	0.389	3	3		
HWRC-627-05	e	537901	7131891	6	7.5		0.0	0.500	3	3		
HWRC-628-05	e	537858	7132128	6	7.5		0.0	0.321	3	3	0.0	0.0
HWRC-628-06	e	537858	7132128	7.5	9		0.0	0.393	3	3		
HWRC-628-07	e	537858	7132128	9	10.5		0.0	0.464	3	3		
HWRC-629-03	e	537897	7132397	3	4.5		0.0	0.417	3	1	0.0	0.0
HWRC-630-02	e	537889	7132698	1.5	3		0.0	0.500	3	1	0.0	0.0
HWRC-635-02	e	538006	7135040	1.5	3		0.0	0.375	3	1	0.0	0.0
HWRC-636-03	e	537888	7135447	1.5	3		0.0	0.375	3	1	0	0.0
HWRC-639-04	e	538010	7136946	4.5	6		2.6	0.292	3	3	33.0	11.0
HWRC-639-05	e	538010	7136946	6	7.5		6.2	0.375	3	3		
HWRC-639-06	e	538010	7136946	7.5	9		24.2	0.458	3	3		
HWRC-645-02	e	537904	7138738	1.5	3		0.7	0.375	3	1	0.7	0.7
HWRC-650-03	e	535255	7135807	3	4.5		0.0	0.417	3	1	0.0	0.0
HWRC-651-05	e	535214	7135302	6	7.5		0.0	0.321	3	3	0.0	0.0
HWRC-651-06	e	535214	7135302	7.5	9		0.0	0.393	3	3		
HWRC-651-07	e	535214	7135302	9	10.5		0.0	0.464	3	3		
HWRC-652-02	e	535331	7135036	1.5	3		0.0	0.375	3	1	0.0	0.0
HWRC-653-03	e	535211	7134342	3	4.5		0.7	0.278	3	3	2.4	0.8
HWRC-653-04	e	535211	7134342	4.5	6		0.7	0.389	3	3		
HWRC-653-05	e	535211	7134342	6	7.5		1.1	0.500	3	3		
HWRC-654-03	e	535275	7134110	3	4.5		0.6	0.313	3	2	1.2	0.6
HWRC-654-04	e	535275	7134110	4.5	6		0.6	0.438	3	2		
HWRC-655-02	e	535233	7133870	1.5	3		0.0	0.500	3	1	0.0	0.0
HWRC-656-02	e	535211	7133536	1.5	3		0.0	0.500	3	1	0.0	0.0
HWRC-657-02	e	535243	7133325	1.5	3		3.2	0.300	3	2	6.0	3.0
HWRC-657-03	e	535243	7133325	3	4.5		2.8	0.500	3	2		
HWRC-658-03	e	535244	7133083	3	4.5		6.5	0.278	3	3	24.0	8.0
HWRC-658-04	e	535244	7133083	4.5	6		4.1	0.389	3	3		
HWRC-658-05	e	535244	7133083	6	7.5		13.5	0.500	3	3		
HWRC-659-02	e	535288	7132866	1.5	3		2.1	0.500	3	1	2.1	2.1
HWRC-660-03	e	535227	7132623	3	4.5		1.9	0.278	3	3	3.5	1.2
HWRC-660-04	e	535227	7132623	4.5	6		1.0	0.389	3	3		
HWRC-660-05	e	535227	7132623	4.5	6		0.6	0.500	3	3		
HWRC-661-02	e	535208	7132332	1.5	3		0.0	0.375	3	1	0.0	0.0
HWRC-732-02	w	514630	7134425	3	4.5		0.4	0.500	3	1	0.4	0.4
HWRC-737-02	w	514630	7135742	3	4.5		0.0	0.300	3	2	0.5	0.2
HWRC-737-03	w	514630	7135742	4.5	6		0.5	0.500	3	2		
HWRC-738-03	w	514529	7136370	3	4.5		0.4	0.278	3	3	1.4	0.5
HWRC-738-04	w	514529	7136370	4.5	6		0.9	0.389	3	3		
HWRC-738-05	w	514529	7136370	6	7.5		0.0	0.500	3	3		
HWRC-740-03	w	511319	7134780	4.5	6		0.0	0.417	3	1	0.0	0.0
HWRC-742-03	w	511249	7133747	4.5	6		0.0	0.357	3	2	1.4	0.7
HWRC-742-04	w	511249	7133747	6	7.5		1.4	0.500	3	2		
HWRC-746-03	w	511215	7131655	4.5	6		0.6	0.417	3	1	0.6	0.6
HWRC-751-02	w	512488	7130241	1.5	3		0.0	0.500	3	1	0.0	0.0
HWRC-754-02	w	512639	7131215	3	4.5		0.0	0.375	3	1	0.0	0.0
HWRC-269-06	w	512866	7135462	7.5	9		0.0	0.611	2	3	1.7	0.6
HWRC-269-07	w	512866	7135462	9	10.5		0.5	0.722	2	3		
HWRC-269-08	w	512866	7135462	9	10.5		1.1	0.722	2	3		Duplicate
HWRC-483-04	e	536943	7131001	5	6.5		0.0	0.583	2	2	0.0	0.0
HWRC-483-05	e	536943	7131001	6.5	8		0.0	0.750	2	2		
HWRC-484-05	e	536834	7131810	6.5	8		0.0	0.563	2	2	0.0	0.0
HWRC-484-06	e	536834	7131810	8	9.5		0.0	0.688	2	2		
HWRC-485-07	e	536416	7135069	9.5	11		0.0	0.542	2	3	0.9	0.3

SampleID	StudyArea	CollarEasting	CollarNorthing	From	To	nKIM	Depth Interval	Depth Interval Bin	Sample Count added	KIM sum	KIM avg	Notes
HWRC-485-08	e	536416	7135069	11	12.5	0.0	0.625	2	3			
HWRC-485-09	e	536416	7135069	12.5	14	0.9	0.708	2	3			
HWRC-486-08	e	536077	7133811	9.5	11	0.0	0.536	2	4	1.8	0.4	
HWRC-486-09	e	536077	7133811	11	12.5	0.8	0.607	2	4			
HWRC-486-10	e	536077	7133811	12.5	14	0.5	0.679	2	4			
HWRC-486-11	e	536077	7133811	14	15.5	0.5	0.750	2	4			
HWRC-487-06	e	536677	7133526	8	9.5	0.5	0.643	2	1		0.5	
HWRC-488-05	e	535945	7135629	8	9.5	0.0	0.643	2	1	0.0	0.0	
HWRC-497-05	e	536580	7138693	6.5	8	2.5	0.563	2	2	3.0	1.5	
HWRC-497-06	e	536580	7138693	8	9.5	0.5	0.688	2	2			
HWRC-503-04	e	539884	7134889	5	6.5	0.5	0.700	2	1	0.5	0.5	
HWRC-516-04	e	542939	7136728	4.5	6	8.5	0.700	2	1	8.5	8.5	
HWRC-627-06	e	537901	7131891	7.5	9	0.0	0.611	2	2	0.0	0.0	
HWRC-627-07	e	537901	7131891	9	10.5	0.0	0.722	2	2			
HWRC-628-08	e	537858	7132128	10.5	11	1.1	0.536	2	4	1.6	0.4	
HWRC-628-09	e	537858	7132128	11	12.5	0.0	0.607	2	4			
HWRC-628-10	e	537858	7132128	12.5	14	0.0	0.679	2	4			
HWRC-628-11	e	537858	7132128	14	15.5	0.5	0.750	2	4			
HWRC-629-04	e	537897	7132397	4.5	6	1.1	0.583	2	2	1.1	0.6	
HWRC-629-05	e	537897	7132397	6	7.5	0.0	0.750	2	2			
HWRC-635-03	e	538006	7135040	3	4.5	0.0	0.625	2	1	0.0	0.0	
HWRC-636-04	e	537888	7135447	3	4.5	0.0	0.625	2	1	0.0	0.0	
HWRC-639-07	e	538010	7136946	9	10.5	0.0	0.542	2	3	0.6	0.2	
HWRC-639-08	e	538010	7136946	10.5	12	0.6	0.625	2	3			
HWRC-639-09	e	538010	7136946	12	13.5	0.0	0.708	2	3			
HWRC-645-03	e	537904	7138738	3	4.5	1.3	0.625	2	1	1.3	1.3	
HWRC-650-04	e	535255	7135807	4.5	6	2.5	0.583	2	2	2.5	1.3	
HWRC-650-05	e	535255	7135807	6	7.5	0.0	0.750	2	2			
HWRC-651-08	e	535214	7135302	10.5	12	0.0	0.536	2	4	0.0	0.0	
HWRC-651-09	e	535214	7135302	12	13.5	0.0	0.607	2	4			
HWRC-651-10	e	535214	7135302	13.5	15	0.0	0.679	2	4			
HWRC-651-11	e	535214	7135302	15	16.5	0.0	0.750	2	4			
HWRC-652-03	e	535331	7135036	3	4.5	0.0	0.625	2	1	0.0	0.0	
HWRC-653-06	e	535211	7134342	7.5	9	0.0	0.611	2	2	1.2	0.6	
HWRC-653-07	e	535211	7134342	9	10.5	1.2	0.722	2	2			
HWRC-654-05	e	535275	7134110	6	7.5	1.5	0.563	2	2	1.5	0.8	
HWRC-654-06	e	535275	7134110	7.5	9	0.0	0.688	2	2			
HWRC-657-04	e	535243	7133325	4.5	6	4.5	0.700	2	1	4.5	4.5	
HWRC-658-06	e	535244	7133083	7.5	9	14.0	0.611	2	2	14.7	7.3	
HWRC-658-07	e	535244	7133083	9	10.5	0.7	0.722	2	2			
HWRC-660-06	e	535227	7132623	6	7.5	2.8	0.611	2	2	5.2	2.6	
HWRC-660-07	e	535227	7132623	7.5	9	2.5	0.722	2	2			
HWRC-661-03	e	535208	7132332	3	4.5	0.0	0.625	2	1	0.0	0.0	
HWRC-737-04	w	514630	7135742	6	7.5	0.0	0.700	2	1	0.0	0.0	
HWRC-738-06	w	514529	7136370	7.5	9	0.0	0.611	2	2	2.2	1.1	
HWRC-738-07	w	514529	7136370	9	10.5	2.2	0.722	2	2			
HWRC-740-04	w	511319	7134780	6	7.5	0.0	0.583	2	2	0.9	0.5	
HWRC-740-05	w	511319	7134780	7.5	9	0.9	0.750	2	2			
HWRC-742-05	w	511249	7133747	7.5	9	0.0	0.643	2	1	0.0	0.0	
HWRC-746-04	w	511215	7131655	6	7.5	0.0	0.583	2	2	0.0	0.0	
HWRC-746-05	w	511215	7131655	7.5	9	0.0	0.750	2	2			
HWRC-754-03	w	512639	7131215	4.5	6	0.0	0.625	2	1	0.0	0.0	
HWRC-269-09	w	512866	7135462	10.5	12	0.6	0.833	1	2	0.6	0.3	
HWRC-269-10	w	512866	7135462	12	13.2	0.0	0.944	1	2			
HWRC-270-03	w	515523	7130261	3	4	0.0	0.833	1	1	0.0	0.0	
HWRC-482-03	e	536774	7129893	3.5	6.8	0.0	0.833	1	1	0.0	0.0	
HWRC-483-06	e	536943	7131001	8	10	0.5	0.917	1	1	0.5	0.5	
HWRC-484-07	e	536834	7131810	9.5	11	0.0	0.813	1	2	0.4	0.2	
HWRC-484-08	e	536834	7131810	11	12.5	0.4	0.938	1	2			
HWRC-485-10	e	536416	7135069	14	15.5	0.0	0.792	1	3	1.4	0.5	
HWRC-485-11	e	536416	7135069	15.5	17	0.5	0.875	1	3			
HWRC-485-12	e	536416	7135069	17	19.5	0.9	0.958	1	3			
HWRC-486-12	e	536077	7133811	15.5	17	1.1	0.821	1	3	1.5	0.5	
HWRC-486-13	e	536077	7133811	17	18.5	0.0	0.893	1	3			



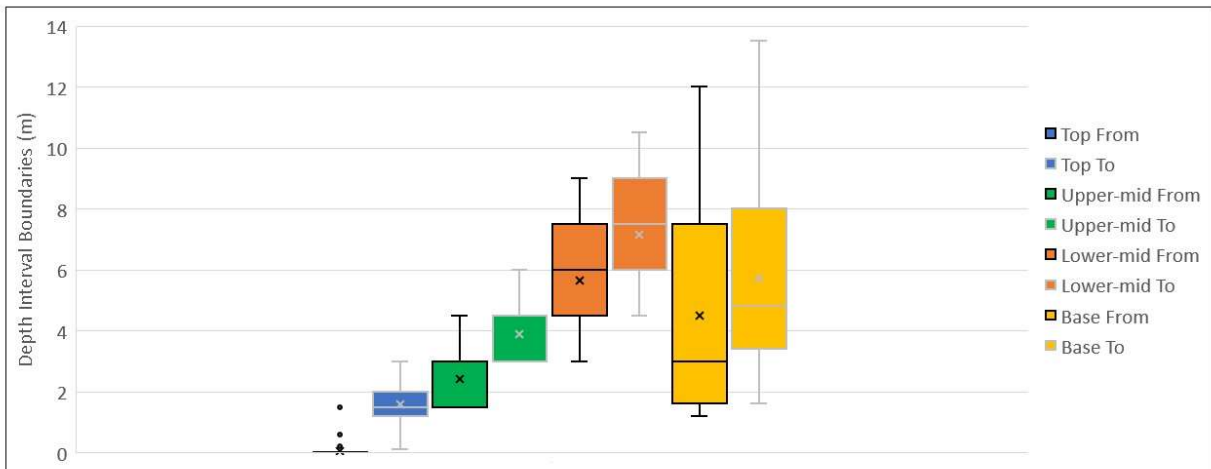
SampleID	StudyArea	CollarEasting	CollarNorthing	From	To	nKIM	Depth Interval	Depth Interval Bin	Sample Count added	KIM sum	KIM avg	Notes
HWRC-486-14	e	536077	7133811	18.5	20.4	0.4	0.964	1	3			
HWRC-487-07	e	536677	7133526	9.5	11	0.0	0.786	1	2	0.6	0.3	
HWRC-487-08	e	536677	7133526	11	12.5	0.6	0.929	1	2			
HWRC-488-06	e	535945	7135629	9.5	11	0.0	0.786	1	2	0.5	0.2	
HWRC-488-07	e	535945	7135629	11	12.5	0.5	0.929	1	2			
HWRC-497-07	e	536580	7138693	9.5	11	0.5	0.813	1	2	0.5	0.2	
HWRC-497-08	e	536580	7138693	11	12	0.0	0.938	1	2			
HWRC-499-02	e	539865	7138821	2	4	0.6	0.750	1	1	0.6	0.6	
HWRC-500-02	e	539921	7137816	2	3.6	0.5	0.750	1	1	0.5	0.5	
HWRC-503-05	e	539884	7134889	6.5	7.5	0.7	0.900	1	1	0.7	0.7	
HWRC-512-02	e	542896	7132936	0.4	1.8	0.0	0.750	1	1	0.0	0.0	
HWRC-516-05	e	542939	7136728	6	7	1.3	0.900	1	1	1.3	1.3	
HWRC-524-03	e	545422	7133178	3	4.2	0.0	0.833	1	1	0.0	0.0	
HWRC-626-02	e	538023	7131613	1.5	2.4	0.0	0.750	1	1	0.0	0.0	
HWRC-627-08	e	537901	7131891	10.5	12	0.0	0.833	1	2	0.0	0.0	
HWRC-627-09	e	537901	7131891	12	13.5	0.0	0.944	1	2			
HWRC-628-12	e	537858	7132128	15.5	17	0.0	0.821	1	3	1.7	0.6	
HWRC-628-13	e	537858	7132128	17	18.5	0.6	0.893	1	3			
HWRC-628-14	e	537858	7132128	18.5	19.8	1.1	0.964	1	3			
HWRC-629-06	e	537897	7132397	7.5	9.2	0.0	0.917	1	1	0.0	0.0	
HWRC-630-03	e	537889	7132698	3	4.2	0.0	0.833	1	1	0.0	0.0	
HWRC-635-04	e	538006	7135040	4.5	5.4	0.0	0.875	1	1	0.0	0.0	
HWRC-636-05	e	537888	7135447	4.5	6.4	0.0	0.875	1	1	0.0	0.0	
HWRC-639-10	e	538010	7136946	13.5	15	0.0	0.792	1	3	0.0	0.0	
HWRC-639-11	e	538010	7136946	15	16.5	0.0	0.875	1	3			
HWRC-639-12	e	538010	7136946	16.5	18.2	0.0	0.958	1	3			
HWRC-644-02	e	537916	7138232	1.5	3	3.5	0.750	1	1	3.5	3.5	
HWRC-645-04	e	537904	7138738	4.5	6.4	0.6	0.875	1	1	0.6	0.6	
HWRC-650-06	e	535255	7135807	7.5	9.2	0.0	0.917	1	1	0.0	0.0	
HWRC-651-12	e	535214	7135302	16.5	18	0.0	0.821	1	3	0.0	0.0	
HWRC-651-13	e	535214	7135302	16.5	18	0.0	0.893	1	3			
HWRC-651-14	e	535214	7135302	18	19.5	0.0	0.964	1	3			
HWRC-652-04	e	535331	7135036	4.5	5.5	0.5	0.875	1	1	0.5	0.5	
HWRC-653-08	e	535211	7134342	10.5	12	1.2	0.833	1	2	1.2	0.6	
HWRC-653-09	e	535211	7134342	12	13.5	0.0	0.944	1	2			
HWRC-654-07	e	535275	7134110	9	10.5	1.3	0.813	1	2	1.9	0.9	
HWRC-654-08	e	535275	7134110	10.5	11.8	0.6	0.938	1	2			
HWRC-655-03	e	535233	7133870	3	4.4	1.8	0.833	1	1	1.8	1.8	
HWRC-656-03	e	535211	7133536	3	4.4	0.0	0.833	1	1	0.0	0.0	
HWRC-657-05	e	535243	7133325	6	7.8	5.7	0.900	1	1	5.7	5.7	
HWRC-658-08	e	535244	7133083	10.5	12	0.0	0.833	1	2	0.0	0.0	
HWRC-658-09	e	535244	7133083	12	13	0.0	0.944	1	2			
HWRC-659-03	e	535288	7132866	3	4.5	0.0	0.833	1	1	0.0	0.0	
HWRC-660-08	e	535227	7132623	9	10.5	2.0	0.833	1	2	2.6	1.3	
HWRC-660-09	e	535227	7132623	10.5	12.2	0.6	0.944	1	2			
HWRC-661-04	e	535208	7132332	4.5	6.4	0.0	0.875	1	1	0.0	0.0	
HWRC-732-03	w	514630	7134425	4.5	5.2	0.0	0.833	1	1	0.0	0.0	
HWRC-737-05	w	514630	7135742	7.5	8	0.0	0.900	1	1	0.0	0.0	
HWRC-738-08	w	514529	7136370	10.5	12	7.9	0.833	1	2	7.9	3.9	
HWRC-738-09	w	514529	7136370	12	12.6	0.0	0.944	1	2			
HWRC-740-06	w	511319	7134780	9	10	0.0	0.917	1	1	0.0	0.0	
HWRC-742-06	w	511249	7133747	9	10.5	0.0	0.786	1	2	1.2	0.6	
HWRC-742-07	w	511249	7133747	10.5	10.8	1.2	0.929	1	2			
HWRC-746-06	w	511215	7131655	9	10.5	0.0	0.917	1	1	0.0	0.0	
HWRC-747-02	w	511245	7131153	3	3.4	0.0	0.750	1	1	0.0	0.0	
HWRC-751-03	w	512488	7130241	3	3.4	0.0	0.833	1	1	0.0	0.0	
HWRC-754-04	w	512639	7131215	6	7.5	0.0	0.875	1	1	0.0	0.0	

### East Study Area Depth Interval Boundaries



	Top From	Top To	Upper-mid From	Upper-mid To	Lower-mid From	Lower-mid To	Base From	Base To
Max	1	3	6	7.5	10.5	12	16.5	18
3rd quartile	0	1.5	3.25	4.75	7.5	9	9.125	10.6
median	0	1.5	2	3.5	5	6.5	4.55	6.4
1st quartile	0	0.6	1.5	3	3.975	5.1	3	4.4
Min	0	0.2	1.5	3	3	4.2	0	0.4

### West Study Area Depth Interval Boundaries



	Top From	Top To	Upper-mid From	Upper-mid To	Lower-mid From	Lower-mid To	Base From	Base To
Max	1.5	3	4.5	6	9	10.5	12	13.5
3rd quartile	0	2	3	4.5	7.5	9	6.75	7.75
Median	0	1.5	1.5	3	6	7.5	3	4.8
1st quartile	0	1.2	1.5	3	4.5	6	2.3	3.4
Min	0	0.1	1.5	3	3	4.5	1.2	1.6

## **Appendix D: Sediment texture results for UW data**

UW lab sample descriptions

UW lab sample weights

UW Analysette results

UW sample: texture Wentworth classification results table

UW sample: texture cumulative weight percent table

Sample number	Lab number	Initial notes	Batch #	Drying notes	Initial weight (kg)	500g split weight	Sieving notes
17-RS-001-B	198	Few thin roots. Bit wet	1. Start dry lvl 4 on Oct 18. Turned down to level 2 at 2pm to go shop for oven mits and spoons. Stirred at 7pm, Oct 19 at 9:15 am, 12:15, took out at 3:15pm dry. Stirred. Covered with tin foil, allowed air gap for heat to escape. Seived Oct 20 around lunchtime.	After 2 hours bit solid on bottom of pan	2.1	500.55	Resieve >1mm.
17-RS-002-B	197	Wet clump. Broke up.	1. Start dry lvl 4 on Oct 18. Turned down to level 2 at 2pm to go shop for oven mits and spoons. Stirred at 7pm, Oct 19 at 9:15 am, 12:15, took out at 3:15pm dry. Stirred. Covered with tin foil, allowed air gap for heat to escape. Seived Oct 20 around lunchtime.	After 2 hours bit solid on bottom of pan	2.13	500.50	
17-RS-003-B	196	Wet clump. Broke up.	1. Start dry lvl 4 on Oct 18. Turned down to level 2 at 2pm to go shop for oven mits and spoons. Stirred at 7pm, Oct 19 at 9:15 am, 12:15, took out at 3:15pm dry. Stirred. Covered with tin foil, allowed air gap for heat to escape. Seived Oct 20 around lunchtime.	After 2 hours bit solid on bottom of pan	2.7	539.49	
17-RS-004-B	195	Few thin roots. More sandy than previous	1. Start dry lvl 4 on Oct 18. Turned down to level 2 at 2pm to go shop for oven mits and spoons. Stirred at 7pm, Oct 19 at 9:15 am, 12:15, took out at 3:15pm dry. Stirred. Covered with tin foil, allowed air gap for heat to escape. Seived Oct 20 around lunchtime.	Dried quick.	2.74	503.11	
17-RS-005-B	194	declump	2 start dry lvl 4 on oct 21 at 10:30. Stir 2pm. Turn to LVL 2. Stir @ 9am oct 23. Took out of oven to cool. 2pm bagged up.	Dry quick	2.97/2.92	503.89	
17-RS-006-B	193	v coarse sand. Near dry	2 start dry lvl 4 on oct 21 at 10:30. Stir 2pm. Turn to LVL 2. Stir @ 9am oct 23. Took out of oven to cool. 2pm bagged up.	Dry quick	3.68	578.45	lots of bug egg casings
17-RS-007-B	192	Oxidized. Roots. Fine sandy near dry.	2 start dry lvl 4 on oct 21 at 10:30. Stir 2pm. Turn to LVL 2. Stir @ 9am oct 23. Took out of oven to cool. 2pm bagged up.	Dry quick	3.21	502.30	
17-RS-008-B	191	Some declump.	2 start dry lvl 4 on oct 21 at 10:30. Stir 2pm. Turn to LVL 2. Stir @ 9am oct 23. Took out of oven to cool. 2pm bagged up.	Minimal stuck. Dry quick.	2.48	512.41	
17-RS-009-B	190	oxidized	3 Start dry 5pm oct 23 on lvl 4. Stir at 6:15 pm. Turn down to lvl 2. Took out at 7am oct 24.		2.52	500.64	v fine and oxidized
17-RS-010-B	189	Wet. Declump. Minor roots	3 Start dry 5pm oct 23 on lvl 4. Stir at 6:15 pm. Turn down to lvl 2. Took out at 7am oct 24.		2.8	509.34	
17-RS-011-B	187	bit clump	3 Start dry 5pm oct 23 on lvl 4. Stir at 6:15 pm. Turn down to lvl 2. Took out at 7am oct 24.		2.3/2.34	505.00	
17-RS-012-B	186	dry, coarse sand. Oxidized. Roots	3 Start dry 5pm oct 23 on lvl 4. Stir at 6:15 pm. Turn down to lvl 2. Took out at 7am oct 24.		2.78	505.00	
17-RS-013-B	185	Sandy. Dry.	4 Put in at 11am oct 24. lvl 4. stir 3pm.		2.7/2.59	545.19	lost some fines due to wet rubber seals
17-RS-014-B	184	Coarse sandy. Roots Oxidized.	4 Put in at 11am oct 24. lvl 4. stir 3pm.		2.98	502.78	despite extensive blow drying, rubber seals caused clumping of fines
17-RS-015-B	183	V wet. Declump	4 Put in at 11am oct 24. lvl 4. stir 3pm.		2.87	510.27	
17-RS-016-C1	N/A	No geochem	10	Nearly dry to start	0.15066	N/A	fine roots. Do not use for geochem. Did not clean sieves between
17-RS-016-C2	N/A	No geochem	10	Nearly dry to start	0.470552	N/A	fine roots. Do not use for geochem. Did not clean sieves between
17-RS-016-C3	N/A	No geochem. Finer grained and lighter col	10	Nearly dry to start	0.059662	N/A	fine roots. Do not use for geochem. Did not clean sieves between
17-RS-017-B	182		4 Put in at 11am oct 24. lvl 4. stir 3pm.		2.93	534.73	
17-RS-018-B	181	Fine sand.	8 in 1:45pm oct 30, lvl 3 turn to 2. out 7:30 am nov 2		2.33	501.86	
17-RS-019-B	180	Oxidized minimal clumping. Sandy, roots	5 lvl 2 at 7:45 pm oct 25, stir 9pm	fast, no clumping	2.19/2.16	503.96	

Sample number	Lab number	Initial notes	Batch #	Drying notes	Initial weight (kg)	500g split weight	Sieving notes
17-RS-020-B	179	fineish sand	6 in 1:30 pm Oct 26. Stir 3:30, stir 5:30 out oct 27 11:30 cool, bag 2:15pm		3.15	501.97	
17-RS-021-B	178	slight oxidation, sandy, roots	7 in 6:15 pm oct 27. Out 11:30 am Oct 30.		2.98	508.88	
17-RS-022-B	176	minor roots, break clumps	9 in 2pm nov 2. out 11:45 am nov 3			509.69	
17-RS-023-B	175	fineish sand	7 in 6:15 pm oct 27. Out 11:30 am Oct 30.		2.63	504.97	
17-RS-024-B	174	minor roots. Rusty	9 in 2pm nov 2. out 11:45 am nov 3			501.62	
17-RS-025-B	173	Oxidized minimal clumps. Sandy	5 In 7:45 pm. Stir 9pm. Lvl 2 2:45 pm cool at 10am oct 26.	Dried fast, no clumping	2.36/2.37	509.15	
17-RS-026-B	172	minor roots. Rusty crusts. Break up.	9 in 2pm nov 2. out 11:45 am nov 3	Mica flashes (flakes)		517.45	
17-RS-027-B	171	oxidized. Minor clumps.. Sandy	5 In 7:45 pm. Stir 9pm. Lvl 2 2:45 pm cool at 10am oct 26.	fast, no clumping	2.81	511.19	
17-RS-028-B	170	minor break-up	9 in 2pm nov 2. out 11:45 am nov 3			510.28	
17-RS-029-B	169	oxidized. Minor clumps. Sandy.. Roots	5 In 7:45 pm. Stir 9pm. Lvl 2 2:45 pm cool at 10am oct 26.	fast, no clumping	2.67	503.15	
17-RS-030-B	168	slight oxidation. Sandy, roots, minor clum	7 in 6:15 pm oct 27. Out 11:30 am Oct 30.		2.64	500.01	
17-RS-031-B	167	oxidized, sandy, roots	6 in 1:30 pm Oct 26. Stir 3:30, stir 5:30 out oct 27 11:30 cool, bag 2:15pm		2.71	530.65	Rubber seal felt dry to touch, but clumped fines. Lots of plant/black rooty
17-RS-032-B	165	oxidized, sandy, roots	6 in 1:30 pm Oct 26. Stir 3:30, stir 5:30 out oct 27 11:30 cool, bag 2:15pm		2.49/2.46	503.14	
17-RS-033-B	164	oxidized, sandy, roots	6 in 1:30 pm Oct 26. Stir 3:30, stir 5:30 out oct 27 11:30 cool, bag 2:15pm		3.41	519.47	Same splitter as 32
17-RS-034-B	163	oxidized with rusty patches and grey spher	8 in 1:45pm oct 30, lvl 3 turn to 2. out 7:30 am nov 2		2.41	513.65	
17-RS-035-B	162	et. Rusty, oxidized, very muddy, minor ro	8 in 1:45pm oct 30, lvl 3 turn to 2. out 7:30 am nov 2		2.57	509.12	
17-RS-037-B	161	Very hard. Sandy, some roots	8 in 1:45pm oct 30, lvl 3 turn to 2. out 7:30 am nov 2		3.17	503.29	
17-RS-039-B	160	fineish sand	7 in 6:15 pm oct 27. Out 11:30 am Oct 30.		2.17/2.16	500.30	Same splitter as 37



Sample number	<0.063 mm (g)	<0.125 mm (g)	<0.25 mm (g)	<0.5 mm (g)	<1.0 mm (g)	<2.0 mm (g)	<4.0 mm (g)	<8.0 mm (g)	>8.0 mm (g)	Sieve total (g)	Initial dried sample weight	Diff initial vs sieve total	% diff
17-RS-001-B	70.270	570.100	222.220	141.070	121.670	111.720	106.020	95.070	122.810	1560.950	2100	38.500	2
17-RS-002-B	280.380	409.880	232.110	145.480	116.440	107.930	93.490	85.850	116.530	1588.090	2130	41.410	2
17-RS-003-B	372.050	611.110	282.500	189.180	149.330	150.460	127.600	112.840	132.480	2127.550	2700	32.960	1
17-RS-004-B	304.320	332.800	265.760	231.920	180.880	186.530	165.910	174.750	396.580	2239.450	2740	-2.560	0
17-RS-005-B	358.430	833.540	394.140	214.060	148.320	128.440	117.790	108.830	124.940	2428.490	2945	12.620	0
17-RS-006-B	47.180	183.750	166.190	102.570	371.180	346.240	352.100	496.520	1029.754	3095.484	3680	6.066	0
17-RS-007-B	210.080	810.482	532.130	315.420	243.770	209.410	151.090	99.650	124.360	2696.392	3210	11.308	0
17-RS-008-B	414.850	528.260	292.630	186.210	150.250	134.950	108.060	74.910	67.660	1957.780	2480	9.810	0
17-RS-009-B	356.340	380.050	245.770	197.350	146.130	132.530	148.520	267.250	119.290	1993.230	2520	26.130	1
17-RS-010-B	384.000	633.482	365.240	255.240	160.350	142.010	104.780	91.020	142.690	2278.812	2800	11.848	0
17-RS-011-B	289.240	445.150	268.680	150.040	107.570	90.790	82.750	85.310	316.030	1835.560	2350	9.440	0
17-RS-012-B	281.330	339.230	244.650	227.200	195.600	192.110	166.360	173.750	416.190	2236.420	2780	38.580	1
17-RS-013-B	200.350	811.372	395.780	254.890	145.830	116.550	78.630	65.550	50.530	2119.482	2650	-14.672	-1
17-RS-014-B	362.152	532.402	442.142	281.222	187.522	173.402	150.202	151.132	173.102	2453.278	2980	23.942	1
17-RS-015-B	252.702	427.632	338.202	251.112	185.912	208.352	261.742	241.662	171.272	2338.588	2870	21.142	1
17-RS-016-C1	10.980	46.230	57.580	24.970	11.010	3.795	1.240	0.940	0.000	156.745	150.66		
17-RS-016-C2	20.490	91.630	136.090	127.630	64.400	14.260	3.840	0.770	0.000	459.110	470.552		
17-RS-016-C3	22.470	26.560	4.190	3.290	2.220	0.290	0.000	0.000	0.000	59.020	59.662		
17-RS-017-B	423.682	892.234	308.502	221.322	153.842	116.612	89.892	53.432	116.802	2376.320	2930	18.950	1
17-RS-018-B	270.692	408.362	348.852	224.252	132.912	131.392	110.212	87.032	95.012	1808.718	2330	19.422	1
17-RS-019-B	384.880	334.740	181.210	144.440	138.550	136.320	115.380	117.340	105.860	1658.720	2175	12.320	1
17-RS-020-B	467.332	592.852	323.472	336.382	216.552	189.102	148.442	135.602	201.972	2611.708	3150	36.322	1
17-RS-021-B	708.814	460.162	261.722	200.662	169.192	150.052	127.172	109.422	256.592	2443.790	2980	27.330	1
17-RS-022-B	554.982	688.874	269.182	198.232	145.142	126.022	87.872	55.572	50.752	2176.630			
17-RS-023-B	474.652	866.694	345.782	173.582	50.292	78.952	31.782	19.472	53.402	2094.610	2630	30.420	1
17-RS-024-B	470.632	585.602	572.092	186.052	138.042	119.212	72.112	40.802	48.722	2233.268			
17-RS-025-B	585.452	447.482	229.302	144.892	130.052	106.262	79.992	53.442	33.622	1810.498	2365	45.352	2
17-RS-026-B	478.732	616.702	277.162	156.382	106.682	108.362	103.432	85.072	58.972	1991.498			
17-RS-027-B	428.102	415.762	304.812	271.752	216.912	189.662	178.292	177.402	107.782	2290.478	2810	8.332	0
17-RS-028-B	377.932	687.804	315.902	223.032	156.092	141.982	117.872	73.652	85.252	2179.520			
17-RS-029-B	698.636	484.012	257.322	181.932	147.402	133.342	106.852	78.962	55.842	2144.302	2670	22.548	1
17-RS-030-B	642.992	637.454	260.452	192.512	145.852	118.662	76.462	33.262	13.232	2120.880	2640	19.110	1
17-RS-031-B	488.712	576.592	216.972	145.102	100.232	75.942	64.762	83.692	376.782	2128.788	2710	50.562	2
17-RS-032-B	447.362	560.792	310.302	172.262	93.672	68.802	61.162	62.792	182.532	1959.678	2475	12.182	0
17-RS-033-B	371.962	286.802	314.512	172.802	130.902	165.372	206.362	297.422	933.614	2879.750	3410	10.780	0
17-RS-034-B	334.202	571.452	276.582	228.032	171.852	129.952	86.882	46.412	18.062	1863.428	2410	32.922	1
17-RS-035-B	645.774	880.234	167.842	96.232	58.712	37.602	29.272	38.212	76.122	2030.002	2570	30.878	1
17-RS-037-B	338.432	917.654	436.382	255.412	175.552	153.962	131.062	112.992	103.392	2624.840	3170	41.870	1
17-RS-039-B	400.082	483.312	241.362	151.592	84.332	64.832	52.732	64.742	124.502	1667.488	2165	-2.788	0

Size High [ $\mu\text{m}$ ]	17-RS-001	17-RS-002	17-RS-003	17-RS-004	17-RS-005	17-RS-006	17-RS-007	17-RS-008	17-RS-009	17-RS-010	17-RS-011	17-RS-012
0.09	0.00	0.00	0.00	0.00	0.00	0.00	0.00	0.00	0.00	0.00	0.00	0.00
0.10	0.00	0.00	0.00	0.00	0.00	0.00	0.00	0.00	0.00	0.00	0.00	0.00
0.11	0.00	0.00	0.00	0.00	0.00	0.00	0.00	0.00	0.00	0.00	0.00	0.00
0.12	0.00	0.00	0.00	0.00	0.00	0.00	0.00	0.00	0.00	0.00	0.00	0.00
0.13	0.00	0.00	0.00	0.00	0.00	0.00	0.00	0.00	0.00	0.00	0.00	0.00
0.15	0.00	0.00	0.00	0.00	0.00	0.00	0.00	0.00	0.00	0.00	0.00	0.00
0.16	0.00	0.00	0.00	0.00	0.00	0.00	0.00	0.00	0.00	0.00	0.00	0.00
0.18	0.00	0.00	0.00	0.00	0.00	0.00	0.00	0.00	0.00	0.00	0.00	0.00
0.20	0.00	0.00	0.00	0.00	0.00	0.00	0.00	0.00	0.00	0.00	0.00	0.00
0.22	0.00	0.00	0.00	0.00	0.00	0.00	0.00	0.00	0.00	0.00	0.00	0.00
0.24	0.00	0.00	0.00	0.00	0.00	0.00	0.00	0.00	0.00	0.00	0.00	0.00
0.26	0.00	0.00	0.00	0.00	0.00	0.00	0.00	0.00	0.00	0.00	0.00	0.00
0.29	0.00	0.00	0.00	0.00	0.00	0.00	0.00	0.00	0.00	0.00	0.00	0.00
0.32	0.01	0.01	0.02	0.01	0.01	0.03	0.02	0.01	0.02	0.01	0.01	0.02
0.36	0.07	0.06	0.08	0.06	0.05	0.12	0.06	0.04	0.07	0.06	0.06	0.06
0.39	0.19	0.18	0.20	0.15	0.14	0.31	0.14	0.13	0.17	0.16	0.18	0.14
0.43	0.39	0.37	0.41	0.32	0.30	0.63	0.28	0.30	0.33	0.33	0.37	0.28
0.48	0.71	0.68	0.71	0.58	0.54	1.09	0.48	0.56	0.57	0.60	0.67	0.48
0.53	1.12	1.08	1.10	0.92	0.85	1.68	0.75	0.91	0.88	0.94	1.07	0.74
0.58	1.63	1.58	1.57	1.33	1.24	2.39	1.06	1.36	1.25	1.37	1.55	1.05
0.65	2.22	2.15	2.11	1.81	1.69	3.18	1.42	1.88	1.67	1.86	2.10	1.41
0.71	2.87	2.78	2.69	2.32	2.17	4.02	1.81	2.45	2.12	2.40	2.71	1.79
0.79	3.56	3.43	3.30	2.85	2.68	4.89	2.22	3.04	2.59	2.97	3.34	2.20
0.87	4.27	4.10	3.91	3.38	3.18	5.75	2.63	3.63	3.05	3.54	3.98	2.61
0.96	4.99	4.76	4.52	3.89	3.66	6.61	3.03	4.20	3.50	4.10	4.62	3.00
1.06	5.71	5.41	5.12	4.38	4.12	7.47	3.42	4.74	3.94	4.66	5.26	3.38
1.17	6.45	6.05	5.73	4.86	4.55	8.35	3.79	5.27	4.36	5.19	5.91	3.74
1.29	7.19	6.69	6.33	5.33	4.95	9.25	4.15	5.77	4.77	5.72	6.56	4.07
1.43	7.96	7.33	6.94	5.79	5.33	10.20	4.49	6.28	5.18	6.23	7.25	4.38
1.58	8.76	8.01	7.59	6.27	5.71	11.21	4.84	6.80	5.60	6.75	7.98	4.69
1.74	9.61	8.73	8.28	6.76	6.10	12.30	5.18	7.35	6.03	7.29	8.77	4.99
1.92	10.52	9.51	9.04	7.30	6.52	13.49	5.54	7.97	6.49	7.86	9.64	5.30
2.13	11.51	10.38	9.88	7.89	7.00	14.78	5.94	8.66	6.99	8.49	10.61	5.64

Size High [ $\mu\text{m}$ ]	17-RS-001	17-RS-002	17-RS-003	17-RS-004	17-RS-005	17-RS-006	17-RS-007	17-RS-008	17-RS-009	17-RS-010	17-RS-011	17-RS-012
2.35	12.57	11.33	10.79	8.54	7.53	16.14	6.35	9.42	7.52	9.17	11.67	6.02
2.59	13.70	12.36	11.79	9.23	8.13	17.58	6.80	10.25	8.08	9.92	12.81	6.43
2.86	14.98	13.56	12.94	10.04	8.85	19.16	7.32	11.23	8.73	10.79	14.10	6.93
3.16	16.35	14.86	14.20	10.94	9.67	20.83	7.88	12.29	9.44	11.75	15.50	7.49
3.49	17.80	16.27	15.57	11.92	10.60	22.58	8.49	13.46	10.19	12.82	16.99	8.11
3.86	19.39	17.82	17.10	13.03	11.68	24.44	9.18	14.76	11.02	14.02	18.62	8.83
4.26	21.09	19.50	18.76	14.27	12.92	26.39	9.94	16.19	11.94	15.35	20.35	9.64
4.71	22.86	21.27	20.55	15.61	14.28	28.39	10.76	17.72	12.91	16.80	22.16	10.52
5.20	24.66	23.11	22.44	17.05	15.77	30.41	11.64	19.35	13.94	18.36	24.02	11.47
5.74	26.53	25.03	24.45	18.61	17.42	32.46	12.59	21.11	15.06	20.05	25.94	12.52
6.34	28.45	27.04	26.56	20.28	19.21	34.53	13.61	22.98	16.26	21.88	27.91	13.66
7.00	30.43	29.13	28.80	22.08	21.17	36.62	14.70	24.97	17.57	23.89	29.95	14.92
7.74	32.49	31.31	31.16	24.01	23.29	38.75	15.89	27.09	19.01	26.07	32.07	16.32
8.54	34.64	33.61	33.65	26.08	25.59	40.92	17.18	29.35	20.60	28.44	34.28	17.86
9.44	36.97	36.08	36.34	28.37	28.13	43.21	18.62	31.81	22.42	31.06	36.67	19.62
10.42	39.49	38.76	39.24	30.91	30.92	45.66	20.25	34.51	24.48	33.95	39.26	21.61
11.51	42.30	41.74	42.43	33.80	34.04	48.36	22.16	37.53	26.92	37.17	42.14	23.96
12.72	45.43	45.06	45.93	37.09	37.52	51.33	24.42	40.92	29.77	40.75	45.34	26.71
14.04	48.91	48.75	49.77	40.81	41.38	54.59	27.09	44.70	33.10	44.70	48.90	29.92
15.51	52.73	52.84	53.97	44.97	45.63	58.16	30.23	48.90	36.95	49.04	52.81	33.64
17.13	56.96	57.40	58.62	49.67	50.39	62.10	33.98	53.60	41.45	53.89	57.14	37.97
18.92	61.67	62.51	63.82	54.97	55.77	66.48	38.45	58.87	46.70	59.37	62.01	43.02
20.90	66.90	68.14	69.56	60.89	61.84	71.30	43.72	64.74	52.79	65.51	67.42	48.87
23.08	72.48	74.07	75.61	67.19	68.37	76.42	49.56	70.95	59.46	72.02	73.19	55.26
25.49	78.30	80.13	81.75	73.78	75.25	81.73	55.93	77.37	66.64	78.71	79.21	62.16
28.16	84.13	86.00	87.61	80.39	82.10	86.96	62.62	83.68	74.01	85.17	85.16	69.33
31.10	89.75	91.40	92.82	86.87	88.67	91.86	69.72	89.67	81.56	91.07	90.75	76.86
34.35	94.35	95.59	96.65	92.29	93.91	95.75	76.39	94.45	88.13	95.54	95.17	83.70
37.94	97.65	98.37	98.96	96.41	97.58	98.38	82.75	97.79	93.59	98.42	98.15	89.81
41.90	99.41	99.70	99.90	98.81	99.43	99.68	88.12	99.50	97.22	99.73	99.60	94.40
46.28	100.00	100.00	100.00	99.81	99.98	100.00	92.50	100.00	99.16	100.00	100.00	97.44
51.11	100.00	100.00	100.00	100.00	100.00	100.00	95.90	100.00	99.90	100.00	100.00	99.15
56.45	100.00	100.00	100.00	100.00	100.00	100.00	98.24	100.00	100.00	100.00	100.00	99.85

Size High [ $\mu\text{m}$ ]	17-RS-001	17-RS-002	17-RS-003	17-RS-004	17-RS-005	17-RS-006	17-RS-007	17-RS-008	17-RS-009	17-RS-010	17-RS-011	17-RS-012
62.35	100.00	100.00	100.00	100.00	100.00	100.00	99.56	100.00	100.00	100.00	100.00	100.00
68.87	100.00	100.00	100.00	100.00	100.00	100.00	100.00	100.00	100.00	100.00	100.00	100.00
76.06	100.00	100.00	100.00	100.00	100.00	100.00	100.00	100.00	100.00	100.00	100.00	100.00
84.01	100.00	100.00	100.00	100.00	100.00	100.00	100.00	100.00	100.00	100.00	100.00	100.00
92.78	100.00	100.00	100.00	100.00	100.00	100.00	100.00	100.00	100.00	100.00	100.00	100.00
102.48	100.00	100.00	100.00	100.00	100.00	100.00	100.00	100.00	100.00	100.00	100.00	100.00
113.18	100.00	100.00	100.00	100.00	100.00	100.00	100.00	100.00	100.00	100.00	100.00	100.00
125.01	100.00	100.00	100.00	100.00	100.00	100.00	100.00	100.00	100.00	100.00	100.00	100.00
138.07	100.00	100.00	100.00	100.00	100.00	100.00	100.00	100.00	100.00	100.00	100.00	100.00
152.50	100.00	100.00	100.00	100.00	100.00	100.00	100.00	100.00	100.00	100.00	100.00	100.00
168.43	100.00	100.00	100.00	100.00	100.00	100.00	100.00	100.00	100.00	100.00	100.00	100.00
186.03	100.00	100.00	100.00	100.00	100.00	100.00	100.00	100.00	100.00	100.00	100.00	100.00
205.46	100.00	100.00	100.00	100.00	100.00	100.00	100.00	100.00	100.00	100.00	100.00	100.00
226.93	100.00	100.00	100.00	100.00	100.00	100.00	100.00	100.00	100.00	100.00	100.00	100.00
250.64	100.00	100.00	100.00	100.00	100.00	100.00	100.00	100.00	100.00	100.00	100.00	100.00
276.82	100.00	100.00	100.00	100.00	100.00	100.00	100.00	100.00	100.00	100.00	100.00	100.00
305.75	100.00	100.00	100.00	100.00	100.00	100.00	100.00	100.00	100.00	100.00	100.00	100.00
337.69	100.00	100.00	100.00	100.00	100.00	100.00	100.00	100.00	100.00	100.00	100.00	100.00
372.97	100.00	100.00	100.00	100.00	100.00	100.00	100.00	100.00	100.00	100.00	100.00	100.00
411.94	100.00	100.00	100.00	100.00	100.00	100.00	100.00	100.00	100.00	100.00	100.00	100.00
454.98	100.00	100.00	100.00	100.00	100.00	100.00	100.00	100.00	100.00	100.00	100.00	100.00
502.51	100.00	100.00	100.00	100.00	100.00	100.00	100.00	100.00	100.00	100.00	100.00	100.00
555.02	100.00	100.00	100.00	100.00	100.00	100.00	100.00	100.00	100.00	100.00	100.00	100.00
613.00	100.00	100.00	100.00	100.00	100.00	100.00	100.00	100.00	100.00	100.00	100.00	100.00
677.05	100.00	100.00	100.00	100.00	100.00	100.00	100.00	100.00	100.00	100.00	100.00	100.00
747.79	100.00	100.00	100.00	100.00	100.00	100.00	100.00	100.00	100.00	100.00	100.00	100.00
825.91	100.00	100.00	100.00	100.00	100.00	100.00	100.00	100.00	100.00	100.00	100.00	100.00
912.20	100.00	100.00	100.00	100.00	100.00	100.00	100.00	100.00	100.00	100.00	100.00	100.00
1,007.51	100.00	100.00	100.00	100.00	100.00	100.00	100.00	100.00	100.00	100.00	100.00	100.00
1,112.77	100.00	100.00	100.00	100.00	100.00	100.00	100.00	100.00	100.00	100.00	100.00	100.00
1,229.04	100.00	100.00	100.00	100.00	100.00	100.00	100.00	100.00	100.00	100.00	100.00	100.00
1,357.44	100.00	100.00	100.00	100.00	100.00	100.00	100.00	100.00	100.00	100.00	100.00	100.00
1,499.27	100.00	100.00	100.00	100.00	100.00	100.00	100.00	100.00	100.00	100.00	100.00	100.00

Size High [ $\mu\text{m}$ ]	17-RS-001	17-RS-002	17-RS-003	17-RS-004	17-RS-005	17-RS-006	17-RS-007	17-RS-008	17-RS-009	17-RS-010	17-RS-011	17-RS-012
1,655.91	100.00	100.00	100.00	100.00	100.00	100.00	100.00	100.00	100.00	100.00	100.00	100.00
1,828.92	100.00	100.00	100.00	100.00	100.00	100.00	100.00	100.00	100.00	100.00	100.00	100.00
2,020.00	100.00	100.00	100.00	100.00	100.00	100.00	100.00	100.00	100.00	100.00	100.00	100.00

Wentworth GSC	17-RS-001	17-RS-002	17-RS-003	17-RS-004	17-RS-005	17-RS-006	17-RS-007	17-RS-008	17-RS-009	17-RS-010	17-RS-011	17-RS-012
63-31 coarse	19.39	17.82	17.10	13.03	11.68	24.44	9.18	14.76	11.02	14.02	18.62	8.83
15.6-31 medium silt	32.49	31.31	31.16	24.01	23.29	38.75	15.89	27.09	19.01	26.07	32.07	16.32
7.8-15.6 fine silt	52.73	52.84	53.97	44.97	45.63	58.16	30.23	48.90	36.95	49.04	52.81	33.64
7.8-3.9 very fine silt	89.75	91.40	92.82	86.87	88.67	91.86	69.72	89.67	81.56	91.07	90.75	76.86
0.06-3.9 clay	100.00	100.00	100.00	100.00	100.00	100.00	99.56	100.00	100.00	100.00	100.00	100.00



Size High [ $\mu\text{m}$ ]	17-RS-013	17-RS-014	17-RS-015	17-RS-017	17-RS-018	17-RS-019	17-RS-020	17-RS-021	17-RS-022	17-RS-023	17-RS-024	17-RS-025
0.09	0.00	0.00	0.00	0.00	0.00	0.00	0.00	0.00	0.00	0.00	0.00	0.00
0.10	0.00	0.00	0.00	0.00	0.00	0.00	0.00	0.00	0.00	0.00	0.00	0.00
0.11	0.00	0.00	0.00	0.00	0.00	0.00	0.00	0.00	0.00	0.00	0.00	0.00
0.12	0.00	0.00	0.00	0.00	0.00	0.00	0.00	0.00	0.00	0.00	0.00	0.00
0.13	0.00	0.00	0.00	0.00	0.00	0.00	0.00	0.00	0.00	0.00	0.00	0.00
0.15	0.00	0.00	0.00	0.00	0.00	0.00	0.00	0.00	0.00	0.00	0.00	0.00
0.16	0.00	0.00	0.00	0.00	0.00	0.00	0.00	0.00	0.00	0.00	0.00	0.00
0.18	0.00	0.00	0.00	0.00	0.00	0.00	0.00	0.00	0.00	0.00	0.00	0.00
0.20	0.00	0.00	0.00	0.00	0.00	0.00	0.00	0.00	0.00	0.00	0.00	0.00
0.22	0.00	0.00	0.00	0.00	0.00	0.00	0.00	0.00	0.00	0.00	0.00	0.00
0.24	0.00	0.00	0.00	0.00	0.00	0.00	0.00	0.00	0.00	0.00	0.00	0.00
0.26	0.00	0.00	0.00	0.00	0.00	0.00	0.00	0.00	0.00	0.00	0.00	0.00
0.29	0.00	0.00	0.00	0.00	0.00	0.00	0.00	0.00	0.00	0.00	0.00	0.00
0.32	0.01	0.02	0.02	0.02	0.01	0.02	0.03	0.02	0.02	0.01	0.01	0.02
0.36	0.08	0.07	0.10	0.08	0.07	0.07	0.11	0.08	0.07	0.05	0.07	0.08
0.39	0.22	0.18	0.28	0.21	0.21	0.19	0.25	0.21	0.19	0.14	0.20	0.20
0.43	0.47	0.36	0.58	0.43	0.44	0.39	0.49	0.43	0.39	0.29	0.42	0.41
0.48	0.87	0.63	1.02	0.76	0.79	0.68	0.84	0.75	0.69	0.54	0.76	0.72
0.53	1.39	0.99	1.60	1.19	1.26	1.06	1.29	1.16	1.08	0.86	1.21	1.12
0.58	2.02	1.42	2.29	1.72	1.83	1.53	1.83	1.67	1.55	1.26	1.75	1.61
0.65	2.76	1.92	3.08	2.33	2.49	2.07	2.44	2.25	2.10	1.73	2.38	2.18
0.71	3.55	2.46	3.92	2.99	3.21	2.65	3.09	2.87	2.69	2.24	3.05	2.80
0.79	4.38	3.01	4.79	3.68	3.95	3.25	3.77	3.52	3.30	2.77	3.74	3.44
0.87	5.20	3.57	5.66	4.38	4.69	3.85	4.45	4.16	3.91	3.30	4.44	4.08
0.96	6.01	4.12	6.53	5.07	5.43	4.43	5.11	4.79	4.50	3.80	5.13	4.72
1.06	6.80	4.66	7.40	5.76	6.16	4.98	5.77	5.39	5.07	4.27	5.80	5.33
1.17	7.58	5.19	8.28	6.46	6.88	5.51	6.42	5.97	5.61	4.70	6.46	5.93
1.29	8.36	5.70	9.18	7.17	7.61	6.01	7.06	6.52	6.11	5.09	7.13	6.50
1.43	9.15	6.21	10.12	7.89	8.34	6.49	7.72	7.06	6.60	5.45	7.82	7.08
1.58	9.96	6.74	11.11	8.64	9.10	6.98	8.40	7.61	7.09	5.79	8.55	7.67
1.74	10.80	7.29	12.17	9.44	9.90	7.50	9.13	8.18	7.60	6.13	9.34	8.28
1.92	11.71	7.89	13.32	10.30	10.75	8.05	9.92	8.80	8.14	6.48	10.22	8.96
2.13	12.69	8.55	14.56	11.24	11.68	8.69	10.81	9.50	8.75	6.87	11.21	9.73

Size High [μm]	17-RS-013	17-RS-014	17-RS-015	17-RS-017	17-RS-018	17-RS-019	17-RS-020	17-RS-021	17-RS-022	17-RS-023	17-RS-024	17-RS-025
2.35	13.73	9.26	15.87	12.23	12.66	9.39	11.78	10.28	9.41	7.29	12.31	10.58
2.59	14.81	10.03	17.26	13.29	13.70	10.19	12.85	11.16	10.16	7.77	13.53	11.53
2.86	16.02	10.92	18.80	14.49	14.87	11.15	14.08	12.20	11.04	8.35	14.93	12.65
3.16	17.30	11.90	20.44	15.77	16.13	12.24	15.44	13.39	12.03	9.01	16.47	13.90
3.49	18.65	12.97	22.16	17.14	17.48	13.46	16.93	14.73	13.15	9.77	18.18	15.29
3.86	20.10	14.19	24.01	18.64	18.97	14.87	18.59	16.29	14.42	10.67	20.06	16.86
4.26	21.64	15.53	25.96	20.24	20.58	16.44	20.42	18.04	15.86	11.71	22.13	18.58
4.71	23.23	16.99	27.98	21.93	22.28	18.17	22.38	19.98	17.45	12.89	24.34	20.45
5.20	24.88	18.55	30.04	23.69	24.07	20.02	24.44	22.09	19.18	14.21	26.66	22.45
5.74	26.61	20.24	32.16	25.54	25.96	22.01	26.62	24.39	21.09	15.70	29.10	24.60
6.34	28.41	22.04	34.32	27.47	27.94	24.16	28.93	26.86	23.19	17.38	31.66	26.89
7.00	30.30	23.98	36.53	29.49	30.02	26.46	31.34	29.52	25.47	19.25	34.31	29.34
7.74	32.30	26.07	38.79	31.62	32.19	28.93	33.87	32.33	27.96	21.34	37.06	31.94
8.54	34.40	28.30	41.10	33.85	34.47	31.56	36.50	35.31	30.64	23.68	39.90	34.71
9.44	36.69	30.77	43.53	36.26	36.93	34.41	39.30	38.49	33.59	26.34	42.89	37.70
10.42	39.18	33.49	46.09	38.86	39.57	37.51	42.28	41.88	36.79	29.32	46.05	40.93
11.51	41.95	36.56	48.84	41.73	42.48	40.92	45.51	45.55	40.33	32.74	49.46	44.47
12.72	45.03	40.02	51.83	44.90	45.68	44.65	49.02	49.52	44.24	36.61	53.16	48.36
14.04	48.46	43.91	55.05	48.37	49.21	48.75	52.83	53.81	48.54	40.97	57.20	52.61
15.51	52.25	48.25	58.53	52.17	53.09	53.22	56.98	58.48	53.28	45.83	61.57	57.26
17.13	56.48	53.14	62.34	56.40	57.40	58.18	61.56	63.59	58.58	51.30	66.34	62.37
18.92	61.22	58.68	66.60	61.17	62.25	63.76	66.67	69.23	64.53	57.47	71.53	67.99
20.90	66.49	64.89	71.32	66.55	67.67	69.93	72.29	75.30	71.06	64.32	77.02	74.03
23.08	72.10	71.48	76.39	72.35	73.48	76.42	78.16	81.45	77.80	71.48	82.54	80.16
25.49	77.95	78.28	81.69	78.47	79.52	82.92	84.05	87.31	84.37	78.70	87.78	86.05
28.16	83.80	84.86	86.94	84.56	85.47	88.94	89.55	92.39	90.24	85.50	92.40	91.28
31.10	89.43	90.90	91.87	90.34	91.02	94.07	94.28	96.34	95.01	91.55	96.09	95.51
34.35	94.07	95.47	95.77	94.92	95.37	97.57	97.58	98.75	98.08	95.98	98.50	98.26
37.94	97.44	98.40	98.39	98.04	98.27	99.43	99.40	99.81	99.60	98.70	99.69	99.63
41.90	99.29	99.71	99.67	99.57	99.67	100.00	100.00	100.00	100.00	99.83	100.00	100.00
46.28	99.95	100.00	100.00	100.00	100.00	100.00	100.00	100.00	100.00	100.00	100.00	100.00
51.11	100.00	100.00	100.00	100.00	100.00	100.00	100.00	100.00	100.00	100.00	100.00	100.00
56.45	100.00	100.00	100.00	100.00	100.00	100.00	100.00	100.00	100.00	100.00	100.00	100.00

Size High [ $\mu\text{m}$ ]	17-RS-013	17-RS-014	17-RS-015	17-RS-017	17-RS-018	17-RS-019	17-RS-020	17-RS-021	17-RS-022	17-RS-023	17-RS-024	17-RS-025
62.35	100.00	100.00	100.00	100.00	100.00	100.00	100.00	100.00	100.00	100.00	100.00	100.00
68.87	100.00	100.00	100.00	100.00	100.00	100.00	100.00	100.00	100.00	100.00	100.00	100.00
76.06	100.00	100.00	100.00	100.00	100.00	100.00	100.00	100.00	100.00	100.00	100.00	100.00
84.01	100.00	100.00	100.00	100.00	100.00	100.00	100.00	100.00	100.00	100.00	100.00	100.00
92.78	100.00	100.00	100.00	100.00	100.00	100.00	100.00	100.00	100.00	100.00	100.00	100.00
102.48	100.00	100.00	100.00	100.00	100.00	100.00	100.00	100.00	100.00	100.00	100.00	100.00
113.18	100.00	100.00	100.00	100.00	100.00	100.00	100.00	100.00	100.00	100.00	100.00	100.00
125.01	100.00	100.00	100.00	100.00	100.00	100.00	100.00	100.00	100.00	100.00	100.00	100.00
138.07	100.00	100.00	100.00	100.00	100.00	100.00	100.00	100.00	100.00	100.00	100.00	100.00
152.50	100.00	100.00	100.00	100.00	100.00	100.00	100.00	100.00	100.00	100.00	100.00	100.00
168.43	100.00	100.00	100.00	100.00	100.00	100.00	100.00	100.00	100.00	100.00	100.00	100.00
186.03	100.00	100.00	100.00	100.00	100.00	100.00	100.00	100.00	100.00	100.00	100.00	100.00
205.46	100.00	100.00	100.00	100.00	100.00	100.00	100.00	100.00	100.00	100.00	100.00	100.00
226.93	100.00	100.00	100.00	100.00	100.00	100.00	100.00	100.00	100.00	100.00	100.00	100.00
250.64	100.00	100.00	100.00	100.00	100.00	100.00	100.00	100.00	100.00	100.00	100.00	100.00
276.82	100.00	100.00	100.00	100.00	100.00	100.00	100.00	100.00	100.00	100.00	100.00	100.00
305.75	100.00	100.00	100.00	100.00	100.00	100.00	100.00	100.00	100.00	100.00	100.00	100.00
337.69	100.00	100.00	100.00	100.00	100.00	100.00	100.00	100.00	100.00	100.00	100.00	100.00
372.97	100.00	100.00	100.00	100.00	100.00	100.00	100.00	100.00	100.00	100.00	100.00	100.00
411.94	100.00	100.00	100.00	100.00	100.00	100.00	100.00	100.00	100.00	100.00	100.00	100.00
454.98	100.00	100.00	100.00	100.00	100.00	100.00	100.00	100.00	100.00	100.00	100.00	100.00
502.51	100.00	100.00	100.00	100.00	100.00	100.00	100.00	100.00	100.00	100.00	100.00	100.00
555.02	100.00	100.00	100.00	100.00	100.00	100.00	100.00	100.00	100.00	100.00	100.00	100.00
613.00	100.00	100.00	100.00	100.00	100.00	100.00	100.00	100.00	100.00	100.00	100.00	100.00
677.05	100.00	100.00	100.00	100.00	100.00	100.00	100.00	100.00	100.00	100.00	100.00	100.00
747.79	100.00	100.00	100.00	100.00	100.00	100.00	100.00	100.00	100.00	100.00	100.00	100.00
825.91	100.00	100.00	100.00	100.00	100.00	100.00	100.00	100.00	100.00	100.00	100.00	100.00
912.20	100.00	100.00	100.00	100.00	100.00	100.00	100.00	100.00	100.00	100.00	100.00	100.00
1,007.51	100.00	100.00	100.00	100.00	100.00	100.00	100.00	100.00	100.00	100.00	100.00	100.00
1,112.77	100.00	100.00	100.00	100.00	100.00	100.00	100.00	100.00	100.00	100.00	100.00	100.00
1,229.04	100.00	100.00	100.00	100.00	100.00	100.00	100.00	100.00	100.00	100.00	100.00	100.00
1,357.44	100.00	100.00	100.00	100.00	100.00	100.00	100.00	100.00	100.00	100.00	100.00	100.00
1,499.27	100.00	100.00	100.00	100.00	100.00	100.00	100.00	100.00	100.00	100.00	100.00	100.00

Size High [ $\mu\text{m}$ ]	17-RS-013	17-RS-014	17-RS-015	17-RS-017	17-RS-018	17-RS-019	17-RS-020	17-RS-021	17-RS-022	17-RS-023	17-RS-024	17-RS-025
1,655.91	100.00	100.00	100.00	100.00	100.00	100.00	100.00	100.00	100.00	100.00	100.00	100.00
1,828.92	100.00	100.00	100.00	100.00	100.00	100.00	100.00	100.00	100.00	100.00	100.00	100.00
2,020.00	100.00	100.00	100.00	100.00	100.00	100.00	100.00	100.00	100.00	100.00	100.00	100.00

Wentworth GSC	17-RS-013	17-RS-014	17-RS-015	17-RS-017	17-RS-018	17-RS-019	17-RS-020	17-RS-021	17-RS-022	17-RS-023	17-RS-024	17-RS-025
63-31 coarse	20.10	14.19	24.01	18.64	18.97	14.87	18.59	16.29	14.42	10.67	20.06	16.86
15.6-31 medium silt	32.30	26.07	38.79	31.62	32.19	28.93	33.87	32.33	27.96	21.34	37.06	31.94
7.8-15.6 fine silt	52.25	48.25	58.53	52.17	53.09	53.22	56.98	58.48	53.28	45.83	61.57	57.26
7.8-3.9 very fine silt	89.43	90.90	91.87	90.34	91.02	94.07	94.28	96.34	95.01	91.55	96.09	95.51
0.06-3.9 clay	100.00	100.00	100.00	100.00	100.00	100.00	100.00	100.00	100.00	100.00	100.00	100.00

Size High [ $\mu\text{m}$ ]	17-RS-026	17-RS-027	17-RS-028	17-RS-029	17-RS-030	17-RS-031	17-RS-032	17-RS-033	17-RS-034	17-RS-035	17-RS-037	17-RS-039
0.09	0.00	0.00	0.00	0.00	0.00	0.00	0.00	0.00	0.00	0.00	0.00	0.00
0.10	0.00	0.00	0.00	0.00	0.00	0.00	0.00	0.00	0.00	0.00	0.00	0.00
0.11	0.00	0.00	0.00	0.00	0.00	0.00	0.00	0.00	0.00	0.00	0.00	0.00
0.12	0.00	0.00	0.00	0.00	0.00	0.00	0.00	0.00	0.00	0.00	0.00	0.00
0.13	0.00	0.00	0.00	0.00	0.00	0.00	0.00	0.00	0.00	0.00	0.00	0.00
0.15	0.00	0.00	0.00	0.00	0.00	0.00	0.00	0.00	0.00	0.00	0.00	0.00
0.16	0.00	0.00	0.00	0.00	0.00	0.00	0.00	0.00	0.00	0.00	0.00	0.00
0.18	0.00	0.00	0.00	0.00	0.00	0.00	0.00	0.00	0.00	0.00	0.00	0.00
0.20	0.00	0.00	0.00	0.00	0.00	0.00	0.00	0.00	0.00	0.00	0.00	0.00
0.22	0.00	0.00	0.00	0.00	0.00	0.00	0.00	0.00	0.00	0.00	0.00	0.00
0.24	0.00	0.00	0.00	0.00	0.00	0.00	0.00	0.00	0.00	0.00	0.00	0.00
0.26	0.00	0.00	0.00	0.00	0.00	0.00	0.00	0.00	0.00	0.00	0.00	0.00
0.29	0.00	0.00	0.00	0.00	0.00	0.00	0.00	0.00	0.00	0.00	0.00	0.00
0.32	0.01	0.02	0.01	0.01	0.02	0.01	0.01	0.03	0.02	0.03	0.01	0.01
0.36	0.06	0.06	0.06	0.06	0.08	0.06	0.05	0.09	0.09	0.10	0.06	0.05
0.39	0.17	0.17	0.16	0.16	0.20	0.15	0.13	0.23	0.23	0.24	0.16	0.14
0.43	0.36	0.34	0.34	0.33	0.39	0.31	0.28	0.45	0.46	0.48	0.34	0.30
0.48	0.64	0.60	0.62	0.60	0.69	0.56	0.49	0.77	0.80	0.82	0.61	0.54
0.53	1.02	0.95	0.99	0.96	1.07	0.89	0.78	1.19	1.24	1.26	0.96	0.86
0.58	1.48	1.37	1.43	1.39	1.53	1.29	1.13	1.69	1.78	1.78	1.40	1.25
0.65	2.02	1.86	1.96	1.90	2.07	1.75	1.55	2.27	2.39	2.37	1.91	1.70
0.71	2.60	2.39	2.52	2.45	2.64	2.25	2.00	2.88	3.06	3.00	2.47	2.20
0.79	3.21	2.95	3.12	3.02	3.24	2.76	2.47	3.52	3.74	3.64	3.05	2.71
0.87	3.82	3.50	3.71	3.59	3.83	3.28	2.94	4.16	4.44	4.29	3.63	3.22
0.96	4.41	4.04	4.29	4.15	4.41	3.77	3.39	4.80	5.13	4.92	4.19	3.72
1.06	4.98	4.56	4.86	4.68	4.98	4.23	3.82	5.43	5.82	5.54	4.72	4.19
1.17	5.53	5.05	5.41	5.19	5.52	4.67	4.22	6.06	6.52	6.15	5.23	4.64
1.29	6.05	5.52	5.94	5.67	6.04	5.07	4.59	6.70	7.23	6.76	5.71	5.05
1.43	6.57	5.97	6.47	6.14	6.56	5.45	4.92	7.35	7.97	7.38	6.16	5.45
1.58	7.09	6.41	7.01	6.60	7.08	5.82	5.24	8.03	8.76	8.02	6.62	5.85
1.74	7.63	6.87	7.57	7.07	7.64	6.18	5.55	8.76	9.62	8.69	7.10	6.25
1.92	8.23	7.36	8.18	7.57	8.25	6.58	5.87	9.55	10.58	9.41	7.62	6.68
2.13	8.91	7.90	8.86	8.13	8.93	7.01	6.22	10.42	11.64	10.19	8.20	7.15



Size High [ $\mu\text{m}$ ]	17-RS-026	17-RS-027	17-RS-028	17-RS-029	17-RS-030	17-RS-031	17-RS-032	17-RS-033	17-RS-034	17-RS-035	17-RS-037	17-RS-039
2.35	9.65	8.49	9.60	8.74	9.70	7.47	6.59	11.36	12.80	11.02	8.85	7.66
2.59	10.48	9.14	10.42	9.41	10.57	7.99	7.00	12.38	14.08	11.90	9.59	8.23
2.86	11.45	9.92	11.37	10.21	11.60	8.61	7.49	13.54	15.52	12.90	10.46	8.90
3.16	12.54	10.78	12.43	11.12	12.78	9.31	8.03	14.81	17.10	13.99	11.44	9.65
3.49	13.75	11.75	13.60	12.14	14.11	10.10	8.63	16.19	18.81	15.17	12.54	10.49
3.86	15.12	12.86	14.93	13.32	15.66	11.01	9.31	17.72	20.70	16.48	13.82	11.47
4.26	16.66	14.11	16.40	14.67	17.40	12.06	10.09	19.40	22.73	17.93	15.26	12.57
4.71	18.35	15.50	18.01	16.17	19.34	13.24	10.95	21.21	24.90	19.50	16.84	13.81
5.20	20.18	17.02	19.73	17.80	21.44	14.55	11.91	23.13	27.17	21.19	18.56	15.17
5.74	22.17	18.71	21.60	19.60	23.73	16.03	12.99	25.19	29.57	23.03	20.45	16.69
6.34	24.34	20.57	23.61	21.58	26.19	17.70	14.20	27.39	32.08	25.03	22.50	18.37
7.00	26.68	22.62	25.77	23.73	28.83	19.60	15.58	29.74	34.71	27.20	24.74	20.23
7.74	29.21	24.87	28.10	26.09	31.63	21.73	17.15	32.27	37.46	29.56	27.15	22.30
8.54	31.91	27.35	30.59	28.64	34.60	24.13	18.94	34.98	40.34	32.13	29.76	24.57
9.44	34.83	30.10	33.31	31.48	37.77	26.86	21.02	37.93	43.41	34.96	32.60	27.14
10.42	37.99	33.16	36.26	34.60	41.17	29.96	23.41	41.15	46.70	38.08	35.70	30.02
11.51	41.45	36.60	39.50	38.09	44.87	33.52	26.23	44.71	50.28	41.57	39.13	33.30
12.72	45.23	40.47	43.05	41.97	48.89	37.60	29.50	48.63	54.18	45.43	42.92	37.02
14.04	49.36	44.78	46.94	46.24	53.22	42.22	33.28	52.90	58.40	49.70	47.09	41.21
15.51	53.85	49.56	51.18	50.93	57.88	47.41	37.57	57.52	62.96	54.38	51.64	45.88
17.13	58.80	54.90	55.88	56.10	62.91	53.29	42.50	62.56	67.87	59.54	56.69	51.12
18.92	64.30	60.86	61.16	61.85	68.35	59.92	48.17	68.05	73.13	65.27	62.32	56.99
20.90	70.33	67.40	67.05	68.15	74.13	67.20	54.65	73.92	78.62	71.49	68.50	63.47
23.08	76.61	74.16	73.32	74.70	79.98	74.66	61.66	79.89	84.04	77.88	74.96	70.25
25.49	82.88	80.88	79.78	81.26	85.64	81.95	69.11	85.67	89.11	84.15	81.46	77.14
28.16	88.74	87.14	86.02	87.42	90.78	88.50	76.65	90.88	93.46	89.85	87.60	83.79
31.10	93.81	92.62	91.70	92.84	95.06	93.95	84.17	95.18	96.82	94.62	93.00	89.97
34.35	97.37	96.58	95.96	96.75	97.97	97.58	90.47	98.06	98.90	97.82	96.87	94.77
37.94	99.35	98.94	98.63	99.04	99.53	99.48	95.39	99.56	99.85	99.50	99.13	98.01
41.90	100.00	99.88	99.78	99.92	100.00	100.00	98.36	100.00	100.00	100.00	99.96	99.60
46.28	100.00	100.00	100.00	100.00	100.00	100.00	99.68	100.00	100.00	100.00	100.00	100.00
51.11	100.00	100.00	100.00	100.00	100.00	100.00	100.00	100.00	100.00	100.00	100.00	100.00
56.45	100.00	100.00	100.00	100.00	100.00	100.00	100.00	100.00	100.00	100.00	100.00	100.00

Size High [μm]	17-RS-026	17-RS-027	17-RS-028	17-RS-029	17-RS-030	17-RS-031	17-RS-032	17-RS-033	17-RS-034	17-RS-035	17-RS-037	17-RS-039
62.35	100.00	100.00	100.00	100.00	100.00	100.00	100.00	100.00	100.00	100.00	100.00	100.00
68.87	100.00	100.00	100.00	100.00	100.00	100.00	100.00	100.00	100.00	100.00	100.00	100.00
76.06	100.00	100.00	100.00	100.00	100.00	100.00	100.00	100.00	100.00	100.00	100.00	100.00
84.01	100.00	100.00	100.00	100.00	100.00	100.00	100.00	100.00	100.00	100.00	100.00	100.00
92.78	100.00	100.00	100.00	100.00	100.00	100.00	100.00	100.00	100.00	100.00	100.00	100.00
102.48	100.00	100.00	100.00	100.00	100.00	100.00	100.00	100.00	100.00	100.00	100.00	100.00
113.18	100.00	100.00	100.00	100.00	100.00	100.00	100.00	100.00	100.00	100.00	100.00	100.00
125.01	100.00	100.00	100.00	100.00	100.00	100.00	100.00	100.00	100.00	100.00	100.00	100.00
138.07	100.00	100.00	100.00	100.00	100.00	100.00	100.00	100.00	100.00	100.00	100.00	100.00
152.50	100.00	100.00	100.00	100.00	100.00	100.00	100.00	100.00	100.00	100.00	100.00	100.00
168.43	100.00	100.00	100.00	100.00	100.00	100.00	100.00	100.00	100.00	100.00	100.00	100.00
186.03	100.00	100.00	100.00	100.00	100.00	100.00	100.00	100.00	100.00	100.00	100.00	100.00
205.46	100.00	100.00	100.00	100.00	100.00	100.00	100.00	100.00	100.00	100.00	100.00	100.00
226.93	100.00	100.00	100.00	100.00	100.00	100.00	100.00	100.00	100.00	100.00	100.00	100.00
250.64	100.00	100.00	100.00	100.00	100.00	100.00	100.00	100.00	100.00	100.00	100.00	100.00
276.82	100.00	100.00	100.00	100.00	100.00	100.00	100.00	100.00	100.00	100.00	100.00	100.00
305.75	100.00	100.00	100.00	100.00	100.00	100.00	100.00	100.00	100.00	100.00	100.00	100.00
337.69	100.00	100.00	100.00	100.00	100.00	100.00	100.00	100.00	100.00	100.00	100.00	100.00
372.97	100.00	100.00	100.00	100.00	100.00	100.00	100.00	100.00	100.00	100.00	100.00	100.00
411.94	100.00	100.00	100.00	100.00	100.00	100.00	100.00	100.00	100.00	100.00	100.00	100.00
454.98	100.00	100.00	100.00	100.00	100.00	100.00	100.00	100.00	100.00	100.00	100.00	100.00
502.51	100.00	100.00	100.00	100.00	100.00	100.00	100.00	100.00	100.00	100.00	100.00	100.00
555.02	100.00	100.00	100.00	100.00	100.00	100.00	100.00	100.00	100.00	100.00	100.00	100.00
613.00	100.00	100.00	100.00	100.00	100.00	100.00	100.00	100.00	100.00	100.00	100.00	100.00
677.05	100.00	100.00	100.00	100.00	100.00	100.00	100.00	100.00	100.00	100.00	100.00	100.00
747.79	100.00	100.00	100.00	100.00	100.00	100.00	100.00	100.00	100.00	100.00	100.00	100.00
825.91	100.00	100.00	100.00	100.00	100.00	100.00	100.00	100.00	100.00	100.00	100.00	100.00
912.20	100.00	100.00	100.00	100.00	100.00	100.00	100.00	100.00	100.00	100.00	100.00	100.00
1,007.51	100.00	100.00	100.00	100.00	100.00	100.00	100.00	100.00	100.00	100.00	100.00	100.00
1,112.77	100.00	100.00	100.00	100.00	100.00	100.00	100.00	100.00	100.00	100.00	100.00	100.00
1,229.04	100.00	100.00	100.00	100.00	100.00	100.00	100.00	100.00	100.00	100.00	100.00	100.00
1,357.44	100.00	100.00	100.00	100.00	100.00	100.00	100.00	100.00	100.00	100.00	100.00	100.00
1,499.27	100.00	100.00	100.00	100.00	100.00	100.00	100.00	100.00	100.00	100.00	100.00	100.00

Size High [ $\mu\text{m}$ ]	17-RS-026	17-RS-027	17-RS-028	17-RS-029	17-RS-030	17-RS-031	17-RS-032	17-RS-033	17-RS-034	17-RS-035	17-RS-037	17-RS-039
1,655.91	100.00	100.00	100.00	100.00	100.00	100.00	100.00	100.00	100.00	100.00	100.00	100.00
1,828.92	100.00	100.00	100.00	100.00	100.00	100.00	100.00	100.00	100.00	100.00	100.00	100.00
2,020.00	100.00	100.00	100.00	100.00	100.00	100.00	100.00	100.00	100.00	100.00	100.00	100.00

Wentworth GSC	17-RS-026	17-RS-027	17-RS-028	17-RS-029	17-RS-030	17-RS-031	17-RS-032	17-RS-033	17-RS-034	17-RS-035	17-RS-037	17-RS-039
63-31 coarse	15.12	12.86	14.93	13.32	15.66	11.01	9.31	17.72	20.70	16.48	13.82	11.47
15.6-31 medium silt	29.21	24.87	28.10	26.09	31.63	21.73	17.15	32.27	37.46	29.56	27.15	22.30
7.8-15.6 fine silt	53.85	49.56	51.18	50.93	57.88	47.41	37.57	57.52	62.96	54.38	51.64	45.88
7.8-3.9 very fine silt	93.81	92.62	91.70	92.84	95.06	93.95	84.17	95.18	96.82	94.62	93.00	89.97
0.06-3.9 clay	100.00	100.00	100.00	100.00	100.00	100.00	100.00	100.00	100.00	100.00	100.00	100.00

Size High [ $\mu\text{m}$ ]
0.09
0.10
0.11
0.12
0.13
0.15
0.16
0.18
0.20
0.22
0.24
0.26
0.29
0.32
0.36
0.39
0.43
0.48
0.53
0.58
0.65
0.71
0.79
0.87
0.96
1.06
1.17
1.29
1.43
1.58
1.74
1.92
2.13

17-RS-016 C1	17-RS-016 C2	17-RS-016 C3
0.00	0.00	0.00
0.00	0.00	0.00
0.00	0.00	0.00
0.00	0.00	0.00
0.00	0.00	0.00
0.00	0.00	0.00
0.00	0.00	0.00
0.00	0.00	0.00
0.00	0.00	0.00
0.00	0.00	0.00
0.00	0.00	0.00
0.00	0.00	0.00
0.00	0.00	0.00
0.01	0.01	0.01
0.04	0.04	0.04
0.11	0.10	0.11
0.21	0.20	0.22
0.36	0.35	0.39
0.57	0.56	0.62
0.82	0.81	0.90
1.10	1.10	1.22
1.42	1.42	1.58
1.75	1.76	1.95
2.08	2.09	2.32
2.39	2.42	2.67
2.70	2.73	3.01
2.99	3.02	3.33
3.26	3.28	3.62
3.50	3.51	3.90
3.74	3.73	4.16
3.97	3.94	4.42
4.20	4.14	4.68
4.44	4.34	4.95

Size High [ $\mu\text{m}$ ]
2.35
2.59
2.86
3.16
3.49
3.86
4.26
4.71
5.20
5.74
6.34
7.00
7.74
8.54
9.44
10.42
11.51
12.72
14.04
15.51
17.13
18.92
20.90
23.08
25.49
28.16
31.10
34.35
37.94
41.90
46.28
51.11
56.45

17-RS-016 C1	17-RS-016 C2	17-RS-016 C3
4.69	4.54	5.23
4.95	4.75	5.52
5.24	4.98	5.83
5.55	5.23	6.17
5.88	5.49	6.52
6.24	5.78	6.90
6.62	6.09	7.32
7.02	6.43	7.76
7.44	6.80	8.23
7.90	7.20	8.74
8.38	7.65	9.28
8.92	8.16	9.87
9.49	8.73	10.51
10.12	9.39	11.20
10.82	10.17	11.99
11.62	11.09	12.91
12.58	12.23	14.05
13.75	13.63	15.46
15.18	15.35	17.20
16.91	17.44	19.31
19.00	19.90	21.81
21.44	22.74	24.68
24.15	25.82	27.84
26.93	28.87	31.06
29.67	31.78	34.29
32.37	34.52	37.60
35.28	37.40	41.33
38.57	40.67	45.66
42.94	45.11	51.27
48.67	51.04	58.19
56.14	58.82	66.45
65.26	68.24	75.59
75.21	78.28	84.50





Sample number	>8.0 mm (wt%)	<8.0 mm (wt%)	<4.0 mm (wt%)	<2.0 mm (wt%)	<1.0 mm (wt%)	<0.5 mm (wt%)	<0.25 mm (wt%)	<0.125 mm (wt%)	>0.063 mm (%)	>0.031 mm (%)	>0.0156 mm (%)	>0.0078 mm (%)	>0.0006 mm (%)
17-RS-001-B	7.867644704	6.090521798	6.792017682	7.157179922	7.794612255	9.037445146	14.23620231	36.52263045	0.872946887	0.589740186	0.911017325	1.666606258	0.461435076
17-RS-002-B	7.337745342	5.405864907	5.886945954	6.79621432	7.332078157	9.160689885	14.6156704	25.80962036	3.146496583	2.382043541	3.801194275	6.807534876	1.517901401
17-RS-003-B	6.226880684	5.303753143	5.997508872	7.071984207	7.018871472	8.891917934	13.27818383	28.72364927	2.989654376	2.459332189	3.988525714	6.7941574	1.255580914
17-RS-004-B	17.70881243	7.803255264	7.408515484	8.329277278	8.076983188	10.35611422	11.86719954	14.86079171	1.770830871	1.49177205	2.84882939	5.693941217	1.783677356
17-RS-005-B	5.144760736	4.481385552	4.8503391	5.288883215	6.107498898	8.81453084	16.22983829	34.32338614	1.724154494	1.713825282	3.296890324	6.351994834	1.672071242
17-RS-006-B	33.2663325	16.04014106	11.37463479	11.18532675	11.99101659	3.313536752	5.368788855	5.936066864	0.372561902	0.217978313	0.295945276	0.513599071	0.124071273
17-RS-007-B	4.612089043	3.695679263	5.603413747	7.766304009	9.040599438	11.69785402	19.73489018	30.05801827	0.715193216	0.523052567	1.117070778	3.076386634	2.324814575
17-RS-008-B	3.455955215	3.826272615	5.519517004	6.893011472	7.674508883	9.511283188	14.94703184	26.98260274	3.127635871	2.612797274	4.622171191	8.638970175	2.188242527
17-RS-009-B	5.984758407	13.40788569	7.451222388	6.649006888	7.331316506	9.901014936	12.33023786	19.06704194	1.970995649	1.428348886	3.207178212	7.974773918	3.296218725
17-RS-010-B	6.261595954	3.994186445	4.59800984	6.231755845	7.036561156	11.20057293	16.02764949	27.79878287	2.362531491	2.03054223	3.870717858	7.081784945	1.505308937
17-RS-011-B	17.21708906	4.647627972	4.508160997	4.946174464	5.8603369	8.174072218	14.63749482	24.2514546	2.933521385	2.119649461	3.267629319	5.979990481	1.456798318
17-RS-012-B	18.60965293	7.769113136	7.43867431	8.590068055	8.746121033	10.15909355	10.93935844	15.16843884	1.110912418	0.941449547	2.179423425	5.436248537	2.911445777
17-RS-013-B	2.38407309	3.09273681	3.709868732	5.498985129	6.880454753	12.02605165	18.67343058	38.28161787	1.899882817	1.153211594	1.885875845	3.514708661	0.999102471
17-RS-014-B	7.055947186	6.160410683	6.122502219	7.068175722	7.643732182	11.4631118	18.02249888	21.70165795	2.094423372	1.75356165	3.274742207	6.295752864	1.343483288
17-RS-015-B	7.323735519	10.33367143	11.19230921	8.909307668	7.949754296	10.73776142	14.46180345	18.28590585	2.594225813	1.597282789	2.132983433	3.602658204	0.878600923
17-RS-016-C1	0	0.59970015	0.791093815	2.421129861	7.024147501	15.9303271	36.73482408	30.55768398	0.436922723	0.228019653	0.519619235	1.286718987	3.469807312
17-RS-016-C2	0	0.167715798	0.836400863	3.106009453	14.02713947	27.79943804	29.64213369	20.51042748	0.257778416	0.131975572	0.388368558	0.891228042	2.241384619
17-RS-016-C3	0	0	0	0.491358861	3.761436801	5.574381566	7.099288377	48.04580828	2.628603597	1.371662275	3.350508232	8.382549801	19.29440221
17-RS-017-B	4.915247105	2.248518718	3.782823862	4.907251549	6.473959736	9.313644627	12.98234245	37.54687921	3.322559041	2.314457538	3.665118084	6.804830219	1.722367868
17-RS-018-B	5.253002403	4.811805931	6.093376635	7.264371782	7.348409205	12.39839489	19.28725208	22.57742272	2.838875097	1.978823675	3.127113656	5.67773297	1.343413916
17-RS-019-B	6.382029517	7.074129449	6.955966046	8.218385261	8.352826276	8.70791936	10.92468892	20.1806212	3.449275725	3.263221265	5.635997606	9.479240865	1.375698512
17-RS-020-B	7.733330066	5.192081197	5.683713493	7.240549097	8.29158543	12.87977063	12.3854581	22.69978114	3.326964074	2.73321972	4.136029336	6.673158798	1.024358918
17-RS-021-B	10.49975653	4.477553309	5.203884131	6.140134791	6.923344477	8.211098335	10.70967636	18.82985036	4.72383971	4.654797423	7.581931838	10.98372367	1.060409077
17-RS-022-B	2.331677869	2.553121109	4.037066474	5.789775938	6.668198086	9.107289709	12.36691583	31.64864952	3.677220829	3.450962105	6.456709077	10.6392362	1.273177258
17-RS-023-B	2.549496088	0.929624131	1.517323034	3.769293568	2.40101976	8.287079695	16.50818052	41.37734471	2.416965927	2.419924153	5.548728859	10.36036391	1.91465205
17-RS-024-B	2.181645911	1.827008671	3.228989982	5.338006903	6.181165897	8.330930278	25.61680909	26.22175216	4.22840058	3.582419163	5.164624643	7.274947334	0.823299391
17-RS-025-B	1.857058113	2.951784537	4.41823189	5.869213885	7.183216993	8.002880975	12.66513412	24.71596213	5.450899505	4.878101938	8.185791198	12.36981111	1.451913605
17-RS-026-B	2.96118801	4.271759249	5.193678327	5.441230672	5.356872063	7.852480896	13.91726228	30.96673961	3.635850828	3.385864312	5.923171405	9.60568472	1.488217627
17-RS-027-B	4.705655326	7.745195544	7.784052062	8.280454997	9.470162997	11.86442306	13.3077899	18.15175697	2.403804511	2.245256605	4.613957212	8.048002706	1.379488108
17-RS-028-B	3.91150345	3.379276171	5.408163265	6.514370137	7.161760388	10.23307884	14.49410879	31.55759066	2.588448493	2.284407177	4.001399092	7.025999949	1.439893578
17-RS-029-B	2.604204072	3.682410407	4.983066751	6.218433784	6.874125007	8.484439225	12.00026862	22.57200711	4.341325322	4.157926467	8.093520566	13.65586151	2.332411156
17-RS-030-B	0.623891969	1.568311267	3.605201614	5.594941722	6.876956735	9.076986911	12.28037418	30.05610879	4.746440732	4.843910675	7.957534693	11.27133751	1.498003199
17-RS-031-B	17.69936696	3.931438922	3.042200539	3.567382003	4.708406849	6.816178971	10.19227842	27.08545896	2.528431774	2.460510077	5.896167727	10.68431539	1.387863404
17-RS-032-B	9.314387364	3.204199874	3.121022944	3.51088291	4.779968954	8.790321675	15.83433605	28.61653802	2.126046661	1.789565246	4.661120683	10.63791884	3.61369078
17-RS-033-B	32.41996701	10.32804931	7.165969268	5.742581821	4.545602917	6.000590329	10.9215036	9.959267298	2.289392314	1.878703205	3.261830312	4.86348822	0.623054392
17-RS-034-B	0.969288859	2.49067847	4.662482264	6.973813853	9.222357934	12.2372316	14.84264485	30.66670674	3.711621575	3.006518969	4.573107206	6.073413088	0.570134604
17-RS-035-B	3.749848522	1.882362677	1.441969023	1.852313446	2.892213899	4.74048794	8.268070672	43.36123807	5.242949403	4.161965752	7.893325534	12.80027492	1.712980148
17-RS-037-B	3.938892948	4.304719526	4.993142439	5.865576568	6.688102894	9.730574054	16.62508953	34.96037854	1.781731352	1.719456448	3.157588027	5.331499375	0.903158303
17-RS-039-B	7.867644704	6.090521798	6.792017682	7.157179922	7.794612255	9.037445146	14.23620231	36.52263045	0.516269164	0.487495195	1.061792082	1.984647489	0.451541801

Sample number	Cumulative weight percent												
	>8.0 mm	<8.0 mm	<4.0 mm	<2.0 mm	<1.0 mm	<0.5 mm	<0.25 mm	<0.125 mm	>0.063 mm	>0.031 mm	>0.0156 mm	>0.0078 mm	>0.0006 mm
17-RS-001-B	7.9	14.0	20.8	27.9	35.7	44.7	59.0	95.5	96.4	97.0	97.9	99.5	100
17-RS-002-B	7.3	12.7	18.6	25.4	32.8	41.9	56.5	82.3	85.5	87.9	91.7	98.5	100
17-RS-003-B	6.2	11.5	17.5	24.6	31.6	40.5	53.8	82.5	85.5	88.0	92.0	98.7	100
17-RS-004-B	17.7	25.5	32.9	41.2	49.3	59.7	71.6	86.4	88.2	89.7	92.5	98.2	100
17-RS-005-B	5.1	9.6	14.5	19.8	25.9	34.7	50.9	85.2	87.0	88.7	92.0	98.3	100
17-RS-006-B	33.3	49.3	60.7	71.9	83.9	87.2	92.5	98.5	98.8	99.1	99.4	99.9	100
17-RS-007-B	4.6	8.3	13.9	21.7	30.7	42.4	62.2	92.2	93.0	93.5	94.6	97.7	100
17-RS-008-B	3.5	7.3	12.8	19.7	27.4	36.9	51.8	78.8	81.9	84.6	89.2	97.8	100
17-RS-009-B	6.0	19.4	26.8	33.5	40.8	50.7	63.1	82.1	84.1	85.5	88.7	96.7	100
17-RS-010-B	6.3	10.3	14.9	21.1	28.1	39.3	55.4	83.1	85.5	87.5	91.4	98.5	100
17-RS-011-B	17.2	21.9	26.4	31.3	37.2	45.4	60.0	84.2	87.2	89.3	92.6	98.5	100
17-RS-012-B	18.6	26.4	33.8	42.4	51.2	61.3	72.3	87.4	88.5	89.5	91.7	97.1	100
17-RS-013-B	2.4	5.5	9.2	14.7	21.6	33.6	52.3	90.5	92.4	93.6	95.5	99.0	100
17-RS-014-B	7.1	13.2	19.3	26.4	34.1	45.5	63.5	85.2	87.3	89.1	92.4	98.7	100
17-RS-015-B	7.3	17.7	28.8	37.8	45.7	56.4	70.9	89.2	91.8	93.4	95.5	99.1	100
17-RS-016-C1	0.0	0.6	1.4	3.8	10.8	26.8	63.5	94.1	94.5	94.7	95.2	96.5	100
17-RS-016-C2	0.0	0.2	1.0	4.1	18.1	45.9	75.6	96.1	96.3	96.5	96.9	97.8	100
17-RS-016-C3	0.0	0.0	0.0	0.5	4.3	9.8	16.9	65.0	67.6	69.0	72.3	80.7	100
17-RS-017-B	4.9	7.2	10.9	15.9	22.3	31.6	44.6	82.2	85.5	87.8	91.5	98.3	100
17-RS-018-B	5.3	10.1	16.2	23.4	30.8	43.2	62.5	85.0	87.9	89.9	93.0	98.7	100
17-RS-019-B	6.4	13.5	20.4	28.6	37.0	45.7	56.6	76.8	80.2	83.5	89.1	98.6	100
17-RS-020-B	7.7	12.9	18.6	25.8	34.1	47.0	59.4	82.1	85.4	88.2	92.3	99.0	100
17-RS-021-B	10.5	15.0	20.2	26.3	33.2	41.5	52.2	71.0	75.7	80.4	88.0	98.9	100
17-RS-022-B	2.3	4.9	8.9	14.7	21.4	30.5	42.9	74.5	78.2	81.6	88.1	98.7	100
17-RS-023-B	2.5	3.5	5.0	8.8	11.2	19.5	36.0	77.3	79.8	82.2	87.7	98.1	100
17-RS-024-B	2.2	4.0	7.2	12.6	18.8	27.1	52.7	78.9	83.2	86.7	91.9	99.2	100
17-RS-025-B	1.9	4.8	9.2	15.1	22.3	30.3	42.9	67.7	73.1	78.0	86.2	98.5	100
17-RS-026-B	3.0	7.2	12.4	17.9	23.2	31.1	45.0	76.0	79.6	83.0	88.9	98.5	100
17-RS-027-B	4.7	12.5	20.2	28.5	38.0	49.8	63.2	81.3	83.7	86.0	90.6	98.6	100
17-RS-028-B	3.9	7.3	12.7	19.2	26.4	36.6	51.1	82.7	85.2	87.5	91.5	98.6	100
17-RS-029-B	2.6	6.3	11.3	17.5	24.4	32.8	44.8	67.4	71.8	75.9	84.0	97.7	100
17-RS-030-B	0.6	2.2	5.8	11.4	18.3	27.3	39.6	69.7	74.4	79.3	87.2	98.5	100
17-RS-031-B	17.7	21.6	24.7	28.2	32.9	39.8	50.0	77.0	79.6	82.0	87.9	98.6	100
17-RS-032-B	9.3	12.5	15.6	19.2	23.9	32.7	48.6	77.2	79.3	81.1	85.7	96.4	100
17-RS-033-B	32.4	42.7	49.9	55.7	60.2	66.2	77.1	87.1	89.4	91.3	94.5	99.4	100
17-RS-034-B	1.0	3.5	8.1	15.1	24.3	36.6	51.4	82.1	85.8	88.8	93.4	99.4	100
17-RS-035-B	3.7	5.6	7.1	8.9	11.8	16.6	24.8	68.2	73.4	77.6	85.5	98.3	100
17-RS-037-B	3.9	8.2	13.2	19.1	25.8	35.5	52.1	87.1	88.9	90.6	93.8	99.1	100
17-RS-039-B	7.9	14.0	20.8	27.9	35.7	44.7	59.0	95.5	96.4	97.0	97.9	99.5	100

## **Appendix E: Clast lithology results for UW and HW data**

UW clast lithology counts

HW granitoid clast content bins

HW clast lithology estimates

UW clast lithology classification pictures – east study area

UW clast lithology classification pictures – west study area

counts/20 class same unit/measurement	White Granitoid				Pink Granitoid				Metasedimentary				Quartz				Other			
	4-8mm		>8mm		4-8mm		>8mm		4-8mm		>8mm		4-8mm		>8mm		4-8mm		>8mm	
	n =	(g)	n =	(g)	n =	(g)	n =	(g)	n =	(g)	n =	(g)	n =	(g)	n =	(g)	n =	(g)	n =	(g)
17-RS-001-B	82	28.58	17	28.52	96	24.74	11	15.49	144	38.51	26	72.83	2	0.72	0	0	34	0	4	7.18
17-RS-002-B	96	21.84	2	3.57	97	22.54	14	43.9	115	34.06	9	44.47	2	0.48	1	0.74	25	5.34	4	23.47
17-RS-003-B	90	20.16	4	34.52	129	32.24	15	33.21	157	41.12	10	29.15	0	0	0	0	58	16.06	14	34.53
17-RS-004-B	162	40.78	13	29.77	139	40.87	28	142.1	280	75.64	19	101.2	3	0.77	0	0	53	15.89	29	124.1
17-RS-005-B	112	28.63	15	17.73	84	25.93	30	80.73	117	27.47	8	18.62	1	0.37	0	0	85	26.11	5	7.91
17-RS-006-B	436	96.2	42	89.48	463	114.7	105	317.7	894	234.4	122	472.8	7	2.25	3	6.98	133	37.94	49	133.3
17-RS-007-B	83	19.71	11	37.88	110	28.25	10	22.08	165	36.51	9	15.38	1	0.15	0	0	45	12.39	16	48.81
17-RS-008-B	76	19.46	5	9.87	80	17.82	8	16.57	115	34.93	3	14.17	0	0	0	0	12	2.49	6	26.58
17-RS-009-B	122	50.33	27	43.72	123	67.33	23	38.67	419	123.3	11	18.85	5	1.26	0	0	88	23.94	15	18.29
17-RS-010-B	87	20.45	11	26.18	114	29.84	19	73.26	124	33.64	10	23.93	3	0.87	0	0	21	4.31	8	18.12
17-RS-011-B	98	25.19	24	94.53	90	21.55	16	75.39	101	31.31	21	99.74	0	0	0	0	19	6.23	12	44.39
17-RS-012-B	135	34.31	17	58.7	140	40.68	41	197.1	267	77.5	30	130.8	0	0	2	2.16	50	18.03	8	25.16
17-RS-013-B	68	17.92	1	1.98	69	17.9	7	14.28	84	23.33	5	21.8	0	0	0	0	13	3.59	4	12.06
17-RS-014-B	131	32.65	8	13.4	156	39.82	30	96.91	121	63.54	8	12.3	4	1.12	1	1.03	45	13.56	17	49.6
17-RS-015-B	144	32.61	13	23.54	126	30.52	14	49.67	209	44.57	6	26.41	0	0	0	0	44	11.26	20	56.36
17-RS-017-B	65	12.74	8	77	70	15.14	6	18.9	88	20.72	8	13.6	5	1.3	0	0	15	3.9	0	0
17-RS-018-B	90	19.83	3	13.31	73	17.5	14	39.97	107	29.08	3	20.14	0	0	0	0	28	8.23	14	19.92
17-RS-019-B	137	28.85	8	20.82	146	38.25	21	55.2	122	34.68	3	5.36	0	0	0	0	51	15.11	10	24.51
17-RS-020-B	148	36.26	11	46.63	162	42.97	22	59.15	149	44.65	10	29.1	6	1.32	0	0	36	10.26	15	67.38
17-RS-021-B	108	24.56	10	15.26	155	38.63	29	104.2	93	27.47	10	18.01	0	0	0	0	68	18.74	15	119.6
17-RS-022-B	49	10.08	1	0.82	59	16.66	7	19.89	99	24.55	3	6.3	2	0.26	0	0	17	4.11	5	23.78
17-RS-023-B	17	4.3	0	0	22	5.36	3	24.81	36	8.45	6	27.49	3	0.53	0	0	3	0.76	1	1.09
17-RS-024-B	34	6.57	5	6.39	33	7.74	2	2.5	97	20.11	10	39.83	1	0.27	0	0	22	5.52	0	0
17-RS-025-B	62	13.54	2	2.35	69	15.93	8	25.71	93	21.28	3	5.64	0	0	0	0	10	2.5	0	0
17-RS-026-B	109	21.71	8	15.77	110	29.18	6	9.22	191	48.32	11	16.78	3	0.47	0	0	15	4.81	5	17.16
17-RS-027-B	114	24.3	6	9.35	214	56.54	10	22.54	309	84.55	30	58.25	2	0.68	0	0	45	12.1	11	16.96
17-RS-028-B	30	6.14	2	2.2	49	11.33	3	8.62	82	23.28	7	15.3	2	0.39	0	0	12	2.78	6	56.88
17-RS-029-B	69	13.78	10	19.91	95	23.27	11	18.04	151	36.87	7	12.43	9	1.63	0	0	15	3.54	3	5.45
17-RS-030-B	29	5.45	0	0	28	5.79	1	1.48	70	17.36	5	11.52	5	1.01	0	0	14	3.73	1	1.27
17-RS-031-B	42	11.02	7	16.12	77	20.75	10	91.84	106	45.01	20	179.8	0	0	0	0	24	6.06	23	89.4
17-RS-032-B	42	11.6	8	28.07	54	16.25	8	44.66	107	31.71	19	89.73	3	0.75	0	0	11	2.08	7	20.13
17-RS-033-B	168	43.06	33	62.18	304	84.21	30	144.4	441	153.5	108	622.2	6	0.93	0	0	47	12.07	27	60.38
17-RS-034-B	41	8.21	0	0	66	14.82	4	11.85	98	20.61	5	4.89	0	0	0	0	13	2.03	2	2.13
17-RS-035-B	29	6.5	9	16.2	27	8.8	10	17.1	49	13.72	22	46.8	1	0.2	0	0	12	3.73	0	0
17-RS-037-B	79	17.47	9	20.75	115	27.64	16	43.62	215	58.7	12	32.63	0	0	0	0	22	6.11	6	8.33
17-RS-039-B	35	10.32	6	23.96	42	11.43	7	32.66	114	36.8	17	64.1	0	0	0	0	21	5.96	1	3.69

Granitoid clast content in bins

Bins (% granitoid)	West # samples	East # samples
0	3	6
5	2	3
10	20	4
20	41	17
30	48	34
40	23	97
50	21	84
60	10	52
70	2	24
80	2	2
90	2	1
95	1	0
	175	324

SampleID	SampleNum	HoleID	CollarEasting	CollarNorthing	StudyArea	Depth Interval Bin	MetaSed (%)	Granitic (%)
HWRC-040-01	1	HW-40	533889	7129918	e	4	50	50
HWRC-041-01	1	HW-41	533865	7130847	e	4	60	40
HWRC-042-01	1	HW-42	533887	7131814	e	4	70	30
HWRC-043-01	1	HW-43	533876	7132854	e	4	80	20
HWRC-044-01	1	HW-44	533886	7133844	e	4	60	40
HWRC-045-01	1	HW-45	533889	7134856	e	4	50	50
HWRC-046-01	1	HW-46	533883	7135833	e	4	50	50
HWRC-047-01	1	HW-47	533881	7136842	e	4	50	50
HWRC-048-01	1	HW-48	533882	7137842	e	4	60	40
HWRC-482-01	1	HW-482	536774	7129893	e	4	60	40
HWRC-483-01	1	HW-483	536943	7131001	e	4	50	50
HWRC-484-01	1	HW-484	536834	7131810	e	4	45	55
HWRC-485-01	1	HW-485	536416	7135069	e	4	50	55
HWRC-486-01	1	HW-486	536077	7133811	e	4	53	47
HWRC-487-01	1	HW-487	536677	7133526	e	4	63	37
HWRC-488-01	1	HW-488	535945	7135629	e	4	50	50
HWRC-489-01	1	HW-489	536636	7136822	e	4	60	40
HWRC-049-01	1	HW-49	530835	7137888	e	4	50	50
HWRC-490-01	1	HW-490	536666	7137283	e	4	60	40
HWRC-491-01	1	HW-491	536455	7137941	e	4	50	50
HWRC-492-01	1	HW-492	535449	7138029	e	4	80	20
HWRC-493-01	1	HW-493	533832	7137060	e	4	60	40
HWRC-494-01	1	HW-494	533768	7138443	e	4	70	30
HWRC-495-01	1	HW-495	535351	7138251	e	4	50	50
HWRC-496-01	1	HW-496	535335	7139007	e	4	50	50
HWRC-497-01	1	HW-497	536580	7138693	e	4	45	55
HWRC-498-01	1	HW-498	536958	7138304	e	4	40	60
HWRC-499-01	1	HW-499	539865	7138821	e	4	30	70
HWRC-050-01	1	HW-50	530929	7138776	e	4	90	10
HWRC-500-01	1	HW-500	539921	7137816	e	4	40	60
HWRC-501-01	1	HW-501	539470	7136684	e	4	40	60
HWRC-502-01	1	HW-502	540076	7135844	e	4	30	70
HWRC-503-01	1	HW-503	539884	7134889	e	4	50	50
HWRC-504-01	1	HW-504	539711	7133744	e	4	95	5
HWRC-505-01	1	HW-505	539928	7132967	e	4	60	40
HWRC-506-01	1	HW-506	539987	7131749	e	4	60	40
HWRC-507-01	1	HW-507	539856	7130818	e	4	50	50
HWRC-508-01	1	HW-508	539974	7129901	e	4	90	10
HWRC-509-01	1	HW-509	542716	7129910	e	4	50	50
HWRC-051-01	1	HW-51	533882	7138721	e	4	100	0
HWRC-510-01	1	HW-510	542884	7130708	e	4	50	50
HWRC-511-01	1	HW-511	542833	7131961	e	4	40	60
HWRC-512-01	1	HW-512	542896	7132936	e	4	50	50
HWRC-513-01	1	HW-513	542837	7133868	e	4	60	40
HWRC-514-01	1	HW-514	542979	7134917	e	4	50	50
HWRC-515-01	1	HW-515	542742	7135996	e	4	60	40
HWRC-516-01	1	HW-516	542939	7136728	e	4	60	40
HWRC-517-01	1	HW-517	542820	7137926	e	4	50	50
HWRC-518-01	1	HW-518	542962	7138795	e	4	60	40
HWRC-519-01	1	HW-519	545809	7138350	e	4	30	70
HWRC-052-01	1	HW-52	530887	7136858	e	4	50	50
HWRC-520-01	1	HW-520	545840	7137544	e	4	30	70
HWRC-521-01	1	HW-521	545814	7136344	e	4	50	50
HWRC-522-01	1	HW-522	545891	7135326	e	4	40	60
HWRC-523-01	1	HW-523	545968	7134302	e	4	50	50



SampleID	SampleNum	HoleID	CollarEasting	CollarNorthing	StudyArea	Depth Interval Bin	MetaSed (%)	Granitic (%)
HWRC-524-01	1	HW-524	545422	7133178	e	4	70	30
HWRC-525-01	1	HW-525	545720	7132292	e	4	70	30
HWRC-526-01	1	HW-526	545641	7131521	e	4	60	40
HWRC-527-01	1	HW-527	545365	7130311	e	4	70	30
HWRC-528-01	1	HW-528	545835	7129364	e	4	60	40
HWRC-053-01	1	HW-53	530890	7135852	e	4	50	50
HWRC-054-01	1	HW-54	530962	7134835	e	4	60	40
HWRC-055-01	1	HW-55	530939	7133753	e	4	95	5
HWRC-056-01	1	HW-56	530861	7132803	e	4	95	5
HWRC-057-01	1	HW-57	530779	7131825	e	4	100	0
HWRC-059-01	1	HW-59	530884	7129853	e	4	40	60
HWRC-626-01	1	HW-626	538023	7131613	e	4	80	20
HWRC-627-01	1	HW-627	537901	7131891	e	4	60	40
HWRC-628-01	1	HW-628	537858	7132128	e	4	70	30
HWRC-629-01	1	HW-629	537897	7132397	e	4	75	25
HWRC-630-01	1	HW-630	537889	7132698	e	4	50	50
HWRC-631-01	1	HW-631	538247	7132882	e	4	80	20
HWRC-632-01	1	HW-632	537898	7133451	e	4	60	40
HWRC-633-01	1	HW-633	537837	7133926	e	4	60	40
HWRC-634-01	1	HW-634	538062	7134569	e	4	60	40
HWRC-635-01	1	HW-635	538006	7135040	e	4	50	50
HWRC-636-01	1	HW-636	537888	7135447	e	4	45	55
HWRC-637-01	1	HW-637	537900	7135946	e	4	50	50
HWRC-638-01	1	HW-638	537881	7136183	e	4	60	40
HWRC-639-01	1	HW-639	538010	7136946	e	4	53	47
HWRC-640-01	1	HW-640	538119	7137327	e	4	10	90
HWRC-641-01	1	HW-641	537833	7137436	e	4	40	60
HWRC-642-01	1	HW-642	537852	7137666	e	4	40	60
HWRC-643-01	1	HW-643	537858	7137933	e	4	30	70
HWRC-644-01	1	HW-644	537916	7138232	e	4	20	80
HWRC-645-01	1	HW-645	537904	7138738	e	4	40	60
HWRC-646-01	1	HW-646	535127	7137062	e	4	40	60
HWRC-647-01	1	HW-647	535174	7136771	e	4	60	40
HWRC-648-01	1	HW-648	535188	7136420	e	4	60	40
HWRC-649-01	1	HW-649	535372	7136078	e	4	80	20
HWRC-650-01	1	HW-650	535255	7135807	e	4	45	55
HWRC-651-01	1	HW-651	535214	7135302	e	4	57	43
HWRC-652-01	1	HW-652	535331	7135036	e	4	50	50
HWRC-653-01	1	HW-653	535211	7134342	e	4	55	45
HWRC-654-01	1	HW-654	535275	7134110	e	4	50	50
HWRC-655-01	1	HW-655	535233	7133870	e	4	50	50
HWRC-656-01	1	HW-656	535211	7133536	e	4	30	70
HWRC-657-01	1	HW-657	535243	7133325	e	4	50	50
HWRC-658-01	1	HW-658	535244	7133083	e	4	40	60
HWRC-659-01	1	HW-659	535288	7132866	e	4	30	70
HWRC-660-01	1	HW-660	535227	7132623	e	4	35	65
HWRC-661-01	1	HW-661	535208	7132332	e	4	40	60
HWRC-662-01	1	HW-662	535191	7131848	e	4	50	50
HWRC-663-01	1	HW-663	530738	7129256	e	4	30	70
HWRC-664-01	1	HW-664	530900	7130060	e	4	50	50
HWRC-665-01	1	HW-665	531006	7130255	e	4	40	60
HWRC-666-01	1	HW-666	530830	7130590	e	4	50	50
HWRC-667-01	1	HW-667	531003	7131149	e	4	60	40
HWRC-668-01	1	HW-668	530780	7131283	e	4	60	40
HWRC-669-01	1	HW-669	530891	7131642	e	4	70	30

SampleID	SampleNum	HoleID	CollarEasting	CollarNorthing	StudyArea	Depth Interval Bin	MetaSed (%)	Granitic (%)
HWRC-670-01	1	HW-670	530805	7132276	e	4	90	10
HWRC-044-02	2	HW-44	533886	7133844	e	3	50	50
HWRC-045-02	2	HW-45	533889	7134856	e	3	60	40
HWRC-046-02	2	HW-46	533883	7135833	e	3	55	45
HWRC-047-02	2	HW-47	533881	7136842	e	3	55	45
HWRC-048-02	2	HW-48	533882	7137842	e	3	70	30
HWRC-482-02	2	HW-482	536774	7129893	e	3	60	40
HWRC-483-03	3	HW-483	536943	7131001	e	3	50	50
HWRC-484-03	3	HW-484	536834	7131810	e	3	40	60
HWRC-485-04	4	HW-485	536416	7135069	e	3	43	50
HWRC-486-05	5	HW-486	536077	7133811	e	3	50	50
HWRC-487-04	4	HW-487	536677	7133526	e	3	80	20
HWRC-488-03	3	HW-488	535945	7135629	e	3	55	45
HWRC-049-02	2	HW-49	530835	7137888	e	3	50	50
HWRC-497-03	3	HW-497	536580	7138693	e	3	40	60
HWRC-503-02	2	HW-503	539884	7134889	e	3	40	60
HWRC-051-02	2	HW-51	533882	7138721	e	3	100	0
HWRC-516-02	2	HW-516	542939	7136728	e	3	50	50
HWRC-524-02	2	HW-524	545422	7133178	e	3	50	50
HWRC-053-02	2	HW-53	530890	7135852	e	3	50	50
HWRC-627-03	3	HW-627	537901	7131891	e	3	63	37
HWRC-628-05	5	HW-628	537858	7132128	e	3	63	37
HWRC-629-03	3	HW-629	537897	7132397	e	3	70	30
HWRC-630-02	2	HW-630	537889	7132698	e	3	50	50
HWRC-635-02	2	HW-635	538006	7135040	e	3	50	50
HWRC-636-03	3	HW-636	537888	7135447	e	3	60	40
HWRC-639-04	4	HW-639	538010	7136946	e	3	43	57
HWRC-645-02	2	HW-645	537904	7138738	e	3	50	50
HWRC-650-03	3	HW-650	535255	7135807	e	3	70	30
HWRC-651-05	5	HW-651	535214	7135302	e	3	53	47
HWRC-652-02	2	HW-652	535331	7135036	e	3	60	40
HWRC-653-03	3	HW-653	535211	7134342	e	3	57	45
HWRC-654-03	3	HW-654	535275	7134110	e	3	50	50
HWRC-655-02	2	HW-655	535233	7133870	e	3	40	60
HWRC-656-02	2	HW-656	535211	7133536	e	3	40	60
HWRC-657-02	2	HW-657	535243	7133325	e	3	35	65
HWRC-658-03	3	HW-658	535244	7133083	e	3	33	67
HWRC-659-02	2	HW-659	535288	7132866	e	3	40	60
HWRC-660-03	3	HW-660	535227	7132623	e	3	37	63
HWRC-661-02	2	HW-661	535208	7132332	e	3	40	60
HWRC-046-04	4	HW-46	533883	7135833	e	2	60	40
HWRC-047-04	4	HW-47	533881	7136842	e	2	60	40
HWRC-048-03	3	HW-48	533882	7137842	e	2	60	40
HWRC-483-04	4	HW-483	536943	7131001	e	2	40	60
HWRC-484-05	5	HW-484	536834	7131810	e	2	60	40
HWRC-485-07	7	HW-485	536416	7135069	e	2	60	40
HWRC-486-08	8	HW-486	536077	7133811	e	2	48	53
HWRC-487-05	5	HW-487	536677	7133526	e	2	70	30
HWRC-488-05	5	HW-488	535945	7135629	e	2	50	50
HWRC-497-05	5	HW-497	536580	7138693	e	2	45	55
HWRC-503-04	4	HW-503	539884	7134889	e	2	60	40
HWRC-051-03	3	HW-51	533882	7138721	e	2	100	0
HWRC-516-04	4	HW-516	542939	7136728	e	2	30	70
HWRC-053-03	3	HW-53	530890	7135852	e	2	60	40
HWRC-627-06	6	HW-627	537901	7131891	e	2	65	35

SampleID	SampleNum	HoleID	CollarEasting	CollarNorthing	StudyArea	Depth Interval Bin	MetaSed (%)	Granitic (%)
HWRC-628-08	8	HW-628	537858	7132128	e	2	70	30
HWRC-629-04	4	HW-629	537897	7132397	e	2	60	40
HWRC-635-03	3	HW-635	538006	7135040	e	2	60	40
HWRC-636-04	4	HW-636	537888	7135447	e	2	50	50
HWRC-639-07	7	HW-639	538010	7136946	e	2	53	47
HWRC-645-03	3	HW-645	537904	7138738	e	2	60	40
HWRC-650-04	4	HW-650	535255	7135807	e	2	67	33
HWRC-651-08	8	HW-651	535214	7135302	e	2	60	40
HWRC-652-03	3	HW-652	535331	7135036	e	2	60	40
HWRC-653-06	6	HW-653	535211	7134342	e	2	50	50
HWRC-654-05	5	HW-654	535275	7134110	e	2	70	30
HWRC-657-04	4	HW-657	535243	7133325	e	2	30	70
HWRC-658-06	6	HW-658	535244	7133083	e	2	35	65
HWRC-660-06	6	HW-660	535227	7132623	e	2	35	65
HWRC-661-03	3	HW-661	535208	7132332	e	2	40	60
HWRC-040-02	2	HW-40	533889	7129918	e	1	70	30
HWRC-041-02	2	HW-41	533865	7130847	e	1	50	50
HWRC-044-03	3	HW-44	533886	7133844	e	1	80	20
HWRC-045-03	3	HW-45	533889	7134856	e	1	60	40
HWRC-046-05	5	HW-46	533883	7135833	e	1	70	30
HWRC-047-05	5	HW-47	533881	7136842	e	1	50	50
HWRC-048-04	4	HW-48	533882	7137842	e	1	100	0
HWRC-482-03	3	HW-482	536774	7129893	e	1	60	40
HWRC-483-06	6	HW-483	536943	7131001	e	1	40	60
HWRC-484-07	7	HW-484	536834	7131810	e	1	65	35
HWRC-485-10	10	HW-485	536416	7135069	e	1	53	47
HWRC-486-12	12	HW-486	536077	7133811	e	1	53	47
HWRC-487-07	7	HW-487	536677	7133526	e	1	50	50
HWRC-488-06	6	HW-488	535945	7135629	e	1	70	30
HWRC-049-03	3	HW-49	530835	7137888	e	1	50	50
HWRC-497-07	7	HW-497	536580	7138693	e	1	75	25
HWRC-499-02	2	HW-499	539865	7138821	e	1	70	30
HWRC-500-02	2	HW-500	539921	7137816	e	1	50	50
HWRC-503-05	5	HW-503	539884	7134889	e	1	70	30
HWRC-051-04	4	HW-51	533882	7138721	e	1	100	0
HWRC-512-02	2	HW-512	542896	7132936	e	1	50	50
HWRC-516-05	5	HW-516	542939	7136728	e	1	70	30
HWRC-052-02	2	HW-52	530887	7136858	e	1	60	40
HWRC-524-03	3	HW-524	545422	7133178	e	1	50	50
HWRC-053-04	4	HW-53	530890	7135852	e	1	70	30
HWRC-059-02	2	HW-59	530884	7129853	e	1	60	40
HWRC-626-02	2	HW-626	538023	7131613	e	1	70	30
HWRC-627-08	8	HW-627	537901	7131891	e	1	70	30
HWRC-628-12	12	HW-628	537858	7132128	e	1	70	30
HWRC-629-06	6	HW-629	537897	7132397	e	1	60	40
HWRC-630-03	3	HW-630	537889	7132698	e	1	80	20
HWRC-635-04	4	HW-635	538006	7135040	e	1	80	20
HWRC-636-05	5	HW-636	537888	7135447	e	1	60	40
HWRC-639-10	10	HW-639	538010	7136946	e	1	47	53
HWRC-644-02	2	HW-644	537916	7138232	e	1	40	60
HWRC-645-04	4	HW-645	537904	7138738	e	1	50	50
HWRC-650-06	6	HW-650	535255	7135807	e	1	60	40
HWRC-651-12	12	HW-651	535214	7135302	e	1	60	40
HWRC-652-04	4	HW-652	535331	7135036	e	1	60	40
HWRC-653-08	8	HW-653	535211	7134342	e	1	65	35

SampleID	SampleNum	HoleID	CollarEasting	CollarNorthing	StudyArea	Depth Interval Bin	MetaSed (%)	Granitic (%)
HWRC-654-07	7	HW-654	535275	7134110	e	1	45	55
HWRC-655-03	3	HW-655	535233	7133870	e	1	40	60
HWRC-656-03	3	HW-656	535211	7133536	e	1	40	60
HWRC-657-05	5	HW-657	535243	7133325	e	1	40	60
HWRC-658-08	8	HW-658	535244	7133083	e	1	50	50
HWRC-659-03	3	HW-659	535288	7132866	e	1	40	60
HWRC-660-08	8	HW-660	535227	7132623	e	1	45	55
HWRC-661-04	4	HW-661	535208	7132332	e	1	50	50
HWRC-166-01	1	HW-166	515887	7128816	w	4	80	20
HWRC-167-01	1	HW-167	515789	7130868	w	4	80	20
HWRC-168-02	2	HW-168	516057	7131840	w	4	50	50
HWRC-169-01	1	HW-169	515936	7132946	w	4	70	30
HWRC-170-01	1	HW-170	516061	7133906	w	4	60	40
HWRC-171-01	1	HW-171	516092	7134904	w	4	80	20
HWRC-172-01	1	HW-172	515891	7135813	w	4	80	20
HWRC-173-01	1	HW-173	515881	7136823	w	4	80	20
HWRC-174-01	1	HW-174	512898	7136861	w	4	80	20
HWRC-175-01	1	HW-175	512910	7134790	w	4	50	50
HWRC-176-01	1	HW-176	512890	7133862	w	4	40	60
HWRC-177-01	1	HW-177	512885	7132870	w	4	60	40
HWRC-178-01	1	HW-178	512891	7131876	w	4	70	30
HWRC-179-01	1	HW-179	512884	7130847	w	4	70	30
HWRC-180-01	1	HW-180	512694	7129949	w	4	90	10
HWRC-181-01	1	HW-181	512765	7128818	w	4	70	30
HWRC-204-01	1	HW-204	509883	7128860	w	4	70	30
HWRC-205-01	1	HW-205	509925	7129741	w	4	70	30
HWRC-206-01	1	HW-206	509770	7130950	w	4	80	20
HWRC-207-01	1	HW-207	509876	7131838	w	4	80	20
HWRC-208-01	1	HW-208	509913	7132927	w	4	67	33
HWRC-209-01	1	HW-209	509986	7133919	w	4	70	30
HWRC-210-01	1	HW-210	509866	7134899	w	4	90	10
HWRC-212-01	1	HW-212	506893	7135833	w	4	70	30
HWRC-213-01	1	HW-213	506987	7134872	w	4	95	5
HWRC-214-01	1	HW-214	506878	7133857	w	4	70	30
HWRC-215-01	1	HW-215	506836	7132756	w	4	80	20
HWRC-216-01	1	HW-216	506862	7131848	w	4	10	90
HWRC-217-01	1	HW-217	506831	7130665	w	4	90	10
HWRC-218-01	1	HW-218	506892	7129838	w	4	50	50
HWRC-219-01	1	HW-219	506929	7128796	w	4	50	50
HWRC-226-01	1	HW-226	505470	7128865	w	4	80	20
HWRC-227-01	1	HW-227	505353	7129839	w	4	50	50
HWRC-228-01	1	HW-228	505522	7130873	w	4	80	20
HWRC-229-01	1	HW-229	505355	7131869	w	4	80	20
HWRC-230-01	1	HW-230	505449	7132678	w	4	50	50
HWRC-231-01	1	HW-231	505486	7133863	w	4	70	30
HWRC-232-01	1	HW-232	505485	7134867	w	4	70	30
HWRC-233-01	1	HW-233	505510	7135880	w	4	40	60
HWRC-234-01	1	HW-234	505387	7136965	w	4	80	20
HWRC-269-01	1	HW-269	512866	7135462	w	4	60	40
HWRC-270-01	1	HW-270	515523	7130261	w	4	90	10
HWRC-727-01	1	HW-727	514544	7132663	w	4	60	40
HWRC-728-01	1	HW-728	514556	7133245	w	4	70	30
HWRC-729-01	1	HW-729	514556	7133245	w	4	50	50
HWRC-730-01	1	HW-730	514550	7133962	w	4	60	40
HWRC-731-01	1	HW-731	514575	7134210	w	4	70	30

SampleID	SampleNum	HoleID	CollarEasting	CollarNorthing	StudyArea	Depth Interval Bin	MetaSed (%)	Granitic (%)
HWRC-732-01	1	HW-732	514630	7134425	w	4	60	40
HWRC-733-01	1	HW-733	514575	7134706	w	4	20	80
HWRC-734-01	1	HW-734	514562	7134945	w	4	30	70
HWRC-735-01	1	HW-735	514487	7135153	w	4	80	20
HWRC-736-01	1	HW-736	514614	7135455	w	4	80	20
HWRC-737-01	1	HW-737	514630	7135742	w	4	80	20
HWRC-738-01	1	HW-738	514529	7136370	w	4	65	35
HWRC-739-01	1	HW-739	514557	7136733	w	4	90	10
HWRC-740-01	1	HW-740	511319	7134780	w	4	55	45
HWRC-741-01	1	HW-741	511342	7134271	w	4	90	10
HWRC-742-01	1	HW-742	511249	7133747	w	4	60	40
HWRC-743-01	1	HW-743	511309	7133266	w	4	50	50
HWRC-744-01	1	HW-744	511309	7132790	w	4	50	50
HWRC-745-01	1	HW-745	511190	7132208	w	4	5	95
HWRC-746-01	1	HW-746	511215	7131655	w	4	70	30
HWRC-747-01	1	HW-747	511245	7131153	w	4	60	40
HWRC-748-01	1	HW-748	511121	7130856	w	4	70	30
HWRC-749-01	1	HW-749	511209	7130199	w	4	40	60
HWRC-750-01	1	HW-750	512488	7130241	w	4	30	70
HWRC-751-01	1	HW-751	512488	7130241	w	4	70	30
HWRC-752-01	1	HW-752	512555	7130814	w	4	40	60
HWRC-753-01	1	HW-753	512432	7131089	w	4	20	80
HWRC-754-01	1	HW-754	512639	7131215	w	4	70	30
HWRC-755-01	1	HW-755	512485	7131486	w	4	50	50
HWRC-756-01	1	HW-756	512484	7131738	w	4	40	60
HWRC-167-02	2	HW-167	515789	7130868	w	3	70	30
HWRC-168-03	3	HW-168	516057	7131840	w	3	80	20
HWRC-169-02	2	HW-169	515936	7132946	w	3	70	30
HWRC-171-02	2	HW-171	516092	7134904	w	3	75	25
HWRC-181-02	2	HW-181	512765	7128818	w	3	80	20
HWRC-205-02	2	HW-205	509925	7129741	w	3	90	10
HWRC-207-03	3	HW-207	509876	7131838	w	3	80	20
HWRC-208-04	4	HW-208	509913	7132927	w	3	63	37
HWRC-218-02	2	HW-218	506892	7129838	w	3	80	20
HWRC-219-02	2	HW-219	506929	7128796	w	3	70	30
HWRC-227-02	2	HW-227	505353	7129839	w	3	50	50
HWRC-231-02	2	HW-231	505486	7133863	w	3	80	20
HWRC-232-02	2	HW-232	505485	7134867	w	3	70	30
HWRC-233-02	2	HW-233	505510	7135880	w	3	70	30
HWRC-234-02	2	HW-234	505387	7136965	w	3	90	10
HWRC-269-03	3	HW-269	512866	7135462	w	3	73	27
HWRC-270-02	2	HW-270	515523	7130261	w	3	90	10
HWRC-732-02	2	HW-732	514630	7134425	w	3	50	50
HWRC-737-02	2	HW-737	514630	7135742	w	3	65	35
HWRC-738-03	3	HW-738	514529	7136370	w	3	77	23
HWRC-740-03	3	HW-740	511319	7134780	w	3	80	20
HWRC-742-03	3	HW-742	511249	7133747	w	3	65	35
HWRC-746-03	3	HW-746	511215	7131655	w	3	60	40
HWRC-751-02	2	HW-751	512488	7130241	w	3	60	40
HWRC-754-02	2	HW-754	512639	7131215	w	3	60	40
HWRC-168-04	4	HW-168	516057	7131840	w	2	80	20
HWRC-169-03	3	HW-169	515936	7132946	w	2	80	20
HWRC-171-04	4	HW-171	516092	7134904	w	2	80	20
HWRC-207-04	4	HW-207	509876	7131838	w	2	70	30
HWRC-208-07	7	HW-208	509913	7132927	w	2	70	30

SampleID	SampleNum	HoleID	CollarEasting	CollarNorthing	StudyArea	Depth Interval Bin	MetaSed (%)	Granitic (%)
HWRC-227-03	3	HW-227	505353	7129839	w	2	90	10
HWRC-269-06	6	HW-269	512866	7135462	w	2	50	50
HWRC-737-04	4	HW-737	514630	7135742	w	2	40	60
HWRC-738-06	6	HW-738	514529	7136370	w	2	80	20
HWRC-740-04	4	HW-740	511319	7134780	w	2	70	30
HWRC-742-05	5	HW-742	511249	7133747	w	2	70	30
HWRC-746-04	4	HW-746	511215	7131655	w	2	55	45
HWRC-754-03	3	HW-754	512639	7131215	w	2	50	50
HWRC-167-03	3	HW-167	515789	7130868	w	1	90	10
HWRC-168-06	6	HW-168	516057	7131840	w	1	80	20
HWRC-169-04	4	HW-169	515936	7132946	w	1	50	50
HWRC-171-05	5	HW-171	516092	7134904	w	1	90	10
HWRC-175-02	2	HW-175	512910	7134790	w	1	70	30
HWRC-176-02	2	HW-176	512890	7133862	w	1	60	40
HWRC-179-02	2	HW-179	512884	7130847	w	1	90	10
HWRC-181-03	3	HW-181	512765	7128818	w	1	80	20
HWRC-205-03	3	HW-205	509925	7129741	w	1	90	10
HWRC-207-06	6	HW-207	509876	7131838	w	1	60	40
HWRC-208-09	9	HW-208	509913	7132927	w	1	70	30
HWRC-209-02	2	HW-209	509986	7133919	w	1	70	30
HWRC-210-02	2	HW-210	509866	7134899	w	1	95	5
HWRC-211-02	2	HW-211	506929	7136728	w	1	80	20
HWRC-214-02	2	HW-214	506878	7133857	w	1	70	30
HWRC-216-02	2	HW-216	506862	7131848	w	1	90	10
HWRC-218-03	3	HW-218	506892	7129838	w	1	70	30
HWRC-219-03	3	HW-219	506929	7128796	w	1	60	40
HWRC-227-04	4	HW-227	505353	7129839	w	1	90	10
HWRC-229-02	2	HW-229	505355	7131869	w	1	70	30
HWRC-231-03	3	HW-231	505486	7133863	w	1	80	20
HWRC-232-03	3	HW-232	505485	7134867	w	1	90	10
HWRC-233-03	3	HW-233	505510	7135880	w	1	80	20
HWRC-234-03	3	HW-234	505387	7136965	w	1	80	20
HWRC-269-09	9	HW-269	512866	7135462	w	1	75	25
HWRC-270-03	3	HW-270	515523	7130261	w	1	100	0
HWRC-732-03	3	HW-732	514630	7134425	w	1	40	60
HWRC-737-05	5	HW-737	514630	7135742	w	1	70	30
HWRC-738-08	8	HW-738	514529	7136370	w	1	55	45
HWRC-740-06	6	HW-740	511319	7134780	w	1	100	0
HWRC-742-06	6	HW-742	511249	7133747	w	1	75	25
HWRC-746-06	6	HW-746	511215	7131655	w	1	70	30
HWRC-747-02	2	HW-747	511245	7131153	w	1	10	90
HWRC-751-03	3	HW-751	512488	7130241	w	1	70	30
HWRC-754-04	4	HW-754	512639	7131215	w	1	70	30



## East Study Area selected clast lithology classification

Note that some samples had minor reclassifications after these photos were taken

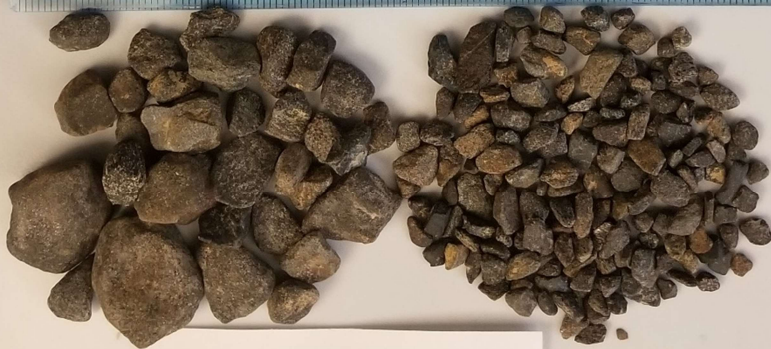
White Granitoid



Pink Granitoid



17-RS-001-B



Quartz



Metasedimentary

White Granitoid



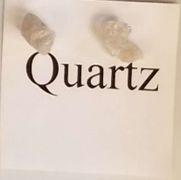
Pink Granitoid



17-RS-002-B



Quartz

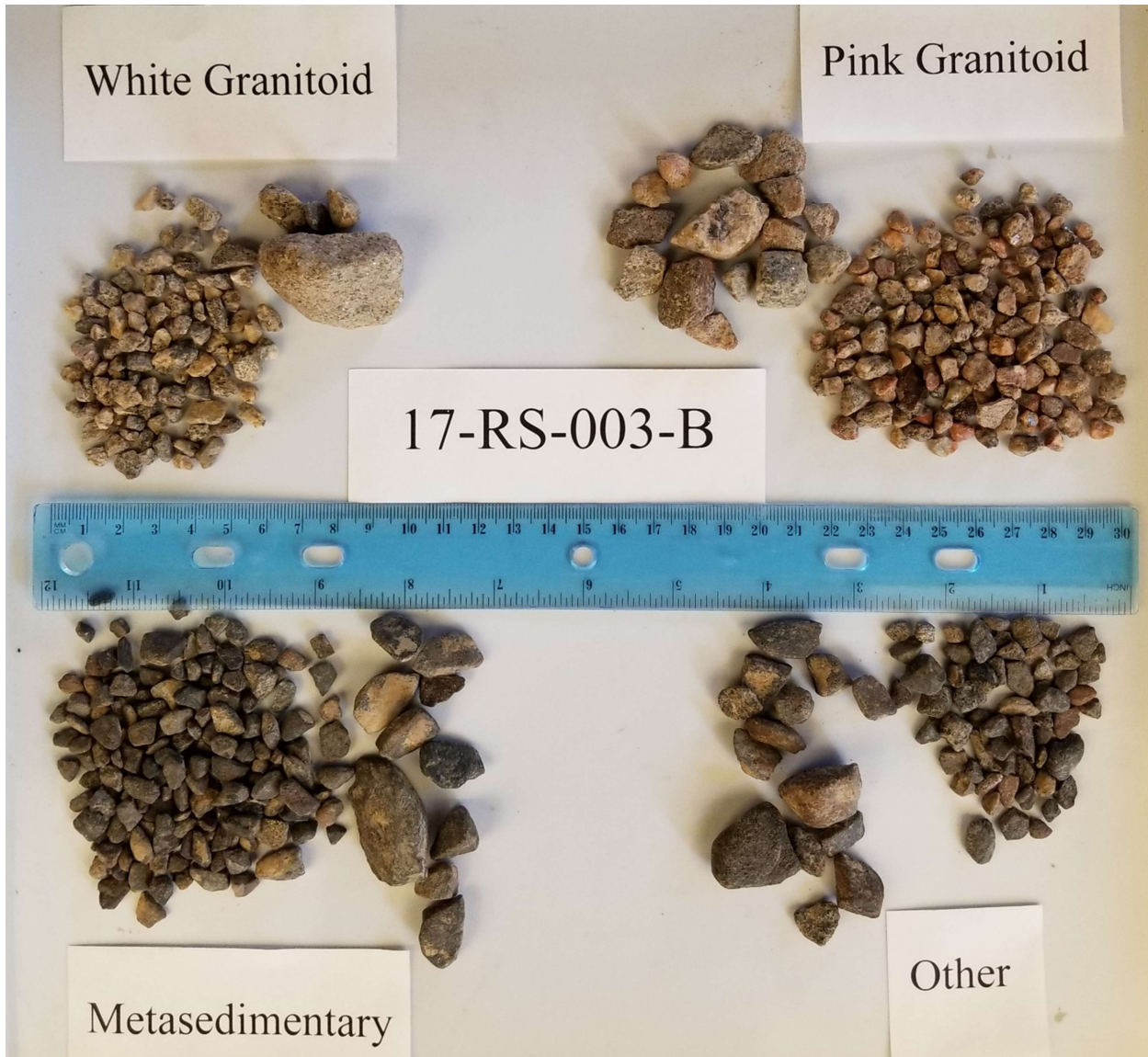


Ultramafic

Metasedimentary





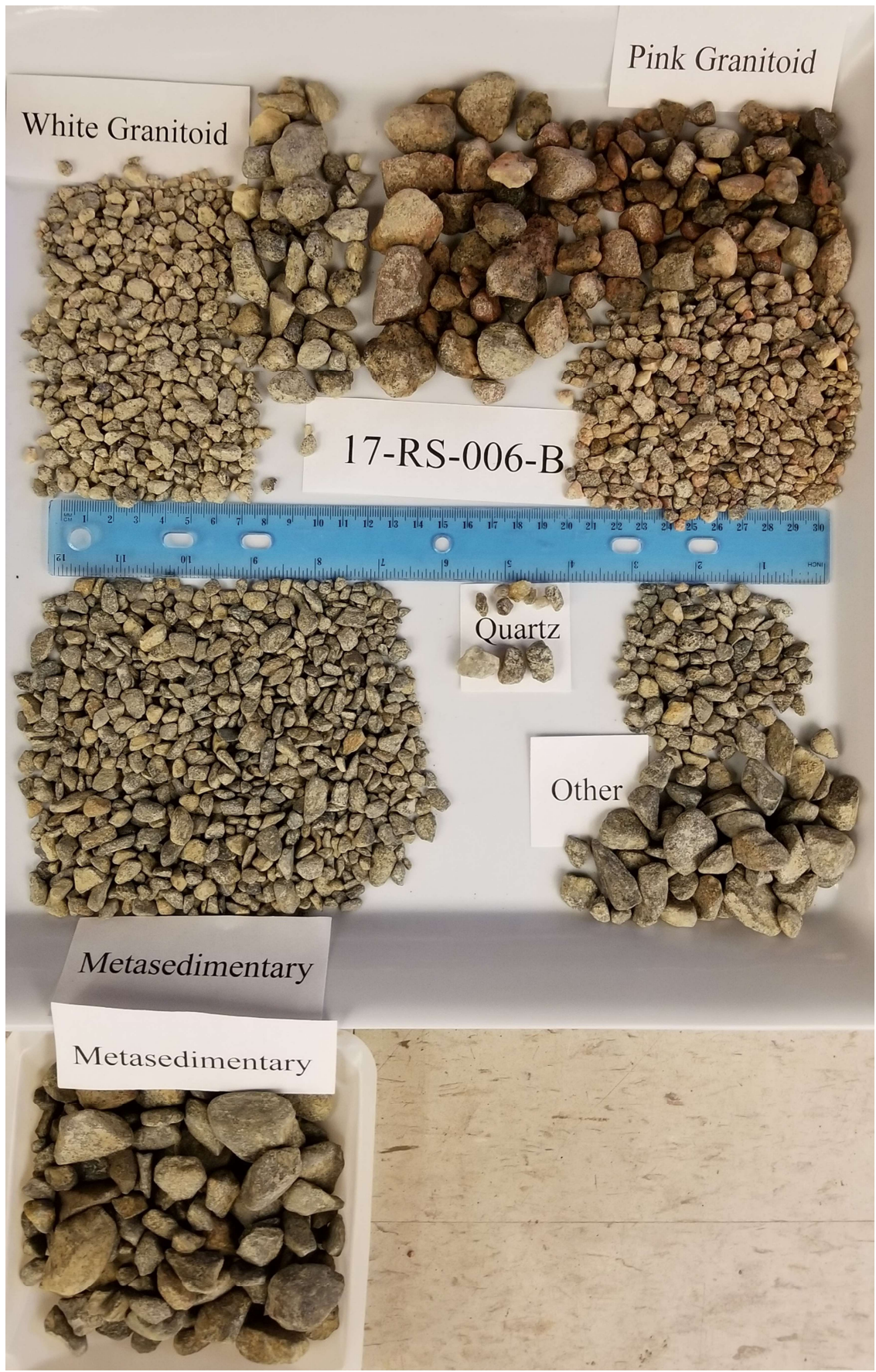












White Granitoid

Pink Granitoid

17-RS-006-B

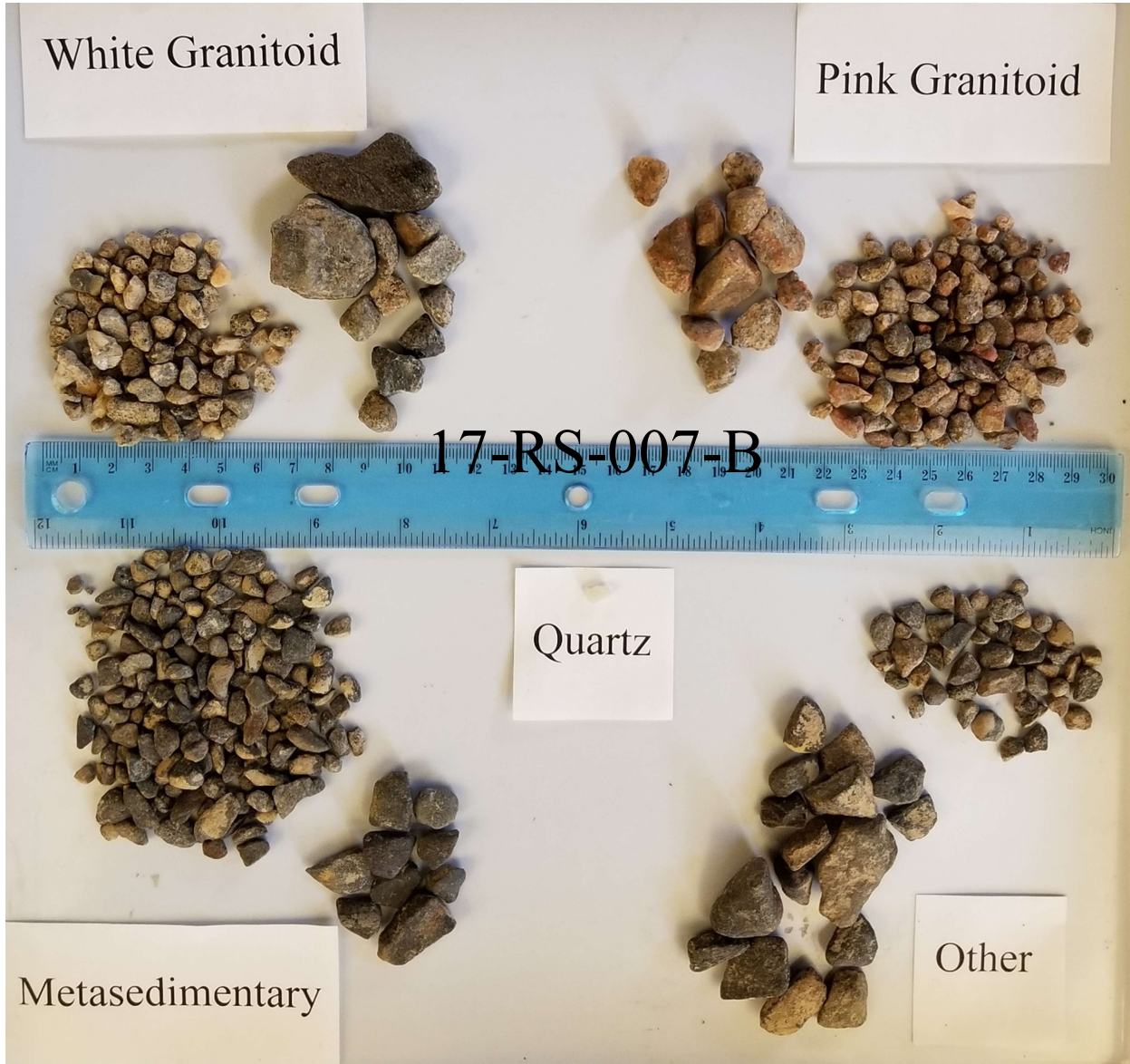
Quartz

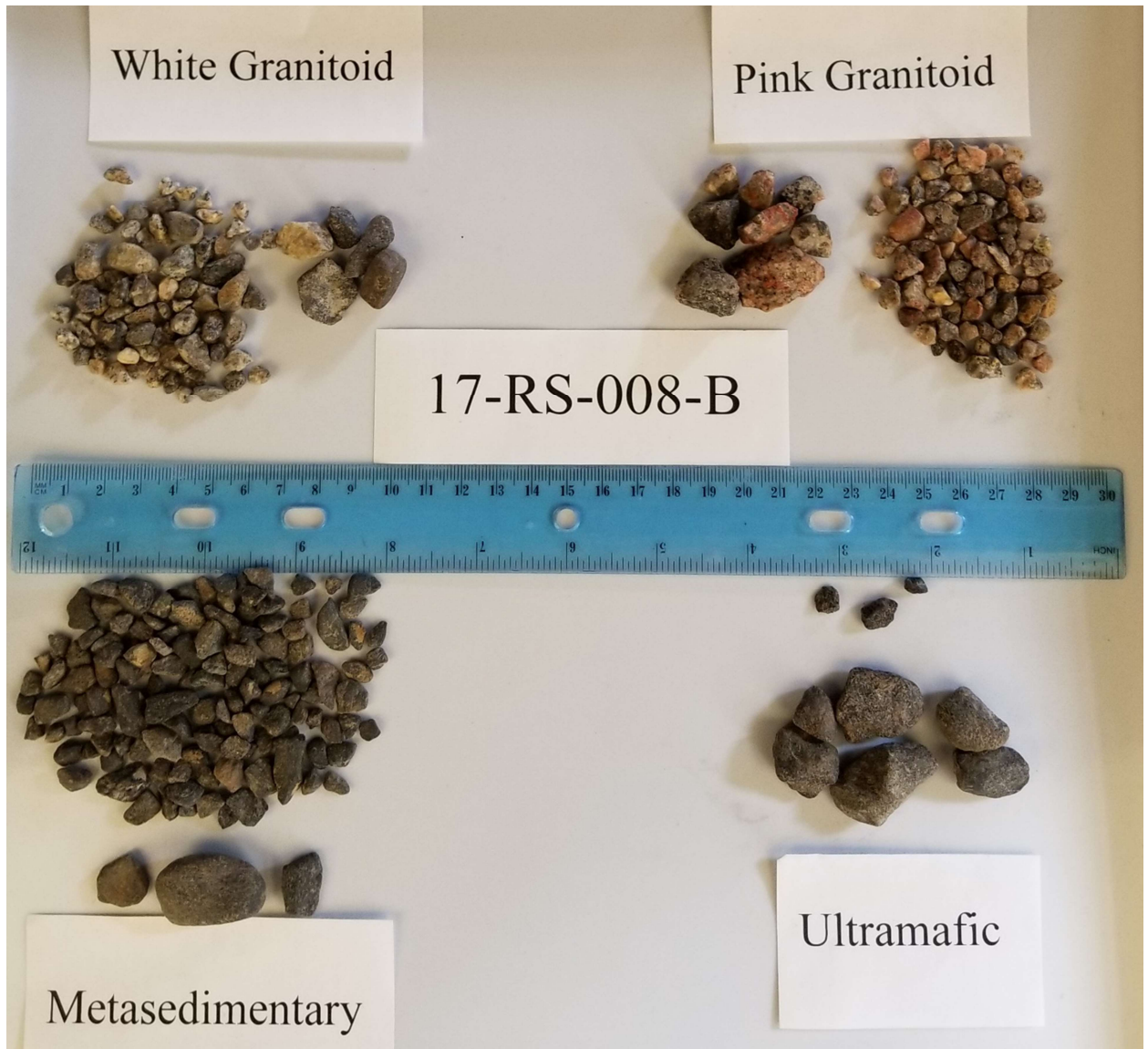
Other

Metasedimentary

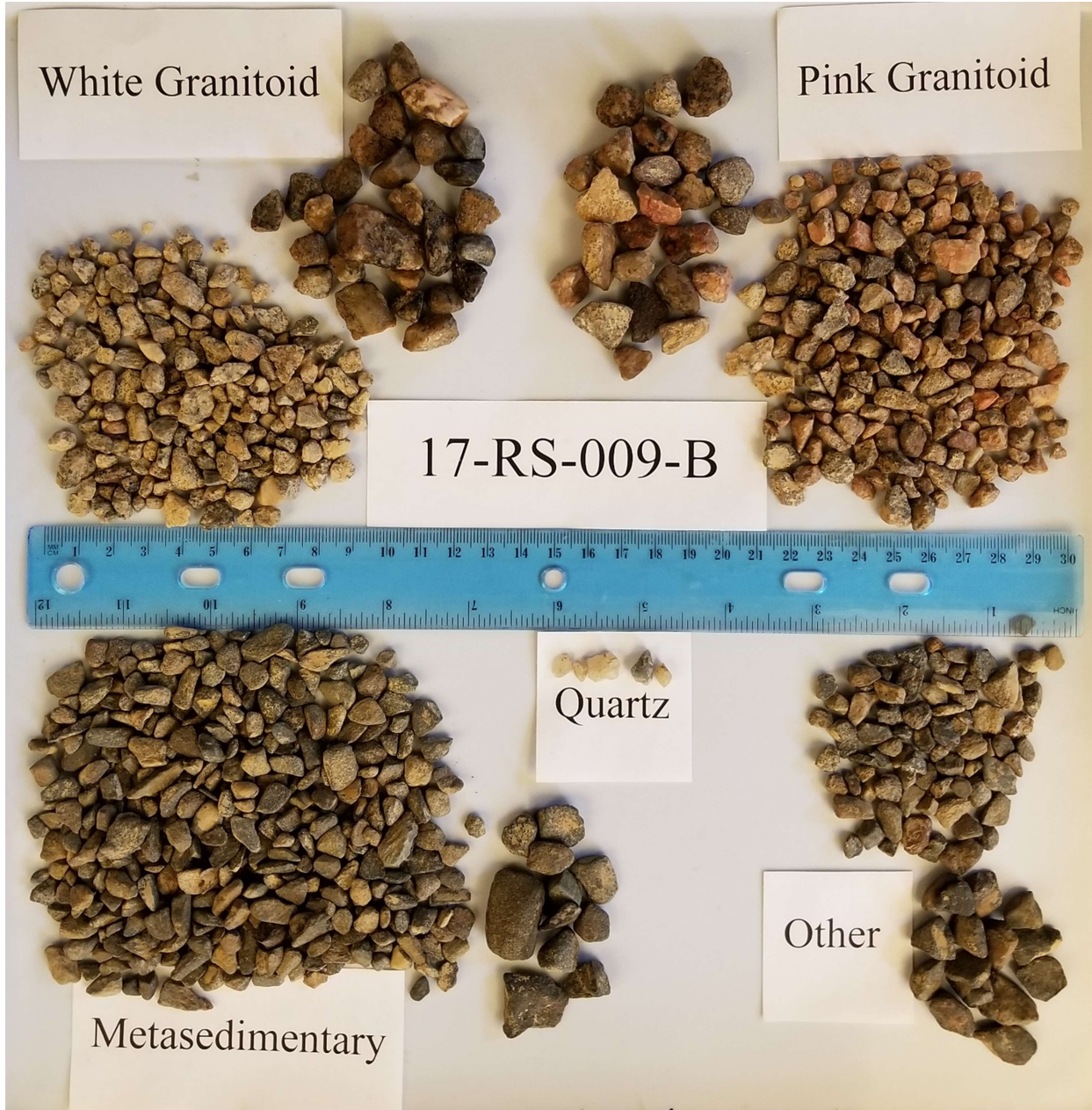
Metasedimentary

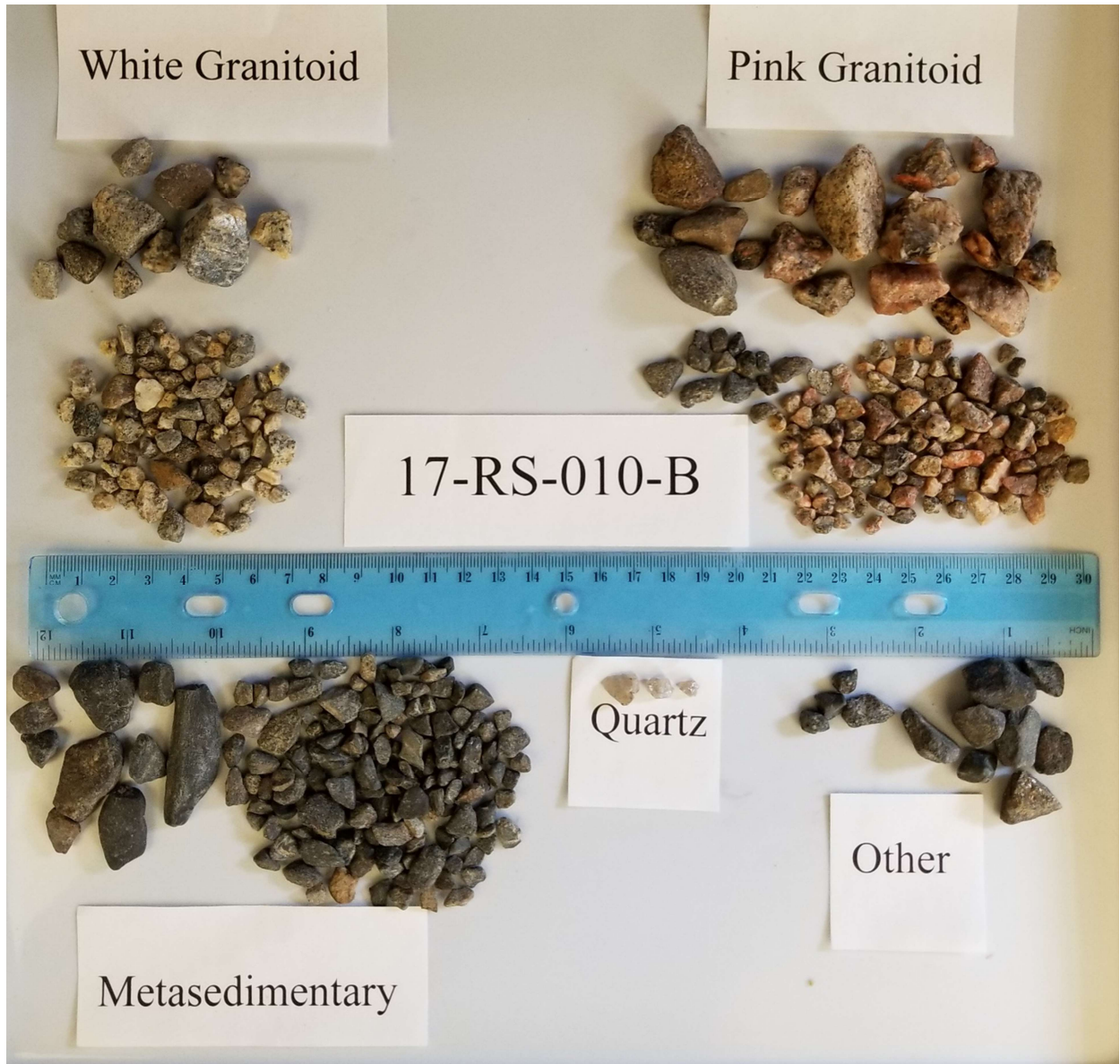




















White Granitoid

Pink Granitoid

17-RS-013-B



Other

Metasedimentary















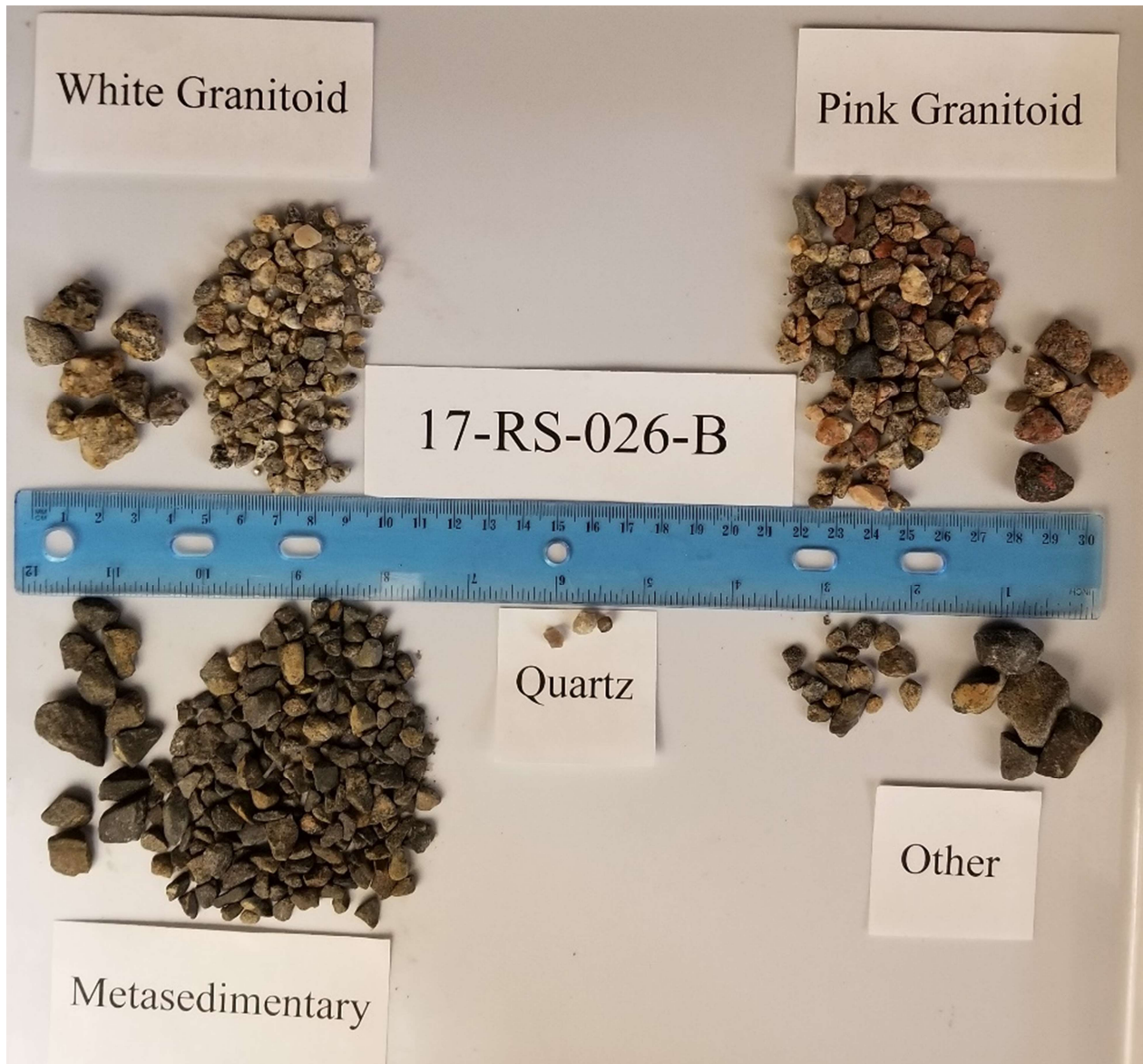




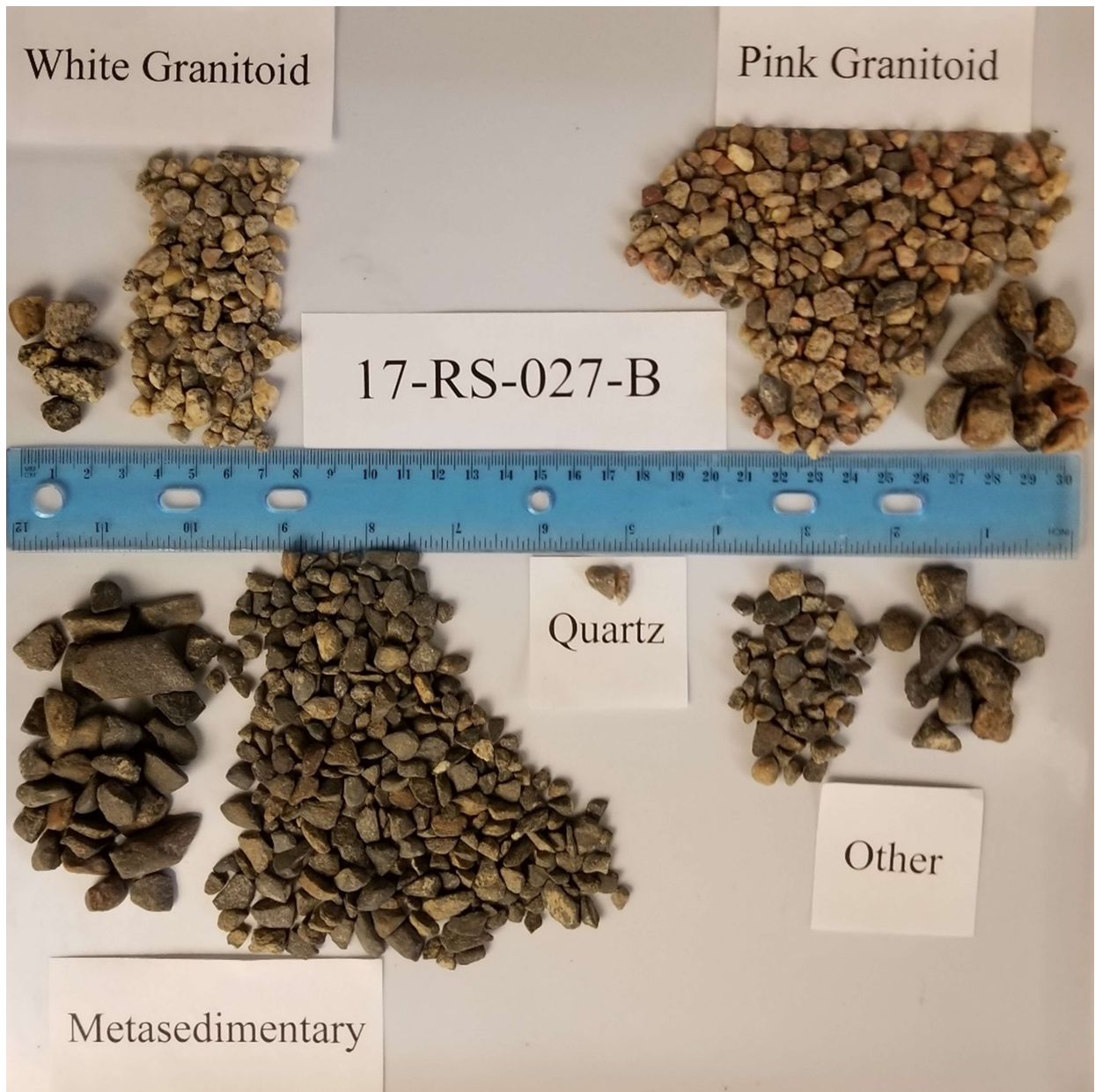


## West Study Area selected clast lithology classifications

Note that some samples had minor reclassifications after these photos were taken

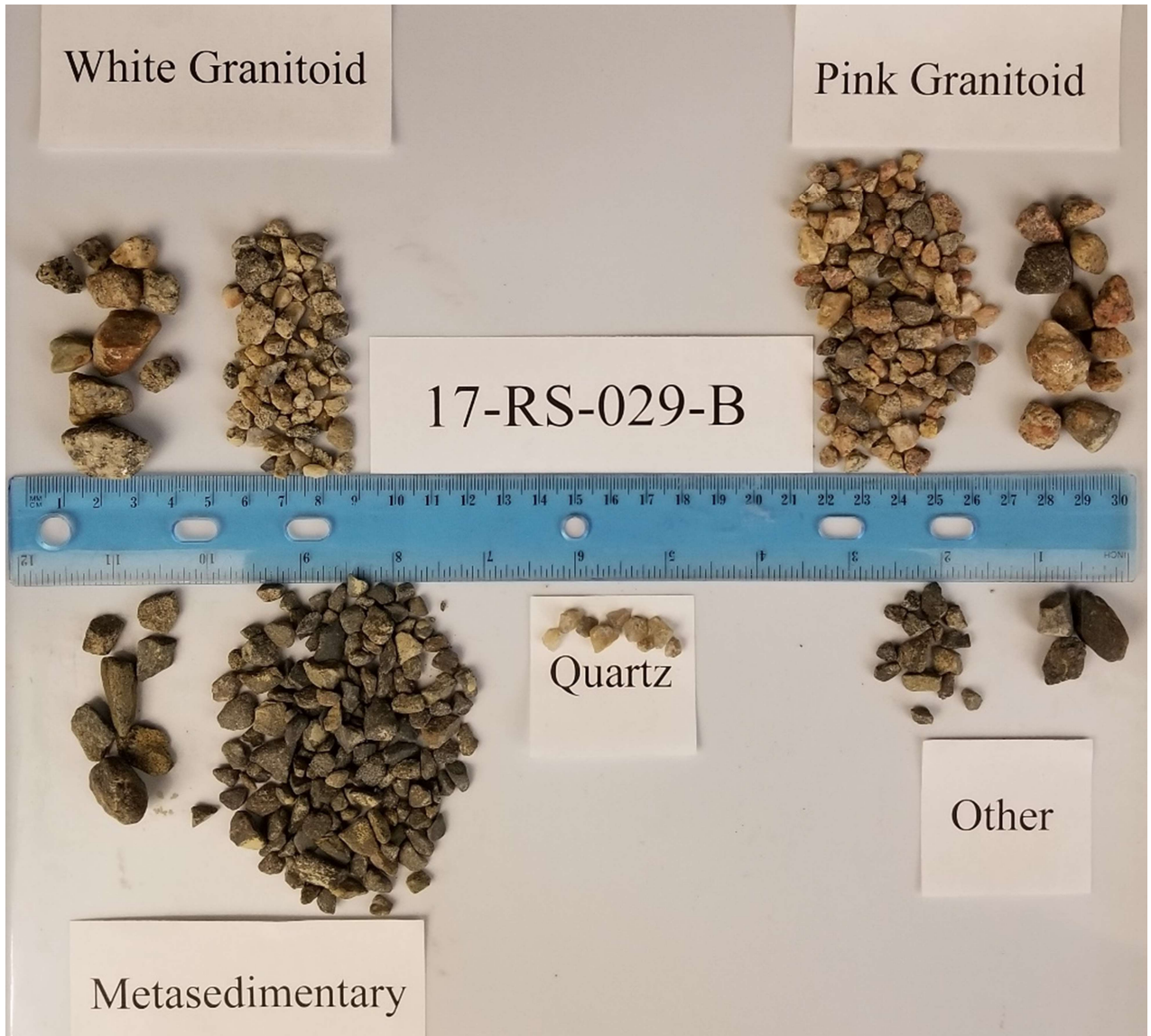






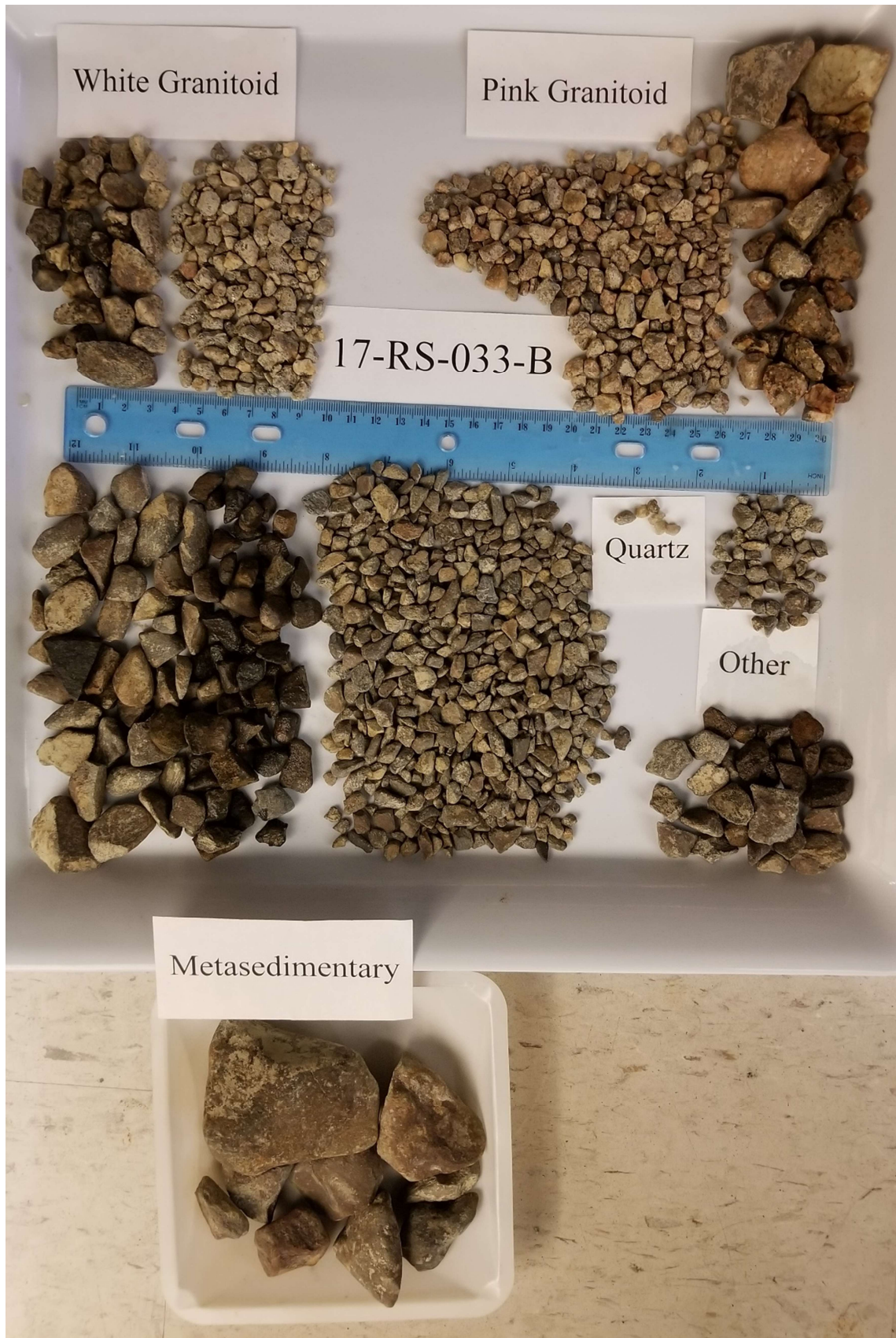






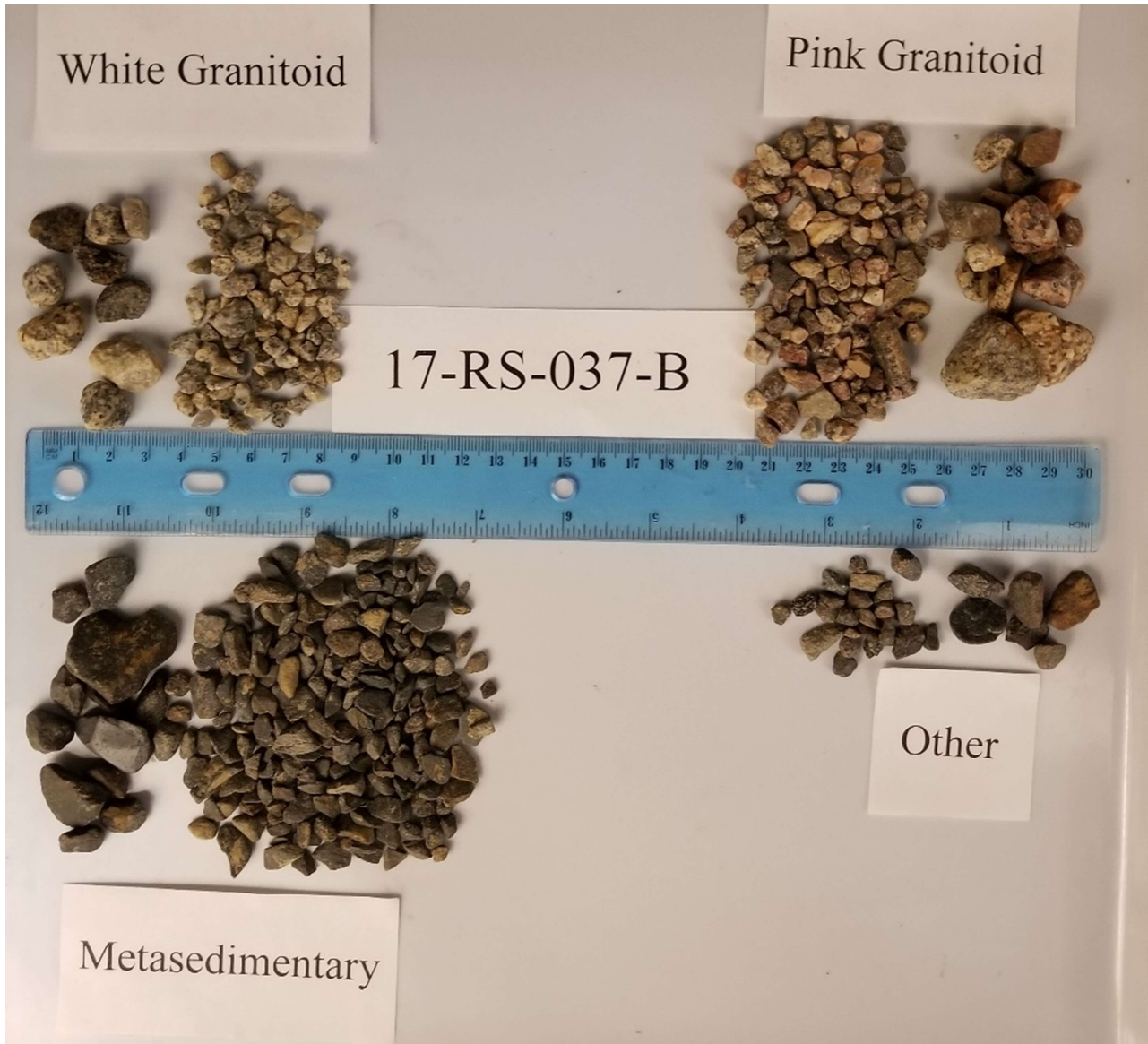














## **Appendix F: Geochemistry results for UW data**

UW SRC G-2018-92 MSTD

UW SRC G-2018-92 TD

UW SRC G-2018-92 PD

UW all SRC geochemistry results with field sample numbers

ICP Total Digestion

Column Header Details

Aluminum in wt % (Al2O3)  
 Barium in ppm (Ba)  
 Calcium in wt % (CaO)  
 Cerium in ppm (Ce)  
 Chromium in ppm (Cr)

Iron in wt % (Fe2O3)  
 Potassium in wt % (K2O)  
 Lanthanum in ppm (La)  
 Lithium in ppm (Li)  
 Magnesium in wt % (MgO)

Manganese in wt % (MnO)  
 Sodium in wt % (Na2O)  
 Phosphorus in wt % (P2O5)  
 Strontium in ppm (Sr)  
 Titanium in wt % (TiO2)

Zirconium in ppm (Zr)

Sample Number	Al2O3 wt %	Ba ppm	CaO wt %	Ce ppm	Cr ppm	Fe2O3 wt %	K2O wt %	La ppm	Li ppm	MgO wt %	MnO wt %	Na2O wt %	P2O5 wt %	Sr ppm	TiO2 wt %	Zr ppm
DCB01	11.1	387	1.50	126	270	3.35	2.43	63	41	1.68	0.036	0.57	0.208	413	0.800	417
160	12.7	414	1.81	70	44	1.95	2.33	35	19	0.820	0.030	3.06	0.209	282	0.509	198
161	12.8	439	1.83	74	44	1.93	2.31	37	22	0.817	0.030	3.10	0.196	299	0.527	214
162	12.5	525	1.53	63	43	2.28	2.35	32	26	0.783	0.028	2.65	0.100	266	0.493	218
163	12.8	497	1.74	74	49	2.40	2.45	38	28	0.975	0.034	2.85	0.193	276	0.545	215
164	13.0	466	1.71	68	54	2.42	2.41	34	28	0.943	0.033	2.89	0.195	276	0.487	197
165	12.6	415	1.84	75	38	1.80	2.26	37	19	0.724	0.029	3.11	0.214	298	0.485	199
166	12.9	459	1.96	96	42	2.11	2.48	49	23	0.851	0.034	3.05	0.247	296	0.571	243
167	13.0	423	1.79	73	40	1.94	2.31	37	22	0.760	0.030	3.10	0.207	297	0.476	203
168	13.2	470	1.75	77	50	2.33	2.34	39	23	0.923	0.032	2.98	0.195	289	0.550	199
169	12.2	451	1.66	68	40	2.17	2.18	35	22	0.772	0.030	2.77	0.154	273	0.507	206
170	13.1	450	1.84	70	46	2.05	2.40	36	22	0.855	0.031	3.11	0.199	303	0.532	200
171	12.8	426	1.73	74	44	2.16	2.20	37	22	0.762	0.031	2.96	0.188	288	0.533	209
172	12.7	452	1.72	61	45	2.02	2.34	31	24	0.849	0.028	2.96	0.199	285	0.464	168
173	12.1	492	1.72	68	47	2.17	2.34	35	23	0.845	0.032	2.77	0.173	267	0.492	203
174	12.4	463	1.65	67	49	2.13	2.35	34	25	0.838	0.029	2.85	0.175	269	0.466	182
175	12.0	383	1.77	69	34	1.61	2.12	35	17	0.611	0.027	3.04	0.204	289	0.462	191
176	12.0	428	1.69	66	36	1.79	2.20	33	19	0.704	0.027	2.87	0.193	272	0.434	191
177	12.3	493	2.59	42	121	3.92	2.40	20	22	1.70	0.062	2.67	0.115	305	0.490	143
178	12.9	476	1.85	91	44	2.20	2.56	46	26	0.855	0.034	2.96	0.236	282	0.520	231

ICP Total Digestion

Sample Number	Al2O3 wt %	Ba ppm	CaO wt %	Ce ppm	Cr ppm	Fe2O3 wt %	K2O wt %	La ppm	Li ppm	MgO wt %	MnO wt %	Na2O wt %	P2O5 wt %	Sr ppm	TiO2 wt %	Zr ppm
DCB01	11.1	387	1.51	124	272	3.36	2.45	64	42	1.70	0.036	0.57	0.205	412	0.794	412
179	13.6	511	1.83	77	45	2.33	2.73	40	33	0.906	0.034	3.06	0.208	289	0.500	216
180	13.3	488	1.86	75	42	2.20	2.64	39	26	0.820	0.032	3.09	0.220	295	0.488	223
181	13.3	480	1.86	82	47	2.33	2.60	43	27	0.962	0.039	3.03	0.235	289	0.526	217
182	13.7	515	1.94	73	51	2.29	2.76	38	30	1.02	0.034	3.15	0.216	298	0.487	196
183	13.6	500	1.83	79	56	2.72	2.71	41	34	1.14	0.039	2.97	0.218	285	0.502	194
184	13.3	463	1.78	73	41	2.20	2.54	38	25	0.816	0.030	3.06	0.201	288	0.450	186
185	13.5	463	1.91	82	47	2.20	2.54	41	26	0.901	0.036	3.17	0.224	307	0.520	213
186	13.0	422	1.84	86	41	2.08	2.34	44	25	0.767	0.033	3.03	0.222	294	0.479	230
187	13.1	447	1.85	73	44	1.95	2.46	37	23	0.790	0.029	3.10	0.223	298	0.459	191
188	12.3	408	1.69	69	38	1.85	2.17	34	21	0.728	0.028	2.91	0.196	278	0.453	181
189	12.9	450	1.88	87	45	1.99	2.45	45	22	0.831	0.032	3.08	0.224	297	0.528	229
190	12.8	422	1.66	78	45	2.40	2.24	40	26	0.747	0.030	2.89	0.143	281	0.484	213
191	12.9	444	1.93	83	39	1.89	2.42	43	22	0.745	0.030	3.16	0.220	304	0.496	221
192	12.3	415	1.77	68	34	1.87	2.21	35	20	0.657	0.028	2.98	0.184	292	0.436	205
193	13.9	504	1.63	72	62	2.85	2.63	36	34	1.11	0.036	2.92	0.188	280	0.472	174
194	13.0	460	1.98	102	45	2.12	2.50	52	23	0.862	0.034	3.09	0.251	299	0.569	245
195	12.2	405	1.70	93	42	2.11	2.19	48	25	0.754	0.032	2.80	0.209	273	0.477	214
196	13.0	483	1.76	77	52	2.30	2.59	40	27	0.951	0.033	2.92	0.222	276	0.498	203
192 R	12.6	421	1.80	70	34	1.90	2.26	36	21	0.660	0.028	3.05	0.186	295	0.439	209
DCB01	11.1	395	1.52	127	271	3.36	2.44	64	42	1.70	0.036	0.57	0.209	413	0.791	411
197	12.9	427	1.87	80	40	1.89	2.37	41	22	0.748	0.032	3.09	0.216	300	0.472	209
198	12.9	444	1.87	77	40	1.89	2.41	39	22	0.746	0.030	3.12	0.214	301	0.461	204
199	12.5	496	2.60	41	125	3.95	2.43	20	21	1.72	0.064	2.65	0.117	307	0.494	144
199 R	12.4	491	2.56	40	122	3.90	2.40	21	20	1.71	0.063	2.64	0.117	304	0.489	142

Total Digestion: A 0.125 g pulp is gently heated in a mixture of ultrapure HF/HNO3/HClO4 until dry and the residue dissolved in dilute ultrapure HNO3. The standard is DCB01.



ICP MS Total Digestion

Column Header Details

Silver in ppm (Ag)  
Beryllium in ppm (Be)  
Bismuth in ppm (Bi)  
Cadmium in ppm (Cd)  
Cobalt in ppm (Co)  
  
Cesium in ppm (Cs)  
Copper in ppm (Cu)  
Dysprosium in ppm (Dy)  
Erbium in ppm (Er)  
Europium in ppm (Eu)  
  
Gallium in ppm (Ga)  
Gadolinium in ppm (Gd)  
Hafnium in ppm (Hf)  
Holmium in ppm (Ho)  
Molybdenum in ppm (Mo)  
  
Niobium in ppm (Nb)  
Neodymium in ppm (Nd)  
Nickel in ppm (Ni)  
Lead204 in ppm (Pb204)  
Lead206 in ppm (Pb206)  
  
Lead207 in ppm (Pb207)  
Lead208 in ppm (Pb208)  
Lead in ppm (PbSUM)  
Praseodymium in ppm (Pr)  
Rubidium in ppm (Rb)  
  
Scandium in ppm (Sc)  
Samarium in ppm (Sm)  
Tin in ppm (Sn)  
Tantalum in ppm (Ta)  
Terbium in ppm (Tb)  
  
Thorium in ppm (Th)  
Uranium in ppm (U)  
Vanadium in ppm (V)  
Tungsten in ppm (W)  
Yttrium in ppm (Y)

**University of Waterloo**  
Attention: Rebecca Stirling  
PO #/Project:  
Samples: 45

**SRC Geoanalytical Laboratories**

Report No: G-2018-92

Date of Report: Feb 02, 2018

**ICP MS Total Digestion**

Ytterbium in ppm (Yb)  
Zinc in ppm (Zn)

ICP MS Total Digestion

Sample Number	Ag ppm	Be ppm	Bi ppm	Cd ppm	Co ppm	Cs ppm	Cu ppm	Dy ppm	Er ppm	Eu ppm	Ga ppm	Gd ppm	Hf ppm	Ho ppm	Mo ppm	Nb ppm	Nd ppm
DCB01	2.79	1.6	7.9	0.7	16.8	1.1	276	4.83	2.32	1.33	14.5	6.0	10.4	0.82	12.3	20.7	51.5
160	0.31	1.6	0.3	0.2	5.49	2.0	15.2	3.28	1.42	1.32	12.7	4.4	5.2	0.51	0.38	6.1	36.2
161	0.29	1.4	0.3	0.2	5.08	2.2	18.3	3.21	1.47	1.45	13.3	4.5	5.4	0.53	0.52	6.4	38.4
162	0.29	1.4	0.3	0.2	6.74	2.6	15.5	2.64	1.24	1.20	13.8	3.7	5.5	0.43	0.62	8.0	31.4
163	0.28	1.5	0.3	0.2	7.52	3.2	21.0	3.11	1.42	1.32	14.2	4.4	5.4	0.50	0.66	7.6	37.7
164	0.26	1.8	0.4	0.2	9.11	2.8	25.7	2.93	1.32	1.30	14.3	4.3	5.1	0.46	0.91	6.6	34.4
165	0.22	1.3	0.3	0.2	5.07	1.9	15.9	3.18	1.37	1.40	12.3	4.6	5.1	0.50	0.40	5.6	38.6
166	0.25	1.5	0.3	0.2	5.87	2.4	15.2	3.97	1.68	1.55	13.4	5.8	6.3	0.62	0.47	7.3	48.9
167	0.22	1.6	0.3	0.2	8.28	2.0	26.2	3.19	1.39	1.36	12.8	4.5	5.1	0.49	0.58	5.8	37.2
168	0.23	1.3	0.3	0.2	6.69	2.4	25.2	3.24	1.46	1.42	13.6	4.6	5.1	0.53	0.51	6.6	39.0
169	0.23	1.6	0.3	0.2	7.15	2.1	18.2	2.87	1.30	1.29	13.2	4.2	5.5	0.46	0.60	7.0	35.0
170	0.22	1.3	0.3	0.2	6.10	2.3	20.7	3.09	1.37	1.33	13.1	4.4	5.2	0.49	0.47	6.3	36.5
171	0.21	1.6	0.3	0.2	7.52	2.0	18.3	3.21	1.46	1.34	12.7	4.5	5.5	0.50	0.64	6.4	37.6
172	0.22	1.4	0.3	0.2	6.44	2.4	25.2	2.87	1.32	1.31	13.4	4.0	4.4	0.48	0.54	6.3	32.4
173	0.22	1.7	0.3	0.2	6.47	2.6	18.2	3.11	1.40	1.32	13.3	4.2	5.4	0.49	0.65	7.2	35.9
174	0.22	1.6	0.3	0.2	6.83	2.5	23.2	2.92	1.27	1.29	12.9	4.1	4.9	0.47	0.57	6.2	34.3
175	0.19	1.3	0.3	0.2	4.07	1.6	12.7	3.05	1.35	1.36	11.5	4.4	5.0	0.48	0.30	5.5	36.2
176	0.18	1.5	0.3	0.2	5.91	2.0	19.3	2.89	1.34	1.28	12.0	4.1	5.1	0.47	0.45	5.6	34.2
177	1.69	1.8	0.5	0.2	14.1	1.9	22.6	2.34	1.29	0.99	14.1	2.5	3.8	0.42	0.73	7.7	17.7
178	0.38	1.9	0.4	0.3	7.54	2.6	18.2	3.79	1.67	1.53	12.7	5.7	6.2	0.60	0.66	7.4	48.2
DCB01	2.91	1.5	7.9	0.8	16.7	1.2	280	4.79	2.31	1.33	14.6	6.0	8.7	0.93	12.5	20.9	52.3
179	0.40	1.7	0.5	0.2	8.14	3.1	21.0	3.26	1.47	1.40	14.8	4.9	5.7	0.52	0.69	7.6	40.9
180	0.60	1.6	0.4	0.2	6.34	2.6	15.9	3.27	1.50	1.38	13.6	4.8	5.9	0.53	0.71	6.8	39.9
181	0.28	1.7	0.3	0.2	10.4	2.8	30.0	3.65	1.58	1.50	14.0	5.2	5.8	0.56	0.79	6.9	44.1
182	0.26	1.7	0.3	0.2	7.04	2.9	25.3	3.23	1.41	1.42	13.8	4.7	5.1	0.50	0.82	6.6	38.1
183	0.24	1.5	0.4	0.2	11.0	3.6	36.9	3.25	1.44	1.43	14.9	4.9	5.1	0.52	0.92	6.8	40.8
184	0.20	1.7	0.4	0.2	6.21	2.6	17.0	3.15	1.37	1.38	13.0	4.7	5.0	0.50	0.70	5.9	38.4
185	0.23	1.5	0.3	0.2	8.80	2.7	28.7	3.60	1.53	1.52	14.1	5.2	5.8	0.55	0.82	6.8	43.6
186	0.23	1.4	0.4	0.3	6.75	2.3	16.3	3.68	1.57	1.46	12.6	5.4	6.1	0.56	0.79	6.0	45.1
187	0.21	1.5	0.4	0.2	5.54	2.5	20.8	3.15	1.39	1.39	12.6	4.6	5.1	0.48	0.54	6.0	38.4
188	0.20	1.6	0.3	0.2	7.82	2.0	25.1	2.94	1.32	1.28	12.0	4.2	4.8	0.47	0.56	5.7	35.5
189	0.22	1.4	0.3	0.2	5.91	2.4	17.4	3.93	1.63	1.50	12.7	5.6	6.0	0.57	0.57	6.7	45.9
190	0.19	1.4	0.4	0.2	6.33	2.3	15.7	3.12	1.34	1.40	12.6	4.8	5.7	0.49	0.96	6.0	40.9
191	0.21	1.6	0.3	0.2	5.02	2.3	21.3	3.53	1.59	1.48	12.6	5.3	5.9	0.55	0.62	6.3	44.6
192	0.21	1.5	0.3	0.2	4.16	2.0	11.2	2.84	1.27	1.30	12.1	4.2	5.1	0.45	0.59	7.1	36.1
193	0.22	1.8	0.5	0.2	10.6	3.6	58.3	3.07	1.40	1.36	14.9	4.4	4.7	0.48	1.12	6.3	36.8
194	0.21	1.4	0.3	0.3	5.68	2.3	14.7	4.08	1.79	1.59	12.6	6.2	6.4	0.63	0.44	7.0	51.8
195	0.19	1.5	0.5	0.2	6.87	2.3	25.1	3.66	1.52	1.48	12.5	5.8	5.7	0.55	0.94	5.7	48.6
196	0.21	1.4	0.3	0.2	6.85	3.0	18.4	3.35	1.54	1.42	13.5	4.8	5.4	0.54	0.71	6.4	40.3
192 R	0.18	1.7	0.3	0.2	4.22	2.0	11.3	2.98	1.27	1.31	12.0	4.4	5.6	0.45	0.57	6.8	37.1

ICP MS Total Digestion

Sample Number	Ag ppm	Be ppm	Bi ppm	Cd ppm	Co ppm	Cs ppm	Cu ppm	Dy ppm	Er ppm	Eu ppm	Ga ppm	Gd ppm	Hf ppm	Ho ppm	Mo ppm	Nb ppm	Nd ppm
DCB01	2.87	1.4	7.6	0.8	16.0	1.2	272	4.69	2.35	1.32	14.5	6.0	10.4	0.80	13.0	20.7	51.7
197	0.26	1.6	0.4	0.2	6.88	2.3	20.2	3.37	1.45	1.45	12.5	5.1	5.7	0.52	0.50	5.8	42.4
198	0.25	1.4	0.3	0.2	5.12	2.3	19.9	3.32	1.42	1.43	13.0	4.8	5.4	0.51	0.74	6.4	39.7
199	1.70	1.7	0.4	0.2	14.5	2.0	23.2	2.46	1.35	1.03	14.4	2.7	3.7	0.45	0.72	8.0	19.8
199 R	1.61	1.8	0.4	0.2	14.0	2.0	23.4	2.38	1.29	1.00	14.1	2.6	3.6	0.44	0.73	7.8	19.2

ICP MS Total Digestion

Sample Number	Ni ppm	Pb204 ppm	Pb206 ppm	Pb207 ppm	Pb208 ppm	PbSUM ppm	Pr ppm	Rb ppm	Sc ppm	Sm ppm	Sn ppm	Ta ppm	Tb ppm	Th ppm	U ppm	V ppm	W ppm
DCB01	99.1	1.28	33.5	19.3	47.7	102	14.0	60.3	6.6	8.0	3.43	1.66	0.82	51.2	127	101	11.0
160	18.2	0.216	3.91	3.22	8.00	15.3	9.2	59.8	6.0	6.4	1.07	0.25	0.57	10.7	3.04	37.9	1.2
161	17.7	0.206	3.81	3.13	7.65	14.8	9.8	62.3	6.3	6.6	1.11	0.29	0.58	10.6	3.08	39.6	1.1
162	21.7	0.202	3.62	3.00	7.62	14.4	8.0	68.9	6.6	5.4	1.25	0.39	0.46	9.46	2.61	43.1	1.3
163	23.8	0.201	3.78	3.07	7.62	14.7	9.7	71.6	7.4	6.4	1.36	0.31	0.55	10.4	3.12	46.8	1.2
164	29.0	0.206	4.02	3.11	7.72	15.0	8.9	70.2	6.8	6.1	1.21	0.35	0.52	10.1	2.81	44.6	1.2
165	17.0	0.218	3.98	3.16	7.89	15.2	9.9	59.8	5.4	6.7	1.00	0.24	0.57	11.2	3.00	35.6	1.0
166	19.5	0.202	4.05	3.10	7.93	15.3	12.7	65.6	6.6	8.5	1.16	0.31	0.73	13.5	3.70	42.2	1.0
167	27.4	0.211	3.91	3.16	7.78	15.1	9.4	60.6	6.0	6.3	1.00	0.26	0.56	10.1	2.96	37.6	1.1
168	22.6	0.209	3.89	3.16	8.00	15.2	10.1	63.0	7.2	6.8	1.19	0.27	0.59	10.2	2.93	46.3	1.3
169	22.1	0.205	3.85	3.00	7.52	14.6	9.0	60.7	6.3	6.0	0.87	0.33	0.52	10.1	2.66	40.5	1.4
170	21.4	0.206	3.84	3.11	7.54	14.7	9.3	62.8	6.3	6.3	1.23	0.25	0.55	9.76	2.94	41.6	1.0
171	23.6	0.213	4.02	3.16	7.88	15.3	9.7	57.4	5.9	6.6	0.85	0.27	0.58	10.9	2.80	39.8	1.2
172	24.4	0.202	3.71	3.09	7.44	14.4	8.2	64.0	6.2	5.8	1.18	0.27	0.50	8.21	2.58	40.9	1.2
173	21.5	0.207	3.71	3.00	7.46	14.4	9.2	70.2	6.5	6.3	1.07	0.31	0.52	9.96	2.76	42.4	0.8
174	24.4	0.200	3.70	2.95	7.36	14.2	8.9	68.1	6.2	5.8	1.00	0.28	0.51	9.60	2.82	41.0	0.9
175	14.3	0.200	3.59	2.96	7.36	14.1	9.3	54.1	4.5	6.3	1.06	0.27	0.54	9.53	2.63	31.5	0.8
176	20.7	0.205	3.76	3.06	7.44	14.5	8.8	60.2	5.3	6.0	0.93	0.25	0.52	9.26	2.54	34.9	1.0
177	47.4	0.389	6.34	5.94	12.7	25.7	4.7	56.7	9.5	3.4	1.86	0.36	0.36	4.91	2.05	63.1	0.7
178	23.9	0.209	4.24	3.21	7.97	15.6	12.3	70.8	6.3	8.3	1.23	0.32	0.70	13.0	3.74	42.0	1.0
DCB01	98.4	1.28	33.2	19.4	47.3	101	14.3	62.7	6.5	8.1	3.60	1.63	0.81	48.8	124	101	10.9
179	24.7	0.236	4.64	3.56	8.64	17.1	10.6	79.3	6.6	7.2	1.64	0.43	0.59	12.0	3.49	44.2	0.9
180	19.8	0.211	4.19	3.16	7.88	15.4	10.2	73.9	6.0	7.1	1.10	0.31	0.61	11.0	3.13	41.8	0.8
181	28.2	0.205	4.00	3.13	7.96	15.3	11.4	73.6	7.3	7.5	1.14	0.31	0.67	12.1	3.70	46.1	1.2
182	26.2	0.219	3.94	3.20	7.69	15.0	10.0	76.7	6.9	6.7	1.44	0.29	0.58	10.3	3.15	46.4	1.0
183	35.9	0.213	4.21	3.24	8.03	15.7	10.6	80.8	7.4	7.2	1.79	0.29	0.59	10.7	3.34	51.2	1.5
184	19.8	0.204	3.94	3.14	7.69	15.0	9.9	68.4	6.0	6.8	1.02	0.25	0.56	10.6	3.05	40.9	1.6
185	25.8	0.214	4.09	3.17	7.97	15.4	11.3	70.2	6.3	7.5	1.13	0.32	0.64	11.5	3.46	42.8	1.2
186	22.1	0.226	4.53	3.40	8.68	16.8	11.6	61.4	5.8	7.9	1.39	0.25	0.65	13.2	3.50	38.1	0.9
187	21.7	0.209	3.92	3.18	7.74	15.0	9.9	66.6	5.8	6.7	0.94	0.30	0.57	10.2	3.12	38.6	0.9
188	26.6	0.198	3.65	2.96	7.34	14.2	9.1	56.5	5.6	6.2	0.84	0.32	0.53	9.12	2.54	36.0	0.9
189	19.6	0.197	3.89	2.97	7.56	14.6	11.8	66.0	6.1	7.9	0.90	0.28	0.66	12.5	3.38	40.4	0.9
190	19.6	0.210	4.04	3.06	7.67	15.0	10.6	58.7	5.8	7.1	0.99	0.27	0.59	11.7	2.94	40.6	1.0
191	18.4	0.209	4.02	3.20	7.95	15.4	11.4	64.6	5.5	7.6	1.08	0.29	0.64	12.0	3.34	37.0	0.9
192	13.1	0.210	3.78	3.08	7.75	14.8	9.0	58.7	5.1	6.4	0.77	0.38	0.53	11.0	2.70	34.0	0.8
193	37.8	0.233	4.51	3.45	8.34	16.5	9.4	75.6	7.7	6.4	1.47	0.26	0.56	10.4	4.34	50.6	1.2
194	18.9	0.197	4.15	3.10	8.05	15.5	13.3	64.3	6.3	9.0	1.17	0.29	0.75	14.4	4.22	42.4	1.3
195	23.5	0.198	4.24	3.04	7.76	15.2	12.6	58.0	5.5	8.7	0.95	0.23	0.70	14.0	4.94	37.8	1.0
196	21.6	0.200	3.97	3.06	7.63	14.9	10.4	70.8	6.7	7.1	1.22	0.27	0.62	11.2	3.23	45.8	0.9
192 R	13.0	0.212	3.81	3.07	7.65	14.7	9.5	59.6	5.0	6.4	0.83	0.22	0.55	11.2	2.73	34.7	0.7



ICP MS Total Digestion

Sample Number	Ni ppm	Pb204 ppm	Pb206 ppm	Pb207 ppm	Pb208 ppm	PbSUM ppm	Pr ppm	Rb ppm	Sc ppm	Sm ppm	Sn ppm	Ta ppm	Tb ppm	Th ppm	U ppm	V ppm	W ppm
DCB01	100	1.30	33.1	19.0	47.3	100	14.1	62.4	6.4	8.2	3.61	1.70	0.82	51.1	126	102	10.4
197	20.6	0.206	3.89	3.10	7.71	14.9	11.1	62.2	5.6	7.3	0.91	0.26	0.62	11.3	3.12	37.1	1.0
198	16.9	0.209	3.88	3.12	7.82	15.0	10.2	65.6	5.5	6.9	0.90	0.28	0.59	10.7	3.08	37.3	1.2
199	47.0	0.395	6.32	5.84	13.2	25.8	5.0	57.1	9.6	3.6	1.75	0.24	0.38	4.82	2.06	62.7	0.7
199 R	47.5	0.385	6.42	5.93	12.7	25.4	4.8	56.9	9.7	3.4	1.81	0.22	0.38	4.46	2.04	63.0	0.8

ICP MS Total Digestion

Sample Number	Y ppm	Yb ppm	Zn ppm
DCB01	21.4	2.05	134
160	13.9	1.21	22
161	14.7	1.24	25
162	11.9	1.05	24
163	13.9	1.23	31
164	13.1	1.10	33
165	13.7	1.17	22
166	16.9	1.37	26
167	14.0	1.17	21
168	14.7	1.24	27
169	13.0	1.10	22
170	13.7	1.13	25
171	14.0	1.20	23
172	12.9	1.10	27
173	13.8	1.20	26
174	12.6	1.08	25
175	13.3	1.12	16
176	13.0	1.09	21
177	12.3	1.27	54
178	16.5	1.36	26
DCB01	21.5	1.97	128
179	14.3	1.20	29
180	14.6	1.25	25
181	16.2	1.36	33
182	13.8	1.20	32
183	14.5	1.19	40
184	13.6	1.13	25
185	15.5	1.30	29
186	15.6	1.29	23
187	13.4	1.18	24
188	13.3	1.07	20
189	16.1	1.34	24
190	13.2	1.14	22
191	15.0	1.30	21
192	12.0	1.04	18
193	13.5	1.18	34
194	17.3	1.42	24
195	14.7	1.21	24
196	14.9	1.25	30
192 R	12.5	1.09	18

ICP MS Total Digestion

Sample Number	Y ppm	Yb ppm	Zn ppm
DCB01	21.2	2.04	131
197	13.9	1.17	23
198	14.2	1.21	21
199	13.0	1.23	53
199 R	12.8	1.26	52

Total Digestion: A 0.125 g pulp is gently heated in a mixture of ultrapure HF/HNO3/HClO4 until dry and the residue dissolved in dilute ultrapure HNO3. The standard is DCB01.

ICP MS Partial Digestion

Column Header Details

Silver in ppm (Ag)  
Arsenic in ppm (As)  
Beryllium in ppm (Be)  
Bismuth in ppm (Bi)  
Cadmium in ppm (Cd)

Cobalt in ppm (Co)  
Cesium in ppm (Cs)  
Copper in ppm (Cu)  
Dysprosium in ppm (Dy)  
Erbium in ppm (Er)

Europium in ppm (Eu)  
Gallium in ppm (Ga)  
Gadolinium in ppm (Gd)  
Germanium in ppm (Ge)  
Hafnium in ppm (Hf)

Mercury in ppm (Hg)  
Holmium in ppm (Ho)  
Molybdenum in ppm (Mo)  
Niobium in ppm (Nb)  
Neodymium in ppm (Nd)

Nickel in ppm (Ni)  
Lead204 in ppm (Pb204)  
Lead206 in ppm (Pb206)  
Lead207 in ppm (Pb207)  
Lead208 in ppm (Pb208)

Lead in ppm (PbSUM)  
Praseodymium in ppm (Pr)  
Rubidium in ppm (Rb)  
Antimony in ppm (Sb)  
Scandium in ppm (Sc)

Selenium in ppm (Se)  
Samarium in ppm (Sm)  
Tin in ppm (Sn)  
Tantalum in ppm (Ta)  
Terbium in ppm (Tb)

ICP MS Partial Digestion

Tellurium in ppm (Te)  
Thorium in ppm (Th)  
Uranium in ppm (U)  
Vanadium in ppm (V)  
Tungsten in ppm (W)

Yttrium in ppm (Y)  
Ytterbium in ppm (Yb)  
Zinc in ppm (Zn)  
Zirconium in ppm (Zr)



ICP MS Partial Digestion

Sample Number	Ag ppm	As ppm	Be ppm	Bi ppm	Cd ppm	Co ppm	Cs ppm	Cu ppm	Dy ppm	Er ppm	Eu ppm	Ga ppm	Gd ppm	Ge ppm	Hf ppm	Hg ppm	Ho ppm
DCB01	2.30	29.6	0.43	6.88	0.45	13.7	0.50	265	1.67	0.82	0.52	1.96	2.39	<0.01	0.71	0.02	0.30
160	0.02	7.81	0.17	0.14	0.02	2.51	0.68	11.1	1.19	0.49	0.29	1.25	1.99	<0.01	0.08	<0.01	0.19
161	0.01	5.70	0.17	0.12	0.02	2.30	0.80	13.7	1.20	0.50	0.31	1.36	2.02	<0.01	0.05	<0.01	0.19
162	0.03	4.78	0.28	0.15	0.03	3.22	0.96	10.7	0.94	0.36	0.29	2.00	1.74	<0.01	0.07	<0.01	0.14
163	0.02	7.23	0.24	0.19	0.03	4.18	1.20	16.2	1.27	0.52	0.36	2.00	2.24	<0.01	0.07	<0.01	0.21
164	0.02	12.0	0.28	0.25	0.04	5.18	1.12	18.2	1.15	0.46	0.29	1.82	1.92	<0.01	0.08	<0.01	0.18
165	0.02	8.31	0.17	0.15	0.03	2.27	0.64	11.1	1.13	0.46	0.27	1.10	1.87	<0.01	0.08	<0.01	0.18
166	0.01	5.50	0.20	0.17	0.03	2.74	0.95	11.7	1.40	0.57	0.33	1.36	2.45	<0.01	0.07	<0.01	0.23
167	0.02	9.82	0.28	0.15	0.04	4.92	0.71	19.5	1.18	0.48	0.30	1.32	1.96	<0.01	0.05	<0.01	0.19
168	0.01	8.99	0.25	0.15	0.03	3.32	0.86	18.1	1.22	0.50	0.34	1.59	2.05	<0.01	0.06	<0.01	0.20
169	0.02	9.84	0.26	0.22	0.05	3.90	0.79	13.2	1.14	0.44	0.30	1.55	2.09	<0.01	0.08	<0.01	0.18
170	0.01	6.77	0.20	0.14	0.02	3.41	0.94	16.8	1.20	0.49	0.32	1.56	2.04	<0.01	0.06	<0.01	0.19
171	0.02	13.2	0.32	0.20	0.04	4.42	0.72	14.0	1.26	0.49	0.32	1.50	2.15	<0.01	0.07	<0.01	0.19
172	0.01	8.49	0.24	0.15	0.02	3.79	0.98	19.4	1.28	0.54	0.34	1.63	2.14	<0.01	0.08	<0.01	0.20
173	0.01	6.65	0.23	0.18	0.03	3.28	0.90	13.3	1.21	0.49	0.33	1.58	2.15	<0.01	0.08	<0.01	0.19
174	0.01	8.12	0.24	0.19	0.03	3.96	0.94	18.0	1.17	0.46	0.30	1.64	2.01	<0.01	0.07	<0.01	0.18
175	0.01	6.47	0.16	0.12	0.03	1.91	0.47	9.92	1.20	0.50	0.29	0.99	2.01	<0.01	0.04	<0.01	0.20
176	0.02	8.19	0.22	0.17	0.03	3.41	0.69	15.2	1.19	0.49	0.31	1.29	1.96	<0.01	0.08	<0.01	0.19
177	1.60	74.7	0.34	0.32	0.07	9.90	0.47	19.7	1.10	0.55	0.37	2.75	1.60	<0.01	0.07	0.06	0.20
178	0.02	7.64	0.29	0.30	0.04	4.36	1.01	13.9	1.46	0.60	0.36	1.65	2.59	<0.01	0.06	<0.01	0.24
DCB01	2.38	27.4	0.41	6.66	0.45	13.6	0.47	265	1.70	0.78	0.52	1.98	2.36	<0.01	0.72	<0.01	0.29
179	0.02	7.05	0.35	0.30	0.04	4.68	1.16	15.6	1.27	0.52	0.32	1.87	2.17	<0.01	0.08	<0.01	0.20
180	0.02	7.28	0.27	0.30	0.04	3.36	0.98	12.1	1.31	0.53	0.32	1.74	2.13	<0.01	0.07	<0.01	0.20
181	0.01	7.96	0.24	0.18	0.03	6.80	1.23	24.3	1.42	0.60	0.36	1.80	2.38	<0.01	0.12	<0.01	0.24
182	0.02	5.02	0.19	0.15	0.03	3.61	1.08	19.5	1.18	0.51	0.31	1.57	1.97	<0.01	0.09	<0.01	0.20
183	0.01	10.4	0.27	0.22	0.03	7.22	1.64	28.9	1.24	0.54	0.32	2.22	2.07	<0.01	0.14	<0.01	0.20
184	0.02	7.99	0.31	0.20	0.04	3.39	0.94	13.2	1.15	0.46	0.28	1.66	1.92	<0.01	0.06	<0.01	0.18
185	0.01	8.74	0.25	0.18	0.03	5.37	1.08	21.9	1.28	0.54	0.32	1.58	2.15	<0.01	0.09	<0.01	0.21
186	0.02	9.82	0.29	0.30	0.03	3.49	0.82	11.5	1.21	0.50	0.30	1.20	2.07	<0.01	0.07	<0.01	0.20
187	0.02	7.97	0.24	0.22	0.03	2.95	0.98	16.4	1.32	0.54	0.32	1.35	2.20	<0.01	0.09	<0.01	0.21
188	0.02	9.72	0.30	0.16	0.03	4.91	0.72	19.5	1.20	0.48	0.32	1.30	2.06	<0.01	0.05	<0.01	0.19
189	0.02	5.24	0.18	0.18	0.03	3.02	0.98	13.7	1.33	0.52	0.33	1.39	2.24	<0.01	0.06	<0.01	0.21
190	0.02	10.4	0.33	0.32	0.03	3.21	0.88	11.8	1.04	0.41	0.28	1.66	1.89	<0.01	0.07	<0.01	0.16
191	0.01	7.11	0.22	0.16	0.03	2.51	0.79	17.0	1.20	0.52	0.30	1.19	1.91	<0.01	0.06	<0.01	0.20
192	0.02	6.53	0.21	0.16	0.04	1.76	0.62	8.33	1.05	0.42	0.24	1.18	1.79	<0.01	0.06	<0.01	0.17
193	0.02	17.8	0.49	0.39	0.04	6.83	1.79	45.6	1.32	0.57	0.38	2.64	2.09	<0.01	0.09	<0.01	0.22
194	0.01	5.73	0.19	0.17	0.04	2.78	1.02	12.0	1.36	0.57	0.33	1.40	2.22	<0.01	0.06	<0.01	0.22
195	0.02	12.8	0.37	0.37	0.04	4.18	0.96	20.6	1.38	0.56	0.35	1.45	2.44	<0.01	0.07	<0.01	0.22
196	0.02	6.97	0.25	0.19	0.03	3.95	1.27	14.9	1.19	0.49	0.29	1.87	1.98	<0.01	0.06	<0.01	0.19
192 R	0.02	6.61	0.22	0.16	0.03	1.80	0.63	8.39	1.02	0.42	0.24	1.21	1.76	<0.01	0.06	<0.01	0.16

ICP MS Partial Digestion

Sample Number	Ag ppm	As ppm	Be ppm	Bi ppm	Cd ppm	Co ppm	Cs ppm	Cu ppm	Dy ppm	Er ppm	Eu ppm	Ga ppm	Gd ppm	Ge ppm	Hf ppm	Hg ppm	Ho ppm
DCB01	2.35	28.1	0.44	6.64	0.42	13.6	0.48	268	1.66	0.81	0.52	1.94	2.40	<0.01	0.71	<0.01	0.30
197	0.01	7.54	0.24	0.21	0.04	4.10	0.85	16.4	1.28	0.52	0.32	1.31	2.17	<0.01	0.08	<0.01	0.21
198	0.01	6.77	0.21	0.16	0.03	2.59	0.78	15.5	1.19	0.49	0.29	1.28	2.02	<0.01	0.06	<0.01	0.19
199	1.62	75.6	0.34	0.31	0.07	9.87	0.46	19.5	1.12	0.54	0.38	2.74	1.59	<0.01	0.07	0.06	0.20
199 R	1.57	75.4	0.33	0.32	0.07	9.82	0.48	19.8	1.08	0.55	0.37	2.71	1.57	<0.01	0.06	0.05	0.19

ICP MS Partial Digestion

Sample Number	Mo ppm	Nb ppm	Nd ppm	Ni ppm	Pb204 ppm	Pb206 ppm	Pb207 ppm	Pb208 ppm	PbSUM ppm	Pr ppm	Rb ppm	Sb ppm	Sc ppm	Se ppm	Sm ppm	Sn ppm	Ta ppm
DCB01	10.9	0.10	16.0	52.0	1.20	29.9	18.3	42.2	91.7	4.34	9.97	0.33	1.9	0.9	2.76	1.02	<0.01
160	0.26	0.08	12.0	8.17	0.030	1.04	0.545	1.52	3.13	3.21	5.88	<0.01	1.1	0.3	2.38	0.19	<0.01
161	0.31	0.10	13.3	7.79	0.022	0.855	0.428	1.23	2.54	3.38	6.31	<0.01	1.2	0.3	2.46	0.13	<0.01
162	0.42	0.28	12.1	9.89	0.034	1.11	0.597	1.68	3.42	3.29	4.37	<0.01	1.3	0.3	2.23	0.18	<0.01
163	0.50	0.14	14.8	11.3	0.038	1.21	0.665	1.84	3.75	4.09	9.16	<0.01	1.6	0.5	2.76	0.28	<0.01
164	0.67	0.24	12.6	14.4	0.037	1.27	0.672	1.80	3.78	3.31	8.11	0.01	1.5	0.4	2.35	0.15	<0.01
165	0.24	0.09	11.4	7.52	0.031	0.999	0.540	1.47	3.04	3.00	5.43	<0.01	1.0	0.5	2.26	0.21	<0.01
166	0.32	0.09	15.3	8.88	0.029	1.17	0.549	1.58	3.32	3.97	7.79	<0.01	1.3	0.5	2.93	0.26	<0.01
167	0.40	0.19	12.1	14.8	0.031	1.12	0.560	1.55	3.26	3.12	4.66	<0.01	1.1	0.3	2.30	0.18	<0.01
168	0.36	0.14	13.1	10.4	0.039	1.16	0.692	1.87	3.76	3.41	6.67	<0.01	1.3	0.4	2.39	0.34	<0.01
169	0.46	0.19	13.6	10.9	0.033	1.15	0.603	1.74	3.53	3.55	5.17	<0.01	1.2	0.3	2.52	0.13	<0.01
170	0.35	0.12	13.3	10.8	0.034	1.05	0.580	1.64	3.31	3.43	7.82	<0.01	1.4	0.5	2.47	0.41	<0.01
171	0.45	0.21	13.8	12.3	0.036	1.24	0.644	1.82	3.75	3.64	5.21	<0.01	1.2	0.3	2.65	0.13	<0.01
172	0.41	0.12	13.4	12.6	0.033	1.08	0.607	1.66	3.38	3.53	7.85	<0.01	1.4	0.4	2.50	0.28	<0.01
173	0.44	0.16	14.4	9.66	0.028	0.986	0.514	1.50	3.03	3.76	5.95	<0.01	1.1	0.5	2.62	0.13	<0.01
174	0.44	0.18	13.2	12.8	0.031	1.09	0.579	1.62	3.31	3.50	7.18	<0.01	1.3	0.4	2.43	0.12	<0.01
175	0.20	0.11	13.0	6.53	0.024	0.908	0.482	1.41	2.83	3.35	3.75	<0.01	0.8	0.4	2.42	0.22	<0.01
176	0.32	0.14	12.6	10.6	0.034	1.07	0.596	1.64	3.34	3.33	5.18	<0.01	1.0	0.6	2.39	0.21	<0.01
177	0.61	0.32	9.74	27.5	0.266	4.19	3.90	8.84	17.1	2.55	6.17	0.26	3.1	0.4	1.78	0.86	<0.01
178	0.50	0.22	16.1	12.0	0.030	1.32	0.594	1.70	3.65	4.23	7.96	<0.01	1.4	0.5	3.10	0.16	<0.01
DCB01	10.8	0.10	15.6	52.9	1.18	29.4	18.4	42.3	91.2	4.16	9.94	0.31	2.0	0.8	2.71	1.05	<0.01
179	0.50	0.23	14.1	12.9	0.047	1.65	0.842	2.30	4.84	3.70	8.58	<0.01	1.5	0.5	2.67	0.38	<0.01
180	0.51	0.24	13.9	9.85	0.029	1.22	0.574	1.60	3.42	3.68	7.61	<0.01	1.3	0.3	2.64	0.15	<0.01
181	0.58	0.06	14.8	15.5	0.030	1.13	0.530	1.48	3.17	3.80	11.1	<0.01	1.8	0.5	2.77	0.18	<0.01
182	0.58	0.06	12.1	13.0	0.028	0.959	0.517	1.42	2.92	3.12	9.75	<0.01	1.5	0.3	2.31	0.27	<0.01
183	0.67	0.05	13.2	20.3	0.045	1.43	0.816	2.09	4.38	3.41	15.0	<0.01	2.3	0.4	2.43	0.47	<0.01
184	0.51	0.30	12.4	9.66	0.028	1.10	0.530	1.51	3.17	3.28	6.81	<0.01	1.4	0.4	2.37	0.18	<0.01
185	0.57	0.05	13.4	13.0	0.026	1.06	0.518	1.44	3.05	3.50	9.37	<0.01	1.6	0.4	2.52	0.14	<0.01
186	0.55	0.23	13.2	10.3	0.048	1.57	0.860	2.20	4.68	3.36	5.95	<0.01	1.2	0.4	2.49	0.46	<0.01
187	0.37	0.12	13.8	11.3	0.024	1.07	0.478	1.38	2.95	3.60	7.87	<0.01	1.3	0.4	2.68	0.12	<0.01
188	0.40	0.19	13.6	14.7	0.031	1.15	0.573	1.60	3.36	3.62	4.74	<0.01	1.1	0.3	2.51	0.20	<0.01
189	0.39	0.11	14.3	8.90	0.020	0.972	0.421	1.30	2.71	3.77	8.10	<0.01	1.3	0.5	2.68	0.14	<0.01
190	0.73	0.33	13.0	8.93	0.034	1.22	0.628	1.73	3.61	3.38	5.02	<0.01	1.2	0.3	2.38	0.20	<0.01
191	0.41	0.08	11.8	8.53	0.029	1.04	0.532	1.46	3.06	3.04	6.47	<0.01	1.1	0.3	2.30	0.27	<0.01
192	0.37	0.24	11.4	5.10	0.022	0.968	0.470	1.36	2.82	3.02	4.19	<0.01	0.8	0.5	2.21	0.14	<0.01
193	0.89	0.18	13.2	21.1	0.055	1.72	1.00	2.41	5.19	3.50	12.6	0.01	2.5	0.3	2.50	0.40	<0.01
194	0.32	0.10	14.1	9.16	0.028	1.12	0.535	1.50	3.18	3.64	7.96	<0.01	1.3	0.5	2.67	0.27	<0.01
195	0.75	0.23	15.5	12.5	0.033	1.41	0.645	1.78	3.87	4.07	6.51	<0.01	1.4	0.5	2.94	0.14	<0.01
196	0.53	0.20	12.4	10.8	0.027	1.12	0.530	1.46	3.13	3.25	10.4	<0.01	1.6	0.4	2.42	0.28	<0.01
192 R	0.38	0.24	11.1	5.30	0.022	0.963	0.444	1.32	2.75	2.99	4.29	<0.01	0.9	0.3	2.17	0.15	<0.01

ICP MS Partial Digestion

Sample Number	Mo ppm	Nb ppm	Nd ppm	Ni ppm	Pb204 ppm	Pb206 ppm	Pb207 ppm	Pb208 ppm	PbSUM ppm	Pr ppm	Rb ppm	Sb ppm	Sc ppm	Se ppm	Sm ppm	Sn ppm	Ta ppm
DCB01	10.6	0.10	16.0	52.2	1.22	29.9	18.7	42.0	91.8	4.14	10.1	0.31	2.0	0.7	2.76	1.07	<0.01
197	0.38	0.10	14.3	10.6	0.024	1.04	0.483	1.40	2.94	3.71	7.08	<0.01	1.2	0.4	2.67	0.13	<0.01
198	0.54	0.10	12.8	8.04	0.022	0.906	0.413	1.21	2.56	3.35	6.64	<0.01	1.1	0.4	2.43	0.12	<0.01
199	0.60	0.30	9.80	27.9	0.265	4.22	3.92	8.86	17.2	2.55	6.14	0.27	3.0	0.4	1.76	0.84	<0.01
199 R	0.58	0.31	9.76	28.1	0.263	4.27	3.86	8.79	17.1	2.51	6.15	0.25	3.2	0.4	1.79	0.85	<0.01

ICP MS Partial Digestion

Sample Number	Tb ppm	Te ppm	Th ppm	U ppm	V ppm	W ppm	Y ppm	Yb ppm	Zn ppm	Zr ppm
DCB01	0.30	0.14	14.2	112	28.8	5.0	7.12	0.62	121	30.0
160	0.23	<0.01	4.15	1.02	10.7	0.3	4.37	0.31	10.7	2.58
161	0.24	<0.01	3.75	1.08	11.7	0.2	4.46	0.32	11.8	1.92
162	0.20	<0.01	4.22	1.49	14.5	0.3	3.11	0.22	10.9	2.49
163	0.26	<0.01	4.56	1.36	16.7	0.2	4.90	0.34	16.9	2.73
164	0.22	<0.01	4.44	1.12	15.0	0.3	4.14	0.29	16.8	3.10
165	0.22	<0.01	3.86	1.04	9.9	0.2	4.25	0.31	9.9	2.45
166	0.28	<0.01	5.04	1.36	13.3	0.2	5.28	0.36	12.8	2.41
167	0.23	<0.01	3.52	1.08	11.2	0.3	4.31	0.32	10.8	1.97
168	0.24	<0.01	3.72	1.04	13.4	0.2	4.59	0.32	12.8	2.34
169	0.23	<0.01	4.67	1.08	13.4	0.3	3.94	0.27	11.0	2.78
170	0.24	<0.01	4.02	1.13	13.8	0.2	4.59	0.32	13.6	2.48
171	0.24	0.01	4.87	1.13	13.2	0.4	4.34	0.31	11.8	2.75
172	0.24	<0.01	3.92	1.14	14.2	0.3	4.82	0.35	15.8	2.86
173	0.24	<0.01	4.41	1.15	14.3	0.2	4.33	0.30	12.0	2.78
174	0.23	<0.01	4.26	1.14	14.1	0.2	4.21	0.30	13.4	2.71
175	0.24	<0.01	3.87	1.00	9.2	0.2	4.55	0.31	7.8	1.83
176	0.23	<0.01	4.02	1.03	11.3	0.3	4.41	0.31	10.6	2.66
177	0.20	<0.01	2.64	1.03	27.1	0.1	5.10	0.43	35.1	2.95
178	0.30	<0.01	5.28	1.43	14.9	0.2	5.47	0.38	14.5	2.44
DCB01	0.30	0.14	13.9	114	28.9	5.2	7.05	0.61	119	30.3
179	0.25	<0.01	4.99	1.39	16.1	0.3	4.69	0.34	15.6	2.99
180	0.26	<0.01	4.66	1.18	15.3	0.2	4.84	0.36	12.8	2.52
181	0.28	<0.01	4.55	1.54	16.8	0.3	5.65	0.41	19.4	4.32
182	0.24	<0.01	3.80	1.23	15.0	0.1	4.73	0.34	17.7	3.30
183	0.24	0.01	4.35	1.42	21.1	0.3	4.98	0.36	25.2	4.88
184	0.22	<0.01	4.18	1.22	14.9	0.2	4.33	0.31	13.9	2.38
185	0.25	<0.01	4.32	1.40	14.8	0.3	5.05	0.36	16.1	3.21
186	0.25	<0.01	4.81	1.28	11.3	0.3	4.62	0.32	10.5	2.56
187	0.26	<0.01	4.74	1.33	12.5	0.2	4.94	0.34	13.2	2.98
188	0.24	<0.01	4.07	1.19	11.4	0.2	4.49	0.33	10.9	2.05
189	0.26	<0.01	4.51	1.48	13.2	0.2	5.05	0.34	12.6	2.17
190	0.21	0.01	4.68	1.16	15.7	0.3	3.65	0.25	10.9	2.40
191	0.24	<0.01	3.73	1.13	11.2	0.2	4.70	0.35	10.1	2.18
192	0.21	<0.01	4.25	1.00	10.3	0.3	3.78	0.27	8.2	1.96
193	0.25	0.02	4.30	2.22	21.2	0.3	4.99	0.40	20.9	3.55
194	0.27	<0.01	4.67	1.31	13.3	0.2	5.20	0.37	12.6	2.37
195	0.27	<0.01	5.42	1.66	13.1	0.3	5.13	0.35	13.3	2.60
196	0.24	<0.01	4.30	1.23	17.0	0.2	4.60	0.32	17.0	2.38
192 R	0.21	<0.01	4.30	0.98	10.9	0.3	3.77	0.26	8.3	1.99



ICP MS Partial Digestion

Sample Number	Tb ppm	Te ppm	Th ppm	U ppm	V ppm	W ppm	Y ppm	Yb ppm	Zn ppm	Zr ppm
DCB01	0.30	0.13	13.8	112	28.6	4.6	7.07	0.61	120	29.9
197	0.26	<0.01	4.62	1.30	12.2	0.3	4.87	0.34	13.1	3.00
198	0.24	<0.01	4.30	1.28	11.6	0.2	4.52	0.32	11.0	2.58
199	0.20	<0.01	2.65	1.05	27.7	0.1	5.07	0.41	35.5	2.94
199 R	0.21	<0.01	2.64	1.04	27.4	<0.1	5.05	0.42	35.7	2.97

Partial Digestion: A 0.5 g pulp is digested with 2.25 ml of 8:1 ultrapure HNO<sub>3</sub>:HCl for 1 hour at 95 C.  
The standard is DCB01.

Group #: G- 2018-92      Date: 1-26-2018			Al2O3 ICP Total Digestion	Ba ICP Total Digestion	CaO ICP Total Digestion	Ce ICP Total Digestion	Cr ICP Total Digestion	Fe2O3 ICP Total Digestion	K2O ICP Total Digestion	La ICP Total Digestion	Li ICP Total Digestion	MgO ICP Total Digestion
Description	Sample Number	Sample Type	wt %	ppm	wt %	ppm	ppm	wt %	wt %	ppm	ppm	wt %
160	17-RS-039-B	Pulp	12.70	414	1.81	70	44	1.95	2.33	35	19	0.820
161	17-RS-037-B	Pulp	12.80	439	1.83	74	44	1.93	2.31	37	22	0.817
162	17-RS-035-B	Pulp	12.50	525	1.53	63	43	2.28	2.35	32	26	0.783
163	17-RS-034-B	Pulp	12.80	497	1.74	74	49	2.40	2.45	38	28	0.975
164	17-RS-033-B	Pulp	13.00	466	1.71	68	54	2.42	2.41	34	28	0.943
165	17-RS-032-B	Pulp	12.60	415	1.84	75	38	1.80	2.26	37	19	0.724
166	17-RS-005-B	Pulp	12.90	459	1.96	96	42	2.11	2.48	49	23	0.851
167	17-RS-031-B	Pulp	13.00	423	1.79	73	40	1.94	2.31	37	22	0.760
168	17-RS-030-B	Pulp	13.20	470	1.75	77	50	2.33	2.34	39	23	0.923
169	17-RS-029-B	Pulp	12.20	451	1.66	68	40	2.17	2.18	35	22	0.772
170	17-RS-028-B	Pulp	13.10	450	1.84	70	46	2.05	2.40	36	22	0.855
171	17-RS-027-B	Pulp	12.80	426	1.73	74	44	2.16	2.20	37	22	0.762
172	17-RS-026-B	Pulp	12.70	452	1.72	61	45	2.02	2.34	31	24	0.849
173	17-RS-025-B	Pulp	12.10	492	1.72	68	47	2.17	2.34	35	23	0.845
174	17-RS-024-B	Pulp	12.40	463	1.65	67	49	2.13	2.35	34	25	0.838
175	17-RS-023-B	Pulp	12.00	383	1.77	69	34	1.61	2.12	35	17	0.611
176	17-RS-022-B	Pulp	12.00	428	1.69	66	36	1.79	2.20	33	19	0.704
177	R1179	Pulp	12.30	493	2.59	42	121	3.92	2.40	20	22	1.700
178	17-RS-021-B	Pulp	12.90	476	1.85	91	44	2.20	2.56	46	26	0.855
179	17-RS-020-B	Pulp	13.60	511	1.83	77	45	2.33	2.73	40	33	0.906
180	17-RS-019-B	Pulp	13.30	488	1.86	75	42	2.20	2.64	39	26	0.820
181	17-RS-018-B	Pulp	13.30	480	1.86	82	47	2.33	2.60	43	27	0.962
182	17-RS-017-B	Pulp	13.70	515	1.94	73	51	2.29	2.76	38	30	1.020
183	17-RS-015-B	Pulp	13.60	500	1.83	79	56	2.72	2.71	41	34	1.140
184	17-RS-014-B	Pulp	13.30	463	1.78	73	41	2.20	2.54	38	25	0.816
185	17-RS-013-B	Pulp	13.50	463	1.91	82	47	2.20	2.54	41	26	0.901
186	17-RS-012-B	Pulp	13.00	422	1.84	86	41	2.08	2.34	44	25	0.767
187	17-RS-011-B	Pulp	13.10	447	1.85	73	44	1.95	2.46	37	23	0.790
188	17-RS-031-B	Pulp	12.30	408	1.69	69	38	1.85	2.17	34	21	0.728
189	17-RS-010-B	Pulp	12.90	450	1.88	87	45	1.99	2.45	45	22	0.831
190	17-RS-009-B	Pulp	12.80	422	1.66	78	45	2.40	2.24	40	26	0.747
191	17-RS-008-B	Pulp	12.90	444	1.93	83	39	1.89	2.42	43	22	0.745
192	17-RS-007-B	Pulp	12.30	415	1.77	68	34	1.87	2.21	35	20	0.657
192 R		Repeat	12.60	421	1.80	70	34	1.90	2.26	36	21	0.660
193	17-RS-006-B	Pulp	13.90	504	1.63	72	62	2.85	2.63	36	34	1.110
194	17-RS-005-B	Pulp	13.00	460	1.98	102	45	2.12	2.50	52	23	0.862
195	17-RS-004-B	Pulp	12.20	405	1.70	93	42	2.11	2.19	48	25	0.754
196	17-RS-003-B	Pulp	13.00	483	1.76	77	52	2.30	2.59	40	27	0.951
197	17-RS-002-B	Pulp	12.90	427	1.87	80	40	1.89	2.37	41	22	0.748
198	17-RS-001-B	Pulp	12.90	444	1.87	77	40	1.89	2.41	39	22	0.746
199	R1179	Pulp	12.50	496	2.60	41	125	3.95	2.43	20	21	1.720
199 R		Repeat	12.40	491	2.56	40	122	3.90	2.40	21	20	1.710
DCB01		Standard	11.10	387	1.50	126	270	3.35	2.43	63	41	1.68
DCB01		Standard	11.10	387	1.51	124	272	3.36	2.45	64	42	1.70
DCB01		Standard	11.10	395	1.52	127	271	3.36	2.44	64	42	1.70

Group #: G- 2018-92      Date: 1-26-2018			MnO ICP Total Digestion	Na2O ICP Total Digestion	P2O5 ICP Total Digestion	Sr ICP Total Digestion	TiO2 ICP Total Digestion	Zr ICP Total Digestion	Ag ICP MS Partial Digestion	As ICP MS Partial Digestion	Be ICP MS Partial Digestion
Description	Sample Number	Sample Type	wt %	wt %	wt %	ppm	wt %	ppm	ppm	ppm	ppm
160	17-RS-039-B	Pulp	0.030	3.06	0.209	282	0.509	198	0.02	7.81	0.17
161	17-RS-037-B	Pulp	0.030	3.10	0.196	299	0.527	214	0.01	5.70	0.17
162	17-RS-035-B	Pulp	0.028	2.65	0.100	266	0.493	218	0.03	4.78	0.28
163	17-RS-034-B	Pulp	0.034	2.85	0.193	276	0.545	215	0.02	7.23	0.24
164	17-RS-033-B	Pulp	0.033	2.89	0.195	276	0.487	197	0.02	12.00	0.28
165	17-RS-032-B	Pulp	0.029	3.11	0.214	298	0.485	199	0.02	8.31	0.17
166	17-RS-005-B	Pulp	0.034	3.05	0.247	296	0.571	243	0.01	5.50	0.20
167	17-RS-031-B	Pulp	0.030	3.10	0.207	297	0.476	203	0.02	9.82	0.28
168	17-RS-030-B	Pulp	0.032	2.98	0.195	289	0.550	199	0.01	8.99	0.25
169	17-RS-029-B	Pulp	0.030	2.77	0.154	273	0.507	206	0.02	9.84	0.26
170	17-RS-028-B	Pulp	0.031	3.11	0.199	303	0.532	200	0.01	6.77	0.20
171	17-RS-027-B	Pulp	0.031	2.96	0.188	288	0.533	209	0.02	13.20	0.32
172	17-RS-026-B	Pulp	0.028	2.96	0.199	285	0.464	168	0.01	8.49	0.24
173	17-RS-025-B	Pulp	0.032	2.77	0.173	267	0.492	203	0.01	6.65	0.23
174	17-RS-024-B	Pulp	0.029	2.85	0.175	269	0.466	182	0.01	8.12	0.24
175	17-RS-023-B	Pulp	0.027	3.04	0.204	289	0.462	191	0.01	6.47	0.16
176	17-RS-022-B	Pulp	0.027	2.87	0.193	272	0.434	191	0.02	8.19	0.22
177	R1179	Pulp	0.062	2.67	0.115	305	0.490	143	1.60	74.70	0.34
178	17-RS-021-B	Pulp	0.034	2.96	0.236	282	0.520	231	0.02	7.64	0.29
179	17-RS-020-B	Pulp	0.034	3.06	0.208	289	0.500	216	0.02	7.05	0.35
180	17-RS-019-B	Pulp	0.032	3.09	0.220	295	0.488	223	0.02	7.28	0.27
181	17-RS-018-B	Pulp	0.039	3.03	0.235	289	0.526	217	0.01	7.96	0.24
182	17-RS-017-B	Pulp	0.034	3.15	0.216	298	0.487	196	0.02	5.02	0.19
183	17-RS-015-B	Pulp	0.039	2.97	0.218	285	0.502	194	0.01	10.40	0.27
184	17-RS-014-B	Pulp	0.030	3.06	0.201	288	0.450	186	0.02	7.99	0.31
185	17-RS-013-B	Pulp	0.036	3.17	0.224	307	0.520	213	0.01	8.74	0.25
186	17-RS-012-B	Pulp	0.033	3.03	0.222	294	0.479	230	0.02	9.82	0.29
187	17-RS-011-B	Pulp	0.029	3.10	0.223	298	0.459	191	0.02	7.97	0.24
188	17-RS-031-B	Pulp	0.028	2.91	0.196	278	0.453	181	0.02	9.72	0.30
189	17-RS-010-B	Pulp	0.032	3.08	0.224	297	0.528	229	0.02	5.24	0.18
190	17-RS-009-B	Pulp	0.030	2.89	0.143	281	0.484	213	0.02	10.40	0.33
191	17-RS-008-B	Pulp	0.030	3.16	0.220	304	0.496	221	0.01	7.11	0.22
192	17-RS-007-B	Pulp	0.028	2.98	0.184	292	0.436	205	0.02	6.53	0.21
192 R		Repeat	0.028	3.05	0.186	295	0.439	209	0.02	6.61	0.22
193	17-RS-006-B	Pulp	0.036	2.92	0.188	280	0.472	174	0.02	17.80	0.49
194	17-RS-005-B	Pulp	0.034	3.09	0.251	299	0.569	245	0.01	5.73	0.19
195	17-RS-004-B	Pulp	0.032	2.80	0.209	273	0.477	214	0.02	12.80	0.37
196	17-RS-003-B	Pulp	0.033	2.92	0.222	276	0.498	203	0.02	6.97	0.25
197	17-RS-002-B	Pulp	0.032	3.09	0.216	300	0.472	209	0.01	7.54	0.24
198	17-RS-001-B	Pulp	0.030	3.12	0.214	301	0.461	204	0.01	6.77	0.21
199	R1179	Pulp	0.064	2.65	0.117	307	0.494	144	1.62	75.60	0.34
199 R		Repeat	0.063	2.64	0.117	304	0.489	142	1.57	75.40	0.33
DCB01		Standard	0.036	0.57	0.208	413	0.800	417	2.30	29.6	0.43
DCB01		Standard	0.036	0.57	0.205	412	0.794	412	2.38	27.4	0.41
DCB01		Standard	0.036	0.57	0.209	413	0.791	411	2.35	28.1	0.44

Group #: G- 2018-92 Date: 1-26-2018			Bi ICP MS Partial Digestion	Cd ICP MS Partial Digestion	Co ICP MS Partial Digestion	Cs ICP MS Partial Digestion	Cu ICP MS Partial Digestion	Dy ICP MS Partial Digestion	Er ICP MS Partial Digestion	Eu ICP MS Partial Digestion
Description	Sample Number	Sample Type	ppm	ppm	ppm	ppm	ppm	ppm	ppm	ppm
160	17-RS-039-B	Pulp	0.14	0.02	2.51	0.68	11.1	1.19	0.49	0.29
161	17-RS-037-B	Pulp	0.12	0.02	2.30	0.80	13.7	1.20	0.50	0.31
162	17-RS-035-B	Pulp	0.15	0.03	3.22	0.96	10.7	0.94	0.36	0.29
163	17-RS-034-B	Pulp	0.19	0.03	4.18	1.20	16.2	1.27	0.52	0.36
164	17-RS-033-B	Pulp	0.25	0.04	5.18	1.12	18.2	1.15	0.46	0.29
165	17-RS-032-B	Pulp	0.15	0.03	2.27	0.64	11.1	1.13	0.46	0.27
166	17-RS-005-B	Pulp	0.17	0.03	2.74	0.95	11.7	1.40	0.57	0.33
167	17-RS-031-B	Pulp	0.15	0.04	4.92	0.71	19.5	1.18	0.48	0.30
168	17-RS-030-B	Pulp	0.15	0.03	3.32	0.86	18.1	1.22	0.50	0.34
169	17-RS-029-B	Pulp	0.22	0.05	3.90	0.79	13.2	1.14	0.44	0.30
170	17-RS-028-B	Pulp	0.14	0.02	3.41	0.94	16.8	1.20	0.49	0.32
171	17-RS-027-B	Pulp	0.20	0.04	4.42	0.72	14.0	1.26	0.49	0.32
172	17-RS-026-B	Pulp	0.15	0.02	3.79	0.98	19.4	1.28	0.54	0.34
173	17-RS-025-B	Pulp	0.18	0.03	3.28	0.90	13.3	1.21	0.49	0.33
174	17-RS-024-B	Pulp	0.19	0.03	3.96	0.94	18.0	1.17	0.46	0.30
175	17-RS-023-B	Pulp	0.12	0.03	1.91	0.47	9.9	1.20	0.50	0.29
176	17-RS-022-B	Pulp	0.17	0.03	3.41	0.69	15.2	1.19	0.49	0.31
177	R1179	Pulp	0.32	0.07	9.90	0.47	19.7	1.10	0.55	0.37
178	17-RS-021-B	Pulp	0.30	0.04	4.36	1.01	13.9	1.46	0.60	0.36
179	17-RS-020-B	Pulp	0.30	0.04	4.68	1.16	15.6	1.27	0.52	0.32
180	17-RS-019-B	Pulp	0.30	0.04	3.36	0.98	12.1	1.31	0.53	0.32
181	17-RS-018-B	Pulp	0.18	0.03	6.80	1.23	24.3	1.42	0.60	0.36
182	17-RS-017-B	Pulp	0.15	0.03	3.61	1.08	19.5	1.18	0.51	0.31
183	17-RS-015-B	Pulp	0.22	0.03	7.22	1.64	28.9	1.24	0.54	0.32
184	17-RS-014-B	Pulp	0.20	0.04	3.39	0.94	13.2	1.15	0.46	0.28
185	17-RS-013-B	Pulp	0.18	0.03	5.37	1.08	21.9	1.28	0.54	0.32
186	17-RS-012-B	Pulp	0.30	0.03	3.49	0.82	11.5	1.21	0.50	0.30
187	17-RS-011-B	Pulp	0.22	0.03	2.95	0.98	16.4	1.32	0.54	0.32
188	17-RS-031-B	Pulp	0.16	0.03	4.91	0.72	19.5	1.20	0.48	0.32
189	17-RS-010-B	Pulp	0.18	0.03	3.02	0.98	13.7	1.33	0.52	0.33
190	17-RS-009-B	Pulp	0.32	0.03	3.21	0.88	11.8	1.04	0.41	0.28
191	17-RS-008-B	Pulp	0.16	0.03	2.51	0.79	17.0	1.20	0.52	0.30
192	17-RS-007-B	Pulp	0.16	0.04	1.76	0.62	8.3	1.05	0.42	0.24
192 R		Repeat	0.16	0.03	1.80	0.63	8.4	1.02	0.42	0.24
193	17-RS-006-B	Pulp	0.39	0.04	6.83	1.79	45.6	1.32	0.57	0.38
194	17-RS-005-B	Pulp	0.17	0.04	2.78	1.02	12.0	1.36	0.57	0.33
195	17-RS-004-B	Pulp	0.37	0.04	4.18	0.96	20.6	1.38	0.56	0.35
196	17-RS-003-B	Pulp	0.19	0.03	3.95	1.27	14.9	1.19	0.49	0.29
197	17-RS-002-B	Pulp	0.21	0.04	4.10	0.85	16.4	1.28	0.52	0.32
198	17-RS-001-B	Pulp	0.16	0.03	2.59	0.78	15.5	1.19	0.49	0.29
199	R1179	Pulp	0.31	0.07	9.87	0.46	19.5	1.12	0.54	0.38
199 R		Repeat	0.32	0.07	9.82	0.48	19.8	1.08	0.55	0.37
DCB01		Standard	6.88	0.45	13.7	0.50	265	1.67	0.82	0.52
DCB01		Standard	6.66	0.45	13.6	0.47	265	1.70	0.78	0.52
DCB01		Standard	6.64	0.42	13.6	0.48	268	1.66	0.81	0.52

Group #: G- 2018-92      Date: 1-26-2018			Ga ICP MS Partial Digestion	Gd ICP MS Partial Digestion	Ge ICP MS Partial Digestion	Hf ICP MS Partial Digestion	Hg ICP MS Partial Digestion	Ho ICP MS Partial Digestion	Mo ICP MS Partial Digestion	Nb ICP MS Partial Digestion
Description	Sample Number	Sample Type	ppm	ppm	ppm	ppm	ppm	ppm	ppm	ppm
160	17-RS-039-B	Pulp	1.25	1.99	<0.01	0.08	<0.01	0.19	0.26	0.08
161	17-RS-037-B	Pulp	1.36	2.02	<0.01	0.05	<0.01	0.19	0.31	0.10
162	17-RS-035-B	Pulp	2.00	1.74	<0.01	0.07	<0.01	0.14	0.42	0.28
163	17-RS-034-B	Pulp	2.00	2.24	<0.01	0.07	<0.01	0.21	0.50	0.14
164	17-RS-033-B	Pulp	1.82	1.92	<0.01	0.08	<0.01	0.18	0.67	0.24
165	17-RS-032-B	Pulp	1.10	1.87	<0.01	0.08	<0.01	0.18	0.24	0.09
166	17-RS-005-B	Pulp	1.36	2.45	<0.01	0.07	<0.01	0.23	0.32	0.09
167	17-RS-031-B	Pulp	1.32	1.96	<0.01	0.05	<0.01	0.19	0.40	0.19
168	17-RS-030-B	Pulp	1.59	2.05	<0.01	0.06	<0.01	0.20	0.36	0.14
169	17-RS-029-B	Pulp	1.55	2.09	<0.01	0.08	<0.01	0.18	0.46	0.19
170	17-RS-028-B	Pulp	1.56	2.04	<0.01	0.06	<0.01	0.19	0.35	0.12
171	17-RS-027-B	Pulp	1.50	2.15	<0.01	0.07	<0.01	0.19	0.45	0.21
172	17-RS-026-B	Pulp	1.63	2.14	<0.01	0.08	<0.01	0.20	0.41	0.12
173	17-RS-025-B	Pulp	1.58	2.15	<0.01	0.08	<0.01	0.19	0.44	0.16
174	17-RS-024-B	Pulp	1.64	2.01	<0.01	0.07	<0.01	0.18	0.44	0.18
175	17-RS-023-B	Pulp	0.99	2.01	<0.01	0.04	<0.01	0.20	0.20	0.11
176	17-RS-022-B	Pulp	1.29	1.96	<0.01	0.08	<0.01	0.19	0.32	0.14
177	R1179	Pulp	2.75	1.60	<0.01	0.07	0.06	0.20	0.61	0.32
178	17-RS-021-B	Pulp	1.65	2.59	<0.01	0.06	<0.01	0.24	0.50	0.22
179	17-RS-020-B	Pulp	1.87	2.17	<0.01	0.08	<0.01	0.20	0.50	0.23
180	17-RS-019-B	Pulp	1.74	2.13	<0.01	0.07	<0.01	0.20	0.51	0.24
181	17-RS-018-B	Pulp	1.80	2.38	<0.01	0.12	<0.01	0.24	0.58	0.06
182	17-RS-017-B	Pulp	1.57	1.97	<0.01	0.09	<0.01	0.20	0.58	0.06
183	17-RS-015-B	Pulp	2.22	2.07	<0.01	0.14	<0.01	0.20	0.67	0.05
184	17-RS-014-B	Pulp	1.66	1.92	<0.01	0.06	<0.01	0.18	0.51	0.30
185	17-RS-013-B	Pulp	1.58	2.15	<0.01	0.09	<0.01	0.21	0.57	0.05
186	17-RS-012-B	Pulp	1.20	2.07	<0.01	0.07	<0.01	0.20	0.55	0.23
187	17-RS-011-B	Pulp	1.35	2.20	<0.01	0.09	<0.01	0.21	0.37	0.12
188	17-RS-031-B	Pulp	1.30	2.06	<0.01	0.05	<0.01	0.19	0.40	0.19
189	17-RS-010-B	Pulp	1.39	2.24	<0.01	0.06	<0.01	0.21	0.39	0.11
190	17-RS-009-B	Pulp	1.66	1.89	<0.01	0.07	<0.01	0.16	0.73	0.33
191	17-RS-008-B	Pulp	1.19	1.91	<0.01	0.06	<0.01	0.20	0.41	0.08
192	17-RS-007-B	Pulp	1.18	1.79	<0.01	0.06	<0.01	0.17	0.37	0.24
192 R		Repeat	1.21	1.76	<0.01	0.06	<0.01	0.16	0.38	0.24
193	17-RS-006-B	Pulp	2.64	2.09	<0.01	0.09	<0.01	0.22	0.89	0.18
194	17-RS-005-B	Pulp	1.40	2.22	<0.01	0.06	<0.01	0.22	0.32	0.10
195	17-RS-004-B	Pulp	1.45	2.44	<0.01	0.07	<0.01	0.22	0.75	0.23
196	17-RS-003-B	Pulp	1.87	1.98	<0.01	0.06	<0.01	0.19	0.53	0.20
197	17-RS-002-B	Pulp	1.31	2.17	<0.01	0.08	<0.01	0.21	0.38	0.10
198	17-RS-001-B	Pulp	1.28	2.02	<0.01	0.06	<0.01	0.19	0.54	0.10
199	R1179	Pulp	2.74	1.59	<0.01	0.07	0.06	0.20	0.60	0.30
199 R		Repeat	2.71	1.57	<0.01	0.06	0.05	0.19	0.58	0.31
DCB01		Standard	1.96	2.39	<0.01	0.71	0.02	0.30	10.9	0.1
DCB01		Standard	1.98	2.36	<0.01	0.72	<0.01	0.29	10.8	0.1
DCB01		Standard	1.94	2.40	<0.01	0.71	<0.01	0.30	10.6	0.1



Group #: G- 2018-92      Date: 1-26-2018			Nd ICP MS Partial Digestion	Ni ICP MS Partial Digestion	Pb204 ICP MS Partial Digestion	Pb206 ICP MS Partial Digestion	Pb207 ICP MS Partial Digestion	Pb208 ICP MS Partial Digestion	PbSUM ICP MS Partial Digestion	Pr ICP MS Partial Digestion
Description	Sample Number	Sample Type	ppm	ppm	ppm	ppm	ppm	ppm	ppm	ppm
160	17-RS-039-B	Pulp	12	8.17	0.030	1.040	0.545	1.52	3.13	3.21
161	17-RS-037-B	Pulp	13.3	7.79	0.022	0.855	0.428	1.23	2.54	3.38
162	17-RS-035-B	Pulp	12.1	9.89	0.034	1.110	0.597	1.68	3.42	3.29
163	17-RS-034-B	Pulp	14.8	11.30	0.038	1.210	0.665	1.84	3.75	4.09
164	17-RS-033-B	Pulp	12.6	14.40	0.037	1.270	0.672	1.80	3.78	3.31
165	17-RS-032-B	Pulp	11.4	7.52	0.031	0.999	0.540	1.47	3.04	3.00
166	17-RS-005-B	Pulp	15.3	8.88	0.029	1.170	0.549	1.58	3.32	3.97
167	17-RS-031-B	Pulp	12.1	14.80	0.031	1.120	0.560	1.55	3.26	3.12
168	17-RS-030-B	Pulp	13.1	10.40	0.039	1.160	0.692	1.87	3.76	3.41
169	17-RS-029-B	Pulp	13.6	10.90	0.033	1.150	0.603	1.74	3.53	3.55
170	17-RS-028-B	Pulp	13.3	10.80	0.034	1.050	0.580	1.64	3.31	3.43
171	17-RS-027-B	Pulp	13.8	12.30	0.036	1.240	0.644	1.82	3.75	3.64
172	17-RS-026-B	Pulp	13.4	12.60	0.033	1.080	0.607	1.66	3.38	3.53
173	17-RS-025-B	Pulp	14.4	9.66	0.028	0.986	0.514	1.50	3.03	3.76
174	17-RS-024-B	Pulp	13.2	12.80	0.031	1.090	0.579	1.62	3.31	3.50
175	17-RS-023-B	Pulp	13	6.53	0.024	0.908	0.482	1.41	2.83	3.35
176	17-RS-022-B	Pulp	12.6	10.60	0.034	1.070	0.596	1.64	3.34	3.33
177	R1179	Pulp	9.74	27.50	0.266	4.190	3.900	8.84	17.10	2.55
178	17-RS-021-B	Pulp	16.1	12.00	0.030	1.320	0.594	1.70	3.65	4.23
179	17-RS-020-B	Pulp	14.1	12.90	0.047	1.650	0.842	2.30	4.84	3.70
180	17-RS-019-B	Pulp	13.9	9.85	0.029	1.220	0.574	1.60	3.42	3.68
181	17-RS-018-B	Pulp	14.8	15.50	0.030	1.130	0.530	1.48	3.17	3.80
182	17-RS-017-B	Pulp	12.1	13.00	0.028	0.959	0.517	1.42	2.92	3.12
183	17-RS-015-B	Pulp	13.2	20.30	0.045	1.430	0.816	2.09	4.38	3.41
184	17-RS-014-B	Pulp	12.4	9.66	0.028	1.100	0.530	1.51	3.17	3.28
185	17-RS-013-B	Pulp	13.4	13.00	0.026	1.060	0.518	1.44	3.05	3.50
186	17-RS-012-B	Pulp	13.2	10.30	0.048	1.570	0.860	2.20	4.68	3.36
187	17-RS-011-B	Pulp	13.8	11.30	0.024	1.070	0.478	1.38	2.95	3.60
188	17-RS-031-B	Pulp	13.6	14.70	0.031	1.150	0.573	1.60	3.36	3.62
189	17-RS-010-B	Pulp	14.3	8.90	0.020	0.972	0.421	1.30	2.71	3.77
190	17-RS-009-B	Pulp	13	8.93	0.034	1.220	0.628	1.73	3.61	3.38
191	17-RS-008-B	Pulp	11.8	8.53	0.029	1.040	0.532	1.46	3.06	3.04
192	17-RS-007-B	Pulp	11.4	5.10	0.022	0.968	0.470	1.36	2.82	3.02
192 R		Repeat	11.1	5.30	0.022	0.963	0.444	1.32	2.75	2.99
193	17-RS-006-B	Pulp	13.2	21.10	0.055	1.720	1.000	2.41	5.19	3.50
194	17-RS-005-B	Pulp	14.1	9.16	0.028	1.120	0.535	1.50	3.18	3.64
195	17-RS-004-B	Pulp	15.5	12.50	0.033	1.410	0.645	1.78	3.87	4.07
196	17-RS-003-B	Pulp	12.4	10.80	0.027	1.120	0.530	1.46	3.13	3.25
197	17-RS-002-B	Pulp	14.3	10.60	0.024	1.040	0.483	1.40	2.94	3.71
198	17-RS-001-B	Pulp	12.8	8.04	0.022	0.906	0.413	1.21	2.56	3.35
199	R1179	Pulp	9.8	27.90	0.265	4.220	3.920	8.86	17.20	2.55
199 R		Repeat	9.8	28.10	0.263	4.270	3.860	8.79	17.10	2.51
DCB01		Standard	16.0	52.0	1.20	29.9	18.3	42.2	91.70	4.34
DCB01		Standard	15.6	52.9	1.18	29.4	18.4	42.3	91.20	4.16
DCB01		Standard	16.0	52.2	1.22	29.9	18.7	42.0	91.80	4.14

Group #: G- 2018-92 Date: 1-26-2018			Rb ICP MS Partial Digestion	Sb ICP MS Partial Digestion	Sc ICP MS Partial Digestion	Se ICP MS Partial Digestion	Sm ICP MS Partial Digestion	Sn ICP MS Partial Digestion	Ta ICP MS Partial Digestion	Tb ICP MS Partial Digestion
Description	Sample Number	Sample Type	ppm	ppm	ppm	ppm	ppm	ppm	ppm	ppm
160	17-RS-039-B	Pulp	5.88	<0.01	1.1	0.3	2.38	0.19	<0.01	0.23
161	17-RS-037-B	Pulp	6.31	<0.01	1.2	0.3	2.46	0.13	<0.01	0.24
162	17-RS-035-B	Pulp	4.37	<0.01	1.3	0.3	2.23	0.18	<0.01	0.20
163	17-RS-034-B	Pulp	9.16	<0.01	1.6	0.5	2.76	0.28	<0.01	0.26
164	17-RS-033-B	Pulp	8.11	0.01	1.5	0.4	2.35	0.15	<0.01	0.22
165	17-RS-032-B	Pulp	5.43	<0.01	1.0	0.5	2.26	0.21	<0.01	0.22
166	17-RS-005-B	Pulp	7.79	<0.01	1.3	0.5	2.93	0.26	<0.01	0.28
167	17-RS-031-B	Pulp	4.66	<0.01	1.1	0.3	2.30	0.18	<0.01	0.23
168	17-RS-030-B	Pulp	6.67	<0.01	1.3	0.4	2.39	0.34	<0.01	0.24
169	17-RS-029-B	Pulp	5.17	<0.01	1.2	0.3	2.52	0.13	<0.01	0.23
170	17-RS-028-B	Pulp	7.82	<0.01	1.4	0.5	2.47	0.41	<0.01	0.24
171	17-RS-027-B	Pulp	5.21	<0.01	1.2	0.3	2.65	0.13	<0.01	0.24
172	17-RS-026-B	Pulp	7.85	<0.01	1.4	0.4	2.50	0.28	<0.01	0.24
173	17-RS-025-B	Pulp	5.95	<0.01	1.1	0.5	2.62	0.13	<0.01	0.24
174	17-RS-024-B	Pulp	7.18	<0.01	1.3	0.4	2.43	0.12	<0.01	0.23
175	17-RS-023-B	Pulp	3.75	<0.01	0.8	0.4	2.42	0.22	<0.01	0.24
176	17-RS-022-B	Pulp	5.18	<0.01	1.0	0.6	2.39	0.21	<0.01	0.23
177	R1179	Pulp	6.17	0.26	3.1	0.4	1.78	0.86	<0.01	0.20
178	17-RS-021-B	Pulp	7.96	<0.01	1.4	0.5	3.10	0.16	<0.01	0.30
179	17-RS-020-B	Pulp	8.58	<0.01	1.5	0.5	2.67	0.38	<0.01	0.25
180	17-RS-019-B	Pulp	7.61	<0.01	1.3	0.3	2.64	0.15	<0.01	0.26
181	17-RS-018-B	Pulp	11.10	<0.01	1.8	0.5	2.77	0.18	<0.01	0.28
182	17-RS-017-B	Pulp	9.75	<0.01	1.5	0.3	2.31	0.27	<0.01	0.24
183	17-RS-015-B	Pulp	15.00	<0.01	2.3	0.4	2.43	0.47	<0.01	0.24
184	17-RS-014-B	Pulp	6.81	<0.01	1.4	0.4	2.37	0.18	<0.01	0.22
185	17-RS-013-B	Pulp	9.37	<0.01	1.6	0.4	2.52	0.14	<0.01	0.25
186	17-RS-012-B	Pulp	5.95	<0.01	1.2	0.4	2.49	0.46	<0.01	0.25
187	17-RS-011-B	Pulp	7.87	<0.01	1.3	0.4	2.68	0.12	<0.01	0.26
188	17-RS-031-B	Pulp	4.74	<0.01	1.1	0.3	2.51	0.20	<0.01	0.24
189	17-RS-010-B	Pulp	8.10	<0.01	1.3	0.5	2.68	0.14	<0.01	0.26
190	17-RS-009-B	Pulp	5.02	<0.01	1.2	0.3	2.38	0.20	<0.01	0.21
191	17-RS-008-B	Pulp	6.47	<0.01	1.1	0.3	2.30	0.27	<0.01	0.24
192	17-RS-007-B	Pulp	4.19	<0.01	0.8	0.5	2.21	0.14	<0.01	0.21
192 R		Repeat	4.29	<0.01	0.9	0.3	2.17	0.15	<0.01	0.21
193	17-RS-006-B	Pulp	12.60	0.01	2.5	0.3	2.50	0.40	<0.01	0.25
194	17-RS-005-B	Pulp	7.96	<0.01	1.3	0.5	2.67	0.27	<0.01	0.27
195	17-RS-004-B	Pulp	6.51	<0.01	1.4	0.5	2.94	0.14	<0.01	0.27
196	17-RS-003-B	Pulp	10.40	<0.01	1.6	0.4	2.42	0.28	<0.01	0.24
197	17-RS-002-B	Pulp	7.08	<0.01	1.2	0.4	2.67	0.13	<0.01	0.26
198	17-RS-001-B	Pulp	6.64	<0.01	1.1	0.4	2.43	0.12	<0.01	0.24
199	R1179	Pulp	6.14	0.27	3.0	0.4	1.76	0.84	<0.01	0.20
199 R		Repeat	6.15	0.25	3.2	0.4	1.79	0.85	<0.01	0.21
DCB01		Standard	9.97	0.33	1.9	0.9	2.76	1.02	<0.01	0.3
DCB01		Standard	9.94	0.31	2.0	0.8	2.71	1.05	<0.01	0.3
DCB01		Standard	10.10	0.31	2.0	0.7	2.76	1.07	<0.01	0.3

Group #: G- 2018-92 Date: 1-26-2018			Te ICP MS Partial Digestion	Th ICP MS Partial Digestion	U ICP MS Partial Digestion	V ICP MS Partial Digestion	W ICP MS Partial Digestion	Y ICP MS Partial Digestion	Yb ICP MS Partial Digestion	Zn ICP MS Partial Digestion
Description	Sample Number	Sample Type	ppm	ppm	ppm	ppm	ppm	ppm	ppm	ppm
160	17-RS-039-B	Pulp	<0.01	4.15	1.02	10.7	0.3	4.37	0.31	10.7
161	17-RS-037-B	Pulp	<0.01	3.75	1.08	11.7	0.2	4.46	0.32	11.8
162	17-RS-035-B	Pulp	<0.01	4.22	1.49	14.5	0.3	3.11	0.22	10.9
163	17-RS-034-B	Pulp	<0.01	4.56	1.36	16.7	0.2	4.90	0.34	16.9
164	17-RS-033-B	Pulp	<0.01	4.44	1.12	15.0	0.3	4.14	0.29	16.8
165	17-RS-032-B	Pulp	<0.01	3.86	1.04	9.9	0.2	4.25	0.31	9.9
166	17-RS-005-B	Pulp	<0.01	5.04	1.36	13.3	0.2	5.28	0.36	12.8
167	17-RS-031-B	Pulp	<0.01	3.52	1.08	11.2	0.3	4.31	0.32	10.8
168	17-RS-030-B	Pulp	<0.01	3.72	1.04	13.4	0.2	4.59	0.32	12.8
169	17-RS-029-B	Pulp	<0.01	4.67	1.08	13.4	0.3	3.94	0.27	11.0
170	17-RS-028-B	Pulp	<0.01	4.02	1.13	13.8	0.2	4.59	0.32	13.6
171	17-RS-027-B	Pulp	0.01	4.87	1.13	13.2	0.4	4.34	0.31	11.8
172	17-RS-026-B	Pulp	<0.01	3.92	1.14	14.2	0.3	4.82	0.35	15.8
173	17-RS-025-B	Pulp	<0.01	4.41	1.15	14.3	0.2	4.33	0.30	12.0
174	17-RS-024-B	Pulp	<0.01	4.26	1.14	14.1	0.2	4.21	0.30	13.4
175	17-RS-023-B	Pulp	<0.01	3.87	1.00	9.2	0.2	4.55	0.31	7.8
176	17-RS-022-B	Pulp	<0.01	4.02	1.03	11.3	0.3	4.41	0.31	10.6
177	R1179	Pulp	<0.01	2.64	1.03	27.1	0.1	5.10	0.43	35.1
178	17-RS-021-B	Pulp	<0.01	5.28	1.43	14.9	0.2	5.47	0.38	14.5
179	17-RS-020-B	Pulp	<0.01	4.99	1.39	16.1	0.3	4.69	0.34	15.6
180	17-RS-019-B	Pulp	<0.01	4.66	1.18	15.3	0.2	4.84	0.36	12.8
181	17-RS-018-B	Pulp	<0.01	4.55	1.54	16.8	0.3	5.65	0.41	19.4
182	17-RS-017-B	Pulp	<0.01	3.80	1.23	15.0	0.1	4.73	0.34	17.7
183	17-RS-015-B	Pulp	0.01	4.35	1.42	21.1	0.3	4.98	0.36	25.2
184	17-RS-014-B	Pulp	<0.01	4.18	1.22	14.9	0.2	4.33	0.31	13.9
185	17-RS-013-B	Pulp	<0.01	4.32	1.40	14.8	0.3	5.05	0.36	16.1
186	17-RS-012-B	Pulp	<0.01	4.81	1.28	11.3	0.3	4.62	0.32	10.5
187	17-RS-011-B	Pulp	<0.01	4.74	1.33	12.5	0.2	4.94	0.34	13.2
188	17-RS-031-B	Pulp	<0.01	4.07	1.19	11.4	0.2	4.49	0.33	10.9
189	17-RS-010-B	Pulp	<0.01	4.51	1.48	13.2	0.2	5.05	0.34	12.6
190	17-RS-009-B	Pulp	0.01	4.68	1.16	15.7	0.3	3.65	0.25	10.9
191	17-RS-008-B	Pulp	<0.01	3.73	1.13	11.2	0.2	4.70	0.35	10.1
192	17-RS-007-B	Pulp	<0.01	4.25	1.00	10.3	0.3	3.78	0.27	8.2
192 R		Repeat	<0.01	4.30	0.98	10.9	0.3	3.77	0.26	8.3
193	17-RS-006-B	Pulp	0.02	4.30	2.22	21.2	0.3	4.99	0.40	20.9
194	17-RS-005-B	Pulp	<0.01	4.67	1.31	13.3	0.2	5.20	0.37	12.6
195	17-RS-004-B	Pulp	<0.01	5.42	1.66	13.1	0.3	5.13	0.35	13.3
196	17-RS-003-B	Pulp	<0.01	4.30	1.23	17.0	0.2	4.60	0.32	17.0
197	17-RS-002-B	Pulp	<0.01	4.62	1.30	12.2	0.3	4.87	0.34	13.1
198	17-RS-001-B	Pulp	<0.01	4.30	1.28	11.6	0.2	4.52	0.32	11.0
199	R1179	Pulp	<0.01	2.65	1.05	27.7	0.1	5.07	0.41	35.5
199 R		Repeat	<0.01	2.64	1.04	27.4	<0.1	5.05	0.42	35.7
DCB01		Standard	0.14	14.2	112	28.8	5.0	7.12	0.62	121
DCB01		Standard	0.14	13.9	114	28.9	5.2	7.05	0.61	119
DCB01		Standard	0.13	13.8	112	28.6	4.6	7.07	0.61	120

Group #: G- 2018-92 Date: 1-26-2018			Zr ICP MS Partial Digestion	Ag ICP MS Total Digestion	Be ICP MS Total Digestion	Bi ICP MS Total Digestion	Cd ICP MS Total Digestion	Co ICP MS Total Digestion	Cs ICP MS Total Digestion	Cu ICP MS Total Digestion	Dy ICP MS Total Digestion
Description	Sample Number	Sample Type	ppm	ppm	ppm	ppm	ppm	ppm	ppm	ppm	ppm
160	17-RS-039-B	Pulp	2.58	0.31	1.6	0.3	0.2	5.49	2.0	15.2	3.28
161	17-RS-037-B	Pulp	1.92	0.29	1.4	0.3	0.2	5.08	2.2	18.3	3.21
162	17-RS-035-B	Pulp	2.49	0.29	1.4	0.3	0.2	6.74	2.6	15.5	2.64
163	17-RS-034-B	Pulp	2.73	0.28	1.5	0.3	0.2	7.52	3.2	21.0	3.11
164	17-RS-033-B	Pulp	3.10	0.26	1.8	0.4	0.2	9.11	2.8	25.7	2.93
165	17-RS-032-B	Pulp	2.45	0.22	1.3	0.3	0.2	5.07	1.9	15.9	3.18
166	17-RS-005-B	Pulp	2.41	0.25	1.5	0.3	0.2	5.87	2.4	15.2	3.97
167	17-RS-031-B	Pulp	1.97	0.22	1.6	0.3	0.2	8.28	2.0	26.2	3.19
168	17-RS-030-B	Pulp	2.34	0.23	1.3	0.3	0.2	6.69	2.4	25.2	3.24
169	17-RS-029-B	Pulp	2.78	0.23	1.6	0.3	0.2	7.15	2.1	18.2	2.87
170	17-RS-028-B	Pulp	2.48	0.22	1.3	0.3	0.2	6.10	2.3	20.7	3.09
171	17-RS-027-B	Pulp	2.75	0.21	1.6	0.3	0.2	7.52	2.0	18.3	3.21
172	17-RS-026-B	Pulp	2.86	0.22	1.4	0.3	0.2	6.44	2.4	25.2	2.87
173	17-RS-025-B	Pulp	2.78	0.22	1.7	0.3	0.2	6.47	2.6	18.2	3.11
174	17-RS-024-B	Pulp	2.71	0.22	1.6	0.3	0.2	6.83	2.5	23.2	2.92
175	17-RS-023-B	Pulp	1.83	0.19	1.3	0.3	0.2	4.07	1.6	12.7	3.05
176	17-RS-022-B	Pulp	2.66	0.18	1.5	0.3	0.2	5.91	2.0	19.3	2.89
177	R1179	Pulp	2.95	1.69	1.8	0.5	0.2	14.10	1.9	22.6	2.34
178	17-RS-021-B	Pulp	2.44	0.38	1.9	0.4	0.3	7.54	2.6	18.2	3.79
179	17-RS-020-B	Pulp	2.99	0.40	1.7	0.5	0.2	8.14	3.1	21.0	3.26
180	17-RS-019-B	Pulp	2.52	0.60	1.6	0.4	0.2	6.34	2.6	15.9	3.27
181	17-RS-018-B	Pulp	4.32	0.28	1.7	0.3	0.2	10.40	2.8	30.0	3.65
182	17-RS-017-B	Pulp	3.30	0.26	1.7	0.3	0.2	7.04	2.9	25.3	3.23
183	17-RS-015-B	Pulp	4.88	0.24	1.5	0.4	0.2	11.00	3.6	36.9	3.25
184	17-RS-014-B	Pulp	2.38	0.20	1.7	0.4	0.2	6.21	2.6	17.0	3.15
185	17-RS-013-B	Pulp	3.21	0.23	1.5	0.3	0.2	8.80	2.7	28.7	3.60
186	17-RS-012-B	Pulp	2.56	0.23	1.4	0.4	0.3	6.75	2.3	16.3	3.68
187	17-RS-011-B	Pulp	2.98	0.21	1.5	0.4	0.2	5.54	2.5	20.8	3.15
188	17-RS-031-B	Pulp	2.05	0.20	1.6	0.3	0.2	7.82	2.0	25.1	2.94
189	17-RS-010-B	Pulp	2.17	0.22	1.4	0.3	0.2	5.91	2.4	17.4	3.93
190	17-RS-009-B	Pulp	2.40	0.19	1.4	0.4	0.2	6.33	2.3	15.7	3.12
191	17-RS-008-B	Pulp	2.18	0.21	1.6	0.3	0.2	5.02	2.3	21.3	3.53
192	17-RS-007-B	Pulp	1.96	0.21	1.5	0.3	0.2	4.16	2.0	11.2	2.84
192 R		Repeat	1.99	0.18	1.7	0.3	0.2	4.22	2.0	11.3	2.98
193	17-RS-006-B	Pulp	3.55	0.22	1.8	0.5	0.2	10.60	3.6	58.3	3.07
194	17-RS-005-B	Pulp	2.37	0.21	1.4	0.3	0.3	5.68	2.3	14.7	4.08
195	17-RS-004-B	Pulp	2.60	0.19	1.5	0.5	0.2	6.87	2.3	25.1	3.66
196	17-RS-003-B	Pulp	2.38	0.21	1.4	0.3	0.2	6.85	3.0	18.4	3.35
197	17-RS-002-B	Pulp	3.00	0.26	1.6	0.4	0.2	6.88	2.3	20.2	3.37
198	17-RS-001-B	Pulp	2.58	0.25	1.4	0.3	0.2	5.12	2.3	19.9	3.32
199	R1179	Pulp	2.94	1.70	1.7	0.4	0.2	14.50	2.0	23.2	2.46
199 R		Repeat	2.97	1.61	1.8	0.4	0.2	14.00	2.0	23.4	2.38
DCB01		Standard	30.0	2.79	1.6	7.9	0.7	16.8	1.1	276	4.83
DCB01		Standard	30.3	2.91	1.5	7.9	0.8	16.7	1.2	280	4.79
DCB01		Standard	29.9	2.87	1.4	7.6	0.8	16.0	1.2	272	4.69

Group #: G- 2018-92 Date: 1-26-2018			Er ICP MS Total Digestion	Eu ICP MS Total Digestion	Ga ICP MS Total Digestion	Gd ICP MS Total Digestion	Hf ICP MS Total Digestion	Ho ICP MS Total Digestion	Mo ICP MS Total Digestion	Nb ICP MS Total Digestion	Nd ICP MS Total Digestion
Description	Sample Number	Sample Type	ppm	ppm	ppm	ppm	ppm	ppm	ppm	ppm	ppm
160	17-RS-039-B	Pulp	1.42	1.32	12.7	4.4	5.2	0.51	0.38	6.1	36.2
161	17-RS-037-B	Pulp	1.47	1.45	13.3	4.5	5.4	0.53	0.52	6.4	38.4
162	17-RS-035-B	Pulp	1.24	1.20	13.8	3.7	5.5	0.43	0.62	8.0	31.4
163	17-RS-034-B	Pulp	1.42	1.32	14.2	4.4	5.4	0.50	0.66	7.6	37.7
164	17-RS-033-B	Pulp	1.32	1.30	14.3	4.3	5.1	0.46	0.91	6.6	34.4
165	17-RS-032-B	Pulp	1.37	1.40	12.3	4.6	5.1	0.50	0.40	5.6	38.6
166	17-RS-005-B	Pulp	1.68	1.55	13.4	5.8	6.3	0.62	0.47	7.3	48.9
167	17-RS-031-B	Pulp	1.39	1.36	12.8	4.5	5.1	0.49	0.58	5.8	37.2
168	17-RS-030-B	Pulp	1.46	1.42	13.6	4.6	5.1	0.53	0.51	6.6	39.0
169	17-RS-029-B	Pulp	1.30	1.29	13.2	4.2	5.5	0.46	0.60	7.0	35.0
170	17-RS-028-B	Pulp	1.37	1.33	13.1	4.4	5.2	0.49	0.47	6.3	36.5
171	17-RS-027-B	Pulp	1.46	1.34	12.7	4.5	5.5	0.50	0.64	6.4	37.6
172	17-RS-026-B	Pulp	1.32	1.31	13.4	4.0	4.4	0.48	0.54	6.3	32.4
173	17-RS-025-B	Pulp	1.40	1.32	13.3	4.2	5.4	0.49	0.65	7.2	35.9
174	17-RS-024-B	Pulp	1.27	1.29	12.9	4.1	4.9	0.47	0.57	6.2	34.3
175	17-RS-023-B	Pulp	1.35	1.36	11.5	4.4	5.0	0.48	0.30	5.5	36.2
176	17-RS-022-B	Pulp	1.34	1.28	12.0	4.1	5.1	0.47	0.45	5.6	34.2
177	R1179	Pulp	1.29	0.99	14.1	2.5	3.8	0.42	0.73	7.7	17.7
178	17-RS-021-B	Pulp	1.67	1.53	12.7	5.7	6.2	0.60	0.66	7.4	48.2
179	17-RS-020-B	Pulp	1.47	1.40	14.8	4.9	5.7	0.52	0.69	7.6	40.9
180	17-RS-019-B	Pulp	1.50	1.38	13.6	4.8	5.9	0.53	0.71	6.8	39.9
181	17-RS-018-B	Pulp	1.58	1.50	14.0	5.2	5.8	0.56	0.79	6.9	44.1
182	17-RS-017-B	Pulp	1.41	1.42	13.8	4.7	5.1	0.50	0.82	6.6	38.1
183	17-RS-015-B	Pulp	1.44	1.43	14.9	4.9	5.1	0.52	0.92	6.8	40.8
184	17-RS-014-B	Pulp	1.37	1.38	13.0	4.7	5.0	0.50	0.70	5.9	38.4
185	17-RS-013-B	Pulp	1.53	1.52	14.1	5.2	5.8	0.55	0.82	6.8	43.6
186	17-RS-012-B	Pulp	1.57	1.46	12.6	5.4	6.1	0.56	0.79	6.0	45.1
187	17-RS-011-B	Pulp	1.39	1.39	12.6	4.6	5.1	0.48	0.54	6.0	38.4
188	17-RS-031-B	Pulp	1.32	1.28	12.0	4.2	4.8	0.47	0.56	5.7	35.5
189	17-RS-010-B	Pulp	1.63	1.50	12.7	5.6	6.0	0.57	0.57	6.7	45.9
190	17-RS-009-B	Pulp	1.34	1.40	12.6	4.8	5.7	0.49	0.96	6.0	40.9
191	17-RS-008-B	Pulp	1.59	1.48	12.6	5.3	5.9	0.55	0.62	6.3	44.6
192	17-RS-007-B	Pulp	1.27	1.30	12.1	4.2	5.1	0.45	0.59	7.1	36.1
192 R		Repeat	1.27	1.31	12.0	4.4	5.6	0.45	0.57	6.8	37.1
193	17-RS-006-B	Pulp	1.40	1.36	14.9	4.4	4.7	0.48	1.12	6.3	36.8
194	17-RS-005-B	Pulp	1.79	1.59	12.6	6.2	6.4	0.63	0.44	7.0	51.8
195	17-RS-004-B	Pulp	1.52	1.48	12.5	5.8	5.7	0.55	0.94	5.7	48.6
196	17-RS-003-B	Pulp	1.54	1.42	13.5	4.8	5.4	0.54	0.71	6.4	40.3
197	17-RS-002-B	Pulp	1.45	1.45	12.5	5.1	5.7	0.52	0.50	5.8	42.4
198	17-RS-001-B	Pulp	1.42	1.43	13.0	4.8	5.4	0.51	0.74	6.4	39.7
199	R1179	Pulp	1.35	1.03	14.4	2.7	3.7	0.45	0.72	8.0	19.8
199 R		Repeat	1.29	1.00	14.1	2.6	3.6	0.44	0.73	7.8	19.2
DCB01		Standard	2.32	1.33	14.5	6	10.4	0.82	12.3	20.7	51.5
DCB01		Standard	2.31	1.33	14.6	6	8.7	0.93	12.5	20.9	52.3
DCB01		Standard	2.35	1.32	14.5	6	10.4	0.80	13.0	20.7	51.7



Group #: G- 2018-92 Date: 1-26-2018			Ni ICP MS Total Digestion	Pb204 ICP MS Total Digestion	Pb206 ICP MS Total Digestion	Pb207 ICP MS Total Digestion	Pb208 ICP MS Total Digestion	PbSUM ICP MS Total Digestion	Pr ICP MS Total Digestion	Rb ICP MS Total Digestion	Sc ICP MS Total Digestion
Description	Sample Number	Sample Type	ppm	ppm	ppm	ppm	ppm	ppm	ppm	ppm	ppm
160	17-RS-039-B	Pulp	18.2	0.216	3.91	3.22	8.00	15.3	9.2	59.8	6.0
161	17-RS-037-B	Pulp	17.7	0.206	3.81	3.13	7.65	14.8	9.8	62.3	6.3
162	17-RS-035-B	Pulp	21.7	0.202	3.62	3.00	7.62	14.4	8.0	68.9	6.6
163	17-RS-034-B	Pulp	23.8	0.201	3.78	3.07	7.62	14.7	9.7	71.6	7.4
164	17-RS-033-B	Pulp	29.0	0.206	4.02	3.11	7.72	15.0	8.9	70.2	6.8
165	17-RS-032-B	Pulp	17.0	0.218	3.98	3.16	7.89	15.2	9.9	59.8	5.4
166	17-RS-005-B	Pulp	19.5	0.202	4.05	3.10	7.93	15.3	12.7	65.6	6.6
167	17-RS-031-B	Pulp	27.4	0.211	3.91	3.16	7.78	15.1	9.4	60.6	6.0
168	17-RS-030-B	Pulp	22.6	0.209	3.89	3.16	8.00	15.2	10.1	63.0	7.2
169	17-RS-029-B	Pulp	22.1	0.205	3.85	3.00	7.52	14.6	9.0	60.7	6.3
170	17-RS-028-B	Pulp	21.4	0.206	3.84	3.11	7.54	14.7	9.3	62.8	6.3
171	17-RS-027-B	Pulp	23.6	0.213	4.02	3.16	7.88	15.3	9.7	57.4	5.9
172	17-RS-026-B	Pulp	24.4	0.202	3.71	3.09	7.44	14.4	8.2	64.0	6.2
173	17-RS-025-B	Pulp	21.5	0.207	3.71	3.00	7.46	14.4	9.2	70.2	6.5
174	17-RS-024-B	Pulp	24.4	0.200	3.70	2.95	7.36	14.2	8.9	68.1	6.2
175	17-RS-023-B	Pulp	14.3	0.200	3.59	2.96	7.36	14.1	9.3	54.1	4.5
176	17-RS-022-B	Pulp	20.7	0.205	3.76	3.06	7.44	14.5	8.8	60.2	5.3
177	R1179	Pulp	47.4	0.389	6.34	5.94	12.70	25.7	4.7	56.7	9.5
178	17-RS-021-B	Pulp	23.9	0.209	4.24	3.21	7.97	15.6	12.3	70.8	6.3
179	17-RS-020-B	Pulp	24.7	0.236	4.64	3.56	8.64	17.1	10.6	79.3	6.6
180	17-RS-019-B	Pulp	19.8	0.211	4.19	3.16	7.88	15.4	10.2	73.9	6.0
181	17-RS-018-B	Pulp	28.2	0.205	4.00	3.13	7.96	15.3	11.4	73.6	7.3
182	17-RS-017-B	Pulp	26.2	0.219	3.94	3.20	7.69	15.0	10.0	76.7	6.9
183	17-RS-015-B	Pulp	35.9	0.213	4.21	3.24	8.03	15.7	10.6	80.8	7.4
184	17-RS-014-B	Pulp	19.8	0.204	3.94	3.14	7.69	15.0	9.9	68.4	6.0
185	17-RS-013-B	Pulp	25.8	0.214	4.09	3.17	7.97	15.4	11.3	70.2	6.3
186	17-RS-012-B	Pulp	22.1	0.226	4.53	3.40	8.68	16.8	11.6	61.4	5.8
187	17-RS-011-B	Pulp	21.7	0.209	3.92	3.18	7.74	15.0	9.9	66.6	5.8
188	17-RS-031-B	Pulp	26.6	0.198	3.65	2.96	7.34	14.2	9.1	56.5	5.6
189	17-RS-010-B	Pulp	19.6	0.197	3.89	2.97	7.56	14.6	11.8	66.0	6.1
190	17-RS-009-B	Pulp	19.6	0.210	4.04	3.06	7.67	15.0	10.6	58.7	5.8
191	17-RS-008-B	Pulp	18.4	0.209	4.02	3.20	7.95	15.4	11.4	64.6	5.5
192	17-RS-007-B	Pulp	13.1	0.210	3.78	3.08	7.75	14.8	9.0	58.7	5.1
192 R		Repeat	13.0	0.212	3.81	3.07	7.65	14.7	9.5	59.6	5.0
193	17-RS-006-B	Pulp	37.8	0.233	4.51	3.45	8.34	16.5	9.4	75.6	7.7
194	17-RS-005-B	Pulp	18.9	0.197	4.15	3.10	8.05	15.5	13.3	64.3	6.3
195	17-RS-004-B	Pulp	23.5	0.198	4.24	3.04	7.76	15.2	12.6	58.0	5.5
196	17-RS-003-B	Pulp	21.6	0.200	3.97	3.06	7.63	14.9	10.4	70.8	6.7
197	17-RS-002-B	Pulp	20.6	0.206	3.89	3.10	7.71	14.9	11.1	62.2	5.6
198	17-RS-001-B	Pulp	16.9	0.209	3.88	3.12	7.82	15.0	10.2	65.6	5.5
199	R1179	Pulp	47.0	0.395	6.32	5.84	13.20	25.8	5.0	57.1	9.6
199 R		Repeat	47.5	0.385	6.42	5.93	12.70	25.4	4.8	56.9	9.7
DCB01		Standard	99.1	1.28	33.5	19.3	47.7	102	14.0	60.3	6.6
DCB01		Standard	98.4	1.28	33.2	19.4	47.3	101	14.3	62.7	6.5
DCB01		Standard	100.0	1.30	33.1	19.0	47.3	100	14.1	62.4	6.4

Group #: G- 2018-92 Date: 1-26-2018			Sm ICP MS Total Digestion	Sn ICP MS Total Digestion	Ta ICP MS Total Digestion	Tb ICP MS Total Digestion	Th ICP MS Total Digestion	U ICP MS Total Digestion	V ICP MS Total Digestion	W ICP MS Total Digestion	Y ICP MS Total Digestion
Description	Sample Number	Sample Type	ppm	ppm	ppm	ppm	ppm	ppm	ppm	ppm	ppm
160	17-RS-039-B	Pulp	6.4	1.07	0.25	0.57	10.7	3.04	37.9	1.2	13.9
161	17-RS-037-B	Pulp	6.6	1.11	0.29	0.58	10.6	3.08	39.6	1.1	14.7
162	17-RS-035-B	Pulp	5.4	1.25	0.39	0.46	9.5	2.61	43.1	1.3	11.9
163	17-RS-034-B	Pulp	6.4	1.36	0.31	0.55	10.4	3.12	46.8	1.2	13.9
164	17-RS-033-B	Pulp	6.1	1.21	0.35	0.52	10.1	2.81	44.6	1.2	13.1
165	17-RS-032-B	Pulp	6.7	1.00	0.24	0.57	11.2	3.00	35.6	1.0	13.7
166	17-RS-005-B	Pulp	8.5	1.16	0.31	0.73	13.5	3.70	42.2	1.0	16.9
167	17-RS-031-B	Pulp	6.3	1.00	0.26	0.56	10.1	2.96	37.6	1.1	14.0
168	17-RS-030-B	Pulp	6.8	1.19	0.27	0.59	10.2	2.93	46.3	1.3	14.7
169	17-RS-029-B	Pulp	6.0	0.87	0.33	0.52	10.1	2.66	40.5	1.4	13.0
170	17-RS-028-B	Pulp	6.3	1.23	0.25	0.55	9.8	2.94	41.6	1.0	13.7
171	17-RS-027-B	Pulp	6.6	0.85	0.27	0.58	10.9	2.80	39.8	1.2	14.0
172	17-RS-026-B	Pulp	5.8	1.18	0.27	0.50	8.2	2.58	40.9	1.2	12.9
173	17-RS-025-B	Pulp	6.3	1.07	0.31	0.52	10.0	2.76	42.4	0.8	13.8
174	17-RS-024-B	Pulp	5.8	1.00	0.28	0.51	9.6	2.82	41.0	0.9	12.6
175	17-RS-023-B	Pulp	6.3	1.06	0.27	0.54	9.5	2.63	31.5	0.8	13.3
176	17-RS-022-B	Pulp	6.0	0.93	0.25	0.52	9.3	2.54	34.9	1.0	13.0
177	R1179	Pulp	3.4	1.86	0.36	0.36	4.9	2.05	63.1	0.7	12.3
178	17-RS-021-B	Pulp	8.3	1.23	0.32	0.70	13.0	3.74	42.0	1.0	16.5
179	17-RS-020-B	Pulp	7.2	1.64	0.43	0.59	12.0	3.49	44.2	0.9	14.3
180	17-RS-019-B	Pulp	7.1	1.10	0.31	0.61	11.0	3.13	41.8	0.8	14.6
181	17-RS-018-B	Pulp	7.5	1.14	0.31	0.67	12.1	3.70	46.1	1.2	16.2
182	17-RS-017-B	Pulp	6.7	1.44	0.29	0.58	10.3	3.15	46.4	1.0	13.8
183	17-RS-015-B	Pulp	7.2	1.79	0.29	0.59	10.7	3.34	51.2	1.5	14.5
184	17-RS-014-B	Pulp	6.8	1.02	0.25	0.56	10.6	3.05	40.9	1.6	13.6
185	17-RS-013-B	Pulp	7.5	1.13	0.32	0.64	11.5	3.46	42.8	1.2	15.5
186	17-RS-012-B	Pulp	7.9	1.39	0.25	0.65	13.2	3.50	38.1	0.9	15.6
187	17-RS-011-B	Pulp	6.7	0.94	0.30	0.57	10.2	3.12	38.6	0.9	13.4
188	17-RS-031-B	Pulp	6.2	0.84	0.32	0.53	9.1	2.54	36.0	0.9	13.3
189	17-RS-010-B	Pulp	7.9	0.90	0.28	0.66	12.5	3.38	40.4	0.9	16.1
190	17-RS-009-B	Pulp	7.1	0.99	0.27	0.59	11.7	2.94	40.6	1.0	13.2
191	17-RS-008-B	Pulp	7.6	1.08	0.29	0.64	12.0	3.34	37.0	0.9	15.0
192	17-RS-007-B	Pulp	6.4	0.77	0.38	0.53	11.0	2.70	34.0	0.8	12.0
192 R		Repeat	6.4	0.83	0.22	0.55	11.2	2.73	34.7	0.7	12.5
193	17-RS-006-B	Pulp	6.4	1.47	0.26	0.56	10.4	4.34	50.6	1.2	13.5
194	17-RS-005-B	Pulp	9.0	1.17	0.29	0.75	14.4	4.22	42.4	1.3	17.3
195	17-RS-004-B	Pulp	8.7	0.95	0.23	0.70	14.0	4.94	37.8	1.0	14.7
196	17-RS-003-B	Pulp	7.1	1.22	0.27	0.62	11.2	3.23	45.8	0.9	14.9
197	17-RS-002-B	Pulp	7.3	0.91	0.26	0.62	11.3	3.12	37.1	1.0	13.9
198	17-RS-001-B	Pulp	6.9	0.90	0.28	0.59	10.7	3.08	37.3	1.2	14.2
199	R1179	Pulp	3.6	1.75	0.24	0.38	4.8	2.06	62.7	0.7	13.0
199 R		Repeat	3.4	1.81	0.22	0.38	4.5	2.04	63.0	0.8	12.8
DCB01		Standard	8.0	3.43	1.66	0.82	51.2	127	101	11.0	21.4
DCB01		Standard	8.1	3.60	1.63	0.81	48.8	124	101	10.9	21.5
DCB01		Standard	8.2	3.61	1.70	0.82	51.1	126	102	10.4	21.2

Group #: G- 2018-92      Date: 1-26-2018			Yb ICP MS Total Digestion	Zn ICP MS Total Digestion
Description	Sample Number	Sample Type	ppm	ppm
160	17-RS-039-B	Pulp	1.21	22
161	17-RS-037-B	Pulp	1.24	25
162	17-RS-035-B	Pulp	1.05	24
163	17-RS-034-B	Pulp	1.23	31
164	17-RS-033-B	Pulp	1.10	33
165	17-RS-032-B	Pulp	1.17	22
166	17-RS-005-B	Pulp	1.37	26
167	17-RS-031-B	Pulp	1.17	21
168	17-RS-030-B	Pulp	1.24	27
169	17-RS-029-B	Pulp	1.10	22
170	17-RS-028-B	Pulp	1.13	25
171	17-RS-027-B	Pulp	1.20	23
172	17-RS-026-B	Pulp	1.10	27
173	17-RS-025-B	Pulp	1.20	26
174	17-RS-024-B	Pulp	1.08	25
175	17-RS-023-B	Pulp	1.12	16
176	17-RS-022-B	Pulp	1.09	21
177	R1179	Pulp	1.27	54
178	17-RS-021-B	Pulp	1.36	26
179	17-RS-020-B	Pulp	1.20	29
180	17-RS-019-B	Pulp	1.25	25
181	17-RS-018-B	Pulp	1.36	33
182	17-RS-017-B	Pulp	1.20	32
183	17-RS-015-B	Pulp	1.19	40
184	17-RS-014-B	Pulp	1.13	25
185	17-RS-013-B	Pulp	1.30	29
186	17-RS-012-B	Pulp	1.29	23
187	17-RS-011-B	Pulp	1.18	24
188	17-RS-031-B	Pulp	1.07	20
189	17-RS-010-B	Pulp	1.34	24
190	17-RS-009-B	Pulp	1.14	22
191	17-RS-008-B	Pulp	1.30	21
192	17-RS-007-B	Pulp	1.04	18
192 R		Repeat	1.09	18
193	17-RS-006-B	Pulp	1.18	34
194	17-RS-005-B	Pulp	1.42	24
195	17-RS-004-B	Pulp	1.21	24
196	17-RS-003-B	Pulp	1.25	30
197	17-RS-002-B	Pulp	1.17	23
198	17-RS-001-B	Pulp	1.21	21
199	R1179	Pulp	1.23	53
199 R		Repeat	1.26	52
DCB01		Standard	2.05	134
DCB01		Standard	1.97	128
DCB01		Standard	2.04	131

## **Appendix G: QA/QC results for UW and HW data**

UW standard certificate of analysis for CANMET 1179 Till 3 reference

SRC standard analytical ranges DCB01 ICP-OES total digestion

SRC standard analytical ranges DCB01 ICP-MS total digestion

SRC standard analytical ranges DCB01 ICP- MS partial digestion

SRC quality control standard checks' comparison for all geochemical results

Relative percent difference charts 1179 Till-3, DCB01

Precision scatterplots

Thompson-Howarth Short Method graphs

Average coefficient of variation chart

SRC EPMA report AMC2017-013: KIM discrimination plots

UW sample preparation guide for the laser particle sizer Analysette 22



# Certificate of Analysis

First Issued: November 1995

Last revision: November 1995

## *Provisional Values*

# ***TILL-1, TILL-2, TILL-3 and TILL-4***

## **Geochemical Soil and Till Reference Materials**

### **Source**

TILL-1, TILL-2, TILL-3 and TILL-4 were collected and characterized in cooperation with the Mineral Resources Division, Minerals and Continental Geoscience Branch, Geological Survey of Canada.

TILL-1 was collected 25 kilometres north-west of Lanark, Ontario; TILL-3 was collected 8 kilometres east of Cobalt, Ontario. These two soil samples were collected from the combined B and C horizons. The two till samples (TILL-2 and TILL-4) were collected near Scission's Brook, New Brunswick. At this location, extensive trenching had been done by the mining company who owned the property in order to expose the till. The company had obtained preliminary analyses of till samples collected at various sites within the trenched areas. These analyses were used as guidelines to sampling. No effort was made to collect any particular horizon. In order to augment the molybdenum levels in TILL-4, a small quantity

of a molybdenite-bearing soil was collected near an old test pit. All sampling was done by shovelling.

### **Description**

These four materials, two soils and two tills, complete a series of reference samples of surficial materials which also includes the lake and stream sediment materials, LKSD-1, LKSD-2, LKSD-3, LKSD-4, STSD-1, STSD-2, STSD-3 and STSD-4, which are already available.

Like the sediment series, the TILL samples are characterised for major element oxides, total elements as well as elements from partial extractions. The partial extractions are concentrated hydrochloride - concentrated nitric acids and dilute hydrochloric-dilute nitric acids. In addition, informational data from a single source are provided for a number of elements derived by EPA digestions 3050 and 3051.

### **Intended Use**

TILL-1, TILL-2, TILL-3 and TILL-4 are intended for quality control in chemical analysis.

### **Instructions for Use**

TILL samples should be used “as is” without drying. The contents of the bottle should be thoroughly mixed before taking samples.

### **Method of Preparation**

In each case, the collected material was spread to a depth of 7.5 to 10 cm over a polyethylene sheet and allowed to dry for several weeks at room temperature. When dry, each sample was sieved through an 80-mesh (177 µm) screen. The +80 mesh fraction was discarded. The -80-mesh fraction was ball milled and sieved through a 200-mesh screen (74 µm). The oversize material from this sieving was retained, ball milled and sieved a second time through the 200-mesh screen. At this point, any oversize fraction (plus-200 mesh) was discarded. The two minus-200-mesh fractions were combined and tumbled as a single batch in a conical blender for eight hours. Each material was bottled in 100-g units.

### **State of Homogeneity**

A method described by Lynch (1) was employed for homogeneity testing. No evidence of inhomogeneity was found.

### **Method of Certification**

TILL-1, TILL-2, TILL-3 and TILL-4 were characterised by an interlaboratory analysis program involving thirty-one laboratories. The provisional values for these soil and till reference materials were assigned from the average of data after a two-step trimming method described by Lynch (1).

### **Legal Notice**

The Canadian Certified Reference Materials Project has prepared these reference materials and statistically evaluated the analytical data of the interlaboratory certification program to the best of its ability. The purchaser, by receipt hereof, releases and indemnifies the Canadian Certified Reference Materials Project from and

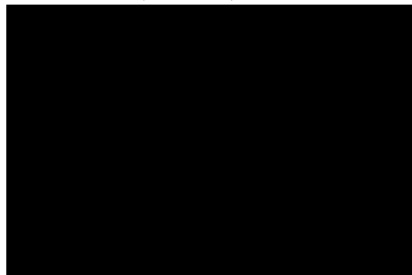
against all liability and costs arising out of the use of these materials and information.

### **References**

(1) J.J. Lynch (1990). Provisional elemental values for eight new geochemical lake sediment and stream sediment reference materials LKSD-1, LKSD-2, LKSD-3, LKSD-4, STSD-1, STSD-2, STSD-3 and STSD-4, *Geostandards Newsletter*, 14: 153-167.

The preparation and certification procedures used for TILL-1, TILL-2, TILL-3 and TILL-4, including values obtained by individual laboratories, are to be published in *Geostandards Newsletter*. This report will be available free of charge on application to:

**Coordinator, CCRMP  
CANMET (NRCan)**





### Material collection locations

Sample	NTS* Desig- nation	Location
TILL-1	31F	Joe Lake, Ontario
TILL-2	21C	5 km West Scisson's Brook, New Brunswick
TILL-3	31M	O'Brien Mine, near Cobalt Ontario
TILL-4	21C 31G	Scisson's Brook, New Brunswick Molybdenite Occurrence near Hull, Québec

\*National topographic system

### Summary of major and minor elements expressed as oxides (%)

	TILL-1	TILL-2	TILL-3	TILL-4
SiO <sub>2</sub>	60.9	60.8	69.1	65.0
Al <sub>2</sub> O <sub>3</sub>	13.7	16.0	12.2	14.4
Fe <sub>2</sub> O <sub>3</sub> (T)	6.82	5.39	3.92	5.63
MgO	2.15	1.83	1.71	1.26
CaO	2.72	1.27	2.63	1.25
Na <sub>2</sub> O	2.71	2.19	2.64	2.46
K <sub>2</sub> O	2.22	3.07	2.42	3.25
MnO	0.18	0.10	0.06	0.06
TiO <sub>2</sub>	0.98	0.88	0.49	0.81
P <sub>2</sub> O <sub>5</sub>	0.22	0.17	0.11	0.20
LOI (1000°C)	7.3	8.1	4.6	5.7
Sum	99.90	99.80	99.88	100.02

Summary of "total" elements in TILL series (in µg/g unless otherwise noted)

	TILL-1	TILL-2	TILL-3	TILL-4
As	18	26	87	111
Au (ppb)	13	2	6	5
Ba	702	540	489	395
Be	2.4	4.0	2.0	3.7
Bi	<5	<5	<5	40
Br	6.4	12.2	4.5	8.6
Ce	71	98	42	78
Co	18	15	15	8
Cr	65	74	123	53
Cs	1.0	12.	1.7	12
Cu	47	150	22	237
Eu	1.3	1.0	<1.0	<1.0
Er	3.6	3.7	1.4	3.2
Fe (%)	4.81	3.84	2.78	3.97
Hf	13	11	8	10
La	28	44	21	41
Li	15	47	21	30
LOI (500°C) %	6.3	6.8	3.6	4.4
Lu	0.6	0.6	0.2	0.5
Mn	1420	780	520	490
Mo	2	14	2	16
Nb	10	20	7	15
Nd	26	36	16	30
Ni	24	32	39	17
P	930	750	490	880
Pb	22	31	26	50
Rb	44	143	55	161
S (%)	<0.05	<0.05	<0.05	0.08
Sb	7.8	0.8	0.9	1.0
Sc	13	12	10	10
Sm	5.9	7.4	3.3	6.1
Sr	291	144	300	109
Ta	0.7	1.9	<0.5	1.6
Tb	1.1	1.2	<0.5	1.1
Th	5.6	18.4	4.6	17.4
Ti	5990	5300	2910	4840
U	2.2	5.7	2.1	5.0
V	99	77	62	67
W	<1	5	<1	204
Y	38	40	17	33
Yb	3.9	3.7	1.5	3.4
Zn	98	130	56	70
Zr	502	390	230	385

**Summary of partial extraction elements; concentrated HNO<sub>3</sub> - concentrated HCl (in µg/g unless otherwise noted)**

	TILL-1	TILL-2	TILL-3	TILL-4
<b>Ag</b>	0.2	0.2	1.6	<0.2
<b>As</b>	13	22	84	102
<b>Ba</b>	84	95	43	71
<b>Bi</b>	<3	4	<3	44
<b>Cd</b>	<0.2	0.3	<0.2	<0.2
<b>Co</b>	12	13	11	6
<b>Cr</b>	30	40	73	26
<b>Cu</b>	48	149	23	254
<b>Fe (%)</b>	3.1	3.2	2.0	3.3
<b>Hg (ppb)</b>	92	74	107	39
<b>Mn</b>	950	530	310	260
<b>Mo</b>	<2	11	<2	14
<b>Ni</b>	18	31	32	15
<b>Pb</b>	12	21	16	36
<b>V</b>	48	38	33	38
<b>Zn</b>	70	116	43	63

**Summary partial extraction elements; dilute HNO<sub>3</sub> - dilute HCl (in µg/g unless otherwise noted)**

	TILL-1	TILL-2	TILL-3	TILL-4
<b>Ag</b>	<0.2	<0.2	1.4	<0.2
<b>Co</b>	12	12	10	6
<b>Cu</b>	49	152	23	252
<b>Fe (%)</b>	3.4	3.4	2.2	3.5
<b>Mn</b>	1020	570	310	260
<b>Mo</b>	1	13	1	15
<b>Ni</b>	17	30	32	14
<b>Pb</b>	14	24	17	37
<b>Zn</b>	71	116	43	62

**Single source data by EPA 3050 digestion - ICP-AES analysis (all values in µg/g)**

<b>Element</b>	<b>TILL - 1</b>	<b>TILL - 2</b>	<b>TILL - 3</b>	<b>TILL - 4</b>
<b>Al</b>	18883	32600	10750	25200
<b>Ba</b>	84.3	104.6	46.4	75.1
<b>Be</b>	1.1	2.1	0.8	1.6
<b>Cd</b>	<0.33	<0.33	<0.33	<0.33
<b>Ca</b>	4145	1940	6240	1438
<b>Cr</b>	29.3	39.3	66.7	25.8
<b>Co</b>	11.7	12.5	10.2	5.8
<b>Cu</b>	44.0	162	17.6	266
<b>Fe</b>	29167	33967	19900	32533
<b>Pb</b>	24.0	35.7	24.0	50.0
<b>Mg</b>	6250	7547	6510	5470
<b>Mn</b>	1060	601	294	243
<b>Mo</b>	8.7	18.7	5.0	20.7
<b>Ni</b>	14.0	27.5	28.0	11.0
<b>P</b>	915	856	470	1150
<b>K</b>	1188	4355	1220	3915
<b>Na</b>	530	527	336	313
<b>V</b>	89	107.2	71.6	82.9
<b>Zn</b>	65.2	111.0	42.5	59.0

**Single source data by EPA 3051 digestion - ICP-AES analysis (all values in µg/g)**

<b>Element</b>	<b>TILL - 1</b>	<b>TILL - 2</b>	<b>TILL - 3</b>	<b>TILL - 4</b>
<b>Al</b>	18050	27550	12000	20400
<b>Ba</b>	77.8	60.8	49.2	102
<b>Be</b>	<0.2	1.7	<0.2	<0.2
<b>Cd</b>	<0.35	<0.3	<0.35	<0.3
<b>Ca</b>	3817	1640	5660	1565
<b>Cr</b>	29.3	34.7	64.7	24.3
<b>Co</b>	12.3	15.5	14.8	8.1
<b>Cu</b>	44.8	176	16.5	332
<b>Fe</b>	37900	38600	21000	40500
<b>Pb</b>	<10.0	31.5	23	42
<b>Mg</b>	6990	8525	7445	5570
<b>Mn</b>	1060	588	317	280
<b>Mo</b>	<2.5	<1.7	6.0	22.5
<b>Ni</b>	18.7	29.5	26.5	11.0
<b>P</b>	834	540	457	1260
<b>K</b>	640	3370	964	3115
<b>Na</b>	575	450	427	485
<b>V</b>	70	111.2	66.1	88.0
<b>Zn</b>	69.8	112.7	42.7	57.6

## CCRMP Reference Materials LKSD, STSD, and TILL

### Explanation of Extraction Methods

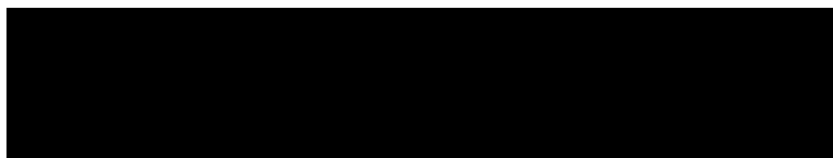
The provisional values for the lake, stream and till reference materials (LKSD, STSD and TILL) were determined from the results of numerous laboratories involved in geochemical exploration using their existing routine methods. Two main types of methods were used.

The first type can be termed total methods wherein the complete amount of a particular element is determined. One subgroup of these total methods involves the sample being analyzed without pretreatment i.e., instrumental neutron activation and powder x-ray diffraction. Another subgroup of total methods includes pretreatments such as a multi acid dissolution with hydrofluoric acid, or fusions followed by, for example, an instrumental finish. This second group of methods may be used to determine the total concentration of numerous elements, but losses of some other elements may occur.

A second type of techniques involves a partial dissolution or extraction of the elements using different combinations of acids at varying strengths. The laboratories that submitted data did not follow established protocols with regards to either the types or amounts of acid utilized. However, two main subgroups of partial extraction or partial dissolution techniques were chosen. The first of these involves the use of both diluted nitric and hydrochloric acids i.e., 2 mL of nitric acid, 1 mL of hydrochloric acid and 5 mL of water; or 3 mL, 2 mL and 1 mL of each component, respectively; or 3 mL, 1 mL and 4 mL of each component, respectively. The second subgroup involves the use of varying amounts of these two acids without the addition of any water i.e., 3 mL of hydrochloric acid plus 1 mL of nitric acid, or 3 mL of nitric acid plus 1 mL of hydrochloric acid. For both of these two subgroups, the sample and acid mixture were heated from 2 to 4 hours at 95°C to 100°C, cooled, diluted to volume and analyzed.



# SRC GEOANALYTICAL LABORATORIES

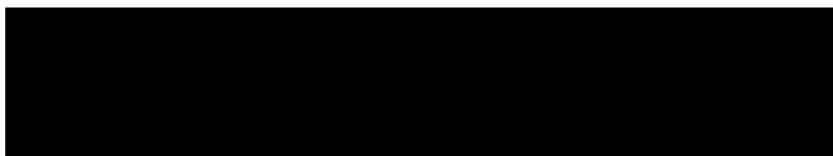


## DCB01 - ICP Total (MS PKG) + S

May 09, 2022

Analyte Name	Value	Range
Al2O3	11.1	10.9 - 11.4
Ba	387	373 - 401
CaO	1.5	1.4 - 1.6
Ce	128	123 - 132
Cr	270	225 - 316
Fe2O3	3.36	3.19 - 3.53
K2O	2.46	2.06 - 2.86
La	66	60 - 73
Li	43	30 - 55
MgO	1.7	1.56 - 1.84
MnO	0.03	0.02 - 0.04
Na2O	0.58	0.5 - 0.65
P2O5	0.21	0.19 - 0.23
Sr	401	350 - 451
TiO2	0.79	0.69 - 0.89
V	101	98 - 104
Zr	419	383 - 454
S	3849	3641 - 4057

# SRC GEOANALYTICAL LABORATORIES



## DCB01 - MS Total

May 09, 2022

Analyte Name	Value	Range
Ag	2.82	2 - 3.64
Be	1.5	0.5 - 2.5
Bi	8.3	6.7 - 9.9
Cd	0.7	0.2 - 1.2
Co	17.2	14.5 - 19.9
Cs	1.1	0.9 - 1.3
Cu	275	253 - 297
Dy	4.16	2.63 - 5.69
Er	2.14	1.4 - 2.88
Eu	1.23	1 - 1.45
Ga	15	11.7 - 18.3
Gd	5.8	4 - 7.6
Hf	11.1	8 - 14.2
Ho	0.77	0.5 - 1.03
Mo	12.4	10.4 - 14.4
Nb	19.5	17.8 - 21.2
Nd	48.4	41.9 - 54.9
Ni	101	86 - 115
Pb204	1.23	1.11 - 1.35
Pb206	33.63	31.29 - 35.97
Pb207	19.12	17.26 - 20.98
Pb208	47.42	42.71 - 52.13
PbSUM	103.2	87.5 - 118.9
Pr	13.3	10.3 - 16.4
Rb	61.4	43.7 - 76
Sc	6.9	5.3 - 8.6
Sm	7.7	5.4 - 10.1
Sn	3.01	1.6 - 4.43
Ta	1.65	0.81 - 2.5
Tb	0.76	0.54 - 0.98
Th	51.9	47.3 - 56.4
U	124	114 - 135
V	98.9	90.2 - 107.7
W	11.6	4.4 - 18.8
Y	21.5	15.2 - 27.8
Yb	1.9	1.51 - 2.29
Zn	126	115 - 137

# SRC GEOANALYTICAL LABORATORIES

## DCB01 - MS Partial

May 09, 2022

Analyte Name	Value	Range
Ag	2.59	2.24 - 2.93
As	28.6	26.1 - 31.1
Be	0.52	0.39 - 0.64
Bi	6.71	6.19 - 7.24
Cd	0.51	0.33 - 0.69
Co	14.3	13.3 - 15.2
Ce	0.4	0.3 - 0.5
Cu	270	261 - 279
Dy	1.65	1.51 - 1.79
Er	0.79	0.73 - 0.85
Eu	0.51	0.47 - 0.54
Ga	2.04	1.92 - 2.15
Gd	2.28	2.14 - 2.43
Ge	0.02	< 0.01 - 0.04
Hf	0.71	0.66 - 0.77
Hg	0.35	0.01 - 0.71
Ho	0.29	0.26 - 0.31
Mo	10.7	10.1 - 11.2
Nb	0.09	0.05 - 0.13
Nd	15.9	15.1 - 16.7
Ni	52.3	49.4 - 55.1
Pb204	1.18	1.11 - 1.25
Pb206	29.8	27.8 - 31.7
Pb207	18.1	17.1 - 19.1
Pb208	42.5	40.1 - 44.8
PbSUM	91.5	86.4 - 96.6
Pr	4.32	4.04 - 4.59
Rb	9.85	9.32 - 10.38
Sb	0.31	0.22 - 0.4
Sc	1.9	1.8 - 2
Se	0.7	0.5 - 1
Sm	2.78	2.59 - 2.96
Sn	1.07	0.99 - 1.14
Ta	0.01	< 0.01 - 0.02
Tb	0.29	0.26 - 0.32
Te	0.12	0.1 - 0.14
Th	13.9	12.9 - 14.9
U	111	105 - 116
V	27.8	26.2 - 29.4
W	4.8	4.3 - 5.3
Y	7.04	6.63 - 7.45
Yb	0.61	0.54 - 0.67
Zn	121	117 - 125

# *SRC GEOANALYTICAL LABORATORIES*



## *DCB01 - MS Partial*

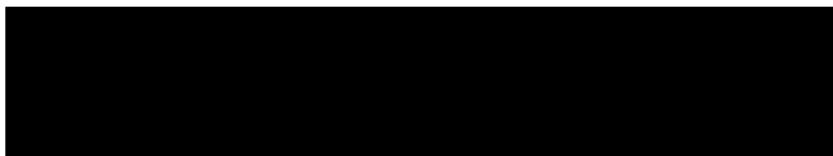
May 09, 2022

Zr

29.1

26.9 - 31.2

# SRC GEOANALYTICAL LABORATORIES



## Standard Checks' Comparisons

Group # 2018-92

Feb 02, 2018

Sample	Analyte Name	Min	Max	Reason	Result
DCB01 for Package # 56 was good ( 111 results checked ).					
DCB01 for Package # 57					
E 1	Sc	1.9	1.8 to 2	>2	2.1
E 21	Gd	2.28	2.14 to 2.43	>2.43	2.46
E 41	Te	0.12	0.1 to 0.14	>0.14	0.15

DCB01 for Package # 59 was good ( 48 results checked ).  
There were 3 errors.

### 2) Repeat Verification

40	192 R				
E W		0.7	1.9	92.31	> 50% diff
45	199 R				

### 3) Total Results must be greater than Partial Results Verification

Sample	Sample ID	Comment
E 45	199 R	Ag (56) 1.61 was less than (57) 1.64

There were 1/1665 Totals less than their Partial results.

### 4) U, Florimetry\_Partial / U, ICP-MS must be less than U, Total Verification

There were no U, Fl/U, ICP-MS or U, Total Results to Check.

### 5) Lower Detection Limit Verification

All 4365 Results are greater than their Detection Limits.

### Upper Detection Limit Verification

All 4365 Results are less than their Detection Limits.

### 7) Oxide Verification

All 90 Al<sub>2</sub>O<sub>3</sub> or Fe<sub>2</sub>O<sub>3</sub> results were less than 40%.

### 8) AS, wt% must be greater than AS, ppm Verification

# *SRC GEOANALYTICAL LABORATORIES*



## *Standard Checks' Comparisons*

**Group # 2018-92**

Feb 02, 2018

Sample	Sample ID	Analyte	Comment
--------	-----------	---------	---------

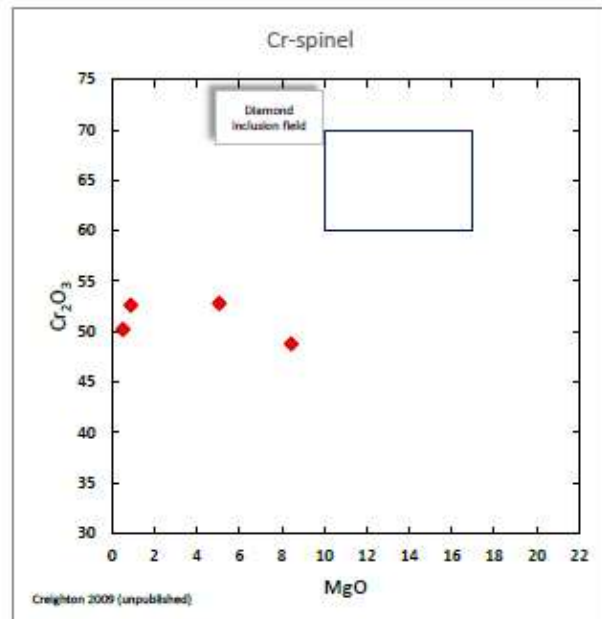
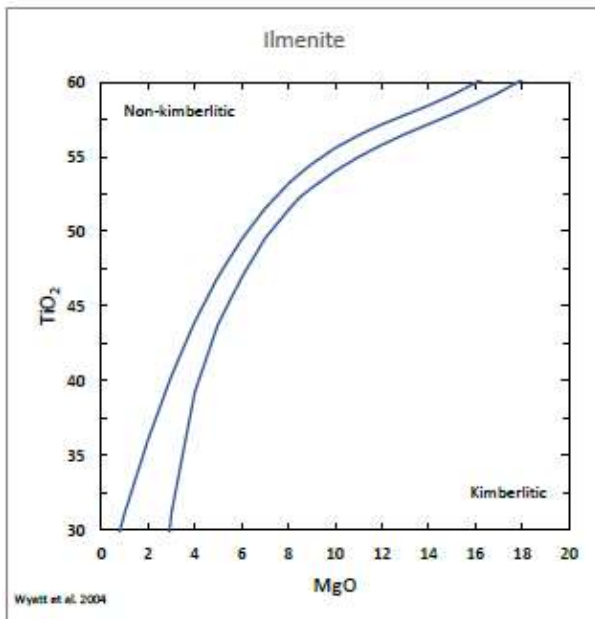
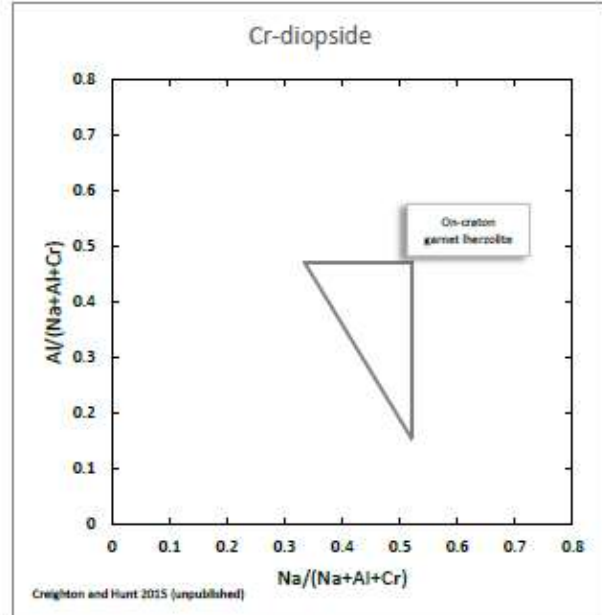
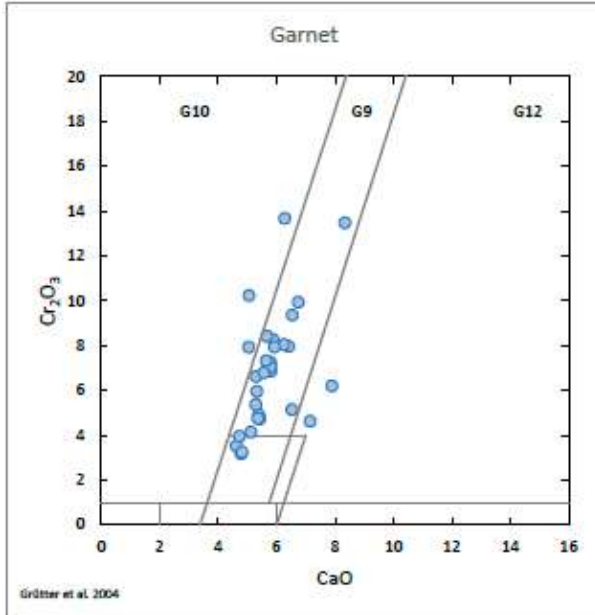
There was no Package ( 135 ) or Packages ( 8, 80 ) to Check.

Verified by: \_\_\_\_\_



SRC Advanced Microanalysis Centre  
Kimberlite Indicator Mineral Discrimination Plots

Group No.: AMC2018-013  
Date of Report: Mar. 26, 2018



GOR128 Glass

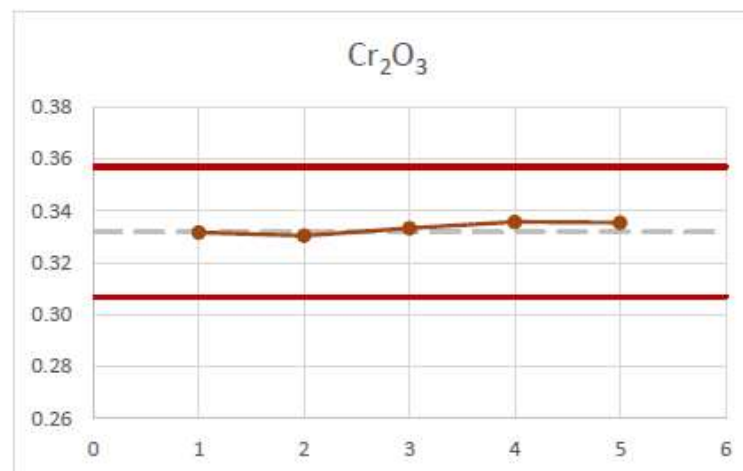
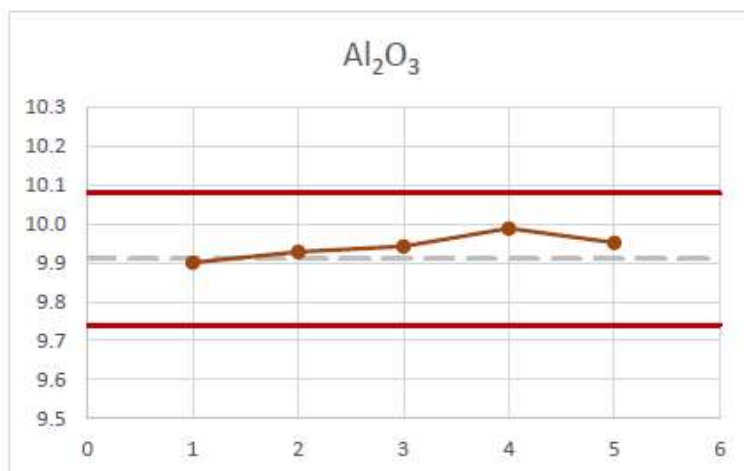
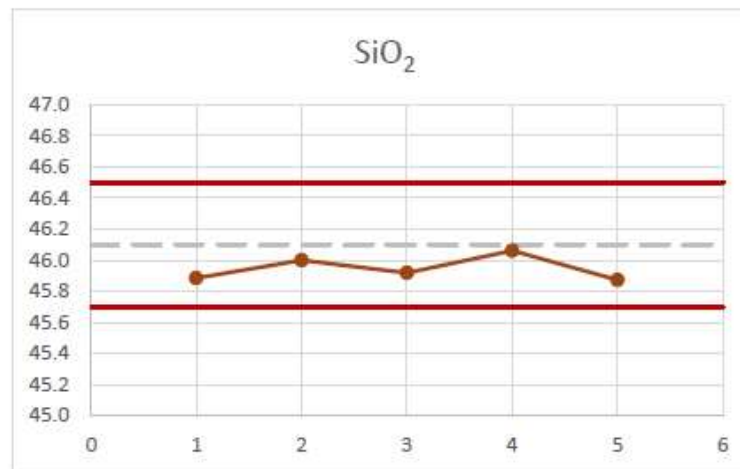


Date of Report: Mar. 26, 2018

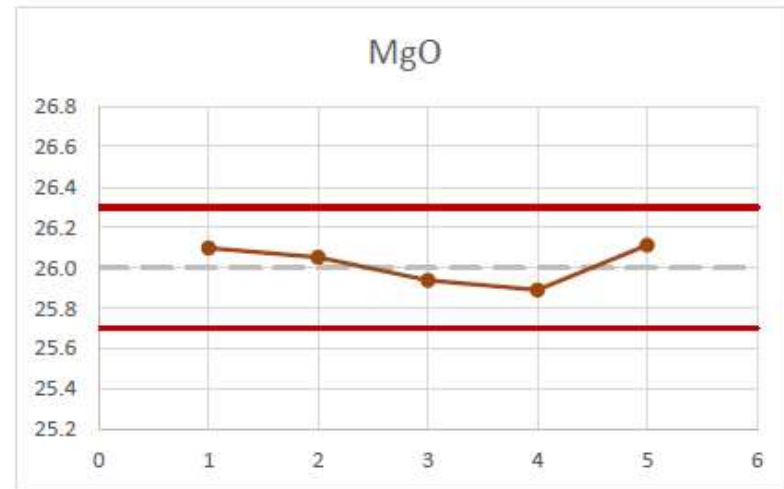
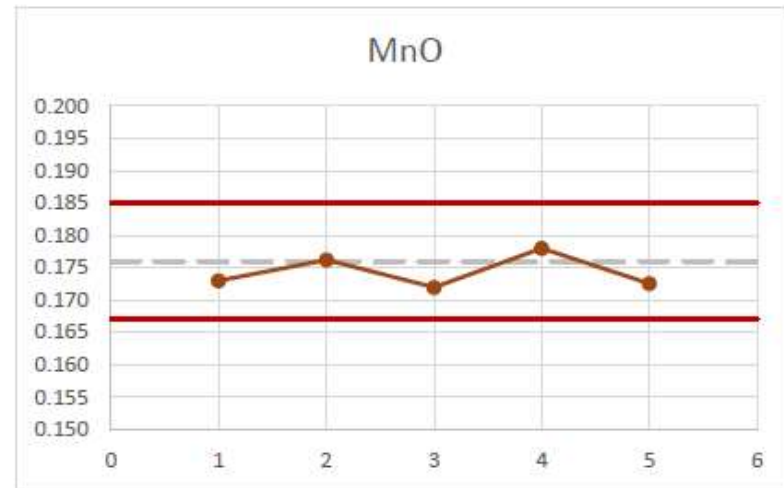
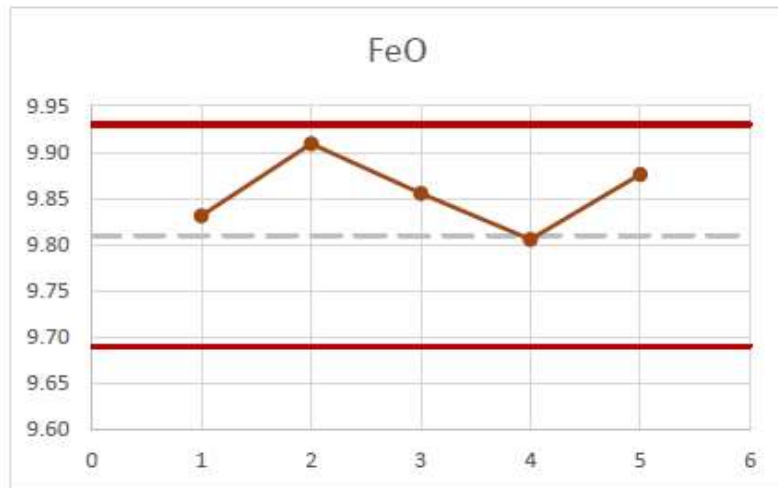
Electron Probe Microanalysis - QC Report

The GOR128 glass is one of eight silicate glasses that were prepared by directly fusing 50-100 of rock powder. The GOR128 was prepared from a komatiite for the purpose of providing a reference material for *in-situ* microanalytical work. The glasses were analysed by a variety of bulk and microanalytical methods in a number of laboratories (Jochum et al. 2006).

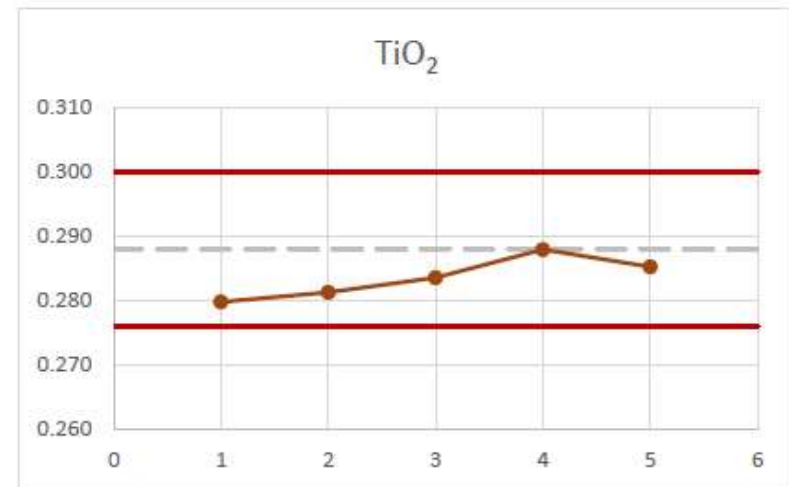
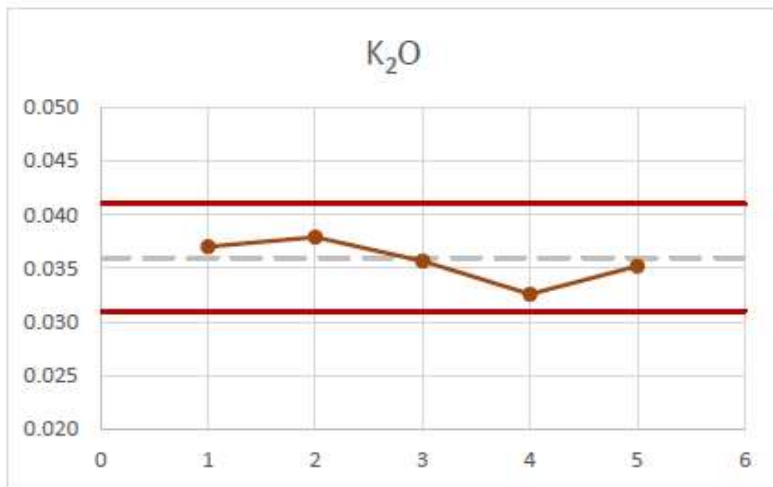
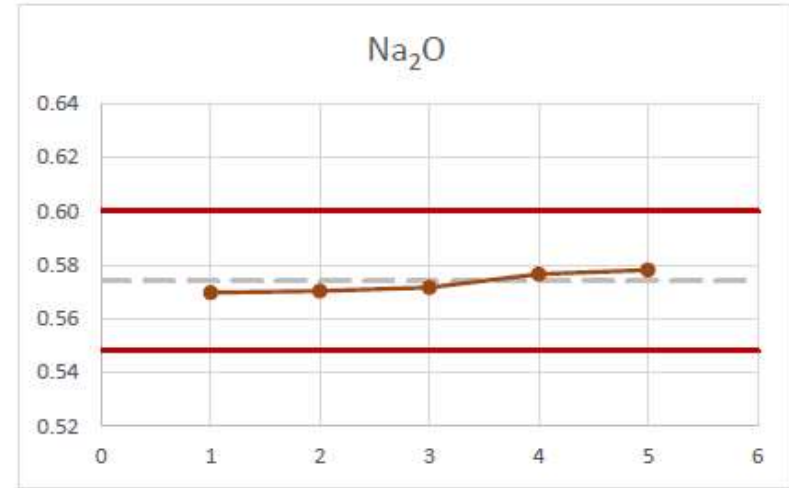
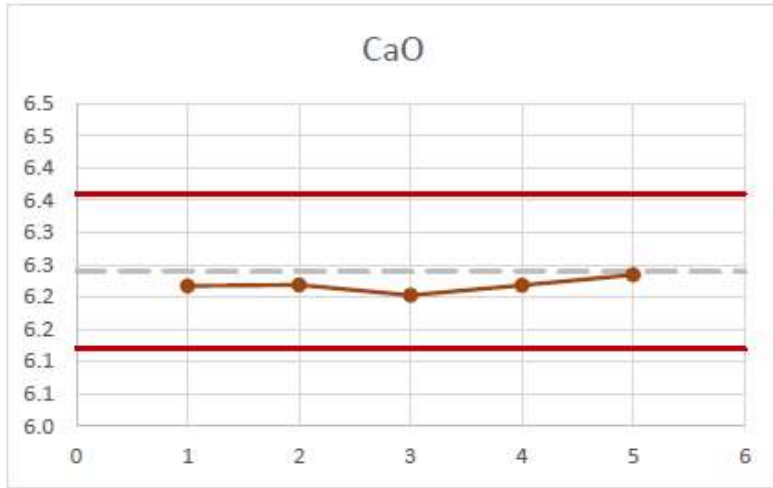
The following plots show the accepted values (dotted line) and the 95% confidence uncertainties (solid lines) with the results of the GOR128 glass analyzed as part of this group of analyses (filled circles).



### Electron Probe Microanalysis - QC Report



### Electron Probe Microanalysis - QC Report



Relative percent difference chart 1179 Till-3

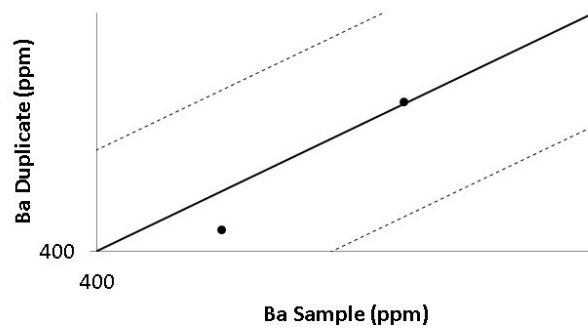
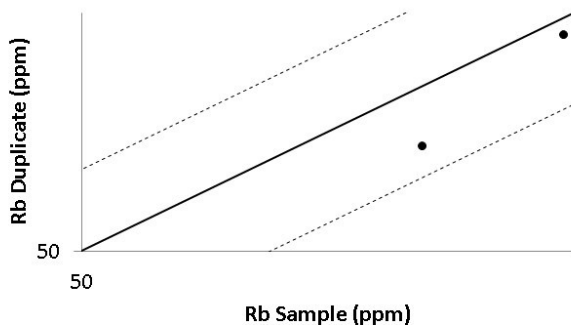
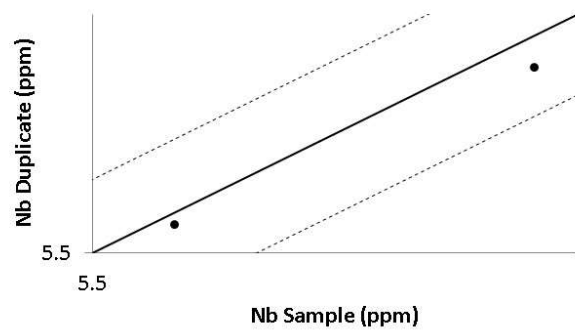
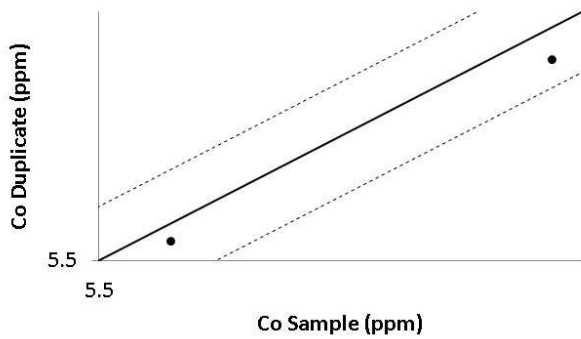
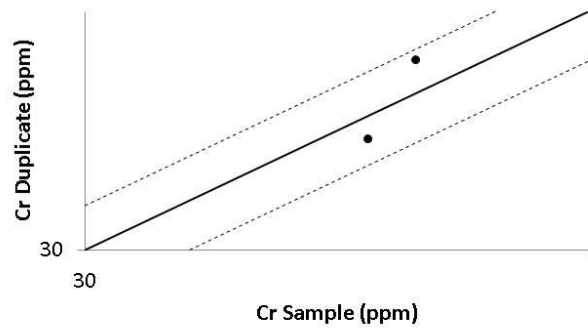
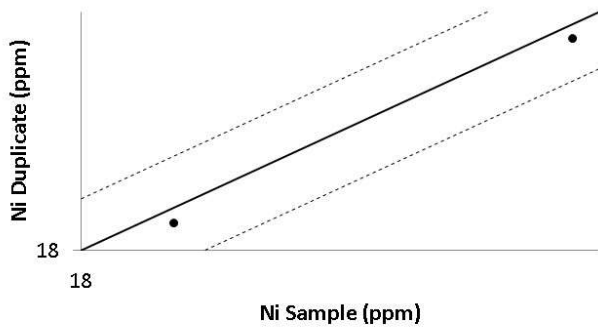
Analyte	SRC method used in study	1179 1	1179 2	1179 2 R	1179 Mean	1179 TILL-3 Reference	%RD	Accuracy (Piercey, 2014)
Ba	Ba ICP Total Digestion	493	496	491	493.3	489	0.9	Excellent
Co	Co ICP MS Total Digestion	14.1	14.5	14	14.2	15	-5.3	Very good
Cr	Cr ICP Total Digestion	121	125	122	122.7	123	-0.3	Excellent
Nb	Nb ICP MS Total Digestion	7.7	8	7.8	7.8	7	11.9	Not precise
Ni	Ni ICP MS Total Digestion	47.4	47	47.5	47.3	39	21.3	Not precise
Rb	Rb ICP MS Total Digestion	56.7	57.1	56.9	56.9	55	3.5	Excellent

Relative percent difference chart DCB01

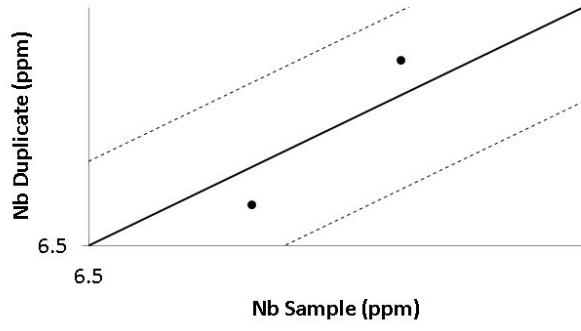
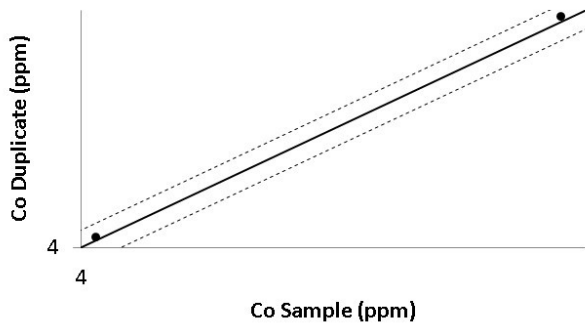
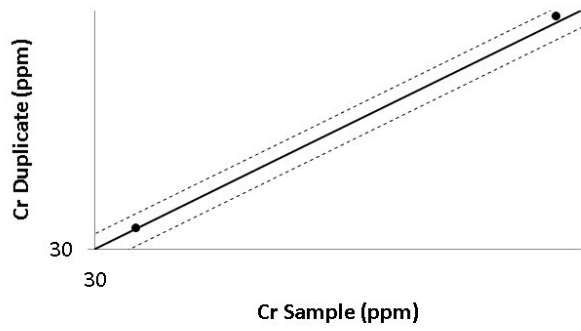
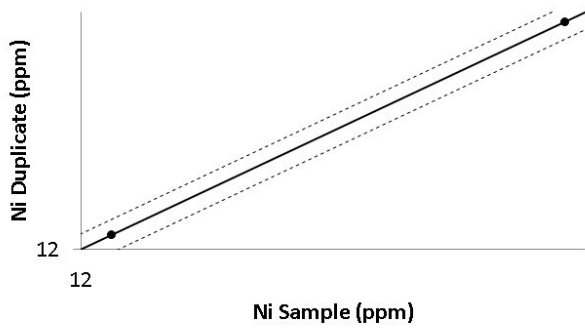
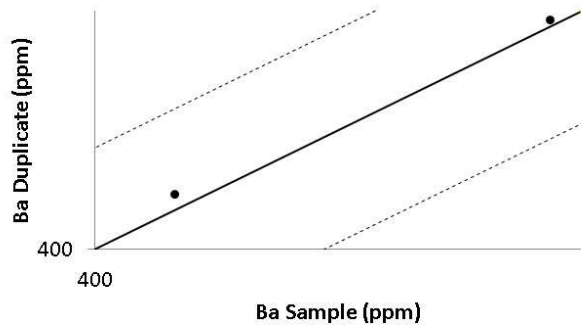
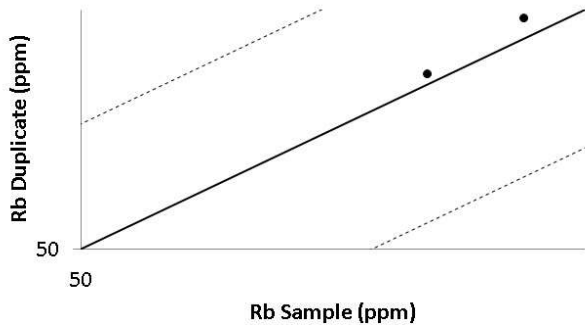
Analyte	SRC method used in study	DCB01 1	DCB01 2	DCB01 3	DCB01 Mean	DCB01 Reference	%RD	Accuracy (Piercey, 2014)
Ba	Ba ICP-OES Total Digestion	387	387	395	389.7	387	0.7	Excellent
Co	Co ICP-MS Total Digestion	16.8	16.7	16	16.5	17.2	-4.1	Very good
Cr	Cr ICP-OES Total Digestion	270	272	271	271.0	270	0.4	Excellent
Nb	Nb ICP-MS Total Digestion	20.7	20.9	20.7	20.8	19.5	6.5	Very good
Ni	Ni ICP-MS Total Digestion	99.1	98.4	100	99.2	101	-1.8	Excellent
Rb	Rb ICP-MS Total Digestion	60.3	62.7	62.4	61.8	61.4	0.7	Excellent



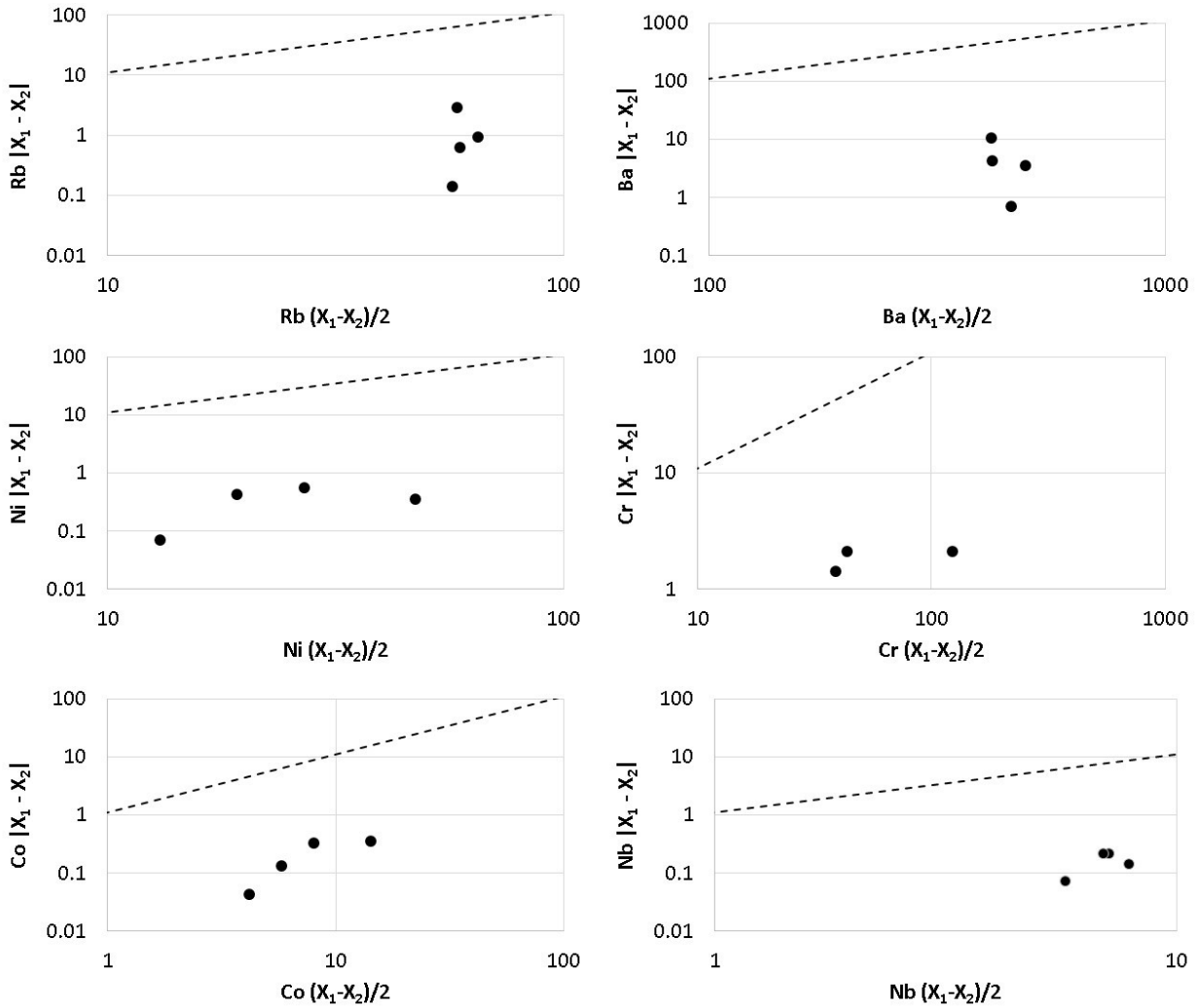
Scatterplots (for duplicates 17-RS-005-B and 17-RS-031-B) in logarithmic scale. 10% Confidence Interval.



Scatterplots (for repeats 17-RS-007-B and 1179) in logarithmic scale.  
10% Confidence Interval.



Thompson-Howarth Short Method graphs with control line at 90% confidence interval for samples 17-RS-005-B, 17-RS-007-B, 17-RS-031-B, and 1179. Note that 17-RS-007-B Cr original and duplicate value are there same, and therefore result in "0", which cannot be displayed on a log scale.



## Coefficient of Variation

Sample ID	Co ICP-MS TD (p	Dup/Rep	Absolute difference between duplicates	Mean of duplicates	Coefficient of Variation
17-RS-005-B	5.87	5.68	0.19	5.775	1.6
17-RS-031-B	8.28	7.82	0.46	8.05	2.9
R1179	14.1	14.5	0.4	14.3	1.4
17-RS-007-B	4.16	4.22	0.06	4.19	0.7

Sample ID	Ba ICP-OES TD	Dup/Rep	Absolute difference between duplicates	Mean of duplicates	Coefficient of Variation
17-RS-031-B	423	408	15	415.5	1.8
17-RS-005-B	460	459	1	459.5	0.1
17-RS-007-B	415	421	6	418	0.7
R1179	496	491	5	493.5	0.5

Sample ID	Cr ICP-OES TD	Dup/Rep	Absolute difference between duplicates	Mean of duplicates	Coefficient of Variation
17-RS-031-B	40	38	2	39	2.6
17-RS-005-B	45	42	3	43.5	3.4
17-RS-007-B	34	34	0	34	0.0
R1179	125	122	3	123.5	1.2

Sample ID	Nb ICP-MS TD	Dup/Rep	Absolute difference between duplicates	Mean of duplicates	Coefficient of Variation
17-RS-031-B	5.8	5.7	0.1	5.75	0.9

17-RS-005-B	7	7.3	0.3	7.15	2.1
17-RS-007-B	7.1	6.8	0.3	6.95	2.2
R1179	8	7.8	0.2	7.9	1.3

Sample ID	Ni ICP MS-TD	Dup/Rep	Absolute difference between duplicates	Mean of duplicates	Coefficient of Variation
17-RS-031-B	27.4	26.6	0.8	27	1.5
17-RS-005-B	18.9	19.5	0.6	19.2	1.6
17-RS-007-B	13.1	13	0.1	13.05	0.4
R1179	47	47.5	0.5	47.25	0.5

Sample ID	Rb ICP-MS TD	Dup/Rep	Absolute difference between duplicates	Mean of duplicates	Coefficient of Variation
17-RS-031-B	60.6	56.5	4.1	58.55	3.5
17-RS-005-B	64.3	65.6	1.3	64.95	1.0
17-RS-007-B	58.7	59.6	0.9	59.15	0.8
R1179	57.1	56.9	0.2	57	0.2

## **Sample Preparation**

### **for the Laser Particle Sizer ANALYSETTE 22**



#### **Sample preparation**

##### **1. Sample division**

##### **2. Sample preparation**

###### **2.1 Dispersion**

###### **2.2 Tips and tricks**

##### **3. Materials and suitable measuring liquids**



## Sample preparation

It is always astounding that the market for highly precise, fully automatic analytical instruments is permanently growing, while no emphasis is placed on the equally important sample preparation or sampling.

One of the most common mistakes during analysis is already made during the sampling stage and drawn into the analytical procedure right from the beginning. Again and again, it surprises process technicians how often samples are drawn carelessly and how the achieved analysis results are readily accepted.

Initially the capabilities of the measuring instrument are often doubted when repeat measurements deviate, but the source of the error is deeper though: in an inhomogeneous sampling.

Therefore the results are only reproducible if the analysed sample **represents** the goods to be tested with a high degree of exactness, i.e. the sample taken can be equated with the entire batch.

### 1. Sample division

The sample for the **Laser Particle Sizer ANALYSETTE 22** (approximately 200 mg – 1 g) shall correspond in the contained particle type and particle distribution with the entire batch of material.

The **Rotary Cone Sample Divider LABORETTE 27** is very well suited for the division of dry laboratory samples or suspensions, since different dividing heads with different division ratios can be selected. Depending on the division head up to 3000 dividing steps per minute can be achieved.

Possible division: 1:8, 1:10 and 1:30

Example: a laboratory sample of 50 ml (g) respectively 100 ml (g), could initially be divided with the dividing head 1:10 and then with the dividing head 1:30, so that for the Laser Particle Sizer ANALYSETTE 22 required amount of 200-400 mg is available.

Now the **representative** sample will be deglomerated.

### 2. Sample preparation

Via pre-tests it must be determined in which manner the sample material can be moistened and dispersed.

The liquid should possibly completely and spontaneously wet the solid matter.

The additional ultrasonic support (if possible with maximum power) in general reduces the dispersion duration.

- The particles of the solid matter shall be individually and free of agglomerates in the suspension.
- The dispersion condition must be *stable* during the entire measurement, coagulating / flocculating of the particles may not occur.
- Coagulating in a suspension can be recognized by a slight, slushy bottom deposit, which will swim in the sample glass at slight movements of the glass, as a second phase respectively layer and displays a *cloudlike* shape.
- Floating of the sample material on the surface of the liquid is a sign of non-wetted sample material, i.e. the already added share of dispersants like tensides/ wetting agents or salts is too low.
- The sample may not be destroyed during the dispersion, respectively comminuted. With thin, platelet shaped material like mica, kaolin, clay and inorganic salts this is especially important.

Here it is also recommended to paste a small sample amount on a specimen holder with a little bit of liquid and wetting agent. Now under the microscope the particle spectrum and the maximum particle size can be determined.

After the finished dispersion it is also microscopically checked if the coarse particles are still present or were destroyed.

- The vehicle liquid/ measuring liquid must in all cases have a smaller, max. equal specific weight (density) than the solid material to be measured.
- The sample may not partially dissolve, dissolve or swell!

## 2.1 Dispersion

Unproblematic samples, which submerge without any great effort directly into the surface of the water and possess no large amount of fine share, are added to the dispersion unit as a *solid material* with a spatula portion by portion and after a brief ultrasonic treatment/ dispersion (30-60s) measured reproducibly.

Shows the conducted *double measurement* too large differences in the particle size distribution it may be attributed to several reasons:

- pump speed too low – the coarse material deposits
- the agitator speed is too great – air bubbles are created, respectively air is stirred in
- dispersion duration is too brief

- Increasing fine share
  - Longer ultrasonic treatment necessary
  - Addition of dispersion aids
  - Fine particles stick to the measuring cell glass
  - Clogging due to coarse particle >2 mm
  - Coarse material deposits: specific weight too high
  
- Seemingly coarser appearing curve
  - Sample swells or flocculates
  - Sample agglomerates
  - Sample is magnetic
  
- Declining coarse- and fine range
  - Sample dissolves
  - Beam absorption drops

Additionally faulty measurements due to jammed or bent hose connections can occur.

Samples hard to disperse may display the following characteristics: static charge (for example plastics), adhesive forces or cohesive powers – samples tend to conglutinate/ agglutinate – (for example clays, soil samples, kaoline), magnetism, hydrophobic characteristics – water repellent molecule components (for example drugs, medications, toner, graphite, titanium dioxide, waxes), coagulation (for example clays, kaoline, chalk, gypsum).

a) *Static charge respectively also hydrophobic characteristics:*

Here a spatula amount of the material should be added to a small 50 ml Erlenmeyer flask and then at first 1 (up to 2) drops of a wetting agent (surfactant or diluted surfactant solution) added, then mixed into a paste until the sample is completely wetted. Water is added drop by drop and stirred. The now created suspension (approximately 20 - 30 ml) is dispersed in an ultrasonic bath.

If the sample is already inside the dispersion unit and floats on top of the surface, the sample can be wetted as follows:

With a glass rod or with the tip of a spatula, a *small* drop of the wetting agent (for example Dusazin 901, Teepol, Tween 80 or dish soap) is added/ touched on the surface of the liquid and distributed. Immediately it can be seen, that the formed skin on the surface breaks open and the fine portion enters the suspension.

b) *Adhesive powers:*

are *clinging* powers of the particle. A reduction of these surface powers can be obtained by creating on the boundary phase areas from solid/ liquid, adsorption layers from surface-active agents or macromolecules. It is considered a covering, a guarding or masking of the solid material respectively wetting. For this reason in most cases for example tetra-Na-diphosphat (sodium pyrophosphate: Na<sub>4</sub>P<sub>2</sub>O<sub>7</sub>) or poly sodium approximately at 0.5-1% are utilized.

c) *Cohesive powers and magnetism:*

The effects of the forces of attraction between atoms or molecules of a body are described as cohesive power or polarity respectively magnetic characteristics. The magnetic characteristics are difficult to eliminate: with only slight magnetism a highly viscous liquid like for example ethylene glycol or a glycerine/ water mixture may be used or the sample is heated above several 100°C.

This is hardly possible in a laboratory and seldom realisable. Therefore are such materials with a high degree of magnetism are not suitable for the particle size analysis.

d) *Coagulation:*

is the flocculation of a sample caused by the agglomeration of colloid particles in a suspension. This can happen with too great amounts of solids or an unfavourable ph-range. By adding several drops of undiluted acid (for example hydrochloric acid) prior to adding the sample!! for the acidic range or through diluted bases (for example caustic lye, ammonia or even soda solution) in the alkaline range, may the ph-value be lowered respectively increased, so it counteracts the reaction of the sample (for example with chalk, kaolin, hydrated lime and clay). Suitable are here also  $\text{Na}_2\text{HPO}_4$  (alkaline) or  $\text{KH}_2\text{PO}_4$  (acidic) as a 0.1-1% solution.

## 2.2 Tips and Tricks

The larger the fine share of a sample, the greater is the dispersion effort. A necessary ultrasonic treatment lasting several minutes (or even longer) should be conducted in the external Ultrasonic Cleaner LABORETTE 17.

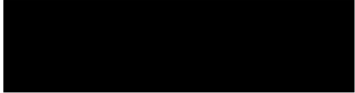
Here it is recommended to add to a 50 ml Erlenmeyer flask a spatula tip full (approximately 0.5-1 g) of sample and via simple wetting adding approximately 20 ml of the measuring liquid + the dissolved/ mixed dispersion aid (surfactant).

We recommend when utilizing surfactants those with low foam tendencies like for example Dusazin 901.

After briefly shaking the Erlenmeyer flask, it is fastened with laboratory clip inside the ultrasonic bath so the inner level of liquid is below the surface of the liquid of the ultrasonic bath.

After during the pre-tests determined deagglomeration period, the necessary suspension amount for the measurement will be added with a shaking motion via a pipette into the dispersion unit of the Laser Particle Sizer ANALYSETTE 22.

If the needed amount of solids is exactly known, it may be weighed directly into the Erlenmeyer flask and after the dispersion the *complete* contents can be conveyed with a wash bottle, so no separation due to sampling with a pipette occurs.



With a few small tricks difficult samples like for example fly ash, sulphur, coal, plastics or pigments can be quickly dispersed even in water.

The sample is mixed with **one** drop of surfactant and after adding **one to two** drops of water with a glass stirrer or spatula mixed to a *paste*. Due to the relatively high share of surfactant compared to the share of water the cavitation is reduced and the sample quickly wetted.

After further addition of several drops of water and stirring at the same time it can be checked if not already wetted particles are swimming on top of the surface of the liquid.

Now the suspension is diluted down to approximately 20-30 ml and deagglomerated in the ultrasonic bath.

When using simple surfactants like dish soap it often occurs that when *pasting* and mixing the sample “foam” evolves which after the dispersion swims on top of the surface and is traversed into the particle sizer.

A too high stirring intensity pulls the foam into the measuring circuit and “*coarse particles*” are measured which are not present.

In order to avoid this “faulty measurement” it is possible to destroy the “foam” inside the Erlenmeyer flask: the tip of a glass stirrer is dipped into *n-butanol* so the glass stirrer is just wetted but no drops are recognizable.

By slightly touching the surface of the foam it collapses and the suspension can easily be analysed for particle size.


An additional possibility – with poor wetting – would be the addition of 2 to 3 drops of alcohol (for example ethyl alcohol) directly on the dry laboratory sample, which immediately absorbs the alcohol like a sponge. Now again water and a wetting agent can be added and dispersed accordingly.

The user, working with the “Small Volume Wet Dispersion Unit” of course has the possibility to utilize alcohol, alkanes, high-boiling benzines or other organic liquids.

It should be mentioned, that the Small Volume Wet Dispersion Unit is **not** explosion protected – please select the corresponding liquids – and only operate in well ventilated areas.

The exchange of the measurement liquid for example alcohols to other organic liquids is relatively easy, since many liquids can be mixed easily amongst each other.

The compatibility of solvents with the connective hoses should also be kept in mind. The seals in the measuring cell and the connective hoses are made of Viton. Acetone (ketones), acetates and enamel thinner cannot be used.



The *resistance lists* available from hose manufacturers contain for the most common elastomers a rating of the chemical resistance against various operating mediums (liquids).


After a conducted measurement with the ANALYSETTE 22 it should become habit to *directly* rinse the measuring system in order to avoid an unnecessary “depositing” or “adhering” of particles in the measuring circuit and especially on the measuring cell.

An „in-between rinsing“ with a surfactant is very helpful.

Residue on the measurement cell may be caused by tap water respectively limy water. Either it should be switched to distilled water or the measurement cell has to be cleaned from time to time.

The lime residue is removed in a few minutes by rinsing with 10% hydrochlorid acid. Afterwards it should be rinsed twice with regular water.

On the following pages you find a list of materials with the suitable dispersion liquids and additives. Please note the list is only available in German. Should you have questions please contact the FRITSCH laboratory:





Materials and suitable measuring liquids

Feststoff		Sedimentations- flüssigkeit	Zusatzstoff	
Art	Dichte g/cm <sup>3</sup>		Art	Konzentration g/l
Ackerboden (s.a. Boden, Erde)		Wasser Wasser Wasser	Tetranatriumpyrophosphat Natriumoxalat Ammoniakwasser	0,45...1,35 0,67 5,8 Vol. %
Aktivkohle (s.a. Kohle)	2,0	Wasser Isopropanol Wasser Wasser Wasser	Ammoniakwasser - Tetranatriumpyrophosphat Natriumlinoleat Natriumoxalat	5,8 Vol. % - o.A. o.A. o.A.
Alaunerde	1,8	Wasser Wasser Wasser Wasser Wasser Tetrachlorkohlenstoff	- Natriumtartrat Natriumoxalat Natriumhexametaphosphat Salzsäure -	- 1,0 ohne Angabe 1,0 ohne Angabe -
Alaunerdezement		Ethylenglycol	Cobaltchlorid	ohne Angabe
Alkalisalze		Leinöl + Xylol n-Butylamin Cyclohexanon Cyclohexanol n-Butanol	- - - - -	- - - - -
Aluminium *	2,7	Tetrachlorkohlenstoff Wasser + 50 Vol.% Ethylenglycol Wasser Wasser Wasser Wasser + Ethylenglycol Ethylenglycol Cyclohexanon Cyclohexanol Chloroform Isopropanol Wasser	- - - - Natriumhexametaphosphat Natriumtartrat Natriumoxalat Trinatriumphosphat Trinatriumphosphat - - - - - Salzsäure	- - - - o.A. o.A. o.A. o.A. o.A. - - - - - pH = 3
Aluminiumfluorid		Ethylenglycol Ethylenglycol Ethylenglycol	Calciumchlorid Strontiumchlorid Cobaltchlorid	0,05 - 0,5 0,05 - 0,5 0,05 - 0,5
Aluminiumhydroxid	2,3...2,4	Wasser Wasser	- Saccharose	- 40 %
Aluminiumoxid (s.a. Tonerde, Korund)	3,5...4,1	n-Butylamin Tetrachlorkohlenstoff Wasser Wasser Wasser Wasser Wasser Wasser n-Butanol Cyclohexanon Leinöl + Xylol	- - Natriumhexametaphosphat Natriumcarbonat Tetranatriumpyrophosphat Kalium/Natriumhexameta- phosphat Natriumtartrat Salzsäure - - -	- - 0,5 - 1,0 o.A. 0,3...1,5 1,0 1,0 pH = 3 - - -

Feststoff		Sedimentations- flüssigkeit	Zusatzstoff	
Art	Dichte g/cm <sup>3</sup>		Art	Konzentration g/l
Aluminiumsilicoid		Wasser Wasser	Tetranatriumpyrophosphat Trinatriumphosphat	0,3...1,5 o.A.
Ammoniumperchlorat	2,0	Isobutanol Benzol	- Naphthalinstearosulfosäure	einige Tropfen
Anhydrit		Methanol	-	-
Anthracenpaste	1,2	Wasser	Trinatriumphosphat	o.A.
Anthracit	1,4...1,7	Wasser Wasser	Trinatriumphosphat Natriumalkylnaphthalen- sulfonat	0,5 1,0
Antimonoxid	3,8...5,3	Wasser Wasser Wasser	Tetranatriumpyrophosphat Kalium/Natriumhexameta- phosphat Natriumhexametaphosphat	0,3 - 1,5 0,5 o.A.
Apatit		Wasser Wasser	Trinatriumphosphat Aluminiumchlorid	7,8 0,24
Arsenate (nicht wasser- löslich)		Wasser	Tetranatriumpyrophosphat	0,45...1,35
Arsenige Säure		Cyclohexanon n-Octanol	- -	- -
Arsentrioxid	3,8	n-Octanol Cyclohexanol Petroleum	- - Ölsäure	- - 1,8
Asche (s.a. Flugasche, Kraft- werkasche)		Wasser	Tetranatriumpyrophosphat	1,0
Bariumcarbonat	4,4	Cyclohexanon Methanol Wasser	- - Tetranatriumpyrophosphat	- - 1,0
Bariumsalze (nicht wasser- löslich)		Wasser	Tetranatriumpyrophosphat	0,45...1,35
Bariumstrontiumcarbonat		Wasser + Ethanol Wasser + Methanol Cyclohexanon	- - -	- - -
Bariumsulfat, Baryt	4,3... 4,5	Wasser Wasser Wasser Wasser + Ethylenglycol Wasser Wasser + Methanol	Alkylphenolethylenoxid- Kondensat Tetranatriumpyrophosphat Tetranatriumpyrophosphat + Salzsäure Trinatriumphosphat - Natriumhexametaphosphat -	1,0 0,3...2,25 0,3...1,5 3,65 o.A. - 0,5 -
Bariumtitanat	5,3...5,8	Wasser Wasser Cyclohexanon Wasser + Ethylenglycol	Natriumhexametaphosphat Kalium/Natriumhexameta- phosphat - -	0,5 1,0 - -
Baurit	3,3	Wasser	Tetranatriumpyrophosphat	o.A.

Feststoff		Sedimentations- flüssigkeit	Zusatzstoff	
Art	Dichte g/cm <sup>3</sup>		Art	Konzentration g/l
Bentonit	2,7	Wasser	Natriumcarbonat	0,5
		Wasser	Ammoniak	0,15 %
		Wasser	Natronlauge	o.A.
		Wasser	Tetranatriumpyrophosphat	o.A.
		Wasser	Natriumoxalat	0,05
		Wasser	Kalium/Natriumhexameta- phosphat	1,0
		Wasser	Natriumsilikat (Wasserglas)	0,2
Berlinerblau		Wasser	Tetranatriumpyrophosphat	0,3...1,5
Beryll		Wasser	Natriumsilikat	o.A.
		Wasser	Natriumhexametaphosphat	o.A.
Bimsstein		Wasser	-	-
Bismutverbindungen		Wasser	Tetranatriumpyrophosphat	1,35
Blanc fixe		Wasser	Tetranatriumpyrophosphat	0,9
Blei	11,3	Wasser	-	-
		Aceton	-	-
		Cyclohexan	-	-
		Cyclohexanol	-	-
		Cyclohexanon	-	-
		Isomylalkohol	-	-
Bleicherde		Wasser	Trinatriumphosphat	o.A.
		Wasser	Tetranatriumpyrophosphat	0,45...1,35
		Wasser	-	-
Bleioyanamid		Wasser	Tetranatriumpyrophosphat	0,3...1,5
Bleifarben (s.a.Bleioxid, Mennige)		Wasser	Tetranatriumpyrophosphat	0,45...1,35
		Cyclohexanol	-	-
Bleioxide (s.a.Bleifarben, Mennige)	8...9,5	Ethylenglycol	-	-
		Wasser	Tetranatriumpyrophosphat	0,5...1,5
		Xylol	-	-
		Cyclohexanon	-	-
		Paraffinöl + Benzol	-	-
		Wasser	Natriumhexametaphosphat	0,5
			Kalium/Natriumhexameta- phosphat	1
Bleisulfat	5,6	Wasser	Trinatriumphosphat	o.A.
Bleisulfid	7,3	Cyclohexanol	-	-
Boden (s.a.Ackerboden, Erde)		Wasser	-	-
		Wasser	Natriumoxalat	0,67...20 g/l
		Butylphthalat + Ethanol	-	-
Boroarbid	2,5	Wasser	Tetranatriumpyrophosphat	o.A.
Braunkohle (s.a.Kohle)	1,2... 1,4	Wasser	Netzmittel	einige Tropfen
		Isobutanol	-	-
		Diethylphthalat	-	-
		Cyclohexanon + 10 Masse-% Methanol	-	-
		Cyclohexanol + 10 Masse-% Methanol	-	-

Feststoff		Sedimentations- flüssigkeit	Zusatzstoff	
Art	Dichte g/cm <sup>3</sup>		Art	Konzentration g/l
Braunstein	4,9	Wasser Wasser + Ethylenglycol	Tetranatriumpyrophosphat Trinatriumphosphat	0,45...1,35 -
Bronze	8,7...8,9	Cyclohexanol Cyclohexanon	- -	- -
Cadmiumarsenat	4,2	Wasser + 50 Vol.-% Methanol	-	-
Cadmiumfarben		Wasser Wasser	Natriumhexametaphosphat Tetranatriumpyrophosphat	1,0 0,45...1,35
Cadmiumsulfid		Wasser Ethylenglycol	Tetranatriumpyrophosphat -	o.A. -
Calciumarsenat		Wasser + 50 Vol.-% Ethanol Wasser + 50 Vol.-% Methanol	- -	- -
Calciumcarbonat, Kalk- spat (s.s.Kreide)	2,7 - 2,9	Ethylenglycol Wasser Wasser Wasser Wasser Wasser Wasser Wasser Wasser Wasser Wasser Wasser Xylol Wasser + 20 Vol.-% Glycerin Cyclohexanon + 10 Vol.-% Isoamyl- alkohol Wasser + 50 Vol.-% Ethylenglycol	- - Ammoniakwasser Trinatriumphosphat Tetranatriumpyrophosphat Natriumsilikat (Wasserglas) Natriumhexametaphosphat Natriumsilikat (Wasserglas) + Kaliumcitrat Natriumsilikat + Tetranatriumpyrophosphat Natriumcitrat + Tetranatriumpyrophosphat Natriummethylendinaphthyl- sulfonat - - - -	- - 5,8 Vol.-% o.A. 0,3...2,25 2,0 0,5...2,0 20,0 32,4 1,0 1,0 1,0 1,0 1,0 -
Calciumfluorid, Flußspat	3,2	Wasser Wasser Wasser Wasser Wasser Methanol Cyclohexanol Cyclohexanon Aceton	Ammoniakwasser Kaliumchlorid Salpetersäure Tetranatriumpyrophosphat Gelatine + Natriumcarbonat Kaliumchlorid - - -	1 Vol.-% 0,074 0,126 (0,002 n) 0,3...1,5 1...2,5 1...2,5 0,074 - - -
Calciumhydroxid	2,3	Cyclohexanol Ethanol Isopropanol Wasser	- - - Natriumhexametaphosphat	- - - 0,5

Feststoff		Sedimentations- flüssigkeit	Zusatzstoff	
Art	Dichte g/cm <sup>3</sup>		Art	Konzentration g/l
Calcium-Magnesium- carbonat, Dolomit	2,9	Wasser	Trinatriumphosphat	o. A.
		Wasser	Tetranatriumpyrophosphat	0,3...1,5
		Wasser	Ammoniak	5,8 Vol. %
Calciumoxid	3,3 - 3,6	Ethylenglycol	-	-
		Chinolin	-	-
		Aceton	-	-
		Cyclohexanon	-	-
		Cyclohexanol	-	-
		Ethylenglycol	-	-
		Petroleum	-	-
		Ethylenglycol	Calciumchlorid	0,05...0,5
Ethylenglycol	Strontiumchlorid	0,05...0,5		
Ethylenglycol	Cobaltchlorid	0,05...0,5		
Calciumphosphat (wasserlöslich)	2,3	Isobutanol	-	-
		Hexan	-	-
		n-Octanol	-	-
Calciumphosphat (nicht wasserlöslich)	2,2...3,2	Wasser	-	-
		Wasser	Tetranatriumpyrophosphat	o.A.
		Wasser	Natriumhexametaphosphat	0,5...1,0
		Wasser	Natriumsilikat (Wasser- glas)	1,0
		Wasser	Trinatriumphosphat	o.A.
		Wasser + Ethanol	-	-
		n-Butanol	-	-
Ethanol	-	-		
Calciumsalze (nicht wasserlöslich)		Wasser	Tetranatriumpyrophosphat	0,9
Calciumstannat		Wasser	Tetranatriumpyrophosphat	1,0
Calciumsulfat (s.u.Gips, Anhydrit)				
Calciumwolframat		Wasser	Natriumcitrat	0,5
Carborundum (s. Siliciumcarbid)				
Cellulose		Benzin	-	-
		Testbenzin	-	-
		Benzol	Trinatriumphosphat	1,0
Cerussit		Wasser	Natriumhexametaphosphat	o.A.
China clay		Wasser	Trinatriumphosphat	-
Chrom		Isobutanol	-	-
Chromfarben		Wasser	Tetranatriumpyrophosphat	0,45...1,35
Chromgelb	3,3	Cyclohexanon	-	-
Chromoxid	2,7...5,3	Wasser	Tetranatriumpyrophosphat	0,3...2,25
		Cyclohexanol + 10 Vol.-% Isomylalkohol	-	-
		Wasser	Kalium/Natriumhexameta- phosphat + Natriumcarbonat	0,6 0,12
Cobalt (s. Kobalt)				
Cordierit	3,0	Wasser	Natriumsalz der polymeri- sierten Carboxylsäure	einige Tropfen einer wäßrigen Lösung

Feststoff Art	Dichte g/cm <sup>3</sup>	Sedimentations- flüssigkeit	Zusatzstoff	
			Art	Konzentration g/l
Diamant	3,5	Olivenöl	-	-
		Wasser	Gelatine + Natriumcarbonat	1,0...2,0 pH = 9
		Wasser	Trinatriumphosphat	o.A.
		Ethanol	-	-
Diatomeenerde		Wasser	Natriumhexametaphosphat	1,0
		Wasser	-	-
Dicalciumphosphat	2,3	Methanol	-	-
		Wasser + Ethanol	-	-
Dolomit (s. Calcium/ Magnesiumcarbonat)	2,9			
Eisen	7,8	Cyclohexan	-	-
		Wasser + Ethylen-Glycol	-	-
		Sojabl + 50 Vol. % Aceton	-	-
		Rüböl + Aceton	-	-
		Wasser + Ethylenglycol	Trinatriumphosphat	o.A.
		Cyclohexanol	-	-
		Cyclohexanon	-	-
		Wasser	Tetranatriumpyro- phosphat	1,0
Eisenoxide	3,4...5,7	Wasser	Kalium/Natriumhexameta- phosphat	0,5
		Wasser	Tetranatriumpyrophos- phat	0,3...1,5
		Paraffinöl + Benzol	-	-
		Wasser	Natriumhexameta- phosphat	0,5
Eisenoxidrot		Wasser	Tetranatriumpyro- phosphat	1,0
		Xylenollösung	-	-
Eisenschwarz	nicht möglich, da magnetische Flockung			
Eisensulfat	1,8...3,0	Isobutanol	-	-
Eisensulfid (s.a. Pyrit)	4,8	Cyclohexanon	-	-
Email		Wasser	Tetranatriumpyro- phosphat	0,3...1,5
Enstatit	3,0...3,3	Wasser	Kalium (Natriumhexameta- phosphat	1,0
		Wasser	Natriumcarbonat	o.A.
		Wasser	Tetranatriumpyro- phosphat	1,0
Erde (s.a. Boden, Ackerboden)		Wasser	-	-
		Wasser	Tetranatriumpyro- phosphat	0,45 - 1,35
		Wasser	Natriumoxalat	20,0
		Wasser + Ethylenglycol	-	-
		Butylphthalat + Etha- nol	-	-
Farben, mineralische		Wasser	Kaliumcitrat	30
		Wasser	Tetranatriumpyro- phosphat	0,3...1,5
Feldspat	2,6	Wasser	-	-
		Wasser	Trinatriumphosphat	o.A.
		Wasser	Natriumoxalat	o.A.
		Wasser	Tetranatriumpyrophos- phat	0,45...1,35



Feststoff		Sedimentations- flüssigkeit	Zusatzstoff	
Art	Dichte g/cm <sup>3</sup>		Art	Konzentration g/l
FeSiCr	4,9	Cyclohexanol Cyclohexanon	- -	- -
Flint	2,7	Wasser Wasser Wasser	- Natriumoxalat Tetranatriumpyro- phosphat	- o.A. 0,45...1,35
Flugasche (s.a.Asche, Kraftwerkasche)	2,2-2,3	Wasser Wasser Wasser	- Tetranatriumpyro- phosphat Na-Salz der polymeri- sierten substituierten Alkylbenzolsulfon- säure	- 0,45...1,35 0,57
Fluoride		Wasser	Natriumcarbonat + Gelatine	1...2,5 1...2,5
Flußspat (s.Calcium- fluorid)				
Formsand		Wasser Wasser Wasser	Natronlauge Tetranatriumpyrophos- phat Trinatriumphosphat	o.A. 0,45...1,35 o.A.
Forsterit		Wasser	Tetranatriumpyro- phosphat	1,0
Fritten		Wasser Wasser Wasser	- Tetranatriumpyro- phosphat Natronlauge	- 0,45...1,35 o.A.
Füller		Wasser	Trinatriumphosphat	o.A.
Getreidemehl	1,5	Isobutanol Isobutanol + Diethyl- phthalat Diethylphthalat Petroleum	- - - -	- - - -
Gips	2,3	Ethanol Ethylenglycol Ethanol Methanol n-Amylalkohol Methanol + Ethylengly- col + Ethanol Ethylenglycol Ethylenglycol Ethylenglycol Ethylenglycol	Calciumchlorid Cobaltcitrat - - - Calciumchlorid Cobaltcitrat Calciumchlorid Strontiumchlorid Cobaltchlorid	10 o.A. - - - o.A. o.A. 0,05...0,5 0,05...0,5 0,05...0,5
Gips (Stuck-)	3,0	Ethylenglycol + 50 Vol.% Ethanol Ethylenglycol + 50 Vol.% Ethanol Ethylenglycol Methanol	Natriumcitrat Calciumcitrat Cobaltcitrat -	1,29 0,5 o.A. -
Gips (Roh-)	2,3	Wasser	Kaliumcitrat	30,0

Feststoff		Sedimentations- flüssigkeit	Zusatzstoff	
Art	Dichte g/cm <sup>3</sup>		Art	Konzentration g/l
Glas	2,4...3,0	Wasser	Tetranatriumpyro- phosphat	0,45...1,35
		Wasser	Trinatriumphosphat	o.A.
		Wasser	-	-
		Wasser	Kalium/Natriumhexameta- phosphat + Natriumcarbonat	0,3 0,06
		Butanol	-	-
		Cyclohexanol	-	-
		Wasser + Ethylenglycol	-	-
		Methanol	-	-
		Ethylenglycol	-	-
		Ligninlösung	-	-
		Wasser	Natriumhexametaphosphat	0,5
Glasuren		Wasser	Tetranatriumpyrophos- phat	0,3...1,5
Glimmer	2,8	Wasser	Tetranatriumpyrophos- phat	o.A.
Granat	3,8-3,9	Wasser	Natriumhexametaphosphat	0,5
Graphit	2,0...2,5	Wasser	Gerbsäure	0,5
		Wasser	Natriumlinoleat	5,0
		Wasser	Ammoniak + Natriumlinoleat	0,8...3,2 o.A.
		Wasser	Trinatriumphosphat	o.A.
		Wasser	Ligninsulfonat	4,0
		Ethanol	Carboxymethylcellulose	10,0
		Wasser	Diocylester der Natrium- sulfobornsteinsäure	0,5 Vol.-%
Hämatit	5,2	Wasser	-	-
		Wasser	Tetranatriumpyrophos- phat	1,0
Hexachlorcyclohexan		Wasser	Trinatriumphosphat	o.A.
Hochofenschlacke	2,5...3,0	Wasser	Natriumhexametaphosphat	1,0
		Wasser	Tetranatriumpyrophos- phat	0,45...1,35
		Chinolin	-	-
		Cyclohexanol	-	-
		Cyclohexanon	-	-
		Isopropanol	-	-
Hydrargillit	2,4	Wasser	Tetranatriumpyrophosphat	1,0
Ilmenit	4,7	Wasser	-	-
Kagrun		Wasser + Ethylenglycol	-	-
Kakao	1,5	Diethylphthalat	-	-
		Isobutanol	-	-
		Benzol	-	-
		Isobutanol + Diethylphthalat	-	-
		Aceton	-	-
		Cyclohexanon	-	-
Kaliumchlorat	2,3	Cyclohexanon	-	-
		Cyclohexanol	-	-

Feststoff		Sedimentations- flüssigkeit	Zusatzstoff	
Art	Dichte g/cm <sup>3</sup>		Art	Konzentration g/l
Kalkhydrat (s. Calciumhydroxid)				
Kalkstein (s. Calcium- carbonat, Kreide)				
Kalomel	7,2	Cyclohexanon Cyclohexanol	- -	- -
Kaolin	2,2...2,6	Wasser	Ammoniak	0,2
		Wasser	Trinatriumphosphat	o.A.
		Wasser	Salzsäure	pH = 3
		Wasser	Tetranatriumpyro- phosphat	0,3...2,25
		Wasser	Tetranatriumpyro- phosphat	2,25
		Wasser	+ Natriumsilikat (Wasserglas)	1,0
		Wasser	Kalium/Natriumhexameta- phosphat	1,0
		Wasser	Kalium/Natriumhexameta- phosphat	0,573
		Wasser	+ Natriumcarbonat	0,127
		Wasser	Natriummetaphosphat + Natriumcarbonat	0,45 0,011
		Wasser	Natriumoxalat	0,67
		Wasser	Natronlauge	einige Tropfen
Wasser	Natriumcarbonat	0,5		
Wasser	Natriumsilikat (Wasserglas)	0,2 - 1		
Wasser	Natriumpolyacrylat	10		
Kartoffelmehl		Isobutanol	-	-
		Cyclohexanon	-	-
		Isobutanol + Diethylphthalat	-	-
		Diethylphthalat	-	-
			-	-
Keramische Massen		Wasser	Tetranatriumpyro- phosphat	0,45...1,4
		Wasser	Kalium/Natriumhexa- metaphosphat	1,0
		Wasser	Kalium/Natriumhexameta- phosphat + Natriumcarbonat	o.A. o.A.
Kieselgur		Wasser	-	-
		Wasser	Natriumsilikat (Wasserglas)	o.A.
		Wasser	Natriumoxalat	0,67
		Wasser	Trinatriumphosphat	o.A.
		Wasser	Ammoniak	2,0
Kieselgut		Wasser	-	-
	2,2...2,3	Wasser	Tetranatriumpyro- phosphat	1,0
Kleie		Wasser	Trinatriumphosphat	o.A.
Knochenasche		Wasser	-	-



Feststoff		Sedimentations- flüssigkeit	Zusatzstoff	
Art	Dichte g/cm <sup>3</sup>		Art	Konzentration g/l
Kobalt	8,8	Isobutanol	-	-
		Cyclohexan	-	-
		Cyclohexanon	-	-
		Diethylphthalat	-	-
		Cyclohexanol	-	-
		Ethanol	-	-
		Müßl + Aceton	-	-
		Wasser + Ethylenglycol	Trinatriumphosphat	o.A.
Ethanol + 5 % Wasser	-	-		
Kobaltoxid		Wasser	Kalium/Natriumhexameta- phosphat	0,6
			+ Natriumcarbonat	0,12
Kohle (s.a. Aktivkohle, Braunkohle, Steinkohle)		Wasser	Calciumchlorid	1,0
		Ethanol	Calciumchlorid	10...15
		Ethylenglycol	Calciumchlorid	0,05...0,5
		Ethylenglycol	Strontiumchlorid	0,05...0,5
		Ethylenglycol	Cobaltchlorid	0,05...0,5
		Cyclohexan	-	-
		Cyclohexanol	-	-
		Cyclohexanon	-	-
		Ethanol	-	-
		Petroleum	Ölsäure	1...10
		Benzin	Ölsäure	1...10
		Cyclohexanol + 50 Vol.% Methanol	-	-
		Koke	1,6...1,9	Isobutanol
Wasser	Natriumalkylnaphthalen- sulfonat			1,0
Wasser	Natriumlinoleat			1,0
Wasser	Natriumoleat			10,0
Wasser	Gerbsäure + Ammoniak			0,5 0,8...3,2
Ethanol	Calciumchlorid			1,0
Ethanol + 50 Vol.% Ethylenglycol	Calciumchlorid			1,0
Korund (s.a. Aluminium- oxid, Tonerde)	4,0			Wasser
		Wasser	Tetranatriumpyrophosphat	0,45...1,35
		Wasser	Trinatriumphosphat	o.A.
Kraftwerkasche (s.a. Asche, Flugasche)		Wasser	Tetranatriumpyrophosphat	1,0
Kreide (s.a. Calcium- carbonat)	2,6	Wasser	-	-
		Wasser	Natriumsilikat (Wasserglas)	2,0
		Wasser	Kaliumcitrat	5,5
		Wasser	Tetranatriumpyrophosphat	0,3...1,5
		Wasser	Ammoniak	2,0
		Aceton	-	-
		Petroleum	-	-
		Isopropanol	-	-
Kreide (gefällt)		Isopropanol	-	-
Kryolith	3,0	Wasser + 20 Vol.% Glycerin	-	-
		Ethylenglycol	-	-
		Wasser	Tetranatriumpyrophosphat	o.A.
		Ethylenglycol	-	-
Kunststoffe		Wasser	Tetranatriumpyrophosphat	0,45...1,35
		Wasser	Trinatriumphosphat	o.A.
		Isobutanol	-	-

Feststoff		Sedimentations- flüssigkeit	Zusatzstoff	
Art	Dichte g/cm <sup>3</sup>		Art	Konzentration g/l
Kupfer	8,9	Wasser	-	-
		Wasser	Tetranatriumpyrophosphat	20
		Aceton	-	-
		Rfööl	-	-
		Rfööl + Aceton	-	-
		Sojaöl + 30 Vol.-% Aceton	-	-
		Cyclohexanon	-	-
		Cyclohexanol	-	-
		Isomylalkohol	-	-
		Kupferhydroxid		Wasser
Kupferoxychlorid		Wasser	-	-
Kupferphthalocyanin		Wasser	-	-
Kupferschlacke		Wasser	Tetranatriumpyrophosphat	1,0
Kupferverbindungen (nicht wasserlösl.)		Wasser	Tetranatriumpyrophosphat	0,45...1,35
		Wasser	Natriumhexametaphosphat	0,5
Lüppulver		Wasser	Trinatriumphosphat	o.A.
Leuchtstoffe		Wasser	Natriumcitrat	0,5
Lignit		Isobutanol	-	-
		Diethylphthalat	-	-
		Cyclohexanol + 10 % Methanol	-	-
Lithopone	4,2	Diethylphthalat	-	-
		Glycerin	-	-
		Wasser	Natriummethylen-dinaphthyl- sulfonat	1,0
		Wasser	Tetranatriumpyrophosphat	0,3...1,5
		Wasser	Trinatriumphosphat	o.A.
		Wasser + 33 % Glycerin	-	-
L88		Wasser	Trinatriumphosphat	o.A.
		Wasser	Ammoniak	0,1
		Wasser	Natriumsilikat (Wasserglas)	o.A.



Feststoff		Sedimentations- flüssigkeit	Zusatzstoff	
Art	Dichte g/cm <sup>3</sup>		Art	Konzentration g/l
Magnesiumcarbonat	3,5	Wasser	Tetranatriumpyrophosphat	0,3...1,5
		Methanol	-	-
		Wasser	Ammoniakwasser	5,8 Vol. %
		Cyclohexanon	-	-
		Ethylenglycol	Calciumchlorid	0,05...0,5
		Ethylenglycol	Strontiumchlorid	0,05...0,5
		Ethylenglycol	Cobaltchlorid	0,05...0,5
		Ethylenglycol	-	-
Magnesiumoxid	2,8...3,6	Ethylenglycol	-	-
		Methanol	-	-
Magnesiumsilicid		Wasser	Tetranatriumpyrophosphat	0,3...1,5
Magnesiumsilikate (s.a. Enstatit)	3,0...3,3	Wasser	Kalium/Natriumhexameta- phosphat	1,0
		Wasser	Natriumcarbonat	s.A.
		Wasser	Tetranatriumpyrophosphat	1,0
		Wasser	Kalium/Natriumhexameta- phosphat + Natriumcarbonat	o.A.
Magnetit		Wasser	-	-
		Ethanol	-	-
		Methanol	-	-
		Nitrobenzol	-	-
Mangan		Cyclohexanon	-	-
		Isobutanol	-	-
Mangancarbonat		Wasser	Kalium/Natriumhexameta- phosphat	1,0
		Wasser	Tetranatriumpyrophosphat	1,0
		Cyclohexanon	-	-
Mangandioxid, Pyro- lysit	4,7...4,8	Wasser	Tetranatriumpyrophosphat	0,3...2,25
Manganoxide	4,5...5,4	Wasser	Tetranatriumpyrophosphat	0,3...2,25
Mehl		Petroleum	Ölsäure	1,0...10,0
		Isobutanol	-	-
		Isobutanol + Diethylphthalat	-	-
		Diethylphthalat	-	-
		Benzin	-	-
		Benzol	-	-
		Cyclohexanon	-	-
		Benzin	Ölsäure	1,0...10,0
Mennige (s.a. Blei- oxide, Bleifarben)	9,0	Paraffinöl + Benzol	-	-
		Cyclohexanon	-	-
		Ethylenglycol	-	-
		Wasser + Ethylen- glycol	Trinatriumphosphat	o.A.
		Cyclohexanon	-	-
		Wasser	Tetranatriumpyrophosphat	0,3...1,5
		Xylol	-	-
		Ethylenglycol	Calciumchlorid	0,05...0,5
Ethylenglycol	Strontiumchlorid	0,05...0,5		
Ethylenglycol	Cobaltchlorid	0,05...0,5		

Feststoff		Sedimentations- flüssigkeit	Zusatzstoff	
Art	Dichte g/cm <sup>3</sup>		Art	Konzentration g/l
Mergel	2,7	Wasser	Tetranatriumpyrophosphat	o.A.
		Wasser	Kalium/Natriumhexameta- phosphat	1,0
		Wasser	Kalium/Natriumhexameta- phosphat + Natriumcarbonat	o.A. o.A.
Metalle (s. direkt unter den Elementen)				
Methylmethacrylat		Wasser	-	-
Milchpulver	1,4	n-Octanol	-	-
		Isobutanol	-	-
Miloriblauf		Wasser	Trinatriumphosphat	o.A.
Mineralfarben		Wasser	Kaliumnitrat	30,6
Mineralwolle		Cyclohexanon	-	-
Molybdän	10,2	Ethanol	-	-
		Aceton	-	-
		Glycerin	-	-
		Wasser + Glycerin	-	-
		Wasser + Ethylengly- col	-	-
		Ethylenglycol	-	-
Molybdänsulfid		Cyclohexanon	-	-
Natriumbicarbonat	2,2	Cyclohexanon	-	-
		Cyclohexanol	-	-
Natriumphosphat		Ethanol	-	-
Nickel	8,8	Cyclohexanon + 10 % Aceton	-	-
		Cyclohexan	-	-
		Cyclohexanon	-	-
		Cyclohexanol	-	-
		Rüßöl + Aceton	-	-
		Wasser + Glycerin	-	-
Nickeloxid	6,8	Wasser + Glycerin	-	-
Organische Pulver		Isobutanol + Diethylphthalat	-	-
		n-Octanol	-	-
		Isoamylalkohol	-	-
Penicillin		Isocetan	-	-
Petrol eumkoks		Methanol	-	-
Phosphate (s.a. Roh- phosphate)		Wasser	Tetranatriumpyrophosphat Natriumhexametaphosphat	0,9 1,0
Phosphor (rot)	2,2	Ethanol	-	-
		Wasser	Kaliumsilikat	0,12 Vol. %
		Wasser	Natriumhexametaphosphat	0,5
Phosphor (weiß)	1,8	Wasser	Natriumsalz der polymeri- sierten, substituierten Alkylbenzolsulfonsäure + Kaliumsilikat	0,2 1,0

Feststoff		Sedimentations- flüssigkeit	Zusatzstoff	
Art	Dichte g/cm <sup>3</sup>		Art	Konzentration g/l
Pigmente		Cyclohexanon	-	-
		Cyclohexanol	-	-
		Isopropanol	-	-
		Wasser	Tetranatriumpyrophosphat	0,45...2,25
		Wasser + Ethylenglycol	-	-
Polymethylmetacrylat		Wasser	Trinatriumphosphat	-
Polyvinylacetat		Wasser	Tetranatriumpyrophosphat	o.A.
Polyvinylchlorid	1,4	Isopropanol	Natriumlinoleat	o.A.
		Isobutanol	-	-
		Wasser	Gerbsäure	1,0
		Wasser	Trinatriumphosphat	o.A.
		Wasser	Natriumlinoleat	o.A.
Polyester		Paraffinöl	-	-
Portlandzement	3,1	n-Butanol	-	-
		Benzylalkohol	-	-
		Uhinolin	-	-
		Cyclohexanol	-	-
		Cyclohexanon	-	-
		Cyclohexanon + Iso- amylalkohol	-	-
		Ethylenglycol	-	-
		Ethanol	Calciumchlorid	0,05...0,2
		Ethanol	Strontiumchlorid	0,08...0,3
		Ethylenglycol	Calciumchlorid	0,11...0,45
		Ethylenglycol	Strontiumchlorid	0,11...0,45
		Ethanol	-	-
		Isobutanol	-	-
		Rizinusöl	-	-
		Steinöl	-	-
Methanol	Tetranatriumpyrophosphat	gesättigt		
Paraffinöl	-	-		
Porzellanpulver	2,4	Wasser	Natriumhexametaphosphat	0,5
Pumicit		Wasser	-	-
Puzzolane		Wasser	Tetranatriumpyrophosphat	0,45...1,35
		Wasser	-	-
Pyrit (s.s. Eisen- sulfid)	4,4	Ethylenglycol	Calciumchlorid	0,05...0,5
		Ethylenglycol	Strontiumchlorid	0,05...0,5
		Ethylenglycol	Cobaltchlorid	0,05...0,5
		Methanol + Tetra- chlorkohlenstoff	-	-
		Wasser	Tetranatriumpyrophosphat	o.A.
Wasser + Glycerin	Tetranatriumpyrophosphat	o.A.		
Quarz (s.s. Sand, Sandstein)	2,65	Wasser	Tetranatriumpyrophosphat	0,45...1,35
		Wasser	Natriumhexametaphosphat	0,5
		Wasser	Natriumoxalat	0,67
		Wasser	Trinatriumphosphat	o.A.
		Wasser	-	-
		Wasser	OH <sup>-</sup> -Ionen	pH = 7...8
Quarzgut		Wasser	Tetranatriumpyrophosphat	1,0

Feststoff		Sedimentations- flüssigkeit	Zusatzstoff	
Art	Dichte g/cm		Art	Konzentration g/l
Quecksilberver- bindungen (nicht wasserlös.)		Wasser	Tetranatriumpyrophosphat	0,45...1,35
Resin		Wasser	Trinatriumphosphat	o.A.
Rohmehl, Rohschlümme (für Zement)		Cyclohexanol	-	-
		Cyclohexanol + 50 Vol. % Isocamyl- alkohol	-	-
		Isobutanol	-	-
		Wasser	-	-
		Wasser	Tetranatriumpyrophosphat	0,45...1,35
Rohphosphate (s.a. Phosphate)		Wasser	Tetranatriumpyrophosphat	0,45...1,35
		Wasser	Trinatriumphosphat	o.A.
Rohrzucker (s.a. Zucker)	1,6	Diethylphthalat	-	-
		Isobutanol	-	-
		Isocamylalkohol	-	-
Ruß	1,7...2,0	Aceton	-	-
		Methanol	-	-
		Wasser	Diocylester der Natrium- sulfobernsteinsäure	1,0...10,0
		Wasser	Natriumlinoleat	10,0
		Wasser	Gerbsäure	1,0
Rutheniumoxid	7,0	Wasser	Natriumhexametaphosphat	0,5
Sand (s.a. Quarz, Sandstein)		Ethanol + Butyl- phthalat	-	-
		Wasser	-	-
		Wasser	Natriumalkilat (Wasserglas)	2,0
		Wasser	Trinatriumphosphat	o.A.
Sandstein (s.a. Quarz, Sand)		Wasser	Tetranatriumpyrophosphat	0,45...1,35
		Wasser	Trinatriumphosphat	o.A.
		Wasser + Cyclohexanon	-	-
Schamotte	2,6	Wasser	Tetranatriumpyrophosphat	0,3...1,5
		Wasser	Kalium/Natriumhexameta- phosphat	1,0
		Wasser	Kalium/Natriumhexameta- phosphat + Natriumcarbonat	o.A.
		Wasser	Natriumhexametaphosphat	o.A.
Schiefer	2,7	Ethanol	Calciumchlorid	o.A.
		Wasser	Tetranatriumpyrophosphat	1,0
Schlacke (s.a. Hoch- ofenschlacke)		Wasser	-	-
		Isopropanol	-	-
		Wasser	Tetranatriumpyrophosphat	0,3...1,5
Schleifmittel (s.a. Si- liciumcarbid, Korund)		Wasser	Tetranatriumpyrophosphat	0,3...1,5
		Wasser	Trinatriumphosphat	o.A.
Schwefel	2,1	Wasser	Natriumlinoleat + Natriumoleat	o.A. o.A.
Schwefelkies		Ethylenglycol	-	-
Schwermetallver- bindungen (nicht wasserlös.)		Wasser	Tetranatriumpyrophosphat	0,45...1,35

Feststoff		Sedimentations- flüssigkeit	Zusatzstoff	
Art	Dichte g/cm <sup>3</sup>		Art	Konzentration g/l
Selen	4,5	Cyclohexanon	-	-
		Cyclohexanol	-	-
		Ethylenglycol	-	-
		Ethylenglycol	Calciumchlorid	0,05...0,5
		Ethylenglycol	Strontiumchlorid	0,05...0,5
		Ethylenglycol	Cobaltchlorid	0,05...0,5
		Wasser	Tetranatriumpyrophosphat	0,45...1,35
Silberhalogenid	6,0	Wasser	Natriumhexametaphosphat	0,5
Silber - Palladium- paste	10,6	Toluol	-	-
Silicium	2,4	Wasser	-	-
		Wasser	Natriumhexametaphosphat	0,5
Siliciumcarbid	3,2	Methanol	Natriumsalz der Ethylen- diamintetraessigsäure	10,0
		Wasser	-	-
		Wasser	Kalium/Natriumhexameta- phosphat	1,0
		Wasser	Kalium/Natriumhexameta- phosphat + Natriumcarbonat	o.A.
		Wasser	Tetranatriumpyrophosphat	0,45...1,35
		Wasser	Natriumhexametaphosphat	0,5
		Wasser	Trinatriumphosphat	o.A.
		Wasser + Ethylen- glycol	Tetranatriumpyrophosphat	o.A.
		Wasser	Nonylphenoxypolyethanol	einige Tropfen
Siliciumoxid (s.a. Quarz, Kiesel- gut)		Wasser + 50 Vol. % Xylol	-	-
		Wasser	Natriumhexametaphosphat	0,5
		Wasser	9-10 Ethoxy-Octylphenol	einige Tropfen
		Wasser + Ethanol	-	-
Silikate (nicht wasserlös.)		Wasser	-	-
		Wasser	Tetranatriumpyrophosphat	0,45...2,25
		Wasser + 50 Vol. % Ethanol	-	-
		Wasser + 50 Vol. % Ethylenglycol	-	-
		Wasser + Ethylen- glycol	Trinatriumphosphat	o.A.
		Wasser	Tetranatriumpyrophosphat + Natriumoxalat + Natriumhexametaphosphat	2,25 0,67 1,0
Sillimanit		Wasser	-	-
		Wasser	Tetranatriumpyrophosphat	24,8
		Wasser + 50 Vol. % Ethanol	-	-
Stahl	7,8	Wasser + Ethylengly- col	-	-
		Wasser + 50 Masse % Ethylenglycol	Cobaltchlorid	0,1
		Wasser	Alkylphenolethylenoxid- Kondensat	1,0

Feststoff		Sedimentations- flüssigkeit	Zusatzstoff	
Art	Dichte g/cm <sup>3</sup>		Art	Konzentration g/l
Stärke	1,5	Isobutanol	-	-
		Diethylphthalat	-	-
		Isobutanol + Diethylphthalat	-	-
		Benzol	-	-
		Methanol	-	-
Steatit	2,7...2,8	Wasser	Kalium/Natriumhexameta- phosphat	1,0
		Wasser	Kalium/Natriumhexameta- phosphat + Kaliumcarbonat	o.A.
		Wasser	Tetranatriumpyrophosphat	o.A.
Steinkohle (s.a. Kohle)	1,4	Aceton	-	-
		Cyclohexanol	-	-
		Cyclohexanol + 50 Vol. % Methanol	-	-
		Cyclohexanon	-	-
		Cyclohexanon + Metha- nol	-	-
		Ethylenglycol	-	-
		Ethanol	Calciumchlorid	11,0
		Ethanol	-	-
		Methanol	-	-
		Petroleum	-	-
		Wasser	Diocylester der Natrium- sulfobernsteinsäure	5,0...10,0
		Wasser + Ethanol	-	-
		Wasser + Ethanol	Natriumlinoleat + Calciumchlorid	o.A. o.A.
		Wasser + 50 Vol. % 1,3 Butylenglycol	-	-
		Wasser + 50 Vol. % 1,3 Butylenglycol	Natriumcitrat	0,362
		Wasser + 50 Vol. % 1,3 Butylenglycol	Netzmittel	0,2...0,3
		Wasser	Natriumlinoleat + sulfoniertes Lorol (Hauptanteil Dodecyl- alkohol)	10,0 o.A.
Wasser	Gerbsäure	o.A.		
Xylol	-	-		
Strontiumcarbonat	3,7	Cyclohexanon	-	-
		Wasser	Tetranatriumpyrophosphat	1,0
Strontiumsalze (nicht wasserlös.)		Wasser	Tetranatriumpyrophosphat	0,45...1,35
Strontiumtitanat		Wasser	Kalium/Natriumhexameta- phosphat	1,0
Sulfide		Ethylenglycol	-	-
		Wasser	Saponin	o.A.
Sulfonamid	1,3	Isopropanol	9-10 Ethoxyoctylphenol	einige Tropfen
Talkum	2,7	Wasser	Tetranatriumpyrophosphat	0,3...1,5
		Wasser	Natriumhexametaphosphat	1,0
Tantal	16,6	Cyclohexanol	-	-
		Cyclohexanon	-	-
		Ethylenglycol	-	0,1
Thiogutt		Cyclohexanon	-	-



Feststoff		Sedimentations- flüssigkeit	Zusatzstoff	
Art	Dichte g/cm <sup>3</sup>		Art	Konzentration g/l
Thorium		Wasser 33 % Glycerin	-	-
Titan	5,0	Wasser Wasser Wasser + 50 Masse % Ethylenglycol	Tetranatriumpyrophosphat Natriumhexametaphosphat -	1,0 1,0 -
Titancarbid	3,8	Wasser Wasser	Tetranatriumpyrophosphat Natriumsalz der polymeri- sierten Carboxylsäure	1,0 einige Tropfen einer 25 %igen wässr. Lösung
Titandioxid (Rutil, Anatas)	3,8...4,2	Leinol Wasser  Wasser + 50 Masse % Ethylenglycol Wasser  Wasser Wasser Cyclohexanon Cyclohexanol + 10 Vol. % Isoamylalkohol Ethylenglycol Xylol	- Kalium/Natriumhexameta- phosphat + Kaliumhydroxid - Natriumsalz der polymeri- sierten Carboxylsäure Tetranatriumpyrophosphat Natriumhexametaphosphat - - - -	- 0,3 pH = 10,7 - einige Tropfen einer 25 %igen wässr. Lösung 1,0 0,5...1,0 - - - -
Titaneisen		Wasser	-	-
Titanweiß		Wasser Xylenollösung	Tetranatriumpyrophosphat -	o.A. -
Foluidinrot		Wasser	Trinatriumphosphat	o.A.
Ton	2,5...2,6	Wasser Wasser Wasser Wasser  Wasser Wasser Wasser Wasser  Butylphthalat + Ethanol Wasser	Natriumcarbonat - Natriumoxalat Natriumsilikat (Wasserglas) Natriumhexametaphosphat Natriumpyrophosphat Trinatriumphosphat Kalium/Natriumhexameta- phosphat - Natriumpolyacrylat	o.A. - 0,67 20,0 1,0 0,3...1,5 o.A. 1,0 - 40
Tonerde (s.a. Korund, Aluminiumoxid)		Wasser Wasser  Wasser Wasser Wasser  Tetrachlor- kohlenstoff Cyclohexanon	- Kalium/Natriumhexameta- phosphat Natriumhexametaphosphat Natriumtartrat Salzsäure Tetranatriumpyro- phosphat - -	- 1,0 1,0 1,0 pH = 3 0,3...1,5 - -

Feststoff		Sedimentations- flüssigkeit	Zusatzstoff	
Art	Dichte g/cm <sup>3</sup>		Art	Konzentration g/l
Tonerdeement (s.a. Zement)	3,2	Ethylenglycol Ethylenglycol Cyclohexanol Chinolin	Calciumchlorid Cobaltchlorid	1,0 0,65
Tonschiefer (s.a. Schiefer)		Wasser	Trinatriumphosphat	o.A.
Traub		Isobutanol	-	-
Tricalciumphosphat		Wasser Methanol Wasser	Tetranatriumpyrophosphat - -	0,45...1,35 - -
Tripolyphosphat		Methanol		
Trockenhefe		Wasser + Ethanol	-	-
Tuff (vulkan.)		Wasser Wasser Wasser	Natriumoxalat Ammoniak Natriumsilikat	0,67 2,0 o.A.
Ultramarin	2,3	Wasser Ethylenglycol	Tetranatriumpyrophosphat	o.A.
Uranerz	7,3	Wasser	Natriumhexametaphosphat	0,5
Uranoxid	7,1 - 11,0	Isobutanol Wasser Wasser Wasser Wasser  Wasser + Glycerin	- Trinatriumphosphat Tetranatriumpyrophosphat Natriumhexametaphosphat Natriumsalz der polymeri- sierten, substituierten Alkylbenzolsulfonsäure -	- o.A. 1,0 0,5 10,0  -
Waschpulver		Wasser + Ethylen- glycol	-	-
Weicheisen (s.a. Eisen)	7,8	Wasser + Glycerin	-	-
Weizenmehl (s.a. Mehl)	1,5	Cyclohexanon Ethanol Diethylphthalat Isobutanol Isobutanol + Diethylphthalat Petroleum	- - - - - - -	- - - - - - -
Wismutverbindungen (s.u. Bismutverbindungen)				
Wolfram	19,1	Wasser Glycerin Aceton + Ruböl Ethanol Aceton Methanol Wasser (Feststoff vorher in HF be- handeln und waschen) Wasser + Ethylen- glycol	Ethoxyliertes Nonylphenol - - - - - - -	einige Tropfen - - - - - - -

Feststoff		Sedimentations- flüssigkeit	Zusatzstoff	
Art	Dichte g/cm <sup>3</sup>		Art	Konzentration g/l
Wolfram	19,1	Wasser	Sacharose + ethoxyliertes Nonyl- phenol	300 einige Tropfen
		Ethylenglycol	Calciumchlorid	0,05...0,5
		Ethylenglycol	Strontiumchlorid	0,05...0,5
		Ethylenglycol	Cobaltchlorid	0,05...0,5
Wolframcarbid	15,9	Pflanzöl	-	-
		Wasser	-	-
		Wasser + Ethylen- glycol	-	-
		Ethylenglycol	-	-
		Ethylenglycol	Calciumchlorid	0,05...0,5
		Ethylenglycol	Strontiumchlorid	0,05...0,5
Wolframoxide	7,2 12,1	Wasser	Tetranatriumpyrophosphat	1,0
		Cyclohexanon	-	-
		Wasser + Glycerin	-	-
Zahnzement		Ethylenglycol	-	-
Zement (s.s. Portland- zement, Tonerde- zement)	2,9...3,2	Pyridin	-	-
		Petroleum	Ölsäure	1,0...10,0
		Benzol	-	-
		Isopropanol	-	-
		Methanol	Tetranatriumpyrophosphat	gesättigt
		n-Butanol	-	-
		Isobutanol	-	-
		Paraffinöl	-	-
		Cyclohexanol	-	-
		Cyclohexanol + 50 Vol. % Iso- amylalkohol	-	-
		Chinolin	-	-
		Ethanol	Calciumchlorid	0,055...5,5
		Ethanol	Strontiumchlorid	0,075...0,32
		Ethylenglycol	-	-
		Ethylenglycol	Calciumchlorid	0,05...0,5
		Ethylenglycol	Strontiumchlorid	0,05...0,5
		Ethylenglycol	Cobaltchlorid	0,05...0,5
		Benzin	-	-
		Benzin	Ölsäure	1,0...10,0
Methanol + Glycerin	-	-		
Zink	7,1	Ethanol	-	-
		n-Butanol	-	-
		Aceton	-	-
		Cyclohexanon	-	-
		Cyclohexanol	-	-
		Ethylenglycol	Calciumchlorid	o.A.
Zinkoxid	5,5...5,8	Isobutanol	-	-
		Wasser	Natriumhexametaphosphat	0,5...1,0
		Wasser	Tetranatriumpyrophosphat	0,3...1,5
		Wasser	Trinatriumphosphat	o.A.
		Wasser	Kalium/Natriumhexameta- phosphat	1,0
		Wasser	Natriumsalz der kondensierten Naphthalinsulfon- säure	5,0

Peststoff		Sedimentations- flüssigkeit	Zusatzstoff	
Art	Dichte g/cm <sup>3</sup>		Art	Konzentration g/l
Zinkeulfid		Cyclohexanon	-	-
Zinkweiß		Wasser	Tetranatriumpyrophosphat	0,9
Zinn	7,3	n-Butanol Isobutanol Isobutanol + n-Butanol	- - -	- - -
Zinndioxid	7,0	Wasser Wasser Wasser Wasser	Tetranatriumpyrophosphat Natriumcitrat Kalium/Natriumhexameta- phosphat Kalium/Natriumhexameta- phosphat + Natriumcarbonat	0,9 o.A. 1,0 0,6 0,12
Zinnweiß		Wasser	Tetranatriumpyrophosphat	0,45...1,35
Zirkon	6,5	Methanol Wasser Wasser + 50 Vol. % Methanol Wasser Wasser Isobutanol	Salzsäure Tetranatriumpyrophosphat - - Kalium/Natriumhexameta- phosphat -	0,036 (0,001 n) 0,3...2,25 - - 1,0 -
Zirkondioxid	5,5-5,7	Wasser Wasser Wasser Wasser	Ölsäure Tetranatriumpyrophosphat Kalium/Natriumhexameta- phosphat Natriumhexametaphosphat	o.A. 0,3...1,5 1,0 o.A.
Zirkonsilikat	4,7	Wasser	Kalium/Natriumhexameta- phosphat + Natriumcarbonat	0,6 0,12
Zucker (s.a. Rohrzucker)	1,6	Isobutanol Diethylphthalat Isoamylalkohol Cyclohexanon Isopropanol	- - - - -	- - - - -